



Understanding the viral molecular factors involved in Zika virus pathogenicity in humans

Sandra Bos

► To cite this version:

Sandra Bos. Understanding the viral molecular factors involved in Zika virus pathogenicity in humans. Health. Université de la Réunion, 2019. English. NNT : 2019LARE0005 . tel-02879562

HAL Id: tel-02879562

<https://theses.hal.science/tel-02879562>

Submitted on 24 Jun 2020

HAL is a multi-disciplinary open access archive for the deposit and dissemination of scientific research documents, whether they are published or not. The documents may come from teaching and research institutions in France or abroad, or from public or private research centers.

L'archive ouverte pluridisciplinaire **HAL**, est destinée au dépôt et à la diffusion de documents scientifiques de niveau recherche, publiés ou non, émanant des établissements d'enseignement et de recherche français ou étrangers, des laboratoires publics ou privés.

Université de la Réunion
Ecole doctorale "Sciences, Technologies et Santé" E.D. 542

THESE DE DOCTORAT

Présentée en vue de l'obtention du grade de :
DOCTEUR EN BIOLOGIE, MEDECINE, SANTE
Spécialité : Virologie

UNDERSTANDING THE VIRAL MOLECULAR FACTORS INVOLVED IN ZIKA VIRUS PATHOGENICITY IN HUMANS

SANDRA BOS

Soutenue le 18 Avril 2019

Composition du Jury :

Pr. Diane GRIFFIN	Johns Hopkins Bloomberg School of Public Health	Rapporteur
Dr. Jean DUBUISSON	Institut Pasteur de Lille	Rapporteur
Dr. Catherine CETRE-SOSSAH	CIRAD, UMR ASTRE	Examineur
Dr. Gilles GADEA	INSERM, UMR PIMIT	Directeur de thèse
Pr. Marie-Lise GOUGEON	Institut Pasteur	Co-directeur de thèse
Pr. Philippe DESPRES	Université de la Réunion	Co-encadrant de thèse

À vous,
qui m'avez tout appris

*Et à vous que j'estimais beaucoup
et qui, même à bout de souffle,
avez su me faire rire*

« Science is a way of thinking
much more than it is a body of knowledge »

Broca's Brain: Reflections on the Romance of Science – **Carl Sagan**

REMERCIEMENTS

Avant toute chose, je voudrai remercier chaque entité ayant consciemment ou inconsciemment participé à ce travail. Tout au long de ma thèse j'ai pu bénéficier du soutien indéfectible de mes proches et rencontrer des gens venus des quatre coins du monde, qui m'ont inspirée, enseignée, épaulée, et encouragée dans mes recherches. Amis, Paul, Zoé, Dorian, B2, Famille.s, Arnaud, collaborateurs et collègues, professeurs et néophytes à qui j'ai pu faire découvrir ma passion pour la Virologie, je n'aurai pas assez de ces quelques lignes pour vous écrire un petit mot à tous mais je tiens sincèrement à vous dire merci !

—

Je tiens également à remercier Patrick Mavingui, directeur de l'unité PIMIT qui m'a accueillie pour mon doctorat, ainsi que Diane Griffin, Jean Dubuisson et Catherine Cetre-Sossah d'avoir accepté d'être rapporteur ou examinateur de ma thèse.

Dear Diane, I particularly want to express my profound respect and gratitude to you. Since we met, you have always been there for me and available during my visits to Baltimore. Many thanks for coming to my defense. Having you on my jury is a great privilege for me.

—

Je voudrai particulièrement remercier mes directeurs et encadrants de thèse, pour leur confiance et leur bienveillance à mon égard et saluer leurs qualités pédagogiques, humaines, et scientifiques. Nul ne peut rêver d'un meilleur soutien et encadrement. Tout au long de ces années, vous m'avez offert une multitude d'opportunités, la possibilité d'assister à des congrès, de nous y représenter seule, mais également une grande liberté vis-à-vis de mes recherches.

Gilles, je suis fière d'avoir été ta première thésarde. Grâce à toi j'ai appris la vie en équipe, la rigueur de la paillasse, et le « on » non-participatif ! Plus

sérieusement, j'ai adoré travailler avec toi. Au-delà d'être mon directeur de thèse tu as également été un « lab partner » idéal ! Je ne sais même plus combien de fous rires on a eus, mais repenser à la pipette (qui coule) du P2+ suffit à me refaire rire. J'espère sincèrement que notre collaboration continuera après mon doctorat.

Philippe, vous représentez tellement pour moi. Apprendre à vos côtés fut un honneur et je ne vous remercierai jamais assez pour tout le précieux temps que vous m'avez accordé. Je ne connaissais rien aux Flavivirus avant de vous rencontrer, ni même à la Virologie. Les yeux pétillants de la passion qui vous anime, vous m'avez enseigné tant de choses. Outre vos qualités scientifiques indéniables, votre humanité est admirable. J'espère du plus profond de moi pouvoir devenir une virologue aussi respectable, et perpétuer tout ce que vous m'avez appris avec autant de passion et de patience.

Marie Lise, vous êtes également une grande dame. Merci d'avoir accepté la co-direction de ma thèse, de m'avoir accueillie à l'Institut Pasteur, soutenue, et fait découvrir votre domaine de recherche durant ces quelques mois. Cette période peut sembler courte, surtout lorsqu'elle est rapportée à l'échelle d'une vie où elle représenterait un peu moins de 1%, mais elle est tout de même équivalente à la fréquence des pDCs dans le sang ; lorsque l'on voit tout ce qu'elles sont capables de faire on se rend compte que moins de 1% c'est important ! Et, qui sait, je continuerai sans doute (plutôt peut-être ?) à étudier les pDCs car malgré la difficulté inhérente à leur rareté et leur culture, c'est un challenge que j'ai beaucoup aimé relever. Enfin, travailler à l'Institut fut un honneur, et c'est avec mille plaisirs que j'y venais chaque matin, boostée par une pensée à ceux et celles qui étaient là avant moi.

—

Enfin, Papa, Maman, Gaëlle, Papis et Mamies, je ne serai rien sans l'amour et les valeurs que vous m'avez tous donné. Qu'importe la couleur de notre ciel, vous m'avez supporté (dans les deux sens du terme) et tant appris. Aujourd'hui ni moi, ni ce travail, n'aurions été ce que nous sommes sans vous.

— PREFACE —

Avant de commencer cette préface de thèse tout à fait inhabituelle, évidemment, je voudrais vous poser cette question : le hasard existe-t-il ? Les rencontres que l'on fait, les choses qui nous arrivent, les livres que l'on lit et les virus que l'on découvre, ne sont-ils pas des rendez-vous, des synchronicités ?

La rencontre. Tout a commencé lors d'un anodin trajet en covoiturage avec mon encadrant de stage de Master 1 : “ David, j'ai découvert un virus incroyable ! C'est un Flavivirus, il s'appelle Zika. Il a l'air différent des autres, il peut faire ça, ou ça, et encore ça ! C'est incroyable tu ne trouves pas ? Je veux absolument en apprendre plus !”. Par chance le Pr Philippe Desprès, dont je ne connaissais alors que vaguement le nom apposé sur des publications scientifiques, venait d'arriver au laboratoire pour diriger l'équipe I2T ; l'équipe sœur de DySIIS, à laquelle j'étais rattachée à ce moment-là. Grâce à David, j'ai pu rencontrer Philippe et discuter un moment avec lui. Bien décidé à en savoir plus sur Zika je lui ai demandé s'il ne connaissait pas quelqu'un qui travaillait sur ce virus chez qui je pourrai postuler pour mon stage de master. Et, comme vous devez vous en douter, ce quelqu'un c'était lui. Car oui, Philippe avait emporté Zika dans ses valises. L'Aventure commença.

The proof of concept. C'est la boule au ventre mais pleine de motivation que je suis arrivée au laboratoire pour mon premier jour de stage. Je ne connaissais rien à la Virologie ni à ses techniques, et je me souviens que “plaque forming assay”, ma technique favorite, sonnait à ce moment-là comme un mot issu d'une langue totalement incompréhensible. A part ça tout se passait bien jusqu'à ce que Philippe me dise que ce n'est pas lui qui allait m'encadrer mais son collègue Gilles Gadea. Maintenant je peux dire que je n'étais pas vraiment super emballée par cette nouvelle ; et il me semble que toi non plus Gilles tu ne l'étais pas... Finalement, le choix du chef était le bon (comme toujours n'est-ce pas ?) et je crois que l'on a réussi à former une super

équipe. Après tout, comment cela aurait-il pu être autrement quand il s'agit de deux êtres matinaux, organisés et pleins de tocs ?

Durant mes débuts au laboratoire, une parole de Philippe résonnait dans ma tête : “La Virologie c’est comme la cuisine. Soit tu as le truc, soit tu ne l’a pas. C’est elle qui te choisit, pas l’inverse.” Quel stress ! Moi qui au plus profond de moi avait le sentiment d’être faite pour ça. Et si je m’étais trompée ? Si je ne l’avais pas, ce truc ? De toute façon il n’y avait qu’un seul moyen de le savoir : essayer. Et puis, le 15 mars 2016, le petit Zika-GFP est né. Même Philippe, qui l’a pourtant conçu, ni croyait pas. Grâce à ce clone, je me suis rendu compte combien j’aimais voir les virus pousser et combien cela m’émerveille. Comme l’a dit Richard Dawkins : “*There's real poetry in the real world.*” Et cette poésie elle était là, sous mes yeux.

La thèse. J’ai pleuré de joie pendant des heures (littéralement) lorsque j’ai compris que j’avais été reçue au concours de la bourse MENRT. Après toutes les épreuves surmontées, avoir l’opportunité de faire une thèse représentait beaucoup pour moi. C’était comme me délester de tous les poids qui me pèsent et ouvrir la porte sur un nouvel Univers : un Univers où je me sens légère et à ma place, et où mes différences sont une force. J’allais enfin avoir la possibilité de faire mes preuves, de devenir chercheur. Ce sentiment reste encore très vif aujourd’hui et difficile à décrire mais j’étais profondément heureuse et reconnaissante d’avoir cette chance. Et puis ma chance ne s’est pas arrêtée là, faisant de ma thèse une aventure humaine et scientifique exceptionnelle dont j’ai beaucoup appris. Tout au long de ces années, j’ai pu rencontrer et travailler avec des gens adorables qui ont cru en moi et ont tout fait pour m’aider et m’encourager dans mes recherches et mon futur. Mais, au-delà de tout, j’ai eu la chance de bénéficier d’un encadrement en or que je souhaite à chaque thésard.

C’est dans un contexte exceptionnel, en plein cœur de l’épidémie de Zika, que j’ai réalisé ma thèse. Car nous, à I2T, nous avons connu Zika avant le grand Boum, pendant, et maintenant que les choses se calment. Au début très peu de données étaient disponibles dans la littérature mais depuis notre caillou

du bout du monde, nous commençons déjà à apprendre à connaître la souche de Polynésie Française. Lorsqu'il explosa, et devint la « star des médias » début 2015, nous étions là, à la fois acteurs et spectateurs, au milieu de ce tourbillon. Nous vivions et faisons la recherche, les découvertes en “live”. En quelques mois à peine, de nouvelles données étaient publiées. Des données à lire, à trier, qui renforçaient nos hypothèses, en soulevaient de nouvelles, ou donnaient une nouvelle perspective d'analyse de nos résultats. C'était incroyable et tellement passionnant. Comprendre ce virus au jour le jour fut un énorme challenge que de nombreuses équipes de recherche partout dans le monde ont relevé. Aujourd'hui une productivité scientifique titanesque résulte de cet effort ; productivité à laquelle nous avons humblement participé.

ABBREVIATIONS

ADE	:	Antibody-dependent enhancement
Ae.	:	<i>Aedes</i>
ATP	:	Adénosine triphosphate
BR15	:	Zika virus strain BeH819015
C	:	Capsid protein
CCR-7	:	C-C chemokine receptor type 7
CD	:	Cluster of differentiation
CDC	:	Center for disease control and prevention
CDP	:	Common dendritic cell progenitor
CHIKV	:	Chikungunya virus
CLPs	:	Common lymphoid progenitors
CLR	:	C-type lectin receptor
CMPs	:	Common myeloid progenitors
CS	:	Conserved sequence
CZS	:	Congenital Zika syndrome
Da	:	Dalton
DC	:	Dendritic cells
DENV	:	Dengue virus
DNA	:	Deoxyribonucleic acid
E	:	Envelope protein
ED	:	Ectodomain
EID	:	Emerging infectious disease
ELISA	:	Enzyme linked immunosorbent assay
ER	:	Endoplasmic reticulum
FLT3L	:	FMS-like tyrosine kinase 3 ligand
GBS	:	Guillain-Barré syndrome
GFP	:	Green fluorescent protein
HAVcr-1	:	Hepatitis A virus cellular receptor
HIV	:	Human immunodeficiency virus
ICTV	:	International committee on taxonomy of viruses
IFN	:	Interferon
IFNAR	:	Interferon- α/β receptor
Ig	:	Immunoglobulin
IL	:	Interleukines
ILT	:	Immunoglobulin-like transcript
IRAK	:	Interleukin-1 receptor-associated kinase
IRF	:	Interferon regulatory factor
ISA	:	Infectious sub-genomic amplicons
ISFV	:	Insect specific flaviviruses
ISG	:	Interferon stimulated gene
ITAM	:	Immunoreceptor tyrosine-based activation motif

JEV	:	Japanese Encephalitis virus
KEDV	:	Kedougou virus
KFDV	:	Kyasanur Forest disease virus
LRR	:	Leucine-rich repeat
M	:	Membrane protein
MBFV	:	Mosquito-borne flaviviruses
mDC	:	myeloid DC
MERS	:	Middle East respiratory syndrome
MHC	:	Major histocompatibility complex
MMR	:	Macrophage mannose receptor
mRNA	:	messenger RNA
Mtase	:	Methyltransferase activity
M-TBFV	:	Mammalian tick-borne flaviviruses
NK	:	Natural killer lymphocyte
NKV	:	No-known vector
NLS	:	Nuclear location signal
NPC	:	Neuronal progenitor cells
NS	:	Non-Structural protein
ODN	:	Oligodeoxynucleotides
OHFV	:	Omsk Hemorrhagic Fever virus
ORF	:	Open reading frame
PAMP	:	Pathogen associated molecular pattern
PBMC	:	Peripheral blood mononuclear cell
PCR	:	Polymerase chain reaction
pDC	:	Plasmacytoid dendritic cell
pH	:	Hydrogen potential
POWV	:	Powassa virus
PRNT	:	Plaque reduction neutralization test
PRR	:	Pattern recognition receptor
pTalpha	:	pre-T cell receptor alpha
RCP	:	Representative concentration pathway
RCS	:	Repeated conserved sequence
RdRp	:	RNA-dependent RNA polymerase activity
RLRs	:	RIG-I-like receptors
RNA	:	Ribonucleic acid
ROS	:	Reactive oxygen species
RT-PCR	:	Reverse-transcriptase polymerase chain reaction
SARS	:	Severe acute respiratory syndrome
sfRNA	:	Subgenomic flaviviral RNA
SL	:	Stem-loop
SPOV	:	Spondweni virus
STAT	:	Signal transducer and activator of transcription
S-TBFV	:	Seabird tick-borne flaviviruses
SVP	:	Subviral particle

TAK	:	transforming-growth-factor- β -activated kinase
TBEV	:	Tick-borne Encephalitis virus
TBFV	:	Tick-borne flaviviruses
TGN	:	<i>Trans</i> -Golgi Network
TIR	:	Toll-IL-1 receptor
TLR	:	Toll-like receptor
TM	:	Transmembrane
TNF	:	Tumor necrosis factor
TRAF	:	TNF receptor associated factor
TRAIL	:	TNF-Related Apoptosis-Inducing ligand
Treg	:	regulatory T lymphocyte
UTR	:	Untranslated transcribed region
WHO	:	World health organization
WNV	:	West Nile virus
Xrn-1	:	5'-3' exorivonuclease 1
YFV	:	Yellow Fever virus
ZIKV	:	Zika virus

LIST OF TABLES

Table 1: Selected arboviruses of medical importance _____	21
Table 2: Reported suspect Zika and GBS cases per location _____	60
Table 3: Determinants of viral pathogenesis and diseases _____	64
Table 4: Factors responsible for cell injuries _____	66
Table 5: Zika virus cellular targets and receptors _____	68
Table 6: Human cell lines permissive to Zika virus infection _____	69
Table 7: Cellular antiviral responses against Zika virus infection _____	74
Table 8: Phenotypic characterization of human myeloid and plasmacytoid dendritic cells__	169
Table 9: Zika virus counteraction of antiviral response _____	220
Table 10: Overview of Zika virus-induced cellular pathogenesis _____	221

LIST OF FIGURES

Figure 1: Classification of viruses from capsid shape to viral RNA	2
Figure 2: The convergence model	4
Figure 3: Climate change and health	8
Figure 4: Projected climate changes	10
Figure 5: Health maps	17
Figure 6: Distribution of extreme poverty in the world	18
Figure 7: Post-earthquake Zika virus surge	19
Figure 8: Global distribution of emerging and re-emerging arboviruses	20
Figure 9: Predicted global distribution of <i>Ae. aegypti</i> and <i>Ae. albopictus</i> .	26
Figure 10: Phylogenetic reconstruction of <i>Flaviviridae</i>	29
Figure 11: Structure of Zika virus	32
Figure 12 : Flavivirus genome structure and protein expression	34
Figure 13 : Flavivirus life cycle	36
Figure 14: How Zika virus spread to the Americas	46
Figure 15: How Zika virus enters the human population	54
Figure 16: Zika symptoms	56
Figure 17: Zika virus vaccine platforms in clinical studies	57
Figure 18: Time until the clearance of Zika virus RNA	58
Figure 19: Congenital Zika syndrome cases in Brazil	60
Figure 20: Zika virus tropism	67
Figure 21: Schematic diagram of extrinsic antibody-dependent enhancement of infection	76
Figure 22: Notable amino acid changes since ZIKV discovery	79
Figure 22: Overall structure of ZIKV C protein	106
Figure 24: Comparison of ZIKV C with other known flavivirus C structures	106
Figure 25: Flavivirus particle at different maturation stages	108

Figure 26: Changes in ZIKV prM _____	110
Figure 27: Overall structure of ZIKV E protein _____	111
Figure 28: Surface-exposed amino acids conservation in flavivirus E protein _____	112
Figure 29: The fusogenic conformational change of the E protein during cell entry _____	113
Figure 30: Diverse functions of plasmacytoid dendritic cells _____	173
Figure 31: Activation pathway in plasmacytoid dendritic cells responding to nucleic acids _	177
Figure 32: Signaling of CpG ODN classes in different endosomal compartments _____	179
Figure 33: Contact between infected cells and plasmacytoid dendritic cells _____	181

LIST OF CONTENT

INTRODUCTION

I. INTRODUCTION TO VIRUSES AND EMERGENCE	1
I.1. Viruses	1
I1.1. Definition of Viruses	1
I1.2. Classification system	1
I.2. Emergence of infectious diseases and viruses	3
I2.1. Microbial adaptation	3
I2.2. Human susceptibility to infection	5
I2.3. Climate and Ecological changes	8
I2.4. Human behaviors and economic development	12
I2.5. Breakdown or absence of Public Health measures	17
II. ARBOVIRUSES TO FLAVIVIRUSES	20
II.1. The threat of Arboviruses	20
II1.1. The cladistic paradox of Arboviruses	22
II1.2. Epidemiology of Human Arbovirosis	22
II1.3. The emergence triangle of mosquito-borne arboviruses	25
II.2. FLAVIVIRUSES	28
II2.1. Flavivirus burden on Human Health	28
II2.2. Classification and Phylogeny of Flaviviruses	30
II.3. MOLECULAR BIOLOGY OF FLAVIVIRUSES	32
II3.1. Virion and Genome Structure	32
II3.2. Viral Cycle	35
II3.3. Features and Role of the Viral Proteins	38
II3.4. Evolutionary advantage of Flaviviruses	42
III. THE FIERY TALE OF ZIKA VIRUS	45
III.1. Classification	45
III.2. Emergence and Global spread	45
III2.1. Zika in the Pacific and Asia	47

III2.2. Situation in the Americas	49
III2.3. Situation in Europe	51
III.3. Zika virus Ecology	52
III3.1. Host and Reservoir	52
III3.2. Vectors and vector-borne transmission	53
III3.3. Non vector-borne transmission	54
III.4. Clinical features of Zika Fever	56
III4.1. Symptomatology	56
III4.2. Treatment	56
III4.3. Diagnosis and Detection	58
III4.4. Complications	59
III.5. Social Impact	62
IV. UNRAVEL THE PUZZLE OF ZIKA VIRUS PATHOGENICITY	63
IV.1. Reminder on Viral Pathogenesis	63
IV1.1. Terminology and Principle of viral pathogenesis	63
IV1.2. Pathogenic Mechanisms and determinants	65
IV.2. First insight on Zika virus Pathogenesis	67
IV2.1. Target cells and tissues	67
IV2.2. Attachment factors and Entry Receptors	70
IV2.3. Host responses to Zika virus infection	73
IV.3. Viral molecular factors involved in Zika virus pathogenesis	77
IV3.1. Molecular epidemiology	78
IV3.2. Objective of the Doctoral Research	81

PART I : DEVELOPMENT OF MOLECULAR VIROLOGY TOOLS FOR THE STUDY OF ZIKV BIOLOGY AND PATHOGENICITY

I. RATIONALE	96
II. ARTICLE n°1	98

PART II : CONTRIBUTION OF ZIKV STRUCTURAL PROTEINS

I. FEATURES OF ZIKA VIRUS STRUCTURAL PROTEINS	105
I.1. Capsid	105
I.2. Pr and Membrane	107
I2.1. The role of prM in the maturation process	107
I2.2. Particle heterogeneity	108
I2.3. Feature of ZIKV prM	109
I.3. Envelope	110
I3.1. Feature of ZIKV E protein	112
I3.2. Potential impact on ZIKV entry and cellular tropism	112
I3.3. The role of ZIKV E in the fusion process	114
I.4. Investigate the impact of ZIKV structural proteins	114
II. ARTICLE n°2	117
III. ARTICLE n°3	126
IV. ARTICLE n°4	147

PART III : ZIKV IMPACT ON PLASMACYTOID DENDRITIC CELLS ANTIVIRAL RESPONSE

I. INTRODUCTION TO PLASMACYTOID DENDRITIC CELLS	167
I.1. Overview of Dendritic Cells	167
I1.1. Main features of Dendritic cells	167
I1.2. Dendritic cell diversity	168
I.2. Plasmacytoid Dendritic Cells: Sentinels and Orchestrators of the Antiviral Immune Response	170
I2.1. Chronology of the plasmacytoid dendritic cells discovery	170
I2.2. Ontogeny of pDCs	171
I2.3. Distribution of plasmacytoid dendritic cells	172
I2.4. Physiological role of plasmacytoid dendritic cells	172
I.3. Virus detection and IFN production signaling pathway	175

13.1. Toll-like receptors and type I interferon production_____	176
13.2. Regulation of TLR activation_____	180
14. Flavivirus infection and Plasmacytoid dendritic cell response _____	180
14.1. Indirect sensing of flavivirus infection_____	180
14.2. Plasmacytoid dendritic cell activation upon flavivirus infection ____	182
II. ARTICLE n°5 _____	189

DISCUSSION

Asian <i>versus</i> African ZIKV lineages: Can less be more? _____	216
Phenotypic differences between ZIKV African and Asian lineage _____	216
The unforeseen effect of ZIKV structural proteins_____	218
Molecular determinant of differential binding rate_____	218
Determinants of ZIKV virulence _____	220
The E-glycosylation: a key factor for a broad diffusion _____	221
Is there only one mutation in prM involved in microcephaly? _____	223
188V: ZIKV boarding pass by NS1 _____	225
Concluding remarks: Did Zika mutate to cause severe diseases in humans and outbreaks?_____	226
Personal remarks _____	228

ANNEX

Annex n°1 _____	233
Annex n°2 _____	235
Annex n°3 _____	237

INTRODUCTION

I. INTRODUCTION TO VIRUSES AND EMERGENCE

I.1. Viruses

Viruses are everywhere, in every imaginable corner of the planet and have been living on Earth for hundreds of millions of years. Long before humans discovered and accepted their existence, at the end of the 19th century, viruses and infectious diseases shaped the history of Humanity; and will undoubtedly continue to do so. Nonetheless, humans, at all times, expressed reservations about them. Does a pathogen smaller than a bacterium exist? Are the viruses alive? What is the Origin of viruses, where do they come from? If some questions have been answered, the contemporary History of Virology, still enlivened by persistent and unanswered debates, illustrates the enigmatic nature of viruses.

I1.1. Definition of Viruses

More than in any other field, terminologies in virology are not an easy exercise as it aims to set boundaries on phenomena that remain misconceived; which sometimes lies on the cusp of philosophy of biology and Science. Viruses are not exempted from that, and have always been difficult to define since their discovery.

Viruses are obligate parasites, infecting all living organisms, and including themselves. They do not possess the ability to capture and store energy. From this arises the fundamental characteristic of their absolute dependence on a living host for reproduction. This way, a “virus” can be defined as an infectious agent composed of an RNA or DNA genome that replicates only within the cells of living hosts. It is an organism producing virions - namely a particle - that protects viral genome during the extracellular phase and allows viruses to infect new cells.

I1.2. Classification system

› The Classical System

In 1962, Lwoff, Robert Horne, and Paul Tournier, proposed a comprehensive scheme for the classification of all viruses (bacterial, plant, and animal) under the classical Linnaean hierarchical system consisting of phylum, class, order, family, genus, and species. The major principle of this classification is that viruses

should be grouped according to their shared properties rather than the one of the cells or organisms they infect. A second principle was a focus on the nucleic acid genome as the primary criterion for classification. Four characteristics were used for the classification of viruses: (i) nature of the nucleic acid genome in the virion, (ii) symmetry of the protein shell (capsid), (iii) presence or absence of a lipid membrane (envelope) and (iv) dimensions of the virion and capsid.

However, the International Committee on Taxonomy of Viruses (ICTV) did not adopt this system *in toto*. Designation of families, genera, and species was applied in both the scientific and medical literature but was only used for the classification of animal viruses (plant virologists use group names derived from the prototype virus of each group).

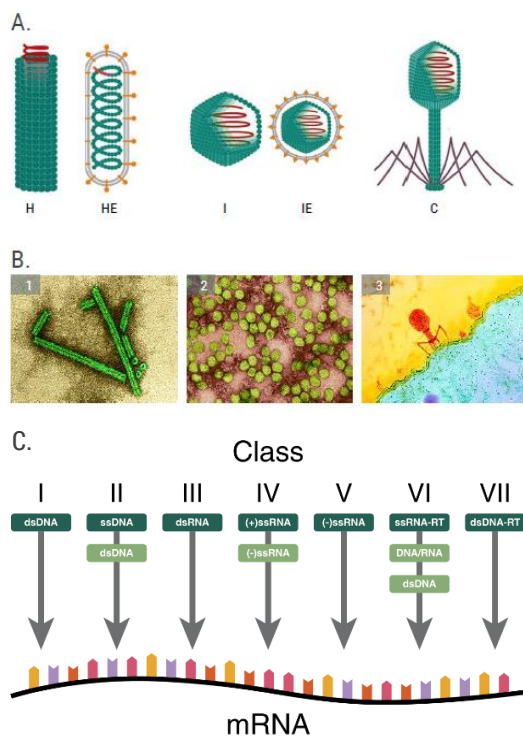


Figure 1: Classification of viruses from capsid shape to viral RNA

(A) Diversity of capsid shape. H helicoidal HE helicoidal enveloped icosahedral IE icosahedral enveloped C complex. Legend: blue = capsid, red = genome, grey = envelop, orange = glycoproteins (*science photo library*)

(B) Virus structure in colored transmission electron micrographs. 1 tobacco mosaic virus, helicoidal structure, unenveloped, 2 Yellow fever virus polyhedral structure, enveloped (Dennis Kunkel microscopy). 3 Bacteriophage T4, complex structure (*science photo library*)

(C) The Baltimore classification of viruses. This classification was created by David Baltimore, based on the nature of the viral genome and is on the method of viral mRNA synthesis. ss = single stranded; ds = double stranded (*Figure source: Wikipedia commons*)

› The Baltimore Classification System

Francis Crick conceptualized the central dogma in which cellular genes are encoded in a double stranded nucleic DNA that will be converted into working proteins carrying out all the functions necessary for life. To be done, information in DNA is first transcribed into a messenger RNA (mRNA) molecule, then mRNAs are transported to the cytoplasm where they are translated by ribosomes and

associated machinery into proteins. But, because viral protein synthesis is completely dependent on the cell's translational machinery, all viruses must direct the synthesis of mRNA to produce proteins. According to the obligatory relationship between the viral genome and its mRNA, David Baltimore proposed an alternative classification that groups viruses into families, depending on their type of genome, strand polarity, and their method of replication. This classification provides virologists with immediate insight into the steps that must take place to initiate replication and expression of viral genome.

1.2. Emergence of infectious diseases and viruses

In the book "A Planet of Viruses", Carl Zimmer wrote: "Viruses are the smallest living thing known to science, yet they hold the entire planet in their sway"¹. However, many of them will remain unknown and will never emerge, raising the question of which parameters facilitate their introduction and spread in human populations.

Emerging infectious diseases (EIDs) are defined as diseases caused by an infectious origin and whose incidence in humans has increased over the last two decades or is likely to increase in the near future. In the past 30 years, more than 30 new infectious diseases have been reported highlighting the growing threat of EIDs to populations. The emergence and spread of infectious diseases are driven by the convergence of a complex set of factors that promote the initiation of an epidemic process. To understand which variables contribute to these phenomenon, Smolinski *et al* developed a model, "The Convergence Model", which illustrates how factors related to (i) genetic and biology, (ii) physical environment, (iii) ecology, and (iv) social, political and economic status, can impact on the human-pathogen interaction². The following paragraphs will address some of the factors that contribute to the emergence of infectious diseases, particularly viral diseases.

12.1. Microbial adaptation

In the "Germ Theory" and Koch's postulates, the scientists of the time assumed that the diseases were caused by a "fixed" microbe species, monomorphic and invariant. Currently, the tremendous mutation capacity of microbes under

selection pressures is well established and can be an important determinant in the emergence or resurgence of many infectious diseases.

Microbes developed many sophisticated survival strategies that allow them to co-evolve with their host and environment, as well as to protect themselves from degradation by the immune system. Among these strategies, several microbes have developed an ability to exchange or incorporate new genetic material into their own genome. This horizontal gene transfer, or lateral transfer, is well described in bacteria and is recognized as a driving process involved in the acquisition of antibiotic resistance genes³. However, recent studies suggest that this process is not limited to this domain of life. Indeed, we now suspect a viral genus, a priori non-pathogenic to humans, the Mimiviruses, to be capable of such a process, as the acquisition of the topoisomerase gene would suggest⁴.

Another way for microbes to adapt very quickly to their environment lies in the speed of the mutation process. The champions in this field are viruses, especially RNA viruses which exhibit mutation rates that are higher in order of magnitude than any other replicative entity⁵. For instance, it is estimated that the mutation rate of RNA viruses is up to a million times higher than their hosts, the record being held (to the best of our knowledge) by the Bacteriophage Q β with $\sim 10^{-3}$ mutations per nucleotide per replication cycle⁶. If RNA viruses are probably the most intriguing biological entities for studying mutation rates, it's because they

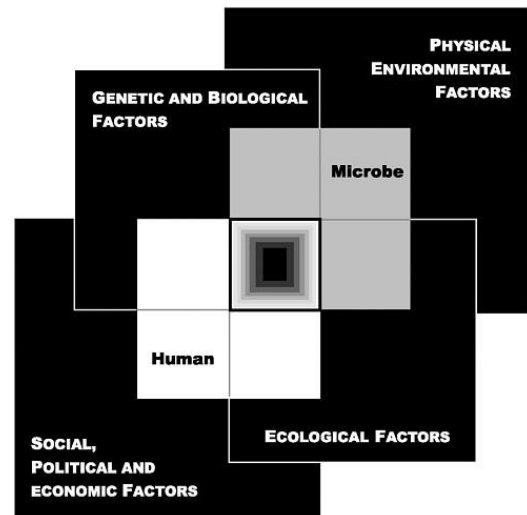


Figure 2: The convergence model

At the center of the model is a box representing the convergence of factors leading to the emergence of an infectious disease. The interior of the box is a gradient flowing from white to black; the white outer edges represent what is known about the factors in emergence, and the black center represents the unknown (similar to the theoretical construct of the "black box" with its unknown constituents and means of operation). Interlocking with the center box are the two focal players in a microbial threat to health—the human and the microbe. The microbe–host interaction is influenced by the interlocking domains of the determinants of the emergence of infection: genetic and biological factors; physical environmental factors; ecological factors; and social, political, and economic factors.

(Figure and caption from the book "Microbial Threats to Health: Emergence, Detection, and Response")

encode their own replication machinery. As a result, they are able to optimize their mutation rate for their fitness (compared to DNA viruses that use hosts polymerases). This incredible mutation capacity, inherently high, combined with their replication rate yields a progeny that differs from the parents by one or two mutations⁷, and thus generates a mutant cloud of descendants. Interestingly, the increase and decrease in the mutation rate of a virus leads to a reduction in the virulence of the viral population⁸. These results suggest a close relationship between the mutation rate of a virus, the diversity created in a viral population, and pathogenesis in an infected host. The perpetual genetic variation of microbes gives them a wide range of strategies to bypass the immune system⁹. Some of these include the antigenic variation, the hiding from the immune system¹⁰ (either by masking key surface antigens or by coating their surface with compounds mimicking host tissue to prevent recognition as "*nonself*"), the mechanisms to downregulate immune system and finally the ability to cause latent infection.

Overall, the high evolutionary potential of microbes makes them organisms able to adapt and develop resistance to even the most potent therapies. Nowadays, microbial adaptation seriously challenges our therapeutic response capacity and stands as the main obstacle to the development of protective vaccines and the discovery of new effective drugs.

12.2. Human susceptibility to infection

If pathogens evolve, so do their hosts. The human body, like a fortress, is full of barriers to prevent invasion by pathogens, which have been selected and conserved by hundred thousand years of co-evolution. These barriers are physical, such as the skin and mucous membranes, or cellular and molecular through the immune system and its effectors. Susceptibility to infection can occur when these defenses are by-passed, altered or compromised by the following factors.

› Transmission route

Infectious agents are transmitted from one host to another by specific means mainly determined by the site of excretion and the physiological stability of a

pathogen. Transmission routes play an important role in the fate of a pathogen and its ability to induce disease. While some pathogens have to deal with a limited number of transmission possibilities, others may use several routes to infect their hosts.

Transmission routes are divided into two main types. (i) Horizontal transmission refers to the spread of a pathogen to other organisms of the same or different species by non-hereditary means. This category includes the vectorial transmission by which an infectious agent is transmitted by the bite of an infected hematophagous vector, usually an insect. In this case, the pathogen is injected directly into the subcutaneous tissues and blood, thus bypassing the first defense of the host: the skin. (ii) Vertical transmission refers to the transfer of a pathogen between parent and offspring. It includes the transmission that occurs during pregnancy, when the infectious agent crosses the placental barrier, or during birth. When an agent is transmitted as a part of the host genome, as in the case of a retrovirus infection, we talk about germline transmission.

› Immunity and Aging

When a foreign organism is detected by the immune system, the innate immune response is induced to eliminate the invader. When this non-specific response is inadequate to control the infection, the adaptive immune response is triggered. The latter one, specific to a given pathogen, is essential to establish the immune memory. Induction and preservation of this response ensures individual immunization against subsequent infections and is the core principle of vaccination. If we consider the example of a viral infection, two major alternatives are possible: either the virus is cleared and the individual is immunized against infection with the same variant, or the virus settles in and persists. Immunization is triggered either following a natural infection or as a result of preventive vaccination. Being aware of this, the prevalence of infected people is a critical parameter in the emergence of viral disease and their epidemic potential, as only the naive immune people will be susceptible to infection.

However, susceptibility to infection varies throughout an individual's life and is strongly influenced by age, with the very young and the elderly at increased risk

of infection. While young people are at high risk of infection because of a fragile immune status, older people are more vulnerable to infection because of a weakened immune system due to chronic diseases and medical treatments. In addition, the senescence process significantly reduces cell-mediated immunity, immunization level, and impairs host defenses. This is highlighted by recent Dengue fever epidemics, in which a significant increase in the incidence of cases among the elderly has been reported¹¹.

› Immunocompromised populations

Thanks to medical advances, the life expectancy of patients has considerably been improved in recent years. But this invaluable benefit is not always priceless and some therapies used to treat or limit the progression of a disease reduce the overall immune capacity of the patients. The most striking example is cancer, whose burden is steadily increasing. Based on data from the World Health Organization, it is estimated that the global incidence of cancer will reach 29.5 million in 2040 compared to 18 million today¹². These patients, usually undergoing heavy treatment such as chemotherapy, are in addition to an ever-growing population of people living with HIV (human immunodeficiency viruses)¹³. This upsurge in immunocompromised people is concomitant with the emergence of opportunistic pathogens, some of which, previously uncommon or unrecognized as pathogenic for humans (e.g. *Aspergillus* spp.¹⁴), are now extending the list.

› Genetic polymorphism

Each of us has a different capacity for immunological reactivity and not all of us are equal against a pathogen. Indeed, individuals and populations are more or less susceptible to infection depending on their genetic determinants. J.B.S. Haldane was the first to suggest that people living in areas where a disease is historically persistent and endemic, such as malaria-laden areas, evolved genetically in order to enhance their ability to survive¹⁵. Research conducted in recent decades supports this hypothesis and allows the discovery of new important genetic determinants. For instance, it's now known that the “S” allelic variant of hemoglobin, which, if homozygous, causes sickle cell disease, confers on the heterozygotes a protection against *P. falciparum* estimated up to 90%¹⁵.

Furthermore, the persistence of this allele, despite its potential disadvantage, attests to the potent selection pressure exerted by pathogens.

12.3. Climate and Ecological changes

In general, environmental changes, both climatic and physical, have a large influence on the transmission dynamics and spread of microbes. Indeed, these perturbations directly impact the biology of pathogens, and the behavior of their hosts. Environmental factors are usually deeply involved in the emergence of vector-borne diseases, which are among the most sensitive.

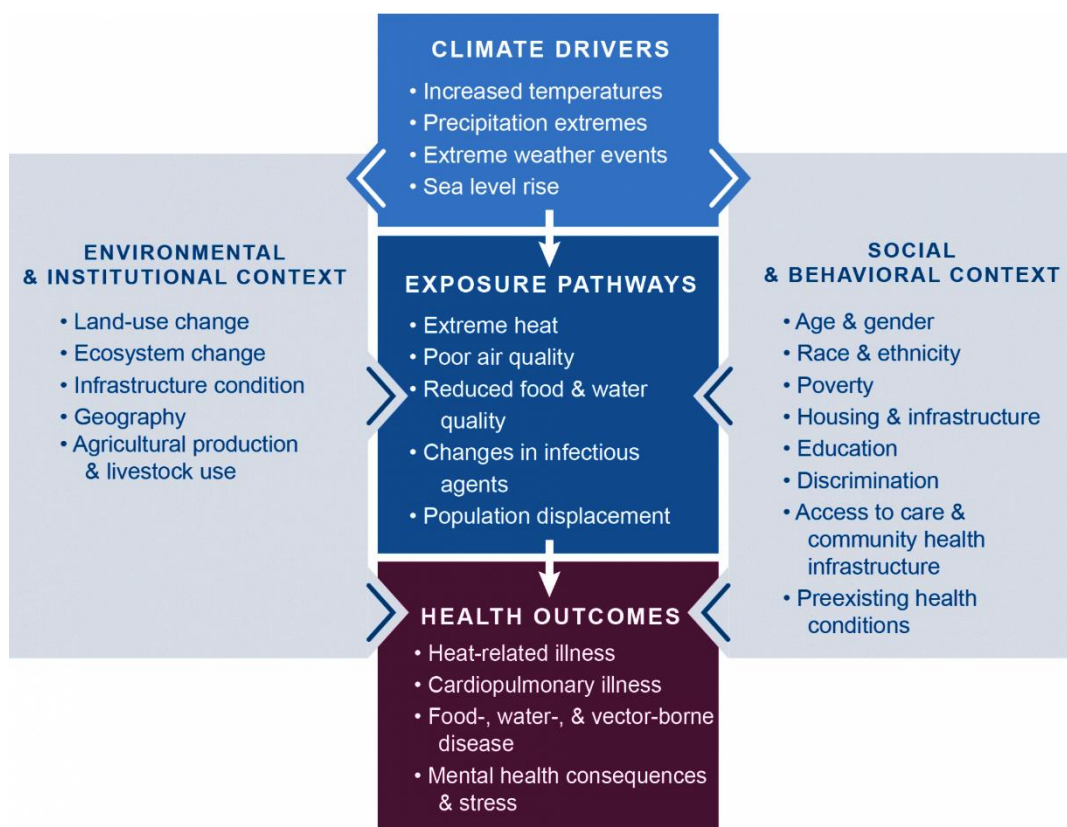


Figure 3: Climate change and health

Conceptual diagram illustrating the exposure pathways by which climate change affects human health. Exposure pathways exist within the context of other factors that positively or negatively influence health outcomes (gray side boxes). Key factors that influence vulnerability for individuals are shown in the right box, and include social determinants of health and behavioral choices. Key factors that influence vulnerability at larger scales, such as natural and built environments, governance and management, and institutions, are shown in the left box. All of these influencing factors can affect an individual's or a community's vulnerability through changes in exposure, sensitivity, and adaptive capacity and may also be affected by climate change (*Figure and caption from "U.S. Global Change Research Program" section Health 2016*)

› Weather and Climate

The seasonal occurrence of certain infectious diseases, in particular respiratory and gastrointestinal diseases, rightly underlines the role of climate. Some pathogens display a different sensitivity to humidity or temperature, for example, which may be involved in the seasonal pattern of infection. It has been demonstrated that the influenza A virus, causing the flu, is more effective at low temperatures and low humidity¹⁶. These properties can explain why, during the winter months, the influenza A virus remains infectious and causes massive flu outbreaks. But, as mentioned above, the range of climate effects is not limited to the pathogen directly, and plays an important role in the biology and distribution of some hosts. Vectors and reservoirs need conditions favorable to their survival that first of all define their own ecological niche and range, but also, as a consequence, those of their infecting pathogens. Thus, geography and climate are a powerful determinant of vector-borne diseases, acting as strong barriers to their distribution; most of the time insurmountable for many species.

› Change in vector ecology

A vector is a living organism that can transmit pathogens, including viruses, bacteria or parasites, from one vertebrate to another when infected itself. Many vectors are blood-sucking insects, which ingest the pathogen(s) by feeding blood from an infected host and inject it to a new host during subsequent blood meals. Among them are mosquitoes, ticks, fleas, sandflies, flies, triatomine bugs and some freshwater aquatic snails¹⁷.

Each vector can be defined through the part of the environment it inhabits, namely in which it fits and is adapted, as well as through the way it interacts with that environment and the other organisms living there. Interactions between vectors and hosts are highly dependent on environmental and climatic factors, and are the root of vector disease transmission and persistence. Temperature (which determines how long it takes for parasites to develop and the survival of mosquito larvae), precipitation (which creates egg-laying sites), wind speed (which affects feeding frequency), abundance and diversity of vegetation, and alternative hosts (which impacts blood meal rates on humans) are all drivers of pathogen transmission.

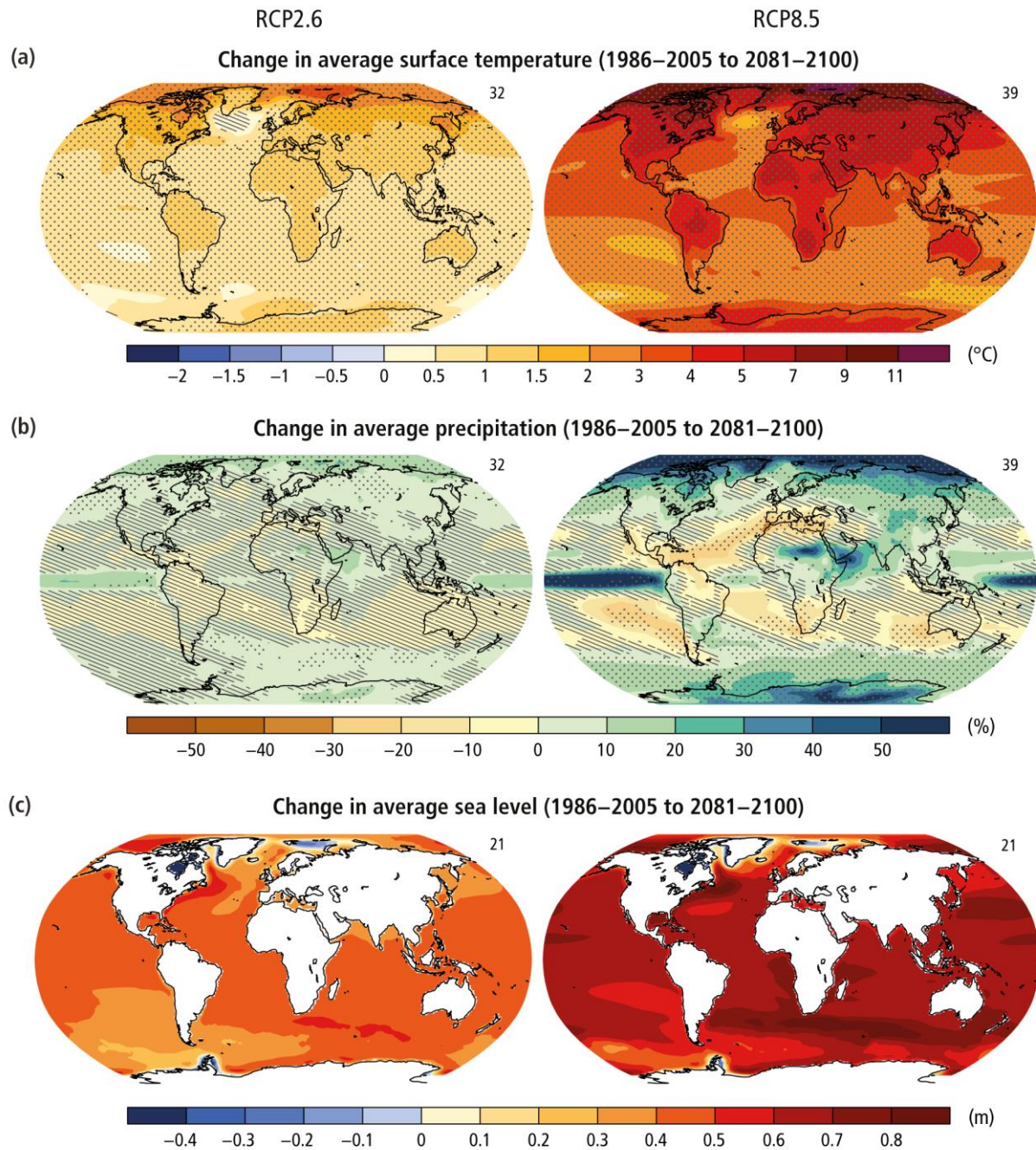


Figure 4: Projected climate changes

Average of the model projections available for the 2081–2100 period under the evolution scenario of the earth radiative balance RCP2.6 (lower) and RCP8.5 (higher) for (a) change in annual mean surface temperature and (b) change in annual mean precipitation, in percentages, and (c) change in average sea level. Changes are shown relative to the 1986–2005 period. The number of models used to calculate the multi-model mean is indicated in the upper right corner of each panel. Stippling (dots) on (a) and (b) indicates regions where the projected change is large compared to natural internal variability (i.e., greater than two standard deviations of internal variability in 20-year means) and where 90% of the models agree on the sign of change. Hatching (diagonal lines) on (a) and (b) shows regions where the projected change is less than one standard deviation of natural internal variability in 20-year means. (Figure and caption from "Summary for Policymakers of IPCC Report 2013")

Although the evolution of a pathogen is usually a key factor in the emergence or resurgence of an infectious vector-borne disease, it's in many cases an environmental co-factor that catalyzes the phenomenon, providing the vector with ideal conditions to ensure its spread. With this in mind, it is natural to worry about the effects of global warming, which could have devastating consequences on the incidence of infectious diseases. Currently, vector-borne diseases account for about 17% of all infectious diseases, with a burden of more than 700,000 deaths per year¹⁷, and are estimated to represent about 30% of EIDs over the past two decades¹⁸.

› Reservoir abundance and distribution

In epidemiology, a reservoir refers to the principal habitat of a pathogen that allows its reproduction and maintenance within an ecosystem. In this way, it can be environmental (e.g. soil for *Clostridium tetani* and the fungus *Histoplasma*, or water for *Legionella pneumophila*) or animal (including humans and vectors species) depending on the given pathogen. In this section, particular emphasis will be placed on animal reservoirs, which represent one of the main reservoir of viruses.

Diseases of non-human animal origin, termed zoonosis, account for the majority of the EIDs events. It is estimated that more than 70% of them are caused by pathogens from wildlife, and this number is expected to rise. As a matter of fact, reservoir species are widely subject to climate change, which in some cases affects their abundance and leads to changes in their behaviors. The emergence of a large number of viruses over the past few decades is a clear indication of this, and highlights the growing threat posed by these changes. As an example, many viruses are maintained in migratory species, such as birds or bats, which live closer to humans and have the potential to spread pathogens over long distances. Changes in migration routes or territory of such reservoir species threaten to occur in response to the global warming¹⁹. As a result, the distribution of the carried-pathogens will be modified and interactions with other species will take place, increasing the risk of transmission and emergence of new pathogens or variants^{19,20}. Another example illustrating how ecological changes of a reservoir species can lead to new EID events is the textbook case of the hantavirus

Sin Nombre²¹. In 1993, in the United States, the southwestern region of the country was hit by an outbreak of acute respiratory distress disease. A lot of Native Americans were affected. The case fatality rate was approximatively 60%; people were dying. To everyone's surprise, a virus belonging to the Hantaviruses, until now not considered as pathogenic for humans, is identified as the etiological agent of the new disease: the virus Sin Nombre. A few years later, the emergence of Sin Nombre virus was correlated with an El Nino Southern Oscillation event in previous years²². This climatic phenomenon, which caused ample rainfalls and warm winters, considerably increased the forage availability resulting in a dramatic high density of deer mouse, the reservoir of Sin Nombre²³.

In a same way as for Hantaviruses, a strong link exists between the emergence and resurgence of Arenaviruses and the density of their rodent reservoir²⁴. The epidemiological history of these two viral groups is enough to highlight the importance of reservoir populations (including vectors) and the disastrous consequences that ecological changes can have on human health. Political will to create programs and public health strategies for the study and control of such populations would be a significant asset in the fight against these diseases. However, although the mechanisms of transmission of a pathogen to humans are generally well described, the identification of its reservoir(s) is complex and remains unclear in many cases. This lack of knowledge seriously hinders our ability to anticipate outbreaks. More epidemiological surveillance studies in wildlife could help to bridge this gap. Furthermore, it would provide new insights that could improve the scientific community's responsiveness in the event of a new zoonosis emergence, as was the case for Zika.

12.4. Human behaviors and economic development

In his book “*Spillover: Animal Infections and the Next Human Pandemic*”, David Quammen argues that the increase in zoonosis observed in the past decades can be directly linked to human behavior and the ways in which we are irrevocably altering the world's ecosystems²⁵. At a time of globalization, most activities related to the economic and demographic development of human populations, from the consumption of natural resources to deforestation, have an impact on the environment and enhance the risk of pathogens emergence. Furthermore,

international exchanges through travel and commerce facilitate a broad spread of pathogens and vectors throughout the world.

› Land use

Now that there are seven billion of us on the planet, humans are changing land use to find more materials, to build or to produce more food. Indeed, humans have extended their territory into wild areas like never before, multiplying interactions with wildlife and, ultimately, finding new infections. In this context, it seems relevant to mention that a growing number of EIDs arise from increased interactions between humans and animal reservoirs due to land-use change. Deforestation and habitat fragmentation in favor of the expansion of living areas or new crops are behind the emergence or recrudescence of several infectious diseases. Ironically, reforestation efforts can also be the origin of these diseases, as shown by the emergence of Lyme disease in the United States^{26,27}. Environmental changes related to water use infrastructure can also be involved in these processes. Dam building and irrigation systems that change water level and flow and create stagnant water pools are, among other things, often associated with the resurgence of mosquito-borne diseases and the spread of schistosomiasis to new areas^{28–30}.

› Animal Husbandry and Food Industry

The ever-growing human population is associated with an expanding need for food and clothes. To meet this demand livestock farming intensifies and farms are established in new areas. These new husbandry practices promote the risks of amplification and emergence of new pathogens enhancing the host-pathogen interaction dynamics. In Australia, the establishment of horse and pig farms in fruit bats living areas led to bats urbanization, due to the degradation of their natural habitat, and the emergence of Hendra and Menangle viruses respectively^{31–33}. At the same time, livestock populations have grown exponentially in response to the demand for meat protein. Animal density per feedlot has increased dramatically, as well as the threat of zoonotic disease, the risk of which inevitably increases in proportion to the animal population. China is probably the country that experienced the most spectacular increase in livestock populations in the last few decades. Poultry and pigs are among the

most prevalent, both of which are hosts of influenza viruses. Intensive poultry production in confined feedlots is a boon for viral amplification. Moreover, poultry markets are a long-standing tradition in China and attract a large number of Chinese people. On this occasion multiple farmers are gathered to sell their poultry, alive, thereby ensuring the virus maintenance and dramatically increasing the probability of its transmission to humans. This optimal combination certainly explains why most of the influenza pandemics of the 20th century originated in China.

› Population mobility

Through the development of new and efficient means of transportation, natural borders, as were the oceans, gradually fade away. The potential for rapid spread of pathogens – and their reservoirs including vectors – around the world is growing as people keep ongoing international travels and expanding global trade markets. Nowadays, an infected host can travel the world, simply by taking a plane, and encounter naive populations that could be extremely susceptible to the carried pathogen. With technological advances, the transportation means are faster and faster and allow to travel long distances within the timeframe of a viremia. In particular, human-to-human infections can easily be spread from one geographical area to another. Pathogens that infect humans asymptotically or are transmissible before the symptomatic period pose a real threat in the absence of a recognized infection and protective measures. Fortunately, vector-borne diseases are in principle less prone to this dissemination pathway. In most cases, not all the factors necessary for the transmission cycle of the pathogen are present (vectors, insufficient number of subsequent infections). Nevertheless, this property tends to disappear gradually due to the increasing distribution of some vectors, typically mosquitoes.

› Urbanization

Currently, more than half of the world's population lives in urban areas³⁴. By 2030, it is estimated that the global urban population will exceed 4.5 billion³⁵ and almost all of this urbanization will take place in the cities of developing countries. The relocation of rural populations to urban areas is a major demographic trend of the 21st century, yet migration to cities not properly equipped with adequate

infrastructure has serious health consequences. Population density is a critical parameter for the maintenance of certain virus populations, especially when the host has a viral immune memory. Depending on the virus route of transmission, vectorial or respiratory, to name a few, the potential for interaction is a limiting factor. Person-to-person transmission of some acute viral infections only occurs if the host population is large and interactive. For example, Measles virus can be maintained only in human populations over 200,000 people, most likely because there is no animal reservoir and infected individuals develop complete and long-lasting immunity. Furthermore, urbanization prompts people into frequent travel between large cities and their villages to visit their relatives. In this way, increasing interactions blur the boundaries of both areas and enhance the risk of pathogen transmission. Lastly, many rural migrants live in overcrowded conditions as a consequence of housing costs and family size. Poor sanitary conditions and lack of access to safe water frequently observed in these areas greatly enhance the probability of disease and facilitate their spread.

› Human High Risk Behaviors

As described in the previous sections, human behavior, individual or collective, plays a major role in the emergence of infectious diseases. Behavior modification is an essential strategy in the prevention of infectious diseases; and for some, it's the only option. However, despite considerable efforts deployed to educate populations, high-risk behaviors are still a burden on public health. New cases of sexually transmitted diseases, such as HIV, contracted as a result of unprotected sex or drug injection appear at first sight easily preventable; yet their incidence is persistent. On the other hand, the current mistrust of vaccination and the rise of "anti-vaxxers" have severe consequences for public health. Heavy lobbying by anti-vaccine activists has led to a drop in the vaccination rate in several countries, mainly among children. Ironically, the immunization campaigns were so well conducted that this generation of parents probably never had to worry about the gravity of these diseases. Nevertheless, although they probably do not fully realize the risks involved in refusing vaccination, the latter actually do exist. Such behavior has already led to the re-emergence of vaccine-preventable diseases in

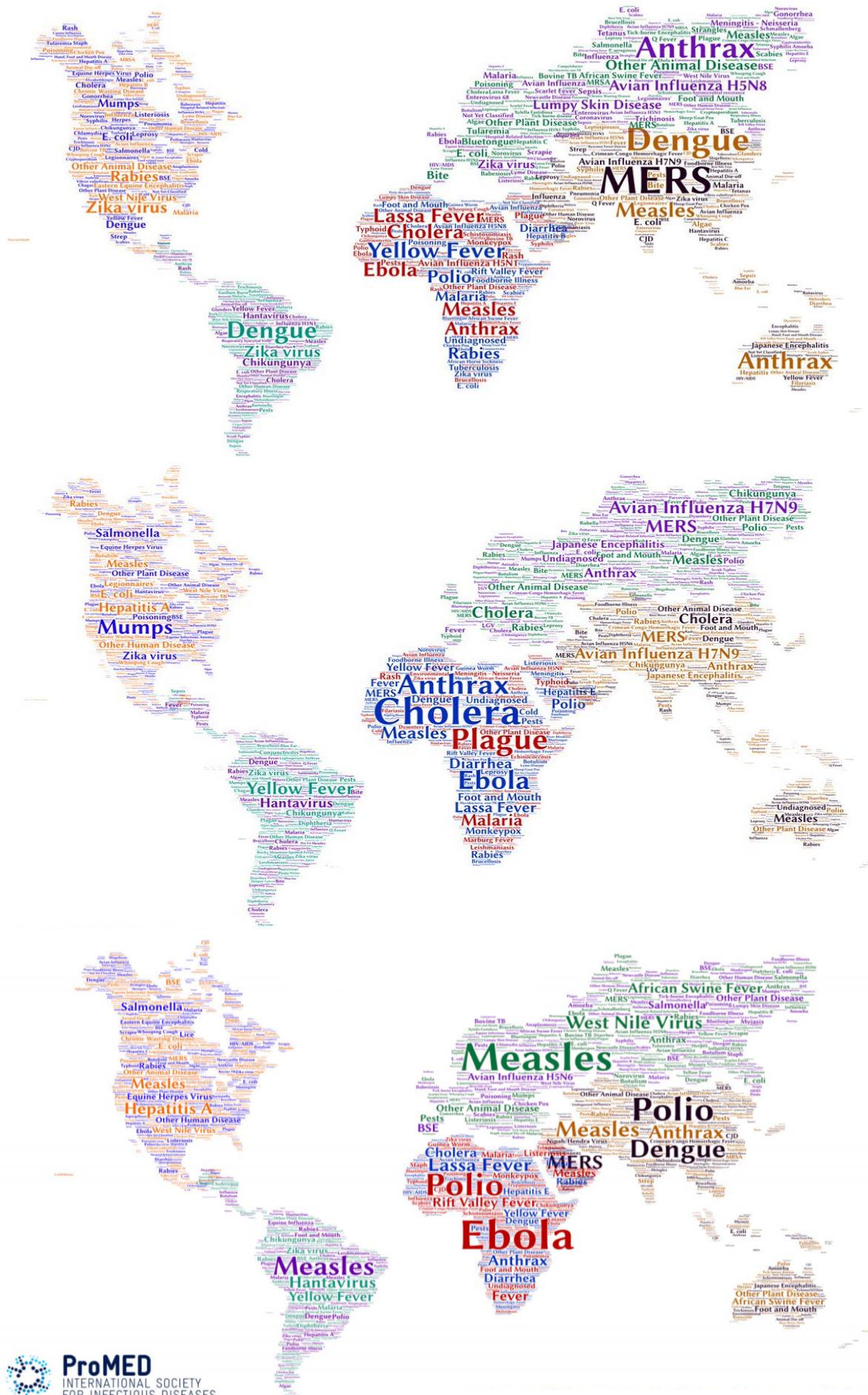


Figure 5: Health maps

Evolution of the ProMED health maps from 2016 to 2018. The international society for infectious diseases publishes annual word clouds based on ProMED's infectious disease surveillance. In the maps the size of each word indicate the number of report but word location does not always correspond to the exact location. (*Maps and caption from "ProMed"*)

several countries. The death due to measles infection of more than 30 people in Europe in 2018 is a tragic illustration of this. If the refusal to vaccinate intensifies, populations could face a serious threat, since a breakdown in immunization coverage would facilitate the re-emergence of virtually eradicated diseases such as polio, involving dramatic consequences.

12.5. Breakdown or absence of Public Health measures

Developing countries bear a disproportionate burden of infectious diseases and emerging events compared to the rest of the world. Poverty creates conditions favorable to the spread of infectious diseases and prevents affected populations from appropriate access to prevention and care. Failure of health systems, instability or lack of political will, as well as natural disasters, are often pointed out as contributing factors to epidemic emergence.

› Poverty

According to the latest World Bank report, nearly 1.1 billion people fewer than in 1990 live in extreme poverty³⁶. In 2015 the overall poverty rate dropped to a record level of 10%. But the decrease was not equal in all regions. While Europe, Central Asia, East Asia and the Pacific, successfully reduced the poverty rate below 3%, the number of poor people in Sub-Saharan Africa has increased. Of the 736 million people still living on less than \$1.90 a day, more than half of them lives in Sub-Saharan Africa. Nevertheless, while the fight against extreme poverty is globally on track, one should not forget that nearly half of the world's population - 3.4 billion people - still struggle to meet their basic needs. Actually, it is estimated that more than a quarter of the world's population lives on \$3.20 a day and nearly half of the world's population on less than \$5.50 a day³⁷.

From a health point of view, I would suggest that poverty should be estimated in terms of more than just a monetary value. The lack of sufficient food, access to safe drinking water, sanitation and proper medical infrastructure are

prerequisites that, if not available, seriously burden human lives. Sanitary poverty is the real plague, opening wide to the emergence of new pathogens and to their persistence in populations.

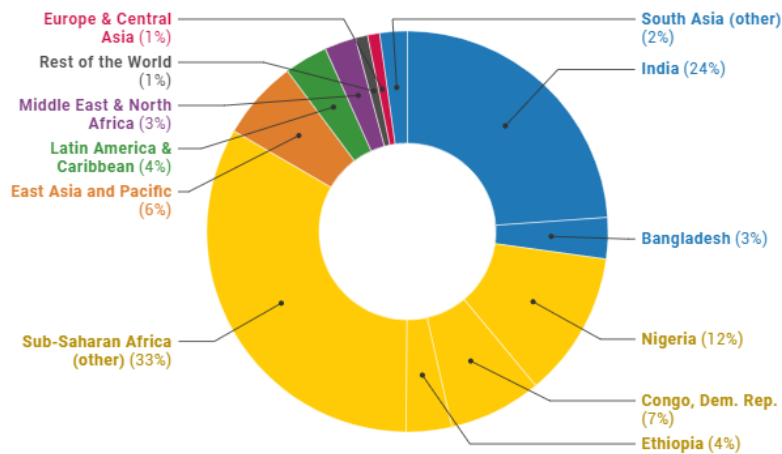


Figure 6: Distribution of extreme poverty in the world

Of the world's 736 million extreme poor (those living on less than \$1.90 a day) in 2015, half of the total lived in just five countries. The five countries with the highest number of extreme poor are (in descending order): India, Nigeria, Democratic Republic of Congo, Ethiopia, and Bangladesh. (Figure and caption from "World Bank.org")

› War and Natural disaster

Wars and natural disasters shake the sanitary conditions of the countries affected, which are in too many cases already precarious. These two situations are not only disastrous, but also create conditions highly conducive to the emergence or resurgence of infectious diseases. Victims of natural disasters and war refugees gather in overcrowded emergency camps to survive. There, sanitary conditions and personal hygiene are very limited, water sources unprotected and often in close proximity to fecal repositories. This chaotic environment has repeatedly been at the core (and is so in Yemen and Zimbabwe currently), of cholera and tuberculosis outbreaks, among others.

EID events are based on multiple factors, the convergence of which leads to epidemics with more severe consequences than if they were dependent on a single factor. The emergence of Ebola virus in Guinea, Liberia and Sierra Leone in 2014 is a recent example. The lack of rapid disease detection, availability of basic care, efficient quarantine, and mobilization of international rescue forces with which people had to cope, demonstrated how the convergence of political instability and poor socio-economic conditions made outbreak management difficult³⁸.

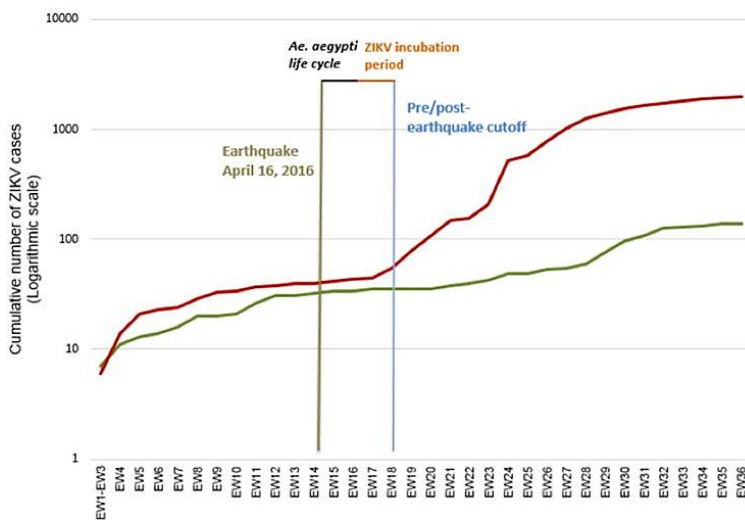


Figure 7: Post-earthquake Zika virus surge

In April 2016, Ecuador experienced a massive 7.8 M earthquake — the strongest seism in almost four decades. Shown are the cumulative number of autochthonous ZIKV cases after a major earthquake (M7.8) that affected Ecuador in 2016. (Cumulative number cases at week 36 of 2016 for mildly affected cantons (green) and severely affected cantons (red)). (Figure and caption from Ortiz et al., 2017)

› Political will

The financial resources that a country can allocate to health and research are also a key component in the fight against infectious diseases and the prevention of emergence. When insufficient budget can lead to inappropriate use of medical equipment and contribute to the spread of a pathogen (e.g. Lassa fever in Nigeria in 1989 due to the reuse of needles in hospitals³⁹), it can also lead to the interruption of surveillance and vector control programs. Additionally, governments tend to fund research activities only once the pathogens or associated diseases are an obvious threat and, more especially, when the latter threatens their own populations. This tardive rise in awareness clearly impairs scientific community responsiveness and could be minimized if research programs focusing on "outsider" pathogens were valued.

Lastly, when national economies are highly dependent on tourism, the political will may be lacking to report a miscontrolled outbreak to the WHO. Some examples include Mauritius, which in 2006 alleged in a press release that the danger of Chikungunya spread was “overplayed”, Saudi Arabia, which took a long time to report the emergence of MERS (Middle East Respiratory Syndrome)⁴⁰, and China, which overlooked the emergence of SARS (Severe Acute Respiratory Syndrome) in 2003⁴¹.

II. ARBOVIRUSES TO FLAVIVIRUSES

II.1. The threat of Arboviruses

Arboviruses are a very heterogeneous group, well known in public health, as many of them cause high morbidity and mortality in both human and animal populations. The term "arbovirus" refers to a virus transmitted to vertebrate hosts by blood-sucking arthropod vectors. It comes from laboratory jargon used in the early 1940s by Californian researchers in reference to "arthropod-borne-virus"⁴².

The study of arboviruses was developed at the initiative of the Rockefeller Foundation, with the collaboration of a reference laboratory at Yale University and various laboratories located in tropical countries. The network of Pasteur Institutes from overseas played a central role in this field of research. In 1930, only 6 arboviruses were known. In 1980, 500 had been identified. Currently 537 arboviruses are listed in the international arbovirus catalogue, but this number is likely to be revised upwards in the near future based on the results of studies investigating virosphere.

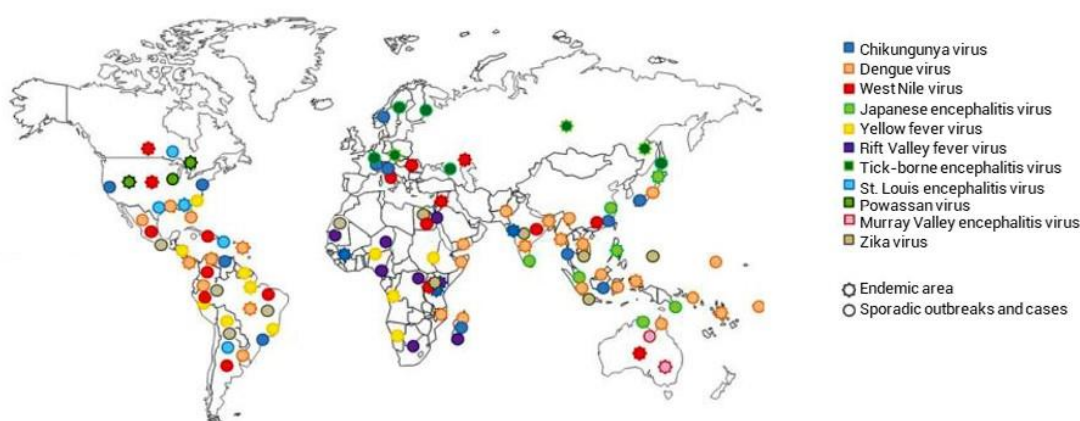


Figure 8: Global distribution of emerging and re-emerging arboviruses

The color symbols indicate the global distribution of the major pathogenic arboviruses for humans as published in 2012, except for Zika virus. Zika virus distribution (brown) has been updated and represented by a circle in view of its recent emergence. (Figure adapted from Anez et al., 2012)

Table 1: Selected arboviruses of medical importance

FAMILY/GENUS	VIRUS	VECTOR
Flaviviridae		
<i>Flavivirus</i>	Dengue viruses (DENV-1 to -4)	Mosquito
	Japanese encephalitis virus (JEV)	Mosquito
	Kunjin virus (KUNV)	Mosquito
	Murray Valley encephalitis virus (MVEV)	Mosquito
	Saint Louis encephalitis virus (SLEV)	Mosquito
	Usutu virus (USUV)	Mosquito
	West Nile virus (WNV)	Mosquito
	Yellow fever virus (YFV)	Mosquito
	Zika virus (ZIKV)	Mosquito
	Alkhumra virus (ALKV)	Tick and mosquito
	Kyasanur forest disease virus (KFDV)	Tick
	Omsk hemorrhagic fever virus (OHFV)	Tick
	Powassan encephalitis virus (POWV)	Tick
	Tick-borne encephalitis virus (TBEV)	Tick
Bunyaviridae		
<i>Orthobunyavirus</i>	La Crosse encephalitis virus (LACV)	Mosquito
	California Encephalitis virus (CEV)	Mosquito
	Jamestown Canyon virus (JCV)	Mosquito
	Oropouche virus (OROV)	Mosquito and flie
<i>Nairovirus</i>	Crimean-Congo hemorrhagic fever virus (CCHFV)	Tick
<i>Phlebovirus</i>	Rift Valley fever virus (RVFV)	Mosquito
	Toscana virus (TOSV)	Flie
Togaviridae		
<i>Alphavirus</i>	Chikungunya (CHIKV)	Mosquito
	Eastern Equine encephalitis virus (EEEV)	Mosquito
	O'nyong-nyong virus (ONNV)	Mosquito
	Ross River virus (RRV)	Mosquito
	Sindbis virus (SINV)	Mosquito
	Venezuelan Equine encephalitis virus (VEEV)	Mosquito
	Western Equine encephalitis virus (WEEV)	Mosquito
Reoviridae		
<i>Coltivirus</i>	Colorado tick fever virus (CTFV)	Tick

II1.1. The cladistic paradox of Arboviruses

In the field of animal viruses, arboviruses form a unique group because of their vector-dependent transmission. This exceptional property reflects the high genetic plasticity of these viruses, which are adapted to both invertebrate and vertebrate hosts (referred to as dual-host tropism afterward). In the past, when molecular analyses were not as accessible as today, arboviruses formed a biological ensemble subdivided into forty serological groups on the basis of their antigenic cross-reactivity. Nowadays, virus classification is established according to genomic criteria, via the alignment of sequence(s) critical to the virus biology, and allows their organization into viral families, each one composed of specific genera. Revision of the initial classification of arboviruses according to this method revealed that arboviruses do not form a single clade, but are rather subdivided into several genera that belong to different families. Moreover, the dual-host tropism of arboviruses is a surprising paraphyletic trait, especially since taxa with arboviruses also include monospecific viruses either from vertebrates or arthropods. This taxonomic diversity is impressive given the highly significant property shared, and represents a major challenge in the understanding of the evolutionary origin of arboviruses.

II1.2. Epidemiology of Human Arbovirosis

› Historical case

The first human virus was identified in 1901. This virus, widespread in tropical countries since the 15th century, was responsible for devastating epidemics associated with very high mortality rates. While the disease can be relatively mild, more-severe cases result in major organ failure such as liver destruction that causes yellowing of the skin. The name of this disease, the Yellow fever, derived from this symptom, and inspired the name of its related virus genus: *Flavivirus*.

Despite its impact, little was known about how Yellow fever was spread, but it was clear that the disease was not directly transferred from person to person. Various speculations about the source of the infection were proposed, as the presence of the virus in the atmosphere or in bedding clothe until 1880, when

Carlos Juan Finlay proposed that a bloodsucking insect played a part in the transmission of the disease: the mosquito. Few years later the Reed Commission's study, established in Cuba in 1899, proved that mosquitoes are the vectors for this disease.

› Transmission cycle

All arbovirus species have an RNA genome, with the exception of African swine fever (*Asfarviridae*). Their transmission cycle alternately involves an arthropod vector and a vertebrate host which is the reservoir or amplifier of the virus. Arbovirus vectors are ticks, culicoids and mainly mosquitoes. After a blood meal on an infected host, the virus multiplies in the midgut and invades surrounding tissues, resulting in a high viral load, particularly in the salivary glands. The time needed for the virus to complete its development in the vector is commonly referred to as the extrinsic period. Then, the arbovirus is transmitted to a vertebrate host by a subsequent bite. To maintain the transmission cycle, the virus must again have the ability to replicate effectively to induce sufficient viremia, during which it can be up taken by another vector. This short-term viremia usually leads to host immunity, which therefore ensures a transient role in the maintenance of the virus. In contrast, the infected vector remains infected throughout its life (one season for mosquitoes, several years for ticks) and can in some cases vertically transmit the virus from one generation to the following one.

Some arbovirosis, such as Yellow fever, can be transmitted through three epidemiological patterns: the sylvatic, urban and intermediate cycles. In the sylvatic form of Yellow fever, the main host is the monkey while the vectors are, in South America, mosquitoes of the genus *Haemagogus* and, in Africa, several species of *Aedes* (*Ae.*). Amplification dynamics of Yellow Fever Virus in sylvatic environments is closely related to the renewal of non-immune simian populations (5-8 years). This situation is behind the periodic occurrence of human epidemics every 5-10 years. In the urban form, mosquitoes acquire infection from contaminated humans and transmit the virus to susceptible humans. The vector is usually *Ae. aegypti*, a domestic mosquito that lives near houses and whose females prefer laying their eggs in the stagnant water of containers. Finally, the intermediate form is carried out by semi-domestic

mosquitoes (which breed in the wild and around households) that infect both monkeys and humans. In this context, the virus can be transmitted from human to human, or from the monkey via the vector. While the latter may also occasionally emerge from the sylvatic cycle during a visit or work in the jungle, it is much more common in the intermediate cycle involving humans living or working in the border areas of the jungle. This epidemiological pattern occurs in the African savannah predominantly.

› Human arbovirolosis

Many arbovirolosis are transmitted essentially by zoonotic cycles, meaning that the associated virus passed from animals to humans via a vector. For these zoonotic viruses, such as West Nile virus (WNV), Japanese encephalitis virus (JEV) and LaCrosse virus, humans are accidental hosts and are usually not important for maintaining transmission cycles. For other arboviruses such as Dengue (DENV), Yellow Fever (YFV), Chikungunya (CHIKV), and more recently Zika (ZIKV), humans are in many cases the main source of virus amplification and vector-borne infection.

Currently, more than 150 arboviruses are known to cause human disease. Of these viruses pathogenic to humans, the majority belong to three families: *Flaviviridae* (genus *Flavivirus*), *Togaviridae* (genus *Alphavirus*) and *Bunyaviridae* (genus *Bunyavirus*, *Orthobunyavirus* and *Nairovirus*), while the others belong to the four additional families, *Phenuiviridae*, *Rhabdoviridae*, *Orthomyxoviridae* and *Reoviridae*. Usually, flaviviruses are transmitted by mosquitoes or ticks, alphaviruses and bunyaviruses by mosquitoes, and phleboviruses by sandflies, with the exception of Rift Valley fever virus which is transmitted by mosquitoes. However, arboviruses can also be transmitted to humans via other non-vectorial transmission routes, more or less anecdotal according to the virus concerned. These are vertical, sexual, nosocomial (blood transfusion⁴³ and organ transplantation⁴⁴) or by drinking infected goat's milk in the case of tick-borne meningoencephalitis virus⁴⁵. Arboviruses causes clinical and subclinical infections in humans resulting in four main clinical syndromes: (i) autolimited acute fevers with or without exanthema, often combined with headache, (ii) polyarthritits and rash, with or without fever of variable duration,

autolimited or with arthralgic sequelae over several weeks to several years (iii) central or peripheral nervous system disorders ranging from aseptic meningitis without severity to encephalitis, microcephaly, Guillain-Barre syndrome or flaccid paralysis, and (iv) hemorrhagic fevers, often associated with capillary leakage, shock and high case-fatality rates. The latter may also be associated with liver damage.

II1.3. The emergence triangle of mosquito-borne arboviruses

Several arbovirosis, long known and formerly considered benign or controlled, are currently on the rise and endangering the populations. This is particularly the case for DENV and YFV. But this persistent threat, which is already significant, is even more so today in an era of globalization. Over the past two decades, an alarming upsurge in the incidence of emerging arboviruses, responsible for spectacular and unprecedented outbreaks in human populations, has been observed. Regardless of the continent where they occur, these viral diseases emerged from a triad of factors, among which anthropogenic environmental changes are considered as the catalyst.

› The Virus

The ability of a virus to infect multiple hosts to ensure its maintenance is inevitably involved in its dispersal potential because the presence of the virus is intrinsically linked to the presence of the host. The dual-host tropism of arboviruses is an important factor, beyond the physical presence of vertebrate or invertebrate hosts. Indeed, the ability of arboviruses to successfully survive through this kind of transmission cycle is based on their remarkable plasticity, which makes them highly adaptable. There are many important differences between vertebrate hosts and invertebrates, including different immune systems and body temperatures, which challenge the survival of viruses. However, the high adaptability and mutation rate of arboviruses and their wide genetic diversity overcome these barriers and turn arboviruses into viruses with a high potential for emergence.

› The Mosquito

Mosquitoes include more than 3500 species that are widely distributed around the world. They are distributed in latitudes from the tropics northwards in the Arctic regions and southwards to the ends of the continents, up to altitudes over 4000 meters above sea level. The main vectors of human arbovirosis belong to three genera: *Aedes*, *Culex* or *Anopheles*.

Virus evolution is oftentimes involved in emergence processes and has the potential to reshape the epidemiological pattern of a disease in a drastic way. A mutation can promote the transmission of a virus by increasing the range of vector species and/or the vectorial competence. In the latter case, the mutation selection is not constant among species and a mutation favorable to one species in a given geographical area will not necessarily be selected by a mosquito of the same species but

from a different geographical area. The most striking example is the Chikungunya virus which caused a pandemic in the Indian Ocean to India, Southeast Asia and parts of Europe. This remarkable outbreak was associated with a single mutation affecting the viral envelope (E1:A226V) that caused

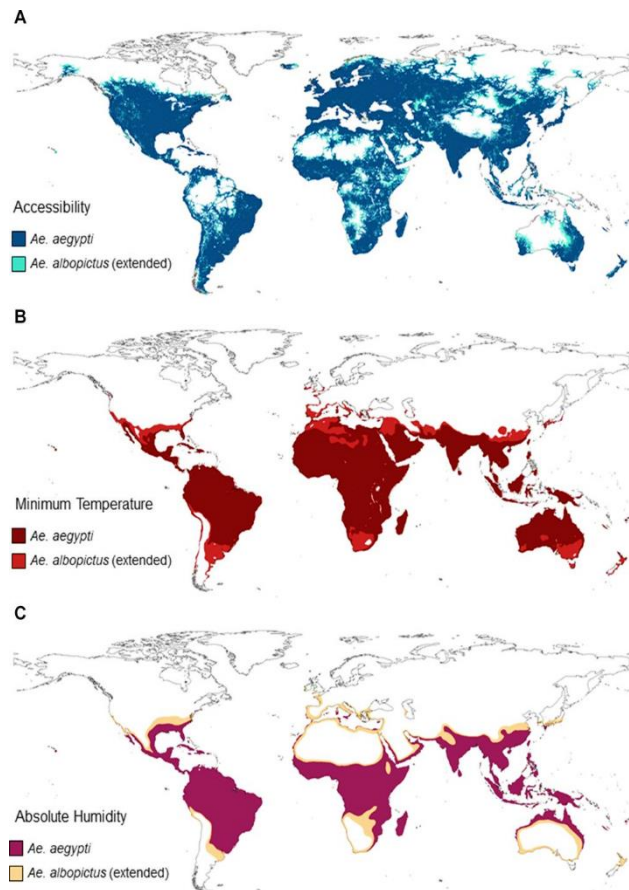


Figure 9: Predicted global distribution of *Ae. aegypti* and *Ae. albopictus*.

Maps indicate areas where, according to the given variable, the vector is predicted to be present. Panel (A) shows the effects of accessibility highlighting the influence of increased transportation, globalization and urban spread. *Ae. albopictus* (light blue) is however able to establish in less accessible areas in comparison with *Ae. aegypti* (blue), being less anthropophilic. Panel (B) shows the effects of temperature on *Ae. aegypti* (dark red) and *Ae. albopictus* (light red). *Ae. albopictus* is able to occupy almost the entire range of *Ae. aegypti* and shows extension beyond these regions into cooler areas. Panel (C) shows that absolute humidity affects *Ae. aegypti* (purple) and *Ae. albopictus* (beige) similarly. (Maps and caption from Dickens et al., 2017)

increased viral transmission by the *Ae. albopictus* mosquitoes from the area but not from Congo or Italy for example^{46–48}. In addition, arthropods such as mosquitoes are frequently infected with bacteria with which they establish a long-term relationship. These endosymbionts have a wide range of effects on their hosts, from their participation in nutritional functions to the manipulation of reproduction. But, mosquito microbiota can also influence and regulate their ability to be infected and transmit viral pathogens to humans, in particular when modulating vectorial competence. While some bacteria enhance vector susceptibility to arbovirus infection, such as *Serratia odofifera* in *Ae. aegypti*, which increases its susceptibility to DENV and CHIKV, others, including *Wolbachia* bacteria, limit transmission of DENV, YFV or ZIKV by mosquitoes of the same species^{49,50}. Besides biological factors, environmental and climatic conditions also affect the abundance and the ability of mosquitoes to transmit and spread a virus. Rainfall, temperature or humidity, play a role in the transmission of arbovirose and the seasonal occurrence of these diseases. Moreover, global warming affects the distribution of mosquito species by expanding their range or by limiting it due to new interspecific competition.

› The Human

In the book "The Geopolitics of the Mosquito" Erik Orsenna tells the "mosquitoes' point of view on globalization" – a global history of abolished borders, as he says. From their travels to straits and dams construction, humans shape the world and scatter mosquitoes as well as viruses. The distribution of *Ae. aegypti* illustrates how powerful is the force that humans exert on their ecosystem. Once endemic to Southeast Asia, *Ae. albopictus* reached the tropics as far as the temperate zones of North America and Europe, due to the transport of eggs contained in lucky bamboos and used tires. Other examples of anthropogenic activities leading to the emergence and spread of infectious diseases abound. The latest one concerns Zika virus which, when arriving in Brazil during a Polynesian pirogue racing competition held in August 2014 in which several Pacific teams participated, found all the optimal conditions for its explosion.

II.2. FLAVIVIRUSES

According to the evaluation of phylogenetic divergence times, flaviviruses probably have a common ancestor and appeared on Earth about 100,000 years ago. The genus *Flavivirus* was named after the word "*flavus*" (which means "yellow" in Latin) in reference to the yellowing of the skin due to liver dysfunction caused by the Yellow Fever virus. This virus was the first human virus discovered, the first flavivirus isolated and propagated *in vitro* and the first full-length flavivirus genome sequenced in 1985. Nowadays, YFV and other flaviviruses are part of a large family of RNA viruses, the *Flaviviridae*, which currently consists of four genera: *Flavivirus*, *Hepacivirus*, *Pestivirus* and recently *Pegivirus*.

II2.1. Flavivirus burden on Human Health

Flaviviruses are a long-standing burden affecting human populations. Some authors, after reviewing ancient texts, found evidence of West Nile fever in the description of Alexander the Great's death in 323 BC written by Plutarch ⁵¹, and the first description of Dengue in a list of symptoms recorded in a Chinese medical encyclopedia of the Jin dynasty (265-420 AD)⁵². But Flaviviruses became a public health issue since the Age of Great Discoveries (15th - 17th century) and during the Colonial Era (17th - 19th century). The first outbreaks of Yellow Fever and Dengue are described in the main port cities of the New World⁵³, taking advantage of the presence of naive population from Europe and the geographical spread of their vector *Ae. aegypti*, through the slave trade and commerce which directly connect the tropical zones of Africa with those of the Americas⁵⁴.

Over the past 20 years, flaviviruses have regularly emerged in various parts of the globe. While some are limited to specific regions of the world, others have conquered both hemispheres displaying exceptional dispersal capacity and epidemic fitness. From the Old World to the New, or from the New World to the Old, viruses previously confined by thousands of years of co-evolution, have been able to spread to the other world causing large outbreaks. It is not uncommon for viruses already known for several years, but considered of low pathogenic potential for humans, to unexpectedly emerge. They are then associated with new or increased symptomatology, sometimes even severe as in the case of Zika

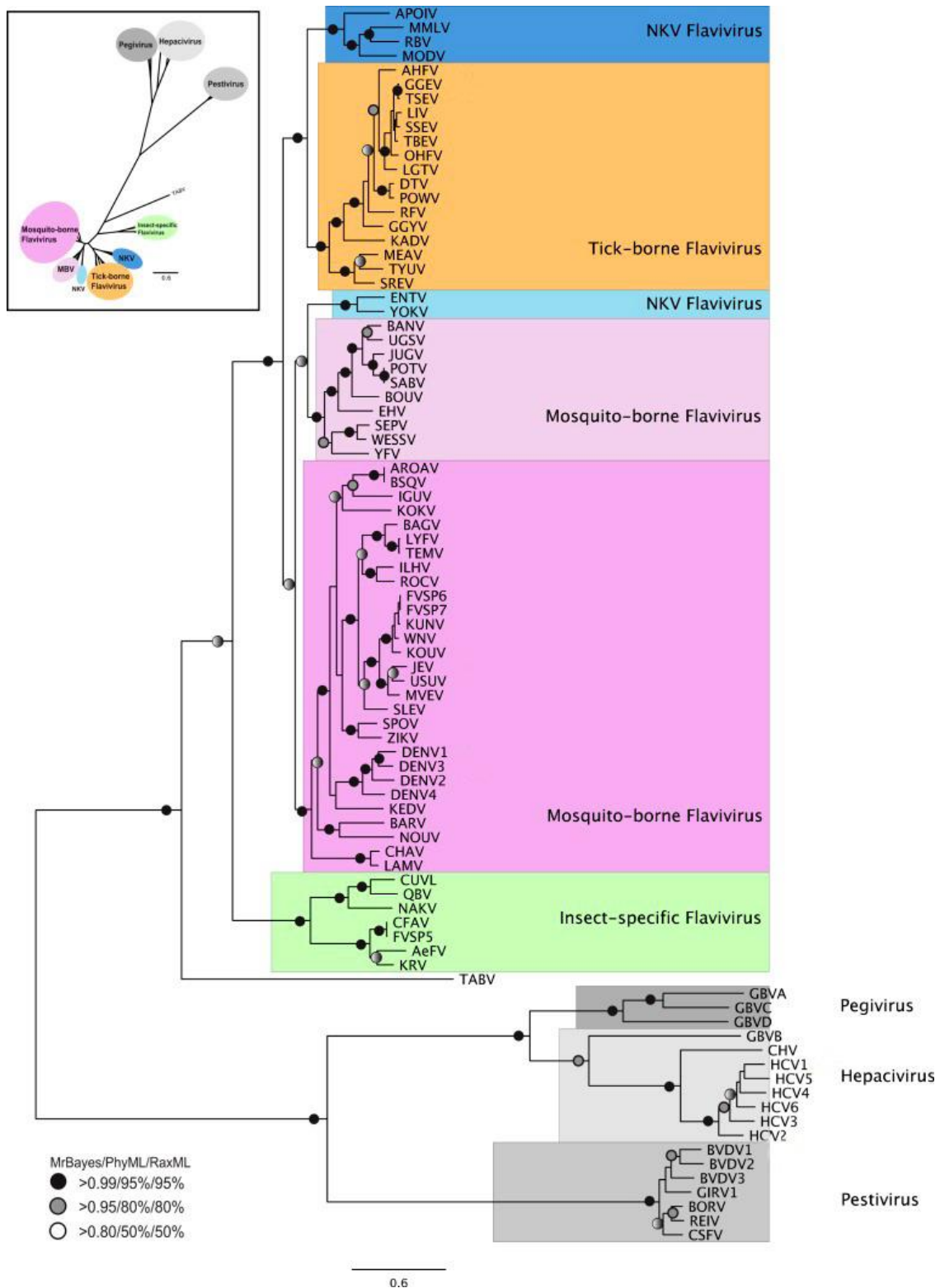


Figure 10: Phylogenetic reconstruction of *Flaviviridae*

Phylogenetic reconstruction of *Flaviviridae* concatenated NS3 and NS5 protein sequences. The tree shown is the best Bayesian topology. Numerical values at the nodes of the tree (x/y/z) indicate statistical support by MrBayes, PhyML and RAXML (posterior probability, bootstrap and bootstrap, respectively). Values for highly supported nodes have been replaced by symbols, as indicated. (Adapted figure and caption from Papageorgiou et al., 2014)

emergence for example. Flaviviruses are probably the most important group of arboviruses from a human health perspective and are found on six different continents. This genus includes a number of viruses of global health concern such as Yellow fever, West Nile, Dengue and Zika viruses and other viruses pathogenic to humans such as Japanese encephalitis, St Louis encephalitis or tick-borne encephalitis viruses, whose impact is currently limited to certain geographical regions.

II2.2. Classification and Phylogeny of Flaviviruses

The first method for studying flavivirus relatedness was provided by the discovery of cross-reactivity between antisera raised against some, but not all, viruses causing similar diseases and heterologous viruses. Subsequently, this method was refined by the development of a standardized hemagglutination inhibition test, which differentiates flaviviruses from alphaviruses referred to at that time as Group A and B arboviruses, respectively⁵⁵. First flaviviruses were grouped among togaviruses according to this serological method, before being classified in the *Flaviviridae* family in the 1980s on the basis of differences in structure, genetic sequence and replication strategy⁵⁶. Over the years, advances in molecular genetics (including viral genome delineation, study of the structure and biology of flaviviruses) have led to a better understanding of the relationships between these viruses and pointed out significant differences with their historical colleagues. A total of 73 viruses of the genus *Flavivirus* (classified into 53 distinct species) have since been identified. Moreover, several viruses have been defined as "non-vectorized" flaviviruses⁵⁷ and a number of insect-specific flaviviruses⁵⁸ (ISFV) have also been discovered.

The taxonomy of flaviviruses is constantly updated to include newly identified viruses and to take into account the advances in analytical methods. According to the current classification, flaviviruses are divided into three groups, in addition to ISFVs, according to the nature of their vector: mosquito-borne (MBFV), tick-borne (TBFV) and flaviviruses without known vector (NKV)⁵⁹. These phyla are secondarily subdivided into groups that remain correlated to both a vector subtype, a vertebrate host and an associated pathology^{60,61}.

› Mosquito-borne Flaviviruses

The MBFVs are subdivided into two groups according to the genus to which their main mosquito vector belongs. One group includes viruses transmitted by *Culex* genus mosquitoes while the other group includes viruses mainly transmitted by *Aedes* genus mosquitoes.

The *Culex*-associated flaviviruses are predominantly neurotropic. They are present in the Old and New World⁶² and generally have an avian reservoir even though they can be amplified by mammals⁶². This subgroup is associated with encephalitis in humans or livestock and includes WNV and JEV.

In contrast, the *Aedes*-associated Flaviviruses are usually viscerotropic and cause hemorrhagic fevers in humans in the most severe forms of infection. They are mainly circulating in the Old World with some exceptions in South America (DENV, YFV) and have a primate reservoir and a sylvatic cycle⁶². Zika virus, which does belong to this group, is quite surprising due to its characteristics commonly assigned to viruses transmitted by *Culex* genus mosquitoes. As a matter of fact, the latter, native of the Old World, displays a marked neurotropism and a quasi-worldwide distribution similar to West Nile virus⁶³.

› Tick-borne Flaviviruses

The TBFV group is divided into three groups: viruses associated with seabird parasitic ticks (seabird tick-borne flaviviruses, S-TBFV), viruses associated with mammalian ticks (mammalian tick-borne flaviviruses, M-TBFV) and Kadam virus which forms a phylogenetic clade on its own even though ecologically associated with the S-TBFV group⁶⁴. Each virus is associated with, and closely linked to, a main tick species. The presence of the virus is correlated with the one of ticks, which is itself geographically determined by the presence of the hosts on which they feed and the type of vegetation⁶⁵. Only viruses belonging to the Tick-borne encephalitis serocomplex are known as human pathogens, with a circulation in the Old World and a clear prevalence in Russia. This serocomplex includes Tick Borne Encephalitis virus (TBEV), Powassan (POWV), Omsk Hemorrhagic Fever virus (OHFV), and Kyasanur Forest Disease virus (KFDV). Human infection occurs via the bite of an infected tick and can lead to serious neurological or visceral damage, sometimes fatal⁶⁶.

› No-known vector Flaviviruses

The NKV group is split into two clusters: one associated with bats and the other with rodents⁶⁷. Bats-associated viruses have been isolated in different continents (Asia, Africa, America) but remain confined to specific sites. Rodent-associated viruses circulate exclusively in the New World, where they also remain confined to well-defined areas. Human infections are often accidental and include few natural infections (Rio Bravo virus, Modoc virus) and several laboratory cases⁶⁸.

II.3. MOLECULAR BIOLOGY OF FLAVIVIRUSES

II.3.1. Virion and Genome Structure

Flaviviruses are enveloped viruses with a positive single-stranded RNA genome classified in Group IV of the Baltimore Classification.

› Structure

Flaviviruses are spherical viral particles, relatively smooth in appearance, about 40-60 nm in diameter. They are enveloped viruses with icosahedral symmetry composed of a capsid that protects the viral genome. There are two forms of virions: mature and immature. The outer shell of the mature virion is made of two viral proteins, the Envelope (E) and the Membrane (M) anchored in the lipid bilayer derived from the membrane of the endoplasmic reticulum (ER) of the host cell, and form heterodimers organized in trimer. The surface of the virion is composed of 180 copies of E, forming dimers flat on the surface of the virion, and arranged in a herringbone array that completely covers the lipid bilayer. Beneath the protein shell, the M protein binds closely to the membrane. No

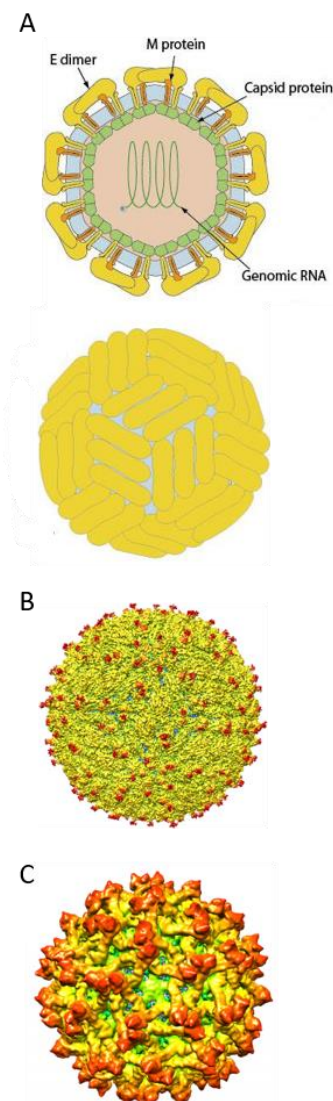


Figure 11: Structure of Zika virus

(A) Schematic representation of a cross-section of ZIKV virion. (Figure from "Viralzone")

Cryo-EM structure of ZIKV. (B) Surface view of mature form of ZIKV (3.8 Å resolution) and (C) immature form (9.1 Å), colored radially according to the code: green, up to 190 Å to red 270 Å and beyond. (Purdue University image courtesy of Kuhn and Rossmann research groups)

noticeable symmetry is observed for the nucleocapsid, and neither E nor M extend through the membrane to connect with.

Immature virions are intracellular, and have a changing appearance throughout their secretion pathway. Immediately after being formed, they are larger in diameter than mature virions (60 nm) and display 60 spikes on their surface. Each protuberance is formed by three E-prM heterodimers, whose precursor "pr" is proteolytically cleaved during maturation⁶⁹. In some cases, partially mature/immature forms are also released from infected cells.

Lastly, a last category of viral particles can be observed. They are small non-infectious particles of about 30 nm in diameter, called noninfectious subviral particles, which contain the E and M proteins but contain neither capsid (C) nor genetic material.

› Genome organization

The flavivirus genome is composed of a positive single-stranded RNA of approximately 11 kb flanked by non-coding 5' and 3' extremity (untranslated transcribed region, UTR). The viral genome is composed of a single open reading frame (ORF) of approximately 3400 codons. In the 5' extremity of the viral genome are the sequences encoding the 3 structural proteins (C, prM and E), followed by those encoding the 7 non-structural proteins (NS1, NS2A, NS2B, NS3, NS4A, NS4B, NS5). The 5' UTR has a cap (type I, m⁷GppAmpN) to stabilize the RNA and initiate translation, which can also subvert the innate antiviral response^{70,71}. Unlike cellular mRNAs, the flavivirus genome lacks a polyadenylate tail at its 3' UTR^{72,73}.

Overall, the 5' UTR is not very well preserved within Flaviviruses apart from common secondary structures such as a bifurcating 5' stem-loop (5' SL). The function of this structure is twofold: (i) initiate translation (ii) act as a promoter to initiate viral RNA replication by binding the viral polymerase^{74–76}. On the other hand, although the organization of the 3' UTR is different for MBFV, TBFV and NKV, the 3' UTR contains several regions, structures and repeated sequences that are extremely conserved throughout the genus *Flavivirus*. Among these sequences, the most conserved is a long sequence of 90 to 120 nucleotides, forming a stem loop (3' SL). Several areas of the 3' SL are essential and influence

viral-host interactions, including replication, translation and RNA synthesis regulation. Thus, 3' SL interacts with multiple viral proteins (NS2A, NS3, NS5)⁷⁷⁻⁷⁹, and host proteins of important functional role (e.g.: the translation elongation factor 1A)^{80,81}. In addition, the MBFVs have, upstream of the 3' SL, the conserved patterns CS1, CS2, RCS2 (conserved sequence 1 and 2 and repeated conserved sequence, respectively), secondary structures and pseudo-knots which form a compact structure giving resistance to the cellular 5' -3' exoribonuclease 1 (Xrn-1). This feature leads to the accumulation of product of incomplete degradation of viral genomic RNA by Xrn-1 (which stops against these highly structured elements) characteristic of flaviviruses called "subgenomic flaviviral RNA" (sfRNA). Lastly, the 5' and 3' UTRs contains regions that interact by sequence complementarities and allow genome circularization required for replication.

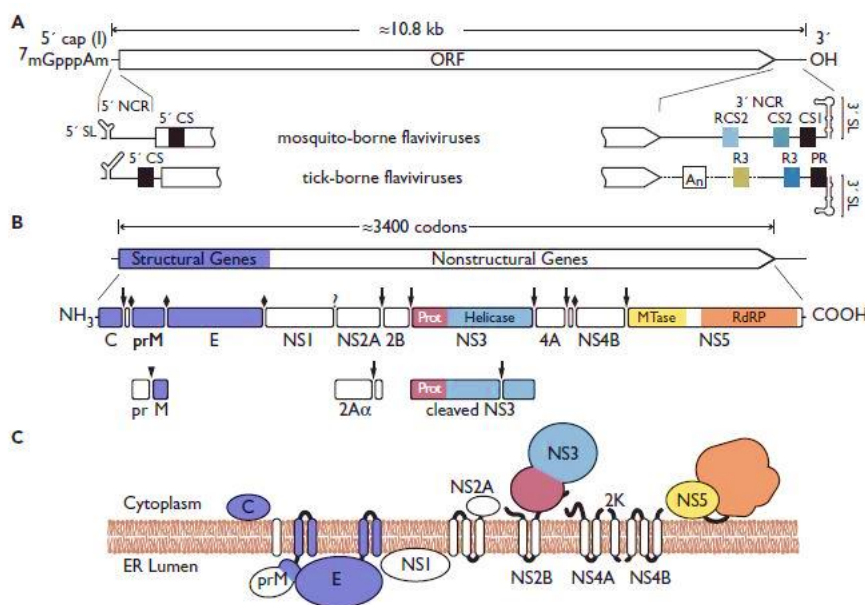


Figure 12 : Flavivirus genome structure and protein expression

(A) Genome structure and RNA elements. The viral genome is depicted with the open reading frame (ORF), the 5' cap, and the 5 and 3 noncoding regions (NCR) indicated. Functionally significant RNA structures within the viral genome are indicated. (B) Polyprotein processing and cleavage products. Boxes below the genome indicate precursors and mature proteins generated by the proteolytic processing cascade. Structural proteins are colored purple, while nonstructural (NS) proteins are white or shaded according to their enzymatic subunits, as indicated. Cleavage sites for host signalase (♦), the viral serine protease (downward arrow), furin or related protease (triangle), or unknown proteases (?) are indicated. (C) Polyprotein membrane topology. The proposed membrane orientation of the flavivirus proteins is shown. The proteins are approximately to scale (areas are proportional to the number of amino acids) and arranged in order (left to right) of their appearance in the polyprotein. (Image and caption from the book "Fields Virology, 6th edition")

II3.2. Viral Cycle

› Entering Cells

Viral infection is initiated by a collision between the viral particle and the cell. The attachment of a virion to the cell surface is a critical and decisive step whose probability can be increased in the presence of a higher concentration of viral particles⁸². However, it is important to note that a virion cannot infect all the cells it encounters, but only those in which it can both enter and replicate. When entry and replication are effective, the tissue is considered permissive to the virus. Flavivirus particles bind to cells by interaction between the viral surface proteins (mainly the E protein) and cellular molecules and receptors, whose distribution plays a major role in the selectivity process. The presence of these receptors determines whether or not the cells are susceptible to the virus, i.e. in which the viral entry process is supported. Thus, a cell can be susceptible without necessarily being permissive. Not all receptors involved in viral entry are well characterized as flaviviruses use a wide range of entry factors and more than one host molecule to enter target cells. Nonetheless, some molecules such as highly sulphated glycosaminoglycans (heparan sulfates), $\alpha_v\beta_3$ integrin, cellular C-type lectin receptors (DC-SIGN/L-SIGN, mannose receptors), phosphatidylserine receptors (TIM, TAM) or heat shock protein (Hsp90/70) have been reported as potential attachment factors for several Flaviviruses⁸³.

After capture by an appropriate receptor, the virions are internalized by endocytosis and reach the cellular cytoplasm in a resulting vesicle called endosome⁸³. Although clathrin-mediated endocytosis is considered to be the major mechanism for flavivirus entry into cells, it is now clear that these viruses can exploit multiple endocytic pathways that could be clathrin or caveol-dependent or independent^{83,84}. Throughout endosomal trafficking, the acidic environment of this compartment induces the fusion between the virion and the host cell membranes. The dimers of protein E dissociate and undergo an irreversible conformational change to form trimers. This reorganization process exposes the fusion peptide, previously buried, which inserts into the endosomal membrane and allows virion opening and nucleocapsid detachment⁸⁵. Fusion requires an optimal pH which varies according to the strain and Flaviviruses. In

addition, its effectiveness is influenced by the lipid composition of the target membranes. Cholesterol, oleic acid and anionic lipids promote fusion, while lysophosphatidylcholine inhibits this process⁵⁵. Finally, the viral genome is dissociated from the capsid and released into the host cytoplasm by the uncoating process⁸⁶.

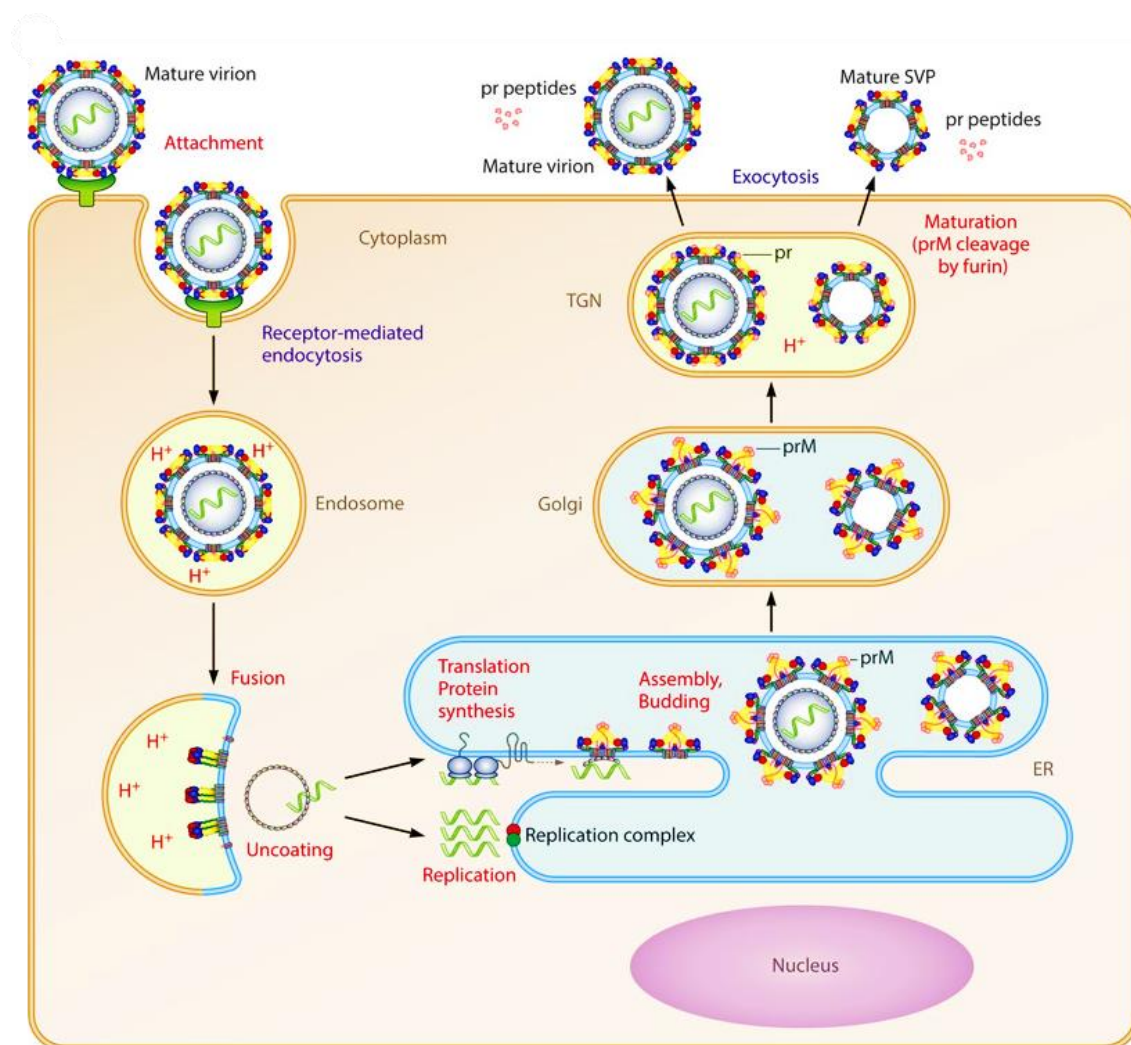


Figure 13 : Flavivirus life cycle

The virus enters cells by receptor-mediated endocytosis and fuses its membrane by an acidic-pH-triggered mechanism in the endosome to release the viral RNA. The positive-stranded genomic RNA serves as the only viral mRNA and leads to the synthesis of a polyprotein that is co- and post-translationally processed into three structural and seven nonstructural proteins. Virus assembly takes place at the ER membrane and leads to the formation of immature virions, which are further transported through the exocytic pathway. The acidic pH in the TGN causes structural changes that allow the cleavage of prM by the cellular protease furin and lead to the herringbone-like arrangement of E. At acidic pH, the cleaved pr part remains associated with the particles (preventing premature fusion in the TGN) and falls off at the neutral pH of the extracellular environment. Subviral particles (SVPs) are formed as a by-product of virion assembly and contain a lipid membrane and prM-E complexes but lack a capsid. SVPs are transported, processed, and released like whole virions. (Image and caption from Heinz and Stiasny, 2017)

› Making Viral Proteins and Copies of Genome

In the cytoplasm, the flavivirus genome functions as an mRNA for the translation of viral proteins. The single open reading frame is translated into a long polyprotein in the endoplasmic reticulum. Then a series of co- and post-translational cleavages is performed by cellular proteases or the viral protease serine (NS2B-NS3) to get the ten viral proteins. The cleavages of the C/prM, prM/E, E/NS1 and 2K-NS4B junctions are performed by the host signal peptidase, while those downstream NS2A are ensured by the viral serine-protease⁵⁵. The NS1-2A cleavage enzyme, on the other hand, remains unknown⁵⁵.

After the translation the RNA synthesis, directed by several structures present in the coding and non-coding regions of flavivirus genome, takes place in complexes formed by all the non-structural proteins and unidentified host proteins assembled around the ER membranes^{86,87}. Although the activity and coordination between the proteins of the replication complex is not yet well identified, NS3 and NS5 appear to constitute the core of this complex⁸⁸. Together, NS3 and NS5, provide the enzymatic activities required to amplify and cap the genome in its 5'UTR.

As previously mentioned, the nature of viral genome determines the replication' strategy. Like all positive-strand RNA viruses, the genomic RNA of flaviviruses is used as a template by the NS5 RNA-dependent RNA-polymerase (RdRp) for the synthesis of a complementary strand of negative polarity (the replicative intermediate)⁸⁶. This allows the production of multiple copies of positive strand during which nucleotide substrates, energy and enzymes are provided by the cell. Thereby, a single input can give rise to multiple daughter genomes. During the replication process, about 10 fold more positive strands are synthesized when compared to negative strands⁸⁶. Moreover, flavivirus replication also leads to the synthesis of 0.2 to 0.6 kb strand, the sfRNA, in addition to these molecules⁸⁹.

› Forming Progeny Virions

Efficient replication of all viruses requires the production of *de novo* assembled infectious particles. The exact process by which flaviviruses assemble into the completed particle is not well known, and some authors suggested that flavivirus assembly differs depending on the type of infected cell. However, this

remarkable process requires considerable specificity in, and coordination among, each following reactions: (i) the formation of structural units of the protective shell, from individual protein molecules, (ii) assembly of the protein coat by appropriate interactions among these structural units, (iii) the incorporation of the nucleic acid genome and other essential virion components in this new structure and (iv) the release of the new assembled progeny virions.

As for replication, flavivirus morphogenesis seems to be carried out in association with the ER membranes in its early stages. The assembly of viral particles is believed to begin with the association of viral RNA (+) and capsid protein dimers^{90,91}, followed by the acquisition of the envelope through budding at the ER membranes^{92–94}. At this stage, immature viral particles are formed and addressed to *trans*-Golgi network (TGN) to complete their maturation. The acidic environment of TGN induces a global rearrangement of the prM-E heterodimers which allows the cleavage of prM into M protein by a furin protease. Once this process completed, the particles, which are now infectious mature virions, are released from the cell through a mechanism that is not yet fully elucidated.

II3.3. Features and Role of the Viral Proteins

The translation of the viral genome results in the production of 10 viral proteins. Of these, the capsid (C), membrane (prM/M) and envelope (E) are structural proteins, while the other seven are non-structural proteins (NS). These latter are referred to as NS1, NS2A, NS2B, NS3, NS4A, NS4B, NS5. After the translation, structural proteins are incorporated into the virion, while non-structural proteins are involved in the coordination of the intracellular aspects of virus replication, assembly and modulation of host defense mechanisms. In this section, the characteristics and role of only non-structural proteins will be discussed. The structural proteins, which are part of my PhD research, will be more extensively detailed in a separate chapter (see part II).

› NS1

The NS1 protein has a molecular weight of ~46 kDa. It contains one to three N-glycosylation sites, depending on the viral species, making NS1 the only NS protein glycosylated known among Flaviviruses⁹⁵. NS1 is partly structured by 12

conserved cysteine residues that mediate intramolecular disulfide bonds^{96,97}. During synthesis, after cleavage of the polyprotein by a cellular protease, NS1 is translocated in the ER by a signal peptide located in the C-terminal region of the E protein⁹⁸. The C-terminal end of NS1 is derived from the cleavage of NS1-2A by an unknown endoplasmic reticulum resident host enzyme.

During the passage through the RE and the Golgi apparatus, NS1 is glycosylated and dimerizes⁹⁹. This dimerized form is predominantly associated with membranes⁹⁹ by a mechanism that remains unknown¹⁰⁰. The intracellular form of NS1 localizes to double-stranded RNA sites and functions as an essential cofactor for viral replication by interacting with the NS4A protein¹⁰¹. When mammalian cells are infected, the NS1 protein is also secreted in a hexameric form. Until recently this form was thought non-existent in mosquito cell infections^{97,102}, however Alcala et al. reported that Dengue NS1 was secreted in a barrel-shaped hexamer from cultured mosquito cells of either *Ae. albopictus* or *aegypti*¹⁰³. The extracellular form of NS1, also known as "viral toxin", accumulates at high levels in human sera and tissues and can be used for the diagnosis of early stage flavivirus infections. In addition, this form is highly antigenic and induces a strong humoral response. The involvement of NS1 in flavivirus pathogenesis is widely described, although the mechanisms implicated remain uncertain. NS1 could facilitate immune complex formation¹⁰⁴, induce autoantibody production¹⁰⁵, damage endothelial cells via the antibody-dependent complement pathway¹⁰⁶, amplify infection in a direct manner¹⁰⁷ or attenuate alternative complement activation pathway by H factor binding¹⁰⁸. In addition, NS1 of WNV plays a modulating role in innate immunity by inhibiting the toll-like receptor 3 (TLR3) dependent signaling pathway¹⁰⁹.

Another form of NS1, longer than the common form, has been described in Japanese encephalitis serogroup flaviviruses: NS1'¹¹⁰. The sequence and presence of a particular secondary structure in the NS1 C-terminal and NS2A N-terminal would cause a frameshift during protein translation and the formation of a new cleavage site in the first 8 nucleotides of NS2A¹¹¹. This would result in a longer NS1' protein which is believed to be involved in the neuro-invasiveness of neurotropic viruses belonging to the JE serogroup¹¹².

› NS2A and NS2B

NS2A is a small hydrophobic multifunctional protein of ~22 kD. The precise topology of this protein is not well determined, although a preliminary model of DENV-2 NS2A topology was proposed in 2013¹¹³. This protein associates with the ER membrane and is involved in viral genome replication⁷⁹. NS2A binds in a specific manner to the 3' UTR of viral RNA and interacts with replication complex effectors. NS2A is likely to transport viral RNA from replication sites to assembly sites via viro-induced membrane structures¹¹⁴, and participates in viral particle assembly mechanisms¹¹⁵ via interaction with NS3^{113,116}. In addition, NS2A from Dengue and West Nile viruses can also inhibit interferon (IFN) signalling^{117,118}.

NS2B is a small protein of ~14kD associated with membranes. It forms a complex with the NS3 protein and anchors this latter in cellular membranes. NS2B acts as a cofactor of the viral serine protease NS2B-NS3^{119,120}.

› NS3

NS3 protein is the second largest protein encoded by flaviviruses. It is a multifunctional protein of ~70 kD whose sequence is highly conserved among Flaviviruses⁵⁵. NS3 supports an helicase/NTPase activity involved in genome replication in association with NS5, and a protease activity required for the maturation of the viral polyprotein^{55,121}. This protein is also believed to play a role in virus assembly, independently of its catalytic functions¹²².

The helicase and NTPase domains are located in the C-terminal part of the NS3 protein. Helicase activity allows the unwinding of the duplex structures of viral RNA. The energy required to dissociate the hydrogen bonds maintaining the two complementary strands is provided by the hydrolysis of a nucleoside triphosphate, usually ATP. This hydrolysis is carried out by the NTPase domain coupled to the helicase domain^{123,124}. The flavivirus helicase/NTPase belongs to the superfamily II of RNA helicases¹²⁵.

The serine protease activity is carried by the N-terminal region of NS3, but the hydrophilic part of NS2B is necessary to form the active protease complex. The NS2B cofactor organizes itself in close proximity to NS3 and this way gives an active or inactive conformation to NS3^{126,127}. The protease preferentially cleaves after adjacent basic residues (Arg or Lys) and before a short side-chain amino

acid (Gly, Ser, or Ala)¹²⁸.

› NS4A and NS4B

NS4A and NS4B are small hydrophobic proteins of ~16 and 27 kD respectively, bound by a conserved 23-amino-acids signal peptide of 2000 Daltons (2K)⁵⁵. The cleavage performed by the viral protease at the NS4A/2K junction is a prerequisite for 2K/NS4B cleavage by a host signalase. NS4A and NS4B are likely to function cooperatively and play multiple roles in viral replication and virus-host interactions.

During replication, NS4A and its peptide 2K induce a rearrangement of the internal cell membranes where viral replicative complexes are located¹²⁹. The latter is conducted according to a process in which 2K regulates the ER membrane modulation function of NS4A by mechanisms intrinsic to each Flaviviruses¹³⁰. In addition, the interaction of NS4A with cellular vimentin regulates the formation of viral replication complexes in Dengue-infected cells¹³¹.

NS4B is a protein rarely documented localized in the ER. If NS4B is known to undergo post-translational modifications resulting in a smaller molecular weight form^{132,133}, the identity and function of this modification remains to be determined⁵⁵. Currently, the structure of NS4B is still not clearly defined, but the study of the NS4B of DENV revealed the presence of three to five potential transmembrane domains depending on the technique used^{134,135}. Dengue virus NS4B interacts with the helicase domain of NS3 and dissociates it from single-stranded RNA¹³⁶. In the case of WNV, it is rather NS4A which interacts with NS3 to regulate its ATPase activity¹³⁷.

Both NS4A and NS4B can inhibit IFN signaling, and induce unfolded protein response^{117,138,139}. In addition, these two proteins interact with NS1 at a genetic level to modulate viral replication. Indeed, replication defects due to mutations in the NS1 of YFV and WNV can be restored/offset by an adaptive mutation in NS4A and NS4B respectively^{101,140}. In addition, mutations in NS4A inhibiting DENV replication are compensated by amino acid changes in NS4B suggesting an interaction between the two proteins¹⁴¹.

› NS5

NS5 protein is a large protein of 103 kDa, multifunctional and strongly conserved within the *Flavivirus* genus⁵⁵. It harbors methyltransferase activity (MTase) in N-terminal^{142,143} and RNA-dependent RNA polymerase activity in C-terminal¹⁴⁴.

Flavivirus genome has a cap in 5'UTR whose production requires several steps carried by the successive action of NS3 and NS5. NS3 provides the RTPase activity needed for the first step of phosphate removal from a 5' triphosphorylated RNA substrate, then NS5 provides the guanylyltransferase, N7 and 2'O-methyltransferase activities involved in the capping of neo-synthesized positive RNAs^{145,146}. The MTase activity of Flavivirus NS5 protein is essential to the viral cycle and differs from the cellular MTase as it preferentially methylates the cap of only viral RNA¹⁴⁶.

The polymerase activity is due to conserved domains within the RdRp family¹⁴⁷, including a GDD triplet indicative of the active polymerase site. Other conserved patterns are involved in the interaction with nucleotides (DxxxxxD) and in the binding with the RNA matrix strand (xGxxxTxxxxN)¹⁴⁸. In the cytoplasm, NS5 forms a complex with NS3 and can thus stimulate the NTPase and RTPase activities of NS3^{78,149}. This protein triggers the initiation of de novo RNA synthesis by binding to the circularized viral genome⁷⁵. While the steps of genome capping and replication take place in the cytoplasm, a nuclear form of NS5 has been observed in mammalian cells infected with certain flaviviruses. Transport to the nucleus is provided by the importin α/β by recognition of a nuclear location signal (NLS) on NS5^{150,151}. This transport protein seems to compete with the viral protein NS3 for NS5 binding. In fact, it transports NS5 to the nucleus while NS3 retains the latter in the cytoplasm¹⁵⁰. The nuclear form of NS5 was reported to negatively modulate the production of pro-inflammatory interleukin 8 (IL-8) at the onset of infection and thus promote viral spread¹⁵². During infection, NS5 is therefore able to pass between cytoplasm and nucleus to participate in both viral replication and transcriptional modulation of the host's cellular genes.

II3.4. Evolutionary advantage of Flaviviruses

Flaviviruses, despite sharing common characteristics in terms of structure or replication cycle, constitute a highly diversified viral genus, infecting a wide

range of vertebrate and arthropod hosts, sometimes even alternating between the two in the case of arboviruses. This dual-host tropism is traditionally associated with genomic flexibility and the high mutation rate of RNA viruses¹⁵³.

› Genetic diversity and Viral fitness

The RdRp of flaviviruses, like other RNA viruses, is characterized by a poor fidelity due to the absence of exonuclease activity. This lack of proofreading activity results in a mutation rate of approximately 10^{-6} to 10^{-4} substitutions per nucleotide and per replication cycle¹⁵⁴. Furthermore, the mutation rate of the same isolate may vary according to the cellular environment, and hence to the host¹⁵⁵. The error rate of the RdRp, coupled with rapid replication and a large population, has given rise to the concept of viral "quasispecies". This term defines the population of genetically related viruses ("the mutant cloud") distributed around a "consensus" sequence defined by the average of the most frequent nucleotide in the population for each position in the genome¹⁵⁶. This quasispecies structure has been shown to be critical for several fundamental aspects of the general fitness of RNA viruses or their pathogenesis¹⁵⁷. For viruses, fitness is often defined as the ability to produce new infectious particles in a given environment¹⁵⁸. This definition, focused on replicative success, doesn't fully integrate the usual definition of the term as it is understood in evolutionary biology where fitness is the amount of genetic material passed on to the next generation¹⁵⁹. Thus, because of their obligatory parasitism, viral fitness also depends on the success of their transmission. The quasi-species structure of RNA viruses has therefore proved important for arboviruses by allowing them to adapt to new cellular environments, selection pressures or hosts¹⁵⁷. Moreover, replication and transmission are integrated into the ability of a virus – whatever the level considered (serotype, genotype, clade, isolate or variant) – to be more prevalent in the field than any other virus. This is called the epidemiological fitness¹⁵⁹.

› Adaptability

While most RNA viruses infect only one or more biologically related host species, arbo-flaviviruses must be able to replicate in two very different host types. Since adaptation to one can affect fitness within the other host, arboviruses must

maintain a "trade-off"¹⁶⁰ that can explain why they evolve more slowly than RNA viruses with a direct transmission¹⁶¹. A fairly large cloud of mutants, by exploring the "genetic space", enables genetic variants more or less adapted to the different types of hosts to be maintained within the same population. Maintaining genetic diversity is therefore crucial for long-term arbovirus transmission. Interestingly, it is worth noting that only a fraction of the viral population diversity is transmitted between different hosts, as well as tissues within the same host^{162,163}. This severe population reduction, called bottleneck, occurs very frequently in the transmission cycle. However, even though it induces a drop in genetic variability and can promote the accumulation of deleterious mutations, the fitness of Flaviviruses is not affected because genetic diversity is quickly restored after dissemination¹⁶².

The dual-host tropism of arbo-flaviviruses involves a number of biological barriers that are *prima facie* restrictive for other viruses. First of all, viruses must be able to overcome the limits of attachment/entry, replication, and assembly/release, underlying a successful infection of arthropod and vertebrate cells. For instance, the receptor complex expressed on the cell surface varies between tissues and species as well as temperature. The latter is a further challenge as the RdRp must be able to operate effectively at temperatures ranging from about 24 (mosquito) to 37 °C, or even higher in case of fever, in order to ensure viral replication. Then these viruses have to face different antiviral pathways that can interfere with their replication and transmission success. Mosquitoes do not have immunoglobulin-based humoral response and rely instead on intrinsic intracellular antiviral mechanisms¹⁶⁴, in particular dsRNA-initiated immune responses, such as RNA interference (RNAi), and canonical immune signaling cascades⁸³, while mammals have both an innate and adaptive immune system to limit viral spread. As a result, flaviviruses have evolved many specific strategies and proteins to counteract or escape the antiviral immune response of their hosts. This capacity is largely involved in flavivirus pathogenicity, which will be further detailed in a following chapter.

III. THE FIERY TALE OF ZIKA VIRUS

“In April 1947, six sentinel platforms were in use at Zika. The temperatures of the rhesus monkeys on the platforms were taken daily. On 18th April, 1947, it was reported that the temperature of one of these monkeys —Rhesus 766— was 39.7°C. On 19th April its temperature was recorded as 40°C.”

Dick G. W. A., Kitchen S. F., Haddock A. J.

« Zika virus (i). Isolations and serological specificity. » 1 September 1952.

Zika virus (ZIKV) is an emerging arthropod-borne virus, transmitted by *Aedes* genus mosquitoes, responsible for Zika fever. It belongs to the *Flaviviridae* family, *Flavivirus* genus, and is related to Dengue, West Nile, Yellow Fever, and Japanese Encephalitis viruses. Discovered in 1947 in Uganda, ZIKV was first isolated from the blood of the sentinel Rhesus monkey No. 766, stationed in the Zika forest during sylvatic Yellow fever surveillance¹⁶⁶. In 1948, the virus was once again isolated from a group of *Ae. africanus* mosquitoes caught in the same forest; giving its name to Zika virus.

III.1. Classification

According to the first phylogenetic studies performed by Kuno *et al* in 1998¹⁶⁷, Zika virus is placed in the cluster of mosquito-borne Flaviviruses, where it forms the clade n°X with the virus Spondweni (SPOV) responsible for fever in Sub-Saharan Africa and Papua New Guinea. Recently, a new phylogenetic tree of *Flavivirus* genus, inferred with complete ORF sequences, confirmed this first classification⁵⁹. Interestingly, the topology of the tree shows that ZIKV and SPOV are grouped along with Kedougou virus (KEDV), and that these viruses are phylogenetically closer to viruses belonging to *Culex-spp* MBFV (Kokobera virus complex) than to DENV serotypes.

III.2. Emergence and Global spread

Until the last few years, ZIKV infection remained relatively less studied due to its low case numbers, and low clinical impact relative to other arboviruses. After its discovery several seroprevalence surveys and entomological studies on non-human primates, human and mosquitoes shown that the ZIKV circulated silently

for decades, through Africa (Nigeria 1971, Gabon 1975, Senegal 1988) and Southeast Asia (Malaysia 1969, Indonesia 1977). At this time, ZIKV was reported to only cause sporadic human infections. The prevalence of Zika virus infection in Uganda was of 6.1% in 1952 among a population of 99 residents¹⁶⁸, and of 7.1% in Java, Indonesia, from 1977-1978 among patients who were hospitalized for fever¹⁶⁹.

In 2007, the first large epidemic was reported in the Yap Island¹⁷⁰, followed by an outbreak of Zika fever in French Polynesia in 2013¹⁷¹. In May 2015, the Brazilian Health authority reported an autochthonous presence of ZIKV in the states of Bahia and Rio Grande de Norte, marking the first emergence of ZIKV in the Americas¹⁷². Since then, Zika virus spread in a spectacular rhythm, creating an unprecedented epidemiological phenomenon. The status of public health emergency of international concern was decreed by the World Health Organization (WHO) on the 1st February 2016 and was withdrawn at the 5th meeting of the Emergency Committee held on the 18th November of the same year¹⁷³. But the Zika has obviously not disappeared after this status was lifted. Beyond the emergence in the Americas, Zika virus was reintroduced into Africa, where it was first discovered, and into several countries in Asia and the Pacific. Between 1st January 2015 and 1st June 2017, 71 countries reported outbreaks or cases of Zika virus disease ; the last one being India¹⁷⁴.

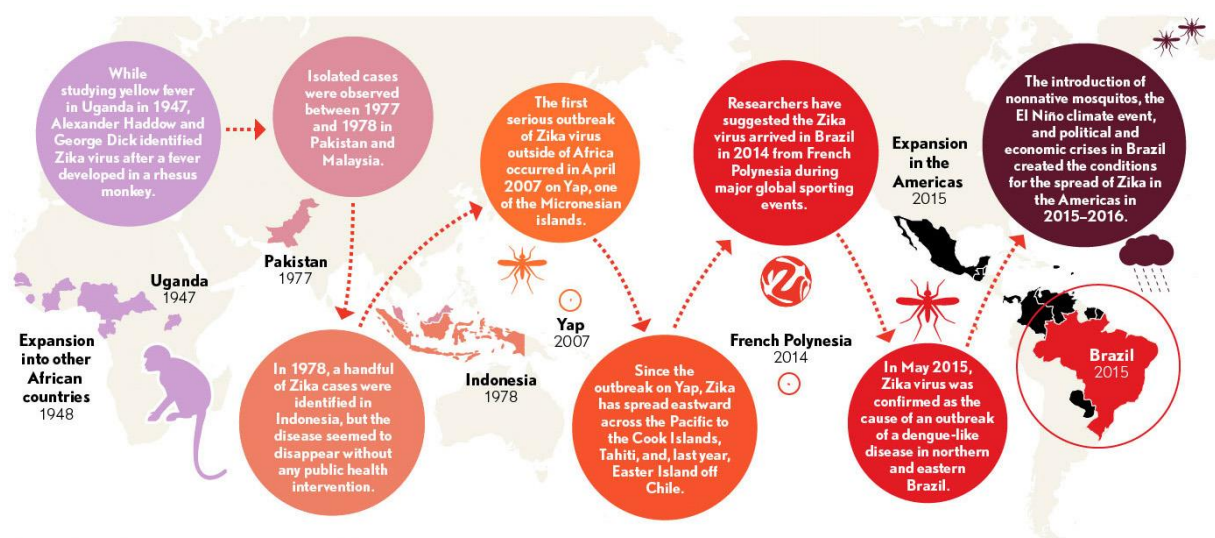


Figure 14: How Zika virus spread to the Americas

(Image from "Council on foreign relations". Sources: CDC, New York Times)

III2.1. Zika in the Pacific and Asia

› The emergence in the Yap Island

In 2007, the first outbreak of Zika fever occurred in the Pacific on the Yap Island in Micronesia. Reports of eruptive syndromes, which do not match the diagnosis of Dengue fever, have led to the identification of the first ZIKV outbreak.

During this epidemic episode, 185 clinically suggestive cases of ZIKV infection were documented. The most frequently described symptoms were moderate fever associated with headaches, maculopapular rashes, arthro-myalgia, and non-purulent conjunctivitis. Thanks to a seroprevalence study based on random samples it was estimated that 73% of Yap residents aged 3 years or older had been infected with the Zika virus. According to these data, the proportion of asymptomatic cases was therefore estimated at about 80%.

The outbreak on the Yap Island represents the largest series of clinical cases of ZIKV infection described in 60 years and marks the beginning of an unexpected geographical expansion.

› The Re-Emergence in French Polynesia

As in Micronesia, Dengue-like symptoms, but different from the usual clinical signs due to the appearance of febrile eruptive syndromes, prompted physicians to report the onset of a new infectious disease. From October 2013 to March 2014, French Polynesia was hit by the largest ZIKV epidemic ever described so far, against a background of Dengue epidemic where serotypes 1 and 3 co-circulated.

During the 6-month epidemic, 8,746 clinically suggestive cases were reported by the sentinel physician network. In addition, it was estimated that 32,000 suspected cases had consulted, bringing the prevalence of Zika infection to about 11.5% of the population. The majority of patients experienced minor clinical signs and no deaths related to the infection were reported. However, during the outbreak, 73 patients had severe neurological or autoimmune manifestations, most of them Guillain-Barré Syndrome (GBS), which led the scientific community to suspect a causal link between ZIKV infection and such complications. The connection was proved afterwards for 42 GBS cases described at the time. This was the first evidence of Zika virus neurotropism.

The reasons for the emergence in French Polynesia are unknown, but the virus encountered conditions favorable to its circulation such as the absence of anti-Zika immunity and the presence of mosquitoes vectors *Ae. aegypti* and *Ae. polynesiensis*. Subsequently, ZIKV autochthonous transmission was reported in several regions of the Pacific.

› Situation in South-East Asia

Zika virus isolation from Malaysian mosquitoes collected in 1966 demonstrates the presence of the virus in Asia for at least several decades¹⁷⁵. In the 1950s-90s, human serology studies suggested that Zika was already circulating in Pakistan¹⁷⁶, India¹⁷⁷, Vietnam¹⁷⁸, the Philippines¹⁷⁹, Malaysia¹⁷⁸ and Indonesia¹⁶⁹, causing *a priori* asymptomatic infections in humans. However, given that the serological tests used in these studies were not designed for the specific detection of Zika, cross-reactions with other widely spread Flaviviruses, in particular Dengue fever and Japanese encephalitis, are not excluded. For these reasons, the first laboratory-confirmed ZIKV infection in Asia dates from 2010 in Cambodia¹⁸⁰. With the emergence of Zika in the Pacific and the detection of autochthonous infection cases on the Asian-Pacific side, the threat of the spread of Zika Fever outbreaks to Southeast Asia was serious. In 2016, active circulation was reported in several countries in Southeast Asia including Indonesia, Thailand, Vietnam and Singapore¹⁸¹. Nevertheless, it is currently difficult to assess whether the transmission intensity and geographical scope of ZIKV in Asia have significantly changed over the past decades. Indeed, phylogenetic analyses suggest that several strains circulated in the area even before the outbreak of Zika Fever was reported¹⁸². WHO alert measures and the implementation of specific diagnostic tests may have uncovered an already existing but undocumented phenomenon, due to the asymptomatic or mild nature of most ZIKV infections. Did any factors limit the successful implementation of Zika before 2016? Were there, on the contrary, any factors exacerbating the pathogenicity of the virus that would lead to its detection? The questions remain open and still unanswered.

III2.2. Situation in the Americas

› From Brazil to South America

In May 2015, a Zika fever outbreak was declared by the Brazilian health authorities, after confirmation of numerous reported cases in northeastern Brazil. Phylogenetic analysis suggests that the strain responsible for the epidemic is linked to the one of French Polynesia. The virus was introduced into Brazil during a Va'a competition in 2014, in which several Pacific countries facing ZIKV outbreak participated. In 2015, the epidemic continued to spread to several states in the country. According to the Ministry of Health the estimated number of suspected cases of ZIKV infection ranges between 440,000 to 1,3 million in early February 2016. At the same time, an increase in serious congenital and neurological anomalies suspected of being linked to ZIKV infection - observed for the first time - compelled the WHO to declare ZIKV as a public health emergency of international concern. By June 2016, the epidemic was on the decline.

In August the Olympic Games took place in Brazil, during the winter season. Even though mosquito activity is reduced towards this period, the influx of travelers from all parts of the World during the Olympics was a potential gateway to the introduction of ZIKV in areas not yet affected. As a result, many worries were voiced and a call for WHO to cancel or postpone the 2016 Olympics was launched by about 200 scientists in view of the potential risk posed by Zika. This appeal was rejected¹⁸³. On the basis of the evaluations carried out, this proposition would not significantly affect the spread of ZIKV. Indeed, a study published in August 2016, found that people attending the Olympics have a negligible risk of infection¹⁸⁴. This risk was assessed according to a mathematical model, whereby in the worst-case scenario studied, 6 to 80 travelers will be infected during their stay, among the hundreds of thousands expected in Brazil, and "only" 3 to 37 people will transport ZIKV into their countries. Nevertheless, the WHO strongly advised pregnant women and travelers to adopt health recommendations and protective measures against mosquito bites.

ZIKV then spread across most of the continent, in a rapid and explosive movement. At the beginning of 2016, South American countries facing ZIKV epidemics included Brazil, Cabo Verde, Colombia, El Salvador, Panama and

Venezuela. Then other countries in South and Central America reported an active circulation of Zika: Barbados, Bolivia, Ecuador, Honduras, Guatemala, Mexico, Paraguay, Puerto Rico, Dominican Republic, Suriname... as well as the French departments of America (Martinique, Guadeloupe, Saint-Martin and Guyana).

› Outbreaks in French Territories

Thanks to the implementation of enhanced surveillance by a network of sentinel physicians, the first indigenous cases of ZIKV infection were reported in Martinique and French Guiana in December 2015¹⁸⁵. Following a significant increase in the incidence of Zika infection, the status of epidemic areas was declared in January 2016. After 10 months, the latter was officially lifted in both territories¹⁸⁵.

Martinique was the French department of the West Indies the most affected by the ZIKV epidemic in 2016. More than 36,000 clinically suggestive cases of infection were reported during the outbreak¹⁸⁶. As in French Polynesia, a high incidence of GBS cases was observed in Martinique. During the event, 5 cases of severe neurological impairment and 29 cases of GBS were reported with laboratory-confirmed ZIKV infection. Among them, one person died. In addition, 830 women were infected during pregnancy and 26 cases of congenital malformation were detected. Thanks to the implementation of pregnancy monitoring, which has been particularly strengthened in the French overseas territories, 21/26 cases were detected by ultrasound¹⁸⁵.

In French Guiana, more than 10,000 clinically suggestive cases and a record of pregnant women exposed to the virus has been established¹⁸⁶. Among them, 2,211 had a laboratory-confirmed Zika virus infection and 22 cases of brain abnormalities were detected, 21 of which by ultrasound. On this department, a total of 7 cases of GBS and 3 cases of other severe neurological syndromes were associated with laboratory-confirmed Zika virus infection¹⁸⁵.

Guadeloupe was also affected by Zika Fever outbreak, and reported the first case of local infection at the end of January 2016. Until July 2017, more than 31,000 people¹⁸⁶, including 815 pregnant women, have been affected by the virus, and 18 fetal malformations have been discovered¹⁸⁵. Again, a high incidence of neurological complications related to Zika was observed in this department.

These include 40 cases of GBS in addition to 15 cases of severe neurological impairment other than GBS. Moreover, 3 deaths that may be attributed to Zika infection are to be deplored¹⁸⁵.

› Zika in the United States

Apart from imported cases, no reports of Zika Fever have been recorded in North America before 2016. Then, in January, the first case of ZIKV infection was detected in the United States Virgin Islands. Since 2016, more than 37,000 confirmed infection cases have been reported in the US territories, including a majority of autochthonous cases. In the United States a total of 5684 cases of ZIKV infection have been reported, with 94% of these cases being imported. The first evidence of active transmission in the continental US was reported in August 2016 in Florida¹⁸⁷. Subsequently, other cases were reported in the state of Texas¹⁸⁵.

The Centers for Disease Control and Prevention (CDC) reported 15 cases of GBS associated with Zika in the US States and 52 cases in the US territories¹⁸⁵. Until 2018, US States reported 2394 pregnancies with Zika confirmed infection and 116 newborns with Zika-associated birth defects¹⁸⁸. In US territories, 4662 pregnancies with laboratory-confirmed infection were recorded, in which 167 cases of birth defects¹⁸⁸.

III2.3. Situation in Europe

As previously discussed, the potential for rapid travel from one part of the world to another, and this throughout the period of viremia, can lead to the introduction of a pathogen into non-epidemic areas. The impact of this kind of mobility was particularly striking during the Zika epidemic and the multiple related introductions have certainly potentiated its spread around the globe¹⁸⁹. For illustrative purpose, the International Air Transport Association revealed that the overall volume of passengers leaving Brazilian hotspots of Zika infection by plane between September 2014 and August 2015 was approximately 9.9 million¹⁹⁰. Of these 9.9 million passengers, 65% concluded their trip in America, 27% in Europe and 5% in Asia¹⁹¹.

According to data obtained from the Surveillance Atlas of the European Center

for Diseases Control, 2341 cases of ZIKV infection were recorded in Europe between 2015 and 2017¹⁹². Of these, 98% were related to travel. In the year 2016 alone, at the peak of the pandemic, 2077 cases of Zika infection were diagnosed among European travelers¹⁹³. Furthermore, France is the country with the highest number of cases (1,141 cases), followed by Spain (306 cases), the United Kingdom (199 cases) and Belgium (128 cases)¹⁹². In a further analysis it was estimated that, among the cases with known areas of residence, 43% were living in areas where *Ae. albopictus* is established.

III.3. Zika virus Ecology

III3.1. Host and Reservoir

Since its discovery from a Rhesus monkey in Uganda, Zika virus has been detected in different monkey species living in Africa and Asia¹⁹⁴. In studies conducted in Borneo, Malaysia, using blood samples from humans and wild and semi-wild orangutans, the prevalence of anti-Zika antibodies in humans was shown to be about 44% compared to 8% in orangutans^{195,196}. According to these data, the authors of the study assumed that the monkeys had been infected either from a human reservoir or from a recently established sylvatic cycle and that non-human primates were a probable Zika reservoir in Asia. Also, many other species from both domestic and wild fauna were found positive for Zika virus in studies conducted in Indonesia in 1978¹⁹⁷ or Pakistan in 1983¹⁷⁶. The most frequently detected animals include bats, rodents, goats and sheep. However, these data are based on antibody tests detection that were not specific to Zika and whose specificity and sensitivity are uncertain, therefore they should be considered with caution.

With the explosion of Zika in America, to determine whether a sylvatic cycle of ZIKV transmission was likely to establish in South America (as was the case centuries ago for Yellow Fever), was an urgent question. Knowing if wildlife and/or domestic animals are involved in virus maintenance is a critical factor in the elaboration of public health strategies for the control of viral infections. In 2018, a study performed by Terzian *et al*¹⁹⁸, demonstrated the presence of Zika in organs collected from 40% of marmosets and capuchin carcasses collected in cities of São Paulo and Minas Gerais States. These findings, and their

experimental verification, highlighted a potential role of free non-human primates in the urban/peri-urban ZIKV dynamics.

III3.2. Vectors and vector-borne transmission

Zika transmission to humans is mainly vectorial and occurs through the bite of an infected female mosquito of the *Aedes* genus. It is mainly urban and sylvatic, where humans are the amplifying host in areas without non-human primates. A wide range of vectors appears to be involved in Zika virus transmission, which emphasizes the strong plasticity of this Flavivirus. ZIKV vectors in Africa are different from those in the Pacific, South America and Southeast Asia. Outside Africa, *Ae. aegypti* is the main vector, while *Ae. albopictus* imposes itself as a competent vector too. In Africa, ZIKV was isolated for the first time from *Ae. africanus* mosquitoes collected in the Zika forest¹⁶⁶. However, viral isolates collected between 1968 and 2002 in West Africa revealed ZIKV in other *Aedes* species, such as *Ae. dalzieli*, *Ae. aegypti* and *Ae. furcifer*¹⁹⁹. Although no estimates of their vectorial competence have been established, other studies conducted from 1962 to 2011 also detected Zika in mosquitoes of the genera *Anopheles*²⁰⁰ and *Culex*²⁰¹.

When the Micronesia epidemic broke out, the prevalence of Zika in mosquitoes collected at the time was higher in *Ae. hensilli*¹⁷⁰. In French Polynesia, *Ae. aegypti* and *Ae. polynesiensis* were considered responsible for the transmission of the virus to humans. However, the results obtained by Calvez *et al.*²⁰², were unexpected since they demonstrated a low Zika transmission by both mosquitoes. Following this, the authors suggested the possible importance of other factors that may have contributed to the rapid spread of the virus in the Pacific, such as the lifespan and density of vectors or the large immunologically naïve fraction of the population.

In Brazil, *Ae. aegypti* and *Ae. albopictus* are the main vectors of ZIKV. Furthermore, investigations of the vector competence of different mosquito species from California have demonstrated that *Ae. aegypti* from the region was an excellent laboratory vector, while the two *Culex* species tested (*Cx. quinquefasciatus* and *Cx. tarsalis*) were refractory²⁰³. However, the competence of *Cx. quinquefasciatus* is actually controversial, as it appears highly dependent

on the geographical area of mosquitoes. Several studies have documented the ability of ZIKV to infect this species in Brazil²⁰⁴, Mexico²⁰⁵ or China²⁰⁶, while others reported an incompetent transmission of *Cx. quiquefasciatus* from North America^{207,208}.

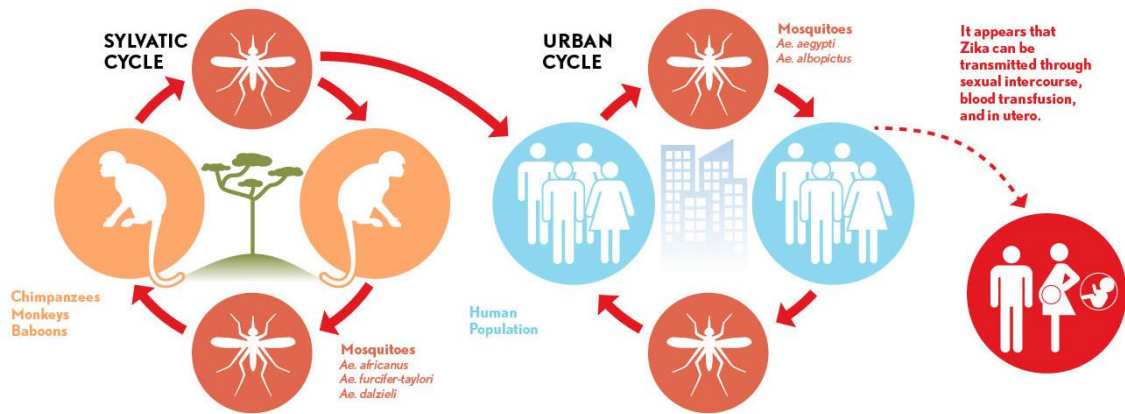


Figure 15: How Zika virus enters the human population
(Image from "Council on foreign relations". Sources: CDC, PLOS)

III3.3. Non vector-borne transmission

In contrast to the initial knowledge, Zika virus transmission is not exclusively vectorial. Intraspecies transmission from human to human can also occur through sexual, or nosocomial routes during blood transfusion^{209,210}. In addition, many cases of vertical transmission have been reported during the recent outbreaks. These modes of transmission, rather unusual for a Flavivirus, were especially evident in countries not affected by Zika but where transmission from imported Zika infections has occurred.

› Sexual Transmission

Unlike other flaviviruses, ZIKV is both arthropod- and sexually-transmitted. The first case of sexual transmission was identified in 2011, in the state of Colorado in the United States, after the return of a scientist on mission in Senegal. His wife, who had not travelled, contracted a ZIKV infection 9 days after her husband's return; an infection that was confirmed by blood serology. The investigation of ZIKV transmission factors identified that transmission by sexual intercourse was

the most likely etiology for this case²¹¹. Following the identification of sporadic cases in 2016, the hypothesis of sexual transmission of ZIKV was accepted. We learn afterwards that the sexual transmission of Zika can be delayed²¹², and can occur up to at least 1 month after the symptoms onset in the partner²¹³. Throughout the case reports and investigations, the presence of Zika was confirmed in the seminal fluid and genital mucosa of woman²¹⁴. The long-term viral shedding in semen, beyond 6 months after symptoms onset²¹⁵, prompted part of the scientific community to undertake investigations to understand this unexpected phenomenon. Today, the findings confirm a marked tropism of the virus for male reproductive tract tissues^{216,217} and alert about a potential long-term detrimental effect of ZIKV infection on human male fertility^{218–220}. In addition, experimental studies in mice and macaques have begun to elucidate the pathogenesis of ZIKV infection in the male genital tract, with the testicles as potential reservoirs for persistent infection²¹⁷.

› Maternal-fetal transmission

A few arboviruses belonging to the genera *Flavivirus* and *Alphavirus* are able to cross the placental barrier in a small proportion of pregnant women. As a result, cases of mother-to-fetus transmission have previously been described for other arbovirosis diseases such as Dengue Fever, Japanese Encephalitis as well as West Nile and Chikungunya. But Zika is the first arbovirus characterized by highly efficient intrauterine transmission.

The alarm signal triggered by Brazil in response to the abnormally high incidence of severe congenital malformation in the newborn, observed during the Zika outbreak, was the first indication of non-anecdotal vertical transmission and severe outcome. Vertical transmission in humans was confirmed when ZIKV RNA was detected in amniotic fluid, placental and fetal tissues^{221,222} and experimental studies demonstrated highly efficient maternal-fetal Zika virus transmission²²³, especially in pregnant rhesus macaques²²⁴. Today, all the clinical, epidemiological and laboratory data published since the beginning of 2016 clearly link the occurrence of adverse events during pregnancy or birth defects to Zika virus infection during pregnancy.

III.4. Clinical features of Zika Fever

III.4.1. Symptomatology

The clinical manifestations of ZIKV infection ranged from asymptomatic infections to mild, self-limited febrile illness, similar to that of a mild dengue-like syndrome for a period of 2-7 days. The incubation period is likely 3-12 days. Zika fever is characterized by non-brutal symptoms onset compared to other arbovirosis, with low-grade fever, headache, muscle and joint pains, retro-orbital pain, conjunctivitis, as well as a characteristic maculopapular rash reminiscent to measles presented by more than 90% of patients.

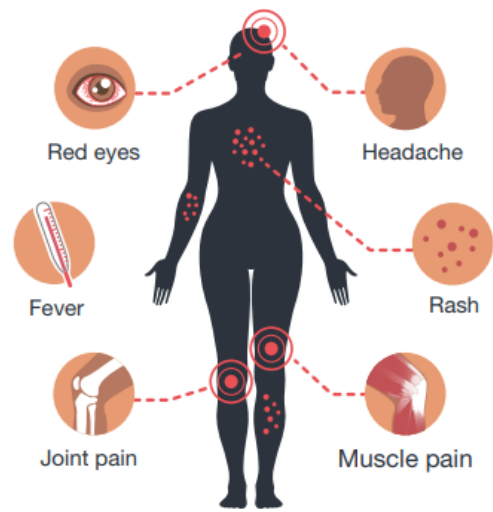


Figure 16: Zika symptoms
(Image from CDC)

However, owing to the mild nature of the disease, asymptomatic patients are frequent, reaching 60 to 80% depending on the affected area and constitute a high-risk source of transmission. Also, the spectrum of Zika fever overlaps that of other arboviral infections, making the diagnostic more confusing, especially in areas of co-circulation, and prevalence surveys of Zika virus infection difficult.

III.4.2. Treatment

There is no vaccine to prevent nor medication to treat ZIKV infection, but only to heal symptoms. The CDC recommendations are to take plenty of rest, drink water to prevent dehydration and take drugs such as paracetamol (acetaminophen) to reduce fever and pain. Furthermore, if the infection occurs in the endemic area of Dengue Fever, avoid aspirin and other non-steroidal anti-inflammatory drugs until Dengue Fever infection can be excluded, in order to reduce the risk of serious bleeding. In response to this lack of therapeutic solution, the WHO called on the global research and product development communities on 1 February 2016, to prioritize the development of preventive and therapeutic solutions.

› Anti-viral drugs

A major challenge in the search for anti-RNA virus therapies is their ability to mutate, allowing them to quickly develop antiviral resistance. Currently, various antivirals or other drugs are being tested to stop Zika virus infection. In parallel, other molecules such as certain nucleoside analogues that integrate into the viral RNA of the virus through the viral polymerase and block its replication, are being studied. Among them, the 7DMA, initially studied against the hepatitis C virus but not yet commercialized in this indication, shows very promising results in mice infected with Zika²²⁵. In addition, other researchers in the field identified molecules with an anti-Zika effect to date tested to verify their effectiveness²²⁶. However, even if promising molecules are identified, their main purpose being the prevention or reduction of fetal pathologies, the use of such experimental drugs in pregnant women remains an important constraint.

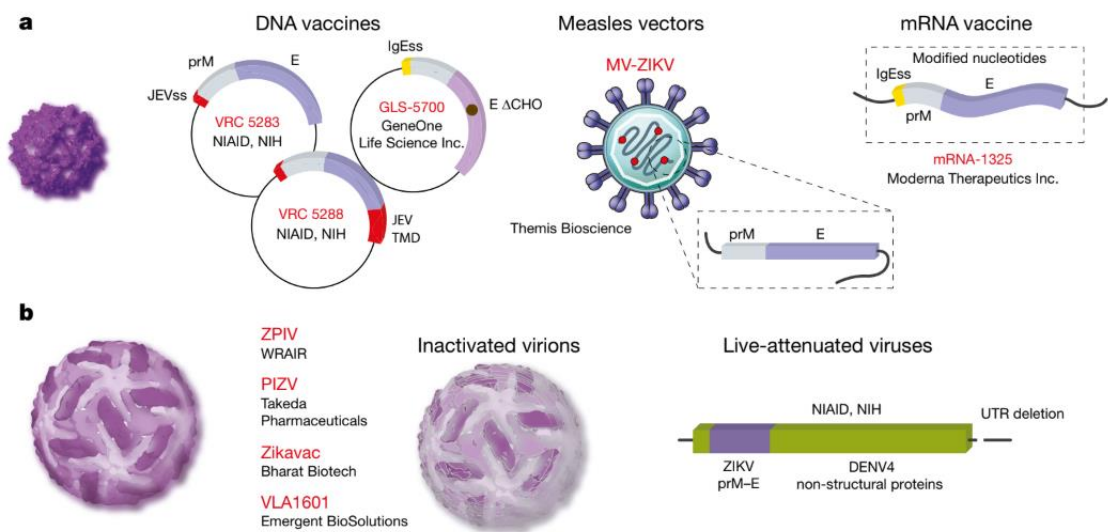


Figure 17: Zika virus vaccine platforms in clinical studies

(a) Flavivirus prM-E proteins form non-infectious subviral particles that share functional and antigenic features with infectious virions. Multiple ZIKV vaccine platforms that encode prM-E proteins have been evaluated in humans. DNA vaccines GLS-5700 (NCT02809443), VRC-5288 (NCT02840487) and VRC 5283 (NCT02996461) differ with respect to ZIKV strain and signal sequence preceding prM. The C terminus of VRC5288 is a chimaera of JEV. Nucleoside-modified mRNAs (mRNA-1325) and a measles vector (MV-ZIKV) expressing prM-E have also been evaluated (NCT03014089 and NCT02996890, respectively). (b) Vaccine candidates derived from infectious ZIKV. Four inactivated vaccine candidates are being assessed. Phase I studies of the ZPIV vaccine construct developed by WRAIR have been conducted (NCT02963909, NCT02952833 and NCT02937233). Studies of the Takeda PIZV (NCT03343626), Emergent Biosolutions VLA1601 (NCT03425149) and Bharat Biotech ZikaVac are underway. Clinical trials of a chimeric live-attenuated vaccine derived from the NIAID DENV vaccine platform are anticipated.

(Image and caption from Pierson and Diamond, 2018)

› Vaccine

Since the WHO call to action, the global research community has rapidly responded by introducing 45 candidate vaccines into the pipeline, initially evaluated in non-clinical studies. At the time of writing, most of them are in development and several have progressed beyond preclinical studies in animals. Of these, 11 entered Phase 1 human trials and 2 candidates entered Phase 2 trials. Progress in vaccine and therapeutic drug development against Zika virus were reviewed by Wilder-Smith *et al* in an article published mid-2018²²⁷.

III.4.3. Diagnosis and Detection

Diagnostic strategies for ZIKV infection have been established based on the state of knowledge concerning the kinetics of the infection (still not clearly established at this time) and adapted as knowledge has evolved. ZIKV infection is usually diagnosed during medical consultation based on symptomology. Also, as ZIKV appears to circulate in the blood for the first three to five days after onset of symptoms, this diagnostic can be ensured by rapid molecular analysis of blood sample using reverse-transcriptase polymerase chain reactions (RT-PCR). Serological tests such as enzyme linked immunosorbent assay (ELISA) based on immunoglobulin (Ig) M or IgG followed by a confirmatory ZIKV plaque reduction

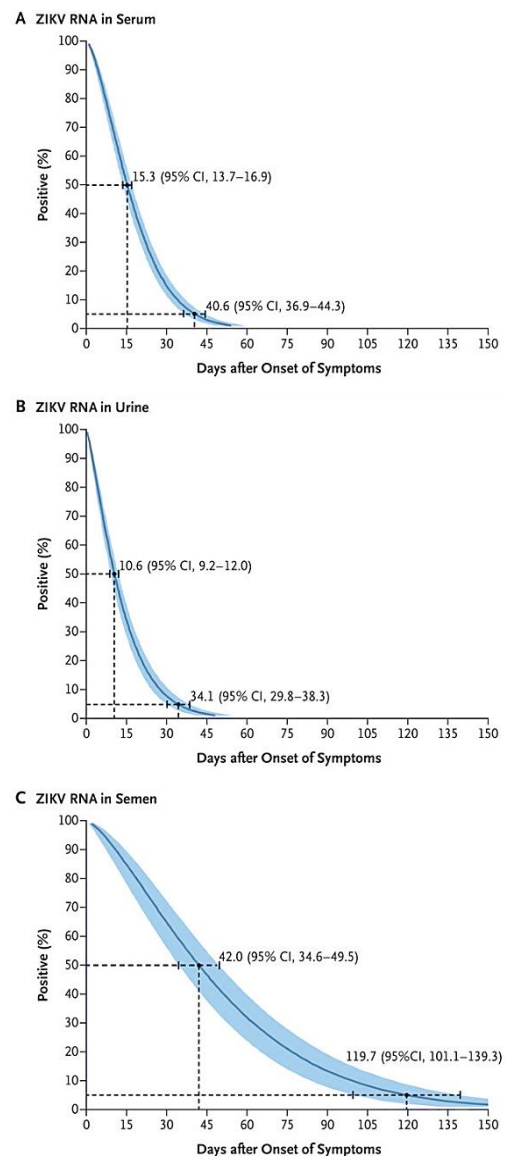


Figure 18: Time until the clearance of Zika virus RNA

Shown are models of the time until the loss of Zika virus (ZIKV) RNA detection after the onset of symptoms in serum (A), urine (B), and semen (C), as estimated with the use of Weibull regression. Also shown are medians and 95th percentiles of the time until the loss of detection, the key values that were reported in this study. Blue shading denotes 95% confidence intervals. (Image and caption from Paz-Bailey *et al.*, 2018)

neutralization test (PRNT) can also be performed²²⁸. The choice of diagnostic test depends on the onset date of clinical signs. Clinical and chronological information is therefore essential for the interpretation of assay results. However, as ZIKV is a member of the Flaviviridae family, a cross-reactivity with other flaviviruses such as Dengue, West Nile, and Yellow fever (including among vaccine recipients) can occur²²⁹. But, as IgM ELISA specificity is known to be limited, particularly during secondary flavivirus infections, a new ELISA based on ZIKV antigen has been developed to minimize cross reaction and by this way enhance the test specificity²³⁰. As well, several research teams worked hard to provide diagnostic tests that are increasingly robust, practical and even inventive. Indeed, most of the existing multiplexed diagnoses are not affordable and are not suitable for use at the point-of-care in resource-limited settings. In order to address this insufficient diagnostic capacity, a team of Californian researchers developed a smartphone-based diagnostic platform for the rapid detection of Zika, Chikungunya, and Dengue viruses²³¹.

Except in serum, ZIKV has been detected in urine and saliva, but also many other tissues. A study published at the beginning of May 2016, compared test results of ZIKV RNA detection in serum, urine and saliva from persons with travel-associated ZIKV infection²³². Results shown that 95% of urine specimens versus 56% of serum specimens collected from persons within 5 days of symptom onset were tested positive by RT-PCR. This suggested that urine (collected non-invasively) might be the preferred specimen type to identify acute Zika fever. This report was then confirmed in a final report published in 2018. Another feature of ZIKV is its detection in semen, with ZIKV RNA clearance after approximately 4 months. The prolonged presence of the virus in semen, reinforces in turn the risk for sexual transmission and could also indicate a prolonged potential risk, higher than thought.

III4.4. Complications

Although the majority of Zika infections are asymptomatic or benign, a more severe pathogenicity has been uncovered in the course of the epidemics. Presently, Zika is recognized as a neurotropic virus with a broad spectrum of complications affecting adults and newborns. Guillain-Barre Syndromes and

Table 2: Reported suspect Zika and GBS cases per location

	ZIKA CASES	GBS CASES	REFERENCE
French Polynesia	31 448	42	233
Bahia, Brazil	30 266	155	234
Salvador, Brazil	16 966	49	235
Colombia	105 027	677	233
Dominican Republic	5 241	285	233
El Salvador	11 054	184	234
Honduras	17 485	71	234
Puerto Rico	73 034	68	233
Suriname	3 097	15	234
Venezuela	32 801	684	234
Martinique	36 701	29	185,186
French Guyana	10 893	7	185,186
Guadeloupe	31 227	40	185,186

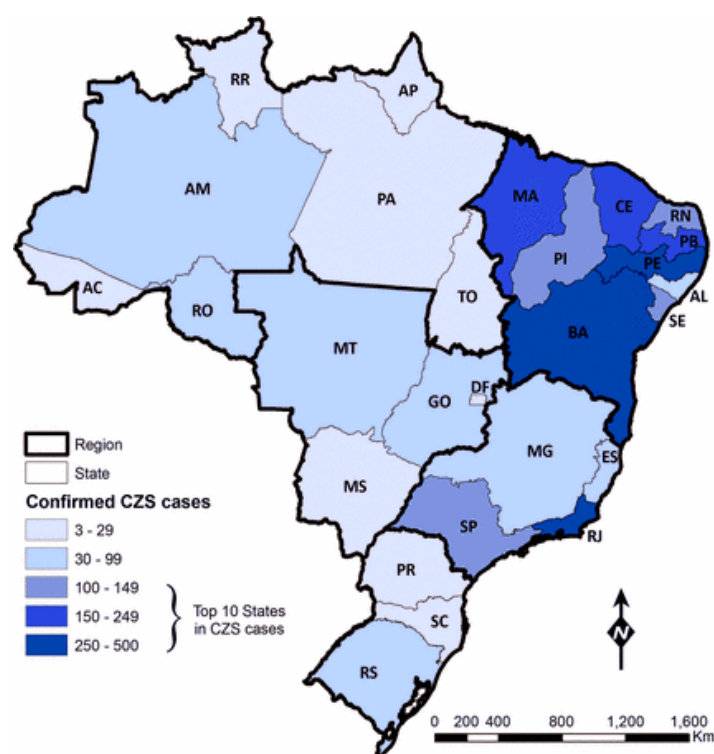


Figure 19: Congenital Zika syndrome cases in Brazil

Confirmed congenital Zika syndrome (CZS) cases from 2015 to 2018 (as of March 3, 2018), by state. States with 100 or more CZS cases ranked among the top 10. Starting from the southern portion of the map, the regional division is as follows: South—Paraná (PR), Santa Catarina (SC), and Rio Grande do Sul (RS); Southeast—Espírito Santo (ES), Minas Gerais (MG), Rio de Janeiro (RJ), and São Paulo (SP); Center-West—Goiás (GO), Mato Grosso do Sul (MS), Mato Grosso (MT), and Distrito Federal (DF); Northeast—Alagoas (AL), Bahia (BA), Ceará (CE), Maranhão (MA), Paraíba (PB), Pernambuco (PE), Piauí (PI), Rio Grande do Norte (RN), and Sergipe (SE); and North—Acre (AC), Amapá (AP), Amazonas (AM), Pará (PA), Roraima (RR), Rondônia (RO), and Tocantins (TO). (Image and caption from Castro et al., 2018)

microcephaly is among the most documented due to their historical report in 2013 and 2016 respectively.

› Autoimmune outcomes and other complications in adult

In a minority of cases, ZIKV infection can lead to serious neurological complications requiring hospitalization. In adults, Guillain-Barre syndrome is the most frequent manifestation. This autoimmune disease is a rare disorder with rapid onset characterized by peripheral nerve demyelination resulting in muscle weakness and ascending flaccid paralysis. In the majority of cases, patients undergo a full recovery after intensive care involving respiratory assistance, plasmapheresis or intravenous immunoglobulin injection. The high probability of GBS cases in epidemic periods was an additional challenge for countries affected by Zika, because health authorities had to work to ensure the equipment, supplies and hospital beds in intensive care units required to treat their populations. In adults, other non-GBS neurological complications have been reported in patients infected with Zika, including meningoencephalitis, myelitis or radiculitis. Moreover, several cases of severe and non-severe immune-mediated idiopathic thrombocytopaenia have been described in Puerto Rico and Guadeloupe. Finally, other anecdotal reports suggest an association between Zika and the development of ophthalmological (uveitis) or cardiac manifestations.

› Congenital Zika Syndrome and other birth defects

Retrospective analysis of events since ZIKV emergence provided insight into the causal association between ZIKV and adverse neurological outcomes, with the feared confirmation that microcephaly was only the tip of the iceberg. The teratogenic potential of Zika is manifested through a constellation of developmental abnormalities grouped under the term "congenital Zika syndrome" (CZS)^{236–238}. Thus, CZS include the following features (i) severe microcephaly and decreased brain tissue with a specific pattern of brain damage, including subcortical calcifications (ii) brain atrophy and asymmetry, abnormally formed or absent brain structures, including ventriculomegaly, lissencephaly, neuronal migration disorders, and hydrocephalus (iii) eye abnormalities, including macular scarring and focal pigmentary retinal mottling, congenital glaucoma, intraocular calcification, optic nerve hypoplasia (iv)

congenital contractures, such as clubfoot or arthrogryposis.

During outbreaks it was estimated that the risk of giving birth to a baby with CZV was 8 to 15%²³⁹ (up to 42% in specific areas²⁴⁰) when the mother's infection occurred during the first trimester of pregnancy. In addition to this devastating possibility for expectant mothers, Zika virus was also responsible for several cases of miscarriage.

III.5. Social Impact

Zika virus is a good example of the complex issue of emerging pathogens that healthcare systems have faced over the past 50 years. The unexpected scale of the "Zika phenomenon" has surprised the world and posed many challenges on several levels. Public health agencies and practitioners were greatly involved and will undoubtedly remain so regarding the future development of parent-support programs for children with CZS.

Like no other Flavivirus before, Zika was at the heart of scientific, ethical and societal debates. One of the most striking example concern the mothers of reproductive age who were advised against going to epidemic zone if they wished to have a child in the near future. But what about the latter living at the epicenter of the epidemic? Faced to the dramatic threat, some people tried to turn the tragedy into an opportunity for women's rights. The United Nations and other human rights advocates have encouraged the establishment of a complete health service (family planning) including expanded access to contraceptive methods, with emergency contraception and safe abortion services. These demands have created a debate between the right to abortion and the right of people with disabilities on the entire Latin American continent and beyond. While many countries in South America have a religious denomination against abortion (punishable by prison), only Colombia has granted access to this practice under the condition of a positive Zika diagnosis²⁴¹, while many others have maintained or even strengthened their position (heavier jail sentence)²⁴². Thus, since most pregnancies in these countries are unwanted, many women sought clandestine abortions or self-induced pregnancy termination, most often under unsafe conditions²⁴².

IV. UNRAVEL THE PUZZLE OF ZIKA VIRUS PATHOGENICITY

Although Zika was discovered 60 years before its emergence, it remained in scientific collections for many years - unstudied - due to its negligible impact on human health. Yet, nowadays, Zika became an unprecedented epidemiological phenomenon; raising the question of why Zika virus suddenly became pathogenic in humans?

Several epidemiological factors non-intrinsic to the virus, including the wide distribution of *Aedes* mosquitoes, favorable weather and climate, immune naïve populations and international travel, to mention a few, were undoubtedly involved in the emergence and rapid spread of Zika virus. Nevertheless, the history of Zika suggests that the virus evolved, acquiring several properties distinct from other flaviviruses, and attesting to its rapid adaptation to human host. As mentioned above, the spectrum of its pathogenicity has gradually been uncovered over the course of epidemics, posing a significant challenge for the scientific community, which worked cooperatively to reveal its facets and mechanisms. In this chapter a first insight on Zika pathogenesis will be discussed before being more extensively reviewed in the discussion section. In addition, the molecular evolution of Zika will be presented and the hypothesis of a contribution of viral molecular factors as a support for Zika pathogenicity will be introduced.

IV.1. Reminder on Viral Pathogenesis

IV1.1. Terminology and Principle of viral pathogenesis

In daily life and through media, we commonly heard about the virulence of viruses but if we all have a cloudy notion of what that might mean, define 'virulence' is not an easy task. Virulence is, in fact, a multifactorial process difficult to study in its entirety, which is much more related to the host than to the virus itself. It's the resulting of an equation comprising both the determinants of viral pathogenesis and those of the disease.

Viral pathogenesis refers to the series of events that occur during viral infection of a host. Determinants of viral pathogenesis could be classified in four

Table 3: Determinants of viral pathogenesis and diseases

VIRAL DISEASE	VIRAL PATHOGENESIS
Nature of the disease	Interaction with target tissue
Target tissue	Access to target tissue
Site of entry	Presence of receptors
Ability of virus to gain access to target tissue	Stability of virus particles in body
Viral tropism	Capacity to establish viremia
Permissivity of cells	Ability to kill cells
Strain of virus	Efficiency of viral replication in the cell
Severity of disease	Best temperature for replication
Ability to kill cells (cytopathic effect)	Cell permissivity
Immunity to virus	Cytotoxic viral protein
Intact immune response	Inhibition of macromolecular synthesis
Immunopathology	Production of viral proteins and structures
Quantity of virions inoculated	Altered cell metabolism
Duration of infection	Host response to infection
General health of the host	Intrinsic cell response
Host nutritional status	Innate and acquired immune responses
Other infections which might affect immune response	Viral immune escape mechanisms
Host genotype	Immunopathology
Age of the host	Manipulation of host immune system

categories: those linked to interaction with target tissue, to the ability to damage or kill cells, to the host response to infection and finally to the immunopathology (Table 3). However, the unique role of viral pathogenesis is insufficient to explain virulence. Indeed, many viruses can infect multiple species, and replicate in their host with noiseless or negligible effects. The cases of reservoir host and asymptomatic people make easier to understand that disease is not an obligate outcome of viral infection.

Disease is a generalized and body scale phenomenon which is in a first time driven by the duration of the infection and by the general health of the host, its nutritional status, age, level of fatigue or genetic background and more. The disease is also dependent on the virus strain, the viral tropism and on the quantity of virions inoculated. The complex interaction between virus-infected cells and host defense system determines the severity of diseases. Consequently, as susceptibility to infection and susceptibility to disease are independent, virulence refers to the capacity of infection to cause disease. It's a quantitative statement of the degree or extent of pathogenesis.

IV1.2. Pathogenic Mechanisms and determinants

Viral pathogenesis is the entire process by which an initial infection leads to a disease. Pathogenic mechanisms include (i) entry and implantation of the virus at a body site thus designated as the portal of entry, (ii) local spread and replication, (iii) dissemination within the organism and (iv) invasion of target organs or sites from which disease and shedding of the virus into the environment occur²⁴³. However, disease is not the outcome of all viral infections and most of them are abortive or subclinical highlighting the existence of factors affecting these mechanisms.

› Accessibility to target tissue

While many factors can influence the pathogenic mechanisms, the extent to which body tissues and organs are accessible to the virus is one of the most critical determinants. From the earliest step, access to a cell capable of supporting efficient amplification of the initial viral inoculum is an absolute prerequisite for any successful infection in an individual host. At a global level, accessibility is

influenced by physical and chemical barriers, by host defense mechanisms and by the distance to cover to reach target organs and tissues²⁴³. Moreover, if a virus successfully reaches an organ, infection will only occur if susceptible cells are present.

› Virulence characteristic

Disease occurrence also depends on the degree of pathogenicity of a virus, namely its virulence. The latter is partly determined by the extent and robustness of the characteristics that allow the virus to alter cell function and overcome the many barriers/inhibitory effects encountered in the host. Virulence characteristics include, for example, the ability of the virus to replicate under adverse conditions (fever, presence of interferon, etc.), in migratory cells, or to induce cell death. On the other hand, it is important to note that, even though virulence characteristics have a genetic basis, viral virulence is a relative property influenced by factors such as the dose or the inoculation route, to mention a few.

› Cellular pathogenesis

Even if successful replication occurs in a target organ, a disease outcome will only result if the infection causes injuries. Cell damage can result from the direct effects of viral replication when it damages essential cells (e. g. structural alteration, permeability, metabolism) or triggers the release of toxic substances from infected tissue, or from the consequences of the host immune responses

Table 4: Factors responsible for cell injuries

CELLULAR PATHOGENESIS

Direct injury - Cytopathic effects
Change in cell morphology
Syncytia formation
Inclusion bodies
Alteration of cell physiology and biochemistry
Diversion of cellular energy
Competition for cellular transcriptional factors
Ions movement and leaky membrane
Manipulation of cell cycle
Formation of secondary messenger
Cascade activation
Shutoff of cell macromolecular synthesis
Change in cellular transcriptional activity
Change in protein-protein interaction
Inhibition of the interferon defense mechanisms
Genotoxic effect
Indirect injury
Integration of viral genome
Induction of host genome mutation
Immunopathological lesion
Tissue damage caused by cytotoxic T lymphocytes
Inflammation
Injury mediated by Free radicals
Antibody-dependent cell-mediated cytotoxicity
Accumulation of immune complex
Antibody-dependent enhancement

(Table 4). In the latter case, we talk about immunopathological lesions.

IV.2. First insight on Zika virus Pathogenesis

Since the beginning of the epidemics, we have learned a great deal about Zika and its etiology. Many studies were conducted, based on cell line or animal models, in order to understand Zika pathogenicity. The knowledge we gained is that the epidemic strains of the virus display a broad tropism and persistence in body fluids and tissues, including those that are ordinarily protected by substantial anatomical barriers. This unexpected potential contributes to the clinical and epidemiological manifestations that have recently been observed, including severe complications caused by ZIKV and its rapid spread. In the following sections, a first insight on the molecular aspects of ZIKV–host interactions, including host target cells, cell surface receptors for viral entry and host cellular and immune responses to ZIKV replications will be discussed.

IV2.1. Target cells and tissues

› The skin

As an arbovirus, Zika virus is mainly acquired through the skin via the bite of an infected mosquito. Once disseminated throughout the epidermis and dermis, the virus has the potential to target several cell types including epidermal keratinocytes, primary dermal fibroblasts and immature dendritic cells which are permissive to ZIKV infection. Human skin, at the site of bite, is therefore the primary replication site of Zika. When infection is initiated in a cell of the vascularized dermis, the virus easily spread to nearby blood and lymphatic vessels, causing viremia and spread to peripheral tissues and organs. A successful implantation at the portal of entry and the establishment of a systemic infection is promoted by the salivary cocktail injected by mosquitoes,

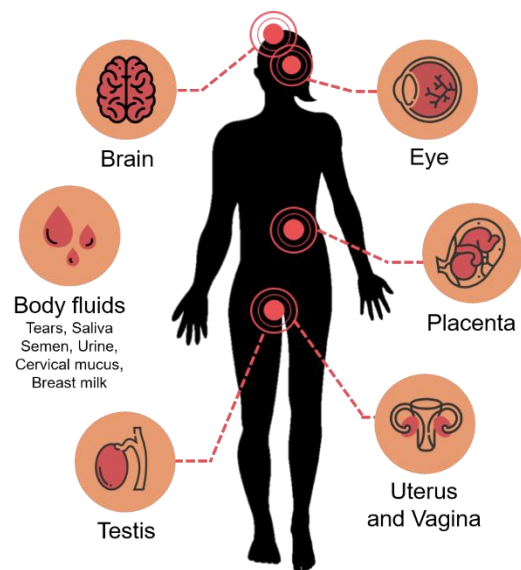


Figure 20: Zika virus tropism

Table 5: Zika virus cellular targets and receptors

PRIMARY CELLS	RECEPTOR	REFERENCE
Brain		
Neural progenitor cells (NPCs)	AXL	244–246
Astroglial cells	AXL	247–250
Microglial cells	AXL	247
Placenta		
Hofbauer cells	AXL, Tyro3, TIM-1	251–253
Trophoblasts	AXL, Tyro3, TIM-1	251–253
Endothelial cells	AXL, Tyro3, TIM-1	253,254
Skin		
Dermal fibroblasts	AXL, Tyro3, TIM-1	255,256
Epidermal keratinocytes	AXL, Tyro3, TIM-1	255
Immune cells		
Immature dendritic cells	DC-SIGN	255,257
Dendritic cells	DC-SIGN	258,259
Plasmacytoid dendritic cells	Unknown	Unpublished data
CD14+ monocytes	Unknown	260–262
CD14+CD16+ monocytes	Unknown	261
Testis		
Sertoli cells	AXL	263–265
Spermatozoa	Tyro3	266,267
Kidney		
Renal mesangial cells	Unknown	268
Glomerular podocytes	Unknown	268
Renal glomerular endothelial cells	Unknown	268
Retina		
Retinal pericytes	AXL, Tyro3	269,270
Retinal microvascular endothelial cells	AXL, Tyro3	269,270
Retinal epithelial cells	Unknown	271
Other		
Osteoblasts	Unknown	272
Oocytes	Unknown	273
Cardiomyocytes	Unknown	274

Table 6: Human cell lines permissive to Zika virus infection

	TISSUE	CELL TYPE	REFERENCE
IMR-32	Brain	Neuroblasts	275
SK-N-SH	Brain/Bone marrow	Neuroblastoma cells	276,277
SH-SY5Y	Brain/Bone marrow	Neuroblastoma cells	278
SF268	CNS	Glioma and Astrocytoma cells	279,280
SNB-19	Brain	Glioblastoma cells	281
HBMEC	Brain	Microvascular Endothelial cells	263,282
hCMEC/D3	Brain	Microvascular Endothelial cells	282,283
HUVEC	Umbilical	Vein Endothelial cells	284
A549	Lung	Epithelial cells	278,285
HFF-1	Skin/Foreskin	Fibroblast	255
Huh-7	Liver	Differentiated Hepatocyte	280,286
HOBIT	Bone	Osteoblast-like cells	287
HPS-19I	Prostate	Stromal cells	288
LNCaP	Prostate	Epithelial cells	288
Tcam-2	Testis	Seminoma cells	289
SEM-1	Testis	Seminoma cells	277
Hs1.Tes	Testis	Fibroblast	277

which enhances the infectivity of the virus, triggers inflammation and alters the local immune response^{290,291}. In blood, the virus is thought to be associated with cells, since viral load and persistence are higher in whole blood than in serum and plasma^{292,293}.

› Urogenital tract

Zika virus can also be transmitted through sexual contacts. This transmission route underlines the ability of the virus to replicate in the urogenital tract, despite the mucus and the low pH that protects it. On the other hand, this is the reflect of a viral shedding via both seminal fluid and vaginal secretions, since male-to-female and female-to-male transmissions are possible. Human cells of the reproductive system, including vaginal epithelial cells, Sertoli cells, spermatogonia, as well as gametes, were all shown permissive for Zika. Interestingly, several renal cell lines, appears to be highly permissive to ZIKV infection. However, kidney has not yet been documented to be a target organ of Zika.

› Placenta

The human placenta is the largest of fetal organs. It has a protective role for the fetus, by forming a selectively-permeable barrier (the trophoblastic barrier) between the maternal and fetal circulations. However, some viruses, including Zika, are able to cross this barrier which then has a permissive function for their transmission to the fetus. Zika virus shows an unusual affinity for the cells at the maternal-fetal interface. Several specific placenta cells have been found to be prone to ZIKV infection, including undifferentiated cytotrophoblasts, placental endothelial cells, and fetal macrophages present in the intervillous space called Hofbauer cells²⁹⁴. The latter have direct access to the blood vessels of the fetus, confirming the important role of the placenta in transmitting ZIKV from blood to the fetal brain. Furthermore, it seems that ZIKV infection induces the proliferation of Hofbauer cells, as suggested by the analysis of placentas from pregnancies complicated by ZIKV infection²⁹⁵.

› Nervous system

In the embryonic brain, ZIKV primarily infects neuronal progenitor cells (NPC). However, if neuronal lineage is a factor in susceptibility, a recent study suggests a differential cellular tropism even within the NPC population²⁹⁶. According to this, Zika seems specifically target glutamatergic neuronal precursors, which will later differentiate into the principal neurons of the cerebral cortex. Zika also infects astrocytes, oligodendrocyte precursor cells, microglia, and to lesser extent neurons. Although Zika neurotropism is mainly concentrated in the central nervous system, the peripheral nervous system has recently been shown susceptible to the infection as well. Studies based on cell lines and murine dorsal root ganglia explant demonstrated that ZIKV replication is cytopathic in peripheral neurons and myelinating Schwann cells, resulting in myelin disruption. These recent results provide an early insight into how ZIKV could cause acute peripheral neuropathies in adults, such as GBS.

IV2.2. Attachment factors and Entry Receptors

Flaviviruses mainly enter host-cells by clathrin-dependent endocytosis, which is initiated when viral particles interact with cell surface receptors. Once bound, the cell surface receptors direct the infectious viral to the endocytic pathway. The

processes of receptor recognition and binding are likely to involve different molecules, which, in combination, allow the virus to enter a host-cell^{297,298}. In doing so, the contact of several attachment factors enhances avidity, and thus strengthens the binding of the viral particle. Attachment factors trap the viral particles on the cell surface until they interact with an entry receptor that generally mediates their internalization²⁹⁸.

Several cell surface receptors facilitate ZIKV entry (Table 5), including the tyrosine-protein kinase receptor AXL, Tyro3, DC-SIGN, and TIM-1^{255,257}. AXL and Tyro3 are part of the TAM receptor tyrosine kinase family that normally binds to Gas6 and Pros1 ligands. These receptors are known to regulate a variety of cellular functions including cell adhesion, migration, proliferation, and survival, as well as the release of inflammatory cytokines, which play pivotal roles in innate immunity²⁹⁹. DC-SIGN is an innate immune receptor present on the surface of both macrophages and dendritic cells (DCs). It recognizes a broad range of pathogen-derived ligands and mediates antigen uptake and signaling³⁰⁰. The TIM-1 receptor, also known as HAVcr-1 (Hepatitis A virus cellular receptor 1), plays an important role in host response to viral infection.

Involvement of AXL, Tyro3, DC-SIGN, and, to a lesser extent, TIM-1 was initially described by Hamel *et al.* when they studied ZIKV entry into skin cells²⁵⁵. AXL was subsequently shown to be a prime target receptor for ZIKV viral entry in a variety of cell types including human endothelial cells³⁰¹, neural stem cells²⁴⁴, microglia and astrocytes²⁴⁷, and oligodendrocyte precursor cells³⁰². Examination of the AXL expression levels of diverse cell types suggests that AXL is highly expressed on the surface of human radial glial cells, astrocytes, human endothelial cells, oligodendrocyte precursor cells, and microglia in the developing human cortex as well as in progenitor cells of the developing retina^{244,302}. Other ZIKV permissive and non-neuronal human cell types, which are known to express AXL, Tyro3, and/or TIM1 and likely to mediate viral entry, include placental cells, explants-cytotrophoblasts, endothelial cells, fibroblasts, and Hofbauer cells in chorionic villi as well as amniotic epithelial cells and trophoblast progenitors in amniochorionic membranes²⁵³.

The susceptibility of human endothelial cells to ZIKV positively correlates with

the cell surface levels of AXL³⁰¹. Gain- and loss-of-function tests revealed that AXL is required for ZIKV entry at a post-binding step, and small-molecule inhibitors of the AXL kinase significantly reduced ZIKV infection of human endothelial cells³⁰¹. In human microglia and astrocytes of the developing brain, like DENV, AXL-mediated ZIKV entry requires the AXL ligand Gas6 to serve as a bridge linking ZIKV particles to glial cells²⁴⁷. Following binding, ZIKV is internalized through clathrin-mediated endocytosis and is transported to Rab5+ endosomes to establish productive infection. Downregulation of AXL by an AXL inhibitor R428 or an AXL decoy receptor MYD1 significantly reduced but did not abolish the ZIKV infection, suggesting the AXL receptor might be the primary but not the only receptor that is required for ZIKV infection²⁴⁷.

Furthermore, it is worth noting that the elimination of any known entry receptor does not result in complete protection against viral infection, as flaviviruses have the capacity to switch to many receptors or entry routes that offer other alternatives. This way, genetic ablation of the AXL receptor by CRISPR-cas9 did not protect human NPCs and cerebral organoids from ZIKV Infection²⁴⁵. In particular, genetic ablation of AXL has no effect on ZIKV entry or ZIKV-mediated cell death in human induced pluripotent stem cell (iPSC)-derived NPCs or cerebral organoids. It is not yet clear what contributes to the observed discrepancy between this and other studies. One possibility is that ZIKV may use different cell surface receptors on iPSC-derived NPCs²⁴⁵ or even entry route. For example, TIM-1 plays a more prominent role than AXL in placental cells²⁵³. Duramycin, a peptide which binds phosphatidylethanolamine in enveloped viral particles and precludes TIM1 binding, reduced ZIKV infection in placental cells and explants. In a mouse study, comparison of homozygous or heterozygous AXL knock-out showed no significant differences in ZIKV viral replication and clinical manifestation, suggesting AXL is dispensable for ZIKV infection in those mice²⁴⁶. Interestingly, a further study demonstrated that the presence of AXL attenuates ZIKV-induced activation of type I IFN signaling genes in human astrocytes via the regulation of SOCS1 expression. Based on their results, the authors suggested that AXL not only serve as an entry receptor, but rather promote ZIKV infection²⁵⁰.

IV2.3. Host responses to Zika virus infection

› Cellular and Immune responses

Inflammation is a first-line defense response of the cellular immune system to viral infection, usually triggered by the release of cytokines, including chemokines. ZIKV triggers various host-cell pro-inflammatory responses^{255,257,285,303}. For example, ZIKV stimulates CD8⁺ T cell-mediated polyfunctional immune responses to induce NF- κ B-mediated production of cytokines such as IL-1 β , IL-6, MIP1 α , as well as chemokines including IP10 and RANTES^{249,303}. In mice, ZIKV-induced T cell immune responses have been proven antiviral by the injection of infected-mice CD8⁺ isolates to naive mice prior to ZIKV infection which led to enhanced viral clearance. Conversely, depletion of CD8⁺ T cells from infected animals compromised viral clearance²⁵⁷. ZIKV structural proteins (C, prM, and E) are the major targets of CD8⁺ T cell and CD4⁺ T cell responses³⁰⁴.

Aside from ZIKV-mediated inflammatory and humoral responses, ZIKV also triggers a series of host-cell innate immune responses, which are crucial for the recognition of viral invasion, activation of antiviral responses and determination of the fate of viral infected cells. Primed by the pathogen-associated molecular pattern (PAMP) of different viruses, host-cells recognize the invading virus by activating different type of pattern recognition receptors (PRRs), which could be cell surface receptors or endosomal receptors. For example, ZIKV is recognized by an endosomal TLR3, a PRR that specifically recognizes dsRNA virus^{255,257,305}. TLR3 belongs to a class of endosomal receptors that can be found in first line of defense cells such as macrophages or Langerhans cells. TLR3 activation plays a key role in host-cell innate immune responses to viral infection. Consistent with the innate immune responses to dsRNA virus, ZIKV-induced TLR3 activation promotes phosphorylation of interferon regulatory factor 3 (IRF3) by TBK1 kinase, leading to induction of type 1 IFN signaling pathways^{257,306}. This initiates a cascade that further activates cytoplasmic RIG-I-like receptors (RLRs) responses, subsequently inducing transcription of RIG-I, MDA5, and several type I and III IFN-stimulated genes including OAS2, ISG15, and MX1²⁵⁵. Activation of the type I IFN signaling pathway results in production and secretion of IFN- β .

Table 7: Cellular antiviral responses against Zika virus infection

CELLULAR RESPONSE	PROTEIN INVOLVED	MOLECULAR ACTION AND CONSEQUENCES	REFERENCE
Pro-inflammatory CD8+ T-cell immune response	IL-1 β , IL-6 MIP1 α IP-10, RANTES	T-cell mediated polyfunctional immune response with release of antiviral cytokines and chemokines	257,303,307,308
CD14+ monocytes and macrophages immune responses	CXCL9, CXCL10, CXCL11, CCL5, IL-15	CD14+ monocytes prime NK cells activities during ZIKV infection	262
Humoral immune response	IgM, IgG	Production of neutralizing and protective antibodies against ZIKV	309,310
TLR3-mediated response	TLR3, TBK1, IRF3, type I IFN	Recognition of ZIKV dsRNA leading to the activation of type I IFN	255,257,305
RIG-1/MDA5-mediated response	RIG-1, MDA5, IRF3, NF κ B, type I IFN	Late response triggered by ZIKV dsRNA which contribute to the of type I IFN	255,257,311
Type I and type III interferon activation	OAS2, ISG15, MX1	Production of IFN β as part of cellular antiviral-response. IFN λ 1 produced by human placental trophoblasts protects against ZIKV	251,255

Secreted IFN- β binding to IFN- β receptor activates JAK1 and Tyk2 kinases that in turn phosphorylate STAT1 and STAT2. Upon ZIKV infection, association of the phosphorylated STAT1/STAT2 heterodimer with IRF9 promotes ISRE3-mediated transcription of antiviral interferon stimulated genes (ISGs)²⁵⁷. One of the ISGs proteins, viperin (virus-inhibitory protein, endoplasmic reticulum-associated, IFN-inducible), shows strong antiviral activity against ZIKV³¹². Specifically, it restricts ZIKV viral replication by targeting the NS3 protein for proteasomal degradation³¹³. Therefore, the production of TLR3- and RIG-1/MDA5-mediated type I IFN production and subsequent activation of the JAK/STAT innate immune pathway confer increased resistance to ZIKV infection³¹⁴.

ZIKV is a membrane-associated virus that utilizes host ER for its replication and morphogenesis along the cellular secretory pathway. Through those cellular membrane interactions, ZIKV can trigger autophagy in a cell-dependent manner. This cellular process is normally involved in removal of aggregated or

erroneously folded proteins through lysosomal degradation. Activation of cellular autophagy is a hallmark of flavivirus infection, which was thought to be part of the host innate immune response to eliminate invading intracellular pathogens^{315–318}. Because autophagy activation could halt cellular growth and trigger apoptosis, ZIKV-induced autophagy was implicated in the ZIKV-mediated microcephaly^{317–319}. Activation of autophagy elicits antiviral activities by removing viral proteins through reticulophagy, a selective form of autophagy that leads to ER degradation, or inclusion of viral proteins in autophagosomes destined for lysosomal degradation³²⁰. The ER-localized reticulophagy receptor FAM134B serves as a host-cell restriction factor to ZIKV and other flaviviruses³²¹. However, ZIKV-induced autophagy could be a double edged sword, which shows activities of both pro- and anti-ZIKV infection³²⁰. Activation of cellular autophagy counteracts ZIKV infection by actively removing viral proteins. As part of the host-cell antiviral responses, type I IFN signaling also limits ZIKV replication by promoting autophagic destruction of the viral NS2B/NS3 protease in a STAT1-dependent manner³²². Conversely, ZIKV takes advantage of autophagosome formation, whose presence was associated with enhanced viral replication²⁵⁵. ZIKV activates autophagy through the cellular mTOR stress pathway that connects oxidative stress and reactive oxygen species (ROS) production. This virus host interaction appears to be highly conserved as, in human fetal neural stem cells, ZIKV triggers autophagy through inhibition of the mammalian mTOR pathway via AKT³¹⁷. Altogether, ZIKV infection elicits RIG-1/MDA5- and TLR3-mediated innate immune responses leading to releases of type I and type III IFNs to protect cells from viral invasion. ZIKV concurrently triggers cellular activation of the stress TOR signaling pathway that induces autophagy. The balance between pro- and anti-ZIKV activities of autophagy, at least in some cells, determines whether infected cells are protected through viral elimination, or destined to apoptosis as the result of viral propagation in host-cells.

› Preexisting anti-flavivirus immunity

Process analogous to antibody-dependent enhancement (ADE) during secondary DENV exposure, may also contribute to the acquired ZIKV virulence³²³. This scenario could occur if individuals have previously been exposed to, or vaccinate

against other flaviviruses and have acquired antibodies that cross-react with ZIKV. Instead of neutralizing, pre-existing cross-reactive antibodies can paradoxically induce viral uptake and infection of Fc gamma receptor-bearing cells. This phenomenon could result in enhanced ZIKV infection, both clinically and immunologically³²³, notably with antibodies targeted to the E protein. As a matter of fact, the opposite scenario has been observed in which pre-exposure of ZIKV was associated with enhanced DENV infection *in vitro*³²⁴ and in monkeys³²⁵. Therefore, enhanced ZIKV infection as the result of prior exposure of other flavivirus could in turn be possible too^{326–329}.

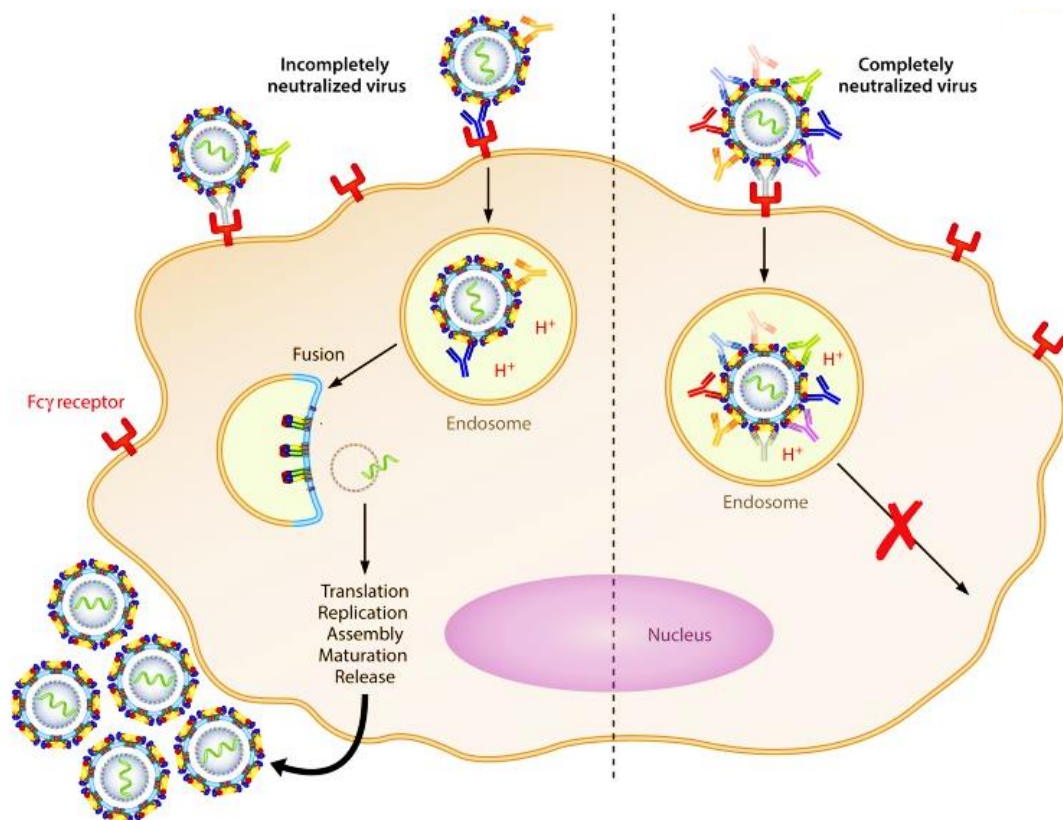


Figure 21: Schematic diagram of extrinsic antibody-dependent enhancement of infection

(Left) Virus-antibody complexes are internalized through Fcγ receptor-mediated endocytosis. Because of incomplete neutralization, the virus can fuse in the endosome and initiate virus production. (Right) Immune complexes containing completely neutralized virus can also be taken up through Fcγ receptor interactions but fail to fuse in the endosome and therefore do not lead to the production of progeny virus. (Image and caption from Heinz and Stiasny., 2017)

Considering DENV endemicity in ZIKV areas, several studies addressed the possibility of exacerbated disease severity due to subsequent infection with a heterologous flavivirus. *In vitro* studies based on isolated human monoclonal antibodies from donors infected with WNV or DENV, as well as recipients of DENV vaccine, reported ADE in human primary monocytes, macrophages and placental tissue explants^{326–328,330,331}. However, while *in vitro* experiments argue in favor of such a phenomenon, the absence of complete humoral response is a major limitation of this approach, since *in vivo* antibodies can interact with immune system components to increase or remove ADE effect. Furthermore, to the best of our knowledge, no evidence of increased ZIKV infection due to previous exposure to DENV has been found in either non-human primates or humans^{332–334}. However, these studies demonstrated that DENV immunity can modulate the immune response, leading to a stronger and faster response to ZIKV, thus providing evidence of a biological outcome.

IV.3. Viral molecular factors involved in Zika virus pathogenesis

Despite its discovery in 1947, it was not until 2007 that Zika virus was recognized as pathogenic to humans. Yet, according to seroprevalence surveys, ZIKV was circulating in Africa and Southeast Asia long before its emergence. In the recent years, the sudden increase in the incidence of symptomatic Zika infection, with possible neurological manifestation that have never been previously observed in endemic area, suggest a modification of ZIKV virulence factors. Additionally, Zika outbreaks and severe complications were reported in several countries from different geographical areas, demonstrating that the virus overcame the populational and environmental factors.

Thanks to the colossal research activity carried out by the scientific community in response to the Zika virus pandemic, numerous viral strains were isolated and sequenced. Currently, more than 400 complete genome sequences are available in GenBank, including epidemic and pre-epidemic Zika virus strains from many countries. The opportunity to analyze a significant number of strains, combined with seroprevalence data, allowed the study of Zika virus evolution and trajectory. Surprisingly, Zika virus strains have a high homology rate, above 85%, even between the most distant ancestral and epidemic isolates. This high

percentage of identity further reinforces the hypothesis that critical divergence events and genetic change have shaped the epidemiology and the biology of Zika virus.

From Zika phylogeny to genetic changes, the molecular features of ancestral and epidemic Zika virus strains will be reviewed in this last introduction section in order to determine what kind of virological changes could have taken place to result in increased viral pathogenicity.

IV3.1. Molecular epidemiology

Zika virus diverged into two lineages, clustering the strains according to their geographical origin either from Africa or from Asia. The African lineage can be sub-divided into two subclades: East African (prototype Uganda strain) and West African (Senegal strains), which group more closely with each other than with the Asian lineage.

According to Faye *et al*³³⁵, Zika virus appeared in East Africa (Uganda) in the 1920s, and subsequently moved to West Africa as a result of at least two introduction events. On the African continent, the virus was mainly maintained in a sylvatic cycle, involving indigenous mosquitoes and monkeys but evidence of Zika infection in humans were found in 29 countries³³⁶. Nevertheless, the African lineage has only been associated with very few human infection cases. The Asian lineage, which probably emerged in the 1940s following ZIKV introduction from East Africa to Southeast Asia, include all epidemic ZIKV strains since 2007^{335,337}. The first introduction of Zika into Asia most likely occurred in the Malaysia-Indonesia region, where the virus mainly circulated between *Ae. aegypti* and humans without recognition³³⁸. During the following decades, ZIKV disseminated to Southeast Asia causing sub-clinical infection, while evolving and adapting to its vector. Human infections were not reported until 1977, in Indonesia, when Zika was suspected to cause a micro-outbreak of fever in Central Java¹⁶⁹. From a molecular point of view, the African lineage and the pre-epidemic strains of the Asian lineage (referred to afterward as ancestral Asian strains) diverge by several amino acid substitutions located throughout the genome, with the exception of the sequence encoding the viral protein NS4A. In particular, structural proteins harbor significant mutations, which probably affected the

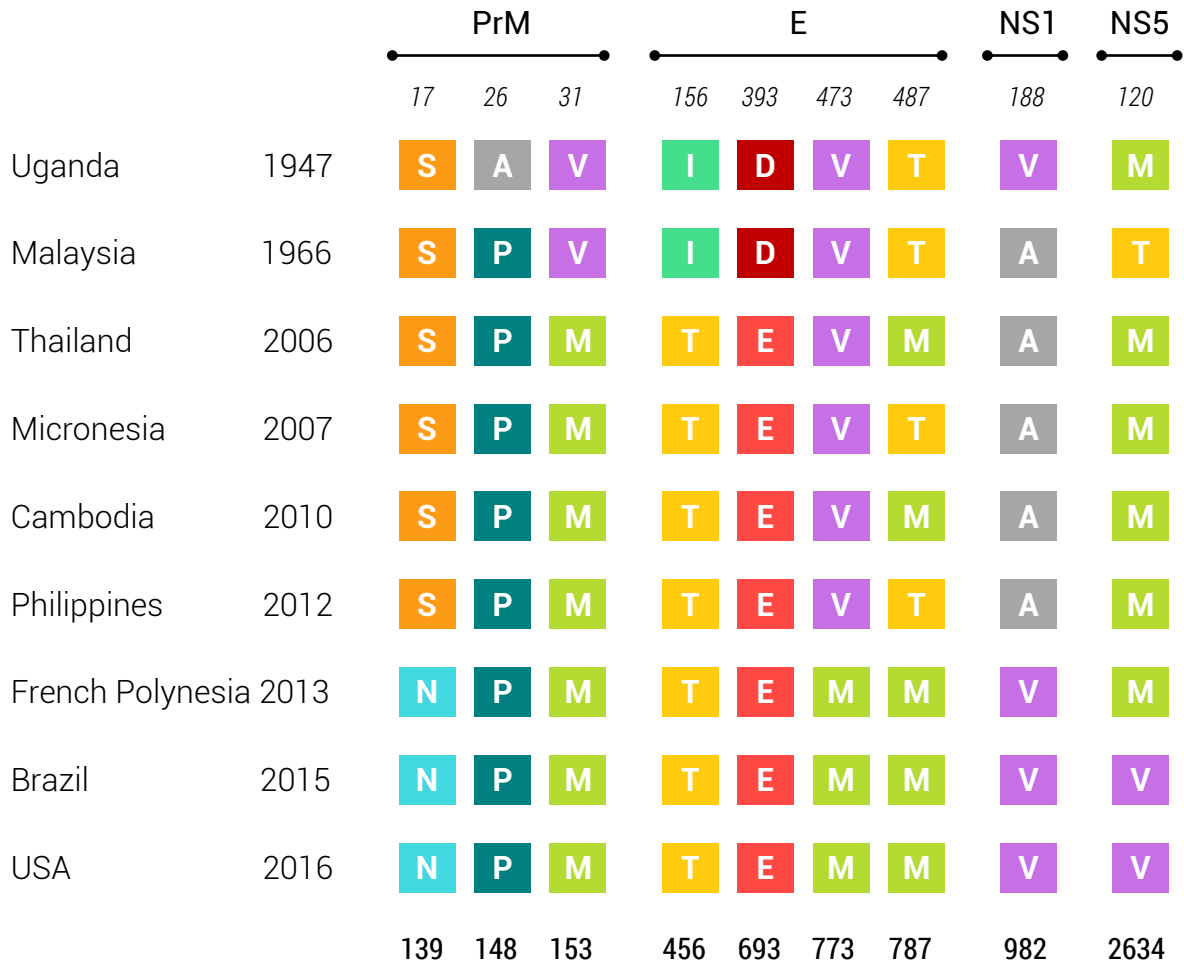


Figure 22: Notable amino acid changes since ZIKV discovery

The italic numbers refer to the substitution position regarding the first nucleotide of the indicated protein while the bold numbers, under the graph, refer to the substitution position regarding the first whole genome nucleotide.

structure and morphogenesis of the virion. Interestingly, a series of amino acid substitutions (I110V, K143E, A148P, H157Y and V158I) characteristic of the prM sequence of the Asian lineage, induced a significant conformational change. The biological impact resulting from this dramatic structural change was addressed during my doctoral research.

Between 1966 (Malaysia strain) and the late 2000s, a new variant appeared in Southeast Asia, with a fifth mutation in prM (V153M) and a remarkable amino acid change at position 693 (D693E) in the domain III of the E protein³³⁹. The latter induced a modification of the viral receptor sequence from VGD, found in the African and ancestral Asian strain, to VGE. These amino acid changes have been conserved in all epidemic ZIKV strains and have probably significantly affected virus-receptor binding and infectivity in humans. In addition, all epidemic ZIKV strains contain an N-linked glycosylation site within the E protein. This motif (153VN~~DT~~156) is absent in African strains as well as in the Malaysian strain, which instead possess an isoleucine in position 156. The emergence of this unique E-glycosylation site over the course of ZIKV evolution is controversial owing to the viral culture methods used in the past that could have suppress it. Nonetheless, this putative mutation was considered by several research teams, including ourselves, for its potential impact on the contemporary ZIKV strains pathogenicity and epidemiological fitness.

Since the 2000s, ZIKV diversified in Southeast Asia where several strains circulated, particularly in Thailand, which apparently experienced multiple introductions³³⁸. These contemporary strains can be subdivided into different genotypes according to the amino acid found at positions 139 (prM), 982 (NS1) and 2634 (NS5) from the start codon of the genome³⁴⁰. According to Liu *et al*³⁴⁰, the SAM variant was transmitted to the Yap Islands of Micronesia, where it was responsible for the first Zika fever outbreak in 2007. Subsequently, the SAM variant diverged again into SVM (982V present in African strains) but in Southeast Asia from where it was imported into the Pacific before the second epidemic. There, it gave rise to the NVM variant which caused the French Polynesia outbreak, spread to the American continent and further diverged into the NVV variant involved in the Western Hemisphere outbreaks. Furthermore, the ZIKV E protein coding sequence underwent two additional mutations over

the elapsed 6 years between the Micronesia and French Polynesia outbreaks³³⁸. These amino acid substitutions were then conserved among epidemic strains since 2013. Interestingly, they are located in transmembrane domains 1 (V763M) and 2 (T777M), and thereby have the potential to affect virion assembly and stability, which could have enhanced ZIKV pathogenicity^{339,341}.

IV3.2. Objective of the Doctoral Research

ZIKV genetic plasticity is undoubtedly at the root of its ability to replicate in multiple vector species and spread among humans. As previously mentioned, this led to the emergence of new viral strains with probable enhanced epidemiological fitness, which were responsible of the recent outbreaks. Concurrently, the shift towards urban transmission cycle, in areas where human is the sole reservoir, compelled the selection of new variants harboring mutations that confer a better adaptation to human host defenses. According to this, molecular viral changes are likely to be involved in the recent pathogenicity of Zika virus in humans.

During my doctoral research I worked, in a collective effort with other researchers, to determine whether the scope of the current epidemic was partly facilitated by viral factors which improved Zika fitness. In particular, the studies conducted aimed to understand if (i) ancestral and epidemic ZIKV strains display the same properties and, (ii) if not, which ZIKV protein(s) supports this divergence and how it would be responsible for the enhanced viral pathogenicity.

REFERENCE

1. Zimmer, C. A Planet of Viruses. (University of Chicago Press, 2012).
2. Institute of Medicine (US) Committee on Emerging Microbial Threats to Health in the 21st Century. Microbial Threats to Health: Emergence, Detection, and Response. (National Academies Press (US), 2003).
3. Martínez, J. L. & Baquero, F. Emergence and spread of antibiotic resistance: setting a parameter space. *Ups. J. Med. Sci.* 119, 68–77 (2014).
4. Benarroch, D., Claverie, J.-M., Raoult, D. & Shuman, S. Characterization of mimivirus DNA topoisomerase IB suggests horizontal gene transfer between eukaryal viruses and bacteria. *J. Virol.* 80, 314–321 (2006).
5. Duffy, S. Why are RNA virus mutation rates so damn high? *PLOS Biol.* 16, e3000003 (2018).
6. Sanjuán, R., Nebot, M. R., Chirico, N., Mansky, L. M. & Belshaw, R. Viral Mutation Rates. *J. Virol.* 84, 9733–9748 (2010).
7. Vignuzzi, M. & Andino, R. Closing the gap: the challenges in converging theoretical, computational, experimental and real-life studies in virus evolution. *Curr. Opin. Virol.* 2, 515–518 (2012).
8. Vignuzzi, M., Stone, J. K., Arnold, J. J., Cameron, C. E. & Andino, R. Quasispecies diversity determines pathogenesis through cooperative interactions in a viral population. *Nature* 439, 344–348 (2006).
9. Schmid-Hempel, P. Parasite immune evasion: a momentous molecular war. *Trends Ecol. Evol.* 23, 318–326 (2008).
10. Ernst, J. D. Antigenic Variation and Immune Escape in the MTBC. *Adv. Exp. Med. Biol.* 1019, 171–190 (2017).
11. Bos, S., Gadea, G. & Despres, P. Dengue: a growing threat requiring vaccine development for disease prevention. *Pathog. Glob. Health* 0, 1–12 (2018).
12. Global Cancer Observatory. Available at: <http://gco.iarc.fr/>. (Accessed: 13th December 2018)
13. WHO | HIV. WHO Available at: <http://www.who.int/hiv/en/>. (Accessed: 13th December 2018)
14. Seyedmousavi, S., Lionakis, M. S., Parta, M., Peterson, S. W. & Kwon-Chung, K. J. Emerging Aspergillus Species Almost Exclusively Associated With Primary Immunodeficiencies. *Open Forum Infect. Dis.* 5, (2018).
15. Weatherall, D. J. Host genetics and infectious disease. *Parasitology* 112 Suppl, S23-29 (1996).
16. Lowen, A. C. & Steel, J. Roles of humidity and temperature in shaping influenza seasonality. *J. Virol.* 88, 7692–7695 (2014).
17. Vector-borne diseases. Available at: <https://www.who.int/news-room/fact-sheets/detail/vector-borne-diseases>. (Accessed: 14th December 2018)
18. Jones, K. E. et al. Global trends in emerging infectious diseases. *Nature* 451, 990–993 (2008).
19. McMichael, C. Climate change-related migration and infectious disease. *Virulence* 6, 548–553 (2015).
20. McMichael, A. J., Woodruff, R. E. & Hales, S. Climate change and human health: present and future risks. *Lancet Lond. Engl.* 367, 859–869 (2006).
21. Nichol, S. T. et al. Genetic identification of a hantavirus associated with an outbreak of acute respiratory illness. *Science* 262, 914–917 (1993).
22. Yates, T. L. et al. The Ecology and Evolutionary History of an Emergent Disease: Hantavirus Pulmonary Syndrome Evidence from two El Niño episodes in the American Southwest suggests that El Niño-driven precipitation, the initial catalyst of a trophic cascade that results in a delayed density-dependent rodent response, is sufficient to predict heightened risk for human contraction of hantavirus pulmonary syndrome. *BioScience* 52, 989–998 (2002).
23. Childs, J. E. et al. Serologic and genetic identification of *Peromyscus maniculatus* as the primary rodent reservoir for a new hantavirus in the southwestern United States. *J. Infect. Dis.* 169, 1271–1280 (1994).
24. Sarute, N. & Ross, S. R. New World Arenavirus Biology. *Annu. Rev. Virol.* 4, 141–158 (2017).
25. Quammen, D. Spillover: Animal Infections and the Next Human Pandemic. (W. W. Norton, 2012).
26. Barbour, A. G. & Fish, D. The biological and social phenomenon of Lyme disease. *Science* 260, 1610–1616 (1993).
27. Ostfeld, R. S. & Keesing, F. Biodiversity and Disease Risk: the Case of Lyme Disease. *Conserv. Biol.* 14, 722–728 (2000).
28. Sang, R. et al. Effects of Irrigation and Rainfall on the Population Dynamics of Rift Valley Fever and Other

- Arbovirus Mosquito Vectors in the Epidemic-Prone Tana River County, Kenya. *J. Med. Entomol.* 54, 460–470 (2017).
29. Leite, M. G. P., Pimenta, E. C., Fujaco, M. a. G. & Eskinazi-Sant'Anna, E. M. Irrigation canals in Melo creek basin (Rio Espera and Capela Nova municipalities, Minas Gerais, Brazil): habitats to *Biomphalaria* (Gastropoda: Planorbidae) and potential spread of schistosomiasis. *Braz. J. Biol. Rev. Brasleira Biol.* 76, 638–644 (2016).
 30. Yang, Y. et al. The Three Gorges Dam: Does the Flooding Time Determine the Distribution of Schistosome-Transmitting Snails in the Middle and Lower Reaches of the Yangtze River, China? *Int. J. Environ. Res. Public. Health* 15, (2018).
 31. Field, H. et al. The natural history of Hendra and Nipah viruses. *Microbes Infect.* 3, 307–314 (2001).
 32. Barr, J. A., Smith, C., Marsh, G. A., Field, H. & Wang, L.-F. Evidence of bat origin for Menangle virus, a zoonotic paramyxovirus first isolated from diseased pigs. *J. Gen. Virol.* 93, 2590–2594 (2012).
 33. Bowden, T. R., Westenberg, M., Wang, L. F., Eaton, B. T. & Boyle, D. B. Molecular characterization of Menangle virus, a novel paramyxovirus which infects pigs, fruit bats, and humans. *Virology* 283, 358–373 (2001).
 34. Dye, C. Health and urban living. *Science* 319, 766–769 (2008).
 35. 68% of the world population projected to live in urban areas by 2050, says UN. UN DESA | United Nations Department of Economic and Social Affairs (2018). Available at: <https://www.un.org/development/desa/en/news/population/2018-revision-of-world-urbanization-prospects.html>. (Accessed: 23rd February 2019)
 36. Poverty. World Bank Available at: <http://www.worldbank.org/en/topic/poverty>. (Accessed: 18th December 2018)
 37. Nearly Half the World Lives on Less than \$5.50 a Day. World Bank Available at: <http://www.worldbank.org/en/news/press-release/2018/10/17/nearly-half-the-world-lives-on-less-than-550-a-day>. (Accessed: 18th December 2018)
 38. Alexander, K. A. et al. What Factors Might Have Led to the Emergence of Ebola in West Africa? *PLoS Negl. Trop. Dis.* 9, e0003652 (2015).
 39. Fisher-Hoch, S. P. et al. Review of cases of nosocomial Lassa fever in Nigeria: the high price of poor medical practice. *BMJ* 311, 857–859 (1995).
 40. Al Shehri, A. M. A lesson learned from Middle East respiratory syndrome (MERS) in Saudi Arabia. *Med. Teach.* 37 Suppl 1, S88-93 (2015).
 41. Braden, C. R., Dowell, S. F., Jernigan, D. B. & Hughes, J. M. Progress in global surveillance and response capacity 10 years after severe acute respiratory syndrome. *Emerg. Infect. Dis.* 19, 864–869 (2013).
 42. Reeves, W. C. Partners: serendipity in arbovirus research. *J. Vector Ecol. J. Soc. Vector Ecol.* 26, 1–6 (2001).
 43. Petersen, L. R. & Busch, M. P. Transfusion-transmitted arboviruses. *Vox Sang.* 98, 495–503 (2010).
 44. Morris, M. I., Grossi, P., Nogueira, M. L. & Azevedo, L. S. Arboviruses Recommendations for Solid-Organ Transplant Recipients and Donors. *Transplantation* 102, S42–S51 (2018).
 45. Hudopisk, N. et al. Tick-borne Encephalitis Associated with Consumption of Raw Goat Milk, Slovenia, 2012. *Emerg. Infect. Dis.* 19, 806–808 (2013).
 46. Fortuna, C. et al. Vector competence of *Aedes albopictus* for the Indian Ocean lineage (IOL) chikungunya viruses of the 2007 and 2017 outbreaks in Italy: a comparison between strains with and without the E1:A226V mutation. *Euro Surveill. Bull. Eur. Sur Mal. Transm. Eur. Commun. Dis. Bull.* 23, (2018).
 47. Vazeille, M. et al. Importance of mosquito 'quasispecies' in selecting an epidemic arthropod-borne virus. *Sci. Rep.* 6, 29564 (2016).
 48. Vega-Rua, A. et al. High efficiency of temperate *Aedes albopictus* to transmit chikungunya and dengue viruses in the Southeast of France. *PloS One* 8, e59716 (2013).
 49. Schultz, M. J. et al. Variable Inhibition of Zika Virus Replication by Different *Wolbachia* Strains in Mosquito Cell Cultures. *J. Virol.* 91, (2017).
 50. Dutra, H. L. C. et al. *Wolbachia* Blocks Currently Circulating Zika Virus Isolates in Brazilian *Aedes aegypti* Mosquitoes. *Cell Host Microbe* 19, 771–774 (2016).
 51. Marr, J. S. & Calisher, C. H. Alexander the Great and West Nile virus encephalitis. *Emerg. Infect. Dis.* 9, 1599–1603 (2003).
 52. Gubler, D. J. Dengue and Dengue Hemorrhagic Fever. *Clin. Microbiol. Rev.* 11, 480–496 (1998).
 53. Nogueira, P. The Early History of Yellow Fever. (2009).

54. Brown, J. E. et al. Human impacts have shaped historical and recent evolution in *Aedes aegypti*, the dengue and yellow fever mosquito. *Evol. Int. J. Org. Evol.* 68, 514–525 (2014).
55. Knipe, D. M. & Howley, P. *Fields Virology*. (Lippincott Williams & Wilkins, 2013).
56. Westaway, E. G. et al. *Flaviviridae*. *Intervirology* 24, 183–192 (1985).
57. Blitvich, B. J. & Firth, A. E. A Review of Flaviviruses that Have No Known Arthropod Vector. *Viruses* 9, (2017).
58. Blitvich, B. J. & Firth, A. E. Insect-specific flaviviruses: a systematic review of their discovery, host range, mode of transmission, superinfection exclusion potential and genomic organization. *Viruses* 7, 1927–1959 (2015).
59. Moureau, G. et al. New Insights into Flavivirus Evolution, Taxonomy and Biogeographic History, Extended by Analysis of Canonical and Alternative Coding Sequences. *PLoS ONE* 10, (2015).
60. Gaunt, M. W. et al. Phylogenetic relationships of flaviviruses correlate with their epidemiology, disease association and biogeography. *J. Gen. Virol.* 82, 1867–1876 (2001).
61. Gould, E. A. & Solomon, T. Pathogenic flaviviruses. *Lancet Lond. Engl.* 371, 500–509 (2008).
62. Gould, E. A., de Lamballerie, X., Zanotto, P. M. & Holmes, E. C. Origins, evolution, and vector/host coadaptations within the genus *Flavivirus*. *Adv. Virus Res.* 59, 277–314 (2003).
63. Wiley, C. A. & Chimelli, L. Human Zika and West Nile virus neurological infections: What is the difference? *Neuropathology* 37, 393–397 (2017).
64. Grard, G. et al. Genetic characterization of tick-borne flaviviruses: new insights into evolution, pathogenetic determinants and taxonomy. *Virology* 361, 80–92 (2007).
65. Randolph, S. E. Tick-borne encephalitis virus, ticks and humans: short-term and long-term dynamics. *Curr. Opin. Infect. Dis.* 21, 462–467 (2008).
66. Gritsun, T. S., Lashkevich, V. A. & Gould, E. A. Tick-borne encephalitis. *Antiviral Res.* 57, 129–146 (2003).
67. Billoir, F. et al. Phylogeny of the genus flavivirus using complete coding sequences of arthropod-borne viruses and viruses with no known vector. *J. Gen. Virol.* 81, 781–790 (2000).
68. Shope, R. E. Epidemiology of other arthropod-borne flaviviruses infecting humans. *Adv. Virus Res.* 61, 373–391 (2003).
69. Stadler, K., Allison, S. L., Schlich, J. & Heinz, F. X. Proteolytic activation of tick-borne encephalitis virus by furin. *J. Virol.* 71, 8475–8481 (1997).
70. Daffis, S. et al. 2'-O methylation of the viral mRNA cap evades host restriction by IFIT family members. *Nature* 468, 452–456 (2010).
71. Cleaves, G. R. & Dubin, D. T. Methylation status of intracellular dengue type 2 40 S RNA. *Virology* 96, 159–165 (1979).
72. Wengler, G. & Wengler, G. Terminal sequences of the genome and replicative-from RNA of the flavivirus West Nile virus: absence of poly(A) and possible role in RNA replication. *Virology* 113, 544–555 (1981).
73. Wengler, G., Wengler, G. & Gross, H. J. Studies on virus-specific nucleic acids synthesized in vertebrate and mosquito cells infected with flaviviruses. *Virology* 89, 423–437 (1978).
74. Dong, H. et al. West Nile virus methyltransferase catalyzes two methylations of the viral RNA cap through a substrate-repositioning mechanism. *J. Virol.* 82, 4295–4307 (2008).
75. Filomatori, C. V. et al. A 5' RNA element promotes dengue virus RNA synthesis on a circular genome. *Genes Dev.* 20, 2238–2249 (2006).
76. Filomatori, C. V., Iglesias, N. G., Villordo, S. M., Alvarez, D. E. & Gamarnik, A. V. RNA sequences and structures required for the recruitment and activity of the dengue virus polymerase. *J. Biol. Chem.* 286, 6929–6939 (2011).
77. Chen, C. J. et al. RNA-protein interactions: involvement of NS3, NS5, and 3' noncoding regions of Japanese encephalitis virus genomic RNA. *J. Virol.* 71, 3466–3473 (1997).
78. Cui, T. et al. Recombinant dengue virus type 1 NS3 protein exhibits specific viral RNA binding and NTPase activity regulated by the NS5 protein. *Virology* 246, 409–417 (1998).
79. Mackenzie, J. M., Khromykh, A. A., Jones, M. K. & Westaway, E. G. Subcellular localization and some biochemical properties of the flavivirus Kunjin nonstructural proteins NS2A and NS4A. *Virology* 245, 203–215 (1998).
80. Blackwell, J. L. & Brinton, M. A. Translation elongation factor-1 alpha interacts with the 3' stem-loop region of West Nile virus genomic RNA. *J. Virol.* 71, 6433–6444 (1997).

81. De Nova-Ocampo, M., Villegas-Sepúlveda, N. & del Angel, R. M. Translation elongation factor-1 α , La, and PTB interact with the 3' untranslated region of dengue 4 virus RNA. *Virology* 295, 337–347 (2002).
82. Flint, S. J., Racaniello, V. R., Rall, G. F., Skalka, A. M. & Enquist, L. W. Principles of Virology: Volume 1: Molecular Biology. (ASM Press, 2015).
83. Laureti, M., Narayanan, D., Rodriguez-Andres, J., Fazakerley, J. K. & Kedzierski, L. Flavivirus Receptors: Diversity, Identity, and Cell Entry. *Front. Immunol.* 9, (2018).
84. Dynamics of Virus-Receptor Interactions in Virus Binding, Signaling, and Endocytosis. PubMed Journals Available at: <https://ncbi-nlm-nih-gov.gate2.inist.fr/labs/articles/26043381/>. (Accessed: 25th June 2017)
85. Mendes, Y. S. et al. The Structural Dynamics of the Flavivirus Fusion Peptide–Membrane Interaction. *PLoS ONE* 7, (2012).
86. Klema, V. J., Padmanabhan, R. & Choi, K. H. Flaviviral Replication Complex: Coordination between RNA Synthesis and 5'-RNA Capping. *Viruses* 7, 4640–4656 (2015).
87. Paul, D. & Bartenschlager, R. Architecture and biogenesis of plus-strand RNA virus replication factories. *World J. Virol.* 2, 32–48 (2013).
88. Apte-Sengupta, S., Sirohi, D. & Kuhn, R. J. Coupling of Replication and Assembly in Flaviviruses. *Curr. Opin. Virol.* 0, 134–142 (2014).
89. Slonchak, A. & Khromykh, A. A. Subgenomic flaviviral RNAs: What do we know after the first decade of research. *Antiviral Res.* 159, 13–25 (2018).
90. Khromykh, A. A. & Westaway, E. G. RNA binding properties of core protein of the flavivirus Kunjin. *Arch. Virol.* 141, 685–699 (1996).
91. Pong, W.-L., Huang, Z.-S., Teoh, P.-G., Wang, C.-C. & Wu, H.-N. RNA binding property and RNA chaperone activity of dengue virus core protein and other viral RNA-interacting proteins. *FEBS Lett.* 585, 2575–2581 (2011).
92. Mackenzie, J. M. & Westaway, E. G. Assembly and maturation of the flavivirus Kunjin virus appear to occur in the rough endoplasmic reticulum and along the secretory pathway, respectively. *J. Virol.* 75, 10787–10799 (2001).
93. Tabata, K. et al. Unique Requirement for ESCRT Factors in Flavivirus Particle Formation on the Endoplasmic Reticulum. *Cell Rep.* 16, 2339–2347 (2016).
94. Welsch, S. et al. Composition and three-dimensional architecture of the dengue virus replication and assembly sites. *Cell Host Microbe* 5, 365–375 (2009).
95. Edeling, M. A., Diamond, M. S. & Fremont, D. H. Structural basis of Flavivirus NS1 assembly and antibody recognition. *Proc. Natl. Acad. Sci. U. S. A.* 111, 4285–4290 (2014).
96. Lee, J. M., Crooks, A. J. & Stephenson, J. R. The synthesis and maturation of a non-structural extracellular antigen from tick-borne encephalitis virus and its relationship to the intracellular NS1 protein. *J. Gen. Virol.* 70 (Pt 2), 335–343 (1989).
97. Mason, P. W. Maturation of Japanese encephalitis virus glycoproteins produced by infected mammalian and mosquito cells. *Virology* 169, 354–364 (1989).
98. Falgout, B., Chanock, R. & Lai, C. J. Proper processing of dengue virus nonstructural glycoprotein NS1 requires the N-terminal hydrophobic signal sequence and the downstream nonstructural protein NS2a. *J. Virol.* 63, 1852–1860 (1989).
99. Winkler, G., Randolph, V. B., Cleaves, G. R., Ryan, T. E. & Stollar, V. Evidence that the mature form of the flavivirus nonstructural protein NS1 is a dimer. *Virology* 162, 187–196 (1988).
100. Jacobs, M. G., Robinson, P. J., Bletchly, C., Mackenzie, J. M. & Young, P. R. Dengue virus nonstructural protein 1 is expressed in a glycosyl-phosphatidylinositol-linked form that is capable of signal transduction. *FASEB J. Off. Publ. Fed. Am. Soc. Exp. Biol.* 14, 1603–1610 (2000).
101. Lindenbach, B. D. & Rice, C. M. Genetic interaction of flavivirus nonstructural proteins NS1 and NS4A as a determinant of replicase function. *J. Virol.* 73, 4611–4621 (1999).
102. Post, P. R., Carvalho, R. & Galler, R. Glycosylation and secretion of yellow fever virus nonstructural protein NS1. *Virus Res.* 18, 291–302 (1991).
103. Alcalá, A. C. et al. The dengue virus non-structural protein 1 (NS1) is secreted efficiently from infected mosquito cells. *Virology* 488, 278–287 (2016).
104. Avirutnan, P. et al. Vascular leakage in severe dengue virus infections: a potential role for the nonstructural viral protein NS1 and complement. *J. Infect. Dis.* 193, 1078–1088 (2006).
105. Chang, H.-H. et al. Facilitation of cell adhesion by

- immobilized dengue viral nonstructural protein 1 (NS1): arginine-glycine-aspartic acid structural mimicry within the dengue viral NS1 antigen. *J. Infect. Dis.* 186, 743–751 (2002).
106. Lin, C.-F. et al. Expression of cytokine, chemokine, and adhesion molecules during endothelial cell activation induced by antibodies against dengue virus nonstructural protein 1. *J. Immunol. Baltim. Md* 1950 174, 395–403 (2005).
107. Alcon-LePoder, S. et al. The secreted form of dengue virus nonstructural protein NS1 is endocytosed by hepatocytes and accumulates in late endosomes: implications for viral infectivity. *J. Virol.* 79, 11403–11411 (2005).
108. Chung, K. M. et al. West Nile virus nonstructural protein NS1 inhibits complement activation by binding the regulatory protein factor H. *Proc. Natl. Acad. Sci. U. S. A.* 103, 19111–19116 (2006).
109. Wilson, J. R., de Sessions, P. F., Leon, M. A. & Scholle, F. West Nile virus nonstructural protein 1 inhibits TLR3 signal transduction. *J. Virol.* 82, 8262–8271 (2008).
110. Blitvich, B. J., Scanlon, D., Shiell, B. J., Mackenzie, J. S. & Hall, R. A. Identification and analysis of truncated and elongated species of the flavivirus NS1 protein. *Virus Res.* 60, 67–79 (1999).
111. Firth, A. E. & Atkins, J. F. A conserved predicted pseudoknot in the NS2A-encoding sequence of West Nile and Japanese encephalitis flaviviruses suggests NS1' may derive from ribosomal frameshifting. *Virol. J.* 6, 14 (2009).
112. Melian, E. B. et al. NS1' of flaviviruses in the Japanese encephalitis virus serogroup is a product of ribosomal frameshifting and plays a role in viral neuroinvasiveness. *J. Virol.* 84, 1641–1647 (2010).
113. Xie, X., Gayen, S., Kang, C., Yuan, Z. & Shi, P.-Y. Membrane topology and function of dengue virus NS2A protein. *J. Virol.* 87, 4609–4622 (2013).
114. Liu, W. J., Chen, H. B. & Khromykh, A. A. Molecular and functional analyses of Kunjin virus infectious cDNA clones demonstrate the essential roles for NS2A in virus assembly and for a nonconservative residue in NS3 in RNA replication. *J. Virol.* 77, 7804–7813 (2003).
115. Leung, J. Y. et al. Role of nonstructural protein NS2A in flavivirus assembly. *J. Virol.* 82, 4731–4741 (2008).
116. Kümmerer, B. M. & Rice, C. M. Mutations in the yellow fever virus nonstructural protein NS2A selectively block production of infectious particles. *J. Virol.* 76, 4773–4784 (2002).
117. Muñoz-Jordan, J. L., Sánchez-Burgos, G. G., Laurent-Rolle, M. & García-Sastre, A. Inhibition of interferon signaling by dengue virus. *Proc. Natl. Acad. Sci. U. S. A.* 100, 14333–14338 (2003).
118. Liu, W. J. et al. A single amino acid substitution in the West Nile virus nonstructural protein NS2A disables its ability to inhibit alpha/beta interferon induction and attenuates virus virulence in mice. *J. Virol.* 80, 2396–2404 (2006).
119. Radichev, I. et al. Structure-based mutagenesis identifies important novel determinants of the NS2B cofactor of the West Nile virus two-component NS2B-NS3 proteinase. *J. Gen. Virol.* 89, 636–641 (2008).
120. Arias, C. F., Preugschat, F. & Strauss, J. H. Dengue 2 virus NS2B and NS3 form a stable complex that can cleave NS3 within the helicase domain. *Virology* 193, 888–899 (1993).
121. Brand, C., Bisailon, M. & Geiss, B. J. Organization of the Flavivirus RNA replicase complex. *Wiley Interdiscip. Rev. RNA* 8, (2017).
122. Patkar, C. G. & Kuhn, R. J. Yellow Fever virus NS3 plays an essential role in virus assembly independent of its known enzymatic functions. *J. Virol.* 82, 3342–3352 (2008).
123. Warrenner, P., Tamura, J. K. & Collett, M. S. RNA-stimulated NTPase activity associated with yellow fever virus NS3 protein expressed in bacteria. *J. Virol.* 67, 989–996 (1993).
124. Frick, D. N. & Lam, A. M. I. Understanding helicases as a means of virus control. *Curr. Pharm. Des.* 12, 1315–1338 (2006).
125. Kadaré, G. & Haenni, A. L. Virus-encoded RNA helicases. *J. Virol.* 71, 2583–2590 (1997).
126. Aleshin, A. E., Shiryayev, S. A., Strongin, A. Y. & Liddington, R. C. Structural evidence for regulation and specificity of flaviviral proteases and evolution of the Flaviviridae fold. *Protein Sci. Publ. Protein Soc.* 16, 795–806 (2007).
127. Erbel, P. et al. Structural basis for the activation of flaviviral NS3 proteases from dengue and West Nile virus. *Nat. Struct. Mol. Biol.* 13, 372–373 (2006).
128. Brecher, M., Zhang, J. & Li, H. The Flavivirus Protease As a Target for Drug Discovery. *Virol. Sin.* 28, 326–336 (2013).
129. Roosendaal, J., Westaway, E. G., Khromykh, A. & Mackenzie, J. M. Regulated cleavages at the West Nile

- virus NS4A-2K-NS4B junctions play a major role in rearranging cytoplasmic membranes and Golgi trafficking of the NS4A protein. *J. Virol.* 80, 4623–4632 (2006).
130. Miller, S., Kastner, S., Krijnse-Locker, J., Bühler, S. & Bartenschlager, R. The non-structural protein 4A of dengue virus is an integral membrane protein inducing membrane alterations in a 2K-regulated manner. *J. Biol. Chem.* 282, 8873–8882 (2007).
 131. Teo, C. S. H. & Chu, J. J. H. Cellular vimentin regulates construction of dengue virus replication complexes through interaction with NS4A protein. *J. Virol.* 88, 1897–1913 (2014).
 132. Preugschat, F. & Strauss, J. H. Processing of nonstructural proteins NS4A and NS4B of dengue 2 virus in vitro and in vivo. *Virology* 185, 689–697 (1991).
 133. Chambers, T. J., McCourt, D. W. & Rice, C. M. Production of yellow fever virus proteins in infected cells: identification of discrete polyprotein species and analysis of cleavage kinetics using region-specific polyclonal antisera. *Virology* 177, 159–174 (1990).
 134. Miller, S., Sparacio, S. & Bartenschlager, R. Subcellular localization and membrane topology of the Dengue virus type 2 Non-structural protein 4B. *J. Biol. Chem.* 281, 8854–8863 (2006).
 135. Li, Y. et al. Secondary Structure and Membrane Topology of the Full-Length Dengue Virus NS4B in Micelles. *Angew. Chem. Int. Ed Engl.* 55, 12068–12072 (2016).
 136. Zou, J. et al. Characterization of dengue virus NS4A and NS4B protein interaction. *J. Virol.* 89, 3455–3470 (2015).
 137. Shiryayev, S. A., Chernov, A. V., Aleshin, A. E., Shiryayeva, T. N. & Strongin, A. Y. NS4A regulates the ATPase activity of the NS3 helicase: a novel cofactor role of the non-structural protein NS4A from West Nile virus. *J. Gen. Virol.* 90, 2081–2085 (2009).
 138. Muñoz-Jordán, J. L. et al. Inhibition of alpha/beta interferon signaling by the NS4B protein of flaviviruses. *J. Virol.* 79, 8004–8013 (2005).
 139. Ambrose, R. L. & Mackenzie, J. M. West Nile virus differentially modulates the unfolded protein response to facilitate replication and immune evasion. *J. Virol.* 85, 2723–2732 (2011).
 140. Youn, S. et al. Evidence for a Genetic and Physical Interaction between Nonstructural Proteins NS1 and NS4B That Modulates Replication of West Nile Virus. *J. Virol.* 86, 7360–7371 (2012).
 141. Tajima, S., Takasaki, T. & Kurane, I. Restoration of replication-defective dengue type 1 virus bearing mutations in the N-terminal cytoplasmic portion of NS4A by additional mutations in NS4B. *Arch. Virol.* 156, 63–69 (2011).
 142. Egloff, M.-P., Benarroch, D., Selisko, B., Romette, J.-L. & Canard, B. An RNA cap (nucleoside-2'-O)-methyltransferase in the flavivirus RNA polymerase NS5: crystal structure and functional characterization. *EMBO J.* 21, 2757–2768 (2002).
 143. Ray, D. et al. West Nile virus 5'-cap structure is formed by sequential guanine N-7 and ribose 2'-O methylations by nonstructural protein 5. *J. Virol.* 80, 8362–8370 (2006).
 144. Ackermann, M. & Padmanabhan, R. De novo synthesis of RNA by the dengue virus RNA-dependent RNA polymerase exhibits temperature dependence at the initiation but not elongation phase. *J. Biol. Chem.* 276, 39926–39937 (2001).
 145. Barrows, N. J. et al. Biochemistry and Molecular Biology of Flaviviruses. *Chem. Rev.* 118, 4448–4482 (2018).
 146. Dong, H. et al. Distinct RNA elements confer specificity to flavivirus RNA cap methylation events. *J. Virol.* 81, 4412–4421 (2007).
 147. Koonin, E. V. The phylogeny of RNA-dependent RNA polymerases of positive-strand RNA viruses. *J. Gen. Virol.* 72 (Pt 9), 2197–2206 (1991).
 148. Poch, O., Sauvaget, I., Delarue, M. & Tordo, N. Identification of four conserved motifs among the RNA-dependent polymerase encoding elements. *EMBO J.* 8, 3867–3874 (1989).
 149. Yon, C. et al. Modulation of the nucleoside triphosphatase/RNA helicase and 5'-RNA triphosphatase activities of Dengue virus type 2 nonstructural protein 3 (NS3) by interaction with NS5, the RNA-dependent RNA polymerase. *J. Biol. Chem.* 280, 27412–27419 (2005).
 150. Johansson, M., Brooks, A. J., Jans, D. A. & Vasudevan, S. G. A small region of the dengue virus-encoded RNA-dependent RNA polymerase, NS5, confers interaction with both the nuclear transport receptor importin-beta and the viral helicase, NS3. *J. Gen. Virol.* 82, 735–745 (2001).
 151. Brooks, A. J. et al. The interdomain region of dengue NS5 protein that binds to the viral helicase NS3

- contains independently functional importin beta 1 and importin alpha/beta-recognized nuclear localization signals. *J. Biol. Chem.* 277, 36399–36407 (2002).
152. Pryor, M. J. et al. Nuclear localization of dengue virus nonstructural protein 5 through its importin alpha/beta-recognized nuclear localization sequences is integral to viral infection. *Traffic Cph. Den.* 8, 795–807 (2007).
153. Weaver, S. C. Evolutionary Influences in Arboviral Disease. in *Quasispecies: Concept and Implications for Virology* (ed. Domingo, E.) 285–314 (Springer Berlin Heidelberg, 2006). doi:10.1007/3-540-26397-7_10
154. Selisko, B., Papageorgiou, N., Ferron, F. & Canard, B. Structural and Functional Basis of the Fidelity of Nucleotide Selection by Flavivirus RNA-Dependent RNA Polymerases. *Viruses* 10, (2018).
155. Combe, M. & Sanjuán, R. Variation in RNA virus mutation rates across host cells. *PLoS Pathog.* 10, e1003855 (2014).
156. Llaure, A. S., Frydman, J. & Andino, R. The role of mutational robustness in RNA virus evolution. *Nat. Rev. Microbiol.* 11, 327–336 (2013).
157. Domingo, E., Sheldon, J. & Perales, C. Viral quasispecies evolution. *Microbiol. Mol. Biol. Rev.* MMBR 76, 159–216 (2012).
158. Domingo, E. & Holland, J. J. RNA virus mutations and fitness for survival. *Annu. Rev. Microbiol.* 51, 151–178 (1997).
159. Wargo, A. R. & Kurath, G. Viral fitness: definitions, measurement, and current insights. *Curr. Opin. Virol.* 2, 538–545 (2012).
160. Ciota, A. T. & Kramer, L. D. Insights into arbovirus evolution and adaptation from experimental studies. *Viruses* 2, 2594–2617 (2010).
161. Jenkins, G. M., Rambaut, A., Pybus, O. G. & Holmes, E. C. Rates of molecular evolution in RNA viruses: a quantitative phylogenetic analysis. *J. Mol. Evol.* 54, 156–165 (2002).
162. Forrester, N. L., Coffey, L. L. & Weaver, S. C. Arboviral bottlenecks and challenges to maintaining diversity and fitness during mosquito transmission. *Viruses* 6, 3991–4004 (2014).
163. Coffey, L. L., Forrester, N., Tsetsarkin, K., Vasilakis, N. & Weaver, S. C. Factors shaping the adaptive landscape for arboviruses: implications for the emergence of disease. *Future Microbiol.* 8, 155–176 (2013).
164. Cheng, G., Liu, Y., Wang, P. & Xiao, X. Mosquito defense strategies against viral infection. *Trends Parasitol.* 32, 177–186 (2016).
165. Flenniken, M. L. Antiviral Defense in Invertebrates. *Viruses* 10, (2018).
166. Dick, G. W. A., Kitchen, S. F. & Haddock, A. J. Zika Virus (I). Isolations and serological specificity. *Trans. R. Soc. Trop. Med. Hyg.* 46, 509–520 (1952).
167. Kuno, G., Chang, G.-J. J., Tsuchiya, K. R., Karabatsos, N. & Cropp, C. B. Phylogeny of the Genus *Flavivirus*. *J. Virol.* 72, 73–83 (1998).
168. Dick, G. W. Epidemiological notes on some viruses isolated in Uganda; Yellow fever, Rift Valley fever, Bwamba fever, West Nile, Mengo, Semliki forest, Bunyamwera, Ntaya, Uganda S and Zika viruses. *Trans. R. Soc. Trop. Med. Hyg.* 47, 13–48 (1953).
169. Olson, J. G., Ksiazek, T. G., Suhandiman, null & Triwibowo, null. Zika virus, a cause of fever in Central Java, Indonesia. *Trans. R. Soc. Trop. Med. Hyg.* 75, 389–393 (1981).
170. Duffy, M. R. et al. Zika virus outbreak on Yap Island, Federated States of Micronesia. *N. Engl. J. Med.* 360, 2536–2543 (2009).
171. Cao-Lormeau, V.-M. et al. Zika virus, French polynesia, South pacific, 2013. *Emerg. Infect. Dis.* 20, 1085–1086 (2014).
172. Zanoluca, C. et al. First report of autochthonous transmission of Zika virus in Brazil. *Mem. Inst. Oswaldo Cruz* 110, 569–572 (2015).
173. Fifth meeting of the Emergency Committee under the International Health Regulations (2005) regarding microcephaly, other neurological disorders and Zika virus. Available at: [https://www.who.int/news-room/detail/18-11-2016-fifth-meeting-of-the-emergency-committee-under-the-international-health-regulations-\(2005\)-regarding-microcephaly-other-neurological-disorders-and-zika-virus](https://www.who.int/news-room/detail/18-11-2016-fifth-meeting-of-the-emergency-committee-under-the-international-health-regulations-(2005)-regarding-microcephaly-other-neurological-disorders-and-zika-virus). (Accessed: 12th January 2019)
174. WHO | Zika virus infection: India. WHO Available at: <http://www.who.int/emergencies/diseases/zika/india-november-2018/en/>. (Accessed: 12th January 2019)
175. Marchette, N. J., Garcia, R. & Rudnick, A. Isolation of Zika virus from *Aedes aegypti* mosquitoes in Malaysia. *Am. J. Trop. Med. Hyg.* 18, 411–415 (1969).
176. Darwish, M. A., Hoogstraal, H., Roberts, T. J., Ahmed, I. P. & Omar, F. A sero-epidemiological survey for certain arboviruses (Togaviridae) in Pakistan. *Trans. R. Soc. Trop. Med. Hyg.* 77, 442–445 (1983).

177. Smithburn, K. C., Kerr, J. A. & Gatne, P. B. Neutralizing antibodies against certain viruses in the sera of residents of India. *J. Immunol. Baltim. Md* 1950 72, 248–257 (1954).
178. Pond, W. L. ARTHROPOD-BORNE VIRUS ANTIBODIES IN SERA FROM RESIDENTS OF SOUTH-EAST ASIA. *Trans. R. Soc. Trop. Med. Hyg.* 57, 364–371 (1963).
179. Hammon, W. M., Schrack, W. D. & Sather, G. E. Serological survey for a arthropod-borne virus infections in the Philippines. *Am. J. Trop. Med. Hyg.* 7, 323–328 (1958).
180. Heang, V. et al. Zika virus infection, Cambodia, 2010. *Emerg. Infect. Dis.* 18, 349–351 (2012).
181. Lim, S.-K., Lim, J. K. & Yoon, I.-K. An Update on Zika Virus in Asia. *Infect. Chemother.* 49, 91–100 (2017).
182. Singapore Zika Study Group. Outbreak of Zika virus infection in Singapore: an epidemiological, entomological, virological, and clinical analysis. *Lancet Infect. Dis.* 17, 813–821 (2017).
183. Codeço, C. et al. Zika is not a reason for missing the Olympic Games in Rio de Janeiro: response to the open letter of Dr Attaran and colleagues to Dr Margaret Chan, Director - General, WHO, on the Zika threat to the Olympic and Paralympic Games. *Mem. Inst. Oswaldo Cruz* 111, 414–415 (2016).
184. Lewnard, J. A., Gonsalves, G. & Ko, A. I. Low Risk of International Zika Virus Spread due to the 2016 Olympics in Brazil. *Ann. Intern. Med.* 165, 286–287 (2016).
185. PAHO/WHO - Home - Pan American Health Organization. Available at: <https://www.paho.org/hq/index.php?lang=en>. (Accessed: 13th January 2019)
186. Hills, S. L., Fischer, M. & Petersen, L. R. Epidemiology of Zika Virus Infection. *J. Infect. Dis.* 216, S868–S874 (2017).
187. Marini, G., Guzzetta, G., Rosà, R. & Merler, S. First outbreak of Zika virus in the continental United States: a modelling analysis. *Eurosurveillance* 22, (2017).
188. CDC. Outcomes of Pregnancies with Possible Zika Virus Infection | CDC. Centers for Disease Control and Prevention (2018). Available at: <https://www.cdc.gov/pregnancy/zika/data/pregnancy-outcomes.html>. (Accessed: 13th January 2019)
189. Grubaugh, N. D. et al. Genomic epidemiology reveals multiple introductions of Zika virus into the United States. *Nature* 546, 401 (2017).
190. Bogoch, I. I. et al. Potential for Zika virus introduction and transmission in resource-limited countries in Africa and the Asia-Pacific region: a modelling study. *Lancet Infect. Dis.* 16, 1237–1245 (2016).
191. Quam, M. B. & Wilder-Smith, A. Estimated global exportations of Zika virus infections via travellers from Brazil from 2014 to 2015. *J. Travel Med.* 23, (2016).
192. Spiteri, G., Sudre, B., Septfons, A., Beauté, J. & The European Zika Surveillance Network. Surveillance of Zika virus infection in the EU/EEA, June 2015 to January 2017. *Euro Surveill. Bull. Eur. Sur Mal. Transm. Eur. Commun. Dis. Bull.* 22, (2017).
193. Wilder-Smith, A., Chang, C. R. & Leong, W. Y. Zika in travellers 1947-2017: a systematic review. *J. Travel Med.* 25, (2018).
194. Buechler, C. R. et al. Seroprevalence of Zika Virus in Wild African Green Monkeys and Baboons. *mSphere* 2, (2017).
195. Wolfe, N. D. et al. Sylvatic transmission of arboviruses among Bornean orangutans. *Am. J. Trop. Med. Hyg.* 64, 310–316 (2001).
196. Kilbourn, A. M. et al. Health evaluation of free-ranging and semi-captive orangutans (*Pongo pygmaeus pygmaeus*) in Sabah, Malaysia. *J. Wildl. Dis.* 39, 73–83 (2003).
197. Olson, J. G. et al. A survey for arboviral antibodies in sera of humans and animals in Lombok, Republic of Indonesia. *Ann. Trop. Med. Parasitol.* 77, 131–137 (1983).
198. Terzian, A. C. B. et al. Evidence of natural Zika virus infection in neotropical non-human primates in Brazil. *Sci. Rep.* 8, 16034 (2018).
199. Berthet, N. et al. Molecular characterization of three Zika flaviviruses obtained from sylvatic mosquitoes in the Central African Republic. *Vector Borne Zoonotic Dis. Larchmt. N* 14, 862–865 (2014).
200. Althouse, B. M. et al. Impact of climate and mosquito vector abundance on sylvatic arbovirus circulation dynamics in Senegal. *Am. J. Trop. Med. Hyg.* 92, 88–97 (2015).
201. Diallo, D. et al. Zika Virus Emergence in Mosquitoes in Southeastern Senegal, 2011. *PLOS ONE* 9, e109442 (2014).
202. Calvez, E. et al. Zika virus outbreak in the Pacific: Vector competence of regional vectors. *PLoS Negl. Trop. Dis.* 12, e0006637 (2018).
203. Main, B. J. et al. Vector competence of *Aedes aegypti*,

- Culex tarsalis*, and *Culex quinquefasciatus* from California for Zika virus. *PLoS Negl. Trop. Dis.* 12, e0006524 (2018).
204. Guedes, D. R. et al. Zika virus replication in the mosquito *Culex quinquefasciatus* in Brazil. *Emerg. Microbes Infect.* 6, e69 (2017).
205. Elizondo-Quiroga, D. et al. Zika Virus in Salivary Glands of Five Different Species of Wild-Caught Mosquitoes from Mexico. *Sci. Rep.* 8, 809 (2018).
206. Guo, X.-X. et al. *Culex pipiens quinquefasciatus*: a potential vector to transmit Zika virus. *Emerg. Microbes Infect.* 5, e102 (2016).
207. Kenney, J. L. et al. Transmission Incompetence of *Culex quinquefasciatus* and *Culex pipiens pipiens* from North America for Zika Virus. *Am. J. Trop. Med. Hyg.* 96, 1235–1240 (2017).
208. Roundy, C. M. et al. Lack of evidence for Zika virus transmission by *Culex* mosquitoes. *Emerg. Microbes Infect.* 6, e90 (2017).
209. Musso, D., Stramer, S. L., AABB Transfusion-Transmitted Diseases Committee, Busch, M. P. & International Society of Blood Transfusion Working Party on Transfusion-Transmitted Infectious Diseases. Zika virus: a new challenge for blood transfusion. *Lancet Lond. Engl.* 387, 1993–1994 (2016).
210. Eick, S. M. et al. Seroprevalence of Dengue and Zika Virus in Blood Donations: A Systematic Review. *Transfus. Med. Rev.* 33, 35–42 (2019).
211. Foy, B. D. et al. Probable Non-Vector-borne Transmission of Zika Virus, Colorado, USA. *Emerg. Infect. Dis.* 17, 880–882 (2011).
212. Turmel, J. M. et al. Late sexual transmission of Zika virus related to persistence in the semen. *The Lancet* 387, 2501 (2016).
213. Counotte, M. J. et al. Sexual transmission of Zika virus and other flaviviruses: A living systematic review. *PLOS Med.* 15, e1002611 (2018).
214. Sánchez-Montalvá, A. et al. Zika virus dynamics in body fluids and risk of sexual transmission in a non-endemic area. *Trop. Med. Int. Health* 23, 92–100 (2018).
215. Nicastri, E. et al. Persistent detection of Zika virus RNA in semen for six months after symptom onset in a traveller returning from Haiti to Italy, February 2016. *Eurosurveillance* 21, 30314 (2016).
216. Robinson, C. L. et al. Male germ cells support long-term propagation of Zika virus. *Nat. Commun.* 9, 2090 (2018).
217. Stassen, L., Armitage, C. W., van der Heide, D. J., Beagley, K. W. & Frentiu, F. D. Zika Virus in the Male Reproductive Tract. *Viruses* 10, (2018).
218. Oliveira, D. B. L. et al. Persistence and Intra-Host Genetic Evolution of Zika Virus Infection in Symptomatic Adults: A Special View in the Male Reproductive System. *Viruses* 10, (2018).
219. Avelino-Silva, V. I. et al. Potential effect of Zika virus infection on human male fertility? *Rev. Inst. Med. Trop. Sao Paulo* 60, e64 (2018).
220. Uraki, R. et al. Zika virus causes testicular atrophy. *Sci. Adv.* 3, e1602899 (2017).
221. Calvet, G. et al. Detection and sequencing of Zika virus from amniotic fluid of fetuses with microcephaly in Brazil: a case study. *Lancet Infect. Dis.* (2016). doi:10.1016/S1473-3099(16)00095-5
222. de Noronha, L. et al. Zika Virus Infection at Different Pregnancy Stages: Anatomopathological Findings, Target Cells and Viral Persistence in Placental Tissues. *Front. Microbiol.* 9, 2266 (2018).
223. Caine, E. A., Jagger, B. W. & Diamond, M. S. Animal Models of Zika Virus Infection during Pregnancy. *Viruses* 10, (2018).
224. Nguyen, S. M. et al. Highly efficient maternal-fetal Zika virus transmission in pregnant rhesus macaques. *PLoS Pathog.* 13, (2017).
225. Zmurko, J. et al. The Viral Polymerase Inhibitor 7-Deaza-2'-C-Methyladenosine Is a Potent Inhibitor of In Vitro Zika Virus Replication and Delays Disease Progression in a Robust Mouse Infection Model. *PLoS Negl. Trop. Dis.* 10, e0004695 (2016).
226. Barrows, N. J. et al. A Screen of FDA-Approved Drugs for Inhibitors of Zika Virus Infection. *Cell Host Microbe* 20, 259–270 (2016).
227. Wilder-Smith, A. et al. Zika vaccines and therapeutics: landscape analysis and challenges ahead. *BMC Med.* 16, 84 (2018).
228. Musso, D. & Gubler, D. J. Zika Virus. *Clin. Microbiol. Rev.* 29, 487–524 (2016).
229. Peters, R. & Stevenson, M. Zika virus diagnosis: challenges and solutions. *Clin. Microbiol. Infect. Off. Publ. Eur. Soc. Clin. Microbiol. Infect. Dis.* (2018). doi:10.1016/j.cmi.2018.12.002
230. Huzly, D., Hanselmann, I., Schmidt-Chanasit, J. & Panning, M. High specificity of a novel Zika virus ELISA in European patients after exposure to different flaviviruses. *Eurosurveillance* 21, (2016).

231. Priye, A. et al. A smartphone-based diagnostic platform for rapid detection of Zika, chikungunya, and dengue viruses. *Sci. Rep.* 7, 44778 (2017).
232. Bingham, A. M. et al. Comparison of Test Results for Zika Virus RNA in Urine, Serum, and Saliva Specimens from Persons with Travel-Associated Zika Virus Disease — Florida, 2016. *MMWR Morb. Mortal. Wkly. Rep.* 65, 475–478 (2016).
233. Mier-Y-Teran-Romero, L., Delorey, M. J., Sejvar, J. J. & Johansson, M. A. Guillain-Barré syndrome risk among individuals infected with Zika virus: a multi-country assessment. *BMC Med.* 16, 67 (2018).
234. Dos Santos, T. et al. Zika Virus and the Guillain-Barré Syndrome - Case Series from Seven Countries. *N. Engl. J. Med.* 375, 1598–1601 (2016).
235. Paploski, I. A. D. et al. Time Lags between Exanthematous Illness Attributed to Zika Virus, Guillain-Barré Syndrome, and Microcephaly, Salvador, Brazil. *Emerg. Infect. Dis.* 22, 1438–1444 (2016).
236. CDC. Congenital Zika Syndrome & Other Birth Defects | CDC. Centers for Disease Control and Prevention (2018). Available at: <https://www.cdc.gov/pregnancy/zika/testing-follow-up/zika-syndrome-birth-defects.html>. (Accessed: 15th January 2019)
237. Hussain, A., Ali, F., Latiwesh, O. B. & Hussain, S. A Comprehensive Review of the Manifestations and Pathogenesis of Zika Virus in Neonates and Adults. *Cureus* 10,
238. Moore, C. A. et al. Characterizing the Pattern of Anomalies in Congenital Zika Syndrome for Pediatric Clinicians. *JAMA Pediatr.* 171, 288–295 (2017).
239. CDC. Centers for Disease Control and Prevention (2018). Available at: <https://www.cdc.gov/pregnancy/zika/data/index.html>. (Accessed: 16th January 2019)
240. Brasil, P. et al. Zika Virus Infection in Pregnant Women in Rio de Janeiro. *N. Engl. J. Med.* 375, 2321–2334 (2016).
241. Carabali, M., Austin, N., King, N. B. & Kaufman, J. S. The Zika epidemic and abortion in Latin America: a scoping review. *Glob. Health Res. Policy* 3, (2018).
242. Castro, M. C., Han, Q. C., Carvalho, L. R., Victora, C. G. & França, G. V. A. Implications of Zika virus and congenital Zika syndrome for the number of live births in Brazil. *Proc. Natl. Acad. Sci.* 115, 6177–6182 (2018).
243. Baron, S., Fons, M. & Albrecht, T. Viral Pathogenesis. in *Medical Microbiology* (ed. Baron, S.) (University of Texas Medical Branch at Galveston, 1996).
244. Nowakowski, T. J. et al. Expression Analysis Highlights AXL as a Candidate Zika Virus Entry Receptor in Neural Stem Cells. *Cell Stem Cell* doi:10.1016/j.stem.2016.03.012
245. Wells, M. F. et al. Genetic Ablation of AXL Does Not Protect Human Neural Progenitor Cells and Cerebral Organoids from Zika Virus Infection. *Cell Stem Cell* 19, 703–708 (2016).
246. Wang, Z.-Y. et al. Axl is not an indispensable factor for Zika virus infection in mice. *J. Gen. Virol.* 98, 2061–2068 (2017).
247. Meertens, L. et al. Axl Mediates ZIKA Virus Entry in Human Glial Cells and Modulates Innate Immune Responses. *Cell Rep.* 18, 324–333 (2017).
248. Hamel, R. et al. African and Asian Zika virus strains differentially induce early antiviral responses in primary human astrocytes. *Infect. Genet. Evol. J. Mol. Epidemiol. Evol. Genet. Infect. Dis.* 49, 134–137 (2017).
249. Stefanik, M. et al. Characterisation of Zika virus infection in primary human astrocytes. *BMC Neurosci.* 19, 5 (2018).
250. Chen, J. et al. AXL promotes Zika virus infection in astrocytes by antagonizing type I interferon signalling. *Nat. Microbiol.* 3, 302–309 (2018).
251. Bayer, A. et al. Type III Interferons Produced by Human Placental Trophoblasts Confer Protection against Zika Virus Infection. *Cell Host Microbe* 19, 705–712 (2016).
252. Quicke, K. M. et al. Zika Virus Infects Human Placental Macrophages. *Cell Host Microbe* 0, (2016).
253. Tabata, T. et al. Zika Virus Targets Different Primary Human Placental Cells, Suggesting Two Routes for Vertical Transmission. *Cell Host Microbe* 20, 155–166 (2016).
254. Miner, J. J. et al. Zika Virus Infection during Pregnancy in Mice Causes Placental Damage and Fetal Demise. *Cell* 165, 1081–1091 (2016).
255. Hamel, R. et al. Biology of Zika Virus Infection in Human Skin Cells. *J. Virol.* 89, 8880–8896 (2015).
256. Persaud, M., Martinez-Lopez, A., Buffone, C., Porcelli, S. A. & Diaz-Griffero, F. Infection by Zika viruses requires the transmembrane protein AXL, endocytosis and low pH. *Virology* 518, 301–312 (2018).

257. Bowen, J. R., Zimmerman, M. G. & Suthar, M. S. Taking the defensive: Immune control of Zika virus infection. *Virus Res.* 254, 21–26 (2018).
258. Sun, X. et al. Transcriptional Changes during Naturally Acquired Zika Virus Infection Render Dendritic Cells Highly Conducive to Viral Replication. *Cell Rep.* 21, 3471–3482 (2017).
259. Vielle, N. J. et al. Silent infection of human dendritic cells by African and Asian strains of Zika virus. *Sci. Rep.* 8, 5440 (2018).
260. Foo, S.-S. et al. Asian Zika virus strains target CD14+ blood monocytes and induce M2-skewed immunosuppression during pregnancy. *Nat. Microbiol.* 2, 1558–1570 (2017).
261. Michlmayr, D., Andrade, P., Gonzalez, K., Balmaseda, A. & Harris, E. CD14+CD16+ monocytes are the main target of Zika virus infection in peripheral blood mononuclear cells in a paediatric study in Nicaragua. *Nat. Microbiol.* 2, 1462–1470 (2017).
262. Lum, F.-M. et al. Zika Virus Infection Preferentially Counterbalances Human Peripheral Monocyte and/or NK Cell Activity. *mSphere* 3, (2018).
263. Siemann, D. N., Strange, D. P., Maharaj, P. N., Shi, P.-Y. & Verma, S. Zika Virus Infects Human Sertoli Cells and Modulates the Integrity of the In Vitro Blood-Testis Barrier Model. *J. Virol.* 91, (2017).
264. Kumar, A. et al. Human Sertoli cells support high levels of Zika virus replication and persistence. *Sci. Rep.* 8, 5477 (2018).
265. Strange, D. P., Green, R., Siemann, D. N., Gale, M. & Verma, S. Immunoprofiles of human Sertoli cells infected with Zika virus reveals unique insights into host-pathogen crosstalk. *Sci. Rep.* 8, 8702 (2018).
266. Salam, A. P. & Horby, P. Isolation of viable Zika virus from spermatozoa. *Lancet Infect. Dis.* 18, 144 (2018).
267. Bagasra, O. et al. Cellular Targets and Receptor of Sexual Transmission of Zika Virus. *Appl. Immunohistochem. Mol. Morphol. AIMM* 25, 679–686 (2017).
268. Alcendor, D. J. Zika Virus Infection of the Human Glomerular Cells: Implications for Viral Reservoirs and Renal Pathogenesis. *J. Infect. Dis.* 216, 162–171 (2017).
269. Roach, T. & Alcendor, D. J. Zika virus infection of cellular components of the blood-retinal barriers: implications for viral associated congenital ocular disease. *J. Neuroinflammation* 14, (2017).
270. Zhao, Z. et al. Viral Retinopathy in Experimental Models of Zika Infection. *Invest. Ophthalmol. Vis. Sci.* 58, 4355–4365 (2017).
271. Salinas, S. et al. Zika Virus Efficiently Replicates in Human Retinal Epithelium and Disturbs Its Permeability. *J. Virol.* 91, e02144-16 (2017).
272. Mumtaz, N. et al. Zika virus infection perturbs osteoblast function. *Sci. Rep.* 8, 16975 (2018).
273. Filho, E. A. et al. Case report of Zika virus during controlled ovarian hyperstimulation: results from follicular fluid, cumulus cells and oocytes. *JBRA Assist. Reprod.* (2019). doi:10.5935/1518-0557.20180081
274. Rajahram, G. S. et al. Postmortem evidence of disseminated Zika virus infection in an adult patient. *Int. J. Infect. Dis. IJID Off. Publ. Int. Soc. Infect. Dis.* (2019). doi:10.1016/j.ijid.2019.01.047
275. Mazar, J. et al. Zika virus as an oncolytic treatment of human neuroblastoma cells requires CD24. *PLoS ONE* 13, (2018).
276. Offerdahl, D. K., Dorward, D. W., Hansen, B. T. & Bloom, M. E. Cytoarchitecture of Zika virus infection in human neuroblastoma and *Aedes albopictus* cell lines. *Virology* 501, 54–62 (2017).
277. Mlera, L. & Bloom, M. E. Differential Zika Virus Infection of Testicular Cell Lines. *Viruses* 11, (2019).
278. Bos, S. et al. The structural proteins of epidemic and historical strains of Zika virus differ in their ability to initiate viral infection in human host cells. *Virology* 516, 265–273 (2018).
279. Tang, H. et al. Zika Virus Infects Human Cortical Neural Progenitors and Attenuates Their Growth. *Cell Stem Cell* 0, (2016).
280. Chan, J. F.-W. et al. Differential cell line susceptibility to the emerging Zika virus: implications for disease pathogenesis, non-vector-borne human transmission and animal reservoirs. *Emerg. Microbes Infect.* 5, e93 (2016).
281. Li, G. et al. The Roles of prM-E Proteins in Historical and Epidemic Zika Virus-mediated Infection and Neurocytotoxicity. *Viruses* 11, 157 (2019).

282. Mladinich, M. C., Schwedes, J. & Mackow, E. R. Zika Virus Persistently Infects and Is Basolaterally Released from Primary Human Brain Microvascular Endothelial Cells. *mBio* 8, (2017).
283. Gong, D. et al. High-Throughput Fitness Profiling of Zika Virus E Protein Reveals Different Roles for Glycosylation during Infection of Mammalian and Mosquito Cells. *iScience* 1, 97–111 (2018).
284. Peng, H. et al. Zika Virus Induces Autophagy in Human Umbilical Vein Endothelial Cells. *Viruses* 10, (2018).
285. Frumence, E. et al. The South Pacific epidemic strain of Zika virus replicates efficiently in human epithelial A549 cells leading to IFN- β production and apoptosis induction. *Virology* 493, 217–226 (2016).
286. Gaudry, A. et al. The Flavonoid Isoquercitrin Precludes Initiation of Zika Virus Infection in Human Cells. *Int. J. Mol. Sci.* 19, 1093 (2018).
287. Colavita, F. et al. ZIKV Infection Induces an Inflammatory Response but Fails to Activate Types I, II, and III IFN Response in Human PBMC. *Mediators Inflamm.* 2018, 2450540 (2018).
288. Spencer, J. L. et al. Replication of Zika Virus in Human Prostate Cells: A Potential Source of Sexually Transmitted Virus. *J. Infect. Dis.* 217, 538–547 (2018).
289. Matusali, G. et al. Zika virus infects human testicular tissue and germ cells. *J. Clin. Invest.* 128, 4697–4710 (2018).
290. Pinggen, M. et al. Host Inflammatory Response to Mosquito Bites Enhances the Severity of Arbovirus Infection. *Immunity* 44, 1455–1469 (2016).
291. Secundino, N. F. C. et al. Zika virus transmission to mouse ear by mosquito bite: a laboratory model that replicates the natural transmission process. *Parasit. Vectors* 10, 346 (2017).
292. Lustig, Y., Mendelson, E., Paran, N., Melamed, S. & Schwartz, E. Detection of Zika virus RNA in whole blood of imported Zika virus disease cases up to 2 months after symptom onset, Israel, December 2015 to April 2016. *Euro Surveill. Bull. Eur. Sur Mal. Transm. Eur. Commun. Dis. Bull.* 21, (2016).
293. Mansuy, J. M. et al. Zika Virus Infection and Prolonged Viremia in Whole-Blood Specimens. *Emerg. Infect. Dis.* 23, 863–865 (2017).
294. Cao, B., Diamond, M. S. & Mysorekar, I. U. Maternal-Fetal Transmission of Zika Virus: Routes and Signals for Infection. *J. Interferon Cytokine Res. Off. J. Int. Soc. Interferon Cytokine Res.* 37, 287–294 (2017).
295. Schwartz, D. A. Viral infection, proliferation, and hyperplasia of Hofbauer cells and absence of inflammation characterize the placental pathology of fetuses with congenital Zika virus infection. *Arch. Gynecol. Obstet.* 295, 1361–1368 (2017).
296. Ho, C.-Y. et al. Differential neuronal susceptibility and apoptosis in congenital Zika virus infection. *Ann. Neurol.* 82, 121–127 (2017).
297. Kaufmann, B. & Rossmann, M. G. Molecular mechanisms involved in the early steps of flavivirus cell entry. *Microbes Infect.* 13, 1–9 (2011).
298. Kim, S. Y., Li, B. & Linhardt, R. J. Pathogenesis and Inhibition of Flaviviruses from a Carbohydrate Perspective. *Pharm. Basel Switz.* 10, (2017).
299. Lemke, G. & Burstyn-Cohen, T. TAM receptors and the clearance of apoptotic cells. *Ann. N. Y. Acad. Sci.* 1209, 23–29 (2010).
300. García-Vallejo, J. J. et al. Multivalent glycopeptide dendrimers for the targeted delivery of antigens to dendritic cells. *Mol. Immunol.* 53, 387–397 (2013).
301. Li, C. et al. Zika Virus Disrupts Neural Progenitor Development and Leads to Microcephaly in Mice. *Cell Stem Cell* 19, 120–126 (2016).
302. Retallack, H. et al. Zika virus cell tropism in the developing human brain and inhibition by azithromycin. *Proc. Natl. Acad. Sci. U. S. A.* 113, 14408–14413 (2016).
303. Tappe, D. et al. Cytokine kinetics of Zika virus-infected patients from acute to reconvalescent phase. *Med. Microbiol. Immunol. (Berl.)* 205, 269–273 (2016).
304. Grifoni, A. et al. Prior Dengue virus exposure shapes T cell immunity to Zika virus in humans. *J. Virol.* (2017). doi:10.1128/JVI.01469-17
305. Dang, J. et al. Zika Virus Depletes Neural Progenitors in Human Cerebral Organoids through Activation of the Innate Immune Receptor TLR3. *Cell Stem Cell* 19, 258–265 (2016).
306. Smith, J. L., Jeng, S., McWeeney, S. K. & Hirsch, A. J. A MicroRNA Screen Identifies the Wnt Signaling Pathway as a Regulator of the Interferon Response during Flavivirus Infection. *J. Virol.* 91, (2017).
307. Zammarchi, L. et al. Zika virus infection in a traveller returning to Europe from Brazil, March 2015. *Euro Surveill. Bull. Eur. Sur Mal. Transm. Eur. Commun. Dis. Bull.* 20, (2015).

308. Elong Ngono, A. et al. Mapping and Role of the CD8+ T Cell Response During Primary Zika Virus Infection in Mice. *Cell Host Microbe* 21, 35–46 (2017).
309. Andrade, D. V. & Harris, E. Recent advances in understanding the adaptive immune response to Zika virus and the effect of previous flavivirus exposure. *Virus Res.* 254, 27–33 (2018).
310. Priyamvada, L. et al. Human antibody responses after dengue virus infection are highly cross-reactive to Zika virus. *Proc. Natl. Acad. Sci. U. S. A.* 113, 7852–7857 (2016).
311. Chazal, M. et al. RIG-I Recognizes the 5' Region of Dengue and Zika Virus Genomes. *Cell Rep.* 24, 320–328 (2018).
312. Vanwalscappel, B., Tada, T. & Landau, N. R. Toll-like receptor agonist R848 blocks Zika virus replication by inducing the antiviral protein viperin. *Virology* 522, 199–208 (2018).
313. Panayiotou, C. et al. Viperin Restricts Zika Virus and Tick-Borne Encephalitis Virus Replication by Targeting NS3 for Proteasomal Degradation. *J. Virol.* 92, (2018).
314. Angleró-Rodríguez, Y. I. et al. *Aedes aegypti* Molecular Responses to Zika Virus: Modulation of Infection by the Toll and Jak/Stat Immune Pathways and Virus Host Factors. *Front. Microbiol.* 8, 2050 (2017).
315. Bell, T. M., Field, E. J. & Narang, H. K. Zika virus infection of the central nervous system of mice. *Arch. Gesamte Virusforsch.* 35, 183–193 (1971).
316. Morán, M. et al. Bulk autophagy, but not mitophagy, is increased in cellular model of mitochondrial disease. *Biochim. Biophys. Acta* 1842, 1059–1070 (2014).
317. Liang, Q. et al. Zika Virus NS4A and NS4B Proteins Deregulate Akt-mTOR Signaling in Human Fetal Neural Stem Cells to Inhibit Neurogenesis and Induce Autophagy. *Cell Stem Cell* 19, 663–671 (2016).
318. Tetro, J. A. Zika and microcephaly: causation, correlation, or coincidence? *Microbes Infect.* 18, 167–168 (2016).
319. Cugola, F. R. et al. The Brazilian Zika virus strain causes birth defects in experimental models. *Nature* 534, 267–271 (2016).
320. Chiramel, A. I. & Best, S. M. Role of autophagy in Zika virus infection and pathogenesis. *Virus Res.* 254, 34–40 (2018).
321. Lennemann, N. J. & Coyne, C. B. Dengue and Zika viruses subvert reticulophagy by NS2B3-mediated cleavage of FAM134B. *Autophagy* 13, 322–332 (2017).
322. Wu, Y. et al. Zika virus evades interferon-mediated antiviral response through the co-operation of multiple nonstructural proteins in vitro. *Cell Discov.* 3, 17006 (2017).
323. Sariol, C. A., Nogueira, M. L. & Vasilakis, N. A Tale of Two Viruses: Does Heterologous Flavivirus Immunity Enhance Zika Disease? *Trends Microbiol.* 26, 186–190 (2018).
324. Kawiecki, A. B. & Christofferson, R. C. Zika Virus-Induced Antibody Response Enhances Dengue Virus Serotype 2 Replication In Vitro. *J. Infect. Dis.* 214, 1357–1360 (2016).
325. George, J. et al. Prior Exposure to Zika Virus Significantly Enhances Peak Dengue-2 Viremia in Rhesus Macaques. *Sci. Rep.* 7, 10498 (2017).
326. Dejnirattisai, W. et al. Dengue virus sero-cross-reactivity drives antibody-dependent enhancement of infection with Zika virus. *Nat. Immunol.* 17, 1102–1108 (2016).
327. Paul, L. M. et al. Dengue Virus Antibodies Enhance Zika Virus Infection. *bioRxiv* 050112 (2016). doi:10.1101/050112
328. Londono-Renteria, B. et al. A relevant in vitro human model for the study of Zika virus antibody-dependent enhancement. *J. Gen. Virol.* 98, 1702–1712 (2017).
329. Cohen, J. Dengue may bring out the worst in Zika. *Science* 355, 1362 (2017).
330. Bardina, S. V. et al. Enhancement of Zika virus pathogenesis by preexisting ant flavivirus immunity. *Science* 356, 175–180 (2017).
331. Hermanns, K. et al. Zika virus infection in human placental tissue explants is enhanced in the presence of dengue virus antibodies in-vitro. *Emerg. Microbes Infect.* 7, 198 (2018).
332. Pantoja, P. et al. Zika virus pathogenesis in rhesus macaques is unaffected by pre-existing immunity to dengue virus. *Nat. Commun.* 8, 15674 (2017).
333. Terzian, A. C. B. et al. Viral Load and Cytokine Response Profile Does Not Support Antibody-Dependent Enhancement in Dengue-Primed Zika Virus-Infected Patients. *Clin. Infect. Dis. Off. Publ. Infect. Dis. Soc. Am.* 65, 1260–1265 (2017).

334. Bhaumik, S. K. et al. Pre-Existing Dengue Immunity Drives a DENV-Biased Plasmablast Response in ZIKV-Infected Patient. *Viruses* 11, 19 (2019).
335. Faye, O. et al. Molecular evolution of Zika virus during its emergence in the 20(th) century. *PLoS Negl. Trop. Dis.* 8, e2636 (2014).
336. Posen, H. J., Keystone, J. S., Gubbay, J. B. & Morris, S. K. Epidemiology of Zika virus, 1947–2007. *BMJ Glob. Health* 1, (2016).
337. Haddow, A. D. et al. Genetic characterization of Zika virus strains: geographic expansion of the Asian lineage. *PLoS Negl. Trop. Dis.* 6, e1477 (2012).
338. Pettersson, J. H.-O. et al. Re-visiting the evolution, dispersal and epidemiology of Zika virus in Asia. *Emerg. Microbes Infect.* 7, 79 (2018).
339. Pettersson, J. H.-O. et al. How Did Zika Virus Emerge in the Pacific Islands and Latin America? *mBio* 7, e01239-16 (2016).
340. Liu, Z.-Y., Shi, W.-F. & Qin, C.-F. The evolution of Zika virus from Asia to the Americas. *Nat. Rev. Microbiol.* 1 (2019). doi:10.1038/s41579-018-0134-9
341. Fritz, R. et al. The unique transmembrane hairpin of flavivirus fusion protein E is essential for membrane fusion. *J. Virol.* 85, 4377–4385 (2011).

PART I:

DEVELOPMENT OF MOLECULAR VIROLOGY
TOOLS FOR THE STUDY OF ZIKV BIOLOGY AND
PATHOGENICITY

I. RATIONALE

The explosive pandemic of Zika virus and its recent association with severe neurological complications posed a global public health emergency. As a consequence, there was an urgent need to develop virological tools that facilitate the study of molecular determinants of Zika virus pathogenicity and allow the testing of potential antiviral compounds.

Methods for the production of infectious viruses from complementary DNA copies of their genome have significantly improved the knowledge on RNA virus biology and pathogenesis. First, the production of a molecular clone enables the study of a virus according to its original sequence deposited in GenBank and thus limits the bias due to genetic drift inherent to the successive passages of isolates. Then, it also provides a viral stock with a reduced number of quasi-species. While the use of a population with poor genetic diversity has significant limitations for the study of virus virulence, it offers the possibility of considering the specific phenotype of a consensus sequence. Finally, the use of molecular clones and other reverse genetic techniques is a considerable asset in determining the effects of specific mutations on the infectious behavior of flaviviruses. For the purposes of my doctoral research, we decided to develop a set of ZIKV molecular clones in order to study the viral factors involved in the human pathogenicity of ZIKV. Thus, infectious molecular clones and chimeras of ZIKV MR766 and BeH819015 (BR15) strains were generated using the “infectious sub-genomic amplicons” method. Owing that the ancestral prototype MR766 strain has never been associated with epidemic in human, this strain was used as a reference in the experiments conducted to highlight epidemic strains features.

The ISA method is based on the electroporation or transfection of overlapping DNA fragments covering the entire genome in a permissive cell. Besides being fast and robust, it offers a multitude of other advantages. In the context of an epidemic crisis, this technique has allowed us to get and share ZIKV strains with other research teams without having to transport infectious materials. In addition to its safety advantage, the ISA method facilitates the rescue of infectious clones with high sequence fidelity by preventing cloning or propagation of cDNA in bacteria. Moreover, the use of overlapping fragments offers great flexibility

which especially enables the production of chimeric clones through the swap of a homologous fragment from another ZIKV strain. The application of ISA method for the study of ZIKV was the subject of a publication (Article No. 1) which describes the design strategy used to develop a reporter ZIKV clone expressing the green fluorescent protein (GFP).

II. ARTICLE N°1

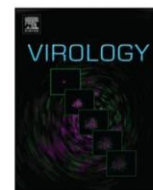
Virology 497 (2016) 157–162



Contents lists available at ScienceDirect

Virology

journal homepage: www.elsevier.com/locate/yviro



A robust method for the rapid generation of recombinant Zika virus expressing the GFP reporter gene



Gilles Gadea, Sandra Bos, Pascale Krejbich-Trotot, Elodie Clain, Wildriss Viranaicken, Chaker El-Kalamouni, Patrick Mavingui, Philippe Desprès*

Université de La Réunion, CNRS UMR 9192, INSERM U1187, IRD UMR 249, Unité Mixte 134 Processus Infectieux Insulaire Tropical (PIMIT), Plateforme Technologique CYROI, 97490 Sainte Clotilde, France

ARTICLE INFO

Article history:

Received 3 June 2016

Returned to author for revisions

13 July 2016

Accepted 18 July 2016

Available online 26 July 2016

Keywords:

Arbovirus

Emerging disease

Flavivirus

Zika virus

Molecular clones

Recombinant virus

GFP reporter

ABSTRACT

Zika virus (ZIKV) infection is a major public health problem with severe human congenital and neurological anomalies. The screening of anti-ZIKV compounds and neutralizing antibodies needs reliable and rapid virus-based assays. Here, we described a convenient method leading to the rapid production of molecular clones of ZIKV. To generate a molecular clone of ZIKV strain MR766^{NIID}, the viral genome was directly assembled into Vero cells after introduction of four overlapping synthetic fragments that cover the full-length genomic RNA sequence. Such strategy has allowed the production of a recombinant ZIKV expressing the GFP reporter gene that is stable over two culturing rounds on Vero cells. Our data demonstrate that the ZIKV reporter virus is a very reliable GFP-based tool for analyzing viral growth and measuring the neutralizing antibody as well as rapid screening of antiviral effect of different classes of inhibitors.

© 2016 Elsevier Inc. All rights reserved.

1. Introduction

Zika virus (ZIKV) is a mosquito-borne, enveloped RNA virus first discovered in Uganda in 1947 (Dick et al., 1952). ZIKV belongs to the *Flaviviridae* family, *Flavivirus* genus, and is related to medically important flaviviruses such as dengue (DENV), West Nile (WNV), yellow fever (YFV), and Japanese encephalitis (JEV) (Plourde and Boch, 2016; Musso and Gubler, 2016; Weaver et al., 2016). Flavivirus genomic RNA contains a single open reading frame, which is translated into a single large polyprotein that is subsequently cleaved into three structural proteins (C, prM/M and E) and seven non structural proteins NS1 to NS5 by cellular and viral proteases.

Until recently, ZIKV outbreaks were sporadic and self-limiting and ZIKV infection remained relatively less studied in view of its low case numbers as well as low clinical impact relative to other mosquito-borne flaviviruses. The first large epidemic was reported from Yap Island in 2007 followed by a major outbreak of its related disease, Zika fever, in French Polynesia in 2013 (Duffy et al., 2009; Roth et al., 2014). Since 2015, Brazil has become the epicenter of the current ZIKV epidemic, which has rapidly spread across the Americas and Caribbean (Gatherer and Kohl, 2015). It is now considered as major public health issue with the clusters of severe

congenital and neurological anomalies urging WHO to declare a Public Health Emergency of International Concern in 2016 (Sikka et al., 2016). Considering the significant increase in ZIKV threat, specific antiviral therapies and vaccines are urgently needed to control ZIKV-related diseases. The development of therapies for ZIKV requires both insights into the viral life cycle and strategies to identify potent antiviral inhibitors.

Virus reporter systems afford the ability to visualize and monitor viral expression inside the infected host cells (Ren et al., 2016). The development of flavivirus reverse technologies has allowed the construction of infectious full-length cDNA molecules containing reporter luciferase or green fluorescent protein (GFP) gene for both DENV and WNV (Pierson et al., 2005; Zou et al., 2011; Aubry et al., 2015). In the present study, we decided to generate a recombinant ZIKV expressing the reporter GFP gene using the reverse genetic method designed ISA (for Infectious-Subgenomic-Amplicons) (Aubry et al., 2014; De Wispelaere et al., 2015).

2. Results and discussion

To generate a molecular clone of ZIKV derived from Uganda 47 (MR766^{NIID}) strain, the full-length viral genome of 10,807 nucleotides was directly assembled into Vero cells after electroporation of the four overlapping synthetic fragments that encode

* Corresponding author.

E-mail address: philippe.despres@univ-reunion.fr (P. Desprès).

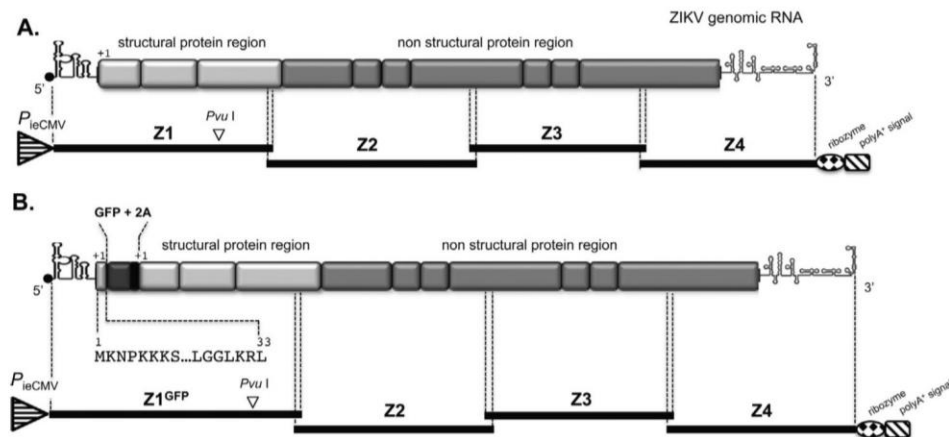


Fig. 1. Schematic representation of the strategy used to construct the molecular clone ZIKV-MR766^{NIID-MC} and its derived mutant ZIKV_{GFP}. Description of overlapping fragments Z1 (or Z1^{GFP}) to Z4 covering the full-length viral genomic RNA. The position of the unique *Pvu* I cleavage site located in the viral E gene is indicated. In (A), Z1 contains the CMV promoter upstream of the viral 5' NTR followed by the structural protein region. Z4 contains a ribozyme followed by a polyadenylation signal downstream of the viral 3' NTR. In (B), the Z1^{GFP} derived from Z1 contains the eGFP gene fused in frame to the first 33 amino acids of the ZIKV C protein. The 2A protease is immediately adjacent to the reporter eGFP gene. The eGFP-2A cassette is juxtaposed to the viral RNA sequence coding for the structural proteins starting with the first amino acid of C (+1) followed by the nonstructural proteins and ended by the 3'NTR.

the different parts of genomic RNA, according to the ISA method. The cDNA sequences have been previously amplified by PCR from plasmids in which synthetic fragments, quoted Z1 to Z4, were inserted (Fig. 1). Primers were designed so that the Z1 to Z4 fragments shared a sequence homology of 41 (Z1 and Z2), 39 (Z2 and Z3), and 34 (Z3 and Z4) nucleotides. The Z1 fragment contains the CMV promoter, which allows transcriptional initiation, immediately adjacent of the 5' non-translated region (NTR) followed by the structural protein region of MR766^{NIID} (Fig. 1A). A silent mutation at positions 1145–1150 located in the E gene that creates the unique restriction site *Pvu* I was introduced into the Z1 fragment. The Z4 fragment contains the hepatitis delta virus ribozyme followed by an SV40 poly(A) signal, which are juxtaposed to ZIKV 3' NTR (Fig. 1A). Five days post-electroporation, cell culture supernatant was collected and used to infect Vero cells in a first round of amplification (P1). Molecular clone of ZIKV-MR766^{NIID} (ZIKV-MR766^{NIID-MC}) was recovered 6 days later and amplified another 3 days on fresh Vero cells in order to grow final virus stocks P2 for further studies. A PCR fragment spanning the engineered *Pvu* I site into the E gene was amplified using RT-PCR from viral RNA (vRNA) extracted from ZIKV-MR766^{NIID-MC}. A similar PCR fragment derived from ZIKV strain PF-2013–18, which should be not cleavable by *Pvu* I, served as a negative control (Frumence et al., 2016). As shown in Fig. 2A, the RT-PCR product obtained from ZIKV-MR766^{NIID-MC}, but not ZIKV strain PF-2013–18, was readily cleaved by *Pvu* I indicating that it is a suitable genetic marker for the molecular clone of ZIKV strain MR-766. The infectivity of ZIKV-MR766^{NIID-MC} was determined by using a standard plaque-forming assay on Vero cells (Frumence et al., 2016). We noted that a majority of virus plaques was of large size (Fig. 2B). The P2 stock of ZIKV-MR766^{NIID-MC} grown on Vero cells reached an infectious titre up to 7.7 log PFU mL⁻¹. Viral growth was next studied on Vero cells infected at multiplicity of infection (MOI) of 1 (Fig. 2C). Virus progeny production increased by 1 log between 24 h and 48 h post-infection (p.i.) to reach almost 8 log PFU mL⁻¹ showing that the replication of molecular clone ZIKV-MR766^{NIID-MC} was greatly efficient in Vero cells.

We decided to produce a GFP-expressing ZIKV derived from molecular clone ZIKV-MR766^{NIID} (Fig. 1B). We used a strategy in which a reporter protein is expressed as an additional part of the structural protein region of flavivirus and then excised from the viral polyprotein by the viral 2A protease factor (Zou et al., 2011; Zhang et al., 2016). To generate a viable reporter ZIKV, the plasmid

pZ1^{GFP} was derived from pZ1 in which the eGFP reporter gene followed by the sequence encoding the protease 2A factor were fused in frame with the amino acids C-1 to C-33 of ZIKV (Fig. 1B) (Zhang et al., 2016). The N-terminal region of the C protein from ZIKV is thought to comprise a potential circularization sequence that is essential for flavivirus RNA replication (Clyde et al., 2008). In the pZ1^{GFP}, the complete coding region of ZIKV-MR766^{NIID-MC} was immediately adjacent to the C-terminus of 2A protease that generates the authentic N-terminus of the C protein.

To generate the GFP-expressing mutant of ZIKV-MR766^{NIID-MC} named ZIKV_{GFP}, the recombinant viral genome of 11,587 nucleotides was directly assembled in Vero cells after electroporation of fragments Z1^{GFP}, Z2, Z3, and Z4. The production of P1 and P2 stocks of ZIKV_{GFP} was made as previously. The PCR fragment spanning the *Pvu* I site into the E gene of ZIKV_{GFP} was readily cleaved by *Pvu* I showing that GFP-expressing mutant of ZIKV-MR766^{NIID-MC} retained the genetic marker (Fig. 2A). We found that the infectious titre of ZIKV_{GFP} stock P2 (6 log PFU mL⁻¹) was 1.5 log lower as compared to ZIKV-MR766^{NIID-MC}. The plaque morphology of ZIKV_{GFP} was different to that of the parent with a phenotype of small plaques (Fig. 2B). We noted that infection of Vero cells with the P2 of ZIKV_{GFP} or ZIKV-MR766^{NIID-MC} at the MOI of 1 resulted in similar virus progeny production at 24 h and 48 h p.i. (Fig. 2C). A rapid generation of wild-type variants could explain the high viral titers of ZIKV_{GFP} observed at P3. The issue regarding the genetic stability of the GFP-expressing mutant of ZIKV-MR766^{NIID-MC} is addressed later in our study.

The expression of GFP in Vero cells infected 48 h with ZIKV_{GFP} at the MOI of 1 was first analyzed by immunofluorescence (IF) assays (Fig. 2D). Infected cells were treated with a low concentration of Triton X-100 (0.01%) leading to a permeabilization of the plasma membrane alone and then incubated with anti-flavivirus E mAb 4G2 (Mertens et al., 2010). There was a marked immunostaining of the E protein in the vicinity of the surface of ZIKV-infected cells (Fig. 2D, ZIKV E). The GFP expression was clearly visualized in Vero cells positive for the ZIKV E protein (Fig. 2D). To study the subcellular distribution of GFP, cells were treated with 0.1% Triton X-100 and then incubated with a specific antibody directed against the ER-resident protein calnexin (CNX). At 48 h p.i., the GFP signal was mainly visualized within a distinct, large dot-like structure in the vicinity of the ER compartment (Fig. 2D, CNX). In the context of viral polyprotein expressed by ZIKV_{GFP}, the 2A protease ensures the release of the adjacent fusion

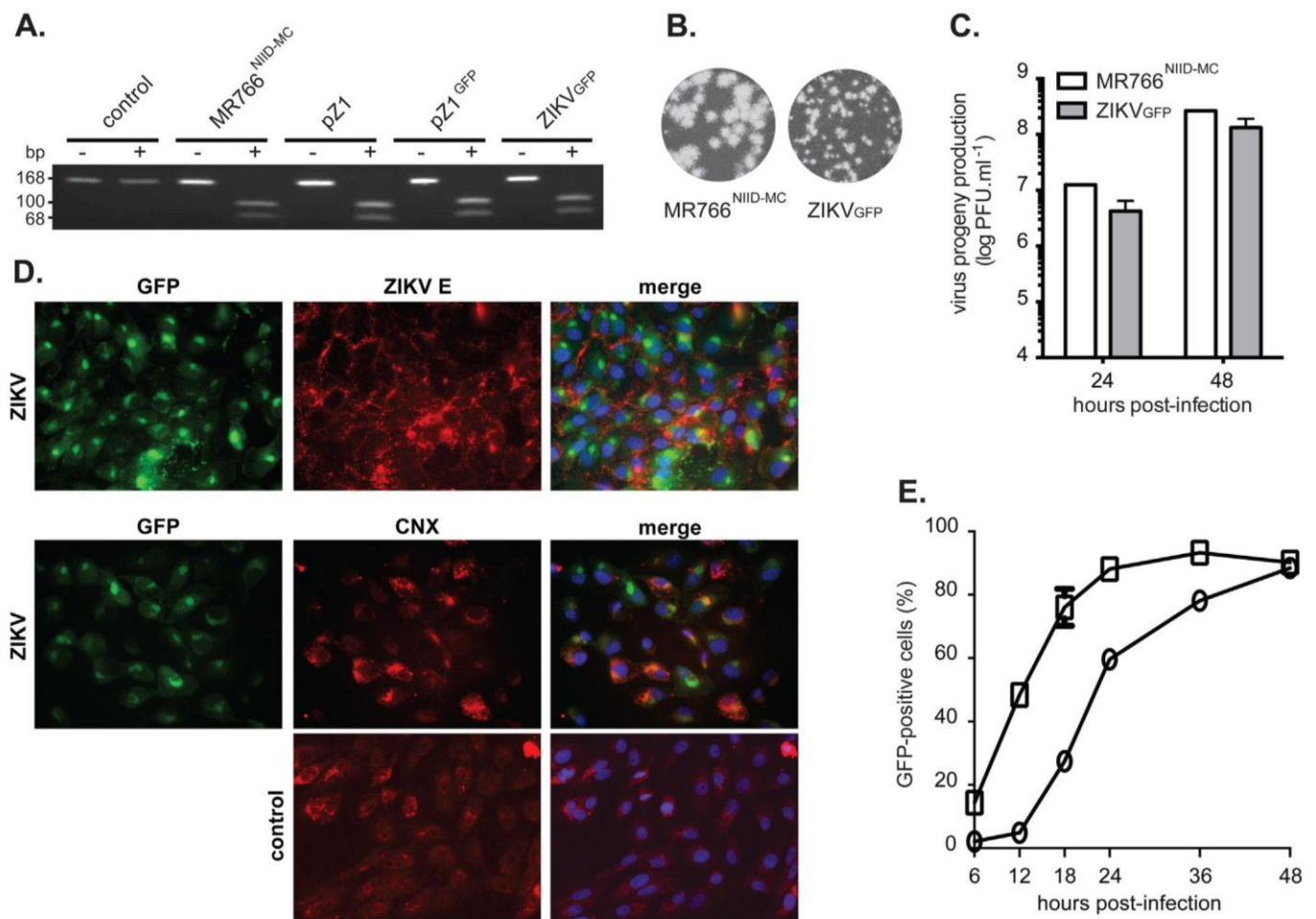


Fig. 2. Characterization of ZIKV-MR766^{NIID-MC} and ZIKV_{GFP}. *In (A)*, RNA was extracted from viral stocks and RT-PCR was performed to amplify a 168-nt fragment into the E gene surrounding the Pvu I cleavage site. The PCR products were subjected to digestion by Pvu I (+) or mock-treated (-). The wild-type ZIKV strain PF-2013-18 (control) served as a negative control for Pvu I cleavage. The expected sizes of the digestion products on a 2.2% agarose gel are indicated. *In (B)*, plaque morphology of ZIKV-MR766^{NIID-MC} and derived mutant ZIKV_{GFP} in Vero cells. *In (C)*, viral growth analysis on Vero cells. Cells were infected at the MOI of 1 and viral titers were determined at 24 h and 48 h p.i. *In (D)*, IF analysis of GFP expression in Vero cells infected with ZIKV_{GFP} or mock-infected (control). Fixed cells were treated 4 min with Triton X-100 at 0.01% (ZIKV E) or 0.1% (CNX) in PBS. The ZIKV E protein and the ER-marker CNX were immunostained with mAb 4G2 or anti-CNXX antibody, respectively. Nuclei were stained with DAPI. The ZIKV E protein or CNX (red), eGFP fluorescence (green), and nuclei (blue) were visualized by fluorescence microscopy. The same magnification of $\times 40$ is used throughout. *In (E)*, time-course analysis of GFP expression in Vero cells infected with ZIKV_{GFP} at MOI of 0.1 (open circle) or 1 (open box). FACS analysis of GFP fluorescence was performed on PFA-fixed cells at various times p.i. Error bars indicate the standard deviations of experiments in triplicate. (For interpretation of the references to color in this figure legend, the reader is referred to the web version of this article.)

protein between the segment (C-1 to C-33) of ZIKV C protein and GFP. The possible association of the N-terminal charged amino acids of C with the cytoplasmic side of the ER membrane could explain the subcellular distribution of GFP in infected cells (Markoff et al., 1997).

We assessed the capacity of ZIKV_{GFP} to grow in human and mosquito cells (Suppl. Fig. S1). Given that South Pacific epidemic ZIKV strain PF-2013-18 exhibited a high level of replication in human epithelial A549 cells (Frumence et al., 2016), we investigated whether the GFP-expressing mutant of ZIKV-MR766^{NIID-MC} has capability to replicate in A549 cells by IF analysis. The GFP expression was readily detected in ZIKV_{GFP}-infected A549 cells (Suppl. Fig. S1). Immunostaining assay with anti-E mAb 4G2 confirmed that GFP is suitable for the monitoring of ZIKV infection in A549 cells (Suppl. Fig. S1). We next analyzed the GFP expression in *Aedes* mosquito C6/36 cells infected 48 h with ZIKV_{GFP} at the MOI of 1. IF analysis detected GFP expression in ZIKV_{GFP}-infected C6/36 cells (Suppl. Fig. S1). Together these results showed that the GFP-expressing mutant of ZIKV-MR766^{NIID-MC} is also a reliable tool for the monitoring of ZIKV replication in human and mosquito cells.

To further validate ZIKV_{GFP}, the kinetic of GFP expression was examined in Vero cells infected with low (0.1) and high (1.0) MOI (Fig. 2E). FACS analysis showed that percentage of GFP-positive Vero cells increased with the time of infection to reach a plateau at 24 h (high MOI) or 48 h (low MOI) p.i. We determined whether increase of GFP signal during the time course of ZIKV_{GFP} infection was associated to an increase in vRNA replication (Suppl. Fig. S2). The production of intracellular vRNA in ZIKV_{GFP}-infected Vero cells was analyzed by quantitative real-time RT-PCR (RT-qPCR) using primer pair specific to the ZIKV E gene or eGFP-2A cassette. The couple of primers targeting the E gene showed that production of vRNA was markedly increased in ZIKV_{GFP}-infected Vero cells since 18 h p.i. (Suppl. Fig. S2; left). Accumulation of intracellular vRNA was also verified using the eGFP-2A cassette primer pair. This is consistent with the assumption that the increase of GFP expression is attributable to an increased production of intracellular vRNA in ZIKV_{GFP}-infected Vero cells. Altogether, these results demonstrate that the GFP-expressing mutant of ZIKV-MR766^{NIID-MC} is a reliable tool to monitor viral growth in host cells infected by ZIKV.

Since ZIKV is sensitive to the antiviral effect of Type-I interferon (IFN) (Frumence et al., 2016), we evaluated the antiviral effect of

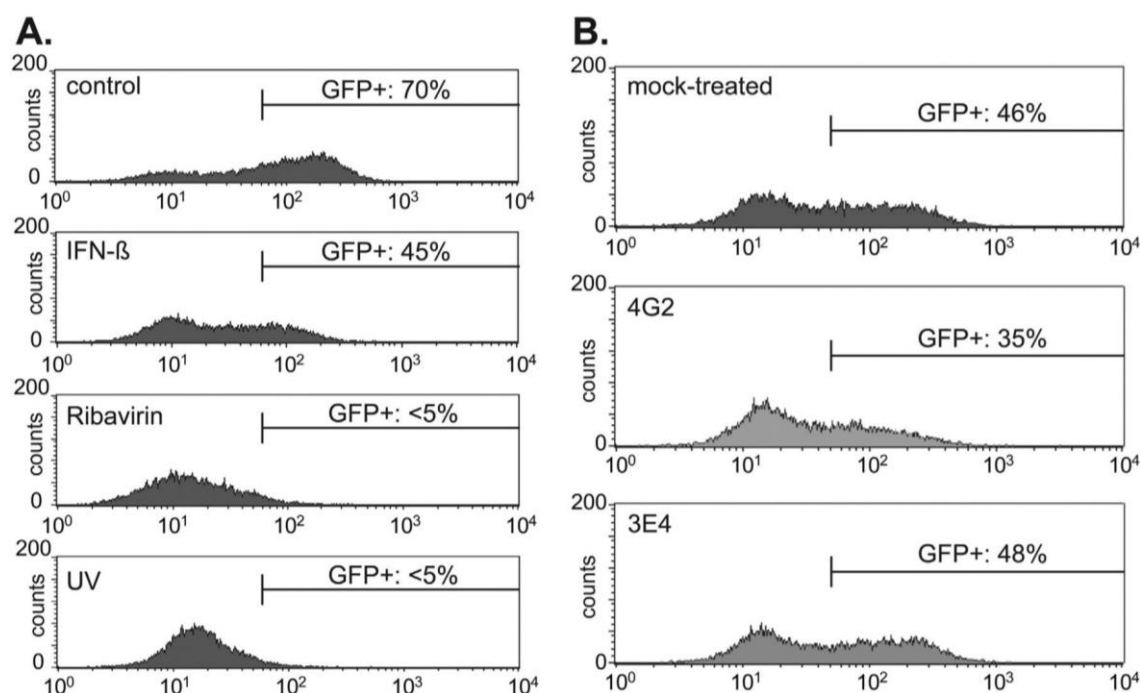


Fig. 3. Inhibition of ZIKV_{GFP} by IFN-β, ribavirin and neutralizing antibody. *In (A)*, the GFP fluorescence in Vero cells infected 24 h with ZIKV_{GFP} was examined by FACS analysis. Vero cells were treated with 10^5 UI mL⁻¹ of IFN-β 2 h prior virus infection (MOI of 0.1) or 100 μM ribavirin 2 h after virus exposure. UV-treated ZIKV_{GFP} served as a positive control. *In (B)*, ZIKV_{GFP} was incubated 2 h with 10 μg mL⁻¹ mAb 4G2 or anti-CHIK. E2 mAb 3E4 (negative control). Vero cells were infected 24 h with mixed virus-antibody and the GFP-positive cells were examined by FACS analysis.

IFN-β on ZIKV_{GFP} by FACS analysis (Fig. 3A). IFN-β treatment of Vero cells 2 h prior ZIKV_{GFP} infection resulted in a significant reduction of GFP-positive cells at 24 h p.i. (Fig. 3A). We next examined whether ZIKV_{GFP} was inhibited by the well-known antiviral inhibitor ribavirin as an analog of guanosine. At the high concentration of ribavirin (1 mM), the progeny production of ZIKV-MR766^{NIID-MC} was reduced at 24 h p.i. by 3 log confirming the potent antiviral effect of ribavirin against ZIKV (Zmurko et al., 2016). Addition of 100 μM ribavirin 2 h after ZIKV_{GFP} exposure resulted in a basal expression level of GFP at 24 h p.i. (Fig. 3A). Furthermore, we tested the neutralizing activity of mouse pan-flavivirus E mAb 4G2 on ZIKV_{GFP} (Fig. 3B). For neutralization test, ZIKV_{GFP} (4.5 log PFU) was mixed with mAb 4G2 (10 μg) for 2 h at 37 °C. The virus-antibody mix was assessed for GFP expression on Vero cells at 24 h p.i. The anti-Chikungunya E2 mAb 3E4 served as a negative control (Bréhin et al., 2008). Incubation of ZIKV_{GFP} with mAb 4G2 resulted in a reduction of GFP-positive Vero cells whereas 3E4 had no effect (Fig. 3B). Altogether, these results showed that ZIKV_{GFP} could be used as GFP-based assay to measure antiviral activity of different classes of inhibitors as well as capturing of neutralizing anti-ZIKV antibodies.

We mentioned earlier the possibility that GFP-expressing mutant of ZIKV-MR766^{NIID-MC} was unstable after a limited number of passages on Vero cells. First, we can exclude the possibility that the recovered ZIKV_{GFP} represented contamination with the wild-type fragment Z1 since the purified PCR product Z1^{GFP} was detected alone (Supplemental Fig. S3). To further the investigation, we decided to perform a continuous culturing ZIKV_{GFP} on Vero cells on four rounds, P1 to P4 (3–4 days by round), P1 being considered as the first viral stock after recovering the viral supernatants from Vero cells in which the fragments Z1^{GFP} to Z4 were introduced. To evaluate the stability of GFP gene, viral supernatants were collected after each round. These supernatants were used to infect Vero cells and the GFP fluorescence was tested by FACS analysis. As shown in Fig. 4A, the number of GFP-expressing cells was dramatically reduced from P3. RT-PCR analysis confirmed

that the eGFP gene was excluded from ZIKV-MR766^{NIID-MC} genomic RNA from P3 (Fig. 4B). Thus, the P2 stock of ZIKV_{GFP} is a powerful GFP-based assay for monitoring viral replication inside the infected cells.

Recently, Shan et al. (2016) described an infectious cDNA clone of ZIKV and derived mutant with a luciferase gene reporter. In the present study, we demonstrated that the ISA method is a very well suited genetic inverse method allowing the rapid implementation of molecular clones of ZIKV. Furthermore, we have easily generated a recombinant live ZIKV expressing GFP with a genomic stability on at least two passages on Vero cells. We demonstrated that our mutant ZIKV_{GFP} is suitable for the study of the dynamics of viral replication within the host cells as well as screening of neutralizing antibodies and antiviral compounds. We believe that both ZIKV-MR766^{NIID-MC} and ZIKV_{GFP} are reliable tools for further investigation on viral determinants that contribute to the pathological effects of ZIKV infection. Such molecular clones of ZIKV will be helpful to the understanding of severe congenital brain malformations and neurological manifestations in humans (Cao-Lor-meau et al., 2016; Quick et al., 2016).

3. Methods

3.1. Cells and reagents

Vero cells (ATCC, CCL-81) were cultured in Dulbecco's modified Eagle's medium (DMEM), supplemented with 10% heat-inactivated fetal bovine serum (FBS). Interferon-β was purchased from Peprotech. Ribavirin was purchased from Sigma. The mouse anti-pan flavivirus envelope E protein mAb 4G2 and anti-CHIK. E2 mAb 3E4 were produced and purified by RD Biotech (Besançon, France). The rabbit anti-calnexin antibody was purchased from Santa-Cruz. Donkey anti-mouse Alexa Fluor 594 IgG (H+L) antibody was purchased from Invitrogen.

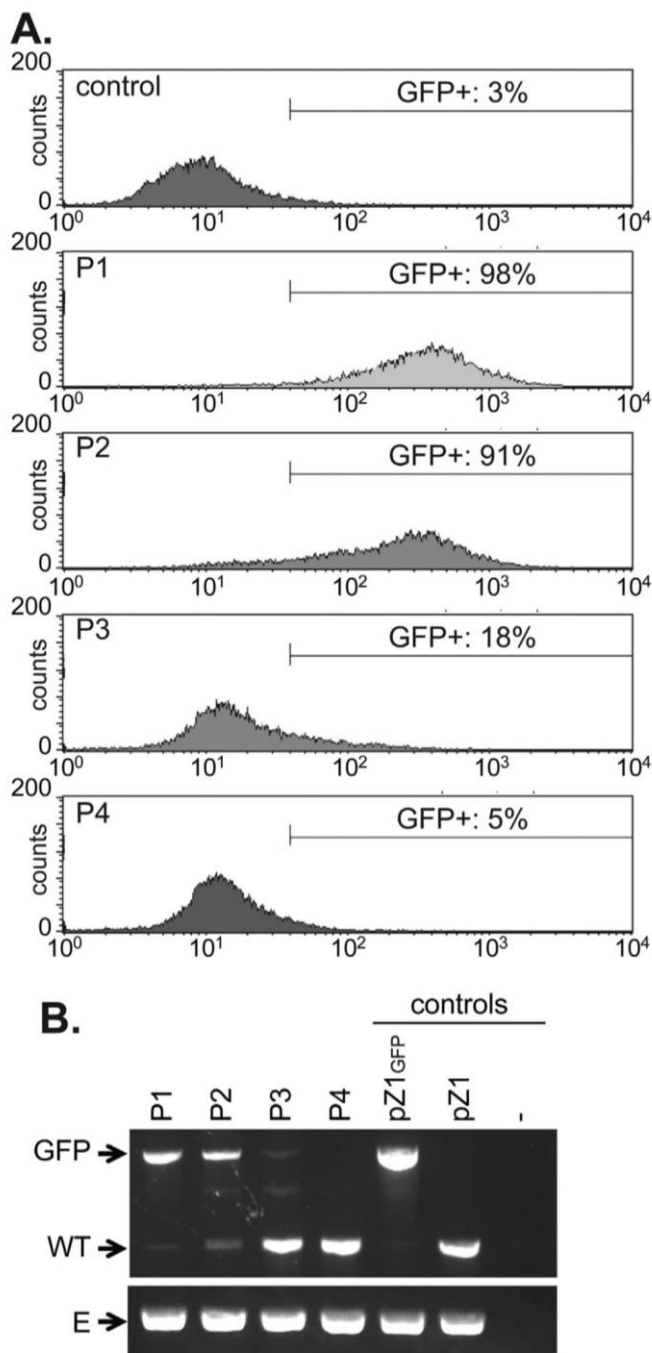


Fig. 4. Stability of GFP reporter gene in ZIKV_{GFP}. In (A), ZIKV_{GFP} was serially passaged on Vero cells and viral supernatants recovered from P1 to P4 were tested for GFP fluorescence 24 h p.i. by FACS analysis. In (B), viral RNA was extracted from viral supernatant recovered from P1 to P4 and RT-PCR was performed with a couple of primers surrounding the eGFP-2A cassette. As controls of fragment sizes, plasmids pZ1 and pZ1-GFP were amplified by PCR using the same primer pair. As a positive control, RT-PCR assay on viral RNA was performed with primers locating at the E gene. The PCR products were analyzed on 0.8% (GFP/WT) or 2% (E) agarose gels.

3.2. Molecular clone design of ZIKV

The construction of molecular clone ZIKV-MR766^{NIID} was based on the sequence of ZIKV strain MR766 Uganda 47-NIID (Genbank access # LC002520) using the ISA method allowing the rapid generation of molecular clones of flaviviruses (Aubry et al., 2014; De Wispelaere et al., 2015). Four synthetic genes Z1 to Z4 covering

the full-length genome of ZIKV strain MR766-NIID were synthesized and cloned into plasmid pUC57 by GeneCust (Luxembourg). The first synthetic fragment (Z1) was designed to contain the ZIKV structural proteins. A cytomegalovirus (CMV) promoter sequence driving the expression of viral fragment from nucleotides 1–2252 of genomic RNA was included in Z1. The three other synthetic genes comprised the portions of the genome coding for the non-structural proteins from nucleotides 2210–5616 (Z2), 5577–8201 (Z3) and 8167–10,801 (Z4) (Fig. 1A). Also, Z4 contained the complete 3' UTR sequence of ZIKV strain MR766-NIID immediately adjacent to the hepatitis delta virus ribozyme and was followed by a simian virus 40 polyadenylation sequence. The Z1 to Z4 sequences cloned into their respective plasmids, pZ1 to pZ4, were amplified by PCR using Phusion High-Fidelity DNA polymerase (Thermo Scientific) and primer pairs, which are listed in Supplemental Table 1. The PCR program is the following: initial PCR activation step at 98 °C (30 s), 35 cycles of denaturation at 98 °C (10 s), annealing at 60 °C (20 s) and elongation at 72 °C (2 min), ended by final elongation step at 72 °C (5 min). The PCR products were purified using RNA mini spin purification kit (QIAGEN) according to the manufacturer's instructions.

The molecular strategy allowing the insertion of a reporter gene in the flavivirus structural proteins region was already described for DENV and WNV (Zou et al., 2011; Zhang et al., 2016). The Z1 sequence was used for the design of a new synthetic fragment Z1^{GFP} that contains the eGFP reporter gene derived from the plasmid pEGFP-N1 (Clontech) followed by the sequence encoding the porcine teschovirus 2A protease factor. The cassette eGFP-2A was fused in-frame downstream the first 99 nucleotides encoding the N-terminal part of C protein from ZIKV strain MR766-NIID (Fig. 1B). The cassette eGFP-2A was followed by the ZIKV structural protein sequence. In this construct, 2A is designed to release the GFP cassette from the N-terminus of C. The Z1^{GFP} sequence was amplified by PCR from plasmid pZ1^{GFP} as described above.

3.3. Rescue of ZIKV molecular clones

To produce an infectious reconstituted ZIKV, 5 µg of each purified PCR products, Z1 or Z1^{GFP} to Z4, were directly introduced within Vero cells as previously described with modifications (De Wispelaere et al., 2015). Vero cells (5.10⁶) were resuspended in 400 µL cold PBS 1X buffer and electroporated by two successive pulses of 100 V, 50 µF for 0.9–1.3 ms and 450 V, 50 µF for 0.6–0.9 ms. The electroporated cells were then transferred to a culture flask containing pre-heated growth medium. After 5 days, cell supernatants were recovered and used to infect a flask of 80% confluent Vero cells. When cytopathic effect was apparent (2–7 days), the virus supernatants were clarified and stored at –80 °C as virus stock passage 1 (P1). A second passage on Vero cells (P2) was used for the studies of ZIKV infection.

3.4. Immunofluorescence assay

Cells grown on coverslips were fixed with 3.7% paraformaldehyde (PFA) at room temperature for 10 min. For permeabilization, fixed cells were incubated with Triton X-100 in PBS for 4 min. Cells were incubated overnight with primary antibody PBS supplemented with bovine serum albumin (BSA). Donkey anti-mouse Alexa Fluor 594 IgG was used as secondary antibody. Nucleus morphology was revealed by DAPI staining. The coverslips were mounted with Vectashield (Vector Labs), and fluorescence was observed using a Nikon Eclipse E2000-U microscope. Images were captured and processed using a Hamamatsu ORCA-ER camera and the imaging software NIS-Element AR (Nikon).

3.5. Flow cytometry assay

To detect GFP-expressing cells, cells were fixed with 3.7% PFA in PBS at room temperature for 10 min. Fixed cells were subjected to a flow cytometric analysis using FACScan flow cytometer (Becton Dickinson). The percentage of GFP-positive cells was determined using FlowJo software.

3.6. Plaque forming assay

Viral titre was determined by a standard plaque-forming assay as previously described with minor modifications (Frument et al., 2016). Briefly, Vero cells grown in 24-well culture plate were infected with tenfold dilutions of virus samples for 2 h at 37 °C and then incubated with 0.4% carboxymethylcellulose (CMC) for 4 days. The cells were fixed by 3.7% PFA in PBS and stained with 0.5% crystal violet in 20% ethanol. Viral titers were expressed as plaque-forming units per mL (PFU mL⁻¹).

3.7. RT-PCR on viral RNA

Genomic RNA was extracted from viral supernatants using Trizol Reagent (Life technologies). RT-PCR was performed using M-MLV Reverse Transcriptase (Invitrogen) and the GoTaq[®] enzyme (Promega) according to manufacturer's recommended procedures. We used the primer pair Z1-E-F and Z1-E-R (listed in Supplemental Table 1) to amplify the 5' region of the genomic RNA between the nucleotides 1046–1213 from ZIKV strain MR766^{NIID-MC} or PF-2013–18. The couple of primers Z1–5'NTR-F and Z1-E-R (listed in Supplemental Table 1) was used to amplify the 5' region of the genomic RNA between the nucleotides 32–2092 from the ZIKV_{GFP} clone. Viral RNA was amplified by RT-PCR with the following program: initial PCR activation step at 95 °C (2 min), 35 cycles of denaturation at 95 °C (30 s), annealing at 62 °C (2 min) and elongation at 72 °C (30 s), ended by final elongation step at 72 °C (5 min). The samples were resolved by agarose gel electrophoresis. Alternatively, the resulting PCR products were purified as described above and then subjected to enzymatic digestion by *Pvu* I. RT-qPCR was performed using M-MLV Reverse Transcriptase and the GoTaq[®] qPCR Master Mix (Promega). All steps were conducted according to manufacturer's instructions. The qPCR data sets were analyzed using the $\Delta\Delta C_t$ method and the results were normalized to Human Glyceraldehyde 3-phosphate dehydrogenase (GAPDH), which was used as internal control. The primers used in this study are listed in Supplemental Table 1.

Acknowledgments

We are grateful to ML. Gougeon, M. de Wispelaere, M. Roche, and E. Frumence, for helpful discussion and assistance during the course of this work. This research was supported in part by the grant ZIKAVAx from the INSERM-transfert, France. EC is supported by a grant Dired from the Conseil Général de La Réunion, France.

Appendix A. Supplementary material

Supplementary data associated with this article can be found in the online version at <http://dx.doi.org/10.1016/j.virol.2016.07.015>.

References

Aubry, F., Nougairède, A., de Fabritus, L., Querat, G., Gould, E.A., de Lamballerie, X., 2014. Single-stranded positive-sense RNA viruses generate in days using

infectious subgenomic amplicons. *J. Gen. Virol.* 95, 2462–2467.

Aubry, F., Nougairède, A., Gould, E.A., de Lamballerie, X., 2015. Flavivirus reverse genetic systems, construction techniques and applications. *Antivir. Res.* 114, 67–85.

Bréhin, A.C., Rubrecht, L., Navarro-Sanchez, M.E., Maréchal, V., Frenkiel, M.P., Lalpud, P., Laune, D., Sall, A.A., Desprès, 2008. Production and characterization of mouse monoclonal antibodies reactive to Chikungunya envelope E2 glycoprotein. *Virology* 371, 185–195. <http://dx.doi.org/10.1016/j.virol.2007.09.028>.

Cao-Lormeau, M., Blake, A., Mons, S., Lastère, S., Roche, C., Vanhomwegen, J., Dub, T., Baudouin, L., Teissier, A., Lare, P., Vial, A.L., Decam, C., Choumet, V., Halstead, S., Willison, H.J., Musset, L., Manuguerra, J.C., Desprès, P., Fournier, E., Mallet, H.P., Musso, D., Fontanet, A., Neil, J., Ghawché, F., 2016. Guillain-barré syndrome outbreak associated with Zika virus infection in French Polynesia: a case-control study. *Lancet*. <http://dx.doi.org/10.1016/j.lancet.2016.05.048>.

Clyde, K., Barrera, J., Harris, E., 2008. The capsid-coding region hairpin element (cHP) is a critical determinant of dengue virus and West Nile virus RNA synthesis. *Virology* 379, 314–323. <http://dx.doi.org/10.1016/j.virol.2008.06.034>.

De Wispelaere, M., Frenkiel, M.P., Desprès, P., 2015. A Japanese encephalitis virus genotype 5 molecular clone is highly neuropathogenic in a mouse model: impact of the structural protein region on virulence. *J. Virol.* 89, 5862–5875. <http://dx.doi.org/10.1128/JVI.00358-15>.

Dick, G.W.A., Kitchen, S.F., Haddock, A.J., 1952. Zika Virus (I). Isolations and serological specificity. *Trans. R. Soc. Trop. Med. Hyg.* 46, 509–520. [http://dx.doi.org/10.1016/0035-9203\(52\)90042-4](http://dx.doi.org/10.1016/0035-9203(52)90042-4).

Duffy, M.R., Chen, T.H., Hancock, W.T., Powers, A.M., Kool, J.L., Lanciotti, R.S., Pre-trick, M., Marfel, M., Holzbauer, S., Dubray, C., Guillaumot, L., Griggs, A., Bel, M., Lambert, A.J., Laven, J., Kosoy, O., Panella, A., Biggerstaff, B.J., Fischer, M., Hayes, E.B., 2009. Zika virus outbreak on Yap Island, Federated States of Micronesia. *N. Engl. J. Med.* 360, 2536–2543. <http://dx.doi.org/10.1056/NEJMoa0805715>.

Frument, E., Roche, M., Krejbich-Trotot, P., El-Kalamouni, C., Nativel, B., Rondeau, P., Missé, D., Gadea, G., Viranackien, W., Desprès, P., 2016. The South Pacific epidemic strain of Zika virus replicates efficiently in human epithelial A549 cells leading to IFN- β production and apoptosis induction. *Virology* 493, 217–226. <http://dx.doi.org/10.1016/j.virol.2016.03.006>.

Gatherer, D., Kohl, A., 2015. Zika virus: a previously slow pandemic spreads rapidly through the Americas. *J. Gen. Virol.* <http://dx.doi.org/10.1099/jgv.0.000381>.

Markoff, L., Falgout, B., Chang, A., 1997. A conserved internal hydrophobic domain mediates the stable membrane integration of the dengue virus capsid protein. *Virology* 233, 105–117.

Mertens, E., Kajaste-Rudnitski, A., Torres, S., Funk, A., Frenkiel, M.P., Iteanu, I., Khromykh, A., Desprès, P., 2010. Viral determinants in the NS3 helicase and 2K peptide that promote West Nile virus resistance to antiviral action of 2',5'-oligoadenylate synthetase 1b. *Virology* 399, 176–185.

Musso, D., Gubler, D.J., 2016. Zika virus. *Clin. Microbiol. Rev.* <http://dx.doi.org/10.1128/CMR.00072-15>.

Pierson, T.C., Diamond, M.S., Ahmed, A.A., Valentine, L.E., Davis, C.W., Samuel, M.A., Hanna, S.L., Puffer, B.A., Doms, R.W., 2005. An infectious West Nile virus that expresses a GFP reporter gene. *Virology* 334, 28–40. <http://dx.doi.org/10.1016/j.virol.2005.01.021>.

Plourde, A.R., Boch, E.M., 2016. A literature review of Zika virus. *Emerg. Infect. Dis.* <http://dx.doi.org/10.3201/eid2207.151990>.

Quick, K.M., Bowen, J.R., Johnson, E.L., Mc Donald, C.E., Hauiliang, M., O'Neal, J.T., Rajakumar, A., Wrammert, J., Rimawi, B.H., Pulendran, B., Shinazi, R.F., Chakraborty, R., Suthar, M.S., 2016. Zika virus infects human placenta macrophages. *Cell Host Microbe* <http://dx.doi.org/10.1016/j.chom.2016.05.015>.

Ren, L., Peng, Z., Chen, X., Ouyang, H., 2016. Live cell reporter systems for positive-sense single strand RNA viruses. *Appl. Biochem. Biotechnol.* 178, 1567–1585. <http://dx.doi.org/10.1007/s12010-015-1968-5>.

Roth, A., Mercier, A., Lepers, C., Hoy, D., Duituturaga, S., Benyon, E., Guillaumot, L., Souarès, Y., 2014. Concurrent outbreaks of dengue, chikungunya and Zika virus infections - an unprecedented epidemic wave of mosquito-borne viruses in the Pacific 2012–2014. *Eurosurveillance* 19, 20929. <http://dx.doi.org/10.2807/1560-7917.ES2014.19.41.20929>.

Shan, C., Xie, X., Muruato, A.E., Rossi, S.L., Roundy, C.M., Azar, S.R., Yang, Y., Tesh, R. B., Bourne, N., Barrett, A.D., Vasilakis, N., Weaver, S.C., Shi, P.Y., 2016. An infectious cDNA clone of Zika Virus to study viral virulence, mosquito transmission, and antiviral inhibitors. *Cell Host Microbe* 0. <http://dx.doi.org/10.1016/j.chom.2016.05.004>.

Sikka, V., Chattu, V.K., Popli, R.K., Galwankar, S.C., Kelkar, D., Sawicki, S.G., Stawicki, S.P., Papadimos, T.J., 2016. The emergence of Zika Virus as a global health security threat: a review and a consensus statement of the INDUSEM joint working group (JWG). *J. Glob. Infect. Dis.* 8, 3–15. <http://dx.doi.org/10.4103/0974-777X.176140>.

Weaver, S.C., Costa, F., Garcia-Blanco, M.A., Ko, A.L., Ribeiro, G.S., Saade, G., Sji, P.Y., Valisakis, N., 2016. Zika virus: History, emergence, biology and prospects for control. *Antivir. Res.* 130, 69–80. <http://dx.doi.org/10.1016/j.antiviral.2016.03.010>.

Zhang, P.T., Shan, C., Li, X.D., Liu, S.Q., Deng, C.L., Ye, H.Q., Shang, B.D., Shi, P.Y., LV, M., Shen, B.F., Qin, C.F., Zhang, B., 2016. Generation of a recombinant West Nile virus stably expressing the Gaussia luciferase for neutralization assay. *Virus Res.* 211, 17–24. <http://dx.doi.org/10.1016/j.virusres.2015.09.015>.

Zmurko, J., Marques, R.E., Schols, D., Verbeken, E., Kaptein, S.J., Neyts, J., 2016. The viral polymerase inhibitor 7-Deaza-2'-C-Methyladenosine is a potent inhibitor of in vitro Zika virus replication and early disease progression in a robust mouse infection model. *PLoS Negl. Trop. Dis.* e0004695.

Zou, G., Xu, H.Y., Qing, M., Wang, Q.Y., Shi, P.Y., 2011. Development and characterization of a stable luciferase dengue virus for high-throughput screening. *Antivir. Res.* 91, 11–19. <http://dx.doi.org/10.1016/j.antiviral.2011.05.001>.

PART II:

CONTRIBUTION OF ZIKA VIRUS
STRUCTURAL PROTEINS

I. FEATURES OF ZIKA VIRUS STRUCTURAL PROTEINS

Phylogenetic analyses of Zika strains revealed that amino acid changes have occurred as the virus emerged from Africa and progressively spread to Asia, to ultimately cause outbreaks¹. Most of these changes are conserved in ZIKV epidemic strains, and thereby probably supported its adaptation to human host and enhanced virulence. These genetic changes arose throughout the entire coding sequence of the genome, with the exception of the sequence coding for the NS4A protein, and more rarely in the non-coding regions¹. Nevertheless, the structural proteins were subject to a higher amino acid substitution rate (proportional to their length) and harbor remarkable genetic changes affecting ZIKV envelope and prM proteins. Structural proteins contribute to virus particle assembly and define virion infectivity. During the different stages of virus replication, structural proteins are mostly involved in virus entry and morphogenesis. In the following paragraph the features of Flavivirus structural proteins will be discussed in the light of the mutations observed in the epidemic strains and their potential impact on ZIKV pathogenicity

I.1. Capsid

Flavivirus capsid is a highly basic protein of ~12 kDa². During the viral cycle, the capsid proteins assemble around the viral genome to form the nucleocapsid. However, a growing number of studies suggests that the flavivirus capsid can also be associated to functions that go beyond its classical structural role, including inhibition of RNA silencing in mosquitoes^{3,4}.

The nascent capsid form contains a hydrophobic C-terminal tail that serves as a signal peptide for the ER translocation of prM. This anchor, of variable size, is first cleaved by the NS2B-3 viral protease at the "capsid dibasic-site" located upstream of the signal peptide, and then by a signal peptidase. This two-step cleavage is important for the efficient processing of prM and the preservation of its chaperone function towards the E protein. Inhibition of viral protease-mediated cleavage or mutation of the signal peptide jeopardizes viral growth and virion infectivity⁵. Despite the low C protein sequence homology, the overall structure of the mature capsid is very conserved among flaviviruses². Capsid

proteins form a twofold symmetric dimer with each monomer containing four α helices interspersed with loops. The "top" layer of the capsid is a hydrophobic membrane-binding interface, while the surface of the "bottom" layer, rich in arginine residues and positively charged under physiological pH, ensures interaction with the virus genome⁶.

Overall, ZIKV capsid has a structure similar to other flaviviruses, albeit closer to WNV capsid⁶. Variations are mainly due to conformational discrepancies in the N terminal region. ZIKV capsid contains a very short $\alpha 1$ helix but a longer pre- $\alpha 1$ loop, which unlike in DENV, are perpendicular to the $\alpha 2$ helix⁶. This conformation results in the formation of tight C protein homodimers due to an extended dimerization interface. Such unique pre- $\alpha 1$ loop creates a hydrophilic site in ZIKV capsid hydrophobic "top" layer which can impact on the binding to the biological membrane⁶. African and Asian ZIKV strains differ in 4 amino acid substitutions within the capsid sequence. Two of these mutations are found in the pre- $\alpha 1$ loop (S25N

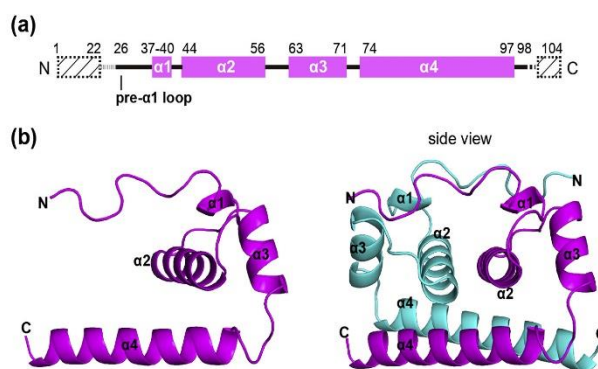


Figure 23: Overall structure of ZIKV C protein

(a) Schematic diagram of the ZIKV C protein organization. Black and gray dashed lines denote regions unresolved in the reconstruction and regions beyond the construct, respectively. (b) Ribbon representation of ZIKV C structure showing the separated monomer and dimer. One monomer is colored in magenta, and the other is colored in cyan. (Figure and caption from Shang et al., 2018)

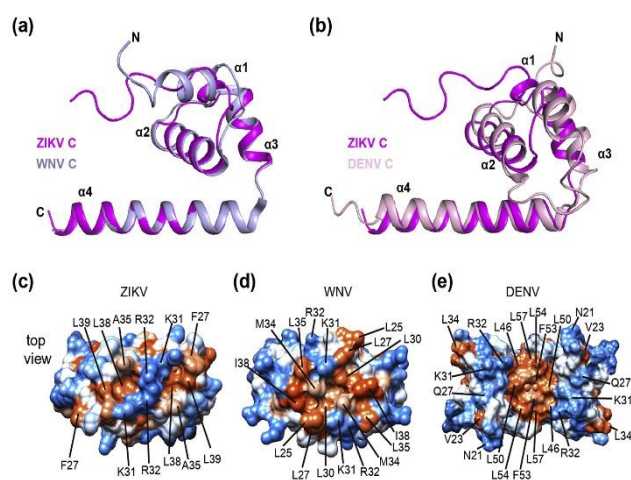


Figure 24: Comparison of ZIKV C with other known flavivirus C structures

(a) Superimposed structures in ribbon representation of C proteins from ZIKV (magenta) and WNV (grey) or (b) DENV (pink). The hydrophobicity surface of C proteins from (c) ZIKV, (d) WNV and (e) DENV in the top view. Molecular surfaces are colored according to their hydrophobicity with blue, white and orange corresponding to the most hydrophilic, neutral and hydrophobic patches, respectively.

(Figure and caption from Shang et al., 2018)

and F27L) while two other ones are located in the capsid dibasic-site (R101K) and the signal peptide (I110V). Nevertheless, since the paired residues share the same properties, it is likely that these changes only have a minor impact on ZIKV biology.

I.2. Pr and Membrane

The prM protein (~ 26 kDa) is the glycosylated precursor of the structural protein M that is embedded in the envelope of mature virions². During the synthesis of the viral proteins, prM is translocated into the ER via the signal sequence of the capsid. The N-terminal region of prM ("pr" domain) contains one to three glycosylation sites (N70 in ZIKV) and six highly conserved cysteine residues which stabilize its structure². The C-terminal region has two transmembrane spanning domains which contain a stop transfer sequence and a signal sequence that anchor prM to the ER membrane and translocate the E protein into its luminal side. prM folds rapidly after the appropriate proteolytic cleavages and assists in the proper folding of E protein. In the lumen of the ER, membrane-anchored prM and E associate to form a prM-E heterodimer and multimeric forms of prM-E compose immature virus particles as part of the viral envelope².

I2.1. The role of prM in the maturation process

The prM protein is the guarantor protein of virion infectivity and integrity during the transport of the immature virus particle into the secretory pathway. It acts as a pH-sensitive switch that can toggle its conformation according to the environmental pH⁷. One of its main functions is to regulate the oligomeric state of E proteins by preventing them from undergoing premature fusogenic rearrangement and fusion during the transit of the virion through the exocytic pathway. This function is partly provided by the "pr" domain of prM and a set of prM-E pH-dependent interactions which vary with virion progression. Following budding in the ER (neutral pH), immature viral particles exhibit a spiky surface. Each spike consists of a trimer of prM-E heterodimers in which the "pr" domain sits at the external tip of the E protein, where it forms a shield that protects the fusion peptide from the cellular environment. In this oligomeric state, the domains "pr", are the main contact links between the three prM-E heterodimers⁸.

This conformation is stable at neutral pH and causes steric hinderance that blocks the prM cleavage site before entering the TGN². Virions transit through acid compartments of the TGN leads to a reorganization of the E proteins which then lie flat to the virus surface. During this rearrangement the domain "pr" remains atop the fusion loop whereas the furin cleavage site is exposed. After prM cleavage, "pr" domain does not immediately dissociate from the mature viral particle but keeps its position until the virion is secreted. This time lag is due to the pr-E junction which consists of complementary electrostatic patches that break upon exposure to the neutral pH of the extracellular medium^{9,10}.

I2.2. Particle heterogeneity

The extent of virion maturation may vary depending on the expression level of furin in infected cell or amino-acid variations in sequence corresponding to pr-M cleavage site¹¹. As a result, a partial maturation takes place resulting in the production of an ensemble of structurally different virions. Indeed, when maturation is not achieved, the neutral pH of extracellular medium turns the prM-E heterodimers back their spiky conformation. Virions thus exhibit a “mosaic” lattice, composed of both mature and immature parts, that allow them to triggered endosomal

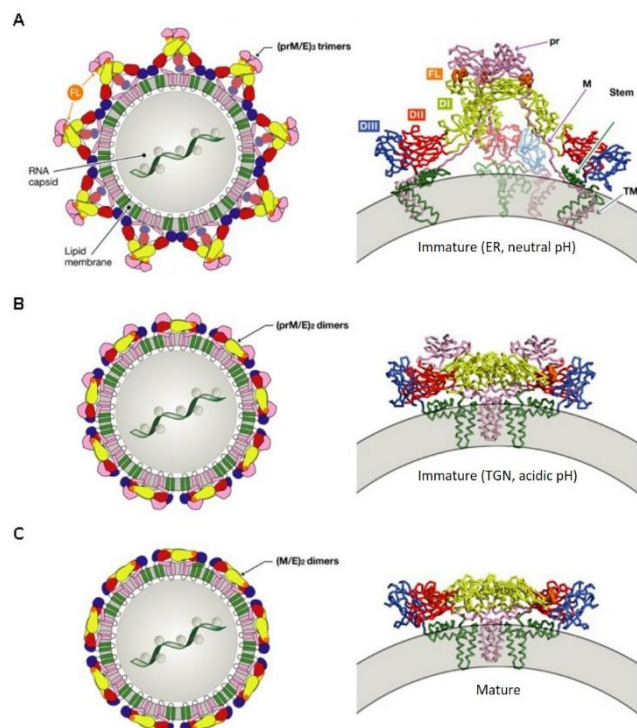


Figure 25: Flavivirus particle at different maturation stages

Protein E is colored according to domains: red, yellow, blue, and green for domains I, II, III, and stem/TM (transmembrane anchor), respectively. The fusion loop is highlighted in orange, and prM/M (including its TM region) is shown in pink. The viral membrane is represented in gray. (A) The immature flavivirus particle as it buds in the ER of the infected cells. Right: A single (prM/E)3 spike is displayed as. (B) The immature flavivirus particle after exposure to the acidic pH of the trans-Golgi network, where the trimeric spikes dissociate and the 180 prM/E heterodimers re-associate into 90 (prM/E)2 dimers. (C) The mature flavivirus particle with 90 (M/E)2 dimers. (Figure and caption adapted from Rey et al., 2017a)

membrane fusion and use different attachment factors and/or receptor to mediated their entry^{11,12}. Such “inefficient” maturation is a typical feature of Flaviviruses, with attested variability including among strains of the same viral species. For instance, DENV is particularly prone to the production of partially mature particles, with a prM content that can be as high as 50% in DENV-2. This singularity is associated with the fact that DENV has evolved a sub-optimal furin cleavage motif, with a conserved acidic residue (D/E) at position P3 where other flaviviruses mainly have a serine (S)^{13,14}. This low maturation extent seems critical for the maintenance of the virus in its environment^{11,13}. Therefore, it is likely that some of the particles in the cloud are more efficient for the infection of different cell type and overcome the limitation imposed by the dual-host tropism of arboviruses. This can reflect the fact that heterogeneous population of particles act synergistically in order to enhance viral tropism and fitness, as the viral genome quasi-species does. Furthermore, partially mature particles have been involved in antibody-dependent enhancement of infection due to possible modulation of E-related antigenicity due to the presence of uncleaved prM forms in virus particles or after binding of specific prM antibodies¹⁵.

12.3. Feature of ZIKV prM

The furin cleavage motif is conserved among ZIKV strains. Nevertheless, the pioneering study in ZIKV structure characterization revealed the presence of particles that, although relatively smooth in appearance, displayed imperfections on their surface¹⁶. If the extent of these imperfections has not been yet assessed, it suggests that ZIKV infection leads to the production of "mosaic" particles whose biological consequences are yet up to be elucidated.

Besides, the comparative analysis of ZIKV sequences revealed that a striking concentration of mutations occurred in prM coding sequence since its discovery in Uganda. Indeed, African strains differ from the ancestral Asian strain (Malaysia 1966) by 4 amino-acid substitutions, including remarkable changes at A26P and H35Y which induce drastic modifications. The first epidemic strain (Micronesia) harbor another mutation (V31M) that is conserved in ZIKV strains since 2007. Finally, an additional mutation is found in the prM sequence of ZIKV strains from the Pacific and Americans at position 17 (S17N). Interestingly, these

seven amino acid substitutions occurred in the "pr" domain of the prM and predominantly cluster at the top of the spikes formed by the prM-E heterodimers of immature viral particles at a neutral pH¹¹.

As a consequence, these mutations can result in a different folding of prM which can display difference in pH-sensitivity and affect its protective function toward the fusion peptide of the E. Moreover, given the production of partially mature particle, this amino-acid divergence can further influence interactions with cellular receptor as well as interactions with the immune system.

I.3. Envelope

The E protein has a molecular weight of ~50 kDa which varies according to the number of glycosylation sites it contains^{2,17}. Like the prM protein, it is translocated in the ER during the processing of structural proteins where it remains membrane-anchored via a double membrane-spanning domain located at its C-terminal anchor. E protein is the main protein exposed on the virion surface and plays a fundamental role in flavivirus life cycle. As a class II fusion protein (see below), E protein mediates both receptor

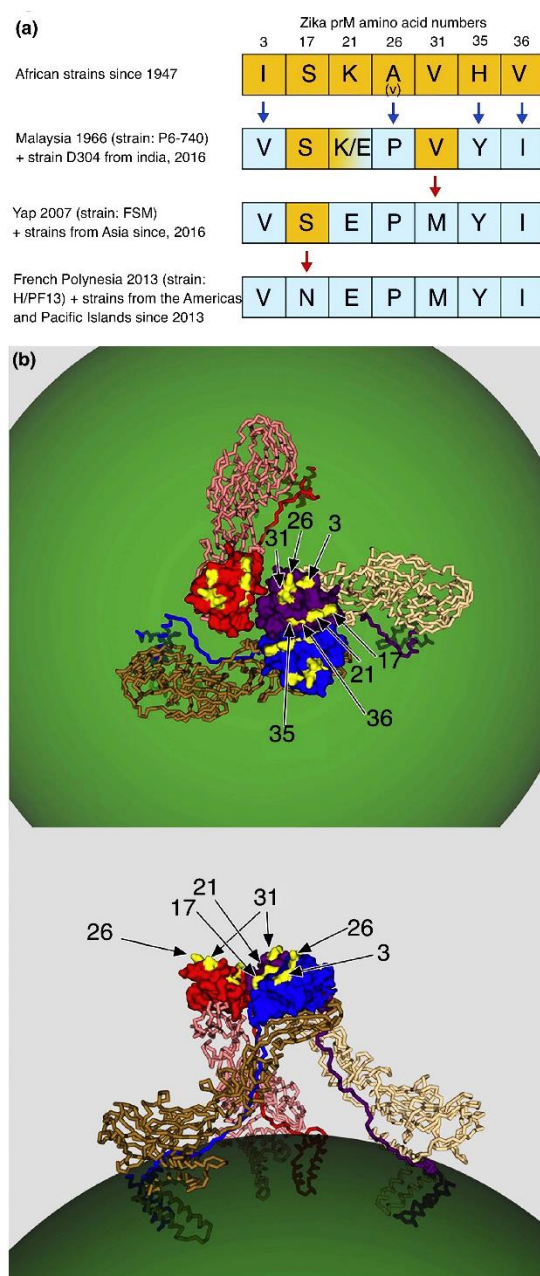


Figure 26: Changes in ZIKV prM

(a) Graphical representation of mutations in prM related to time and location of isolation. Changes in the ZIKV prM amino acid sequence over time was observed at seven positions, as indicated at the top of the figure. (b) Structure of a trimer of prM-E heterodimers (PDB code 4B03). The mutations observed in the ZIKV prM protein over time since its discovery in Uganda 1947 (see panel a) are displayed in yellow and labelled with arrows by their amino acid numbers. (Figure and caption adapted from Rey et al., 2017b)

binding and fusion to target cell¹⁸. In addition, E protein also elicits antibody response being the major antigen of mature viral particles¹⁹.

The E protein of flaviviruses folds into an elongated structure determined by the presence of conserved cysteine residues allowing the formation of six disulfide bonds^{2,17}. Each E ectodomain contains three beta-barrel domains referred to as E domains (ED) I to III, and may be modified or not by the addition of one or two N-bound carbohydrates depending on flavivirus strains. The central structural domain, EDI, is a discontinuous peptide which contains the N-terminal end and connects ED II and III via short flexible loops. Its main roles are to stabilize the general orientation of E protein and assist in conformational changes. But this central domain is also important for the biology of pathogenic flaviviruses since it contains a relatively well-conserved N-glycosylation NxT/S site at position N154²⁰. The finger-like dimerization domain II is formed by the two elongated loops that interspaced the three segments of EDI. At its distal end, EDII contains a highly conserved fusion loop which is involved in interaction with host-cell membrane and mediates viral fusion^{2,20}. On the other hand, the EDIII is an immunoglobulin-like domain of a rather glomerular structure which forms small protrusions on the smooth surface of mature virions²⁰. This domain is mainly implicated in viral entry and appears to include putative receptor binding sites². Moreover, EDIII represents the major antigenic structure of flaviviruses²¹. It contains a panel of epitopes recognized by antibodies, including neutralizing antibodies, making EDIII an excellent target for serologic diagnostic or vaccine development²¹.

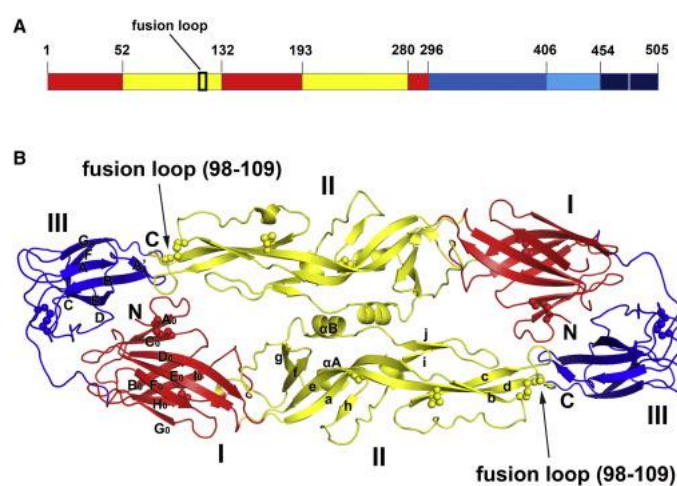


Figure 27: Overall structure of ZIKV E protein

(A) Schematic diagram of domain organization. Domain I (red), domain II (yellow), and domain III (blue). A 48-residue stem segment links the stably folded ZIKV-E ectodomain with the C-terminal transmembrane anchor.

(B) Dimer structure of ZIKV-E. ZIKV-E has three distinct domains: β-barrel-shaped domain I, finger-like domain II, and immunoglobulin-like domain III. The fusion loop is buried by the domains I and II of the other ZIKV E monomer.

(Figure and caption adapted from Dai et al., 2016)

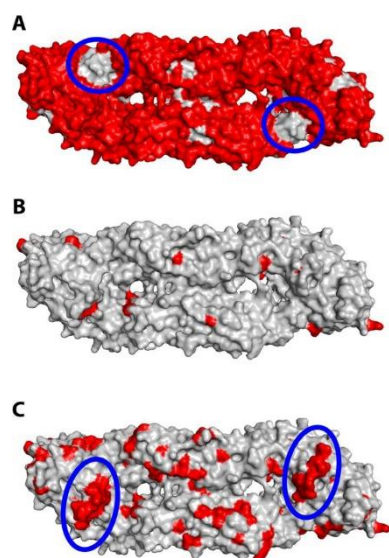


Figure 28: Surface-exposed amino acids conservation in flavivirus E protein

Representation of variable surface-exposed amino acids highlighted in red on the background of the Zika virus E dimer (gray). (A) All amino acids that differ in a comparison between Zika virus and the other mosquito-borne flaviviruses (POWV, TBEV, YFV, WNV, JEV, SPOV, ZIKV, DENV 1 to 4). Circles highlight the conserved patch of amino acids around the fusion loop. (B) Amino acids that differ between Zika virus strains H/PF/2013 and MR766. (C) All amino acids that differ between 111 Zika virus strains. Circles highlight the variability around the glycan loop in domain I. (Figure and caption adapted from Heinz et al., 2017)

I3.1. Feature of ZIKV E protein

The structural comparison of ZIKV E protein with the one of other flaviviruses shows a highly conserved organization with minor discrepancies only visible at the atomic level²². For example, ZIKV and DENV-2 E proteins exhibit a modest root mean square deviation between equivalent carbon alpha atoms of 1.8 Å, yet their sequence has a homology rate of only 54%²³. The most important difference (6 Å) is observed in the region of the glycosylation site which, in the case of ZIKV, is 5 amino acids longer. The glycosylated amino acid, in N153 for DENV or N154 for ZIKV, is proximal to the fusion loop contained in EDIII of the neighboring E protein²³. Interestingly, this specific region has a high sequence variability when compared among flaviviruses species as well as between ZIKV strains¹⁵. Indeed, the E proteins of ZIKV strains of African lineage as well as ancestral Asian strains but not epidemic strain do not bear a NxT/S motif at positions E-154 to E-156. This difference is, depending on the given strain, either due to the presence of a no residue Thr or Ser at position 156 or to the deletion of 4 amino acids covering the N-glycosylation site. It is not well understood whether the loss of the N-glycosylation site at position N-154 is an intrinsic characteristic of African strains or due to an extensive adaptation of the virus as it was subjected to many passages in brain mice and cell lines.

I3.2. Potential impact on ZIKV entry and cellular tropism

The N-glycosylation site at N153 or 154 is surprisingly well preserved among other mosquito-borne flaviviruses pathogenic to humans, except for African

strains of YFV whose E is not N-glycosylated. In the case of ZIKV-related neurotropic flaviviruses, this glycosylation site was important for the neuroinvasiveness and neurovirulence of WNV or JEV respectively^{24,25}. Given the recent association of epidemic ZIKV strains with severe neurological outcome, one can speculate that ZIKV E-glycosylation site may be involved in neuronal tissue infection as well. In addition, glycans are potential binding sites for lectin-type receptors, which can further influence the tropism of ZIKV. In the same way, amino acid substitutions occurring in the EDIII of ZIKV could influence interactions with cellular receptors. In particular, ZIKV strains since 2007 present a mutation which modifies the putative viral receptor binding sequence (D393E). It is also interesting to mention that virus particles are dynamic. Indeed, E dimers metastability gives rise to a phenomenon called "breathing" which leads to the exposure of surfaces that seem cryptic *a priori*¹¹. As a result, it is possible that mutations found in the E protein may modulate ZIKV breathing dynamics and thus influence interactions with attachment factors and entry receptors.

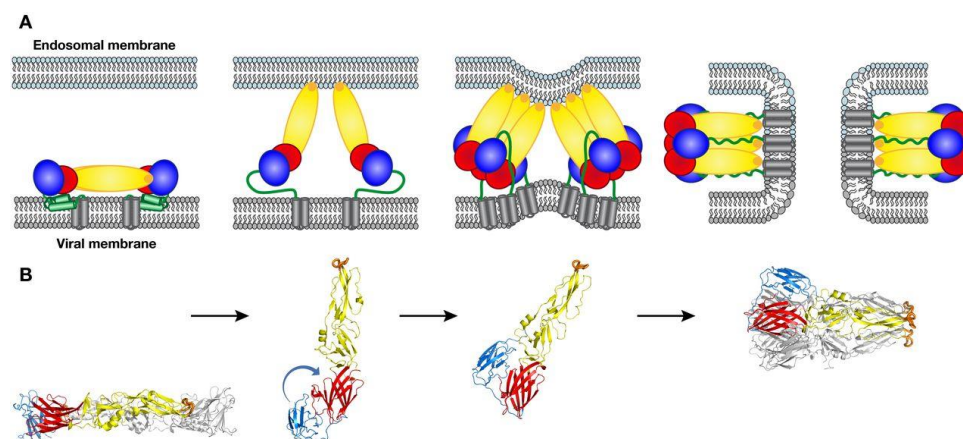


Figure 29: The fusogenic conformational change of the E protein during cell entry

(A) Schematic of the fusion process: A mature E dimer anchored in the viral membrane is represented in the left panel. The dimer dissociates upon exposure to acidic pH in the endosome, inserting the fusion loop into the endosomal membrane (second panel). The aligned E monomers then trimerize, thereby creating a binding site for domain III at the sides of a "core trimer". Domain III then flips to the sides of the trimer, pulling the stem and TM segments toward the endosomal membrane (third panel). The final, post-fusion conformation, brings the viral TM segment next to the fusion loop, inducing first hemi-fusion (i.e., fusion of only the outer leaflets of the two membranes) followed by opening of a fusion pore (fourth panel). The final post-fusion conformation of E is achieved only after fusion pore formation. (B) 3D structures of the dengue virus 2 E ectodomains (lacking the stem/TM regions) matching the steps indicated in (A). (Figure and caption from Rey et al., 2017a)

13.3. The role of ZIKV E in the fusion process

The E protein of flaviviruses is also a class II fusion protein¹⁸ meaning that, unlike class I fusion protein, the protein is not cleaved after synthesis and contains an internal fusion peptide. In mature virus particles, the E proteins are present in the form of 90 homodimers organized into herringbone patterns which completely cover the viral surface. This oligomeric state corresponds to a metastable form of the E protein that is highly sensitive to the physico-chemical environment, particularly temperature and pH. When virions are exposed to an acidic environment, this property leads to an irreversible rearrangement of E proteins, known as "fusogenic conformational change", which results in either the release of the viral genome into the cytoplasm or the inactivation of the virions when it occurs in the absence of a target cell¹⁸. The fusion mechanism is based on the dissociation of E dimer and the exposure of the fusion loop located at the tip of EDIII^{18,19}. During the internalization of flaviviruses by receptor-mediated endocytosis, this process is catalyzed by the acidification of the endosome. The fusion loop then inserts into the inner leaflet of the endosome membrane so that the E protein forms a bridge between the viral and endosomal membranes. Once this bridge is established, other structural changes lead to the fusion of the two lipid bilayers^{18,19}. Since the glycosylation site is in direct proximity to the fusion loop, the fusion process of epidemic ZIKV strains may also be impacted by the presence of glycans. Moreover, it is likely that the amino acid substitutions found in the E protein of epidemic strains may trigger differential pH sensitivity²⁶, which in turn could influence pH-dependent conformational changes, such as viral fusion.

1.4. Investigate the impact of ZIKV structural proteins

As mentioned in this chapter, the structural proteins play an essential role in the biology of flaviviruses. Notably, prM and E ensure the virions ability to infect host cells and are therefore important determinants of viral tropism. Given the high mutation rate of ZIKV structural proteins and its recent association with severe neurological complications, one hypothesis is that epidemic ZIKV strains acquired virulence factors that allow access to neural tissues. In this way, the first part of my doctoral research aimed to investigate the contribution of the

structural proteins in the phenotype of epidemic ZIKV strains. For this purpose, a set of molecular clones, chimeras and mutants of the African strain MR766 and the epidemic strain BR15 ZIKV were generated using reverse genetic methods.

REFERENCE

- Pettersson, J. H.-O. *et al.* How Did Zika Virus Emerge in the Pacific Islands and Latin America? *mBio* **7**, e01239-16 (2016).
- Knipe, D. M. & Howley, P. *Fields Virology*. (Lippincott Williams & Wilkins, 2013).
- Oliveira, E. R. A., Mohana-Borges, R., de Alencastro, R. B. & Horta, B. A. C. The flavivirus capsid protein: Structure, function and perspectives towards drug design. *Virus Res.* **227**, 115–123 (2017).
- Samuel, G. H., Wiley, M. R., Badawi, A., Adelman, Z. N. & Myles, K. M. Yellow fever virus capsid protein is a potent suppressor of RNA silencing that binds double-stranded RNA. *Proc. Natl. Acad. Sci. U. S. A.* **113**, 13863–13868 (2016).
- Amberg, S. M. & Rice, C. M. Mutagenesis of the NS2B-NS3-mediated cleavage site in the flavivirus capsid protein demonstrates a requirement for coordinated processing. *J. Virol.* **73**, 8083–8094 (1999).
- Shang, Z., Song, H., Shi, Y., Qi, J. & Gao, G. F. Crystal Structure of the Capsid Protein from Zika Virus. *J. Mol. Biol.* **430**, 948–962 (2018).
- Zheng, A., Yuan, F., Kleinfelter, L. M. & Kielian, M. A toggle-switch controls the low pH-triggered rearrangement and maturation of the dengue virus envelope proteins. *Nat. Commun.* **5**, 3877 (2014).
- Mukhopadhyay, S., Kuhn, R. J. & Rossmann, M. G. A structural perspective of the flavivirus life cycle. *Nat. Rev. Microbiol.* **3**, 13–22 (2005).
- Li, L. *et al.* The Flavivirus Precursor Membrane-Envelope Protein Complex: Structure and Maturation. *Science* **319**, 1830–1834 (2008).
- Oliveira, E. R. A., de Alencastro, R. B. & Horta, B. A. C. New insights into flavivirus biology: the influence of pH over interactions between prM and E proteins. *J. Comput. Aided Mol. Des.* **31**, 1009–1019 (2017).
- Rey, F. A., Stiasny, K. & Heinz, F. X. Flavivirus structural heterogeneity: implications for cell entry. *Curr. Opin. Virol.* **24**, 132–139 (2017).
- Pierson, T. C. & Diamond, M. S. Degrees of maturity: The complex structure and biology of flaviviruses. *Curr. Opin. Virol.* **2**, 168–175 (2012).
- Junjhon, J. *et al.* Influence of pr-M Cleavage on the Heterogeneity of Extracellular Dengue Virus Particles. *J. Virol.* **84**, 8353–8358 (2010).
- Junjhon, J. *et al.* Differential modulation of prM cleavage, extracellular particle distribution, and virus infectivity by conserved residues at nonfuran consensus positions of the dengue virus pr-M junction. *J. Virol.* **82**, 10776–10791 (2008).
- Heinz, F. X. & Stiasny, K. The Antigenic Structure of Zika Virus and Its Relation to Other Flaviviruses: Implications for Infection and Immunoprophylaxis. *Microbiol. Mol. Biol. Rev. MMBR* **81**, (2017).
- Sirohi, D. *et al.* The 3.8 Å resolution cryo-EM structure of Zika virus. *Science* aaf5316 (2016). doi:10.1126/science.aaf5316
- Winkler, G., Heinz, F. X. & Kunz, C. Studies on the glycosylation of flavivirus E proteins and the role of carbohydrate in antigenic structure. *Virology* **159**, 237–243 (1987).
- Heinz, F. X. & Allison, S. L. Structures and mechanisms in flavivirus fusion. *Adv. Virus Res.* **55**, 231–269 (2000).
- The bright and the dark side of human antibody responses to flaviviruses: lessons for vaccine design | EMBO Reports. Available at: <http://embor.embopress.org/content/early/2017/12/27/embr.201745302>. (Accessed: 10th January 2019)
- Zhang, X. *et al.* Structures and Functions of the Envelope Glycoprotein in Flavivirus Infections. *Viruses* **9**, (2017).
- Chávez, J. H., Silva, J. R., Amarilla, A. A. & Moraes Figueiredo, L. T. Domain III peptides from flavivirus envelope protein are useful antigens for serologic diagnosis and targets for immunization. *Biologicals* **38**, 613–618 (2010).
- Kostyuchenko, V. A. *et al.* Structure of the thermally stable Zika virus. *Nature* **533**, 425–428 (2016).
- Sirohi, D. & Kuhn, R. J. Zika Virus Structure, Maturation, and Receptors. *J. Infect. Dis.* **216**, S935–S944 (2017).
- Moudy, R. M., Zhang, B., Shi, P.-Y. & Kramer, L. D. West Nile virus envelope protein glycosylation is required for efficient viral transmission by *Culex* vectors. *Virology* **387**, 222–228 (2009).
- Liang, J.-J., Chou, M.-W. & Lin, Y.-L. DC-SIGN Binding Contributed by an Extra N-Linked Glycosylation on Japanese Encephalitis Virus Envelope Protein Reduces the Ability of Viral Brain Invasion. *Front. Cell. Infect. Microbiol.* **8**, 239 (2018).
- Rawle, R. J., Webster, E. R., Jelen, M., Kasson, P. M. & Boxer, S. G. pH Dependence of Zika Membrane Fusion Kinetics Reveals an Off-Pathway State. *ACS Cent. Sci.* **4**, 1503–1510 (2018).

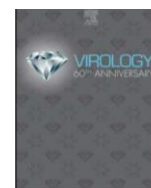
II. ARTICLE N°2



Contents lists available at [ScienceDirect](http://www.sciencedirect.com)

Virology

journal homepage: www.elsevier.com/locate/virology



The structural proteins of epidemic and historical strains of Zika virus differ in their ability to initiate viral infection in human host cells

Sandra Bos, Wildriss Viranaicken, Jonathan Turpin, Chaker El-Kalamouni, Marjolaine Roche, Pascale Krejbich-Trotot, Philippe Desprès*, Gilles Gadea*

Université de la Réunion, INSERM U1187, CNRS UMR 9192, IRD UMR 249, Unité Mixte Processus Infectieux en Milieu Insulaire Tropical, Plateforme Technologique CYROI, 94791 Sainte Clotilde, La Réunion, France

ARTICLE INFO

Keywords:

Arbovirus
Flavivirus
Zika virus
Viral strains
Infectious cDNA
Chimeric virus
Viral infection
Virus binding
Host-cell activation
Structural proteins
Innate immunity

ABSTRACT

Mosquito-borne Zika virus (ZIKV) recently emerged in South Pacific islands and Americas where large epidemics were documented. In the present study, we investigated the contribution of the structural proteins C, prM and E in the permissiveness of human host cells to epidemic strains of ZIKV. To this end, we evaluated the capacity of the epidemic strain BeH819015 to infect epithelial A549 and neuronal SH-SY5Y cells in comparison to the African historical MR766 strain. For that purpose, we generated a molecular clone of BeH819015 and a chimeric clone of MR766 which contains the BeH819015 structural protein region. We showed that ZIKV containing BeH819015 structural proteins was much less efficient in cell-attachment leading to a reduced susceptibility of A549 and SH-SY5Y cells to viral infection. Our data illustrate a previously underrated role for C, prM, and E in ZIKV epidemic strain ability to initiate viral infection in human host cells.

1. Introduction

Zika virus (ZIKV) is an emerging mosquito-borne *flavivirus* (*Flaviviridae* family) that became a major medical concern worldwide. In 2007, the first ZIKV epidemic occurred in the Yap Island affecting more than 70% of the inhabitants (Duffy et al., 2009). Subsequently, ZIKV continued to spread in the South Pacific islands and widely emerged in the Americas from 2015 (Gatherer and Kohl, 2016). Phylogenetic analysis of viral sequences identified the African and Asian genotypes of ZIKV (Haddow et al., 2012), the Asiatic strains being the leading cause of the major current epidemics with millions of infection cases (Giovannetti et al., 2016). While a large majority of infections caused by ZIKV are asymptomatic, or result in dengue-like symptoms, epidemiological studies have pointed out that ZIKV infection can also cause severe diseases in humans including Guillain-Barre syndrome and congenital neurological defects (microcephaly) (Cao-Lormeau et al., 2016; Cugola et al., 2016; Merfeld et al., 2017; Parra et al., 2016). Unlike most other flaviviruses, a component of the spread of ZIKV may reflect its potential for human-to-human transmission. ZIKV is believed to disseminate using both sexual and non-sexual routes including body fluids such as tears, saliva or blood (D'Ortenzio et al., 2016; Motta et al., 2016; Musso et al., 2016). The risk of human infection by solid organ

transplantation has also been suggested (Alcendor, 2017).

ZIKV contains a single-strand positive sense genomic RNA, which is translated into a large and unique polyprotein. The polyprotein is then processed by host and viral proteases into three structural proteins (C, prM/M and E), and seven nonstructural (NS) proteins (NS1 to NS5). Recently, we reported the generation of an infectious cDNA clone of MR766 (hereafter MR766^{MC}) based on the GenBank access number LC002520 (MR766-NIID) after electroporation of four overlapping synthetic fragments that cover the genomic RNA sequence using the ISA method (Atieh et al., 2016; Gadea et al., 2016). The African historical ZIKV strain MR766 was initially collected from a rhesus monkey in Uganda in 1947 and serially propagated in new-born mouse brains (Dick et al., 1952). It is not known whether the mouse neuroadaptation of MR766 resulted in accumulation of mutations in viral sequence.

Epidemic strains of ZIKV have the capacity to replicate in diverse cell types of human origin including epithelial and neuronal cells (Hamel et al., 2017; Pagani et al., 2017; Sheridan et al., 2017; Simonin et al., 2016; Tripathi et al., 2017). We reported that infection of human lung epithelial A549 cells with ZIKV strain PF-25013-18 of Asian lineage isolated during the epidemic in French Polynesia in 2013 (Cao-Lormeau et al., 2014; Frumence et al., 2016) resulted in the activation of Interferon Stimulated Genes (ISGs), the production of Type-I

* Corresponding authors.

E-mail addresses: philippe.despres@univ-reunion.fr (P. Desprès), gilles.gadea@inserm.fr (G. Gadea).

<https://doi.org/10.1016/j.virol.2017.12.003>

Received 22 October 2017; Received in revised form 4 December 2017; Accepted 6 December 2017

Available online 01 February 2018

0042-6822/ © 2018 The Authors. Published by Elsevier Inc. This is an open access article under the CC BY-NC-ND license (<http://creativecommons.org/licenses/by-nc-nd/4.0/>).

interferon (IFN) associated to expression of pro-inflammatory cytokines, and induction of apoptosis. Several reports highlighted the preponderant role of the NS proteins in the responsiveness of human host cells to ZIKV infection. Here, we studied the role of the structural proteins in the permissiveness of human neuroblastoma SH-SY5Y and A549 cells to infection with epidemic strains of ZIKV. Using the ISA method, we generated a molecular clone of ZIKV strain BeH819015 isolated from a human serum specimen in Brazil in 2015 and a chimeric clone of MR766 in which the structural protein region was replaced with the one of BeH819015. Comparative analysis between the three viral clones revealed that ZIKV containing BeH819015 structural proteins are less efficient in the initiation of viral infection in human cells when compared to MR766^{MC}.

2. Methods

2.1. Cells and reagents

Vero cells (ATCC, CCL-81) were cultured at 37 °C under a 5% CO₂ atmosphere in MEM medium, supplemented with 5% heat-inactivated foetal bovine serum (FBS), A549-DualTM cells (InvivoGen, a549d-nfis) designated hereafter as A549^{DUAL} cells and SH-SY5Y cells (ATCC, CRL2266) in MEM medium, supplemented with 10% heat-inactivated FBS and non-essential amino acids. A549-DualTM (A549^{DUAL}) cells were maintained in growth medium supplemented with 10 µg mL⁻¹ blasticidin and 100 mg mL⁻¹ zeocin (InvivoGen). The mouse anti-pan flavivirus envelope E protein mAb 4G2 was produced by RD Biotech. The rabbit anti-BAX and anti-caspase 3 antibodies were purchased from Cell Signalling Technology, the anti-cleaved PARP antibody from Promega, donkey anti-mouse Alexa Fluor 488 and anti-rabbit Alexa Fluor 594 IgG antibodies from Invitrogen. Horseradish peroxidase-conjugated anti-rabbit and anti-mouse antibodies were purchased from Vector Labs.

2.2. Design of ZIKV molecular clones

The molecular clone design and production strategies for ZIKV were previously described by Gadea et al. (2016). The viral clone BR15^{MC} was produced as described for MR766^{MC} (Gadea et al., 2016). BR15^{MC} was based on the sequence of epidemic ZIKV strain BeH819015 (GenBank access KU365778) isolated in Brazil in 2015. MR766 was passaged more than hundred times in new-born mouse brain, and BeH819015 was isolated from blood patient and sequenced after one passage on C6/36 (Dick et al., 1952; Faria et al., 2016). Because the sequences of the untranslated regions (UTRs) deposited in GenBank were partial and also showed abnormalities, the 5'UTR of MR766^{MC} and the 3'UTR of contemporary clinical isolate Paraiba of ZIKV (GenBank access KX280026) were chosen to generate BR15^{MC}. The 3'UTRs from BR15^{MC} and MR766^{MC} perfectly matched on the last 150 nucleotides. Based on our previous experience with molecular clone of ZIKV that used overlapping PCR products (Gadea et al., 2016), the design of viral genome into four viral genomic fragments Z1^{BR15}, Z2^{BR15}, Z3^{BR15} and Z4^{BR15} was chosen to mimic those used to construct MR766^{MC}. The fragment Z1^{BR15} contains the CMV promoter immediately adjacent to the 5'UTR of ZIKV followed by the structural protein region of strain BeH819015. Two synonymous mutations at positions 2200 (a -> g) and 2215 (t -> c) of the structural protein region of ZIKV strain BeH819015 were introduced for a perfect matching of the fragments Z1^{BR15} and Z2^{NIID-MC} on 42 nucleotides. A silent mutation in the E gene that creates the unique restriction site *Pvu* I was introduced into the Z1^{BR15} fragment. The fragment Z4^{BR15} consists of a hepatitis delta virus ribozyme immediately following the last ZIKV nucleotide and a SV40 poly(A) signal. The synthetic genes Z1^{BR15}, Z2^{BR15}, Z3^{BR15}, and Z4^{BR15} were synthesized and cloned into plasmid pUC57 by GeneCust (Luxembourg). The fragments Z1^{BR15} to Z4^{BR15} were amplified by PCR from their respective plasmids using a set of primer pairs that were designed so that Z1^{BR15} and Z2^{BR15} or Z3^{BR15} and Z4^{BR15} matched on about

30–40 nucleotides.

2.3. Recovering of molecular clone BR15^{MC} and chimeric virus CHIM

The molecular clone BR15^{MC} was produced as previously described for MR766^{MC}. Briefly, the purified PCR fragments Z1^{BR15}, Z2^{BR15}, Z3^{BR15}, and Z4^{BR15} were electroporated into Vero cells. After 5 days, cell supernatants were recovered and used to infect fresh Vero cells in a first round of amplification (P1). Viral clone BR15^{MC} was recovered 7 days later and amplified for another 2 days on Vero cells to produce a P2 for further studies. The viral clone BR15^{MC} derived from ZIKV strain BeH819015 is available to BEI Resources (Manassas, VA) under the catalog number NR-51129 (www.beiresearch.org). To produce the viral clone CHIM, Vero cells were electroporated with the PCR fragments Z1^{BR15}, Z2^{MR766-MC}, Z3^{MR766-MC}, and Z4^{MR766-MC}. The recovered virus CHIM consists of the viral sequence of MR766 in which the coding region for the structural proteins was replaced with the counterpart of ZIKV strain BeH819015. The viral clone CHIM contains a chimeric E protein between BeH819015 (amino acids 1–436) and MR766 (amino acids 437–504).

2.4. Plaque forming assay

Viral titers were determined by a standard plaque-forming assay as previously described with minor modifications (Frumence et al., 2016). Briefly, Vero cells grown in 48-well culture plate were infected with tenfold dilutions of virus samples for 2 h at 37 °C and then incubated with 0.8% carboxymethylcellulose (CMC) for 4 days. The cells were fixed by 3.7% FA in PBS and stained with 0.5% crystal violet in 20% ethanol. Viral titers were expressed as plaque-forming units per mL (PFU.mL⁻¹).

2.5. Quantification of viral stocks

Zika virus samples were analyzed by titration on Vero cells while genomic viral RNA was quantified by RT-qPCR. For viral genome quantification, viral RNA was extracted from virus particles using QIAmp kit (QIAGEN). The PCR standard curve used for the quantification of ZIKV copy numbers was obtained with a pUC57/ZIKV-E amplicon plasmid containing a synthetic cDNA encompassing nucleotides 961–1301 of genomic RNA (GenBank accession number LC002520). The couple of ZIKV E primers was used to equally amplify pUC57/ZIKV-E amplicon and the cDNA encompassing nucleotides 1046–1213 from genomic RNA of ZIKV molecular clones used in this study.

2.6. Immunoblot assay

Cell lysates were performed in RIPA lysis buffer. All subsequent steps of immunoblotting was performed as described (Nativel et al., 2013; Viranaicken et al., 2011). Primary antibodies were used at 1:500 dilutions. Anti-rabbit immunoglobulin-horseradish peroxidase and anti-mouse immunoglobulin-horseradish peroxidase conjugates were used as secondary antibodies (dilution 1:2000). Blots were revealed with ECL detection reagents. Bands were quantified by densitometry using ImageJ software.

2.7. Immunofluorescence assay

A549^{DUAL} cells grown on glass coverslips were fixed with 3.7% formaldehyde at room temperature for 10 min. Fixed were permeabilized with 0.1% Triton X-100 in PBS for 4 min. Cells were stained using the mouse anti-pan flavivirus envelope E protein mAb 4G2 (1:1000 dilution), rabbit anti-Caspase 3 mAb (1:1000 dilution) and rabbit anti-BAX mAb (1:1000 dilution). Antigen staining was visualized with Alexa Fluor-conjugated class specific secondary antibodies (1:1000, Invitrogen). Nucleus morphology was revealed by DAPI staining. The

coverslips were mounted with VECTASHIELD® (VECTOR Laboratories), and fluorescence was observed using a Nikon Eclipse E2000-U microscope. Images were captured and processed using a Hamamatsu ORCA-ER camera and the imaging software NIS-Element AR (Nikon).

2.8. Flow cytometry assay

A549^{Dual} cells were grown on 6-well plates at 5.10^5 cells per well and infected at a multiplicity of infection (MOI) of 1. Infected cells were harvested and fixed with 3.7% formaldehyde in PBS for 20 min, permeabilized with 0.1% Triton-X100 in PBS for 4 min and then blocked with PBS-BSA for 10 min. Cells were stained with anti-E 4G2 (1:1000) for 1 h. Antigen staining was visualized with goat anti-mouse Alexa Fluor 488 IgG (1:1000) for 20 min. Cells were subjected to a flow cytometric analysis using FACScan flow cytometer (BD Bioscience). The percentage of positive cells was determined using FlowJo software.

2.9. RT-qPCR

Total RNA including genomic viral RNA was extracted from cells (Qiagen) and reverse transcription was performed using 500 ng of total RNA, random hexamer primers (intracellular viral RNA) or E reverse primer (virus particles) and MMLV reverse transcriptase (Life Technologies) at 42 °C for 50 min. Quantitative PCR was performed on a ABI7500 Real-Time PCR System (Applied Biosystems). Briefly, 10 ng cDNA was amplified using 0.2 μM of each primer and 1X GoTaq Master Mix (Promega). When appropriate, data were normalized to the internal standard GAPDH. For each single-well amplification reaction, a threshold cycle (Ct) was calculated using the ABI7500 program (Applied Biosystems) in the exponential phase of amplification. Relative changes in gene expression were determined using the $2^{-\Delta\Delta C_t}$ method and reported relative to the control. The primers used in this study are listed in Frumence et al. (2016). ZIKV E primers were designed to match both MR766-NIID and BeH819015 sequences (forward 5-gtcttgaacatggagg-3' and reverse 5'-ttcacttggtgtggc-3').

2.10. Virus binding assay

Cells were cultured at subconfluent density in 60 mm dishes. Cell monolayers were washed in cold PBS and cooled at 4 °C at least 20 min in presence of cold MEM supplemented with 2% FBS. Pre-chilled cells were incubated at 4 °C with ZIKV at MOI of 1 (A549^{Dual} cells) or 10 (SH-SY5Y cells) in 1.5 or 3.0 mL of cold MEM supplemented with 2% FBS. After 1 h of incubation, the virus inputs were removed and the cells were washed with cold MEM supplemented with 2% FBS. Total cellular RNA was extracted using the RNeasy kit (Qiagen) and RT-qPCR analysis on viral RNA was performed using primers for ZIKV E gene as above described.

2.11. Cytotoxicity assay

Cell damages were evaluated measuring lactate dehydrogenase (LDH) release. Supernatants of infected cells were recovered and subjected to a cytotoxicity assay, performed using CytoTox 96® non-radioactive cytotoxicity assay (Promega) according to manufacturer instructions. Absorbance of converted dye was measured at 490 nm (Tecan). Results of LDH activity are presented with subtraction of control values.

2.12. NF-κB and IFN-β pathway activation

The activation of the NF-κB and IRF pathways were monitored measuring the SEAP and *Lucia* luciferase activities, respectively. The SEAP activity was evaluated using the QUANTI-blue substrate (InvivoGen) according to the manufacturer's instructions. NF-κB-induced SEAP levels were quantified using a microplate

spectrophotometer at 620 nm (TECAN). The *Lucia* luciferase activity was evaluated using the QUANTI-Luc substrate (InvivoGen) according to the manufacturer's recommendations. IRF-induced luciferase levels were quantified using a FLUOstar Omega Microplate Reader (BMG LABTECH). Results are presented with subtraction of control values.

2.13. Statistical analysis

All values are expressed as mean ± SD of at least two experiments, or as mean ± SEM of triplicates. Comparisons between different treatments have been analyzed by a one-way or two-way ANOVA tests as appropriate. Values of $p < 0.05$ were considered statistically significant for a post-hoc Tukey's test. All statistical tests were done using the software Graph-Pad Prism version 7.01.

3. Results

3.1. Characterization of viral clones

In an effort to better understand the role of C, prM, and E in the permissiveness of human cells to ZIKV infection, we generated the molecular clones BR15^{MC} based on the sequence of the ZIKV strain BeH819015 and CHIM, a chimera derived from MR766^{MC} in which the structural protein region of MR766 was replaced with the one of BeH819015 (Fig. 1A). BR15^{MC} and CHIM sequence design into four overlapping large fragments was chosen to mimic those initially used to generate MR766^{MC} using the ISA method (Gadea et al., 2016). The chimeric MR766, referred as CHIM, had the 5' and 3'-UTR sequences and the nonstructural proteins coding sequence of MR766, and the structural proteins C-1 to E-436 derived from BeH819015. The genomes of BR15^{MC} and CHIM were assembled in Vero cells by electroporation of the four overlapping fragments corresponding to the full-length genomic RNA. The viruses recovered in the cell supernatants were twice amplified on Vero cells. The titers of viral stocks P2 were determined on Vero cells (Table 1). We noted that BR15^{MC} generated plaques on Vero cells of smaller size than MR766^{MC} or CHIM (Fig. 1B). Also, BR15^{MC} stock had a lower infectious titer than MR766^{MC} and CHIM stocks. There was a constant infectivity ratio of about 1000 viral RNA copies/PFU regardless viral clones (Table 1). Accordingly, the viral stocks P2 of MR766^{MC}, BR15^{MC} and CHIM were suitable for further comparative analysis.

3.2. Susceptibility of A549 and SH-SY5Y cells to viral clones

The study of ZIKV progeny production in A549^{Dual} cells infected with viral clones at MOI of 1 showed that BR15^{MC} and CHIM replicated more slowly than MR766^{MC} (Fig. 2A). A such delay in viral growth was corroborated with the percentage of positive cells determined by FACS assay as well as rate of intracellular viral RNA at early infection times (Fig. 3). In SH-SY5Y cells infected with BR15^{MC} or CHIM at MOI of 10, progeny production of both viral clones was reduced at, at least, 3 log when compared to MR766^{MC} at viral growth plateau (Fig. 2A). Thus, ZIKV containing BeH819015 structural proteins were less efficient in their capacity to infect A549^{Dual} and SH-SY5Y cells when compared to African strain.

The attachment of virus particles to cell surface is a pre-requisite for the initiation of ZIKV infection in the host cells. Virus binding assays were performed to determine whether the lower capacity of BR15^{MC} and CHIM to infect human host cells was due to a difference in cell-attachment (Fig. 2B). A549^{Dual} and SH-SY5Y cells were incubated with viral clones and virus particles binding was evaluated by RT-qPCR. A reduction of at least 80% of BR15^{MC} and CHIM binding was observed compared to MR766^{MC} regardless of the human cell lines tested. Thus, ZIKV containing BeH819015 structural proteins significantly differed from MR766 in their capacity to initiate viral infection in A549^{Dual} and SH-SY5Y cells. These results suggested that permissiveness of human

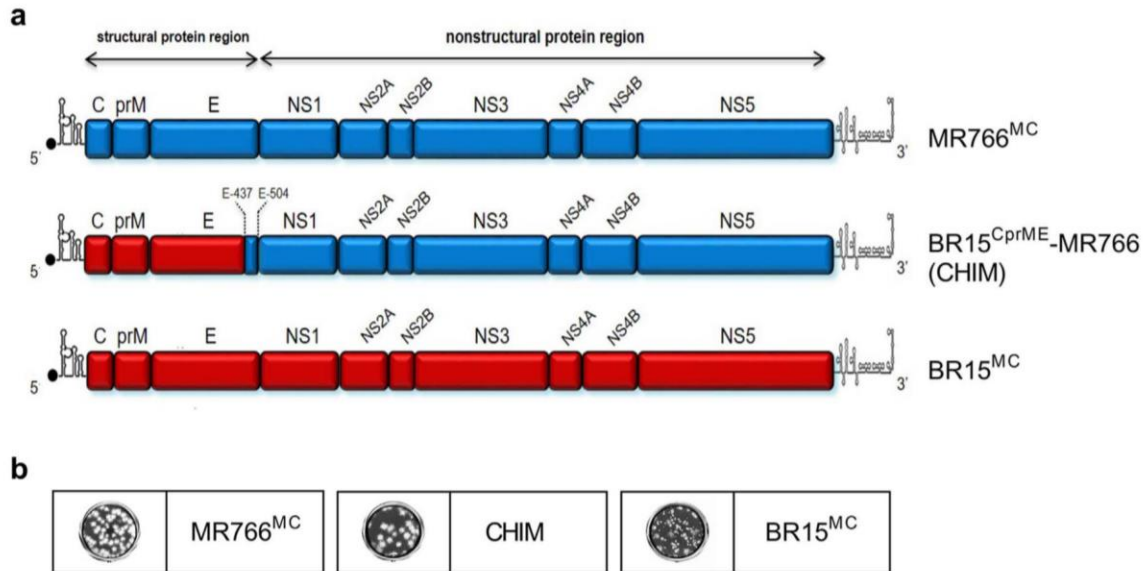


Fig. 1. ZIKV molecular clones MR766, BR15 and CHIM. *In (A)*, schematic representation of viral clone BR15^{MC} derived from ZIKV strain BeH819015 and MR766^{MC} which had been described elsewhere (Gadea et al., 2016). The chimeric clone CHIM expresses most of the structural proteins (C, prM, and E [amino acid sequence 1–436]) of BeH819015 fused to part of the E protein (amino acids 437–504) and the non-structural proteins (NS1 to NS5) of MR766^{MC}. *In (B)*, examples of infectious plaques developed for MR766^{MC}, BR15^{MC}, and CHIM, after plaque forming assay on Vero cells.

Table 1
Infectivity of viral clones.

Virus stocks	vRNA copies.mL ⁻¹	PFU.mL ⁻¹	Ratio ^a
MR766 ^{MC}	5.3 × 10 ¹⁰	5 × 10 ⁷	1008
CHIM	2.3 × 10 ¹⁰	2 × 10 ⁷	1084
BR15 ^{MC}	4.5 × 10 ⁹	5 × 10 ⁶	853

^a Viral RNA copies/PFU ratio was determined for each virus stock P2 produced in Vero cells by dividing the number viral RNA copies as measured by RT-qPCR with the number of PFU determined in Vero cells.

cells to ZIKV infection is related, in part, to the binding efficacy of viral structural proteins to host cell membrane.

3.3. Apoptosis in A549 cells infected with viral clones

Given that BR15^{MC} and CHIM reached a plateau of virus progeny production in A549^{Dual} cells 24 h later than M766^{MC} (Fig. 2A), we assessed whether this delay in viral growth was associated with variations in host-cell responses to ZIKV infection. Analysis of LDH release in A549^{Dual} cells infected 48 h with ZIKV revealed a severe loss of cell integrity in response to MR766^{MC} infection but not to BR15^{MC} and CHIM (Fig. 4A). Thus, the viability of A549^{Dual} cells infected with ZIKV containing BeH819015 structural proteins was mostly preserved at 48 h post-infection. ZIKV infection can trigger apoptosis in various cell types and cell death occurred at maximum of progeny virus production (Frumence et al., 2016; Huang et al., 2016; Souza et al., 2016). Our previous study showed that ZIKV infection induces BAX-dependent apoptosis in A549 cells (Frumence et al., 2016). A low number of A549^{Dual} positive cells for BAX or Caspase 3 activation at 48 h post BR15^{MC} or CHIM infection was observed when compared to cells infected with MR766^{MC} (Fig. 4B and C). Immunoblot assay using an antibody directed against the 85 kDa-cleaved form of PARP showed that PARP cleavage occurred in A549^{Dual} cells infected with MR766^{MC} since 24 h post-infection but not with BR15^{MC} and CHIM. At 48 h post-infection, PARP cleavage was still moderated for BR15^{MC} and CHIM (Fig. 4D). Given that at least 85% of ZIKV-infected A549 cells were positive for expression of E at 48 h p.i. regardless the virus strains tested, the differences in efficiency of PARP cleavage was not related to

a lower percentage of cells infected with ZIKV containing BeH819015 structural proteins (Fig. 3A). Taken together, these results showed that ZIKV-induced apoptosis in A549^{Dual} cells is rather delayed in response to viral clones containing BeH819015 structural proteins.

3.4. Expression of ISGs and cytokines in A549 cells infected with viral clones

There is mounting evidence that ZIKV infection leads to the induction of ISGs and expression of pro-inflammatory cytokines in human host cells (Frumence et al., 2016; Hamel et al., 2015, 2017; Quicke et al., 2016). To determine whether viral clones differ in their capacity to activate host-cell responses, we took advantages of A549^{Dual} cells which derive from A549 cells by stable integration of two reporter genes: the SEAP and *Lucia* luciferase reporter genes under the transcriptional control of the IFN-β minimal promoter fused to NF-κB binding sites or an ISG54 minimal promoter in conjunction with ISREs, respectively.

We examined the kinetic of interferon regulatory factor (IRF) pathway activation in ZIKV-infected A549^{Dual} cells by monitoring *Lucia* luciferase activity. BR15^{MC} and CHIM were poorly efficient at inducing IRF pathway at 24 h and 48 h post-infection when compared to MR766^{MC} (Fig. 5A). At 72 h post-infection, activation of the IRF pathway was detected in A549^{Dual} cells infected with BR15^{MC} or CHIM indicating that significant production of IFN-β can also occur in response to ZIKV containing BeH819015 structural proteins. This IFN-β production is even higher than the one measured in MR766-infected cells most probably due to the earlier MR766-mediated cytotoxicity in A549^{Dual} cells (Fig. 4). At 24 h post-infection, RT-qPCR analysis showed that IFN-β gene was up-regulated in response to the three viral clones but to higher level during MR766 infection (Fig. 5B).

We and others reported that ZIKV infection resulted in activation of Interferon-induced proteins with tetratricopeptide repeats (IFIT) family genes (Frumence et al., 2016; Bowen et al., 2017). By RT-qPCR analysis, we showed that ZIKV infection resulted in a minimal (*ISG54/IFIT2* gene) to moderate (*ISG56/IFIT1* gene) expression level of *IFIT* family genes in A549^{Dual} cells (Fig. 6A). There were no differences in *ISG54/IFIT2* transcript levels with the three viral clones whereas MR766^{MC} and CHIM induced a stronger *ISG56/IFIT1* gene expression than BR15^{MC}.

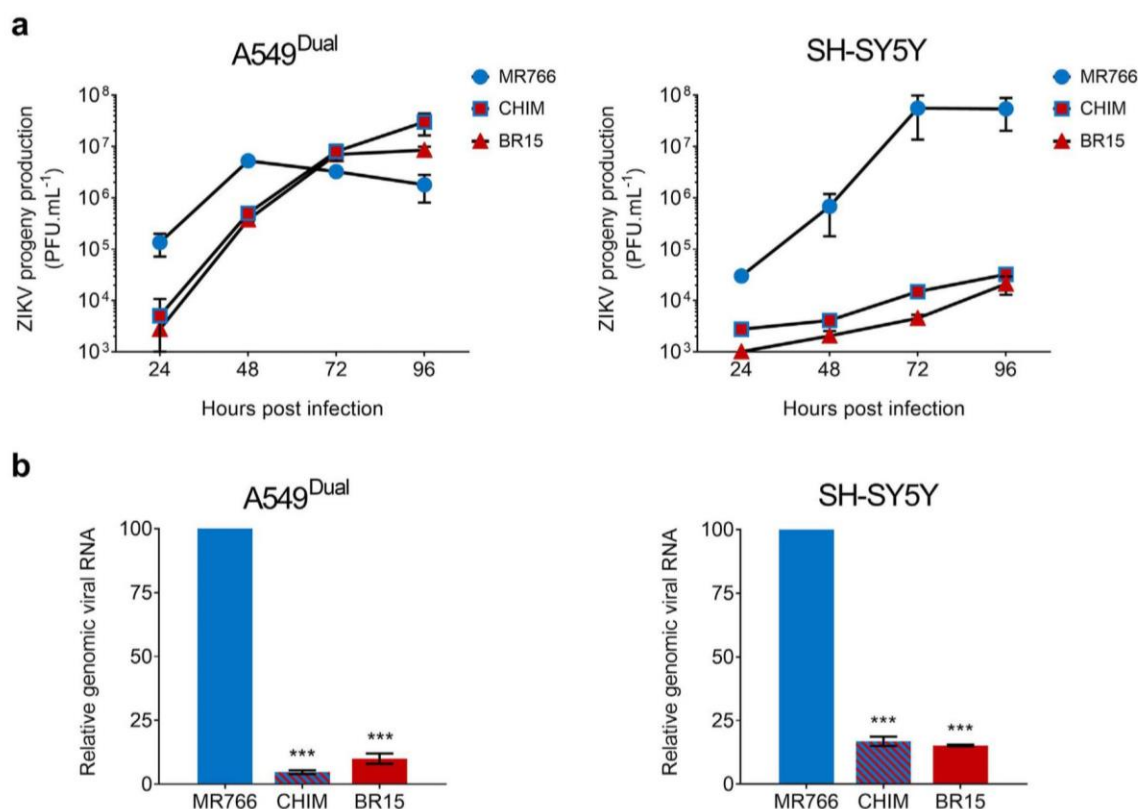


Fig. 2. Analysis of viral growth and virus binding in A549 and SH-SY5Y cells. *In (A)*, A549^{Dual} cells were infected with MR766^{MC}, BR15^{MC}, or CHIM at MOI of 1 and SH-SY5Y cells at MOI of 10. The infectious virus released into the supernatants of infected cells at 24, 48, 72, and 96 h were quantified on Vero cells. The error bars represent the standard deviations of three independent experiments. *In (B)*, for virus binding assays, cells were incubated with viral clones at the MOI of 1 (A549^{Dual} cells) or 10 (SH-SY5Y cells) for 1 h at 4 °C. The number of virus particles bound to cell surface was measured by RT-qPCR. Values represent the mean and standard deviations of two to four independent experiments.

Thus, infection with ZIKV containing the non-structural proteins of MR766^{MC} resulted in stronger induction of *ISG56/IFIT1* gene that has been reported to act as an antagonist of RIG-I-mediated IFN- β induction (Fensterl and Sen, 2011). This result suggests that the nonstructural protein region is capable of initiating expression of some ISGs in human epithelial cells infected with ZIKV.

We examined the expression pattern of genes commonly involved in the synthesis of pro-inflammatory cytokines by RT-qPCR analysis. At 24 h post-infection, ZIKV infection of A549^{Dual} cells resulted in a very weak to no activation of *IL-6* and *IL-1 β* regardless of the viral clone examined (Fig. 6B). This could be corroborated with absence of

detectable NF- κ B activity in A549^{Dual} cells infected with viral clones (Fig. S1). Thus, infection with MR766^{MC} or BR15^{MC} did not result in early activation of *IL-6* and *IL-1 β* genes in A549 cells as it has been previously observed with clinical isolate PF-25013-18 of ZIKV (Frumence et al., 2016). At 24 h post-infection, activation of *IL-8* gene was observed in A549^{Dual} cells infected with the three viral clones. However, the expression level of *IL-8* gene was significantly higher in response to ZIKV containing nonstructural proteins of MR766 (Fig. 6B). This raises the issue on the role of the nonstructural protein region in the activation of some pro-inflammatory cytokines in human epithelial cells infected with ZIKV.

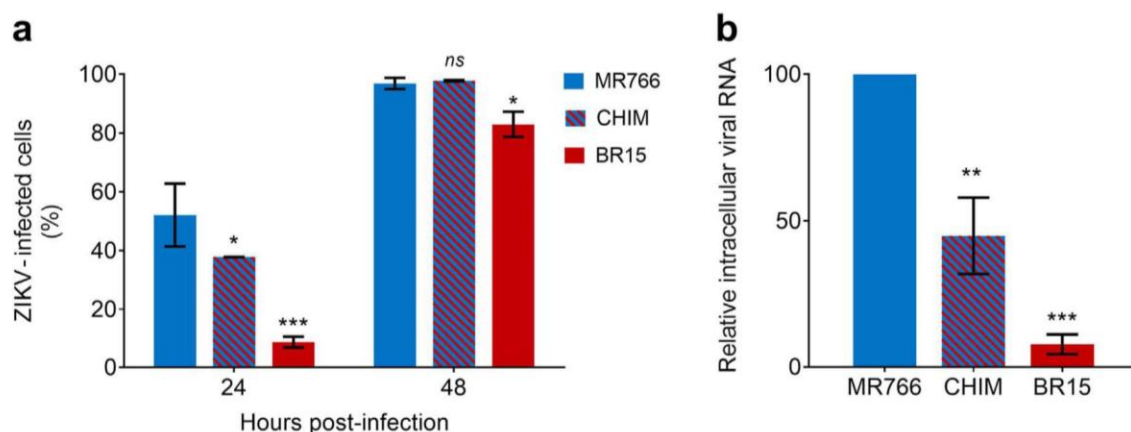


Fig. 3. Viral replication in A549 cells. A549^{Dual} cells were infected with MR766^{MC}, BR15^{MC}, or CHIM at MOI of 1. *In (A)*, the percentages of ZIKV-infected cells at 24 and 48 h were determined by FACS analysis using anti-E mAb 4G2 as primary antibody. The error bars represent the standard deviations of three independent experiments. *In (B)*, intracellular viral RNA production was determined by RT-qPCR at 24 h p.i. Values represents the mean and the standard deviations of two independent experiments (n.s. $p > 0.5$, * $p < 0.5$, ** $p < 0.1$).

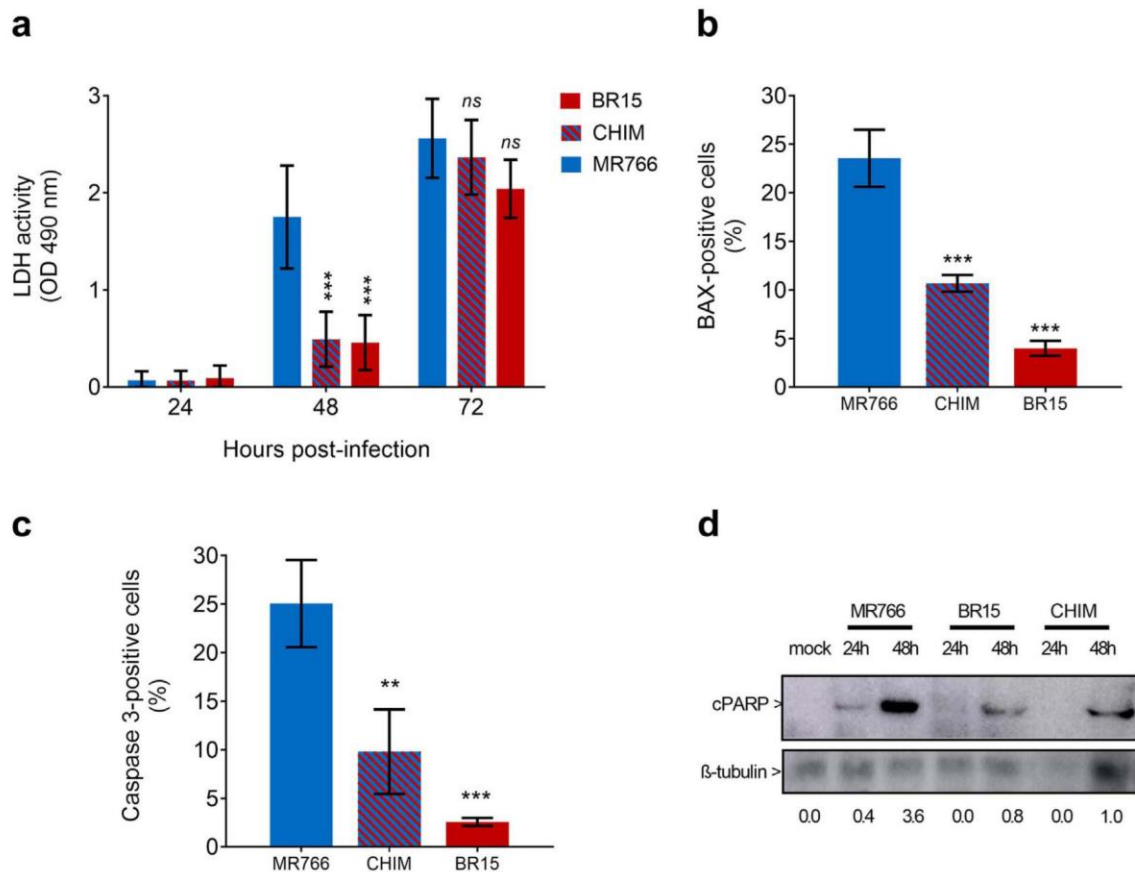


Fig. 4. Kinetics of apoptosis in A549 cells infected with viral clones. A549^{Dual} cells were infected with MR766^{MC}, BR15^{MC}, or CHIM at MOI of 1. *In (A)*, LDH activity was measured at 24, 48 and 72 h p.i. Values represent the mean and the standard deviations of three independent experiments (n.s. $p > 0.5$, * $p < 0.5$, ** $p < 0.1$, *** $p < 0.01$). *In (B)*, percentage of infected cells immunostained with anti-BAX antibody at 48 h p.i. Values represent the mean and the standard deviations of three independent experiments (*** $p < 0.01$). *In (C)*, percentage of infected cells immunostained with anti-caspase 3 antibody at 48 h p.i. Values represent the mean and the standard deviations of three independent experiments (** $p < 0.1$, *** $p < 0.01$). *In (D)*, lysate samples of cells infected 24 and 48 h by viral clones were analyzed by immunoblot assay using anti-cleaved PARP antibody. Antibody against β-tubulin served as protein loading control. The head arrows indicate the cleaved form of PARP (cPARP) and β-tubulin. Values below represent cPARP/β-tubulin ratios.

4. Discussion

The association of contemporary ZIKV strains with epidemics and severe forms of disease in humans warrants the need for further characterization of their biological characteristics. The purpose of our study was to better understand the role of the structural proteins in the

permissiveness of human cells to ZIKV infection. To this end, two ZIKV molecular clones derived from the Brazilian epidemic strain BeH819015 of Asian lineage and the African historical strain MR766 were compared on their capacity to infect human epithelial A549 and neuroblastoma SH-SY5Y cells. We also generated a chimeric clone derived from MR766 in which C, prM and the first 436 amino acids of E

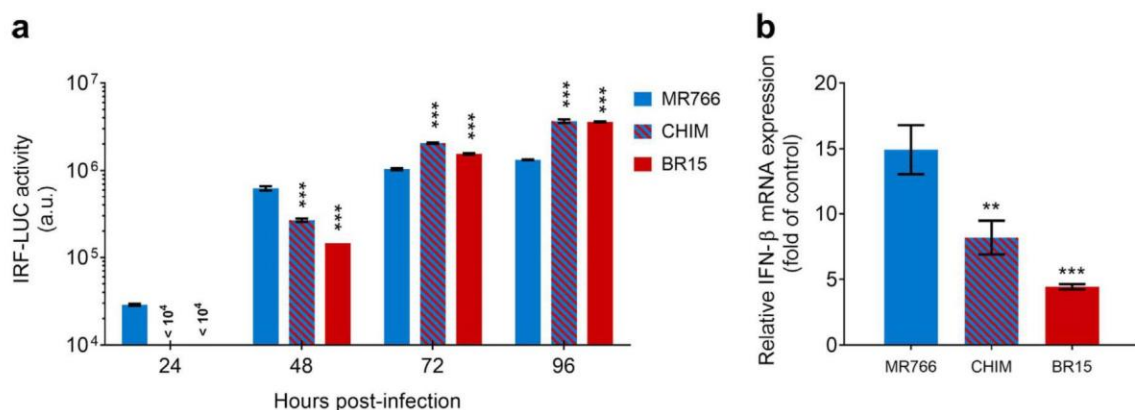


Fig. 5. Activation of IRF and IFN-β pathways in A549 cells infected with viral clones. A549^{Dual} cells were infected with MR766^{MC}, BR15^{MC}, or CHIM at MOI of 1. *In (A)*, analysis of IRF pathway activation in response to viral infection. Activity of the secreted *Lucifera* was measured using QUANTI-Luc substrate. Results are expressed as crude data of arbitrary units of luminescence. The results from a representative experiment (n = 3 repeats) are shown (*** $p < 0.01$). *In (B)*, production of IFN-β mRNA in response to viral infection. The amount of IFN-β transcripts was determined at 24 h p.i. by RT-qPCR. GAPDH mRNA served as an internal reference. Results are expressed as the fold-induction of IFN-β transcripts in ZIKV-infected cells relative to those in mock-infected cells. Values represent the mean and standard deviations of two independent experiments (** $p < 0.1$, *** $p < 0.01$).

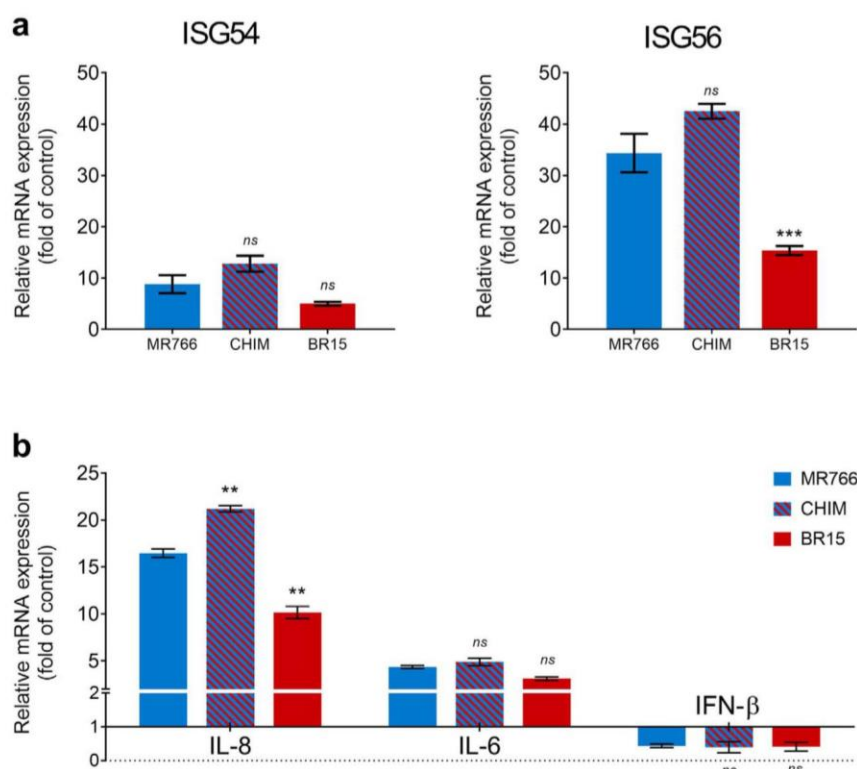


Fig. 6. Activation of ISG54/56 and pro-inflammatory cytokine genes in A549 cells infected with viral clones. A549^{Dual} cells were infected 24 h with MR766^{MC}, BR15^{MC}, or CHIM at MOI of 1. *In* (A) the amounts of ISG54 and ISG56 transcripts were determined by RT-qPCR. GAPDH mRNA served as internal reference. Results are expressed as the fold induction of transcripts relative to those in mock-infected cells. Values represent the mean and standard deviations of triplicates (ns $p > 0.5$, *** $p < 0.01$). *In* (B), the amounts of IL-8, IL-6 and IL-1 β transcripts were determined by RT-qPCR. GAPDH mRNA served as internal reference. Results are expressed as the fold induction of transcripts relative to those in mock-infected cells. Values represent the mean and standard deviations of triplicates (ns $p > 0.5$, ** $p < 0.1$).

from MR766 were replaced with those of BeH819015.

Virus binding assay showed that ZIKV containing BeH819015 structural proteins were much less efficient in cell-attachment when compared to MR766. The lower binding capacity of BeH819015 structural proteins was associated with a delay (A549 cells) or severe restriction (SH-SY5Y cells) in viral growth, arguing for an important role of the structural proteins in human epithelial and neuronal cells permissiveness to ZIKV infection. In A549^{Dual} cells, the growth of ZIKV containing BeH819015 structural proteins was deferred resulting in a delayed activation of mitochondrial apoptosis as well as a lower expression level of ISGs and cytokines as compared to African historical strain MR766. We observed that ZIKV containing MR766 nonstructural proteins induced stronger *ISG56/IFIT1* and *IL-8* gene expression in A549^{Dual} cells as compared to the viral clone derived from epidemic BeH819015 strain. It is interesting to speculate that nonstructural protein region of ZIKV has a direct role in the activation of some ISGs and cytokines that might explain differential susceptibility to ZIKV infection.

Binding to cell surface is an absolute pre-requisite for the initiation of viral infection in the host-cell. Attachment and receptor recognition are likely to be processes in which multiples molecules are used in combination or consecutively for virus entry. ZIKV binding assay performed in our study highlighted a critical role of structural proteins in cell attachment. Among the C and prM proteins of MR766 and BeH819015, we found four divergent amino acids in C and ten in prM (Table 2). Flavivirus prM protein, which is essential for viral particle formation, is cleaved by furin protease into “pr” peptide and mature M protein. Several residues of prM have been reported to play an important role in flavivirus replication (Hsieh et al., 2014; Kim et al., 2008; Yoshii et al., 2004, 2012), and N-terminal residues of West Nile prM have been shown essential in virus assembly inside the intracellular membranes (Calvert et al., 2012; Setoh et al., 2015). A lower cleavage efficacy at the pr-M junction could affect the generation of infectious virus particles in promoting the production of prM-containing viruses (Elshuber et al., 2003; Junjhon et al., 2010). We noted that the pr-M junction with the amino acid sequence YGTCH HKKG

Table 2
Comparative sequence analysis of viral clones.

Viral protein	Amino acid position	Residue MR766 ^{MC}	Residue BR15 ^{CprME} -MR766	Residue BR15 ^{MC}
C	25	N	S	S
	27	L	F	F
	101	R	K	K
	110	I	V	V
prM	3	I	V	V
	17	S	N	N
	21	K	E	E
	26	A	P	P
	31	V	M	M
	35	H	Y	Y
	36	V	I	I
	124	K	R	R
	138	V	A	A
	140	V	A	A
E	120	T	A	A
	152	T	I	I
	156	I	T	T
	158	Y	H	H
	169	V	I	I
	283	K	R	R
	285	F	S	S
	317	V	I	I
	341	I	V	V
	343	V	A	A
	393	D	E	E
	437	V	V	A
	438	F	F	L
	473	V	V	M
	487	T	T	M
	495	M	M	L

Amino acid substitutions in BR15^{MC} and CHIM relative to MR766^{MC} are listed.

ARRSR R/AVTL PSHSS is strictly conserved between ZIKV strains MR766 and BR15 as well as CHIM. Thus, it seems rather unlikely that differences in binding observed among the three virus variants were

correlated with a reduced prM cleavage in ZIKV-infected Vero cells in the course of virus progeny production. On the other hand, the ZIKV prM also contains a single N-glycosylation site at the position prM-70, which is conserved in both historical and epidemic strains. Among the ten amino acid changes between MR766 and BR15 prM proteins, seven are located within the forty N-terminal amino acids (Table 2). Recently, a single Ser to Ala substitution at the position prM-139 protein has been presumed to affect the neuropathogenic properties of ZIKV (Yuan et al., 2017). It remains to be investigated whether the cluster of amino acid changes in the N-terminal region of BeH819015 prM, could contribute to ZIKV strain differences in cell-attachment.

Envelope protein is assumed to bind attachment factors and cellular receptors directing virus particles to the endocytic pathway. ZIKV E protein consists in a four hundred amino acid-long ectodomain which encloses a central β -barrel shaped domain I (EDI), a finger-like domain II (EDII), and a C-terminal immunoglobulin-like domain III (EDIII) followed by a stem region and two transmembrane domains (Sirohi et al., 2016). Analysis of the chimeric ZIKV MR766 containing BeH819015 structural proteins identified eleven amino acid substitutions that could be potentially involved in the less permissiveness of human host cells to ZIKV strain BeH819015 (Table 2). Three substitutions E-T152I, E-I156T and E-Y158H were identified in EDII. The presence of Thr at position E-156 introduces a potential N-glycosylation site in BeH819015 E protein. The N-glycosylation status of the ZIKV E protein may have a major impact on virus particles assembly and infectivity of epidemic strains as well as virus progeny production (Mossenta et al., 2017; Widman et al., 2017). The role of the three residues at positions E-152, E-156, and E-158 in the biological properties of ZIKV strain BeH819015 requires further analysis. The substitutions E-V317I, E-I341V, E-V343A, and E-D393E were identified in EDIII. It has been shown that ZIKV was impaired in virus particle assembly after the removing of residue E-346 which shortens the extended loop of EDIII (Xie et al., 2017). Whether the four amino acid substitutions mapped into the EDIII are involved in the epidemic ZIKV BeH819015 strain capacity to infect human host cells is an important issue to be investigated.

In conclusion, our study showed differences in host-cell susceptibility to the historical strain MR766 and the epidemic strain BeH819015 and highlighted a potential role of the structural proteins in the permissiveness of human epithelial and neuronal cells to ZIKV infection. It was striking to observe that the growth of Asian epidemic strain BeH819015 was poorly efficient in neuroblastoma SH-SY5Y cells whereas infection with African historical strain MR766 was highly productive. The attenuated replication of BeH819015 in human neuronal cells was associated to a minimal loss of cell viability on at least one week (data not shown and Fig. S2). The greater capacity of epidemic strains of ZIKV to initiate persistent infection in specialized human cells is a critical issue that must be urgently investigated. (Bhatnagar et al., 2017; Epelboin et al., 2017; Mladinich et al., 2017).

It is not well understood whether ZIKV strains of African and Asian lineages use the same factors for attachment to cell surface with different affinities, or authorize distinct molecules for endocytosis of virus particles. To date, little is known on attachment factors and entry receptors that contribute to the permissiveness of SH-SY5Y cells to ZIKV. It has been reported that the TIM-receptor AXL binds ZIKV via Gas 6 and mediates viral entry in neural cells of human origin (Meertens et al., 2017). Among the diverging residues identified between MR766 and BeH819015 structural proteins, it is therefore urgent to determine which ones could contribute to the permissiveness of human neural cells to ZIKV infection.

Acknowledgements

We gratefully knowledge P. Mavingui and REACTing consortium for their support. We thank J.-J. Hoarau for helpful discussions. This work was supported by the ZIKAlliance project (European Union-Horizon

2020 programme under grant agreement no 735548) and the ZIKAlert project (POE FEDER 2014-2020 Ile de la Réunion action 1.05 under grant agreement no SYNERGY-RE0001902). SB has PhD degree scholarship from La Réunion Island University (Ecole Doctorale STS), funded by French ministry MEESR.

Appendix A. Supplementary material

Supplementary data associated with this article can be found in the online version at <http://dx.doi.org/10.1016/j.virol.2017.12.003>.

References

- Alcendor, D.J., 2017. Zika virus infection of the human glomerular cells: implications for viral reservoirs and renal pathogenesis. *J. Infect. Dis.* 216, 162–171. <http://dx.doi.org/10.1093/infdis/jix171>.
- Atieh, T., Baronti, C., de Lamballerie, X., Nougairède, A., 2016. Simple reverse genetics systems for Asian and African Zika viruses. *Sci. Rep.* 6, 39384. <http://dx.doi.org/10.1038/srep39384>.
- Bhatnagar, J., Rabeneck, D.B., Martinez, R.B., Reagan-Steiner, S., Ermias, Y., Estetter, L.B.C., Suzuki, T., Ritter, J., Keating, M.K., Hale, G., Gary, J., Muehlenbachs, A., Lambert, A., Lanciotti, R., Oduyibo, T., Meaney-Delman, D., Bolaños, F., Saad, E.A.P., Shieh, W.-J., Zaki, S.R., 2017. Zika virus RNA replication and persistence in brain and placental tissue. *Emerg. Infect. Dis.* 23, 405–414. <http://dx.doi.org/10.3201/eid2303.161499>.
- Calvert, A.E., Huang, C.Y.-H., Blair, C.D., Roehrig, J.T., 2012. Mutations in the West Nile prM protein affect VLP and virion secretion in vitro. *Virology* 433, 35–44. <http://dx.doi.org/10.1016/j.virol.2012.07.011>.
- Cao-Lormeau, V.-M., Blake, A., Mons, S., Lastère, S., Roche, C., Vanhomwegen, J., Dub, T., Baudouin, L., Teissier, A., Larre, P., Vial, A.-L., Decam, C., Choumet, V., Halstead, S.K., Willison, H.J., Musset, L., Manuguerra, J.-C., Despres, P., Fournier, E., Mallet, H.-P., Musso, D., Fontanet, A., Neil, J., Ghawché, F., 2016. Guillain-Barré Syndrome outbreak associated with Zika virus infection in French Polynesia: a case-control study. *Lancet* 387, 1531–1539. [http://dx.doi.org/10.1016/S0140-6736\(16\)00562-6](http://dx.doi.org/10.1016/S0140-6736(16)00562-6).
- Cao-Lormeau, V.-M., Roche, C., Teissier, A., Robin, E., Berry, A.-L., Mallet, H.-P., Sall, A.A., Musso, D., 2014. Zika virus, French polynesia, South pacific, 2013. *Emerg. Infect. Dis.* 20, 1085–1086. <http://dx.doi.org/10.3201/eid2006.140138>.
- Cugola, F.R., Fernandes, I.R., Russo, F.B., Freitas, B.C., Dias, J.L.M., Guimarães, K.P., Benazzato, C., Almeida, N., Pignatari, G.C., Romero, S., Polonio, C.M., Cunha, I., Freitas, C.L., Brandão, W.N., Rossato, C., Andrade, D.G., Faria, D., de, P., Garcez, A.T., Buchpiguel, C.A., Braconi, C.T., Mendes, E., Sall, A.A., Zanotto, P.M., de, A., Peron, J.P.S., Muotri, A.R., Beltrão-Braga, P.C.B., 2016. The Brazilian Zika virus strain causes birth defects in experimental models. *Nature* 534, 267–271. <http://dx.doi.org/10.1038/nature18296>.
- Dick, G.W.A., Kitchen, S.F., Haddock, A.J., 1952. Zika Virus (I). Isolations and serological specificity. *Trans. R. Soc. Trop. Med. Hyg.* 46, 509–520. [http://dx.doi.org/10.1016/0035-9203\(52\)90042-4](http://dx.doi.org/10.1016/0035-9203(52)90042-4).
- D'Ortenzio, E., Matheron, S., Yazdanpanah, Y., de Lamballerie, X., Hubert, B., Piorkowski, G., Maquart, M., Descamps, D., Damond, F., Leparce-Goffart, I., 2016. Evidence of sexual transmission of Zika virus. *N. Engl. J. Med.* 374, 2195–2198. <http://dx.doi.org/10.1056/NEJMc1604449>.
- Duffy, M.R., Chen, T.-H., Hancock, W.T., Powers, A.M., Kool, J.L., Lanciotti, R.S., Pretrick, M., Marfel, M., Holzbauer, S., Dubray, C., Guillaumot, L., Griggs, A., Bel, M., Lambert, A.J., Laven, J., Kosoy, O., Panella, A., Biggerstaff, B.J., Fischer, M., Hayes, E.B., 2009. Zika virus outbreak on Yap Island, Federated States of Micronesia. *N. Engl. J. Med.* 360, 2536–2543. <http://dx.doi.org/10.1056/NEJMoa0805715>.
- Elshuber, S., Allison, S.L., Heinz, F.X., Mandl, C.W., 2003. Cleavage of protein prM is necessary for infection of BHK-21 cells by tick-borne encephalitis virus. *J. Gen. Virol.* 84, 183–191. <http://dx.doi.org/10.1099/vir.0.18723-0>.
- Epelboin, S., Dulioust, E., Epelboin, L., Benachi, A., Merlet, F., Patrat, C., 2017. Zika virus and reproduction: facts, questions and current management. *Hum. Reprod. Update* 23, 629–645. <http://dx.doi.org/10.1093/humupd/dmx024>.
- Faria, N.R., Azevedo, R., do, S., da, S., Kraemer, M.U.G., Souza, R., Cunha, M.S., Hill, S.C., Théze, J., Bonsall, M.B., Bowden, T.A., Rissanen, I., Rocco, I.M., Nogueira, J.S., Maeda, A.Y., Vasami, F.G., da, S., Macedo, F.L., de, L., Suzuki, A., Rodrigues, S.G., Cruz, A.C.R., Nunes, B.T., Medeiros, D.B., de, A., Rodrigues, D.S.G., Queiroz, A.L.N., da Silva, E.V.P., Henriques, D.F., da Rosa, E.S.T., de Oliveira, C.S., Martins, L.C., Vasconcelos, H.B., Casseb, L.M.N., Smith, D., de, B., Messina, J.P., Abade, L., Lourenço, J., Alcantara, L.C.J., de Lima, M.M., Giovanetti, M., Hay, S.I., de Oliveira, R.S., Lemos, P., da, S., de Oliveira, L.F., de Lima, C.P.S., da Silva, S.P., de Vasconcelos, J.M., Franco, L., Cardoso, J.F., Vianez-Júnior, J.L., da, S.G., Mir, D., Bello, G., Delatorre, E., Khan, K., Creatore, M., Coelho, G.E., de Oliveira, W.K., Tesh, R., Pybus, O.G., Nunes, M.R.T., Vasconcelos, P.F.C., 2016. Zika virus in the Americas: early epidemiological and genetic findings. *Science* 352, 345–349. <http://dx.doi.org/10.1126/science.aaf5036>.
- Fensterl, V., Sen, G.C., 2011. The ISG56/IFIT1 gene family. *J. Interferon Cytokine Res.* 31, 71–78. <http://dx.doi.org/10.1089/jir.2010.0101>.
- Frument, E., Roche, M., Krejbich-Trotot, P., El-Kalamouni, C., Nativel, B., Rondeau, P., Missé, D., Gadea, G., Viranick, W., Després, P., 2016. The South Pacific epidemic strain of Zika virus replicates efficiently in human epithelial A549 cells leading to IFN- β production and apoptosis induction. *Virology* 493, 217–226. <http://dx.doi.org/10.1016/j.virol.2016.03.006>.

- Gadea, G., Bos, S., Krejbich-Trotot, P., Clain, E., Viranaicken, W., El-Kalamouni, C., Mavingui, P., Desprès, P., 2016. A robust method for the rapid generation of recombinant Zika virus expressing the GFP reporter gene. *Virology* 497, 157–162. <http://dx.doi.org/10.1016/j.virol.2016.07.015>.
- Gatherer, D., Kohl, A., 2016. Zika virus: a previously slow pandemic spreads rapidly through the Americas. *J. Gen. Virol.* 97, 269–273. <http://dx.doi.org/10.1099/jgv.0.000381>.
- Giovanetti, M., Milano, T., Alcantara, L.C., Carcangiu, L., Cella, E., Lai, A., Lo Presti, A., Pascarella, S., Zehender, G., Angeletti, S., Ciccozzi, M., 2016. Zika virus spreading in South America: evolutionary analysis of emerging neutralizing resistant Phe279Ser strains. *Asian Pac. J. Trop. Med.* 9, 445–452. <http://dx.doi.org/10.1016/j.apjtm.2016.03.028>.
- Haddow, A.D., Schuh, A.J., Yasuda, C.Y., Kasper, M.R., Heang, V., Huy, R., Guzman, H., Tesh, R.B., Weaver, S.C., 2012. Genetic characterization of Zika virus strains: geographic expansion of the Asian lineage. *PLoS Negl. Trop. Dis.* 6, e1477. <http://dx.doi.org/10.1371/journal.pntd.0001477>.
- Hamel, R., Dejarnac, O., Wichit, S., Ekcharyawat, P., Neyret, A., Luplertlop, N., Perera-Lecoin, M., Surasombattana, P., Talignani, L., Thomas, F., Cao-Lormeau, V.-M., Choumet, V., Briant, L., Desprès, P., Amara, A., Yssel, H., Missé, D., 2015. Biology of Zika Virus infection in human skin cells. *J. Virol.* 89, 8880–8896. <http://dx.doi.org/10.1128/JVI.00354-15>.
- Hamel, R., Ferraris, P., Wichit, S., Diop, F., Talignani, L., Pompon, J., Garcia, D., Liégeois, F., Sall, A.A., Yssel, H., Missé, D., 2017. African and Asian Zika virus strains differentially induce early antiviral responses in primary human astrocytes. *Infect. Genet. Evol.* 49, 134–137. <http://dx.doi.org/10.1016/j.meegid.2017.01.015>.
- Hsieh, S.-C., Wu, Y.-C., Zou, G., Nerurkar, V.R., Shi, P.-Y., Wang, W.-K., 2014. Highly conserved residues in the helical domain of dengue virus type 1 precursor membrane protein are involved in assembly, precursor membrane (prM) protein cleavage, and entry. *J. Biol. Chem.* 289, 33149–33160. <http://dx.doi.org/10.1074/jbc.M114.610428>.
- Huang, W.-C., Abraham, R., Shim, B.-S., Choe, H., Page, D.T., 2016. Zika virus infection during the period of maximal brain growth causes microcephaly and corticospinal neuron apoptosis in wild type mice. *Sci. Rep.* 6, 34793. <http://dx.doi.org/10.1038/srep34793>.
- Junjhon, J., Edwards, T.J., Utaipat, U., Bowman, V.D., Holdaway, H.A., Zhang, W., Keelapang, P., Puttikunt, C., Perera, R., Chipman, P.R., Kasinrerk, W., Malasit, P., Kuhn, R.J., Sittisombut, N., 2010. Influence of pr-M cleavage on the heterogeneity of extracellular dengue virus particles. *J. Virol.* 84, 8353–8358. <http://dx.doi.org/10.1128/JVI.00696-10>.
- Kim, J.-M., Yun, S.-I., Song, B.-H., Hahn, Y.-S., Lee, C.-H., Oh, H.-W., Lee, Y.-M., 2008. A single N-linked glycosylation site in the Japanese encephalitis virus prM protein is critical for cell type-specific prM protein biogenesis, virus particle release, and pathogenicity in mice. *J. Virol.* 82, 7846–7862. <http://dx.doi.org/10.1128/JVI.00789-08>.
- Meertens, L., Labeau, A., Dejarnac, O., Cipriani, S., Sinigaglia, L., Bonnet-Madin, L., Le Charpentier, T., Hafirassou, M.L., Zamborlini, A., Cao-Lormeau, V.-M., Couplier, M., Missé, D., Jouvencet, N., Tabibiazar, R., Gressens, P., Schwartz, O., Amara, A., 2017. Axl mediates ZIKA virus entry in human glial cells and modulates innate immune responses. *Cell Rep.* 18, 324–333. <http://dx.doi.org/10.1016/j.celrep.2016.12.045>.
- Merfeld, E., Ben-Avi, L., Kennon, M., Cerveny, K.L., 2017. Potential mechanisms of Zika-linked microcephaly. *Wiley Interdiscip. Rev. Dev. Biol.* <http://dx.doi.org/10.1002/wdev.273>.
- Mladinich, M.C., Schwedes, J., Mackow, E.R., 2017. Zika virus persistently infects and is basolaterally released from primary human brain microvascular endothelial cells. *mBio* 8. <http://dx.doi.org/10.1128/mBio.00952-17>.
- Mossentia, M., Marchese, S., Poggianella, M., Slon Campos, J.L., Burrone, O.R., 2017. Role of N-glycosylation on Zika virus E protein secretion, viral assembly and infectivity. *Biochem. Biophys. Res. Commun.* <http://dx.doi.org/10.1016/j.bbrc.2017.01.022>.
- Motta, I.J.F., Spencer, B.R., Cordeiro da Silva, S.G., Arruda, M.B., Dobbin, J.A., Gonzaga, Y.B.M., Arcuri, I.P., Tavares, R.C.B.S., Atta, E.H., Fernandes, R.F.M., Costa, D.A., Ribeiro, L.J., Limonte, F., Higa, L.M., Voloch, C.M., Brindeiro, R.M., Tanuri, A., Ferreira, O.C., 2016. Evidence for transmission of Zika virus by platelet transfusion. *N. Engl. J. Med.* 375, 1101–1103. <http://dx.doi.org/10.1056/NEJMc1607262>.
- Musso, D., Stramer, S.L., 2016. AABB Transfusion-Transmitted Diseases Committee, Busch, M.P., International Society of Blood Transfusion Working Party on Transfusion-Transmitted Infectious Diseases. Zika virus: a new challenge for blood transfusion. *Lancet.* 387, 1993–1994. [http://dx.doi.org/10.1016/S0140-6736\(16\)30428-7](http://dx.doi.org/10.1016/S0140-6736(16)30428-7).
- Nativel, B., Marimoutou, M., Thon-Hon, V.G., Gunasekaran, M.K., Andries, J., Stanislas, G., Planesne, C., Da Silva, C.R., Césari, M., Iwema, T., Gasque, P., Viranaicken, W., 2013. Soluble HMGB1 is a novel adipokine stimulating IL-6 secretion through RAGE receptor in SW872 preadipocyte cell line: contribution to chronic inflammation in fat tissue. *PLoS One* 8, e76039. <http://dx.doi.org/10.1371/journal.pone.0076039>.
- Pagani, I., Ghezzi, S., Ulisse, A., Rubio, A., Turrini, F., Garavaglia, E., Candiani, M., Castilletti, C., Ippolito, G., Poli, G., Broccoli, V., Panina-Bordignon, P., Vicenzi, E., 2017. Human endometrial stromal cells are highly permissive to productive infection by Zika virus. *Sci. Rep.* 7, 44286. <http://dx.doi.org/10.1038/srep44286>.
- Parra, B., Lizarazo, J., Jiménez-Arango, J.A., Zea-Vera, A.F., González-Manrique, G., Vargas, J., Angarita, J.A., Zuñiga, G., Lopez-Gonzalez, R., Beltran, C.L., Rízcala, K.H., Morales, M.T., Pacheco, O., Ospina, M.L., Kumar, A., Cornblath, D.R., Muñoz, L.S., Osorio, L., Barreras, P., Pardo, C.A., 2016. Guillain-Barré syndrome associated with Zika virus infection in Colombia. *N. Engl. J. Med.* 375, 1513–1523. <http://dx.doi.org/10.1056/NEJMoa1605564>.
- Quicke, K.M., Bowen, J.R., Johnson, E.L., McDonald, C.E., Ma, H., O'Neal, J.T., Rajakumar, A., Wrammert, J., Rimawi, B.H., Pulendran, B., Schinazi, R.F., Chakraborty, R., Suthar, M.S., 2016. Zika virus infects human placental macrophages. *Cell Host Microbe* 20, 83–90. <http://dx.doi.org/10.1016/j.chom.2016.05.015>.
- Setoh, Y.X., Tan, C.S.E., Prow, N.A., Hobson-Peters, J., Young, P.R., Khromykh, A.A., Hall, R.A., 2015. The I22V and L72S substitutions in West Nile virus prM protein promote enhanced prM/E heterodimerisation and nucleocapsid incorporation. *Virol. J.* 12, 72. <http://dx.doi.org/10.1186/s12985-015-0303-7>.
- Sheridan, M.A., Yunusov, D., Balaraman, V., Alexenko, A.P., Yabe, S., Verjovski-Almeida, S., Schust, D.J., Franz, A.W., Sadovsky, Y., Ezashi, T., Roberts, R.M., 2017. Vulnerability of primitive human placental trophoblast to Zika virus. *Proc. Natl. Acad. Sci. USA* 114, E1587–E1596. <http://dx.doi.org/10.1073/pnas.1616097114>.
- Simonin, Y., Loustalot, F., Desmetz, C., Foulongne, V., Constant, O., Fournier-Wirth, C., Leon, F., Molès, J.-P., Goubaud, A., Lemaître, J.-M., Maquart, M., Leparç-Goffart, I., Briant, L., Nagot, N., Van de Perre, P., Salinas, S., 2016. Zika virus strains potentially display different infectious profiles in human neural cells. *EBioMedicine* 12, 161–169. <http://dx.doi.org/10.1016/j.ebiom.2016.09.020>.
- Sirohi, D., Chen, Z., Sun, L., Klose, T., Pierson, T.C., Rossmann, M.G., Kuhn, R.J., 2016. The 3.8 Å resolution cryo-EM structure of Zika virus. *Science* 352, 467–470. <http://dx.doi.org/10.1126/science.aaf5316>.
- Souza, B.S.F., Sampaio, G.L.A., Pereira, C.S., Campos, G.S., Sardi, S.I., Freitas, L.A.R., Figueira, C.P., Paredes, B.D., Nonaka, C.K.V., Azevedo, C.M., Rocha, V.P.C., Bandeira, A.C., Mendez-Otero, R., Dos Santos, R.R., Soares, M.B.P., 2016. Zika virus infection induces mitosis abnormalities and apoptotic cell death of human neural progenitor cells. *Sci. Rep.* 6, 39775. <http://dx.doi.org/10.1038/srep39775>.
- Tripathi, S., Balasubramaniam, V.R.M.T., Brown, J.A., Mena, I., Grant, A., Bardina, S.V., Maringer, K., Schwarz, M.C., Maestre, A.M., Sourisseau, M., Albrecht, R.A., Krammer, F., Evans, M.J., Fernandez-Sesma, A., Lim, J.K., García-Sastre, A., 2017. A novel Zika virus mouse model reveals strain specific differences in virus pathogenesis and host inflammatory immune responses. *PLoS Pathog.* 13, e1006258. <http://dx.doi.org/10.1371/journal.ppat.1006258>.
- Viranaicken, W., Gasmí, L., Chaumet, A., Durieux, C., Georget, V., Denoulet, P., Larcher, J.-C., 2011. L-Ilf3 and L-NF90 traffic to the nucleolus granular component: alternatively-spliced exon 3 encodes a nucleolar localization motif. *PLoS One* 6, e22296. <http://dx.doi.org/10.1371/journal.pone.0022296>.
- Widman, D.G., Young, E., Yount, B.L., Plante, K.S., Gallichotte, E.N., Carbaugh, D.L., Peck, K.M., Plante, J., Swanson, J., Heise, M.T., Lazear, H.M., Baric, R.S., 2017. A reverse genetics platform that spans the Zika virus family tree. *mBio* 8. <http://dx.doi.org/10.1128/mBio.02014-16>.
- Xie, X., Yang, Y., Muruato, A.E., Zou, J., Shan, C., Nunes, B.T.D., Medeiros, D.B.A., Vasconcelos, P.F.C., Weaver, S.C., Rossi, S.L., Shi, P.-Y., 2017. Understanding Zika virus stability and developing a chimeric vaccine through functional analysis. *mBio* 8. <http://dx.doi.org/10.1128/mBio.02134-16>.
- Yoshii, K., Igarashi, M., Ichii, O., Yokozawa, K., Ito, K., Kariwa, H., Takashima, I., 2012. A conserved region in the prM protein is a critical determinant in the assembly of flavivirus particles. *J. Gen. Virol.* 93, 27–38. <http://dx.doi.org/10.1099/vir.0.035964-0>.
- Yoshii, K., Konno, A., Goto, A., Nio, J., Obara, M., Ueki, T., Hayasaka, D., Mizutani, T., Kariwa, H., Takashima, I., 2004. Single point mutation in tick-borne encephalitis virus prM protein induces a reduction of virus particle secretion. *J. Gen. Virol.* 85, 3049–3058. <http://dx.doi.org/10.1099/vir.0.80169-0>.
- Yuan, L., Huang, X.-Y., Liu, Z.-Y., Zhang, F., Zhu, X.-L., Yu, J.-Y., Ji, X., Xu, Y.-P., Li, G., Li, C., Wang, H.-J., Deng, Y.-Q., Wu, M., Cheng, M.-L., Ye, Q., Xie, D.-Y., Li, X.-F., Wang, X., Shi, W., Hu, B., Shi, P.-Y., Xu, Z., Qin, C.-F., 2017. A single mutation in the prM protein of Zika virus contributes to fetal microcephaly. *Science* eam7120. <http://dx.doi.org/10.1126/science.aam7120>.

III. ARTICLE N°3



Article

The Roles of prM-E Proteins in Historical and Epidemic Zika Virus-Mediated Infection and Neurocytotoxicity

Ge Li ^{1,†}, Sandra Bos ^{2,†}, Konstantin A. Tsetsarkin ³, Alexander G. Pletnev ³,
Philippe Desprès ^{2,*}, Gilles Gadea ^{2,*} and Richard Y. Zhao ^{1,4,5,6,*}

¹ Department of Pathology, University of Maryland School of Medicine, Baltimore, MD 21201, USA; lige_cn@hotmail.com

² Unité Mixte Processus Infectieux en Milieu Insulaire Tropical, Plateforme Technologique CYROI, Université de La Réunion, INSERM U1187, CNRS UMR 9192, IRD UMR 249, Sainte-Clotilde, 97400 La Réunion, France; SandraBos.Lab@gmail.com (S.B.); philippe.despres@univ-reunion.fr (P.D.)

³ Laboratory of Infectious Diseases, NIAID, NIH, Bethesda, MD 20892, USA; konstantin.tsetsarkin@nih.gov (K.A.T.); apletnev@niaid.nih.gov (A.G.P.)

⁴ Department of Microbiology-Immunology, University of Maryland School of Medicine, Baltimore, MD 21201, USA

⁵ Institute of Global Health, University of Maryland School of Medicine, Baltimore, MD 21201, USA

⁶ Institute of Human Virology, University of Maryland School of Medicine, Baltimore, MD 21201, USA

* Correspondence: gilles.gadea@inserm.fr (G.G.); rzhao@som.umaryland.edu (R.Y.Z.); Tel.: +410-706-6301 (R.Y.Z.)

† These authors contributed equally to this work.

Received: 18 December 2018; Accepted: 9 February 2019; Published: 14 February 2019



Abstract: The Zika virus (ZIKV) was first isolated in Africa in 1947. It was shown to be a mild virus that had limited threat to humans. However, the resurgence of the ZIKV in the most recent Brazil outbreak surprised us because it causes severe human congenital and neurologic disorders including microcephaly in newborns and Guillain-Barré syndrome in adults. Studies showed that the epidemic ZIKV strains are phenotypically different from the historic strains, suggesting that the epidemic ZIKV has acquired mutations associated with the altered viral pathogenicity. However, what genetic changes are responsible for the changed viral pathogenicity remains largely unknown. One of our early studies suggested that the ZIKV structural proteins contribute in part to the observed virologic differences. The objectives of this study were to compare the historic African MR766 ZIKV strain with two epidemic Brazilian strains (BR15 and ICD) for their abilities to initiate viral infection and to confer neurocytopathic effects in the human brain's SNB-19 glial cells, and further to determine which part of the ZIKV structural proteins are responsible for the observed differences. Our results show that the historic African (MR766) and epidemic Brazilian (BR15 and ICD) ZIKV strains are different in viral attachment to host neuronal cells, viral permissiveness and replication, as well as in the induction of cytopathic effects. The analysis of chimeric viruses, generated between the MR766 and BR15 molecular clones, suggests that the ZIKV E protein correlates with the viral attachment, and the C-prM region contributes to the permissiveness and ZIKV-induced cytopathic effects. The expression of adenoviruses, expressing prM and its processed protein products, shows that the prM protein and its cleaved Pr product, but not the mature M protein, induces apoptotic cell death in the SNB-19 cells. We found that the Pr region, which resides on the N-terminal side of prM protein, is responsible for prM-induced apoptotic cell death. Mutational analysis further identified four amino-acid residues that have an impact on the ability of prM to induce apoptosis. Together, the results of this study show that the difference of ZIKV-mediated viral pathogenicity, between the historic and epidemic strains, contributed in part the functions of the structural prM-E proteins.

Keywords: Zika virus; prM-E proteins; viral pathogenicity; virus attachment; viral replication; viral permissiveness; viral survival; apoptosis; cytopathic effects; mutagenesis; chimeric viruses; human brain glial cells

1. Introduction

The 2015 Zika virus (ZIKV) outbreak in South America has a tremendous impact on public health. It was estimated that it left more than three thousand babies who were born with microcephaly, due to ZIKV infection in Brazil alone [1]. Monitoring those babies after birth continue to show various developmental and neurologic disorders that are now known as the congenital ZIKV syndrome [2,3]. Even though the causal relationship between ZIKV infection and ZIKV-induced microcephaly and other neurologic disorders have been firmly established [4–6], the reason for the sudden ZIKV virulence, and resulting neurologic disorders in humans, remain largely unknown.

ZIKV was originally isolated in 1947 from caged monkeys in the Zika forest of Uganda, Africa [7]. It was thought to be a mild virus that causes mild flu-like symptoms [7,8] and having a limited threat to humans [9,10]. A number of small-scale ZIKV outbreaks, with increasing number of individuals affected, took place in Asia and in Pacific Islands in past years [11,12] until it reached the Americas in a large-scale outbreak in 2015 [1]. In the most recent ZIKV outbreak, the virus spread to eighty-four countries, territories, or sub-national areas, with an estimate of over 1.5 million affected individuals [13]. Brazil was the most affected country, with an estimated 440,000 to 1.3 million cases reported [14]. The fact that the epidemic ZIKV causes severe human congenital and neurologic disorders, suggests that the epidemic ZIKV must have acquired enhanced viral pathogenicity through adaptive viral gene mutations.

ZIKV is a member of the flaviviruses (the family of *Flaviviridae*), which include a number of well-known human pathogens such as Dengue Virus (DENV), West Nile Virus (WNV), and Japanese Encephalitis Virus (JEV). It is a single-stranded, positive-sense RNA virus with a viral genome of approximately 10.7 kilobases (kb). The ZIKV genome encodes a single large open reading frame that produces a polyprotein, which is subsequently processed by viral and host proteases to produce a total of fourteen immature proteins, mature proteins, and small peptides [10,15]. A total of ten mature viral proteins, i.e., three structural proteins and seven non-structural proteins are produced after viral processing [16,17]. The structural proteins consist of an anchor capsid (anaC) protein, a precursor membrane (prM) protein, and an envelope (E) protein. In non-infectious and immature viral particles, the prM protein forms a heterodimer with the E protein [18,19]. The E protein, composed of the majority of the virion surface, is involved in binding to the host cell surface and triggering subsequent membrane fusion and endocytosis [10,20,21]. For virus maturation, the mature capsid (C) protein is produced by the proteolytic cleavage of the anaC protein in a post-Golgi compartment, which in turn triggers the cleavage of the prM protein by a host protease furin to produce a mature membrane (M) protein (75 a.a) and a Pr protein product (93 a.a) [15,22,23]. The transition of prM to M by furin cleavage results in mature and infectious particles [19,24]. Thus, one of our research interests here was to examine the effect of prM and its processed proteins, the mature M protein and a cleaved Pr protein product, on ZIKV-mediated cytopathic effect.

Based on phylogenetic analysis, ZIKV can be classified into two viral lineages, i.e., the African lineage, that includes ZIKV strains from Africa; and the Asian lineage that includes both Asian strains and those ZIKV strains that were isolated from the Americas, such as the Brazilian strains [25,26]. Comparative studies of the African and Asian ZIKV strains in vivo, ex vivo, and in animal models suggest that these two ZIKV lineages are intrinsically different in their pathogenicity and virulence [10,25,27,28]. Those virologic differences could potentially explain why the Brazilian ZIKV, which belongs to the Asian lineage, has acquired the epidemic potential and become highly virulent in humans. Conceivably, those epidemic and virologic potentials to cause the observed congenital ZIKV syndromes could be

acquired through evolution by adaptive viral gene mutations [10,28,29]. Nevertheless, which viral gene(s) is responsible for the observed phenotypic transition, and what type of viral gene mutations were adapted for this transition remain elusive.

Potential virologic differences between the African and Asian ZIKV lineages could be elucidated by exchanging different components of the ZIKV genome between the two viral lineages by generating chimeric viruses. Through such analysis of chimeric viral infection, any virologic changes, due to the swapping alteration would allow us to correlate a virologic change with a specific domain or gene of the ZIKV genome. By using this strategy and comparative analysis of a historic African ZIKV MR766 strain and an epidemic Brazilian BR15 strain in human host cells, we discovered in our earlier study that the structural proteins of the BR15 and MR766 ZIKV strains differ in their ability to initiate viral infection [30]. In line with our findings, an earlier comparative study of the ZIKV protein evolution from the pre-epidemic to the epidemic ZIKV, suggested that some of the amino acid (a.a.) sites in the E protein were negatively selected during ZIKV evolution, indicating possible functional alterations might have occurred during evolution [29]. In addition, another evolutionary study suggested that the S139N substitution in the prM protein was positively selected for in the pre-epidemic to the epidemic transition, and this single mutation alone led to more severe microcephaly than the pre-epidemic ZIKV strain [31]. The objectives of this study were (1) to further compare the historic African MR766 ZIKV strain with two epidemic Brazilian strains (molecular clones of BR15 and ICD) for their abilities to initiate viral infection and to confer neurocytopathic effects in human brain SNB-19 glial cells, and (2) to evaluate the contribution of prM-E proteins in the susceptibility of human brain glial cells to ZIKV infection.

2. Materials and Methods

2.1. Cell Culture

The SNB-19 (RRID:CVCL_0535), provided by Dr. HL Tang [32], is a human astrocytoma cell line, which was maintained in Corning RPMI 1640 medium (Product number: 10-040-CV, Mediatech, Inc., Manassas, VA, USA) supplemented with 10% fetal bovine serum (FBS) and 100 units/mL penicillin plus 100 µg/mL streptomycin. Vero76 cell is a derivative of the original Vero cells, which were originally isolated from the kidney of a normal adult African green monkey. Vero76 cells (ATCC-CRL-1587, Manassas, VA) were grown in Dulbecco's Modified Eagle Medium (DMEM) medium (Product number: 10-017-CV, Mediatech, Inc., Manassas, VA, USA), supplemented with 10% FBS and 100 units/mL penicillin, plus 100 µg/mL streptomycin.

2.2. Zika Virus Molecular Clones and Infection

The MR766 ZIKV strain was the first documented Zika strain that was isolated from caged monkey in the Zika forest in Uganda in 1947 [9]. Hence, it is called the historical strain. This viral strain has been passaged countless times in new-born mouse brains. The molecular clone of ZIKV-ZIKV-MR766-NIID was generated, based on the sequence of ZIKV strain MR766 Uganda 47-NIID (Genbank access # LC002520), using the infectious sub-genomic amplicon (ISA) method as described previously [33]. The BR15 ZIKV strain (BeH819015) was isolated from a blood sample of a patient and sequenced after one passage in mosquito C6/36 cells. It was one of the earliest Zika viral sequences that was isolated from one of the Northern states of Brazil (Pará) in July 2015 from a large clade [34,35]. The molecular clone of BR15 was generated, based on the BeH819015 sequence (Genbank Accession number: KU365778), using the same strategy as that of the ZIKV-MR766-NIID [30,33]. BR15 is available to BEI resources (Manassas, VA, USA) under the catalog number NR-51129. The ZIKV Paraíba_01/2015 strain (Genbank Accession number: KX280026) was originally isolated from the northeast state of Paraíba (Brazil) in 2015 from a serum sample of a febrile female. The virus was passed twice in Vero cells, and a molecular clone (ZIKV-ICD *aka* 674v4) was generated as described [36].

For viral infection, the cells were seeded in culture plates and incubated at 37 °C/5% CO₂ overnight to allow the cells to attach to the wells. The second day, ZIKV was added to the cells with the multiplicity of infection (MOI) of 1.0, unless specifically indicated. The cells were incubated for 2 h at 37 °C, with gentle agitation every 30 min. Next, the inoculum was removed, and the cells were washed twice with PBS. The culture medium was added to each well, and the cells were incubated at 37 °C/5% CO₂ for the duration of the experiment.

2.3. Generation and Production of the Chimeric Viruses

Two chimeric ZIKV molecular clones were generated. The M/B chimeric virus consisted of the C-prM viral sequence of MR766, with the rest of the viral genome replaced with the counterpart sequence of BR15 ZIKV molecular clone. Conversely, the B/M chimeric virus consists of the C-prM viral sequence of BR15 with the rest of the viral genome replaced with the counterpart sequence of MR766 ZIKV molecular clone. The general approach used for the construction of chimeric molecular clones was previously described [30,33]. To generate the M/B or B/M chimeric molecular clones, the respective C-prM regions from the MR766 or from the BR15 were extracted from the Z1 fragment. It was then introduced into the BR15 or the MR766 backbone respectively, by using the following shared primers: 5'-GCCAAAAAGTCATATACTTGGTCATGATACTGCTGATTGCCCGGC-3' and 5'-GCCGGGGCAATCAGCAGTATCATGACCAAGTATGACTTTTGGC-3'.

The procedure to generate and produce chimeric ZIKV viruses was essentially the same as described [30,33]. Briefly, the purified PCR fragments were electroporated into Vero76 cells. After 5 days, cell supernatants were recovered, usually in absence of cytopathic effects and were used to infect fresh Vero76 cells (DMEM with 2% FBS) in a first round of amplification (P1). Viral clones M/B or B/M were recovered 3–7 days later until cytopathic effect was observed under microscope and amplified for another 2 days on Vero76 cells to produce working P2 stocks of the viruses that were used for all studies. The viral titers were determined using the standard plaque-forming assay, as described previously, and expressed as plaque-forming units per mL (PFU/mL) [30]. The sequences of all the viruses and plasmid used in the study are available from the authors upon request.

2.4. Adenoviral Constructs and Cell Transduction

All of the Adenoviral (Adv) constructs, that were used in this study, were custom-made by ViGene (Rockville, MD, USA). The viral titers were determined using an ELISA Adeno-X rapid titer kit (Cat#: 631028, Clontech, Mountain View, CA, USA), which detects the Adenoviral Hexon surface antigen. For Adv transduction, SNB-19 cells in the concentration of 1×10^4 /well in 96 well plate were seeded and incubated at 37 °C/5% CO₂ overnight to allow the cells to attach to the wells. The second day, the SNB-19 cells were transduced with Adv with the MOI of 1000. The Adv transduced cells were incubated at 37 °C/5% CO₂ and the cells were collected at indicated times for analyses.

2.5. Viral Binding Assay

SNB-19 cells were cultured at sub-confluent density in 60 mm dishes. Cell monolayers were washed in cold PBS and cooled at 4 °C for at least 20 min in the presence of RPMI 1640, supplemented with 2% FBS. Pre-chilled cells were then incubated at 4 °C with ZIKV at MOI of 1.0 in 1.5 mL of RPMI 1640 medium supplemented with 2% FBS. After 1 h of incubation, the virus inputs were removed, and the cells were washed with RPMI 1640 medium, supplemented with 2% FBS. Total cellular RNA was extracted using TRIzol reagent (Life technologies, Carlsbad, CA, USA). The RT-qPCR analysis on viral RNA was performed using the primers amplifying a conserved ZIKV region between the NS5 and 3'UTR. The nucleotide sequences of these primer pairs are ZIKV-F: 5'-AGGATCATAGGTGATGAAGAAAAGT-3' and ZIKV-R: 5'-CCTGACAACACTAAGATTG-GTGC-3'. For viral binding assay in A549 cells, the RT-qPCR analysis on viral RNA was performed using the primers amplifying a region of the E protein, as described [30]. ZIKV E primers were designed to match both MR766-NIID and BeH819015

sequences. A house-keeping gene glyceraldehyde 3-phosphate dehydrogenase (GAPDH) was used as an endogenous control for the measurement of viral bindings.

2.6. Immunofluorescence Staining

The immunostaining method was used to determine ZIKV infectivity and induction of apoptosis, as described in [32]. Briefly, SNB-19 cells were infected with ZIKV, as described above. ZIKV-infected cells were fixed at 48 h post-infection (p.i.) with 3.7% paraformaldehyde in PBS for 1 h at room temperature on Labtek II slides. After washing three times for 5 min in PBS, the cells were blocked and permeabilized for 30 min in blocking buffer (10% FBS, 0.25% Triton X-100 in PBS). To determine viral infectivity, i.e., the percent of cells infected with ZIKV with MOI of 1.0, cells were first incubated with mouse anti-Flaviviridae group antigen (clone name: D1-4G2-15, Cat# MAB10216, MilliporeSigma, Burlington, MA) primary antibody with proper dilutions in the incubation buffer (1% BSA in PBS) for 2 h at 37 °C. After washing, cells were incubated with Texas Red-conjugated goat anti-mouse IgG secondary antibody (Cat# T-862, ThermoFisher, Waltham, MA, USA) at suggested concentration in the incubation buffer for 1 h at room temperature. After washing, cells were stained with DAPI for 5 min and washed again. Cells were then mounted with mounting medium and visualized on a Leica DM4500B microscope (Leica Microsystems, Buffalo Grove, IL) with Openlab software (Improvision, Lexington, MA, USA). ZIKV-induced caspase-3 cleavage, a hallmark of cellular apoptosis, was measured, by using the same immunostaining method, as described except cells was tested at 72 h p.i., and the primary antibody used was Cleaved Caspase-3 (Asp175) (5A1E) Rabbit mAb (Cat#9664, Cell Signaling, Danvers, MA, USA). The secondary antibody used was the FITC-conjugated goat anti-rabbit IgG secondary antibody (Cat# 31635, ThermoFisher, Waltham, MA, USA).

2.7. Measurement of ZIKV Viral Replication

ZIKV viral replication was measured over time, by using real-time reverse transcription polymerase chain reaction (RT-PCR) analysis, essentially as described previously [37]. Briefly, the total RNA was extracted from SNB-19 cells using TRIzol reagent (Life technologies, Carlsbad, CA, USA) according to the manufacturer's protocol. The RNA pellet was re-suspended in RNase-free distilled water and stored at −80 °C. Five hundred nanograms of RNA was used for real-time RT-PCR analysis, using iTaq universal SYBR Green one-step kit (BioRad, Hercules, CA, USA), according to the manufacturer's instruction. The primer sequences used here are the same conserved ZIKV region between the NS5 and 3'UTR as that described in the Section 2.5. The amplification in BioRad CFX96 real-time PCR system involved a reverse transcription reaction at 50 °C for 10 min, activation and DNA denaturation at 95 °C for 1 min, followed by 40 amplification cycles of 95 °C for 15 s and 60 °C for 30 s. The mRNA expression (fold-induction) was quantified by calculating the $2^{-\Delta CT}$ value, with GAPDH mRNA as an endogenous control.

Besides the RT-PCR, the conventional plaque forming assay was also used to measure viral replication. Viral titers were determined by a standard plaque-forming assay, as previously described, with minor modifications [38]. Briefly, Vero76 cells, grown in 48-well culture plate, were infected with tenfold dilutions of virus samples for 2 h at 37 °C and then incubated with 0.8% carboxymethylcellulose (CMC) for 4 days. CMC was removed from plate. The cells were washed two times with PBS and fixed by 3.7% FA in PBS and stained with 0.5% crystal violet in 20% ethanol. Viral titers were expressed as PFU/mL.

2.8. MTT Assay

The MTT assay was used to measure cell proliferation and viability as described previously [39]. SNB-19 cells were plated in 100 µL media in 96-well plate, with 10,000 cells per well, and incubated at 37 °C/5% CO₂ overnight to allow the cells to attach to the wells. At the indicated time intervals post-treatment, 10 µL of MTT solution (Thiazolyl Blue Tetrazolium Bromide, 5mg/mL in PBS) was added to each well, thoroughly mixed and incubated at 37 °C for 4 h to allow the MTT to be

metabolized. Then the media was removed and resuspended in 100 μ L DMSO to solubilize formazan (the MTT metabolized product). After shaking at 150 rpm for 5 min, the plate was subjected to optical density measurement at 562 nm by a SYNERGY-H1 microplate reader (BioTek Instruments, Winooski, VT, USA).

2.9. Measurement of Cellular Necrosis and Apoptosis

Cellular necrosis and apoptosis were measured by a RealTime-Glo™ Annexin V Apoptosis and Necrosis Assay kit (Promega, Madison, WI, USA) according to manufacturer's instruction. Briefly, 1×10^4 SNB-19 cells/well were seeded into a 96-well plate (Costar 3610, Corning, NY, USA) and cultured at 37 °C/5% CO₂ overnight. The cells were transduced with adenovirus, and 2x detection reagent (which included Annexin V NanoBiT®substrate, CaCl₂, Necrosis Detection Reagent, Annexin V-SmBiT and Annexin V-LgBiT) was added into each tested well of 96-well plate. The plates were incubated at 37 °C/5%, followed by measurements of luminance (RLU) for apoptosis, and fluorescence (RFU, 485 nm_{Ex}/520–30 nm_{Em}) for necrosis at the indicated time intervals post infection using a SYNERGY-H1 microplate reader.

2.10. Statistical Analysis

Unless indicated, two-tailed and paired student *t*-test was used for a pair-wise comparison of data, using Microsoft Excel software. Two-way ANOVA analysis was used to analyze results generated for Figure 1B, Figure 2A, Figure 3C, Figure 4A, Figure 5B,C and Figure 6C,D, respectively using Prism 7 (GraphPad Software, San Diego, CA, USA). A difference is considered statistically significant if $p \leq 0.1$ (*), $p \leq 0.05$ (**) or $p \leq 0.01$ (***) according to conventional definitions.

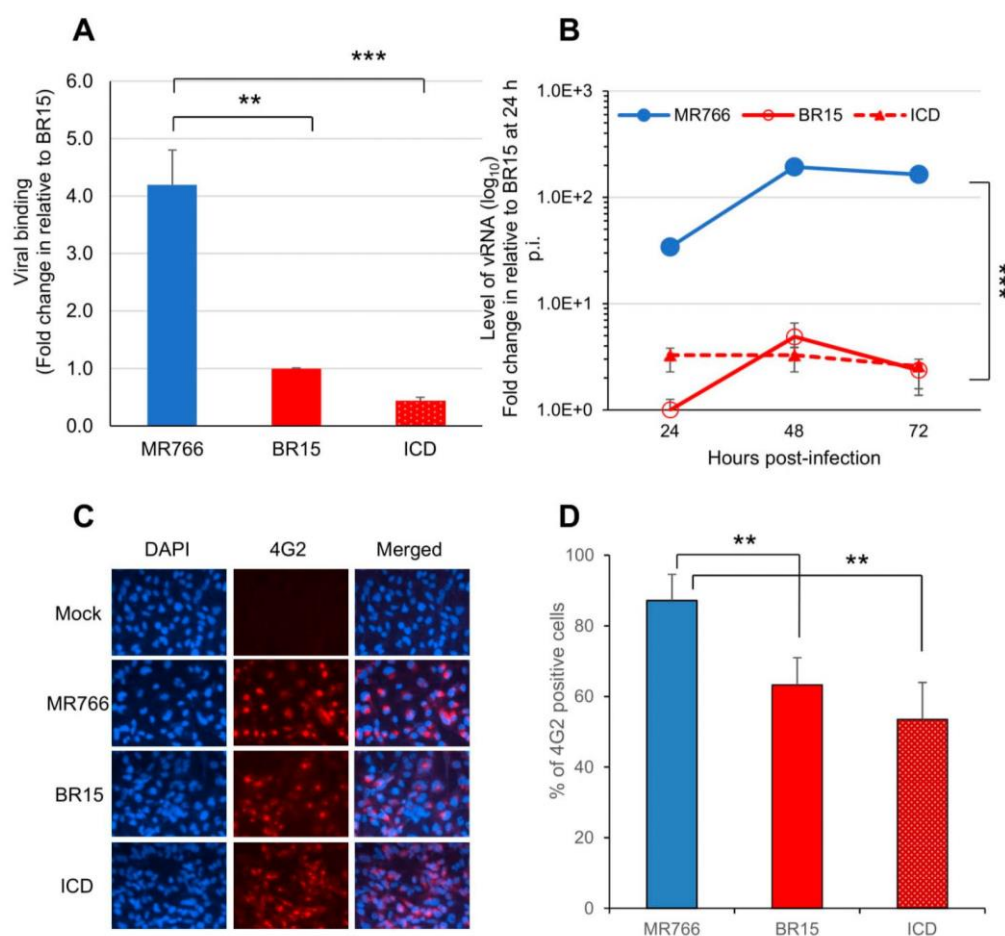


Figure 1. Different infectivity between the epidemic Brazilian Zika virus (BR15 and ICD) molecular clones and the historical African MR766 molecular clone in human brain glial SNB-19 cells. **(A)** Viral binding to SNB-19 cells was measured by presence of cell-associated vRNA one-hour post-infection (p.i.). A housekeeping gene GAPDH was used as an endogenous control for the measurement of viral bindings. **(B)** Zika virus (ZIKV) replication was measured by quantitative RT-PCR with timeframe as indicated. SNB-19 cells were infected by Zika viruses with multiplicity of infection (MOI) 1.0. Results represent average and standard deviation ($X \pm SD$) of four independent experiments. **(C)** Viral infectivity measured by anti-E mAb 4G2 at 48 h p.i. **(D)** Viral infectivity is shown as an average of three different experiments, each carried out in triplicates. Average cell number counted was about 100–200. Results represent average and standard deviation ($X \pm SD$). Levels of statistical significance were calculated by two-tailed and paired t-test for **(A)**, and Two-way ANOVA was used for **(B)**. **, $p < 0.05$; ***, $p < 0.01$.

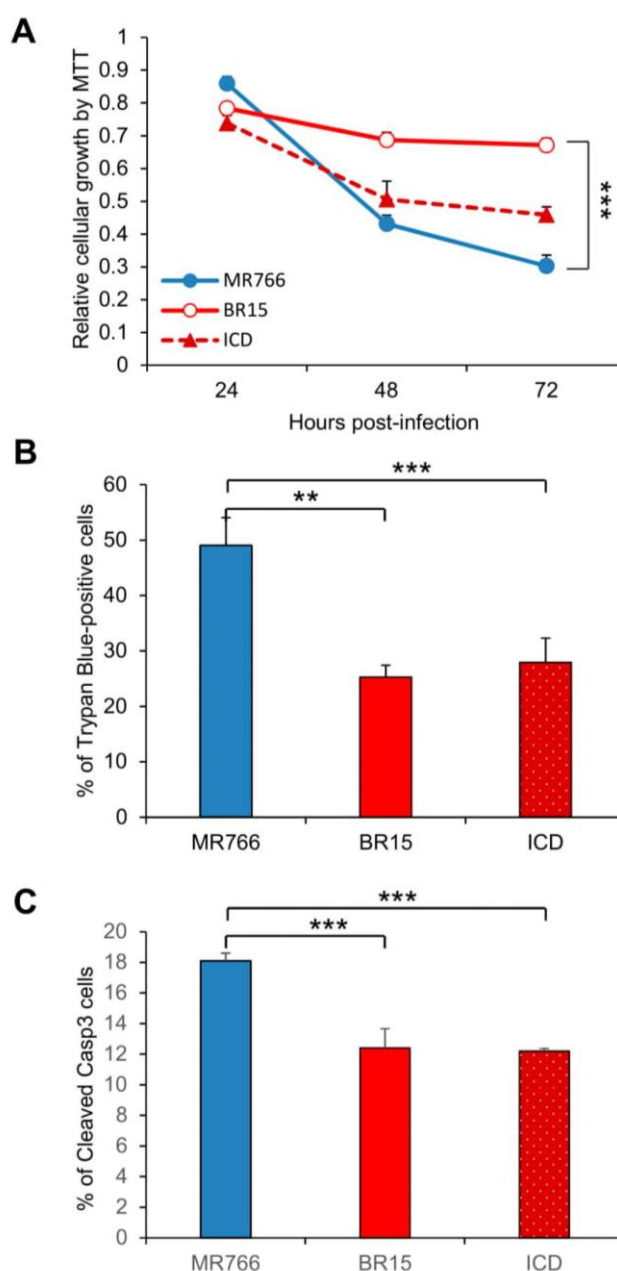


Figure 2. Different neuro-cytopathic effects of epidemic and historical molecular clones of Zika viruses on human brain glial SNB-19 cells. **(A)** Cellular survival was measured by the MTT assay. The graph is plotted as the relative growth in relevance to mock infected SNB19 cells. Statistic t-test shows that the differences among three viruses are not statistically significant. **(B)** ZIKV-induced cell death as measured by the Trypan blue assay. **, $p < 0.05$ for BR15 and ***, $p < 0.01$ for ICD. Three different experiments were carried out. Average cell number counted was about 100–200. **(C)** ZIKV-induced apoptosis was measured by caspase-3 cleavages using immunostaining as reported previously [32]. Cells were collected at 72 h p.i. Two experiments were conducted and cells showing caspase-3 cleavages were counted at 10 different areas with an average number of cells counted at 25–75. All results represent average and standard deviation ($\bar{X} + SD$). Levels of statistical significance were calculated by Two-way ANOVA for **(A)**. The difference between MR766 and BR15 is highly significant with $p < 0.01$ (**).

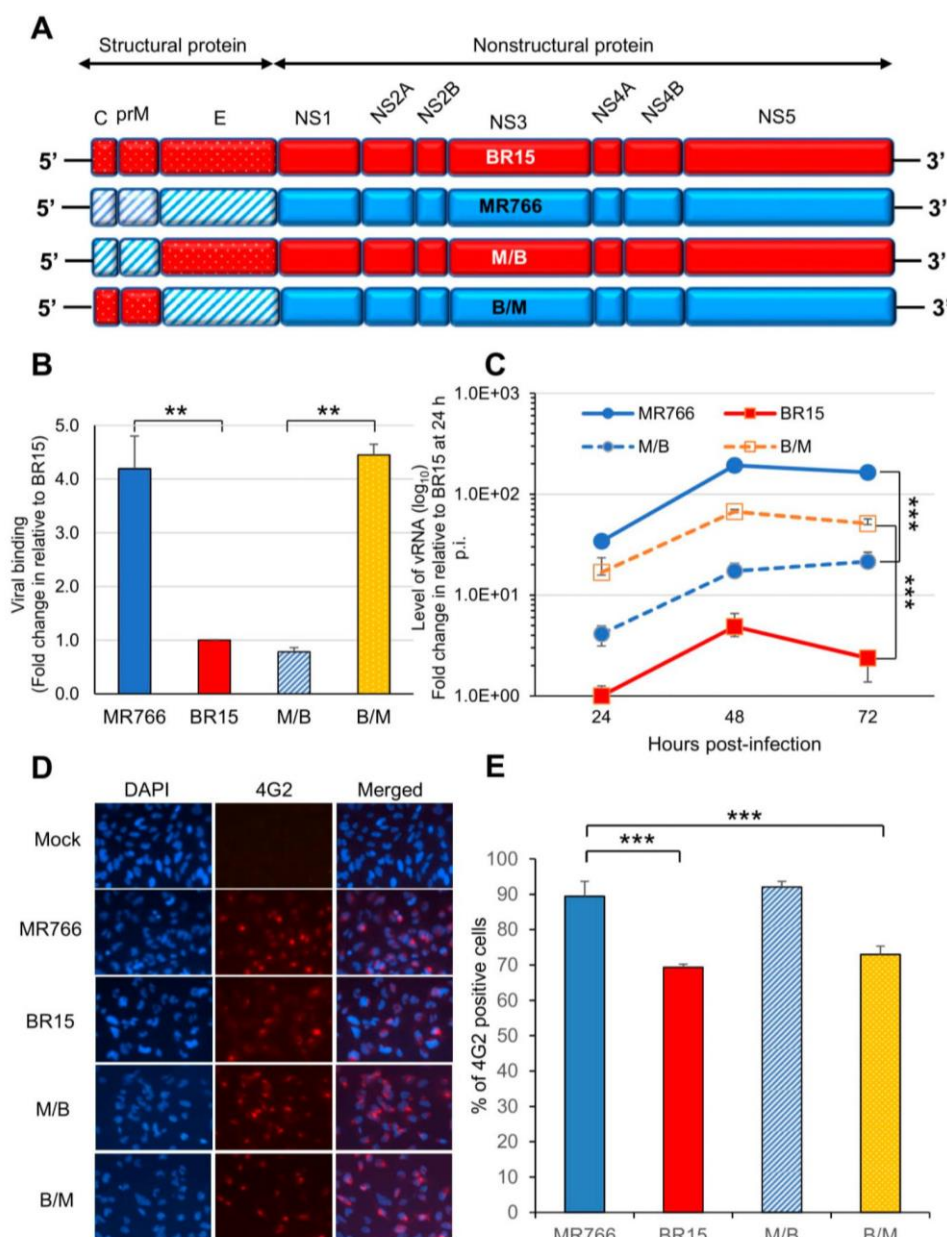


Figure 3. Correlation of the ZIKV C-prM with viral attachment and viral infection. **(A)** Generation of chimeric ZIKV molecular clones are shown along with their parental clones. The chimeric viruses were made between the MR766 and the BR15 ZIKV molecular clones. The viral genome exchange is at the junction of prM and E protein. **(B)** Viral binding was measured by presence of cell-associated vRNA 1 h p.i. A housekeeping gene GAPDH was used as an endogenous control for the measurement of viral bindings. Results represent average and standard deviation ($X \pm SD$) of four independent experiments. **(C)** ZIKV viral replication was measured by RT-qPCR with timeframe as indicated. **(D)** Viral infection was measured by anti-E mAb 4G2 at 48 h p.i. **(E)** Quantification of the results shown in **(D)**. SNB-19 cells were infected with Zika viruses with MOI of 1.0. Three different experiments were carried out in triplicates. Average cell number counted was about 100–200. All quantitative results represent average and standard deviation ($X \pm SD$). Levels of statistical significance were calculated by two-tailed and paired t-test for **(B)**, and Two-way ANOVA was used for **(C)**. **, $p < 0.05$; ***, $p < 0.01$.

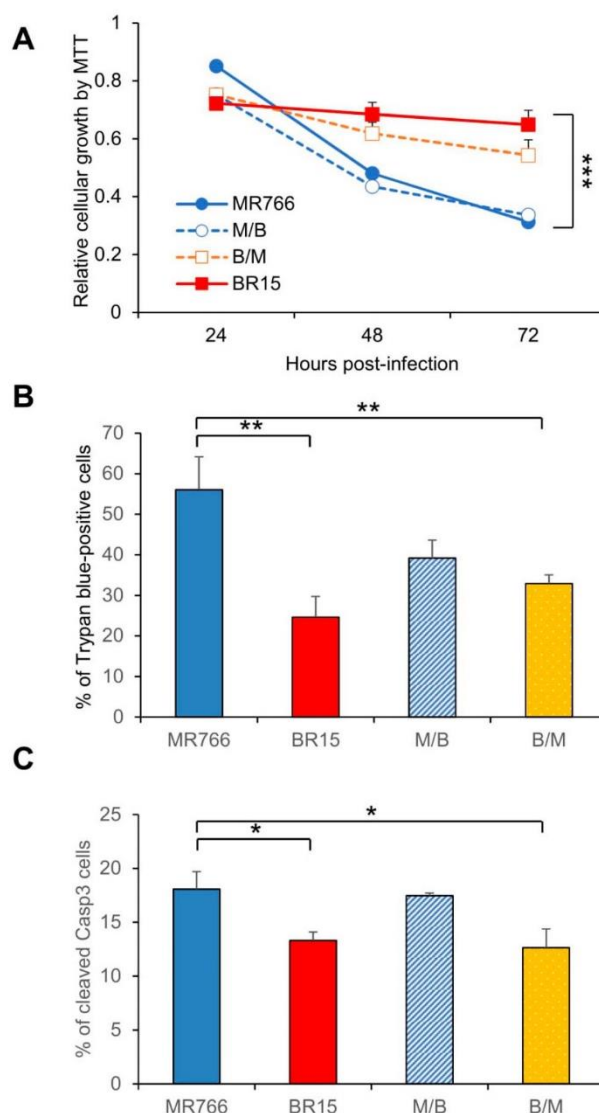


Figure 4. Correlation of the C-prM with ZIKV-induced growth restriction and apoptotic cell death. (A) Cell proliferation was measured by the MTT assay. Statistic t-test shows the differences shown among three viruses are not significant. (B) ZIKV-induced cell death was measured by the Trypan blue assay 72 h p.i. Two different experiments were carried out. Average number of cells counted was about 100–200. Differences between MR766 vs. BR15, and MR766 vs. B/M were both high significant with $p \leq 0.05$ (**) for both comparisons. The difference between MR766 and M/B was not significant with $p = 0.11$. (C) ZIKV-induced apoptosis was measured by cleavage of caspase-3. Cells were collected at 72 h p.i. All results represent average and standard deviation ($X \pm SD$). Levels of statistical significance were calculated by Two-way ANOVA for (A). The difference between MR766 and BR15 is highly significant with $p < 0.01$ (***).

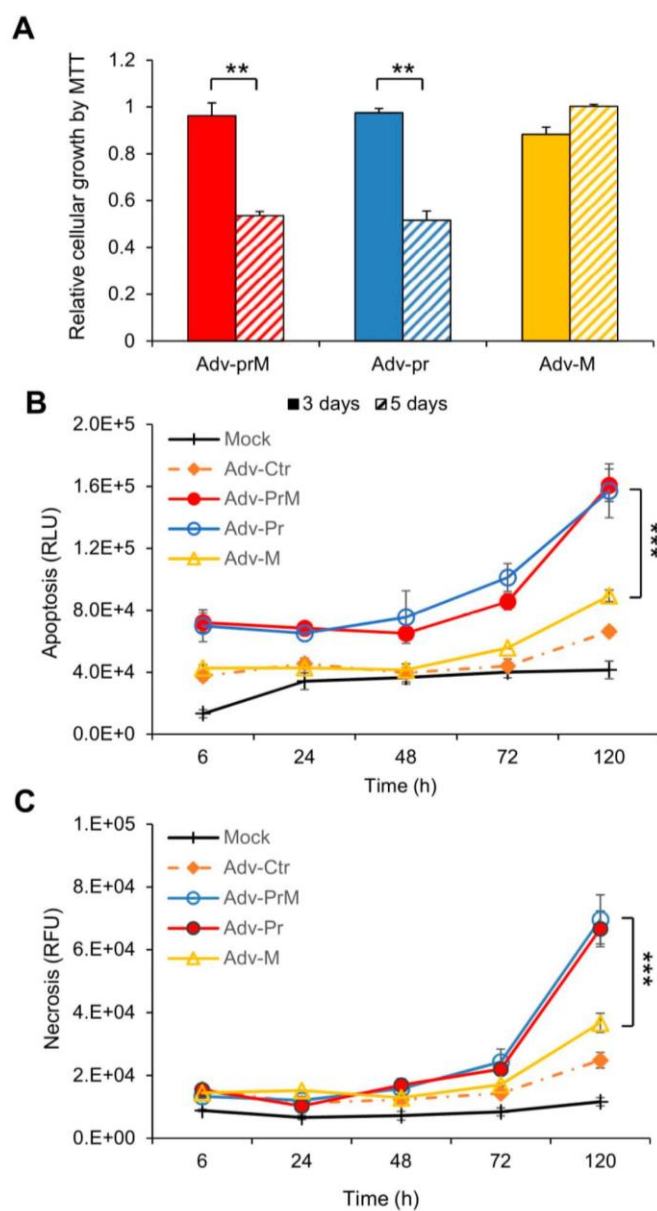


Figure 5. Effect of prM protein processing on ZIKV-induced neurocytotoxicity. (A) Cell proliferation and viability was measured overtime by the MTT assay. The graph is plotted as the relative growth in relevance to mock infected SNB-19 cells. The differences shown were highly significant with $p < 0.05$ (**). (B) Measurement of apoptosis by Annexin V over time. The difference between Adv-prM and Adv-M was highly significant with $p < 0.01$ (***), but the difference between Adv-prM and Adv-Pr was not significant with $p = 0.84$. (C) Measurement of cellular necrosis over time. Two-way ANOVA was used to calculate the difference between Adv-prM and Adv-M for (B) and (C). The differences between Adv-prM and Adv-M were highly significant with $p < 0.01$ (***). More than two different experiments were conducted to evaluate apoptosis and necrosis. All results represent average and standard deviation ($X \pm SD$).

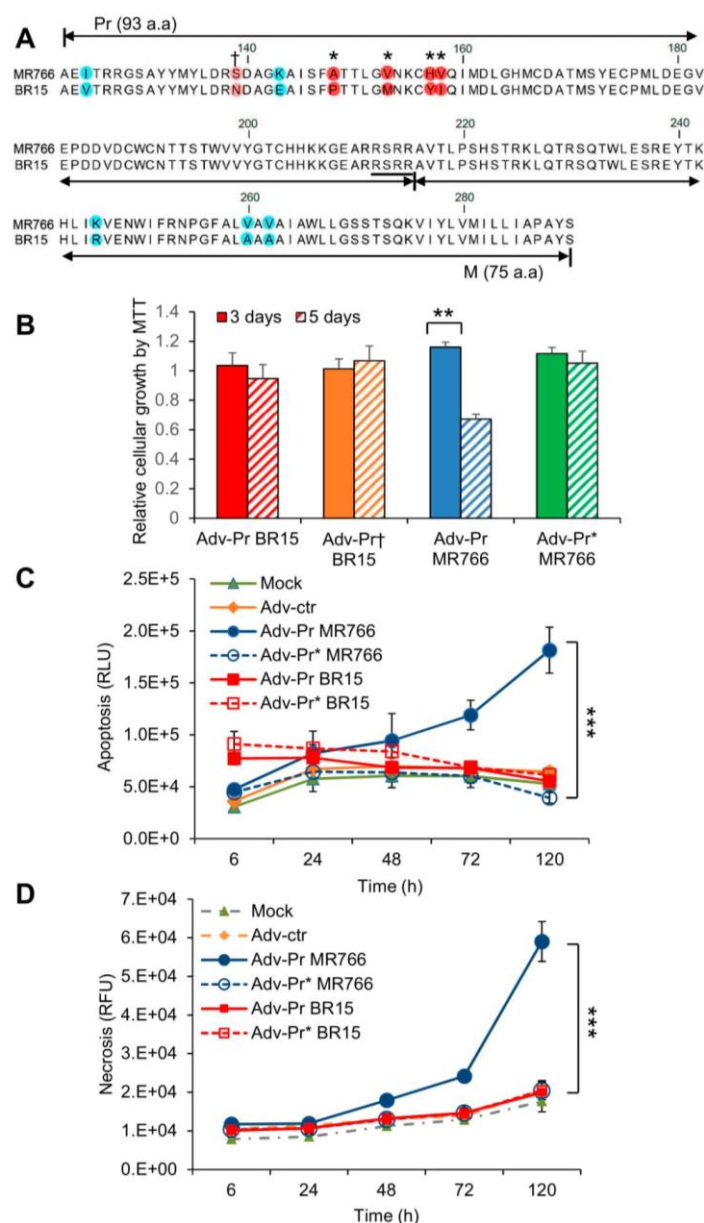


Figure 6. Mutational analysis of the Pr region of the prM protein. **(A)** Mutagenesis of the Pr protein. Four amino acids mutations (A148P, V153M, H157Y and V158I) were generated as shown by “*” on the top of the prM sequence alignments between MR766 (top) and BR15 (bottom). The resulting mutant adenoviral construct is labeled as Adv-Pr*_{MR766}. The site of the reverse N139S mutation is shown by “+” on the top of the prM sequence. The corresponding mutant adenoviral construct is labeled as Adv-Pr†_{BR15}. **(B)** Cell proliferation and viability by the MTT assay. Only Adv-prM showed significant differences overtime with $p < 0.05$ (**). Adv-Pr-induced cell death was measured by **(C)** apoptosis, and **(D)** necrosis over time. The underlined RSRR sequence indicates the putative furin cleavage site on the prM protein, based on its consensus target site Arg-X-Lys/Arg-Arg↓, where the arrow indicates the location of furin cleavage site. Two-way ANOVA was used to calculate the differences between Adv-prM and Adv-M for **(C)** and **(D)**. The differences between Adv-Pr MR766 and Adv-Pr* MR766 were highly significant with $p < 0.01$ (***). However, the difference between Adv-Pr BR15 and Adv-Pr† BR15 was not significant with $p > 0.99$ for both apoptosis and necrosis. All quantitative results represent average and standard deviation ($\bar{X} \pm \text{SD}$).

3. Results

3.1. Comparison of Viral Infectivity Between the Historical African Zika Virus and the Epidemic Brazilian Zika Viruses in Human Brain Glial SNB-19 Cells

Viral infectivity is defined as the ability of the ZIKV to bind, enter, and to replicate in host cells over time [40]. The goal of this experiment was to compare the viral infectivity between the epidemic Brazilian ZIKV molecular clones (BR15 and ICD) and the historical African ZIKV molecular clone (MR766). We first compared the viral attachment between molecular clones derived from epidemic Brazilian ZIKV strains (BR15 and ICD) and from the historical African ZIKV strain (MR766). All three ZIKV molecular clones have been reported previously [30,36]. The historical MR766 ZIKV strain is the first documented Zika strain that was isolated from caged monkey in the Zika forest in Uganda in 1947 [9]. Two epidemic ZIKV strains, BR15 (BeH819015) and ICD (Paraiba_01/2015) were isolated from Brazil in 2015 during the ZIKV epidemic [34,36]. A human brain glial cell line SNB-19 was used in this study because it is highly permissive to ZIKV infection [32].

The SNB-19 cells were infected with these three ZIKV molecular clones at the MOI of 1.0. After 1 h of incubation on ice, the free viruses were removed by washing the infected cells with cold RPMI 1640 medium supplemented with 2% FBS. Cell-associated viral RNA (vRNA), which represents the viruses attached to the cell surface, was isolated and quantified by real-time RT-PCR. A housekeeping gene, GAPDH, was used as an endogenous control for the measurement of viral bindings. As shown in Figure 1A, statistically significant differences in the virus binding to the SNB-19 cells were observed. Specifically, the numbers of ZIKV ICD or BR15 viral particles, that bound to the cells were about 4.2- to 9.5-fold lower, compared to the MR766 molecular clone.

We next monitored ZIKV viral replication over a time period of 3 days by real-time RT-PCR analysis (Figure 1B). The infection of the MR766 results, in consistently high viral RNA levels, were about 30-fold higher than that of BR15 or ICD over time. Both MR766 and BR15 displayed comparable replication kinetics, with a replication rate of 5.9 ± 0.71 fold-increase, and 4.4 ± 0.47 fold-increase, from 24 h, to 48 h p.i., respectively. The rate of vRNA decreased thereafter, presumably due to cytotoxicity. Notably, the vRNA in the ICD-infected cells was relatively stable over time, with an average replication rate of 1.3 ± 0.27 fold-increase, from 24 h to 48 h p.i.

Since there were clearly differences in the levels of viral bindings and the rates of vRNA production between the two types of molecular clones, we tested whether they were due to the viral permissiveness to SNB-19 cells, which typically represents the result of viral circumvention to host antiviral responses. The percentage of cells producing ZIKV particles was measured at 48 h p.i. Cells were immune-stained using the monoclonal antibody 4G2, which is directed against the flavivirus E protein [32]. The results of the immunostaining are shown in (Figure 1C), and the percentages of infected cells with each molecular clone are shown in (Figure 1D). Infection with the MR766 molecular clone resulted in statistically higher percentages of infected cells, with an average of 81.9% than the two Brazilian molecular clones, that displayed 57.8% for BR15 and 46.1% for ICD.

Together, these data indicate that the historical African strain MR766 showed a higher rate vRNA production and better infectivity in SNB-19 cells than that of the epidemic Brazilian ZIKV molecular clones (BR15 and ICD) presumably due to, at least in part, higher level of virus binding.

3.2. Comparison of the Historical Zika Virus with the Brazilian Epidemic Zika Viruses in Their Abilities to Induce Cytotoxicity

We next tested ZIKV-mediated cytotoxicity of the three ZIKV molecular clones. The SNB-19 cells were infected with the three molecular clones separately, as described in the Materials and Methods section. The MTT assay, which measures cell proliferation and viability [39], was used to measure the impacts of ZIKV infection on cellular metabolic activities. As shown in Figure 2A, cell proliferation and viability decreased rather rapidly in the MR766-infected cells between 24 h to 72 h p.i., whereas BR15- and ICD-infected cells were less affected. Even though the trend was clear, the differences are not

statistically significant. ZIKV-mediated cell death was then measured over the same period of time by Trypan blue staining that specifically detects dead cells. Time-dependent cell death was observed in cells infected with all three molecular clones. ZIKV-induced cell death was the most pronounced at 72 h p.i., in which the rate of MR766-induced cell death was significantly increased with $49.0 \pm 5.0\%$ of Trypan blue-positive cells than that of BR15 or ICD both with $25.3 \pm 2.1\%$, and $27.9 \pm 4.4\%$ of dead cells, respectively (Figure 2B; two-tailed *t*-test). To further assess whether ZIKV-induced cell death in the SNB-19 cells was caused by apoptosis, we carried out an immunostaining assay to measure in situ Caspase-3 (Casp-3) cleavages, a hallmark of apoptosis [30,32]. In mock-infected cells, little or no cells showed background staining (Supplemental Figure S1A); whereas ZIKV-infected cells showed Casp-3 cleavages, and MR766-infected cells showed significantly higher percentage of apoptotic cells (Figure 2C; two-tailed *t*-test, $p \leq 0.001$). These data show that the historical MR766 molecular clone is more apoptotic than the two Brazilian molecular clones (BR15 and ICD), suggesting that mutations within the epidemic strains might contribute to the reduced cytotoxicity.

3.3. Effects of the C-prM Region on Viral Infectivity

Since there were clear differences in viral infectivity between the historic and epidemic ZIKV strains in SNB-19 cells (Figure 1), we were interested in identifying which part of the ZIKV genome is responsible for the observed differences. Hereafter, we only focused on MR766 and BR15 molecular clones, as BR15 and ICD were very similar. Our previous study showed that the structural protein region (C-prM-E) of the ZIKV genome contributed to initiation of viral infection [30]. In this study, we decided to generate chimeric viruses, by separating the C-prM region from the E region of the structural proteins, using the ISA method [33]. In this way, we were able to differentiate the possible contribution of the C-prM region to viral infectivity or cytotoxicity from that of the E region. Specifically, the C-prM region of the MR766 was exchanged with that of the BR15 molecular clone, or vice versa. The two resulting new chimeric viruses were designated as M/B or B/M, in which the chimeric M/B virus carries the C-prM region of the MR766 with the rest of viral genome from the BR15; conversely, the chimeric B/M virus carries the BR15 C-prM region and the rest of the genomic structure is from MR766 (Figure 3A). These two chimeric viral genomes were assembled separately in Vero 76 cells, as previously described [30]. The viruses were recovered from cell supernatants, and were then amplified twice in Vero76 cells. The final viral titers were determined using the plaque-forming assay [38].

The ability of the two chimeric viruses to bind SNB-19 cells was firstly evaluated (Figure 3B). As the E protein is responsible for viral attachment to cells [10,21], the levels of cell attachment indeed corresponded to which ZIKV strain the E region originated from. For example, as we previously demonstrated [30], significantly high levels of cell-attached vRNA were observed with ZIKV clones harboring the MR766 structural proteins. Similar levels of cell-associated vRNA were detected with the B/M virus, in which the MR766-derived E protein is presented. In contrast, both the BR15 and the M/B viruses were less efficient in attaching to SNB-19 cells. The same viral binding test was also conducted in a different cell line A549, and similar results were observed (Supplemental Figure S2A). These results confirm the link between the E protein and cell attachment, and demonstrate that C-prM region is not directly involved in viral attachment to the host-cells. In addition, the initial levels of ZIKV viral replication as measured by RT-PCR correlated with the levels of virus attachment to SNB-19 cells (Figure 3C). MR766 and B/M showed significantly higher levels of vRNA over time than BR15 and M/B, with similar kinetics. Consistently, the conventional plaque-forming assay was also used to test viral infectivity of newly generated chimeric viruses in A549 cells. The test results showed a strong correlation between 4G2-positive cell percentages and viral progeny productions (Supplemental Figure S2B).

We next analyzed the percentages of SNB-19 cells infected with these two chimeric viruses and their parental controls. As shown in (Figure 3D,E), both chimeric viruses were able to infect the SNB-19 cells. Interestingly, an opposite correlation was observed between the chimeric viruses and

the parental viruses in the percentages of viral infection to the SNB-19 cells. Statistical two-tailed and paired *t*-test analyses showed that the differences between MR766 vs. BR15, and MR766 vs. B/M were highly significant with $p \leq 0.01$ (***) for both comparisons; whereas the difference between MR766 and M/B was not significant with $p = 0.64$. Thus, the levels of infected cells, with a given chimeric virus, correlated with the C-prM region of its parental virus, not the E region. Indeed, in the cells infected by the M/B chimeric virus, the percentage of infected cells was significantly higher than that of BR15, but it was comparable with that of MR766 ($p = 0.64$, two-tailed and paired *t*-test). A similar correlative relationship was also observed between the B/M chimeric virus and the BR15 virus (Figure 3E).

These results confirm that ZIKV E region correlates with viral attachment to the host cells, and suggest that ZIKV C-prM region contributes to the permissiveness of viral infection.

3.4. Contribution of the ZIKV C-prM Region to ZIKV-Induced Growth Restriction and Apoptotic Cell Death

The data shown in Figure 3D,E were unexpected. It is believed that if the virus has high binding efficiency to the host cells, it should result in higher percentage of viral infected cells. Since ZIKV induces cytotoxicity, we reasoned that the C-prM region could contribute to ZIKV-induced cytotoxicity, which affects the outcome of the measured levels of viral infection. To test this possibility, we measured the effects of chimeric viruses on cell proliferation and viability. As shown in Figure 4A, genetic determinant(s) of cell viability was associated with of the C-prM region of the viral genome. For instance, both MR766 and M/B showed similar cell growth pattern, which was clearly distinguishable from that of BR15 and B/M. Nevertheless, a statistical *t*-test showed those differences were not statistically significant. However and consistent with the trend shown in Figure 4A, a similar but statistically significant correlation was detected in ZIKV-induced cell death (Figure 4B), and in apoptosis, as shown by the casp-3 cleavages (Figure 4C). Together, these data supported the idea that the C-prM domain of African ZIKV molecular clone contributes to ZIKV-induced growth restriction and apoptotic cell death.

3.5. Effect of prM Protein and Its Processed Protein Products (M and Pr) on ZIKV-Induced Cytotoxicity

Considering the association of the C-prM region of ZIKV genome with virus-induced cytotoxicity, it was interesting to evaluate whether the proteolytic processing of the C-prM protein precursor relates to cytotoxicity. Here, we focused on testing prM protein and its processed protein products (M and Pr). The C protein was studied separately. The proteolytic cleavage of prM by furin protease generates two proteins: a virion-associated M protein of 75 a.a. and an extracellularly released Pr polypeptide of 99 a.a. The M protein is only found in mature and fully infectious virus particles [10,41].

The SNB-19 cells were transduced with MOI of 1000 by Adv-prM, Adv-Pr or Adv-M, that were derived from MR766. They represent the precursor prM and a processed mature M protein and a Pr protein product, respectively. Mock-transduced cells were used as a background control. Cell viability was first measured at day 3 and day 5 p.i. as shown in Figure 5A. Both the prM and the Pr caused approximately 50% reduction of the cell viability while no clear change in cell viability was observed in the Adv-M-transduced cells. The prM effect on cell viability was further confirmed in different cell lines including human brain microvascular endothelial cells (HBMEC) and a neuronal cell line SH-SY5Y (Supplemental Figure S3A). Time-dependent measurements of cellular necrosis (Figure 5B) and apoptosis (Figure 5C), by real-time Annexin V Apoptosis and Necrosis assays, showed comparable results, in total agreement with the MTT assay at end of the time course. Note that the differences among the three Adv constructs were relatively small at early time points and only became significant at 120 h p.i.

Overall, our data indicated that ZIKV prM protein and its cleaved Pr protein product, but not the matured M protein, induced apoptotic cell death in SNB-19 cells.

3.6. Mutational Analysis of the Pr Region of the prM Protein and Their Effects on ZIKV-Induced Cytotoxicity

In Figure 2, we showed that the MR766 was more cytotoxic than the BR15. Our data further showed that the MR766 prM, and its cleaved product, Pr protein contributed to ZIKV-induced

cytotoxicity, suggesting that the Pr region of the prM protein might be the source of prM-mediated cytotoxicity (Figure 5). However, we did not know whether Pr-induced apoptosis is ZIKV strain-specific. There is a total of 10 known divergent a.a. mutations of prM protein between MR766 and BR15 (Figure 6A) [31]. Seven of those mutations are within the Pr region. Thus, we tested whether the Pr-induced cell death is only restricted to MR766, or whether we could alter the Pr-induced cell death by introducing divergent genetic mutations, that are present in the Pr protein of the BR15 molecular clone into the MR766 Pr protein. The residue 139 was first selected for reverse genetic analysis because the pre-epidemic to epidemic mutational transition from S to N at the residue 139 (S139N) of the Pr region was reported to be a crucial site for ZIKV-induced microcephaly [31]. Here, we reversed this mutational transition by generating the N139S mutation on the backbone of the BR15 Pr nucleotide sequence (Adv-Pr_{BR15}) to generate the Pr mutant (Adv-Pr⁺_{BR15}). Another four additional a.a. mutational sites (A148P, V153M, H157Y and V158I) were selected for the forward genetic mutagenesis. This region was of particular interest because the A148P mutation could have a major impact on protein folding. We decided to replace the entire cluster 148->158 as adjacent mutations could support putative structure changes associated with A148P mutation. The wildtype MR766 Pr nucleotide sequence (Adv-Pr_{MR766}) was used to generate the MR766 Pr mutant clone (Adv-Pr^{*}_{MR766}), that carries the four selected mutants to represent forward genetic mutations.

The effect of Adv-Pr⁺_{BR15} or Adv-Pr^{*}_{MR766} on the SNB-19 cell viability was measured by the MTT assay and compared to the wild type Adv-Pr_{BR15} or the Adv-Pr_{MR766}. The expression of Adv-Pr_{BR15} showed comparable proliferation and viability at day 3 and day 5 p.i., suggesting that the BR15 Pr is not as cytotoxic as the MR766 (Figure 6B). Next, we analyzed the effect of the N139S reverse mutation in the BR15 Pr protein. The introduction of the N139S substitution into the BR15 Pr protein showed little or no significant changes of BR15 Pr-induced growth restriction and cell death. In contrast and similar to what we showed in Figure 5A, about 50% decrease of cellular growth was observed in cells transduced with the wildtype Adv-Pr_{MR766} at 5 days p.i. (Figure 6B). However, cells infected with the mutant Adv-Pr^{*}_{MR766} displayed no viability decrease in cellular growth, in marked contrast with cells transduced with the wildtype Adv-Pr_{MR766} at 5 days p.i. (Figure 6B). Similarly, the induction of necrosis (Figure 6C) and apoptosis (Figure 6D) by Adv-Pr_{MR766} was completely blocked by the four a.a. mutations generated in the Pr region.

These data suggest that the Pr region of the MR766 prM protein is indeed responsible for prM-induced cytotoxicity. By introducing the four epidemic and divergent a.a. variants (A148, V153, H157 and V158) to the MR766 Pr region of the prM protein, by forward mutagenesis, alleviated MR766 Pr-induced apoptotic cell killing. This suggests that the acquisition of these four a.a. in BR15 could be responsible for its attenuated cytotoxic phenotype. However, reverse genetic mutation at the residue 139 (N139S) did not improve Adv-Pr_{BR15}-induced cytotoxicity, indicating the N139S mutation does not seem to play a role in prM-induced cytotoxicity.

4. Discussion

In this study, we showed that the historic African MR766 ZIKV strain displays different characteristics from that of the epidemic Brazilian strains BR15 and ICD. Those differences include the levels of virus attachment to the human brain glial SNB-19 cells, viral infection and replication overtime (Figure 1), as well as cytotoxicity, as measured by cell proliferation and apoptotic cell death (Figure 2). Since our early study showed that the structural protein region is responsible for the initiation of viral infection, in this study, we further examined the contribution of ZIKV structural prM-E proteins to viral infectivity and cytopathic effects. This was accomplished by generating chimeric viruses (M/B and B/M) that swap the C-prM and E regions of the structural proteins between the MR766 and the BR15 viral genomes. We showed that the E protein is associated with viral attachment to host cells (Figure 3B,C) and the C-prM region is correlated with viral permissiveness and ZIKV-induced cytotoxicity (Figure 3D,E; Figure 4). Further analysis of the prM and its processed protein product, the mature M protein and the Pr protein, indicated that the Pr region of the prM is responsible for

the prM-induced cytopathic effects (Figure 5). To further pinpoint where exactly the specific changes occurred in the Pr region of the prM protein, which contributes to the differences observed between MR766 and BR15, we carried out genetic mutagenesis (Figure 6A) to test whether we could reverse or mimic the respective effects observed in MR766 or BR15. As a result, we showed that the forward genetic mutation at four a.a. changes (A148P, V153M, H157Y and V158I) reversed MR766 Pr-induced cytopathic effects (Figure 6B–D). However, the reverse genetic mutation at the residue of 139 (S139N) did not show any clear effect (Figure 6B–D).

Differences between the historic African MR766 strain and the epidemic Brazilian ZIKV strains have been reported previously [for reviews, see [27,28]]. Although the specific causes of those differences are currently unknown, it is possible that the neurological defects caused by the epidemic Brazilian ZIKV in humans were attributed by subtle but important changes. Those newly adapted changes could include the alteration of viral infection patterns to human brain cells, the ability to establish replication in host cells, and the induction of neuropathic damages that lead to those observed ZIKV-associated neurological disorders [27]. Overall, the historic African MR766 strain has been shown to be more virulent and to cause more severe brain damage than that of the epidemic Asian lineages, including the Brazilian strains [25,42–44]. Indeed, the results of our comparative studies, described here between the historic African MR766 and the epidemic Brazilian BR15 and ICD molecular clones, supported this general notion that MR766 strain is more pathogenic than Brazilian strains.

One of our earlier studies suggested that the structural proteins contribute in part to the differences we observed between historical MR766 and epidemic BR15 strains of Zika viruses [30]. Following that lead, we further dissected the structural proteins of those two ZIKV molecular clones and evaluated the effect of separating the C-prM proteins from the E protein in viral infectivity and induction of cytotoxicity. This objective was achieved by swapping the C-prM region of the viral genome between the two viruses (Figure 3A). Our results suggested that the E protein is likely associated with viral attachment to host cells (Figure 3B,C) whilst the C-prM region is responsible for ZIKV permissiveness and ZIKV-induced cytopathic effects (Figure 3D,E; Figure 4). The finding that, E protein is linked to viral attachment to host cells, is expected because E protein is a major viral surface protein that is responsible for the viral entry. It is a crucial that the viral determinant for initiating the ZIKV-host interaction and for determining viral pathogenesis, and further investigations are needed [10,21]. Our study also suggests a possible relationship between ZIKV permissiveness and ZIKV-induced apoptosis, which would be based on the Pr, a processed protein product by furin cleavage of the prM protein. It would be interesting to clarify the exact contribution of the Pr protein in this relationship.

Here, we provide evidences showing that the function of the prM protein is linked to ZIKV-induced cytotoxicity that could affect the outcome of viral infection (Figure 3D,E; Figure 4). This finding is consistent with our previous reporting showing that the prM protein induces cytopathic effects in fission yeast cells [15]. The dissection analysis of the prM processing further indicated that the functional domain of the prM-mediated cytotoxicity resides within the Pr region of the protein (Figure 5). Most interestingly, reverse genetic analysis by converting asparagine (N) at residue 139 of the BR15 molecular clone to serine (S) of the MR766 molecular clone (N139S) did not significantly alter the cytopathic effects of BR15 Pr (Figure 6B–D). In contrast, forward genetic mutation analysis completely reversed the MR766 Pr-induced cell growth restriction and apoptotic cell death (Figure 6B–D), by replacing four divergent a.a. at residues 148, 153, 157 and 158 presented in MR766, with that of BR15 (A148P, V153M, H157Y and V158I). Note that, ideally, a reciprocal mutant construct should also be generated using BR15 backbone to test whether the opposite effect can be observed. However, the presence of additional divergent amino acids in the Pr protein (Fig. 6A) could contribute to the observed phenotypes that will complicate the interpretation of the experimental results using reciprocal constructs. Similarly, to confirm the mutant effect of Pr during viral infection, it would be desirable to generate a MR766 mutant molecular clone that contains the four described a.a. and test their mutant effect in the context of viral infection. This is not possible because, besides the prM, the ZIKV-induced apoptotic phenotype is also contributed by other viral proteins, such as

non-structural proteins during viral infection. For these reasons, we decided not to generate this reciprocal adenoviral mutant construct or the mutant viral molecular clones.

It should be mentioned that an early study indicates that the pre-epidemic to epidemic mutational transition (S139N) of the prM protein is a crucial site for ZIKV-induced microcephaly [31]. This forward genetic substitution in the viral polyprotein of a presumably less neurovirulent Cambodian ZIKVFSS13025 strain [45], substantially increased ZIKV infectivity in both human and mouse neuronal cells, that led to more severe microcephaly in the mouse fetus, as well as higher mortality rates in neonatal mice [31]. The results of this study suggested an important contribution of prM to fetal microcephaly. However, the molecular mechanism in which prM contributes to microcephaly, and the functional impact of S139N mutation on the prM function in human host cells, are presently unknown. It is intriguing to note that residue 139 is located in the Pr region of the prM protein. Since neither prM nor Pr are present in the mature and infectious viral particles [24,46], it would be interesting to test whether the N139S substitution in the MR766 strain or the four divergent mutations in the BR15 strain will have any effects on their abilities to infect human brain cells.

Supplementary Materials: The following are available online at <http://www.mdpi.com/1999-4915/11/2/157/s1>, Figure S1: Representative pictures of the immunostaining assay to measure caspase 3 cleavages (A) as shown in Figure 2C; Figure S2: Correlation of viral attachment and viral infection between chimeric viruses and their parental viruses in A549 cells; Figure S3: Effect of Adv-prM expression on ZIKV-induced cell viability in different cell lines.

Author Contributions: Conceptualization, P.D., G.G. and R.Z.; Formal analysis, R.Z.; Investigation, G.L. and S.B.; Methodology, K.T. and A.P.; Writing—original draft, R.Z.; Writing—review and editing, P.D. and G.G.

Funding: This study was funded in part by National Institute of Health (NIH R21 AI129369) and the University of Maryland Medical Center (to R.Y.Z.). A.P. and K.T. were supported by National Institute of Allergy and Infectious Diseases (NIAID) Intramural Program. This work was also supported by the ZIKAlert project (European Union-Région Réunion program under grant agreement n SYNERGY: RE0001902). S.B. is the recipient of a PhD degree scholarship from La Réunion Island University (Ecole Doctorale STS), funded by the French ministry MEESR (Ministère de l'Éducation, de l'Enseignement Supérieur et de la Recherche).

Acknowledgments: The authors would like to thank: Hengli Tang from Florida State University for providing the SNB-19 cell line, Kim Kwang Sik from Johns Hopkins University for the human brain microvascular endothelial cells (HBMEC) cell line, and Mohammed Rahman from University of Maryland School of Medicine for the Vero76 cells.

Conflicts of Interest: The authors declare no conflict of interest.

References

1. Victora, C.G.; Schuler-Faccini, L.; Matijasevich, A.; Ribeiro, E.; Pessoa, A.; Barros, F.C. Microcephaly in Brazil: How to interpret reported numbers? *Lancet* **2016**, *387*, 621–624. [\[CrossRef\]](#)
2. Melo, A.S.; Aguiar, R.S.; Amorim, M.M.; Arruda, M.B.; Melo, F.O.; Ribeiro, S.T.; Batista, A.G.; Ferreira, T.; Dos Santos, M.P.; Sampaio, V.V.; et al. Congenital Zika Virus Infection: Beyond Neonatal Microcephaly. *JAMA Neurol.* **2016**, *73*, 1407–1416. [\[CrossRef\]](#) [\[PubMed\]](#)
3. Del Campo, M.; Feitosa, I.M.; Ribeiro, E.M.; Horovitz, D.D.; Pessoa, A.L.; Franca, G.V.; Garcia-Alix, A.; Doriqui, M.J.; Wanderley, H.Y.; Sanseverino, M.V.; et al. The phenotypic spectrum of congenital Zika syndrome. *Am. J. Med. Genet. A* **2017**, *173*, 841–857. [\[CrossRef\]](#) [\[PubMed\]](#)
4. Mlakar, J.; Korva, M.; Tul, N.; Popovic, M.; Poljsak-Prijatelj, M.; Mraz, J.; Kolenc, M.; Resman Rus, K.; Vesnaver Vipotnik, T.; Fabjan Vodusek, V.; et al. Zika Virus Associated with Microcephaly. *N. Engl. J. Med.* **2016**. [\[CrossRef\]](#) [\[PubMed\]](#)
5. Driggers, R.W.; Ho, C.Y.; Korhonen, E.M.; Kuivanen, S.; Jaaskelainen, A.J.; Smura, T.; Rosenberg, A.; Hill, D.A.; DeBiasi, R.L.; Vezina, G.; et al. Zika Virus Infection with Prolonged Maternal Viremia and Fetal Brain Abnormalities. *N. Engl. J. Med.* **2016**. [\[CrossRef\]](#) [\[PubMed\]](#)
6. Qian, X.; Nguyen, H.N.; Song, M.M.; Hadiono, C.; Ogden, S.C.; Hammack, C.; Yao, B.; Hamersky, G.R.; Jacob, F.; Zhong, C.; et al. Brain-Region-Specific Organoids Using Mini-bioreactors for Modeling ZIKV Exposure. *Cell* **2016**, *165*, 1238–1254. [\[CrossRef\]](#) [\[PubMed\]](#)
7. Dick, G.W. Zika virus. II. Pathogenicity and physical properties. *Trans. R Soc. Trop. Med. Hyg.* **1952**, *46*, 521–534. [\[CrossRef\]](#)

8. Bell, T.M.; Field, E.J.; Narang, H.K. Zika virus infection of the central nervous system of mice. *Arch. Gesamte Virusforsch.* **1971**, *35*, 183–193. [[CrossRef](#)]
9. Dick, G.W.; Kitchen, S.F.; Haddow, A.J. Zika virus. I. Isolations and serological specificity. *Trans. R Soc. Trop. Med. Hyg.* **1952**, *46*, 509–520. [[CrossRef](#)]
10. Lee, I.; Bos, S.; Li, G.; Wang, S.; Gadea, G.; Despres, P.; Zhao, R.Y. Probing Molecular Insights into Zika Virus(-)Host Interactions. *Viruses* **2018**, *10*. [[CrossRef](#)]
11. Musso, D.; Nhan, T.; Robin, E.; Roche, C.; Bierlaire, D.; Zisou, K.; Shan Yan, A.; Cao-Lormeau, V.M.; Broult, J. Potential for Zika virus transmission through blood transfusion demonstrated during an outbreak in French Polynesia, November 2013 to February 2014. *Eurosurveillance* **2014**, *19*. [[CrossRef](#)]
12. Duffy, M.R.; Chen, T.H.; Hancock, W.T.; Powers, A.M.; Kool, J.L.; Lanciotti, R.S.; Pretrick, M.; Marfel, M.; Holzbauer, S.; Dubray, C.; et al. Zika virus outbreak on Yap Island, Federated States of Micronesia. *N. Engl. J. Med.* **2009**, *360*, 2536–2543. [[CrossRef](#)] [[PubMed](#)]
13. Hennessey, M.; Fischer, M.; Staples, J.E. Zika Virus Spreads to New Areas-Region of the Americas, May 2015-January 2016. *Morb. Mortal. Wkly. Rep.* **2016**, *65*, 55–58. [[CrossRef](#)] [[PubMed](#)]
14. Talero-Gutierrez, C.; Rivera-Molina, A.; Perez-Pavajeau, C.; Ossa-Ospina, I.; Santos-Garcia, C.; Rojas-Anaya, M.C.; de-la-Torre, A. Zika virus epidemiology: From Uganda to world pandemic, an update. *Epidemiol. Infect.* **2018**, *146*, 673–679. [[CrossRef](#)] [[PubMed](#)]
15. Li, G.; Poulsen, M.; Fenyvuesvolgyi, C.; Yashiroda, Y.; Yoshida, M.; Simard, J.M.; Gallo, R.C.; Zhao, R.Y. Characterization of cytopathic factors through genome-wide analysis of the Zika viral proteins in fission yeast. *Proc. Natl. Acad. Sci. USA* **2017**, *114*, E376–E385. [[CrossRef](#)] [[PubMed](#)]
16. Chambers, T.J.; Hahn, C.S.; Galler, R.; Rice, C.M. Flavivirus genome organization, expression, and replication. *Annu. Rev. Microbiol.* **1990**, *44*, 649–688. [[CrossRef](#)]
17. Harris, E.; Holden, K.L.; Edgil, D.; Polacek, C.; Clyde, K. Molecular biology of flaviviruses. *Novartis. Found. Symp.* **2006**, *277*, 23–39, discussion 40, 71–23, 251–253.
18. Yu, I.M.; Zhang, W.; Holdaway, H.A.; Li, L.; Kostyuchenko, V.A.; Chipman, P.R.; Kuhn, R.J.; Rossmann, M.G.; Chen, J. Structure of the immature dengue virus at low pH primes proteolytic maturation. *Science* **2008**, *319*, 1834–1837. [[CrossRef](#)]
19. Mecharles, S.; Herrmann, C.; Poullain, P.; Tran, T.H.; Deschamps, N.; Mathon, G.; Landais, A.; Breurec, S.; Lannuzel, A. Acute myelitis due to Zika virus infection. *Lancet* **2016**. [[CrossRef](#)]
20. Faye, O.; Freire, C.C.; Iamarino, A.; Faye, O.; de Oliveira, J.V.; Diallo, M.; Zannotto, P.M.; Sall, A.A. Molecular evolution of Zika virus during its emergence in the 20(th) century. *PLoS Negl. Trop Dis.* **2014**, *8*, e2636. [[CrossRef](#)]
21. Fontes-Garfias, C.R.; Shan, C.; Luo, H.; Muruato, A.E.; Medeiros, D.B.A.; Mays, E.; Xie, X.; Zou, J.; Roundy, C.M.; Wakamiya, M.; et al. Functional Analysis of Glycosylation of Zika Virus Envelope Protein. *Cell Rep.* **2017**, *21*, 1180–1190. [[CrossRef](#)] [[PubMed](#)]
22. Lobigs, M.; Lee, E.; Ng, M.L.; Pavy, M.; Lobigs, P. A flavivirus signal peptide balances the catalytic activity of two proteases and thereby facilitates virus morphogenesis. *Virology* **2010**, *401*, 80–89. [[CrossRef](#)] [[PubMed](#)]
23. Amberg, S.M.; Nestorowicz, A.; McCourt, D.W.; Rice, C.M. NS2B-3 proteinase-mediated processing in the yellow fever virus structural region: In vitro and in vivo studies. *J. Virol.* **1994**, *68*, 3794–3802. [[PubMed](#)]
24. Elshuber, S.; Allison, S.L.; Heinz, F.X.; Mandl, C.W. Cleavage of protein prM is necessary for infection of BHK-21 cells by tick-borne encephalitis virus. *J. Gen. Virol.* **2003**, *84*, 183–191. [[CrossRef](#)] [[PubMed](#)]
25. Anfasa, F.; Siegers, J.Y.; van der Kroeg, M.; Mumtaz, N.; Stalin Raj, V.; de Vrij, F.M.S.; Widagdo, W.; Gabriel, G.; Salinas, S.; Simonin, Y.; et al. Phenotypic Differences between Asian and African Lineage Zika Viruses in Human Neural Progenitor Cells. *mSphere* **2017**, *2*. [[CrossRef](#)] [[PubMed](#)]
26. Abushouk, A.I.; Negida, A.; Ahmed, H. An updated review of Zika virus. *J. Clin. Virol.* **2016**, *84*, 53–58. [[CrossRef](#)] [[PubMed](#)]
27. Simonin, Y.; van Riel, D.; Van de Perre, P.; Rockx, B.; Salinas, S. Differential virulence between Asian and African lineages of Zika virus. *PLoS Negl. Trop Dis.* **2017**, *11*, e0005821. [[CrossRef](#)] [[PubMed](#)]
28. Beaver, J.T.; Lelutiu, N.; Habib, R.; Skountzou, I. Evolution of Two Major Zika Virus Lineages: Implications for Pathology, Immune Response, and Vaccine Development. *Front. Immunol.* **2018**, *9*, 1640. [[CrossRef](#)] [[PubMed](#)]

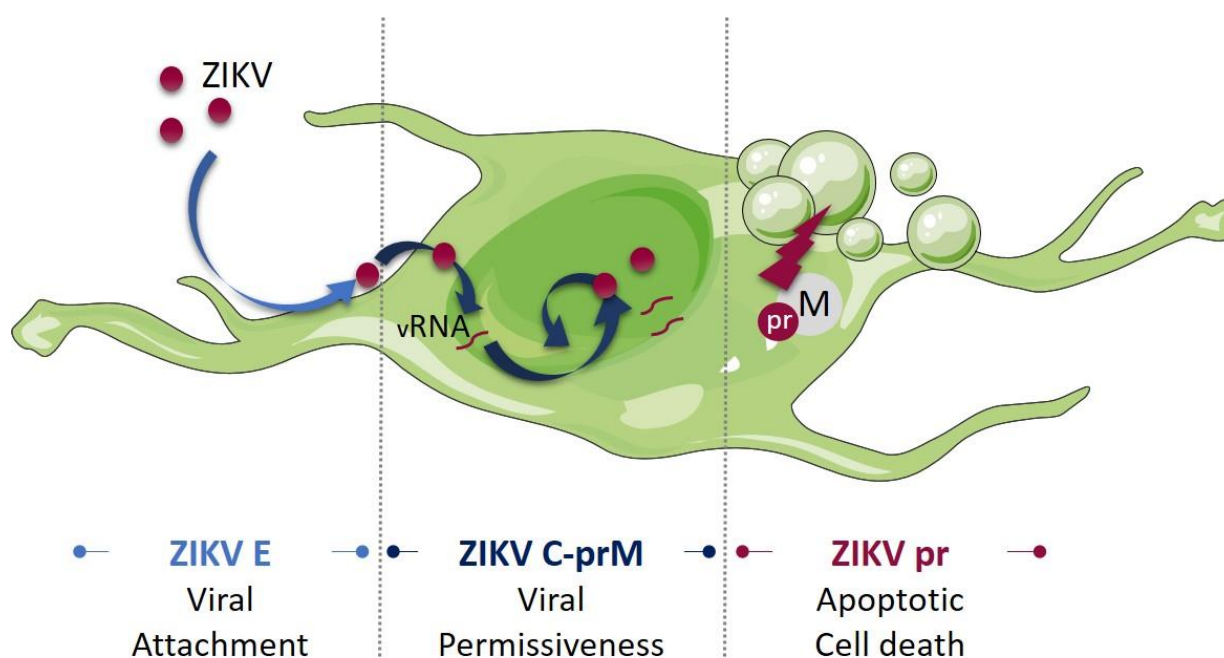
29. Ramaiah, A.; Dai, L.; Contreras, D.; Sinha, S.; Sun, R.; Arumugaswami, V. Comparative analysis of protein evolution in the genome of pre-epidemic and epidemic Zika virus. *Infect. Genet. Evol.* **2017**, *51*, 74–85. [[CrossRef](#)] [[PubMed](#)]
30. Bos, S.; Viranaicken, W.; Turpin, J.; El-Kalamouni, C.; Roche, M.; Krejbich-Trotot, P.; Despres, P.; Gadea, G. The structural proteins of epidemic and historical strains of Zika virus differ in their ability to initiate viral infection in human host cells. *Virology* **2018**, *516*, 265–273. [[CrossRef](#)] [[PubMed](#)]
31. Yuan, L.; Huang, X.Y.; Liu, Z.Y.; Zhang, F.; Zhu, X.L.; Yu, J.Y.; Ji, X.; Xu, Y.P.; Li, G.; Li, C.; et al. A single mutation in the prM protein of Zika virus contributes to fetal microcephaly. *Science* **2017**, *358*, 933–936. [[CrossRef](#)] [[PubMed](#)]
32. Tang, H.; Hammack, C.; Ogden, S.C.; Wen, Z.; Qian, X.; Li, Y.; Yao, B.; Shin, J.; Zhang, F.; Lee, E.M.; et al. Zika Virus Infects Human Cortical Neural Progenitors and Attenuates Their Growth. *Cell Stem. Cell* **2016**, *18*, 587–590. [[CrossRef](#)] [[PubMed](#)]
33. Gadea, G.; Bos, S.; Krejbich-Trotot, P.; Clain, E.; Viranaicken, W.; El-Kalamouni, C.; Mavingui, P.; Despres, P. A robust method for the rapid generation of recombinant Zika virus expressing the GFP reporter gene. *Virology* **2016**, *497*, 157–162. [[CrossRef](#)] [[PubMed](#)]
34. Faria, N.R.; Azevedo Rdo, S.; Kraemer, M.U.; Souza, R.; Cunha, M.S.; Hill, S.C.; Theze, J.; Bonsall, M.B.; Bowden, T.A.; Rissanen, I.; et al. Zika virus in the Americas: Early epidemiological and genetic findings. *Science* **2016**, *352*, 345–349. [[CrossRef](#)]
35. Widman, D.G.; Young, E.; Yount, B.L.; Plante, K.S.; Gallichotte, E.N.; Carbaugh, D.L.; Peck, K.M.; Plante, J.; Swanstrom, J.; Heise, M.T.; et al. A Reverse Genetics Platform That Spans the Zika Virus Family Tree. *MBio* **2017**, *8*. [[CrossRef](#)]
36. Tsatsarkin, K.A.; Kenney, H.; Chen, R.; Liu, G.; Manukyan, H.; Whitehead, S.S.; Laassri, M.; Chumakov, K.; Pletnev, A.G. A Full-Length Infectious cDNA Clone of Zika Virus from the 2015 Epidemic in Brazil as a Genetic Platform for Studies of Virus-Host Interactions and Vaccine Development. *MBio* **2016**, *7*. [[CrossRef](#)] [[PubMed](#)]
37. Xu, M.Y.; Liu, S.Q.; Deng, C.L.; Zhang, Q.Y.; Zhang, B. Detection of Zika virus by SYBR green one-step real-time RT-PCR. *J. Virol. Methods* **2016**, *236*, 93–97. [[CrossRef](#)] [[PubMed](#)]
38. Frumence, E.; Roche, M.; Krejbich-Trotot, P.; El-Kalamouni, C.; Nativel, B.; Rondeau, P.; Misse, D.; Gadea, G.; Viranaicken, W.; Despres, P. The South Pacific epidemic strain of Zika virus replicates efficiently in human epithelial A549 cells leading to IFN-beta production and apoptosis induction. *Virology* **2016**, *493*, 217–226. [[CrossRef](#)]
39. Mosmann, T. Rapid colorimetric assay for cellular growth and survival: Application to proliferation and cytotoxicity assays. *J. Immunol. Methods* **1983**, *65*, 55–63. [[CrossRef](#)]
40. Rodriguez, R.A.; Pepper, I.L.; Gerba, C.P. Application of PCR-based methods to assess the infectivity of enteric viruses in environmental samples. *Appl. Environ. Microbiol.* **2009**, *75*, 297–307. [[CrossRef](#)]
41. Zheng, A.; Umashankar, M.; Kielian, M. In vitro and in vivo studies identify important features of dengue virus pr-E protein interactions. *PLoS Pathog.* **2010**, *6*, e1001157. [[CrossRef](#)]
42. Shao, Q.; Herrlinger, S.; Zhu, Y.N.; Yang, M.; Goodfellow, F.; Stice, S.L.; Qi, X.P.; Brindley, M.A.; Chen, J.F. The African Zika virus MR-766 is more virulent and causes more severe brain damage than current Asian lineage and dengue virus. *Development* **2017**, *144*, 4114–4124. [[CrossRef](#)] [[PubMed](#)]
43. Simonin, Y.; Loustalot, F.; Desmetz, C.; Foulongne, V.; Constant, O.; Fournier-Wirth, C.; Leon, F.; Moles, J.P.; Goubaud, A.; Lemaitre, J.M.; et al. Zika Virus Strains Potentially Display Different Infectious Profiles in Human Neural Cells. *EBioMedicine* **2016**, *12*, 161–169. [[CrossRef](#)] [[PubMed](#)]
44. McGrath, E.L.; Rossi, S.L.; Gao, J.; Widen, S.G.; Grant, A.C.; Dunn, T.J.; Azar, S.R.; Roundy, C.M.; Xiong, Y.; Prusak, D.J.; et al. Differential Responses of Human Fetal Brain Neural Stem Cells to Zika Virus Infection. *Stem Cell Rep.* **2017**, *8*, 715–727. [[CrossRef](#)] [[PubMed](#)]

45. Shan, C.; Xie, X.; Muruato, A.E.; Rossi, S.L.; Roundy, C.M.; Azar, S.R.; Yang, Y.; Tesh, R.B.; Bourne, N.; Barrett, A.D.; et al. An Infectious cDNA Clone of Zika Virus to Study Viral Virulence, Mosquito Transmission, and Antiviral Inhibitors. *Cell Host Microbe* **2016**, *19*, 891–900. [[CrossRef](#)]
46. Stadler, K.; Allison, S.L.; Schalich, J.; Heinz, F.X. Proteolytic activation of tick-borne encephalitis virus by furin. *J. Virol.* **1997**, *71*, 8475–8481.



© 2019 by the authors. Licensee MDPI, Basel, Switzerland. This article is an open access article distributed under the terms and conditions of the Creative Commons Attribution (CC BY) license (<http://creativecommons.org/licenses/by/4.0/>).

Graphical abstract



IV. ARTICLE N°4

The N-glycosylation motif on epidemic Zika virus envelope protein potentiates virus fusion

Sandra Bos¹, Wildriss Viranaicken¹, Etienne Frumence¹, Philippe Desprès¹, Richard Zhao^{2,3,4,5,#} and Gilles Gadea^{1,#}.

1. Université de la Réunion, INSERM U1187, CNRS UMR 9192, IRD UMR 249, Unité Mixte Processus Infectieux en Milieu Insulaire Tropical, Plateforme Technologique CYROI, 94791 Sainte Clotilde, La Réunion, France

2. Department of Pathology, University of Maryland School of Medicine, Baltimore, MD 21201, USA

3. Department of Microbiology and Immunology, University of Maryland, Baltimore, MD 21201, USA

4. Institute of Global Health, University of Maryland, Baltimore, MD 21201, USA

5. Institute of Human Virology, University of Maryland, Baltimore, MD 21201, USA

both authors contributed equally to this work.

(Draft. Not yet submitted.)

ABSTRACT

Mosquito-borne Zika virus (ZIKV) emerged in South Pacific islands and Americas where large epidemics were documented. We recently illustrated a previously underrated role for the structural proteins C, prM, and E in ZIKV epidemic strain ability to initiate viral infection in human host cells. In addition, we found that C-prM region contributes to permissiveness and ZIKV-induced cytopathic effects. In the present study, to further characterize ZIKV structural proteins, we investigated the contribution of the N-glycosylation motif of the E protein in the permissiveness of human host cells to epidemic strains of ZIKV. For that purpose, we generated mutant molecular clones of the epidemic BeH819015 and historical MR766 strains in the E N-glycosylation site. We showed that ZIKV molecular clones containing the BR15 N-glycosylation site were more infectious and more efficient in viral fusion leading to an increase susceptibility of A549 cells to viral infection.

INTRODUCTION

Mosquito-borne flaviviruses, that include Zika (ZIKV), Dengue (DENV), Yellow fever (YFV) and Japanese Encephalitis (JEV) viruses, are pathogens of significant public health concerns¹⁻³. The recent ZIKV global outbreaks, with Brazil as epicenter, highlighted how a previously neglected virus can turn into a severe threat for human health. While ZIKV infection cases remained only sporadic and with a limited impact for decades⁴⁻⁷, the recent outbreaks revealed that ZIKV can cause clusters of severe congenital and neurological abnormalities in infants and peripheral nervous system impairment in adults⁸⁻¹¹. Considering the dramatic increase of ZIKV pathogenicity, strategies to efficiently control this virus, either in terms of antiviral therapies or vaccines, are urgently needed and granted the requirement for more extensive studies.

Flaviviruses are positive single-stranded RNA viruses typically transmitted by the bite of an arthropod vector. Their genomic RNA contains a single large polyprotein that is subsequently cleaved by cellular and viral proteases into seven non-structural proteins (NS1 to NS5) and three structural proteins (C, prM/M and E). The non-structural proteins are responsible for the virus replication, assembly and escape from host immune system, while the structural proteins form the viral particles that include the genomic viral RNA. Among the structural proteins, the envelope (E) protein is responsible for viral entry into host-cells and represents a major determinant for viral pathogenesis. The viral E protein first binds to the cellular attachment factors and receptors, leading to virion internalisation through the endocytic pathway¹². In the endosomes, fusion of the viral and cellular membranes occurs after E protein conformational changes triggered by low pH¹³. The peptide chain of the E protein folds into three distinct domains: a central beta-barrel (DI domain), an elongated dimerization region (DII domain), which includes the fusion loop, and a C-terminal, immunoglobulin-like module (DIII domain)¹⁴. The E protein of most flaviviruses is post-translationally modified by N-linked glycosylation of the glycan loop in the DI domain¹⁵. The contribution of the N-glycan in the ZIKV viral cycle, including in the mosquito vector, has been recently highlighted. The N-linked glycosylation of the E protein was shown as an important determinant of ZIKV virulence and

neuro-invasion in a mouse model¹⁶. In mosquitoes, the lack of N-glycosylation was associated with a reduction of oral infectivity for the *Aedes aegypti* vector¹⁷. Although the N-glycosylation is highly conserved among flaviviruses, which suggests of its biological importance, the E protein of some flavivirus strains remains unglycosylated. To date, the exact mechanism by which the E protein N-glycosylation motif contributes to ZIKV infectivity still remains poorly understood.

Using reverse genetic strategy to generate chimeric ZIKV clones, we recently established the contribution of the structural proteins in the permissiveness of human host cells to epidemic strains of ZIKV¹⁸. We were able to illustrate the role for C, prM and E in ZIKV epidemic strain ability to initiate viral infection. Analysis of chimeric viruses also permitted to establish that the C-prM region contributes to permissiveness and ZIKV-induced cytopathic effects¹⁹. In the present study, to further characterise structural protein contribution, focusing on ZIKV E protein, we investigated the role of the N-glycosylation motif using mutant molecular clones. Comparative analysis of these newly engineered ZIKV clones revealed that the N-glycosylation motif potentiates virus infectivity. ZIKV E protein N-glycosylation motif was shown not to affect cellular binding or immune responses but rather virus entry, with an impact on amounts of viral RNA penetrating into host-cells and viral progeny production.

RESULTS

Characterization of the molecular mutant ZIKV clones

To determine the contribution of the N-glycosylation motif in ZIKV E protein functions, we generated two mutant molecular clones. MR766^{+GLY}, in which the region coding for the glycosylation site of the epidemic strain BeH819015 (BR15) has been introduced, and BR15^{-GLY}, in which the region coding for the N-glycosylation site has been replaced with its counterpart from MR766 historical strain (Figure 1A). The genomes were assembled using the ISA method²⁰. Briefly, Vero cells were electroporated with four overlapping fragments, in which appropriate mutations have been previously introduced. The two recovered

clones were viable and twice amplified on Vero cells. The titres of the second amplification run corresponding to the working viral stocks were determined on Vero cells and were ranging from 5.10^6 to 5.10^7 PFU.mL⁻¹ (Figure 1B). MR766^{+GLY} and BR15^{-GLY} gave plaque morphologies that resembled the ones of their respective parental clones MR766 and BR15 (Figure 1C), in agreement with previously published data¹⁷.

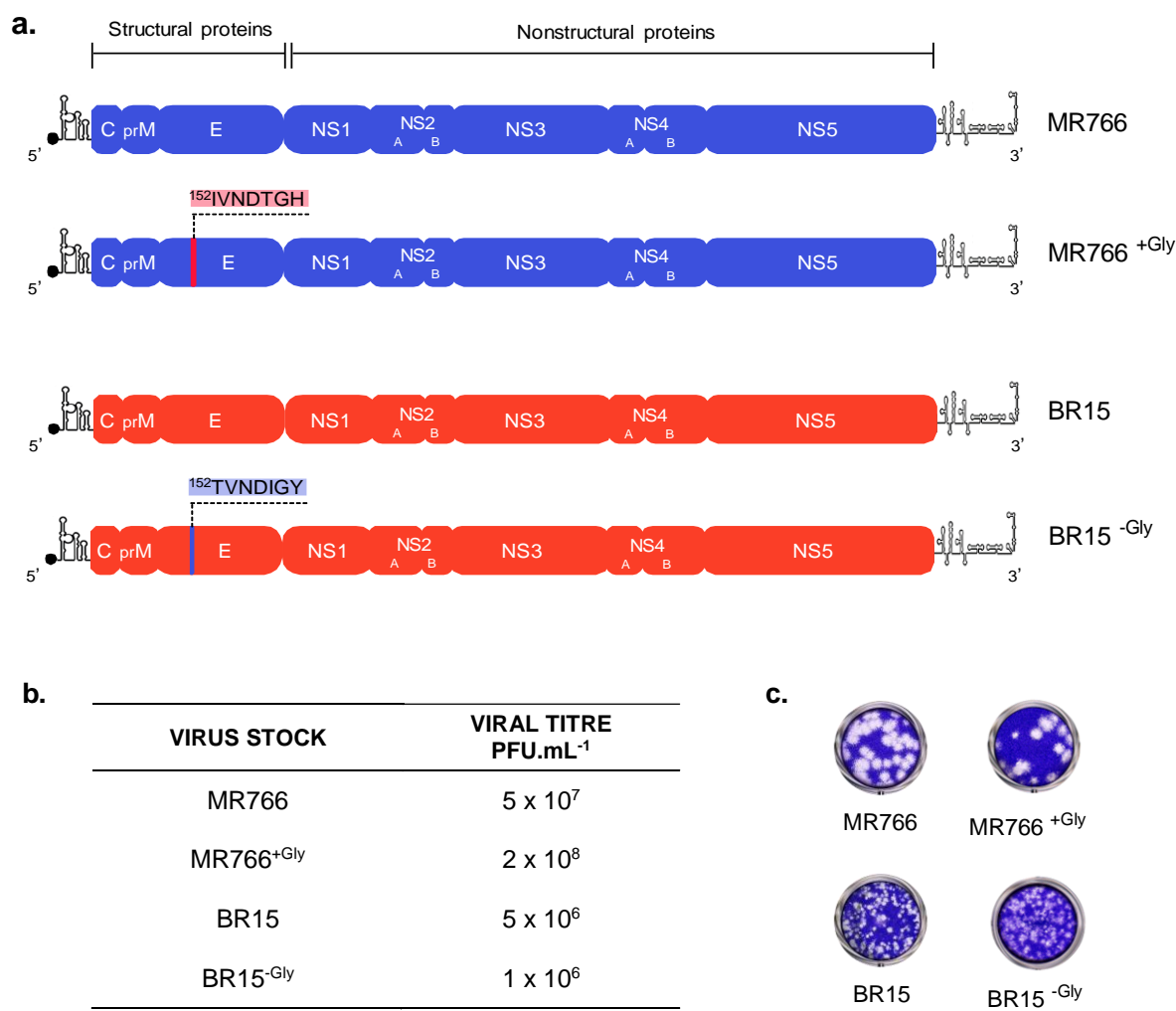






Figure 1: ZIKV mutant molecular clones.

In (A), schematic representation of mutant viral clones BR15^{-GLY} and MR766^{+GLY} and their respective parental clones. In (B), table showing viral titres. In (C), examples of infectious plaques developed for BR15^{-GLY} and MR766^{+GLY}, and parental clones, after plaque-forming assay on Vero cells.

Table showing particles-to-PFU ratios.

CONSTRUCTION	VIRUS STOCK	ENVELOPE	PARTICLE-TO-PFU RATIO
	MR766	Unglycosylated	997 ± 36
	MR766 ^{+Gly}	Glycosylated	419 ± 87
	BR15	Glycosylated	918 ± 91
	BR15 ^{-Gly}	Unglycosylated	11 237 ± 720

ZIKV E protein N-glycosylation site potentiates viral infectivity

We first analyzed the infectivity of our virus stocks. Particles-to-PFU ratios obtained from parental clones were around 900-1000 (Table) and confirmed our previous observations¹⁸. We then compared with E mutant clone particles-to-PFU ratios. The addition of a N-glycosylation site on MR766 strain resulted in a 2.5-fold decrease in the particles-to-PFU ratio. In contrast, for the mirror construct, in which the N-glycosylation site of BR15 has been reverted, the particles-to-PFU ratio was strongly increased (more than ten folds). These results suggest that ZIKV E N-glycosylation site significantly improves virion infectivity.

We previously showed that ZIKV strains of historical or epidemic lineages display differences in their binding properties leading to differences in cell susceptibility to the infection. We investigated the capacity of our mutant clones to bind to A549^{DUAL} cells. Virus binding assays were performed to determine by RT-qPCR the virus particle binding onto the cell surface after an incubation period of 1 hour. Panels A and B show no difference between the mutant clones and their respective parental clones (Figure 2). Conflicting results were obtained in other studies in mosquito cells¹⁷, indicating that, as expected, virus binding ability is cell-dependent. We could not exclude as well that design of the mutant could itself generate discrepancies (point mutation versus motif shifting). We conclude that the N-glycosylation site of ZIKV E protein does not affect virus binding properties in A549^{DUAL} cells.

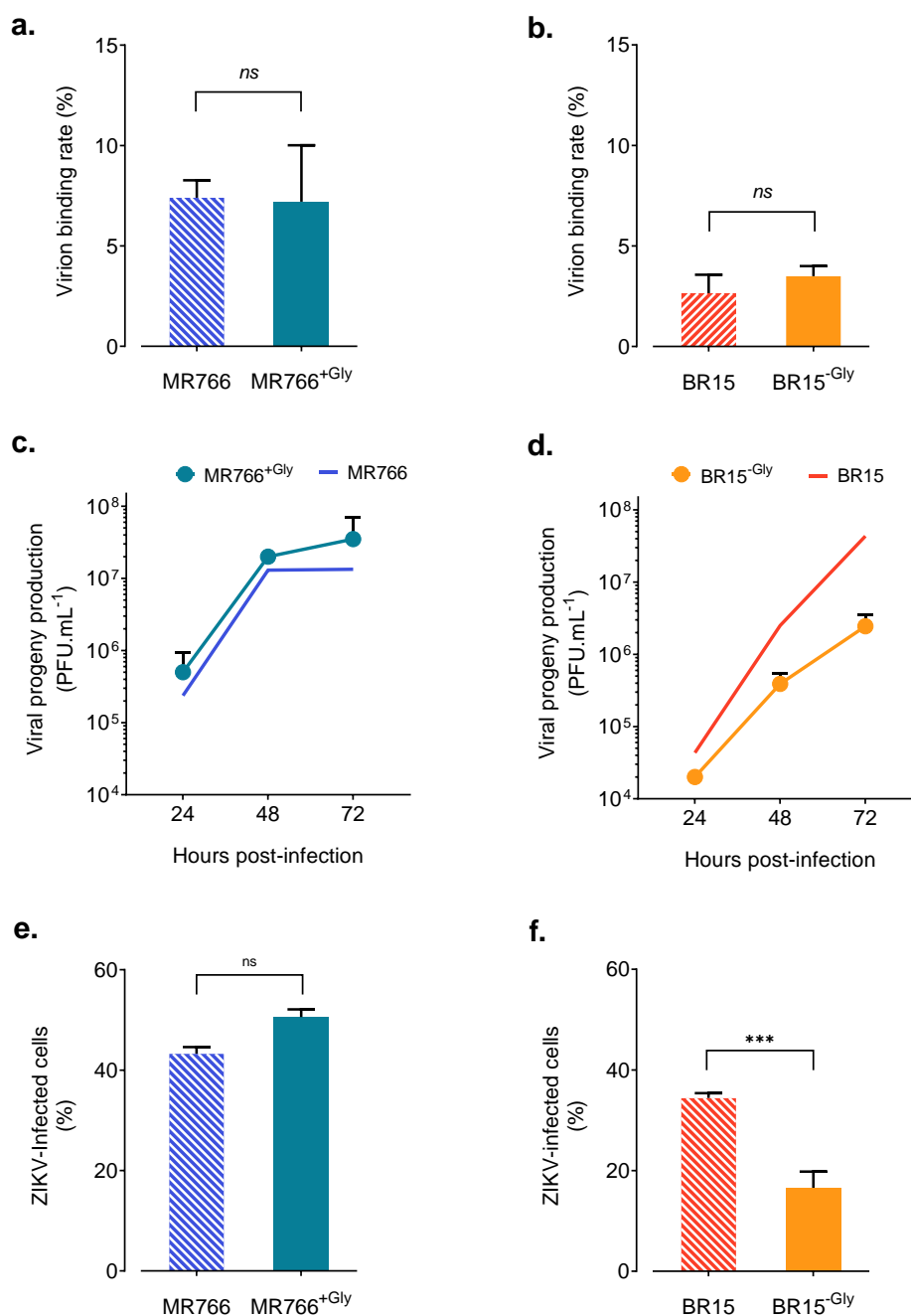


Figure 2: Analysis of virus binding and viral growth in A549^{DUAL}

In (A) and (B), for virus binding assays, cells were incubated with viral clones at the MOI of 1 for 1 h at 4°C. The number of virus particles bound to cell surface was measured by RT-qPCR. Values represent the mean and standard deviations of 3 independent experiments. In (C) and (D), A549^{DUAL} were infected with BR15^{-GLY} and MR766^{+GLY} and parental clones at MOI of 1. The infectious virus released into the supernatants of infected cells at 24 and 48 h were quantified on Vero cells. The error bars represent the standard deviations of at least 2 independent experiments. In (E) and (F), A549^{DUAL} were infected with BR15^{-GLY} and MR766^{+GLY} and parental clones at MOI of 1. The percentages of ZIKV-infected cells at 48 h were determined by flow cytometry using anti-E mAb 4G2 as primary antibody. The error bars represent the standard deviations of 2 independent experiments in duplicates.

The study of A549^{DUAL} cells infected with the different clones at MOI of 1 revealed that E protein N-glycosylation influences ZIKV progeny production resulted in a modest but reproducible increase in ZIKV progeny production. In contrast, deletion of the N-glycosylation site on BR15 strongly altered its progeny production kinetics. The differences were observed as soon as 24h post-infection. Similarly, addition of a N-glycosylation site on MR766 resulted in a modest increase of the infected cell percentage at 48h post-infection, although non-statistically significant. In contrast, deletion of the N-glycosylation site on BR15 strongly altered its ability to infect cells. Taken together, these results indicate that ZIKV E protein N-glycosylation site potentiates viral infectivity, independently of virus binding onto A549^{DUAL} host-cells.

ZIKV E protein N-glycosylation does not change cell death and immune responses

To determine whether the differences in mutant virus properties were associated with specific host-cell responses, we first analyzed virus-induced cell death at 24 h and 48 h post-infection. No difference in cytotoxicity measured by LDH release was observed between wild-type and mutant viruses (MR766 and BR15) (Figure 3A and B). We then took advantages of A549^{DUAL} cells to test virus capacity to activate the innate immunity. A549^{DUAL} cells derive from A549 cells by stable integration of two reporter genes: the Secreted Embryonic Alkaline Phosphatase and Lucia luciferase under the respective transcriptional control of the IFN- β minimal promoter fused to NF- κ B binding sites or an ISG54 minimal promoter in conjunction with Interferon-Sensitive Response Elements. We examined the interferon regulatory factor pathway activation by monitoring Lucia luciferase at 24 h and 48 h post-infection and detected equivalent responses (Figure 3C and D). NF- κ B pathway was not investigated as we previously reported no activation. These results suggest that differences in mutant virus properties could not be explained by specific host-cell responses and are consistent with previous observations suggesting a link between host-cell responses and ZIKV non-structural proteins¹⁸.

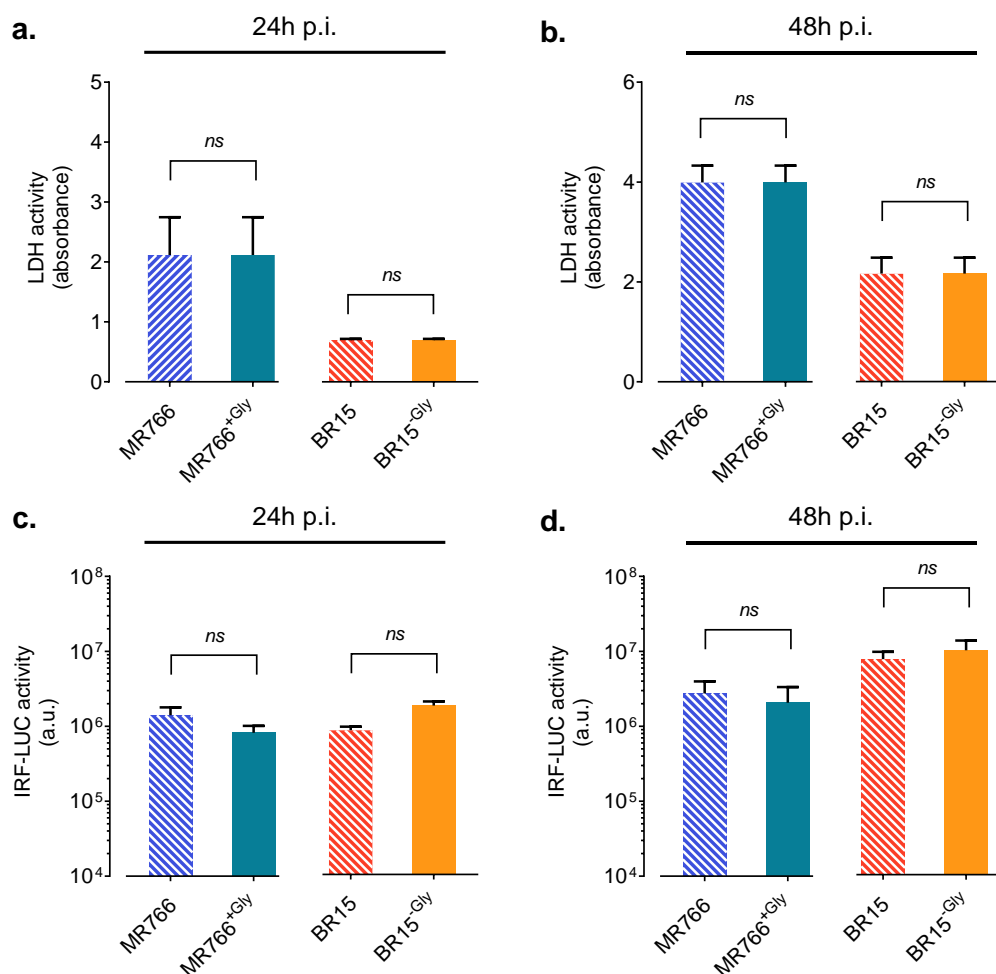


Figure 3: Analysis of infection-induced cell death and immune responses.

A549^{Dual} were infected with BR15^{-GLY} and MR766^{+GLY} and parental clones at MOI of 1. In (A) and (B), LDH activity was measured at 24 and 48h p.i. respectively. Values represents the mean and the standard deviations of 3 independent experiments in triplicates. In (C) and (D), analysis of IRF pathway activation in response to viral infection. Activity of the secreted Lucia luciferase was measured using QUANTI-Luc substrate at 24 and 48h p.i. Results are expressed as crude data of arbitrary units of luminescence. The error bars represent the standard deviations of 3 independent experiments in triplicates.

ZIKV E protein N-glycosylation facilitates viral fusion.

We previously observed that BR15 N-glycosylation site gives a growth advantage without apparent association with cellular attachment or host-cell responses. We then decided to study the viral fusion. Viral fusion of flaviviruses is commonly triggered from the endosomes upon low-pH by a series of molecular changes within the E protein resulting in release of the nucleocapsid into the cell cytoplasm. We wondered whether the observed conformational changes could affect virus fusion and explain the progeny production kinetics. Chloroquine, a 4-aminoquinoline, is a weak base that increases acidic vesicle pH and, in consequence, restricts the viral replication of many viruses through inhibition of pH-dependent steps. Recently, chloroquine has been shown to inhibit Zika virus infection in different cellular models²¹. We performed a chloroquine treatment on A549^{DUAL} cells infected with wild-type or mutant BR15. 100μM of chloroquine were added 60 minutes post-infection for two hours and then cells were put back in regular medium. 30 hours post-infection intracellular viral RNA was quantified by RT-qPCR. BR15^{-GLY} was significantly more restricted by chloroquine treatment than BR15 (Figure 4), suggesting that E N-glycosylation site favours viral fusion with the cell membranes.

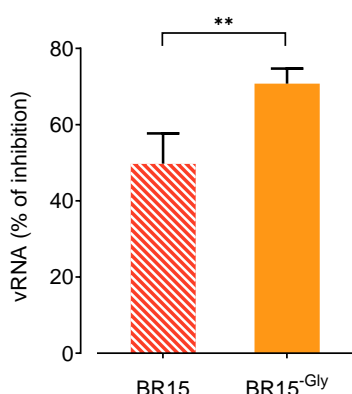


Figure 4: Viral fusion in A549^{DUAL} cells.

Pre-chilled cells were incubated at 4°C with ZIKV at MOI of 1. After 1-hour incubation, cells were shifted to 37°C. 1 hour after temperature shifting, chloroquine was added to the culture medium. Viral RNA was measured by RT-qPCR 30 hours post temperature shift. The error bars represent the standard deviations of 3 independent experiments.

N-glycosylation favours conformational changes in the fusion loop

The reduced fusion observed with the mutant molecular clone lacking the N-glycosylation site could be the consequence of impaired folding. In order to test this hypothesis, wild-type and mutant sequences coding for prM-E (BR15, mutant BR15 and MR766) were codon-optimised for expression in mammalian cells and cloned into pcDNA3.1 vector (Figure 5A). HEK-293 cells were transfected with the

different plasmids and positive cells were selected with antibiotics. Resulting stable cell lines were fractionated and the fractions were subjected to an immunoblot analysis. We first used an in-house developed rat antibody specifically raised against the E protein Domain III²². Figure 5B revealed that the lack of N-glycosylation site resulted in a greater E protein propensity to accumulate in the insoluble compartments. Interestingly, the differences observed between BR15 and mutant BR15 suggested that ZIKV E proteins bear different conformations depending on their glycosylation status. To confirm these observations, we performed an immunoblot using the 4G2 monoclonal antibody, which recognises the highly conserved fusion loop sequence of most flaviviruses. As shown in Figure 5C, the 4G2 monoclonal antibody reactivity against the N-glycosylated E protein is strong, whereas we could barely detect any signal with the two E proteins lacking the N-glycosylation site. These data confirm that the N-glycosylation site of the E protein, in the Domain I, supports conformational changes that could be detected in the fusion loop environment (Domain II). From these results, we conclude that conformational changes occurring in the E protein after changing the N-glycosylation site affect viral fusion, the N-glycosylation site giving the viruses an advantage in terms of membrane fusion.

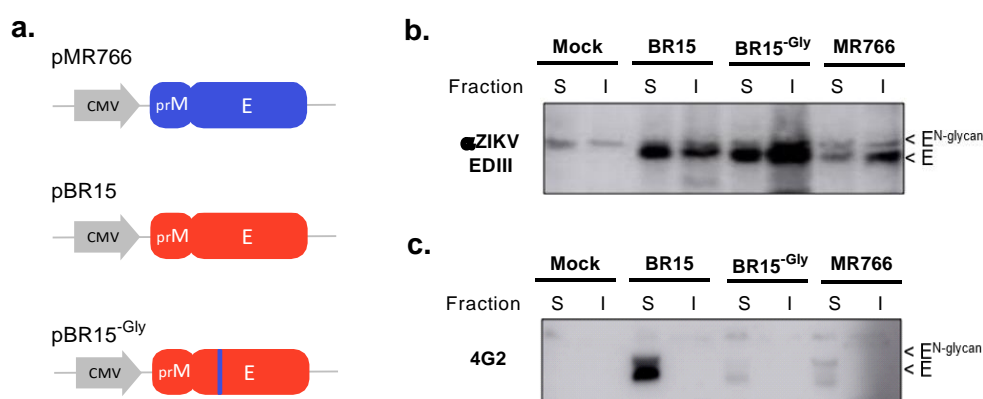


Figure 5: Conformational changes induced by the N-glycosylation site of ZIKV E protein.

In (A), schematic representation of prM-E constructs for MR766, BR15 and BR15^{-GLY}. In (B) and (C), A549^{DUAL} cells were transfected with prM-E constructs and antibiotics-selected to raise stable cell lines. Cells were harvested and proteins extracts subjected to a fractionation. Protein fractions were immunoblotted with anti-ZIKV EDIII (B) or anti-E 4G2 (C) antibodies.

DISCUSSION

The role of the structural protein region in the permissiveness of human cells to ZIKV infection has been previously reported¹⁸. ZIKV strains of historical or epidemic lineages display differences in their binding properties leading to differences in cell susceptibility to the infection. In order to further characterise the biological properties of contemporary ZIKV strains, which have been associated with recent epidemics and severe forms of disease in humans, we investigated the role of ZIKV E protein N-glycosylation site. Our data show differences in virus infectivity and progeny production kinetics without affecting viral attachment or host-cell responses. Further characterisations identified E protein conformational changes, triggered by the N-glycosylation site, as major events in virus fusion and release of the viral RNA into the cytoplasm.

The first step in the viral entry pathway involves non-specific binding to attachment factors. Negatively charged glycosaminoglycans, which are abundantly expressed on numerous cell types, are often used as low-affinity attachment factors by flaviviruses. These interactions serve to concentrate the virus at the cells surface and are mediated by the domain III of the E protein²³. Our data demonstrate that the N-glycosylation site of ZIKV E protein does not influence virus binding, which suggests that Domain III is not strongly affected by N-glycosylation site-induced conformational changes. We conclude that this initial step of ZIKV entry into cells is not dependent on the E protein N-glycosylation site.

Despite the different entry routes of viral particle internalisation, genome release into the cytoplasm always occurs through E protein-mediated membrane fusion²⁴. The low-pH environment within endosomes triggers a series of molecular changes within the E protein resulting in fusion of the viral membrane with the endosomal membrane and subsequent release of the nucleocapsid into the cell cytoplasm^{12,13}. One interesting finding is the fact that chloroquine treatment does alter less BR15 virus entry than it does for mutant BR15. This suggests that the N-glycosylated site increases the pH sensitivity of the E protein. To generate the mutant BR15, the sequence was modified so that the coding region of the E protein IVNDTGH (amino acids 152 to 158) in BR15 was replaced

with the TVNDIGY motif from MR766, meaning that not only the N-glycosylation motif was abrogated but the H158 was also changed into a tyrosine. Histidine residues have been described as pH sensors in flavivirus membrane fusion²⁵. The initiation of fusion is crucially dependent on the protonation of conserved histidine residues at the interface between domains I and III of the E protein, leading to the dissolution of domain interactions and to the exposure of the fusion peptide. Given the fusion differences we observed between the wildtype and the mutant BR15 molecular clones, further investigations on the protonation of H158 are required to determine its contribution in membrane fusion.

Our analysis of virus inocula generated in Vero cells showed differences in particles-to-PFU ratios indicating that the E protein N-glycosylation facilitates the release of more infectious particles. In addition, we demonstrated with recombinant proteins that the N-glycosylation site of ZIKV E protein also facilitates production of more soluble proteins. These results are supported by the work of Mossenta and colleagues²⁶. Whether these observations are due to conformational changes occurring during virion production remains undetermined. However, in a study on flavivirus cross-reactive epitopes, Crill and Chang²⁷ suggested that the close packing of the fusion peptide against its subunit partner and the glycan on the upper surface protects the fusion loop from irreversible pH-induced conformational changes during maturation and secretion. All these observations suggest that the N-glycosylation site on ZIKV E protein could also be an advantage during the virion maturation process.

Finally, our data indicate that N-glycosylation site of the E protein is crucial in ZIKV evolution towards an epidemic behaviour and also highlight conformational changes that further support viral fusion. These new findings could help to design innovative strategies for ZIKV infection control.

MATERIAL AND METHODS

Cells and reagents

Vero cells (ATCC, CCL-81) were cultured at 37°C under a 5% CO₂ atmosphere in MEM medium, supplemented with 5% heat-inactivated foetal bovine serum (FBS), A549-Dual™ cells (InvivoGen, a549d-nfis) in MEM medium, supplemented with 10% heat-inactivated FBS and non-essential amino acids. A549-Dual™ (A549^{Dual}) cells were maintained in growth medium supplemented with 10 µg.mL⁻¹ blasticidin and 100 mg.mL⁻¹ zeocin (InvivoGen). The chloroquine phosphate was purchased from Sigma-Aldrich. The rat antibody specifically raised against the E protein Domain III was developed in-house²². The mouse anti-pan flavivirus envelope E protein mAb 4G2 was produced by RD Biotech. Horseradish peroxidase-conjugated anti-rabbit and anti-mouse antibodies were purchased from Vector Labs.

Design of ZIKV molecular clones

The molecular clone (MR766, GenBank accession number LC002520, and BR15, GenBank accession number KU365778) design and production strategies for ZIKV were previously described^{18,20}. To introduce the BR15 glycosylation site into MR766^{MC}, we used mutagenesis primers (forward primer: 5'-ggctcccagcacagtgggatgatcgtaatgacacaggacatgaaactg-3' and reverse primer: 5'-cagtttcatgtcctgtgtcattaacgatcatcccactgtgtctgggagcc-3') to generate two overlapping fragments

Z1^{MR766-EGLY-1} and Z1^{MR766-EGLY-2} from the Z1^{MR766} fragment encoding the MR766 structural proteins in which the coding region of the E protein received the IVNDTGH motif (amino acids 152 to 158) from BR15. To remove the glycosylation site from BR15^{MC}, a new Z1^{BR15-EmutGLY} fragment was designed for which the sequence was modified so that the encoding region of the E protein received the TVNDIGY motif (amino acids 152 to 158) from MR766. The synthetic genes were cloned into plasmid pUC57 by GeneCust (Luxembourg). The fragments were amplified by PCR from their respective plasmids using sets of primer pairs that were designed so that fragments overlapped on about 30 to 50 nucleotides.

Recovering of molecular clones BR15^{-GLY} and MR766^{+GLY}

The molecular clones were produced as previously described by Gadea *et al.* and Bos *et al.*^{18,20}. Briefly, the purified PCR fragments were electroporated into Vero cells. After 5 days, cell supernatants were recovered usually in absence of cytopathic effect and used to infect fresh Vero cells in a first round of amplification (P1). Viral clones were recovered at the cytopathic effect onset and amplified for another round on Vero cells to produce a P2 for further studies. To produce MR766^{+GLY} and BR15^{-GLY} E mutant viral clones, Vero cells were respectively electroporated with the PCR fragments Z1^{MR766-EGLY-1}, Z1^{MR766-EGLY-2}, Z2^{MR766}, Z3^{MR766}, and Z4^{MR766} and with the PCR fragments Z1^{BR15-EmutGLY}, Z2^{BR15}, Z3^{BR15}, and Z4^{BR15}. The recovered mutant viruses MR766^{+GLY} and BR15^{-GLY} respectively consist of the viral sequence of MR766 in which the glycosylation site of ZIKV strain BR15 was introduced and the viral sequence of BR15 in which the glycosylation site was replaced with its counterpart of ZIKV strain MR766.

Plaque forming assay

Viral titres were determined by a standard plaque-forming assay as previously described with minor modifications²⁸. Briefly, Vero cells grown in 24 or 48-well culture plate were infected with tenfold dilutions of virus samples for 2 hours at 37 °C and then incubated with 0.8% carboxymethylcellulose (CMC) for 4 days. The cells were fixed by 3.7% FA in PBS and stained with 0.5% crystal violet in 20% ethanol. Viral titres were expressed as plaque-forming units per mL (PFU.mL⁻¹).

Quantification of viral stocks

Zika virus samples were analyzed by titration on Vero cells while genomic viral RNA was quantified by RT-qPCR as previously described¹⁸. Briefly, viral RNA was extracted from virus particles using QIAmp kit (QIAGEN). The PCR standard curve used for the quantification of ZIKV copy numbers was obtained with a pUC57/ZIKV-E amplicon plasmid containing a synthetic cDNA encompassing nucleotides 961 to 1301 of genomic RNA (MR766). The couple of ZIKV E primers was used to equally amplify pUC57/ZIKV-E amplicon and the cDNA encompassing nucleotides 1046 to 1213 from genomic RNA of ZIKV molecular clones used in this study.

Immunoblot assay

Cell lysates were performed in RIPA lysis buffer. All subsequent step of immunoblotting was performed as described²⁹. Primary antibodies were used at 1:500 dilutions. Anti-mouse immunoglobulin-horseradish peroxidase and anti-rat immunoglobulin-horseradish peroxidase conjugates were used as secondary antibodies (dilution 1:2000). Blots were revealed with ECL detection reagents.

Flow cytometry assay

A549^{Dual} cells were grown on 6-well plates at $5 \cdot 10^5$ cells per well and infected at a MOI of 1. Infected cells were harvested and fixed with 3.7% formaldehyde in PBS for 20 min, permeabilized with 0.1% Triton-X100 in PBS for 4 min and then blocked with PBS-BSA for 10 min. Cells were stained with anti-E 4G2 (1:1000) for 1 hour. Antigen staining was visualized with goat anti-mouse Alexa Fluor 488 IgG (1:1000) for 20 min. Cells were subjected to a flow cytometric analysis using a CytoFLEX flow cytometer (Beckman). The percentage of positive cells was determined using FlowJo software.

RT-qPCR

Total RNA including genomic viral RNA was extracted from cells (Qiagen) and reverse transcription was performed using 500 ng of total RNA, random hexamer primers (intracellular viral RNA) or E reverse primer (virus particles) and MMLV reverse transcriptase (Life Technologies) at 42°C for 50 minutes. Quantitative PCR was performed on a CFX96 qPCR System (Bio Rad). Briefly, 10 ng cDNA was amplified using 0.2 μ M of each primer and 1X GoTaq Master Mix (Promega). When appropriate, data were normalized to the internal standard GAPDH. For each single-well amplification reaction, a threshold cycle (Ct) was calculated using the ABI7500 program (Applied Biosystems) in the exponential phase of amplification. Relative changes in gene expression were determined using the $2^{-\Delta\Delta C_t}$ method and reported relative to the control. The primers used in this study are listed in Frumence *et al*²⁸. ZIKV E primers were designed to match both MR766-NIID and BeH819015 sequences (forward 5'-gtcttggaacatggagg-3' and reverse 5'-ttcacctgtgttgggc-3').

Virus binding assay

Cells were cultured at subconfluent density in 24-well plates. Cell monolayers were washed in cold PBS and cooled at 4°C at least 20 min in presence of cold MEM supplemented with 2% FBS. Pre-chilled cells were incubated at 4°C with ZIKV at MOI of 1 in 1.5 mL of cold MEM supplemented with 2% FBS. After 1 hour of incubation, the virus inputs were removed and the cells were washed with cold MEM supplemented with 2% FBS. Total cellular RNA was extracted using the RNeasy kit (Qiagen) and RT-qPCR analysis on viral RNA was performed using primers for ZIKV E gene as above described.

Fusion assay

Cells were cultured at subconfluent density in 12-well plates. Cell monolayers were cooled at 4°C at least 20 min in presence of cold MEM supplemented with 10% FBS. Pre-chilled cells were incubated at 4°C with ZIKV at MOI of 1 in 1 mL of cold MEM supplemented with 10% FBS. After 1-hour incubation, cells were shifted to 37°C. 1 hour after temperature shifting, chloroquine was added to the culture medium at 100µM for a 2-hour period. Culture medium was then replaced to avoid cytotoxic effects of the drug. 30 hours post temperature shifting, cells were harvested for RNA extraction. Total RNA were subjected to RT-qPCR analysis.

Cytotoxicity assay

Cell damages were evaluated measuring lactate dehydrogenase (LDH) release. Supernatants of infected cells were recovered and subjected to a cytotoxicity assay, performed using CytoTox 96® non-radioactive cytotoxicity assay (Promega) according to manufacturer instructions. Absorbance of converted dye was measured at 490 nm (Tecan). Results of LDH activity in the cell supernatants are presented with subtraction of control values.

IRF pathway activation

The activation of the IRF pathway was monitored measuring the Lucia luciferase activity. It was evaluated using the QUANTI-Luc substrate (InvivoGen) according

to the manufacturer's recommendations. IRF-induced luciferase levels were quantified using a FLUOstar Omega Microplate Reader (BMG LABTECH). Results are presented with subtraction of control values.

prM-E expression

To express the recombinant E proteins from ZIKV in mammalian cells, the prM and E genes from MR766 and BR15, as well as a mutant BR15 lacking the N-Glycosylation motif, were synthesised by GeneCust (Luxembourg). The prM protein plays the role of chaperone to ensure the proper folding of the E protein. Modifications that optimize the expression of viral envelope proteins in human cells were done on the original sequences. Then, mammalian codon-optimised sequences coding for prM signal peptide followed by the prM and E proteins were cloned into the Nhe I and Not I restriction sites of the pcDNA3.1(-) plasmid to generate pMR766, pBR15 and pBR15^{GLY} respectively. Each plasmid was transfected in human HEK-293T cells using lipofectamine 3000 according to the manufacturer's instructions.

Cell fractionation

Cells were washed with PBS and lysed at the concentration of 1.10^4 cells/ μ l in protein separation buffer A (0.2% Triton X-100, 50 mM Tris-HCl pH 7.5, 150 mM NaCl, 2.5 mM EDTA). The Triton X-100-insoluble fraction was separated by centrifugation at 3,400 g for 10 minutes. Pellets were enriched in non-folded proteins.

Statistical analysis

All values are expressed as mean \pm SD of at least two experiments, or as mean \pm SEM of triplicates. Comparisons between different treatments have been analyzed by a one-way or two-way ANOVA tests as appropriate. Values of $p < 0.05$ were considered statistically significant for a post-hoc Tukey's test. All statistical tests were done using the software Graph-Pad Prism version 7.01.

REFERENCE

1. Lee, I. et al. Probing Molecular Insights into Zika Virus–Host Interactions. *Viruses* 10, 233 (2018).
2. Douam, F. & Ploss, A. Yellow Fever Virus: Knowledge Gaps Impeding the Fight Against an Old Foe. *Trends Microbiol.* 26, 913–928 (2018).
3. Lindquist, L. Recent and historical trends in the epidemiology of Japanese encephalitis and its implication for risk assessment in travellers. *J. Travel Med.* 25, S3–S9 (2018).
4. MacNamara, F. . Zika virus : A report on three cases of human infection during an epidemic of jaundice in Nigeria. *Trans. R. Soc. Trop. Med. Hyg.* 48, 139–145 (1954).
5. Fagbami, A. H., Monath, T. P. & Fabiyi, A. Dengue virus infections in Nigeria: a survey for antibodies in monkeys and humans. *Trans. R. Soc. Trop. Med. Hyg.* 71, 60–65 (1977).
6. Jan, C., Languillat, G., Renaudet, J. & Robin, Y. [A serological survey of arboviruses in Gabon]. *Bull. Soc. Pathol. Exot. Filiales* 71, 140–146 (1978).
7. Renaudet, J., Jan, C., Ridet, J., Adam, C. & Robin, Y. [A serological survey of arboviruses in the human population of Senegal]. *Bull. Soc. Pathol. Exot. Filiales* 71, 131–140 (1978).
8. Cao-Lormeau, V.-M. et al. Guillain-Barré Syndrome outbreak associated with Zika virus infection in French Polynesia: a case-control study. *Lancet Lond. Engl.* 387, 1531–1539 (2016).
9. Cugola, F. R. et al. The Brazilian Zika virus strain causes birth defects in experimental models. *Nature* 534, 267–271 (2016).
10. Merfeld, E., Ben-Avi, L., Kennon, M. & Cervený, K. L. Potential mechanisms of Zika-linked microcephaly. *Wiley Interdiscip. Rev. Dev. Biol.* (2017). doi:10.1002/wdev.273
11. Parra, B. et al. Guillain-Barré Syndrome Associated with Zika Virus Infection in Colombia. *N. Engl. J. Med.* 375, 1513–1523 (2016).
12. Smit, J., Moesker, B., Rodenhuis-Zybert, I. & Wilschut, J. Flavivirus Cell Entry and Membrane Fusion. *Viruses* 3, 160–171 (2011).
13. Stiasny, K., Fritz, R., Pangerl, K. & Heinz, F. X. Molecular mechanisms of flavivirus membrane fusion. *Amino Acids* 41, 1159–1163 (2011).
14. Rey, F. A., Heinz, F. X., Mandl, C., Kunz, C. & Harrison, S. C. The envelope glycoprotein from tick-borne encephalitis virus at 2 Å resolution. *Nature* 375, 291–298 (1995).
15. Pierson, T. C. & Diamond, M. S. Degrees of maturity: The complex structure and biology of flaviviruses. *Curr. Opin. Virol.* 2, 168–175 (2012).
16. Annamalai, A. S. et al. Zika Virus Encoding Nonglycosylated Envelope Protein Is Attenuated and Defective in Neuroinvasion. *J. Virol.* 91, (2017).
17. Fontes-Garfias, C. R. et al. Functional Analysis of Glycosylation of Zika Virus Envelope Protein. *Cell Rep.* 21, 1180–1190 (2017).
18. Bos, S. et al. The structural proteins of epidemic and historical strains of Zika virus differ in their ability to initiate viral infection in human host cells. *Virology* 516, 265–273 (2018).
19. Li, G. et al. The Roles of prM-E Proteins in Historical and Epidemic Zika Virus-mediated Infection and Neurocytotoxicity. *Viruses* 11, 157 (2019).
20. Gadea, G. et al. A robust method for the rapid generation of recombinant Zika virus expressing the GFP reporter gene. *Virology* 497, 157–162 (2016).
21. Delvecchio, R. et al. Chloroquine, an Endocytosis Blocking Agent, Inhibits Zika Virus Infection in Different Cell Models. *Viruses* 8, 322 (2016).
22. Viranaicken, W. et al. ClearColi BL21(DE3)-based expression of Zika virus antigens illustrates a rapid method of antibody production against emerging pathogens. *Biochimie* 142, 179–182 (2017).
23. Chen, Y. et al. Dengue virus infectivity depends on envelope protein binding to target cell heparan sulfate. *Nat. Med.* 3, 866–871 (1997).
24. Pierson, T. C. & Kielian, M. Flaviviruses: braking the entering. *Curr. Opin. Virol.* 3, 3–12 (2013).
25. Fritz, R., Stiasny, K. & Heinz, F. X. Identification of specific histidines as pH sensors in flavivirus membrane fusion. *J. Cell Biol.* 183, 353–361 (2008).
26. Mossenta, M., Marchese, S., Poggianella, M., Slon Campos, J. L. & Burrone, O. R. Role of N-glycosylation on Zika virus E protein secretion, viral assembly and infectivity. *Biochem. Biophys. Res. Commun.* (2017). doi:10.1016/j.bbrc.2017.01.022

27. Crill, W. D. & Chang, G.-J. J. Localization and Characterization of Flavivirus Envelope Glycoprotein Cross-Reactive Epitopes. *J. Virol.* 78, 13975–13986 (2004).
28. Frumence, E. et al. The South Pacific epidemic strain of Zika virus replicates efficiently in human epithelial A549 cells leading to IFN- β production and apoptosis induction. *Virology* 493, 217–226 (2016).
29. Nativel, B. et al. Soluble HMGB1 is a novel adipokine stimulating IL-6 secretion through RAGE receptor in SW872 preadipocyte cell line: contribution to chronic inflammation in fat tissue. *PloS One* 8, e76039 (2013).

PART III:

ZIKA VIRUS IMPACT ON PLASMATYCOID DENDRITIC CELLS ANTIVIRAL RESPONSE

I. INTRODUCTION TO PLASMACYTOID DENDRITIC CELLS

I.1. Overview of Dendritic Cells

Despite being first observed in humans by Paul Langerhans in 1968, dendritic cells were actually discovered in 1973 by R. Steinman and Z. Cohn while these latter sought to understand how an immune response was induced in a mouse spleen¹. At that time the immunologists knew that for an immune response to develop, lymphocytes were needed as well as an "accessory" cell able to present antigens. This cell was long supposed to be a macrophage, until Steinman and Cohn discovered a rare and unusually shaped population of cells, scattered with long tree-like extensions. These cells were then called "dendritic cells" from greek "*dendreon*" meaning "tree"^{1,2}. Their in-depth characterization was long slowed down by the technical difficulties related to their rarity and the lack of specific markers to identify them. The implementation of protocols providing the facility to generate functional DCs from progenitors or precursors *in vitro* was a major step in improving knowledge of DCs over the past twenty years.

I1.1. Main features of Dendritic cells

In vivo, DCs represent only a small proportion of the leukocytes and are of low proliferative activity. However, they are regularly renewed in order to maintain a constant pool of cells whose presence is essential for the initiation and orientation of the immune response²⁻⁴. DCs are indeed potent stimulators of T lymphocytes and are considered as professional antigen presenting cells. Immature DCs derived from progenitors (myeloid or lymphoid) residing in the bone marrow. They are able to internalize antigens from dying *self*-cells or pathogens and circulating protein antigens, which regulate their role. In non-pathological situations, immature DCs constantly sample *self*-antigens and are thereby involved in the central and peripheral T cells tolerance in order to avoid inappropriate autoimmune responses⁵. Inactivated immature DCs then induce T cell depletion or anergy and promote the development of regulatory T cells (Treg)^{5,6}. On the contrary, in the presence of pathogens, DCs detect danger signals present in the surrounding environment. Indeed, DCs possess a set of receptors specialized in the detection of motifs unique to pathogens or cellular damage⁷⁻⁹.

Thus, in the presence of danger signals or pro-inflammatory cytokines, DCs will evolve towards a mature phenotype. Their maturation is associated with phenotypic changes and characterized by the modulation of their chemokine receptor expression. For example, DCs will express CCR7 (C-C chemokine receptor type 7) which will promote their migration to secondary lymphoid organs¹⁰. In parallel, DCs will also increase the expression of co-stimulation molecules associated with T lymphocytes as well as the production of cytokines involved in the orientation of the immune response^{11,12}. Such secreted cytokines depend on the stimuli encountered and the subpopulation of activated DC.

11.2. Dendritic cell diversity

DCs are a very heterogeneous group of cells, with various functions and origins. Phenotypically, DCs express the CD45 molecule (common antigen lymphocyte) like any other leukocytes and are devoid of cellular lineage markers such as CD3 (T lymphocytes), CD14 (monocytes), CD19 (B lymphocytes), CD16 and CD56 (NK cells). Nevertheless, unlike B and T cells, there is no marker that is both DC-specific and common to all subpopulations.

As the discoveries were made, DCs were subdivided into multiple subpopulations based on their phenotype. However, this classification was revised owing to its lack of homogeneity, sometimes leading to the presence of duplicates (various names for the same population). To overcome these difficulties, the three main following approaches currently prevail: (i) histological classification, (ii) subdivision of DCs according to their ontogeny and factors essential to their development, or (iii) according to transcriptomic homologies^{13,14}. These complementary approaches provide a frame for defining the distinct DC subpopulations, although these latter are still evolving and not fixed currently¹⁵.

In the absence of a real consensus, the usual method consists in dividing DCs into two main functional subtypes: the plasmacytoid DCs (pDC) and the myeloid DCs (mDC), also known as conventional DCs. Despite significant phenotypic differences, this classification is applicable to both humans and mice. In addition, recent advances refined the characterization of homologous DC populations between the two species, allowing a better understanding and/or transfer of the results obtained in mice and humans.

Table 8: Phenotypic characterization of human myeloid and plasmacytoid dendritic cells

PHENOTYPE	Myeloid Dendritic cells	Plasmacytoid Dendritic cells
Myeloid markers		
CD11b	+	–
CD11c	+	–
CD13	+	–
Lymphoid markers		
Pre-Tα	–	+
Ig1-like 14.1	–	+
Spi-B	–	+
Pattern Recognition receptors		
BDCA-1 (CD1c)	+	–
HLA-DR	++	+
CD303 (BDCA2)	+	++
DC-SIGN	+	–
MMR (CD206)	±	–
CD205 (DEC-205)	±	–
Dectin-1	+	+
Dectin-2	++	–
TLR1	+	±
TLR2, TLR4, TLR5	+	–
TLR3	++	–
TLR6	+	+
TLR7	–	++
TLR8	++	–
TLR9	–	++
TLR10	+	±
Other receptors		
CD4	+	++
CD45RA	–	+
CD45RO	+	–
CD123 (IL-3R)	+	++
GM-CSFR	++	+
CCR7	+	+
BDCA3	+	–
BDCA4	–	+
ILT1	+	–
ILT3	–	+
ILT7	–	+

I.2. Plasmacytoid Dendritic Cells: Sentinels and Orchestrators of the Antiviral Immune Response

Plasmacytoid dendritic cells form a very distinctive population to the other DCs, and were long not considered as a fully-fledged DC population. Morphologically, they do not resemble mDCs. In contrast, pDCs are of small size, ranging from 8 to 10 μm , with a round and smooth shape in their basal state from which they get their appellation. The term "plasmacytoid dendritic cell" would therefore seem antinomic but is widely accepted in the field. The main feature of pDCs is their capacity to rapidly produce large quantities of type I IFNs, predominantly IFN α , in particular after exposure to a virus.

I2.1. Chronology of the plasmacytoid dendritic cells discovery

While pDCs were first observed in 1958 by the pathologists K. Lennert and W. Remmele¹⁶, their identification as dendritic cells only dates to the late 1990s^{17–19}. During this period, pDCs had different names, once attributed to T cells and other times to monocytes. In the early 1980s, the research of Trinchieri *et al.* showed that type I IFN is a powerful agent produced by the leukocytes exposed to a virus or to an infected cell, which enhances the NK-induced cytotoxicity. Based on their analyses, they also conclude that the majority of type I IFN would in fact be produced by only a small portion of leukocytes²⁰. These cells, which were known to express HLA-DR, a molecule of the class II major histocompatibility complex (MHC), but were negative for all other markers of lymphocyte and myelomonocyte lines known at that time, have been called "natural IFN producing cells"²¹. At the same time, some pathologists confirmed the previous observations made in 1958, and described once again the abundant presence of cluster-forming cells in the T-zones of the lymph nodes. They reported cells of plasma-cell like morphology and expressing the CD4, a marker associated with T helper cells, that they called "plasmacytoid T cells" in 1983²². Later, a comprehensive study of their phenotype, carried out with a broad panel of monoclonal antibodies, revealed that these cells have markers common with the monocyte-macrophage line such as CD31, CD36, CD68 and express the IL-3 receptor alpha chain (IL-3R α , CD123). These findings led to another new appellation of "plasmatoid monocytes" while their role remained enigmatic at that time.

Finally, the plasma cell-like cells of the peripheral blood and secondary lymphoid organs were identified as being the "IFN-producing cells " in the late 1990s. They were ultimately classified as a subpopulation of DC capable of stimulating T lymphocytes, under the name of plasmacytoid dendritic cells.

12.2. Ontogeny of pDCs

The hematopoietic differentiation pathway of pDCs and its regulating molecular mechanisms are still poorly understood. However, the cytokine FLT3L (FMS-like tyrosine kinase 3 ligand) appears to play a critical role in the development of pDCs and allows the generation of human pDCs from CD34⁺ hematopoietic stem cells *in vitro*^{23,24}. Among the transcription factors involved in the development of pDCs, IRF8, PU.1 and STAT3 are essential for pDCs emergence, as well as for mDCs too^{25,26}. PU.1 and STAT3 are necessary since they allow expression and signaling of the Flt3 receptor respectively^{27,28,29}. Lastly, SpiB and E2-2 proteins, which are both important in the development of B cells, are also required for pDCs³⁰. Several observations emphasize the importance of the E2-2 factor due to its ability to bind to IRF-8 and SpiB promoters, as well as genes encoding the proteins CD303 (BDCA-2), ILT7 (immunoglobulin-like transcript 7) and IRF-7, which are essential for the functions of pDCs.

Unlike mDC, whose myeloid origin is well defined and accepted, a doubt remains about the origin and the nature of the precursor of pDCs. The first hypothesis put forward is that pDCs have a lymphoid origin. The latter is due to the fact that they have transient markers (mRNAs) characteristic of the early phases of lymphoid development which encode pT α (pre-T cell receptor α), $\lambda 5$ and Spi-B, but mDC do not³¹. The lymphoid origin of pDCs is reinforced by the observation that the overexpression of dominant-negative transcription factor Id2 or Id3 blocks the development of pDCs, T and B lymphocytes, but not the one of mDCs³². However, recent data indicating that pDCs can be generated from both common myeloid progenitors (CMPs) and common lymphoid progenitors (CLPs) have challenged this assumption³³. Ishikawa *et al.* further studied the differentiation of human hematopoietic stem cells and progenitors *in vivo* using a murine xenotransplantation system³⁴. They demonstrated that intravenous injection of purified human CMP and CLP into newborn NOD-scid mice resulted in both cases

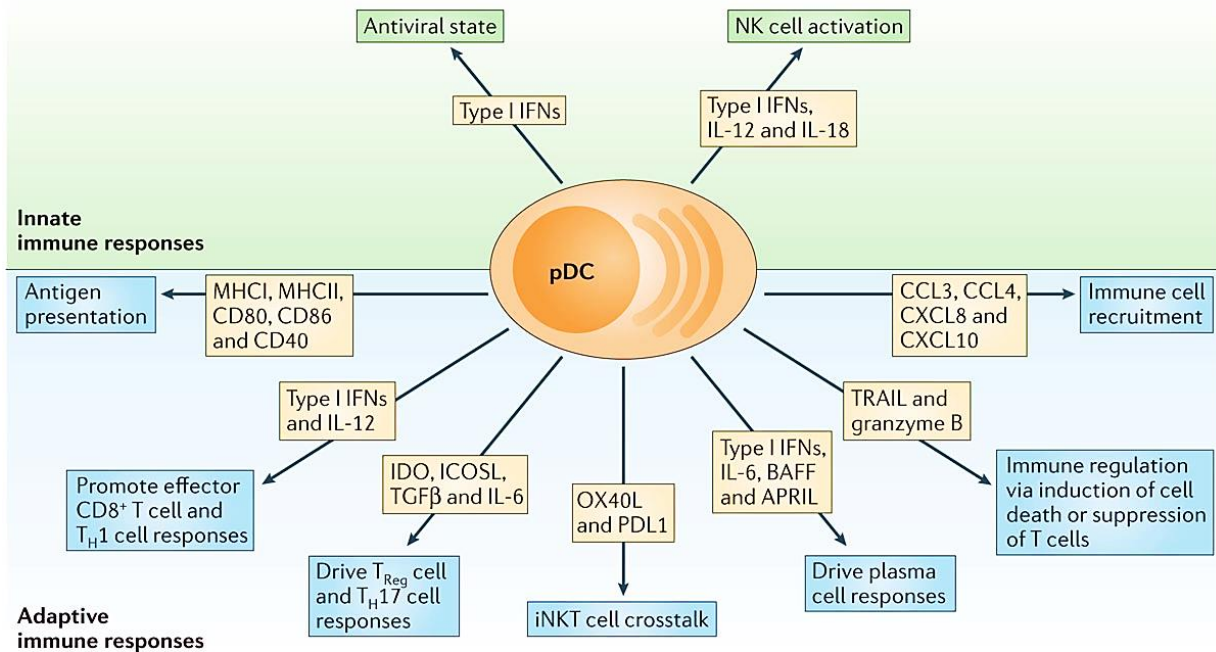
in the phenotypic differentiation of mDC and pDC³⁵. As a consequence, they concluded that human DCs use a unique and flexible differentiation program which cannot be categorized in the classical myeloid and lymphoid pathways. More recently, FLT3L stimulated murine bone marrow culture has been shown to generate DC precursors called " pro-DC " which are capable to split and to differentiate into all DC sub-populations³⁶. These results are in favor of an independent and DC-specific hematopoietic differentiation pathway involving a common dendritic cell progenitor (CDP). However, the authors did not consider the possibility that progenitors of a given line can dedifferentiate into pluripotent cells and then re-differentiate into progenitors of another lineage when injected *in vivo*. Such a mechanism, already observed *in vitro* with early hematopoietic progenitors in mice, would then explain the possible generation of pDC from CMP and CLP, and would therefore reduce the origin of these cells to the lymphoid line³⁷.

I2.3. Distribution of plasmacytoid dendritic cells

The presence of pDCs in fetal organs such as the liver, thymus and bone marrow suggests that they develop from these primary lymphoid tissues³². In adults, they are continuously produced in the bone marrow and circulate in the blood where they represent about 0.5% of PBMC (peripheral blood mononuclear cells). They are also located in paracortical extrafollicular T-zones (but not at the germinative centers) of the lymph nodes, tonsils, thymus, and lung tissue³⁸. Conversely, they have never been observed at effector sites directly exposed to antigens, such as mucous membranes or skin, in normal physiological conditions. In the lymph nodes, pDCs are observed in areas close to the postcapillary veinlets, suggesting their extravasation from the blood in the lymph nodes, without passing through the lymphatic circuit.

I2.4. Physiological role of plasmacytoid dendritic cells

The mammalian immune system consists of the innate and adaptive response. Innate immunity cells, such as DCs, macrophages, NK, neutrophils and other polynuclear cells, have receptors capable to detect and recognize the invariant structures typical of some families of microbes. The adaptive immune response,



Nature Reviews | Immunology

Figure 30: Diverse functions of plasmacytoid dendritic cells

Plasmacytoid dendritic cells (pDCs) are important drivers of both innate (top of figure in green) and adaptive (bottom of figure in blue) immune responses. Their ability to rapidly produce type I interferons (IFNs) during viral infections promotes an antiviral state by inducing cellular expression of IFN- stimulated genes and apoptosis of infected cells. Moreover, type I IFNs, interleukin-12 (IL-12) and IL-18 enhance natural killer (NK) cell activation and effector functions such as IFN γ secretion and lysis of target cells. Expression of MHC class I (MHCI) and MHC class II (MHCII) molecules along with co-stimulatory markers including CD80, CD86 and CD40 enables pDCs to cross-prime CD8⁺ T cells and present antigen to CD4⁺ T cells. Production of type I IFNs and IL-12 by pDCs supports the accumulation and effector functions of CD8⁺ T cells, as well as the polarization of CD4⁺ T cells into T helper 1 (TH1) cells. pDC expression of indoleamine 2,3-dioxygenase (IDO) and inducible T cell co-stimulator ligand (ICOSL) and pDC production of transforming growth factor- β (TGF β) and IL-6 promote regulatory T (Treg) cell or TH17 cell commitment, respectively. Crosstalk between pDCs and invariant NKT (iNKT) cells occurs via OX40–OX40L (also known as TNFRSF4–TNFSF4) and programmed cell death protein 1 (PD1)–PD1 ligand 1 (PDL1) interactions and dampens antiviral adaptive immune responses. pDCs influence B cell activation, plasma cell generation and antibody secretion through production of type I IFNs, IL-6, B cell-activating factor (BAFF) and a proliferation-inducing ligand (APRIL). TNF-related apoptosis inducing ligand (TRAIL) and granzyme B serve as immunoregulatory factors that endow pDCs with the capacity to kill tumor cells, induce apoptosis of infected CD4⁺ T cells and suppress T cell proliferation. Finally, pDCs secrete chemokines such as CXC-chemokine ligand 8 (CXCL8), CXCL10, CC-chemokine ligand 3 (CCL3) and CCL4, which attract immune cells to sites of infection or inflammation (Figure and caption from Swiecki and Colonna, 2015)

ensured by B and T lymphocytes, is more effective being antigen-specific but requires a latency phase to promote the clonal expansion and the T lymphocytes differentiation into effectors. However, the random generation of lymphocyte receptors does not allow them to differentiate between *self* and *non-self* antigens, as it requires an education in which the innate system participates. Such cooperation between innate and adaptive immunity allows the immune system to determine the origin of antigens and establish an effective targeted response.

pDCs are a rare population, representing less than one percent of total blood mononuclear cells, yet they are responsible for 95% of the IFN α/β produced during viral infections¹⁹. They can produce up to a thousand times more IFNs than any other cell type, and dedicate nearly 60% of their transcriptome to the expression of genes encoding type I IFNs. This unique ability makes them crucial cells for the antiviral responses^{39–42}. pDCs are capable of expressing all subtypes of type I IFNs (IFN α , IFN β , IFN ω and IFN τ except IFN κ), type III (IFN λ) but not type II (IFN γ). Type I interferons, in addition to their interference role in viral replication, have a wide field of action on other immune cells^{43,44}. They increase the cytolytic functions of NK and cytotoxic T cells^{39,40,45}, increase B cell antibody production⁴⁶, stimulate cDC production of IL-12, IL-15, IL-18 and IL-23 cytokines, and promote monocyte differentiation into inflammatory DC (i.e. which are recruited to the site of inflammation)⁴⁷. In addition, pDCs also produce inflammatory cytokines, such as IL-6 and IL-12 (in mice) which, in combination with IFN α/β , allow the differentiation of naive and memories B cells into plasma cells^{48,49} and the production of IFN- γ by T cells and NK cells respectively^{39,50}. After activation by TLR-7 or 9, pDCs are able to initiate effective Th1 responses^{43,50,51}. However, they can also be activated by IL-3 and the CD40L, a molecule expressed by activated T cells. In these cases they produce only a small amount of type I IFNs but overexpress the OX40L co-stimulation molecule, which leads to the activation of Th2 cytokine production by T cells: IL-4, IL-5 and IL-10^{52,53}. While activated by TLRs or IL-3 and CD40L, pDCs retain the ability to induce regulatory responses^{54,55}. Consequently, their role in the induction of tolerance is increasingly studied, leading to the recent identification of the molecule responsible for this ability in humans. After maturation, ICOS-L is overexpressed

on pDCs, but not on mDCs. This molecule allows the development of IL-10-producing Treg lymphocytes in Th1 or Th2 responses⁵⁶. This function could be involved in the negative regulation of immune responses to prevent excessive inflammation that could cause damage to healthy body tissues^{57,58}. Lastly, cytotoxicity completes the range of functions that pDCs can perform. Activated by viruses, CpG or IL-3 and CD40L, pDCs express cytolytic molecules such as granzyme B and TRAIL (TNF-Related Apoptosis-Inducing Ligand) and are able to lyse tumor cells^{59–62}.

1.3. Virus detection and IFN production signaling pathway

To be effective, DCs must be able to recognize the *"self"* of the *"infectious non-self"* to determine the origin of the captured antigens and initiate either tolerance or immune response onset. More than twenty years ago, Charles Janeway hypothesized that this capacity was based on the recognition of conserved patterns expressed by pathogens⁶³. These motifs, called PAMP (pathogen-associated molecular pattern), are as expected unique to microorganisms and therefore absent from eukaryotic cells. They are detected by receptors called "pattern recognition receptors" (PRRs) which include many families of proteins such as TLR (Toll-like receptor), RLR (RIG-I-like receptor) and some CLR (C-type lectin receptor). Once detected, PRR activation induces a cascade of intracellular signals which regulate many biological processes, such as cytoskeleton and endosome dynamics, as well as cytokine and chemokine expression.

Janeway's *"self"* and *"non-self"* model explains immune responses against external antigens, but cannot account for antitumor responses, transplant rejections or autoimmune diseases. Consequently, it was replaced in 1994 by the one of Polly Matzinger, which introduces the concept of danger signals⁶⁴. In this model, not only the origin of the stimulating entity matters, but rather if this entity causes injury or not. Thus, danger signals are released by damaged cells due to bacterial, viral, fungal infections, but also during non-infectious processes such as tumor formation or tissue necrosis. These signals are sensed by the organism as threats and lead to the activation of immune cells. Such endogenous danger signals, also known as alarmins, are mediated by proteins that are otherwise sequestered in cells, such as uric acid, heat-shock protein, nucleic acids

or DNA complexed molecules such as HMGB-1⁶⁵. In experimental studies, these molecules induced the maturation of DC and enhanced antigen presentation and cytokine secretion^{66–68}. For instance, Saïdi et *al.* reported that HBGB1 is required for TRAIL translocation and IFN- α production by pDCs exposed to HIV infection⁶⁹.

I3.1. Toll-like receptors and type I interferon production

pDCs express several types of PRRs in their cytosol such as DHX9 and DHX36 helicases which can recognize viral DNA⁷⁰, and RIG-1 (constitutively expressed at low level but inducible) which can detect viral RNA⁷¹. However, TLR activation is thought to be the main response pathway of pDCs to microbial infections. While human mDCs express a range of TLRs, pDCs selectively express TLR7 and -9 in their endosomal compartments^{43,72,73}. These two receptors are involved in the recognition of (i) single-stranded RNA viruses and synthetic imidazoquinoline antiviral compounds such as imiquimod and resiquimod R-848^{74–76} and (ii) natural or synthetic CpG motifs characteristic of viral and bacterial DNA^{42,77}.

TLRs are type 1 transmembrane proteins, carefully conserved during evolution^{78,79}. Each TLR contains an extracellular domain rich in repeated leucine sequences involved in ligand recognition, and an intracellular domain containing a region called Toll-IL-1 receptor (TIR) homology domain, required for the initiation of intracellular signaling⁸⁰. The extracellular region of TLRs contains LRRs (leucine-rich repeat), responsible for PAMP recognition⁸⁰.

› TLR7/9 Signaling

Once the antigen binds to TLR7 or TLR9, different cell transduction pathways are activated, leading to the maturation of pDCs and to the production of cytokines such as type I IFNs. The latter is dependent on the adaptive protein MyD88 and requires the translocation of the factor IRF7 in the nucleus. In most cells, IFN α production depends on the previous activation of type I IFN receptor (IFNAR) by IFN β ligand, which then induces expression of IRF7⁸¹. In pDCs IRF7 is constitutively expressed, thus allowing a rapid production of type I IFNs independently to IFNAR-mediated pre-sensitization^{82,83}.

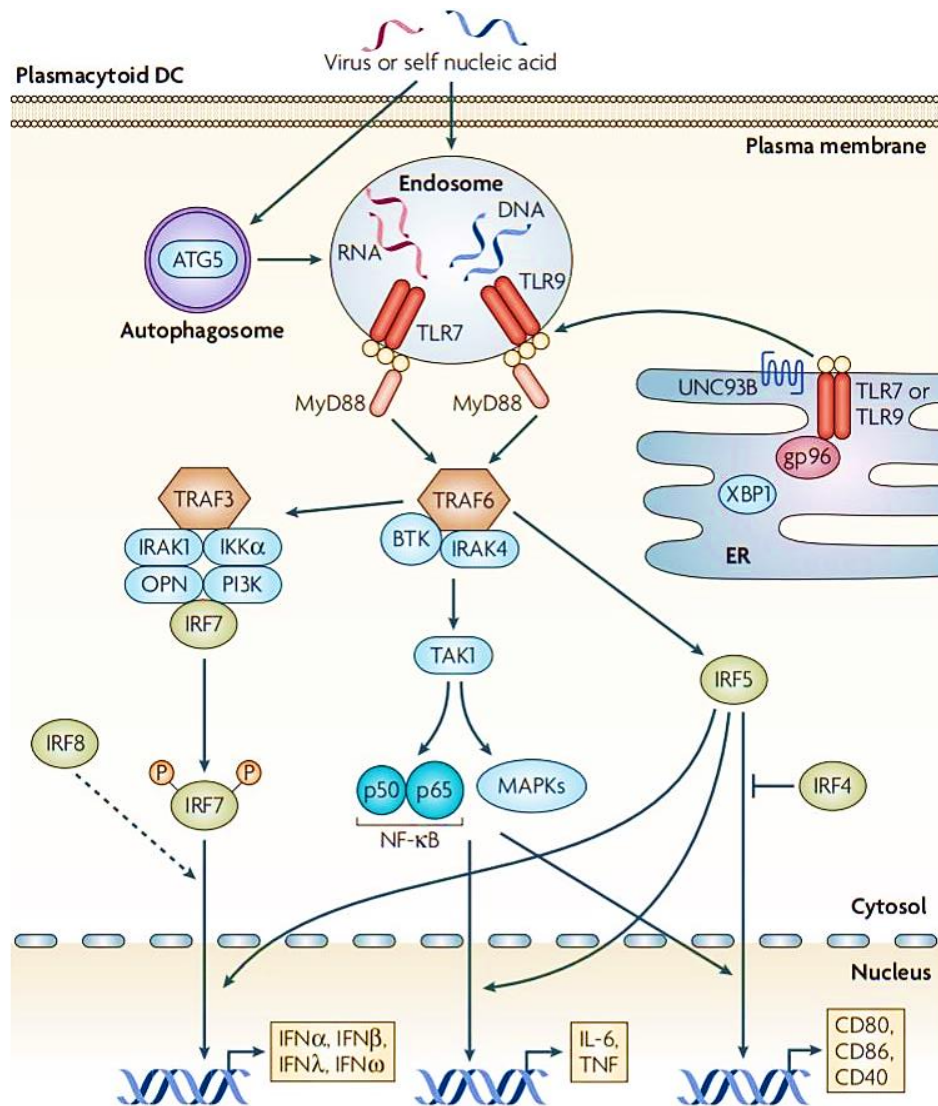


Figure 31: Activation pathway in plasmacytoid dendritic cells responding to nucleic acids

Resting plasmacytoid dendritic cells predominantly express TLR7 and TLR9, which reside in the ER with UNC93B and gp96. Following exposure to virus or nucleic acids, TLR7 and TLR9 relocate from the ER to the endosomes to engage with their RNA or DNA agonists. Conformational changes in the TLRs lead to the activation of MyD88 (myeloid differentiation primary-response gene 88) and its further association with TRAF6 (tumor-necrosis factor (TNF) receptor-associated factor 6), BTK (Bruton's tyrosine kinase) and IRAK4 (interleukin-1-receptor-associated kinase 4). The MyD88–TRAF6–IRAK4 complex then activates IRF7 (interferon-regulatory factor 7), TAK1 (transforming-growth-factor-β-activated kinase 1), nuclear factor-κB (NF-κB) and IRF5 to propagate the downstream signals. Most importantly, IRF7 is activated through TRAF3, IRAK1, IKKα (inhibitor of NF-κB kinase α), osteopontin (OPN) and phosphoinositide 3-kinase (PI3K). Following ubiquitylation and phosphorylation, IRF7 translocates to the nucleus and initiates the transcription of type I IFNs. TAK1 triggers the activation of NF-κB and MAPKs (mitogen-activated protein kinases) and, together with IRF5, leads to the production of pro-inflammatory cytokines and the expression of co-stimulatory molecules. IRF8, although not involved in the initial induction of IFN, magnifies IFN production through a feedback mechanism. By contrast, IRF4 inhibits the function of IRF5 through direct competition. Autophagosomes, which are constitutively formed in pDCs via ATG5 (autophagy-related gene 5), are probably involved in transferring the nucleic-acid agonists to endosomal TLRs for the production of IFNs. IL-6, interleukin-6; XBP1, X-box-binding protein 1. (Figure and caption from Gilliet et al., 2008)

In pDCs, the choice of the induced responses seems correlated with the degree of maturity of the endosome containing the activated TLR7/9. Thus, TLR7/9 activation in early endosome will engage MyD88 and the formation of a signalosome composed of TRAF3, TRAF6, IRAK1 and IRAK4. This signalosome will then lead to the phosphorylation of the transcription factor IRF7 via the involvement of IKK α and PI3K. The latter is subsequently translocated in the nucleus where it induces the production of type I IFNs⁸⁴⁻⁸⁶. In the late stages, MyD88 involvement will trigger the recruitment of TRAF6 and IRAK4 which will activate NF- κ B and p38MAPK. These transcription factors will then induce the production of pro-inflammatory cytokines such as IL-6 and TNF, and the expression of co-stimulation molecules such as CD40, CD80 and CD86^{84,87}.

› TLR9 differential signaling

Synthetic oligodeoxynucleotides rich in CpG are immunostimulatory sequences, referred to as CpG ODNs, which bind TLR9. They are commonly used in pDC studies as a positive control of cytokine production and/or pDC maturation. Three different classes of ODN (CpG A, B and C) exist which differ in terms of sequence and biological activity. Indeed, CpG -B ODNs (e.g. ODN 2006), single-stranded, induce a low IFN α production but a strong pDC maturation with increased co-stimulatory molecule expression. On the other hand, multimeric CpG-A ODNs (e.g. ODN 2216) are excellent inducers of IFN α production but poorly stimulate pDCs maturation⁸⁸. CpG-C ODNs, double-stranded, combine the properties of class A and B CpGs. Such differential TLR9-dependent pDC activation is due to three-dimensional structure and subcellular location of ODNs. Indeed, multimeric class-A CpG ODNs form aggregates and are located in early endosomes while monomeric class-B CpG ODNs are transported to late endosomes and lysosomal compartments^{85,89}. Thus, after binding to TLR9, they probably induce the activation of different signal factors resulting in the previously mentioned phenotypes.

› TLR7 Differential signaling

Concerning TLR7, no concrete studies were conducted to address differential signaling nevertheless discrepancies seems also exist after pDC activation through TLR7 ligands^{90,91}. Furthermore, Wang *et al.* demonstrated that the three-

dimensional structure of the viral genome is important for TLR7 activation in pDCs⁹². Indeed, they reported that Influenza virus, composed of a negative RNA of 2 kb, induces a higher type I IFN production than DENV which consist of an 11 kb positive RNA.

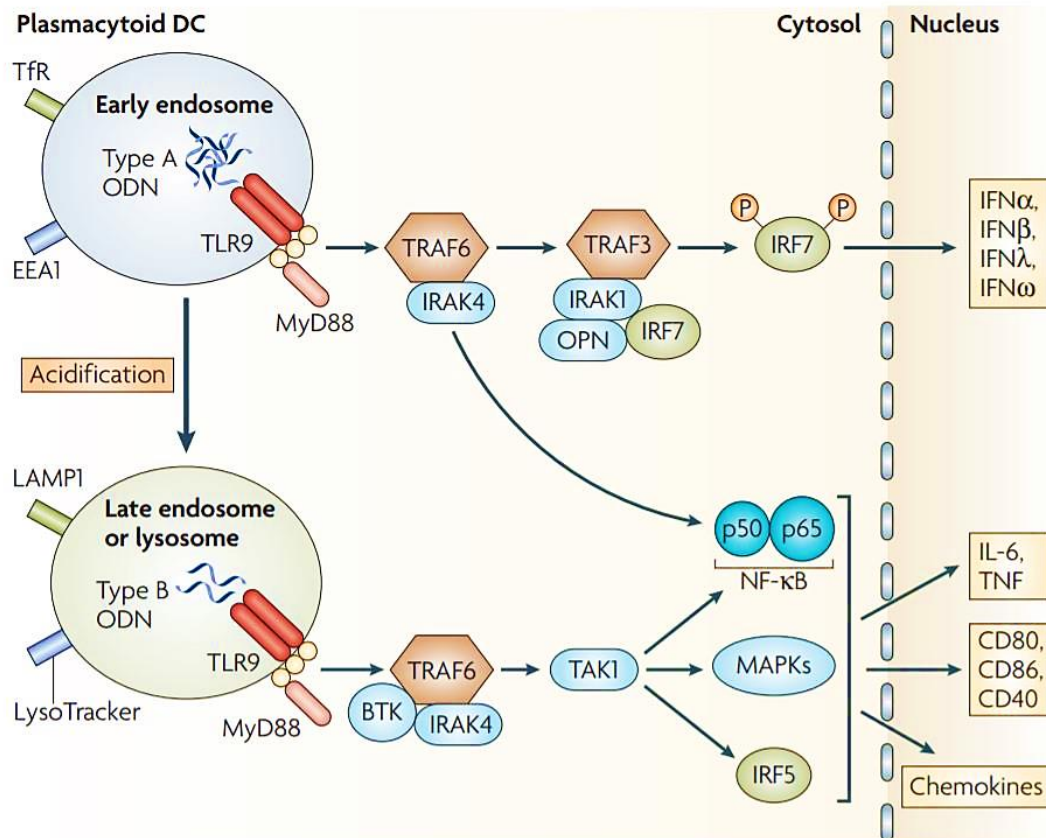


Figure 32: Signaling of CpG ODN classes in different endosomal compartments

In plasmacytoid dendritic cells, the binding of aggregated A-type CpG ODN to TLR9 occurs in the early endosomes, which express markers such as transferrin receptor (Tfr) and early endosomal antigen1 (EEA1). Prolonged TLR9 signaling from the early endosomes activates MyD88 (myeloid differentiation primary-response gene 88) and other signal mediators, importantly IRF7, which promote strong type I IFN production. By contrast, monomeric B-type CpG ODNs that bind to the TLR9 complex quickly traffic through the early endosomes and into the more acidic late endosomes or lysosomes, which are marked by the presence of LAMP1 (lysosomal-associated membrane protein 1) and LysoTracker. This presumably activates a different set of signal mediators, particularly NF-κB and probably MAPKs and IRF5, and thereby leads to distinct outcomes of pDC activation without high levels of IFN production.

(Figure and caption from Gilliet et al., 2008)

I3.2. Regulation of TLR activation

Given type I IFN potency to activate innate and adaptive immune systems, IFN production signaling should be regulated in order to avoid aberrant and deleterious immune responses. To this end, pDCs express a wide range of surface receptors associated with specific signaling pathway capable of modulating and inhibiting cytokines production⁸⁴. CD303 (BDCA2), a type C lectin receptor, was the first receptor demonstrated to suppress the capacity of pDCs to produce type I IFNs in response to TLR ligands⁹³. It has been shown that another receptor specific for human pDCs, ILT7, is also responsible for the inhibition of type I IFN and pro-inflammatory cytokines production by pDCs activated via TLR7/9⁹⁴. CD303 and ILT7 both associate with FcεRIγ and induce a signaling pathway via an ITAM pattern (Immunoreceptor tyrosine-based activation motif)⁹⁴. Other receptors signaling via ITAM patterns were shown to have a similar inhibitory effect. In addition, IgG binding to the FcγRIIA receptor (CD32) decreases IFNα production by activated pDCs^{95,96}.

I.4. Flavivirus infection and Plasmacytoid dendritic cell response

When host-cells detect invasive viruses, they produce type I IFN, which in turn leads to the expression of a set of IFN-stimulated genes (ISG). This first-line response is supposed to suppress viral spread by generating an antiviral state to protect host cells, and by promoting the initiation of adaptive immunity. However, given the potency of these innate responses, flaviviruses have developed mechanisms to counter their detection and subvert the signaling innate response pathways of target cells. In particular, many flaviviruses are able to manipulate the interferon pathways in order to block its production and promote their dissemination within the host⁹⁷. But what about the crucial cells of immunity, such as pDCs?

I4.1. Indirect sensing of flavivirus infection

As wrote Silvin *et al.*, "infection of DCs with viruses can be considered a dilemma for the immune system: it allows activation of the innate and adaptive immune response, but it simultaneously facilitates manipulation by the viruses of the immune system itself"⁹⁸. As a result, pDCs evolved a resistance mechanism

against infection with certain viruses, including enveloped viruses such as flaviviruses. This feature is most likely due to their constitutive expression of RAB15 (common with CD141⁺ DCs) which likely impairs endocytosis processes commonly used for their entry⁹⁸. According to the authors, RAB15 would allow the disruption of conventional vesicular traffic by redirecting virus-containing vesicles towards retrograde transport and/or accumulation in the Golgi, thus impairing the fusion capacity of enveloped viruses within the pDCs⁹⁸. As a consequence, pDCs are generally not susceptible to cell-free virions during flavivirus infection⁹⁹. However, they are nonetheless able to detect the presence of flaviviruses through an indirect alternative mechanism involving physical contact with infected cells. Recent studies with Dengue and Yellow Fever viruses have shown that pDCs can be activated in a cell-cell contact-dependent manner, particularly through the establishment of filopods^{100–102}. These remarkable cytoplasmic extensions enable the transport of viral RNA from infected cells to pDCs. At present, the exact nature of the "carrier " and the mechanism transporting viral RNA to the pDCs is not well determined, however, it seems that pDCs uptake of immature viral particles triggers their activation when infected with DENV and YFV viruses^{100,101}.

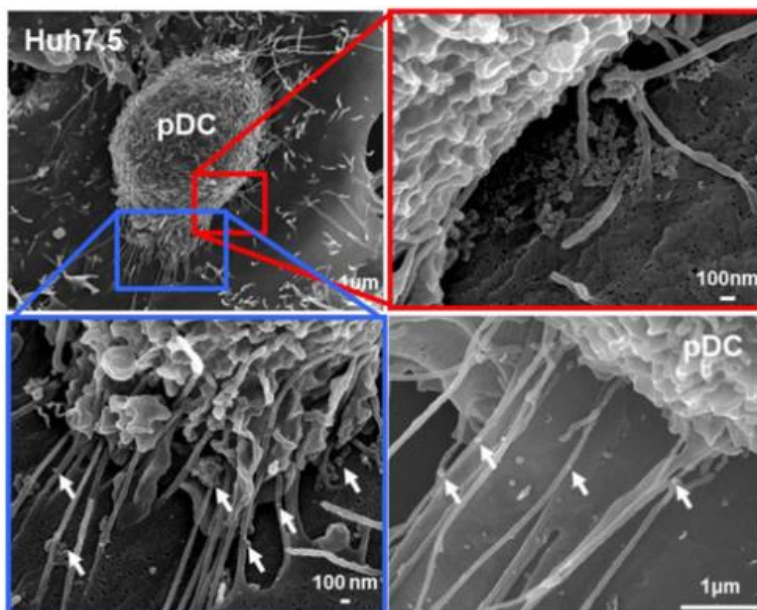


Figure 33: Contact between infected cells and plasmacytoid dendritic cells

Examples of plasmacytoid dendritic cell bound to YFV-infected Huh7.5 cells imaged by scanning electron microscopy. Filopodia-like structures, which might originate from both cell types, were observed between plasmacytoid dendritic cell and Huh7.5 cells. White arrows show objects resembling viruses. (Figure and caption from Sinigaglia et al., 2018)

I4.2. Plasmacytoid dendritic cell activation upon flavivirus infection

pDCs activation is mediated by flavivirus RNA recognition through TLR7¹⁰³. The signaling cascade is *a priori* similar to the one previously described. Interestingly, however, the recognition of cells infected with DENV and YFV induces the production of a large quantity of type I interferon, mainly alpha, but few to no other defensive molecules, such as pro-inflammatory cytokines^{100,101}. This peculiar response is also reported with CHIKV infection¹⁰³, but differs from the one observed with HIV or Influenza A virus which trigger pDC activation either by direct infection or indirect virus stimulation^{50,69,104}. On the other hand, despite the limited research on flavivirus-induced pDC maturation, DENV-2 sensing by humans pDCs has been shown to trigger membrane TRAIL relocalization⁵⁹. The presence of TRAIL-expressing killer pDC, reported following both *in vivo* and *in vitro* DENV-2 infection, suggests that these cytotoxic pDCs may play a role in the pathology associated with this flavivirus⁵⁹.

Finally, as far as we know, pDCs are resistant to direct flavivirus infection but are able to detect infection through an alternative mechanism. Through physical contact with infected cells, pDCs can uptake viral antigens, which triggers their activation and massive IFN α production. In this way, pDCs seem to have an indirect pathogen-sensing mechanisms which *a priori* circumvents cell-intrinsic immune evasion of flaviviruses. But what happens during Zika virus infection?

REFERENCE

1. Steinman, R. M. & Cohn, Z. A. Identification of a novel cell type in peripheral lymphoid organs of mice. I. Morphology, quantitation, tissue distribution. *J. Exp. Med.* 137, 1142–1162 (1973).
2. Steinman, R. M. & Cohn, Z. A. Identification of a novel cell type in peripheral lymphoid organs of mice. II. Functional properties in vitro. *J. Exp. Med.* 139, 380–397 (1974).
3. Hart, D. N. Dendritic cells: unique leukocyte populations which control the primary immune response. *Blood* 90, 3245–3287 (1997).
4. Steinman, R. M., Gutchinov, B., Witmer, M. D. & Nussenzweig, M. C. Dendritic cells are the principal stimulators of the primary mixed leukocyte reaction in mice. *J. Exp. Med.* 157, 613–627 (1983).
5. Steinman, R. M., Hawiger, D. & Nussenzweig, M. C. Tolerogenic dendritic cells. *Annu. Rev. Immunol.* 21, 685–711 (2003).
6. Mowat, A. M. Anatomical basis of tolerance and immunity to intestinal antigens. *Nat. Rev. Immunol.* 3, 331–341 (2003).
7. Iwasaki, A. & Medzhitov, R. Toll-like receptor control of the adaptive immune responses. *Nat. Immunol.* 5, 987–995 (2004).
8. Sancho, D. & Reis e Sousa, C. Sensing of cell death by myeloid C-type lectin receptors. *Curr. Opin. Immunol.* 25, 46–52 (2013).
9. Takeda, K. & Akira, S. TLR signaling pathways. *Semin. Immunol.* 16, 3–9 (2004).
10. Caux, C. et al. Dendritic cell biology and regulation of dendritic cell trafficking by chemokines. *Springer Semin. Immunopathol.* 22, 345–369 (2000).
11. Banchereau, J. & Steinman, R. M. Dendritic cells and the control of immunity. *Nature* 392, 245–252 (1998).
12. Mellman, I. & Steinman, R. M. Dendritic cells: specialized and regulated antigen processing machines. *Cell* 106, 255–258 (2001).
13. Guillemins, M. et al. Dendritic cells, monocytes and macrophages: a unified nomenclature based on ontogeny. *Nat. Rev. Immunol.* 14, 571–578 (2014).
14. Haniffa, M. et al. Human tissues contain CD141^{hi} cross-presenting dendritic cells with functional homology to mouse CD103⁺ nonlymphoid dendritic cells. *Immunity* 37, 60–73 (2012).
15. Vu Manh, T.-P., Bertho, N., Hosmalin, A., Schwartz-Cornil, I. & Dalod, M. Investigating Evolutionary Conservation of Dendritic Cell Subset Identity and Functions. *Front. Immunol.* 6, 260 (2015).
16. Lennert, K. & Remmele, W. [Karyometric research on lymph node cells in man. I. Germinalblasts, lymphoblasts & lymphocytes]. *Acta Haematol.* 19, 99–113 (1958).
17. Cella, M. et al. Plasmacytoid monocytes migrate to inflamed lymph nodes and produce large amounts of type I interferon. *Nat. Med.* 5, 919–923 (1999).
18. Grouard, G. et al. The enigmatic plasmacytoid T cells develop into dendritic cells with interleukin (IL)-3 and CD40-ligand. *J. Exp. Med.* 185, 1101–1111 (1997).
19. Siegal, F. P. et al. The nature of the principal type 1 interferon-producing cells in human blood. *Science* 284, 1835–1837 (1999).
20. Trinchieri, G., Santoli, D., Dee, R. R. & Knowles, B. B. Anti-viral activity induced by culturing lymphocytes with tumor-derived or virus-transformed cells. Identification of the anti-viral activity as interferon and characterization of the human effector lymphocyte subpopulation. *J. Exp. Med.* 147, 1299–1313 (1978).
21. Fitzgerald-Bocarsly, P. Human natural interferon-alpha producing cells. *Pharmacol. Ther.* 60, 39–62 (1993).
22. Vollenweider, R. & Lennert, K. Plasmacytoid T-cell clusters in non-specific lymphadenitis. *Virchows Arch. B* 44, 1 (1983).
23. Blom, B., Ho, S., Antonenko, S. & Liu, Y. J. Generation of interferon alpha-producing predendritic cell (Pre-DC)2 from human CD34(+) hematopoietic stem cells. *J. Exp. Med.* 192, 1785–1796 (2000).
24. Chen, W. et al. Thrombopoietin cooperates with FLT3-ligand in the generation of plasmacytoid dendritic cell precursors from human hematopoietic progenitors. *Blood* 103, 2547–2553 (2004).
25. Schiavoni, G. et al. ICSBP Is Essential for the Development of Mouse Type I Interferon-producing Cells and for the Generation and Activation of CD8 α ⁺ Dendritic Cells. *J. Exp. Med.* 196, 1415–1425 (2002).
26. Tsujimura, H., Tamura, T. & Ozato, K. Cutting edge: IFN consensus sequence binding protein/IFN regulatory factor 8 drives the development of type I IFN-producing plasmacytoid dendritic cells. *J. Immunol. Baltim. Md* 1950 170, 1131–1135 (2003).

27. Carotta, S. et al. The transcription factor PU.1 controls dendritic cell development and Flt3 cytokine receptor expression in a dose-dependent manner. *Immunity* 32, 628–641 (2010).
28. Esashi, E. et al. The signal transducer STAT5 inhibits plasmacytoid dendritic cell development by suppressing transcription factor IRF8. *Immunity* 28, 509–520 (2008).
29. Laouar, Y., Welte, T., Fu, X.-Y. & Flavell, R. A. STAT3 is required for Flt3L-dependent dendritic cell differentiation. *Immunity* 19, 903–912 (2003).
30. Satpathy, A. T., Wu, X., Albring, J. C. & Murphy, K. M. Re(de)fining the dendritic cell lineage. *Nat. Immunol.* 13, 1145–1154 (2012).
31. Corcoran, L. et al. The lymphoid past of mouse plasmacytoid cells and thymic dendritic cells. *J. Immunol. Baltim. Md* 1950 170, 4926–4932 (2003).
32. Spits, H., Couwenberg, F., Bakker, A. Q., Weijer, K. & Uittenbogaart, C. H. Id2 and Id3 inhibit development of CD34(+) stem cells into predendritic cell (pre-DC)2 but not into pre-DC1. Evidence for a lymphoid origin of pre-DC2. *J. Exp. Med.* 192, 1775–1784 (2000).
33. Karsunky, H. et al. Developmental origin of interferon-alpha-producing dendritic cells from hematopoietic precursors. *Exp. Hematol.* 33, 173–181 (2005).
34. Ishikawa, F. et al. Development of functional human blood and immune systems in NOD/SCID/IL2 receptor {gamma} chain(null) mice. *Blood* 106, 1565–1573 (2005).
35. Ishikawa, F. et al. The developmental program of human dendritic cells is operated independently of conventional myeloid and lymphoid pathways. *Blood* 110, 3591–3660 (2007).
36. Naik, S. H. et al. Development of plasmacytoid and conventional dendritic cell subtypes from single precursor cells derived in vitro and in vivo. *Nat. Immunol.* 8, 1217–1226 (2007).
37. Knaän-Shanzer, S. et al. Phenotypic and functional reversal within the early human hematopoietic compartment. *Stem Cells Dayt. Ohio* 26, 3210–3217 (2008).
38. Demedts, I. K., Brusselle, G. G., Vermaelen, K. Y. & Pauwels, R. A. Identification and characterization of human pulmonary dendritic cells. *Am. J. Respir. Cell Mol. Biol.* 32, 177–184 (2005).
39. Dalod, M. et al. Dendritic cell responses to early murine cytomegalovirus infection: subset functional specialization and differential regulation by interferon alpha/beta. *J. Exp. Med.* 197, 885–898 (2003).
40. Krug, A. et al. TLR9-dependent recognition of MCMV by IPC and DC generates coordinated cytokine responses that activate antiviral NK cell function. *Immunity* 21, 107–119 (2004).
41. Krug, A. et al. Herpes simplex virus type 1 activates murine natural interferon-producing cells through toll-like receptor 9. *Blood* 103, 1433–1437 (2004).
42. Lund, J., Sato, A., Akira, S., Medzhitov, R. & Iwasaki, A. Toll-like receptor 9-mediated recognition of Herpes simplex virus-2 by plasmacytoid dendritic cells. *J. Exp. Med.* 198, 513–520 (2003).
43. Kadowaki, N., Antonenko, S., Lau, J. Y. & Liu, Y. J. Natural interferon alpha/beta-producing cells link innate and adaptive immunity. *J. Exp. Med.* 192, 219–226 (2000).
44. Samuel, C. E. Antiviral actions of interferons. *Clin. Microbiol. Rev.* 14, 778–809, table of contents (2001).
45. Gerosa, F. et al. The reciprocal interaction of NK cells with plasmacytoid or myeloid dendritic cells profoundly affects innate resistance functions. *J. Immunol. Baltim. Md* 1950 174, 727–734 (2005).
46. Le Bon, A. et al. Type I interferons potently enhance humoral immunity and can promote isotype switching by stimulating dendritic cells in vivo. *Immunity* 14, 461–470 (2001).
47. Paquette, R. L. et al. Interferon-alpha and granulocyte-macrophage colony-stimulating factor differentiate peripheral blood monocytes into potent antigen-presenting cells. *J. Leukoc. Biol.* 64, 358–367 (1998).
48. Jego, G. et al. Plasmacytoid dendritic cells induce plasma cell differentiation through type I interferon and interleukin 6. *Immunity* 19, 225–234 (2003).
49. Poeck, H. et al. Plasmacytoid dendritic cells, antigen, and CpG-C license human B cells for plasma cell differentiation and immunoglobulin production in the absence of T-cell help. *Blood* 103, 3058–3064 (2004).
50. Cella, M., Facchetti, F., Lanzavecchia, A. & Colonna, M. Plasmacytoid dendritic cells activated by influenza virus and CD40L drive a potent TH1 polarization. *Nat. Immunol.* 1, 305–310 (2000).
51. Boonstra, A. et al. Macrophages and myeloid dendritic cells, but not plasmacytoid dendritic cells, produce IL-10 in response to MyD88- and TRIF-dependent TLR signals, and TLR-independent signals. *J. Immunol. Baltim. Md* 1950 177, 7551–7558 (2006).

52. Ito, T. et al. Plasmacytoid dendritic cells regulate Th cell responses through OX40 ligand and type I IFNs. *J. Immunol. Baltim. Md* 1950 172, 4253–4259 (2004).
53. Rissoan, M. C. et al. Reciprocal control of T helper cell and dendritic cell differentiation. *Science* 283, 1183–1186 (1999).
54. Gilliet, M. & Liu, Y.-J. Generation of Human CD8 T Regulatory Cells by CD40 Ligand-activated Plasmacytoid Dendritic Cells. *J. Exp. Med.* 195, 695–704 (2002).
55. Moseman, E. A. et al. Human Plasmacytoid Dendritic Cells Activated by CpG Oligodeoxynucleotides Induce the Generation of CD4+CD25+ Regulatory T Cells. *J. Immunol.* 173, 4433–4442 (2004).
56. Ito, T. et al. Plasmacytoid dendritic cells prime IL-10-producing T regulatory cells by inducible costimulator ligand. *J. Exp. Med.* 204, 105–115 (2007).
57. de Heer, H. J. et al. Essential role of lung plasmacytoid dendritic cells in preventing asthmatic reactions to harmless inhaled antigen. *J. Exp. Med.* 200, 89–98 (2004).
58. Smit, J. J., Rudd, B. D. & Lukacs, N. W. Plasmacytoid dendritic cells inhibit pulmonary immunopathology and promote clearance of respiratory syncytial virus. *J. Exp. Med.* 203, 1153–1159 (2006).
59. Gandini, M. et al. Dengue Virus Activates Membrane TRAIL Relocalization and IFN- α Production by Human Plasmacytoid Dendritic Cells In Vitro and In Vivo. *PLoS Negl. Trop. Dis.* 7, (2013).
60. Hardy, A. W., Graham, D. R., Shearer, G. M. & Herbeuval, J.-P. HIV turns plasmacytoid dendritic cells (pDC) into TRAIL-expressing killer pDC and down-regulates HIV coreceptors by Toll-like receptor 7-induced IFN- α . *Proc. Natl. Acad. Sci.* 104, 17453–17458 (2007).
61. Chaperot, L. et al. Virus or TLR Agonists Induce TRAIL-Mediated Cytotoxic Activity of Plasmacytoid Dendritic Cells. *J. Immunol.* 176, 248–255 (2006).
62. Matsui, T. et al. CD2 distinguishes two subsets of human plasmacytoid dendritic cells with distinct phenotype and functions. *J. Immunol. Baltim. Md* 1950 182, 6815–6823 (2009).
63. Janeway, C. A. Approaching the asymptote? Evolution and revolution in immunology. *Cold Spring Harb. Symp. Quant. Biol.* 54 Pt 1, 1–13 (1989).
64. Matzinger, P. Tolerance, danger, and the extended family. *Annu. Rev. Immunol.* 12, 991–1045 (1994).
65. Lotze, M. T. & Tracey, K. J. High-mobility group box 1 protein (HMGB1): nuclear weapon in the immune arsenal. *Nat. Rev. Immunol.* 5, 331–342 (2005).
66. Gallucci, S., Lolkema, M. & Matzinger, P. Natural adjuvants: endogenous activators of dendritic cells. *Nat. Med.* 5, 1249–1255 (1999).
67. Sauter, B. et al. Consequences of cell death: exposure to necrotic tumor cells, but not primary tissue cells or apoptotic cells, induces the maturation of immunostimulatory dendritic cells. *J. Exp. Med.* 191, 423–434 (2000).
68. Tian, J. et al. Toll-like receptor 9-dependent activation by DNA-containing immune complexes is mediated by HMGB1 and RAGE. *Nat. Immunol.* 8, 487–496 (2007).
69. Saïdi, H., Melki, M.-T. & Gougeon, M.-L. HMGB1-dependent triggering of HIV-1 replication and persistence in dendritic cells as a consequence of NK-DC cross-talk. *PLoS One* 3, e3601 (2008).
70. Kim, T. et al. Aspartate-glutamate-alanine-histidine box motif (DEAH)/RNA helicase A helicases sense microbial DNA in human plasmacytoid dendritic cells. *Proc. Natl. Acad. Sci. U. S. A.* 107, 15181–15186 (2010).
71. Szabo, A. et al. TLR ligands upregulate RIG-I expression in human plasmacytoid dendritic cells in a type I IFN-independent manner. *Immunol. Cell Biol.* 92, 671–678 (2014).
72. Jarrossay, D., Napolitani, G., Colonna, M., Sallusto, F. & Lanzavecchia, A. Specialization and complementarity in microbial molecule recognition by human myeloid and plasmacytoid dendritic cells. *Eur. J. Immunol.* 31, 3388–3393 (2001).
73. Krug, A. et al. Toll-like receptor expression reveals CpG DNA as a unique microbial stimulus for plasmacytoid dendritic cells which synergizes with CD40 ligand to induce high amounts of IL-12. *Eur. J. Immunol.* 31, 3026–3037 (2001).
74. Diebold, S. S., Kaisho, T., Hemmi, H., Akira, S. & Reis e Sousa, C. Innate antiviral responses by means of TLR7-mediated recognition of single-stranded RNA. *Science* 303, 1529–1531 (2004).
75. Lund, J. M. et al. Recognition of single-stranded RNA viruses by Toll-like receptor 7. *Proc. Natl. Acad. Sci. U. S. A.* 101, 5598–5603 (2004).
76. Hemmi, H. et al. Small anti-viral compounds activate immune cells via the TLR7 MyD88-dependent signaling pathway. *Nat. Immunol.* 3, 196–200 (2002).
77. Hemmi, H. et al. A Toll-like receptor recognizes

- bacterial DNA. *Nature* 408, 740–745 (2000).
78. Akira, S., Takeda, K. & Kaisho, T. Toll-like receptors: critical proteins linking innate and acquired immunity. *Nat. Immunol.* 2, 675–680 (2001).
79. Medzhitov, R. Toll-like receptors and innate immunity. *Nat. Rev. Immunol.* 1, 135–145 (2001).
80. Akira, S., Uematsu, S. & Takeuchi, O. Pathogen recognition and innate immunity. *Cell* 124, 783–801 (2006).
81. Taniguchi, T. & Takaoka, A. The interferon-alpha/beta system in antiviral responses: a multimodal machinery of gene regulation by the IRF family of transcription factors. *Curr. Opin. Immunol.* 14, 111–116 (2002).
82. Ito, T., Kanzler, H., Duramad, O., Cao, W. & Liu, Y.-J. Specialization, kinetics, and repertoire of type 1 interferon responses by human plasmacytoid dendritic cells. *Blood* 107, 2423–2431 (2006).
83. Barchet, W. et al. Virus-induced interferon alpha production by a dendritic cell subset in the absence of feedback signaling in vivo. *J. Exp. Med.* 195, 507–516 (2002).
84. Bao, M. & Liu, Y.-J. Regulation of TLR7/9 signaling in plasmacytoid dendritic cells. *Protein Cell* 4, 40–52 (2013).
85. Honda, K. et al. Spatiotemporal regulation of MyD88-IRF-7 signalling for robust type-I interferon induction. *Nature* 434, 1035–1040 (2005).
86. Kawai, T. et al. Interferon-alpha induction through Toll-like receptors involves a direct interaction of IRF7 with MyD88 and TRAF6. *Nat. Immunol.* 5, 1061–1068 (2004).
87. Karrich, J. J., Jachimowski, L. C. M., Uittenbogaart, C. H. & Blom, B. The plasmacytoid dendritic cell as the Swiss army knife of the immune system: molecular regulation of its multifaceted functions. *J. Immunol. Baltim. Md* 1950 193, 5772–5778 (2014).
88. Kerkmann, M. et al. Activation with CpG-A and CpG-B oligonucleotides reveals two distinct regulatory pathways of type I IFN synthesis in human plasmacytoid dendritic cells. *J. Immunol. Baltim. Md* 1950 170, 4465–4474 (2003).
89. Guiducci, C. et al. Properties regulating the nature of the plasmacytoid dendritic cell response to Toll-like receptor 9 activation. *J. Exp. Med.* 203, 1999–2008 (2006).
90. Berghöfer, B., Haley, G., Frommer, T., Bein, G. & Hackstein, H. Natural and synthetic TLR7 ligands inhibit CpG-A- and CpG-C-oligodeoxynucleotide-induced IFN-alpha production. *J. Immunol. Baltim. Md* 1950 178, 4072–4079 (2007).
91. Birmachu, W. et al. Transcriptional networks in plasmacytoid dendritic cells stimulated with synthetic TLR 7 agonists. *BMC Immunol.* 8, 26 (2007).
92. Wang, J. P. et al. Flavivirus activation of plasmacytoid dendritic cells delineates key elements of TLR7 signaling beyond endosomal recognition. *J. Immunol. Baltim. Md* 1950 177, 7114–7121 (2006).
93. Dzionek, A. et al. BDCA-2, a novel plasmacytoid dendritic cell-specific type II C-type lectin, mediates antigen capture and is a potent inhibitor of interferon alpha/beta induction. *J. Exp. Med.* 194, 1823–1834 (2001).
94. Cao, W. et al. Plasmacytoid dendritic cell-specific receptor ILT7-Fc epsilonRI gamma inhibits Toll-like receptor-induced interferon production. *J. Exp. Med.* 203, 1399–1405 (2006).
95. Green, D. S., Lum, T. & Green, J. A. IgG-derived Fc down-regulates virus-induced plasmacytoid dendritic cell (pDC) IFNalpha production. *Cytokine* 26, 209–216 (2004).
96. Bâve, U. et al. Fc gamma RIIa is expressed on natural IFN-alpha-producing cells (plasmacytoid dendritic cells) and is required for the IFN-alpha production induced by apoptotic cells combined with lupus IgG. *J. Immunol. Baltim. Md* 1950 171, 3296–3302 (2003).
97. Chen, S., Wu, Z., Wang, M. & Cheng, A. Innate Immune Evasion Mediated by Flaviviridae Non-Structural Proteins. *Viruses* 9, 291 (2017).
98. Silvín, A. et al. Constitutive resistance to viral infection in human CD141+ dendritic cells. *Sci. Immunol.* 2, eaai8071 (2017).
99. Bruni, D. et al. Viral entry route determines how human plasmacytoid dendritic cells produce type I interferons. *Sci. Signal.* 8, ra25 (2015).
100. Décembre, E. et al. Sensing of immature particles produced by dengue virus infected cells induces an antiviral response by plasmacytoid dendritic cells. *PLoS Pathog.* 10, e1004434 (2014).
101. Sinigaglia, L. et al. Immature particles and capsid-free viral RNA produced by Yellow fever virus-infected cells stimulate plasmacytoid dendritic cells to secrete interferons. *Sci. Rep.* 8, 10889 (2018).
102. Webster, B., Assil, S. & Dreux, M. Cell-Cell Sensing of Viral Infection by Plasmacytoid Dendritic Cells. *J. Virol.* 90, 10050–10053 (2016).

103. Webster, B. et al. Plasmacytoid dendritic cells control dengue and Chikungunya virus infections via IRF7-regulated interferon responses. *eLife* 7, (2018).
104. Saïdi, H. et al. HMGB1 Is Involved in IFN- α Production and TRAIL Expression by HIV-1-Exposed Plasmacytoid Dendritic Cells: Impact of the Crosstalk with NK Cells. *PLoS Pathog.* 12, e1005407 (2016)

II. ARTICLE N°5

Human plasmacytoid dendritic cells exposed to Zika virions or Zika virus-infected cells fail to produce IFN α and inflammatory cytokines

Sandra Bos^{1,2}, Béatrice Poirier-Beaudouin¹, Maria Manich³, Philippe Desprès², Gilles Gadea² and Marie-Lise Gougeon¹

1. Institut Pasteur, Innate Immunity and Viruses Unit, Infection and Epidemiology Department, 25 rue du Dr. Roux, F-75015 Paris, France

2. Université de la Réunion, INSERM U1187, CNRS UMR 9192, IRD UMR 249, Unité Mixte Processus Infectieux en Milieu Insulaire Tropical, Plateforme Technologique CYROI, 94791 Sainte Clotilde, La Réunion, France

3. Institut Pasteur, BioImage Analysis Unit, Department of Cell Biology and Infection, 25 rue du Dr. Roux, F-75015 Paris, France

(First draft)

ABSTRACT

After a silent circulation period of decades, epidemics of Zika spread in South Pacific islands and then South America where infection has been associated with severe neurological complications in adult and newborn respectively. While a few studies examined Zika virus (ZIKV) interaction with conventional dendritic cells, very limited data are available on ZIKV impact on plasmacytoid dendritic cells (pDCs), a key sensor and initiator of the antiviral immune response. Here, we investigated the susceptibility of human pDCs to different strains of ZIKV and their impact on pDCs functions. We found that human pDCs were refractory to infection with cell-free ZIKV virions regardless viral strains tested. However, infection of pDCs can take place upon co-culture with epithelial or neuronal cells infected by ZIKV. We noted that pDCs exposure to ZIKV-infected cells resulted in a limited maturation phenotype with significant down regulation of CD303 expression. Also, we demonstrated that pDCs infection with ZIKV unexpectedly

resulted in a severe impairment of inflammatory cytokine production, including IFN α . Overall, our data indicate that ZIKV could anergize pDCs suggesting a potential novel immune evasion strategy, atypical for a flavivirus.

INTRODUCTION

Zika virus (ZIKV) belongs to the *flavivirus* genus of the Flaviviridae family which includes a number of medically-important mosquito-borne viruses such as Dengue virus (DENV), Japanese Encephalitis virus (JEV), Yellow fever virus (YFV) and West Nile virus (WNV) [1]. ZIKV strains belonging to Asian lineage have emerged as a global public health threat with a series of epidemics which first hit the Micronesian island of Yap in 2007 [5]. In 2015 the largest Zika pandemic to date began in Brazil [6] and has since rapidly spread throughout the Americas [7]. Manifestations of neurological disorders such as the Guillain-Barre Syndrome (GBS) [8], associated with a dramatic increase in the number of microcephaly and other birth defects in newborns [9] was detected during these recent outbreaks, and the causal relationship with ZIKV infection was established [10, 11]. Recently we compared molecular clones derived from historical ZIKV strain MR766 of African lineage and epidemic contemporary strain BeH819015 of Asian lineage for their abilities to initiate viral infection and confer neurocytopathic effects in the human brain's SNB-19 glial cells, and further determine which part of the ZIKV structural proteins is responsible for the observed differences [28, 29]. MR766 was established after a series of *in vitro* and *in vivo* passages and has been found neuropathogenic in a mouse model of viral encephalitis [3, 4] whereas BeH819015 was isolated from a human serum specimen in Brazil in 2015. We demonstrated that MR766 and BeH819015 (BR15) differ for viral attachment to host neuronal cells, viral permissiveness and replication, as well as in the induction of cytopathic effects [29].

Acute ZIKV infection induces systemic inflammatory responses associated with pro-inflammatory cytokines (IL-1 β , IL-6, MIP1 α), chemokines (IP-10 and RANTES) and cytokines that promote polyfunctional T cell responses (IL-2, IL-4, IL-9 and IL-17) [12, 13]. However, in contrast to DENV acute infection, no significant increase of IFN γ and TNF α levels were observed in ZIKV infection,

pointing toward a Th2 bias [12]. ZIKV infection induces broadly neutralizing and protective humoral immune responses against both African and Asian lineage ZIKV strains [14]. Moreover, individuals with high neutralizing antibody response against ZIKV have expanded clones of B cells that express the same heavy and light immunoglobulin genes and that are cross-reactive against DENV of serotype-1 [15]. CD8⁺ T cell immunity appears to be important during the acute phase, and in mice ZIKV-specific CD8⁺ T cells expand, are polyfunctional and exhibit in vivo cytotoxicity [16]. A recent transcriptional profiling of human CD8⁺ T cells responding to ZIKV infection in donors in the convalescent phase of infection showed functional IFN γ signature with upregulation of TNF α , TNF receptors, as well as a cytotoxic signature characterized by strong upregulation of GZMB and CRTAM [17]. By contrast, the early events that contribute to the establishment of ZIKV infection in humans are unclear. It is believed that ZIKV infects keratinocytes, skin Langerhans cells and dendritic cells as early targets of viral replication. Bowen *et al.* [18] recently reported that human monocyte-derived dendritic cells support the replication of ZIKV of African and Asian lineages but the infection led to a limited secretion of inflammatory cytokines. Moreover, inhibition of type I interferon (IFN) protein translation was observed, and all strains antagonized type I IFN-mediated phosphorylation of STAT1 and STAT2. ZIKV evasion of interferon-mediated antiviral response was also reported in epithelial cell lines, involving the nonstructural proteins NS1 and NS4B, which inhibit IFN- β signaling at TANK-binding kinase 1 level, and NS2B-NS3 which impair JAK-STAT signaling pathway [19]. However, another study reported that an epidemic ZIKV strain induced strong type I IFN and inflammatory cytokine and chemokine production in the monocytic cell line THP-1 and PBMC [20]. From these studies, it seems that the type of inflammatory response induced by ZIKV is cell-specific.

Plasmacytoid dendritic cells (pDCs), the most potent producer of type I IFN, represent a rare cell type in the peripheral blood, their response is rapid and triggered by the endosomal sensors Toll-like receptor (TLR) 7 and TLR9, which recognize viral nucleic acids (RNA and DNA, respectively) [21, 22, 23]. The interactions of pDCs with flaviviruses have been mostly studied in response to DENV and YFV. pDCs were found to poorly support DENV replication but they

were able to trigger a quick and vigorous IFN-I and TNF α cytokine response, which was dependent on TLR7 signaling pathway [24]. However, the detection of DENV-infected cells is a much more potent activator of pDC, particularly through the uptake of immature particles that trigger the IFN-I response of pDC, even more potently than mature virus capable of fusion [25]. Similarly, cells infected with YFV or Chikungunya (CHIKV) virus, an alphavirus, also stimulated pDCs to produce IFNs in a TLR7- and cell contact-dependent manner [26, 27], in the absence of other inflammatory cytokines [27]. To date, human pDCs have not yet been studied in the context of ZIKV infection. In the present study, we investigated the permissiveness of human pDCs to ZIKV strains MR766 and BeH819015.

RESULTS

Limited pDC maturation in response to ZIKV infection

pDCs were purified from freshly isolated PBMC from healthy donors and their phenotype was characterized. Ex-vivo sorted pDCs were all CD123⁺ CD303⁺ HLA-DR⁺, and they scarcely expressed CD83, CD86 and CCR7, thus exhibiting the phenotype of immature pDCs, as we showed in a previous study [30]. TLR9-dependent stimulation of pDCs with CpG ODN 2006 for 24 hours induced their maturation, as evidenced by the increased expression of CCR7, HLA-DR and CD83 markers, (Figure 1A). The decreased expression of CD303 following TLR9 triggering is also a hallmark of pDC maturation [31], as shown in Figure 1A.

FSC/SSC parameters and the expression of maturation markers was then analyzed following 2h exposure of pDCs to ZIKV BR15 or MR766 at a MOI of 1 and 5, followed by overnight incubation in complete medium, as described in Material and Methods. Controls were freshly isolated immature pDCs, pDCs incubated 24h in complete medium (Mock), or with the supernatant of uninfected Vero cells whose volume was that of the viral inoculum of BR15 at MOI of 5. Figure 1B shows that, while freshly isolated immature pDCs appeared in majority as a SSC^{low} population, as expected for living cells, pDCs incubated overnight in complete medium only (Mock) were SSC^{high}, indicating that they were dying because of the lack of survival signals such as IL-3 [32].

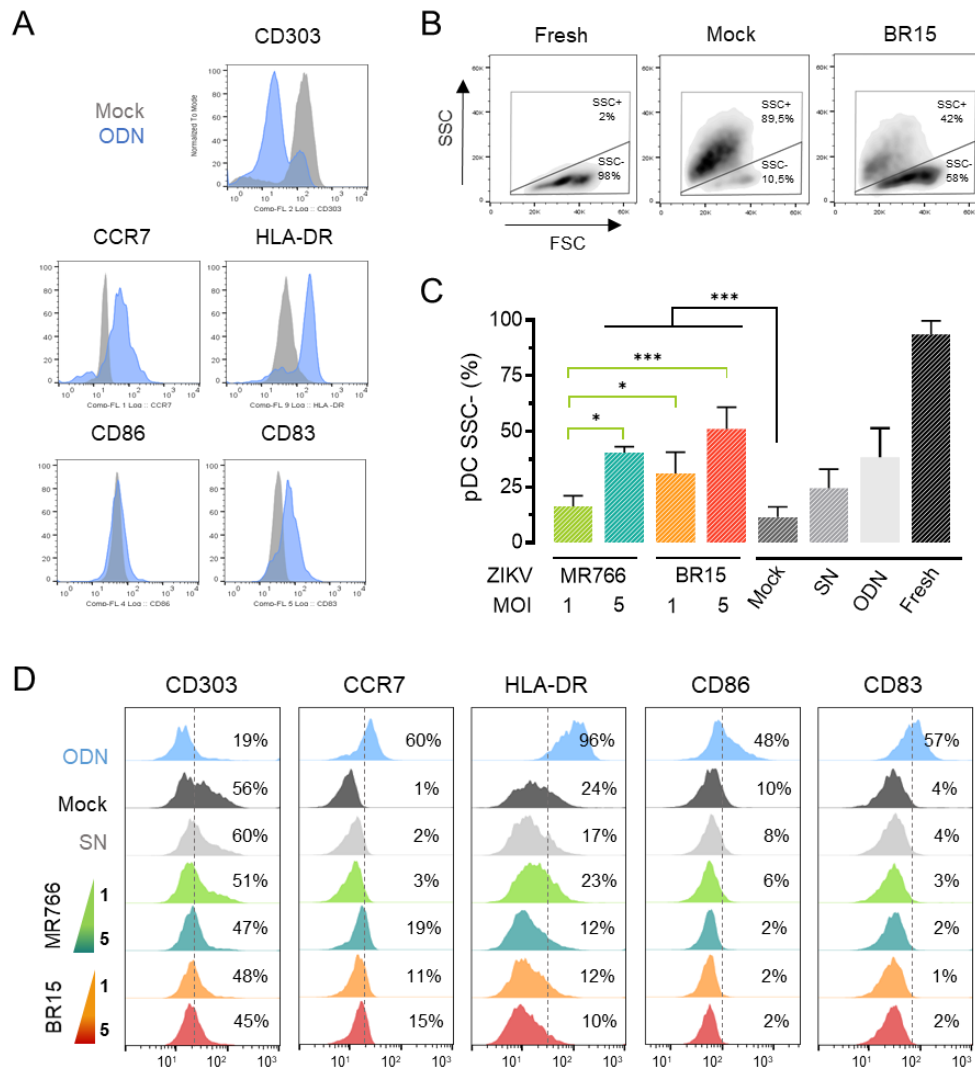


Figure 1.

(A): Phenotypic characterization of mature pDCs. Sorted pDCs were either incubated with medium (Mock) or stimulated with ODN 2216 for 24h and the expression of the indicated markers was analyzed. (B): Repartition of pDCs within two sub-populations referred to as SSC+ and SSC- according to flow cytometry acquisition observed in forward scatter (FSC) and side scatter (SSC). Shown are representative density plots of pDCs freshly isolated, incubated with medium, or exposed to ZIKV BR15 at MOI of 5. (C): Proportion of freshly isolated pDCs or pDCs cultured for 24h clustered within the SSC- populations. Cultured cells were either incubated with medium (mock), stimulated with ODN 2216, or exposed to different MOI of indicated ZIKV strain or to virus-free supernatant (SN). The error bars represent the standard deviations of at least three experiments conducted with primary cells from distinct donors, except for ZIKV MOI of 5 (2 donors in duplicate). (D): Phenotypic characterization of pDCs cultured for 24h. pDCs cultured cells were either incubated with medium (mock), stimulated with ODN 2216, or exposed to different MOI of indicated ZIKV strain or to virus-free supernatant (SN), and the expression of the indicated maturation markers was analyzed. The dotted line represents the positive expression limit of the specified marker and the percentage of cells expressing it is indicated. Results shown in panel (A), (B), and (D) are representative of at least three experiments conducted with primary cells from distinct donors, except for ZIKV MOI of 5 (2 donors in duplicate).

Interestingly, exposure of pDCs to ZIKV BR15 at MOI of 5 was associated with the features of living cells, as shown by the FSC/SSC dot plot. The mean data obtained from three independent experiments are shown in Figure 1C. A dose-dependent influence of ZIKV MR766 or BR15 on the frequency of SSC^{low} pDCs is observed, with a significant positive effect of both ZIKV at MOI of 5 and BR15 at MOI of 1 as compared to Mock infection. This survival effect was associated with a limited degree of pDC maturation as shown in Figure 1D. Among the maturation markers tested, only one of them was modified upon exposure of pDCs to ZIKV: CCR7 expression was induced by MR766 and BR15 at MOI of 5 in 19% and 15% of pDCs respectively. CD303 expression was not modified after exposure to both viruses (Figure 1D). No expression of HLA-DR, CD86 or CD83 was induced. In contrast, overnight CpG stimulation of pDC induced their full maturation as illustrated by the high expression of CCR7 (60%), HLA-DR (96%), CD86 (48%), and CD83 (57%).

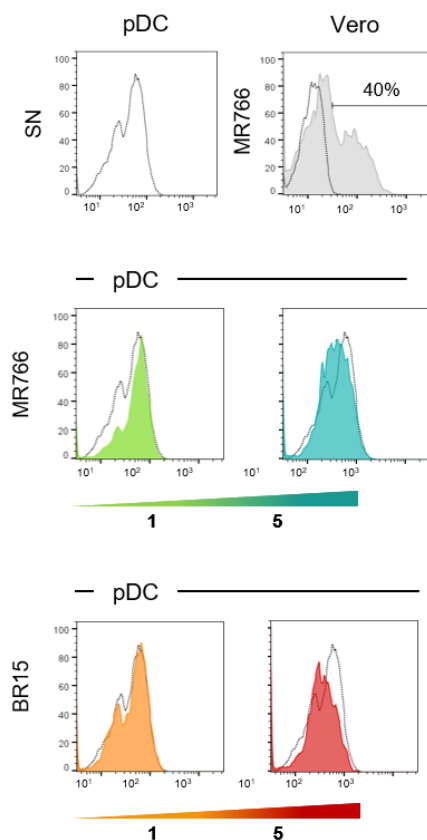


Figure 2.

Cells expressing ZIKV envelope protein (4G2) after 24h of culture. Histograms on the top represents pDCs exposed to virus-free supernatant (right) and Vero cells mock-infected (dotted line) or infected (grey) with ZIKV MR766 at MOI of 1. The percentage of Vero cells expressing 4G2 antibody is indicated. The histograms below shown pDCs exposed to ZIKV MR766 or BR15 at MOI 1 and 5. The dotted line represents pDCs exposed to SN, as negative control. These results are representative of at least two experiments in duplicate conducted with primary cells of distinct donors or Vero cells.

Susceptibility of pDCs to ZIKV infection

We first examined whether pDCs freshly isolated from healthy donors were susceptible to infection by cell-free ZIKV virions. Infection of pDCs was conducted for 24h at MOI of 1. Figure 2 shows that, while 4G2 mAb detected 40% of infected Vero cells, no staining was detected in pDCs, whether infected by MR766, or BR15. Since pDCs appeared to be poorly susceptible to free ZIKV, we then tested their susceptibility to infection when exposed to infected cells. Due to their lack of IFN production, Vero cells were first used in co-culture experiments. Figure 3 summarizes the data indicating that Vero cells were susceptible to infection by either MR766 or BR15. Vero cells were infected at MOI of 1 and the frequency of infected cells was assessed by flow cytometry at 36h p.i. using the antibody J2 specific for dsRNA. As a control of infection, Vero cells were infected under the same conditions with YF-17D. Figure 3A shows that 40-50% of Vero cells were dsRNA+ cells after infection with BR15 and YF-17D strain, while a significant higher infection rate (over 80%) was detected upon infection with MR766. To assess the amount of infectious ZIKV released from Vero cells, viral titers were determined in culture supernatants collected at 36h and 48h p.i. (Figure 3B). Viral progeny production was comparable

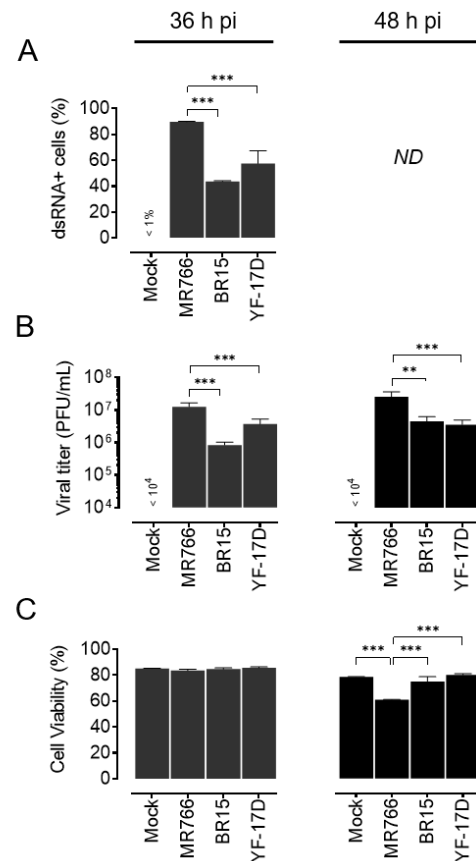


Figure 3.

Vero cells were left uninfected (mock) or infected with the indicated flavivirus strain at MOI of 1 for 36 and 48 hours. (A): Percentage of Vero cells hosting viral replication according to flow cytometry analysis using anti-dsRNA antibody (J2) at 36h post infection. Error bars represent the standard deviation of two experiments performed in triplicate. (B): Quantification of viral progeny production. The infectious virus release into the supernatant of infected cells were titrated on Vero cells. (C): Analysis of Vero cell viability upon infection. Virus-induced cell death was assessed by LDH release measurement. Cell viability is expressed as percentage relative to maximum LDH release. Error bars in panel (B) and (C) represent the standard deviation of three experiments.

after infection with BR15 and YF-17D at both time points, but was significantly higher with MR766. Such observation was consistent with the higher frequency of dsRNA⁺ cells detected 36 h p.i (Figure 3A). ZIKV was shown to induce massive vacuolization followed by "implosive" cell death in human epithelial

cells, primary skin fibroblasts and astrocytes [33]. Therefore, we investigated the viability of Vero cells during these infection experiments (Figure 3C). At 36h p.i. cytopathic effect of the three viruses was low (less than 20%) and infected-cell viability was similar to that of mock-infected. In contrast, a significant higher mortality, although not massive, was induced by MR766 at 48h p.i. as compared with mock control. Neither BR15 nor YF-17D virus had this effect. The cytopathic effect of MR766 was likely the consequence of the important viral replication shown in Figure 2B. Together, these data show that under the conditions used, infected Vero cells are susceptible to infection by both MR766 and BR15 strains, the infection is productive and the release of virions occurs with a minimal cell death.

To determine whether pDCs were susceptible to ZIKV infection when brought in close contact with infected cells, 24 h coculture of pDCs with Vero cells infected at MOI of 1 were performed and the frequency of dsRNA⁺ pDCs was determined by flow cytometry (Figure 4A). 5 to 10 % of pDCs were dsRNA⁺ when exposed to either MR766 or BR15, suggesting their permissiveness to ZIKV infection. The frequency of pDCs infected with YF-17D was a little higher. To visualize pDCs in close proximity to infected Vero cells, deep-red-labeled pDCs were cocultured 24 h with Vero cells infected with BR15 at a MOI of 1, and analyzed by confocal microscopy. Cells were stained with a polyclonal ZIKV-specific antibody, and with NucBlue to visualize nuclei (blue). Figure 4B shows a pDC in close proximity with an infected Vero cell that is positive for ZIKV staining. Intracytoplasmic staining of pDC with ZIKV specific antibody is also evidenced in the 3D reconstitution presented in Figure 4C.

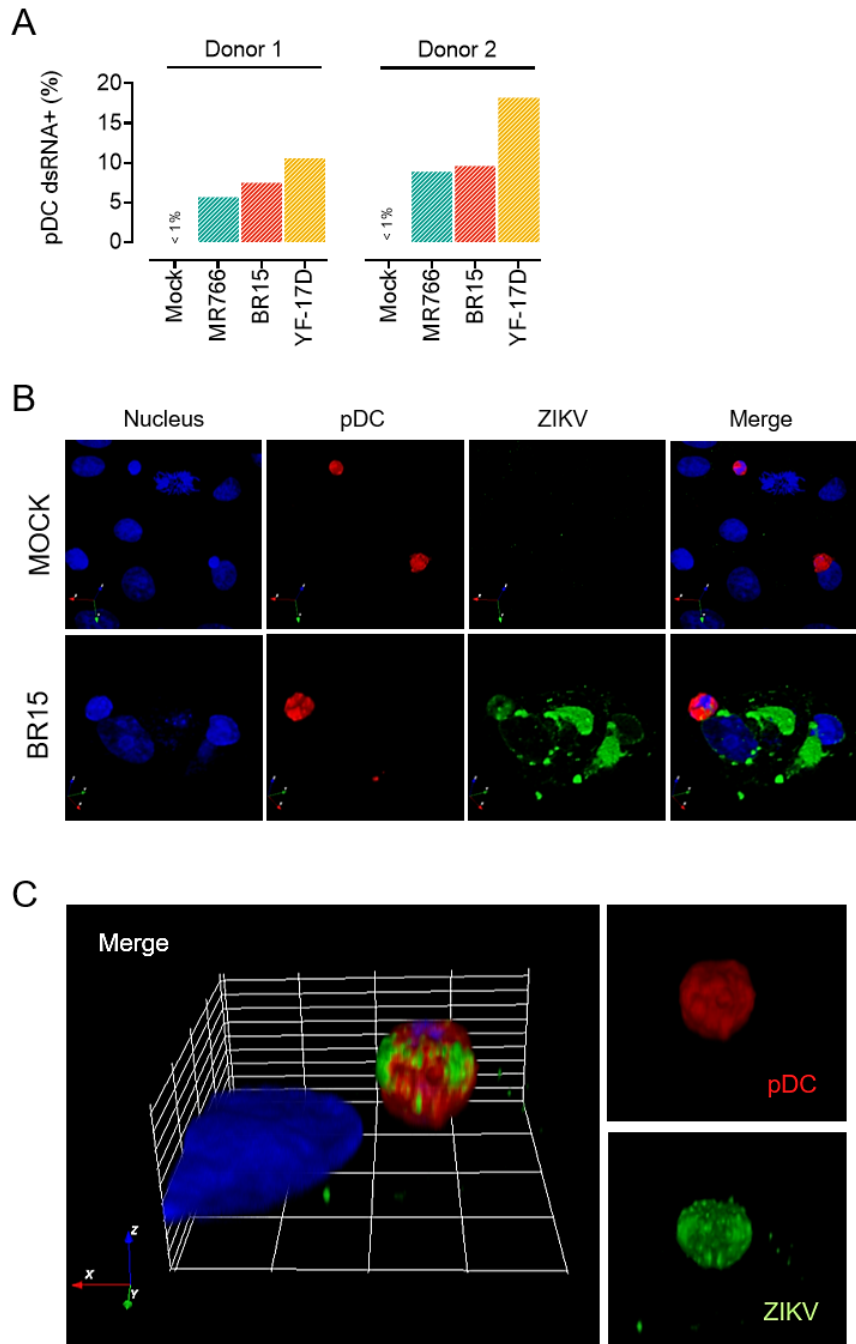


Figure 4.

Vero cells were left uninfected (mock) or infected with the indicated flavivirus strain at MOI of 1 for 12h and then co-cultured with deep-red labelled pDCs for a further 24 hours. (A): Percentage of infected pDCs co-cultured with Vero cells for 24 hours. Infection rate among labelled pDCs was assessed by flow cytometry using the anti-dsRNA antibody (J2). Shown are the results obtained from two distinct donors. (B) and (C): 3D reconstitutions of confocal microscopy acquisition of uninfected or ZIKV-BR15 infected Vero cells and labelled pDCs after 24h of co-culture. ZIKV (green), labelled pDCs (red), nuclei (blue). ZIKV was detected using a polyclonal antibody. Images are representative of three independent experiments conducted with primary cells from distinct donors.

Suppression by ZIKV of IFN α response in pDCs

pDCs are specialized in the production of IFN α triggered by viral sensing or viral infection, and this innate response is of central importance to protect the host. We first examined whether pDCs produce IFN α in the presence of cell-free YF-17D or ZIKV virions. While CpG ODN 2216 triggered a strong IFN α response, as expected, YFV-infected pDCs failed to produce IFN α (Figure 5A), in agreement with data reported by Sinigaglia *et al.* [26] on YF-17D-infected PBMCs. If co-cultured for 24 hours with YFV-infected Vero cells, pDCs produced abundant IFN α . More than 1000 pg/ml were secreted by pDCs exposed to YF-17D 36h p.i. (Figure 5B). In contrast, pDCs failed to produce IFN α (<10 pg/ml) when exposed to MR766- or BR15- infected Vero cells (Figure 5B). A very weak IFN α response (around 100 pg/ml) was detected 48h p.i. in pDCs exposed to ZIKV-infected Vero cells, while YF-17D-infected cells triggered a strong response with the secretion of more than 3000 pg/ml (Figure 5B). Suppression of IFN α by both ZIKV was highly reproducible in the four donors tested, as shown in Figure 5C.

No inflammatory response induced by ZIKV in pDCs

pDCs are critical in bridging innate and adaptive immune responses in the context of systemic viral infections, in part by the production of IFN α , but also through their role in establishing an inflammatory microenvironment, characterized by broad array of cytokines/chemokines. Specifically, TLR-7 or -9 agonists engagement on pDCs trigger a pro-inflammatory response, which was characterized by four distinct cytokine loops in respect to the pDCs ability to produce type I interferons [34]. In the first, activated pDCs secrete factors such as TNF α and MIP1 α independently of IFN α / β receptor (IFNAR), in contrast to IL-8 that is the only one in the second class, whose production is inhibited by IFNAR signaling. In the third class of molecules, such as IP-10 and MIP1 β , their expression is enhanced by autocrine IFN α , while cytokines in the fourth loop (MCP1, IL1Ra, IL1 β , and IL-12p70) are not produced by pDCs in response to TLR engagement but instead induce their production by other cell. Taking advantage of multianalyte profiling (MAP) technology, we have performed an in-depth analysis of the cytokines and chemokines secreted by pDCs activated by CpG ODN 2216, and compared their pattern that induced by cell-free and cell-associated YF-

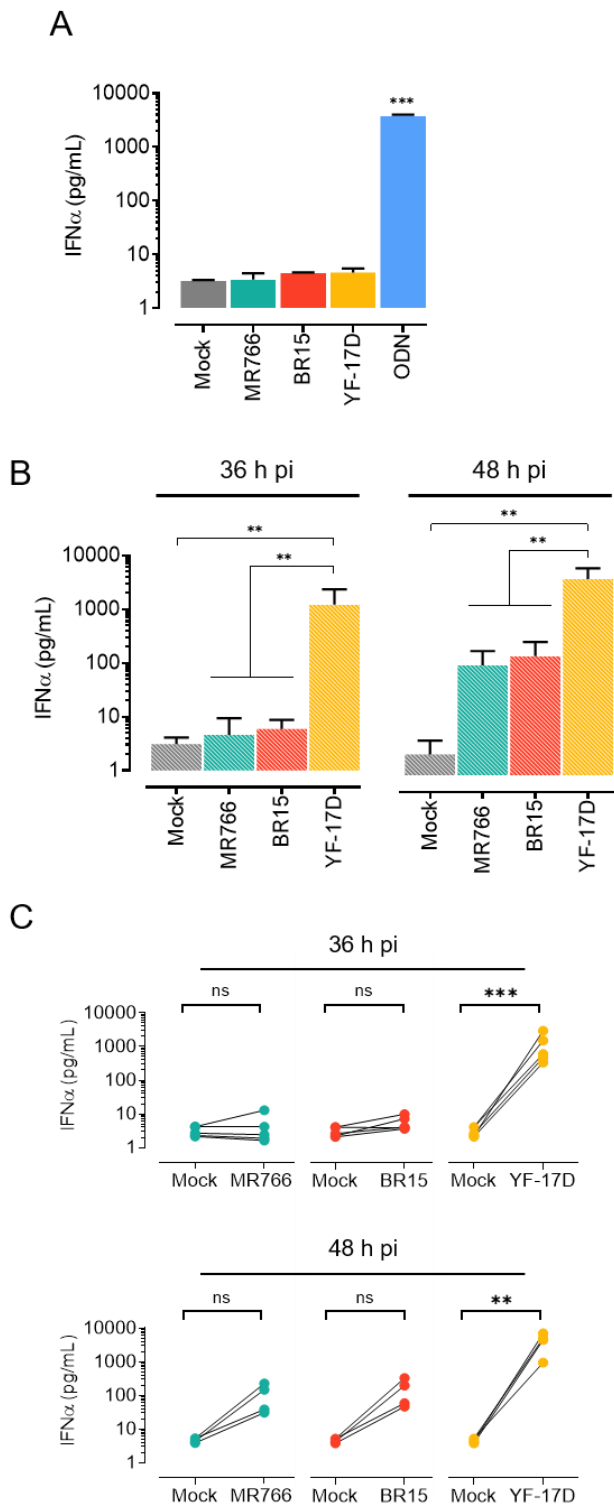


Figure 5.

(A): Quantification of IFN α in the supernatant of pDCs. Freshly isolated pDCs were either incubated with medium (mock), stimulated with ODN 2216, or exposed to indicated flavivirus strain at MOI of 1 for 24 hours. Error bars represent the standard deviation of at least three experiments conducted with primary cells from distinct donors. (B): Quantification of IFN α in the supernatant of pDCs co-cultured with Vero cells. Vero cells were left uninfected (mock) or infected with the indicated flavivirus strain at MOI of 1 for 12h and then co-cultured with pDCs for a further 24 hours. Error bars represent the standard deviation of results obtained from five (36 h pi) and four (48 h pi) distinct donors, detailed below.

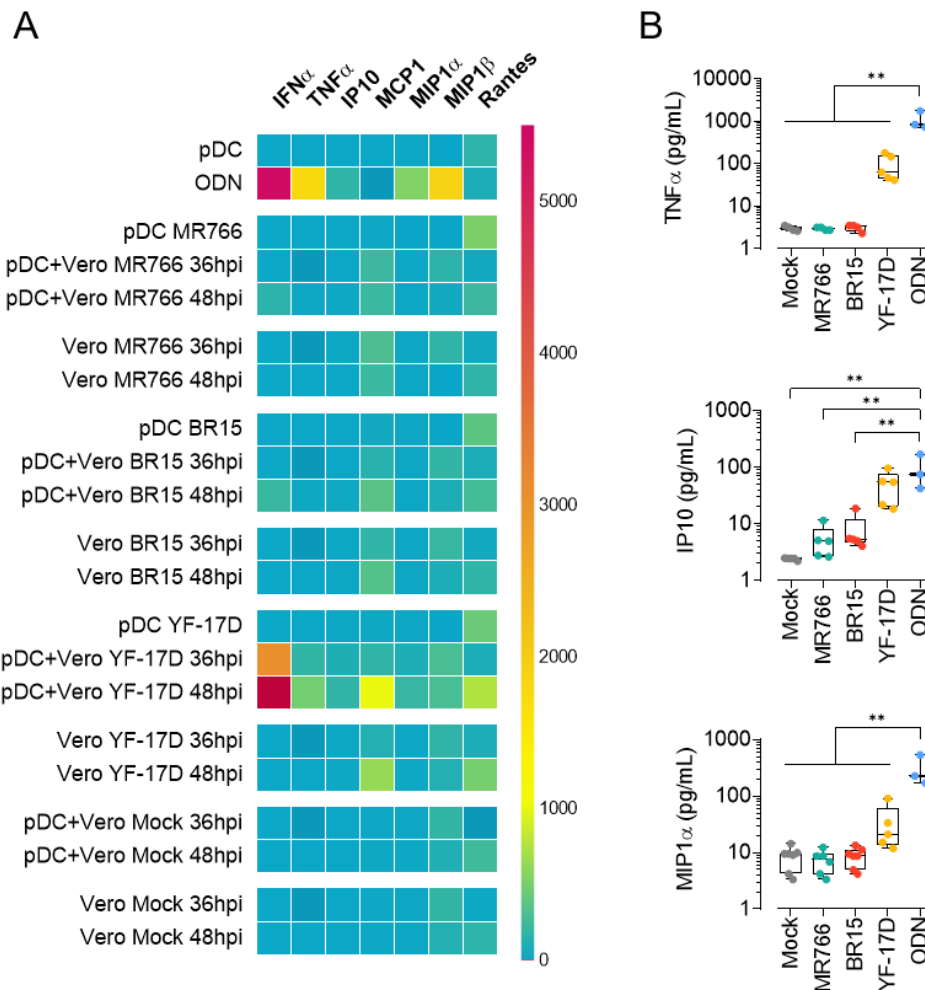


Figure 6.

(A): Quantification of cytokines and chemokines in the supernatant of pDCs, co-cultured pDCs and Vero cells. Heat map was used to visualize the broad array of cytokines and chemokines produced by pDCs upon ZIKVs and YF-17D exposure. The coloured scale bar indicates concentration expressed in microgram per millilitres ($\mu\text{g/mL}$). Supernatants of uninfected pDCs, pDCs stimulated with ODN 2216 or exposed to indicated flavivirus strain at MOI of 1 were collected after 24h of culture. Supernatants of co-cultured pDCs (pDC+Vero) and Vero cells were collected at 36 hours and 48 hours, as indicated, post Vero cell infection at MOI of 1. Concentrations shown are those from one representative donor. (B): Detailed concentration of TNF α , IP10 and MIP1 α produced by co-cultured and pDCs stimulated with ODN 2216 for 24 hours. pDCs were co-cultured with Vero cells left uninfected or infected with the indicated flavivirus strain at MOI of 1. Error bars represent the standard deviation of three (ODN) to five distinct donors.

17D, cell-free and cell-associated MR766 or BR15 ZIKV. The pattern of molecules produced by Vero cells infected with corresponding viruses and that of mock infected cells was also determined. A heat map of the immune mediators detected under these various conditions is shown in Figure 6A. In addition to confirming the weak IFN α response induced by cell-free and cell-associated ZIKV, this MAP analysis reveals that no inflammatory cytokines and chemokines are produced by pDCs in response to ZIKV. The data in Figure 6B compare the mean concentrations of TNF α , IP-10, and MIP1 α secreted by pDC in response to either ODN 2216, or YFV, or ZIKV from experiments performed with pDCs sorted from 6 donors.

Lack of IFN α production by pDCs exposed to ZIKV-infected human neuroblastoma cells

Because ZIKV is a neurotropic virus, and pDCs can be recruited in CNS infections, as shown for WNV [35], we thought interesting to study the interaction of freshly isolated pDCs with ZIKV-infected neuroblastoma cells IMR-32. IMR-32 cells were infected with the two strains of ZIKV or YF-17D at MOI of 4 under the same conditions as those described above for Vero cells, and the viral titers were measured at 36h p.i. Figure 7A shows that IMR-32 cells were poorly permissive to BR15, while the other strain MR766 highly replicated in these cells, as also observed for YF-17D. A weak cytopathic effect was detected under these conditions of infection, although cell viability of IMR-32 was significantly lower after infection with MR766 or YF-17D as compared to BR15, probably as a consequence of the very high levels of viral replication of these two viruses (Figure 7B). pDC IFN α response after exposure to ZIKV-infected neuronal cells was assessed, and Figure 7C shows that no IFN α was detected in the culture supernatant. In contrast, pDCs exposed to YF-17D-infected IMR-32 cells showed a vigorous IFN α response.

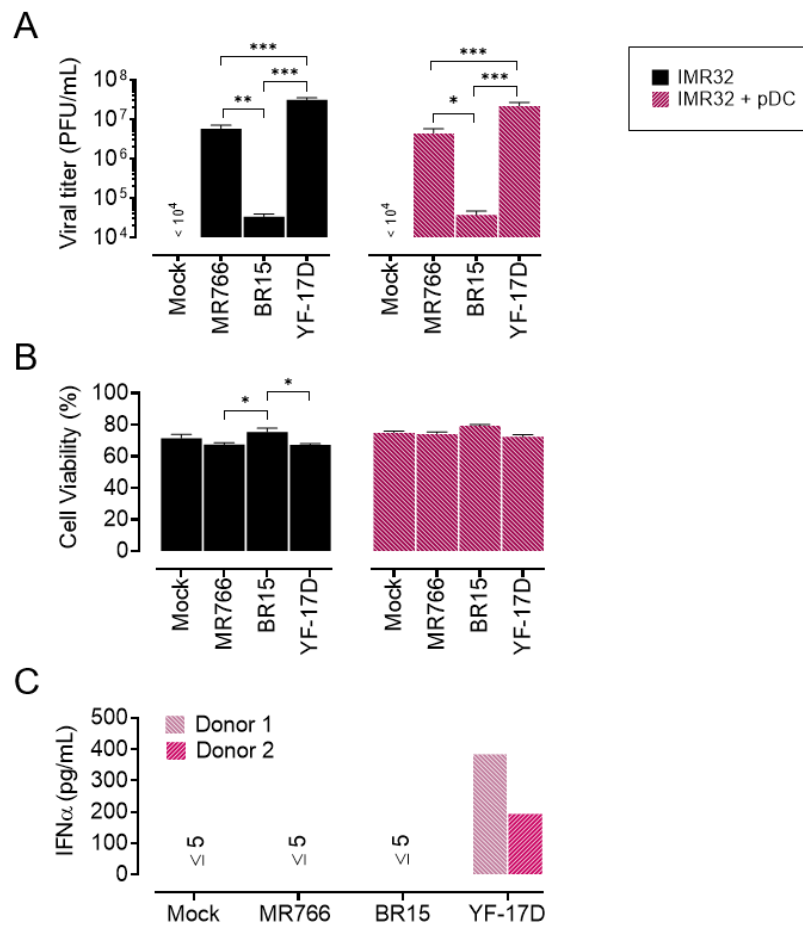


Figure 6.

IMR32 cells were left uninfected (mock) or infected with the indicated flavivirus strain at MOI of 4 for 36 hours. In co-culture experiment (IMR32 + pDC), IMR32 cells were infected for 12 hours and then co-culture with pDCs were co-cultured with IMR32 for a further 24 hours. (A): Quantification of viral progeny production. The infectious virus release into the supernatant of infected cells were titrated on Vero cells. (B): Analysis of IMR32 cells viability upon infection. Virus-induced cell death at 36 hours post IMR32 cells infection was assessed by LDH release measurement. Cell viability is expressed as percentage relative to maximum LDH release. Error bars in panels (A) and (B) represent the standard deviation of two experiments in duplicate. (C) Quantification of IFNα in the supernatant of pDCs co-cultured 24 hours with IMR32 cells for 24 hours. Shown are the results obtained from two distinct donors.

DISCUSSION

The interferon (IFN) response plays a critical role in the control of flaviviruses, as shown by the increased susceptibility of mice lacking components of the IFN pathway to flavivirus infection [36, 37] and the numerous mechanisms employed by flaviviruses to counteract this control [38, 39]. We report here that human sorted pDCs are not susceptible to infection by cell-free ZIKV virions, while they can be infected when exposed to ZIKV-infected cells, as evidenced by intracellular dsRNA expression and confocal microscopy. However, pDCs were unable to mount an IFN α response, whether exposed to infected-epithelial Vero cells or -neuroblastoma IMR-32 cells. In addition, they were suppressed for the secretion of inflammatory cytokines and chemokines.

pDCs are not permissive to most viral infections and recent studies exploring pDC activation by flaviviruses have revealed that sensing of virus-infected cells by pDCs was more effective than sensing of circulating cell-free viruses. This requirement for cell-cell contact is increasingly recognized as a hallmark of the pDC-mediated antiviral state, triggered by evolutionarily divergent enveloped RNA viruses [40]. It was reported for DENV [25, 27], WNV [25], YFV [26] and CHIKV [27]. We report that primary human pDCs are not permissive to infection by ZIKV virions. However, cell-cell contact between pDCs and Vero cells infected with the epidemic strains led to the infection of a small fraction of pDCs, detected by the intracellular expression of viral dsRNA. Our observations are consistent with a recent study assessing the frequency of ZIKV-infected cells in circulating cell populations from individuals with naturally-acquired acute infection. Indeed, Sun *et al.* reported that ZIKV RNA was mainly detected in sorted mDCs, while sorted pDCs from these patients contained no ZIKV RNA, as also observed for B cells, NK cells, CD4 and CD8 T cells. This was corroborated by in vitro infection experiments on PBMCs, since highest levels of ZIKV transcripts were observed in mDCs and lower levels of ZIKV transcripts were detected in the other subsets, including pDCs [41].

Several features characterize the antiviral state of pDCs, such as a robust production of IFN α , concomitant with additional antiviral responses, including inflammatory cytokine secretion. While the lack of cytokine response was

expected in pDCs exposed to cell-free virions [42, 26], it was striking to observe that pDCs co-cultured with ZIKV-infected cells only triggered a very low IFN α response and no production of inflammatory mediators. This surprising observation is in sharp contrast to previous studies conducted with related flaviviruses such as YFV [43], DENV [25] and WNV [42] in which co-culture experiments induced a robust interferon response. Nevertheless, our results are consistent with a recent report assessing ZIKV-induced IFN response in human PBMC, which showed the complete lack of type I and type III IFN induction by ZIKV, suggesting the ability of ZIKV to evade the IFN system [44]. In addition, a remarkable downregulation of antiviral interferon-stimulated genes and innate immune sensors in mDCs was reported [41], suggesting that ZIKV can actively suppress Interferon-dependent immune responses. The importance of type I IFN in mediating host restriction of ZIKV is evident through studies in murine models, which have consistently shown that immune competent adult mice do not support efficient ZIKV replication [36]. A genetic deficiency in type I IFN signaling shifts the balance to sustained viral replication and disseminated disease, promoting spread to the CNS and lethal infection [36, 45]. ZIKV has developed several strategies to antagonize type I IFN signaling to evade the pressures of host innate immune responses. Bowen *et al.* recently reported that human myeloid DCs, targets of mosquito-borne flaviviruses, are susceptible to productive viral replication, yet these cells failed to secrete type I or III IFN. The defect was due to a selective inhibition of translation of type I IFN proteins, while translation of other antiviral host proteins remained intact [18]. ZIKV non-structural proteins, NS1, NS4A, and NS5, may also inhibit type I IFN through inhibition of IRF3 and NF- κ B signaling [46]. ZIKV also counteracts type I IFN responses by blocking phosphorylation of STAT1 and STAT2, thus antagonizing JAK/STAT signaling [18]. Thus, ZIKV targets multiple points within the type I IFN induction signaling cascade [47]. Altogether, these studies illustrate the remarkable ability of ZIKV to evade the pressures of host innate immune responses.

Upon sensing of viral pathogen, pDCs undergo maturation with coordinated regulation of surface markers that mediate important pDCs functions such as interaction with other immune cells or migration to secondary lymphoid tissues. While exposure to ZIKV did not trigger an increase in the surface expression of

CD83, CD86 and HLA-DR in pDCs, a slight upregulation of CCR7 and a slight downregulation of CD303 were observed. CD303, also known as BDCA-2, is an endocytic C-type lectin receptor able to bind and internalize glycosylated antigens [48]. Flaviviruses, including ZIKV, can encode up to three glycosylated proteins depending on the viral strain, including the non-structural protein 1 (NS1) and two structural proteins: the envelope (E) and the membrane precursor (prM). During flavivirus maturation, the latter is cleaved so that only M but not its glycosylated peptide product “pr” remain expressed on the virion [49]. Nevertheless, incomplete maturation commonly occurs during flaviviruses processing leading to the production of “mosaic” virions expressing both E and prM on their surface, as reported for ZIKV [50, 51]. Furthermore, a hallmark of epidemic ZIKV strains is the presence of a N-glycosylation motif in the sequence coding for the envelope protein. Therefore, ZIKV BR15 particles but not ZIKV MR766 particles harbor a glycosylated envelope protein expressed on the virion surface. The presence of glycans associated to prM and/or envelope protein is known to mediated flavivirus entry through binding to DC-SIGN/DC-SIGNR [52, 53, 54, 55], mannose receptor [56] as well as CLEC5A [57, 58] in immune and epithelial mammalian cells. In this way, it is likely that the reduced CD303 expression on the surface of pDCs exposed to ZIKV was mediated by a ligation with ZIKV's glycosylated protein(s). Interestingly, ligand binding to CD303 has been shown to lead to its rapid internalization and subsequent inhibition of type I IFN production of pDCs [59]. In addition, CD303 signaling cascade is also a putative regulator of the canonical NF- κ B pathway activity, and thereby subsequent inflammatory cytokine gene expression [48]. Thus, it is conceivable that the inhibition of pDCs antiviral response induced by ZIKV may, at least partially, involve CD303 signaling.

The mechanism by which ZIKV enters the central nervous system through the peripheral entry route remains to be determined. However, it is likely that the virus gains access to target neural tissue either as cell-free virus, through disruption of the blood-brain barrier for example, or through infected immune cells, able to circumvent this latter. This possibility is supported by the fact that ZIKV can infect pDCs, as we showed. These cells are present in the skin, the main entry route of ZIKV infection, but they are also able to infiltrate the CNS, as

reported in the setting of autoimmune diseases [60]. Based on our results, it is conceivable that pDCs could be an important ZIKV target cell at the portal of entry. Through ZIKV-induced expression of CCR7, a receptor involved in pDC trafficking involving its interaction with the ligands CCL19 and CCL21, infected pDCs could migrate from primary infected to secondary lymphoid tissues. Interestingly, CCL19 and CCL21 are expressed in the blood vessels of the CNS, albeit in smaller amounts. Therefore, it is possible that infected pDCs serve as a Trojan horse for ZIKV entry into the CNS by taking advantage of the ability of specific blood-brain barrier components to attract CCR7-expressing cells.

MATERIALS AND METHODS

Cells and viruses

Vero cells (ATCC, CCL-81) and IMR32 cells (ATCC, CCL-127) were cultured at 37°C in a humidified 5% CO₂ chamber in complete culture medium composed of MEM supplemented with 5% or 10% FBS respectively, 1% penicillin-streptomycin, 2 mmol L⁻¹ l-Glutamine and 1 mmol L⁻¹ sodium pyruvate (PAN Biotech). The culture medium of IMR32 cells was enriched with 5% non-essential amino acids (PAN Biotech). Zika virus molecular clones of Brazilian BeH819015 strain (BEI resources product n°NR-51129), referred to as BR15, and historical MR766 Uganda 47-NIID (Genbank access LC002520) have previously been described [28]. YF-17D stock was prepared on Vero cells inoculated with the YFV vaccine strain (YF-17D-204 STAMARIL, Sanofi Pasteur, Lyon) provided by the Institut Pasteur Medical Center. Viral titers were determined by a standard plaque-forming assay on Vero cells as previously described [28].

Isolation and preparation of pDCs

Peripheral Blood Mononuclear Cells (PBMCs) were separated from the blood of healthy adult donors on a Ficoll-Hypaque density gradient. Blood was obtained through the EFS (Etablissement Français du Sang) in the setting of EFS-Institut Pasteur Convention. pDCs were isolated from fresh PBMCs as previously reported [30], using the Human Plasmacytoid DC Negative Isolation Kit (EASYstep,

StemCell Technologies). The enriched cells were assessed for more than 95% purity using the following antibodies: CD123–APC (clone AC145), CD3-V500 (clone UCHT1) purchased from BD Horizon and CD303–PE (clone REA693) purchased from MACS. pDCs were cultured in complete medium, composed of RPMI 1640 (Invitrogen, Gaithersburg, MD, USA), 10% FBS and 1% penicillin-streptomycin, at 37°C in a humidified 5% CO₂ chamber according to protocol. When indicated, pDCs were stimulated overnight with CpG ODN 2006 or CpG ODN 2216 (InvivoGen, USA) at 3 ug/ml.

Infection of pDCs

Freshly isolated pDCs were incubated with ZIKV molecular clones at a multiplicity of infection (MOI) of 1 to 5, with YF-17D at MOI of 1, or with virus-free supernatant from Vero cells in a volume equal to the highest volume of viral inoculum used in the experiment. After 2h of incubation, the virus (or supernatant) inputs were removed. pDCs were washed and cultured in complete medium for 24 hours.

Co-culture experiments

Vero and IMR32 cells were infected at MOI of 1 and 4 respectively. Twelve hours post-infection the culture medium was removed and replaced with complete RPMI medium containing 5×10^4 pDCs. Cells were co-cultured for 24 to 48 hours as indicated.

Flow cytometry analyses

The phenotype of pDCs was assessed with the following primary mAbs (BD Horizon): CCR7-FITC (clone 3D12), CD83-PE-Cy7 (clone HB15e), CD86-PE-Cy5 (clone 233), HLA-DR-APC-H7 (clone L243), CD123-PerCP-Vio 700 (clone AC145). CD303-PE (clone REA693) was purchase from MACS. Cells were fixed with 4% PFA for 20 min, stained for 30 minutes at 4°C and washed before being subjected to FACS analysis. ZIKV infectivity was assessed with the mouse anti-pan flavivirus envelope protein mAb 4G2 (RD Biotech) or the mouse anti-dsRNA IgG2a mAb J2 (Scicons) as indicated. Cells were fixed with 4% PFA for 20 min at room temperature (RT) and permeabilized with 0.1% Triton X-100 in PBS for 4 min at

RT. Fixed cells were stained overnight at 4°C using 4G2 or J2 (1:500) in PBS-BSA. Then, cells were stained 20 min at RT with secondary antibody donkey anti-mouse Alexa Fluor 488 IgG (1:1000, Invitrogen) or donkey anti-mouse Cy3 (1:500, Jackson immunoResearch) in PBS-BSA, and washed before being subjected to FACS analysis. At least, 5 000 events were acquired using Cyan cytometer (Beckman Coulter). Stained cells were analyzed using FlowJo software (Tree Star, Inc., Ashland, OR). pDCs survival was assessed using the 7-AAD assay as previously described [61]

Cell viability assay

Cell viability was determined using the CytoTox 96® Non-Radioactive Cytotoxicity Assay (Promega) according to the manufacturer's recommendations. This assay is based on LDH release quantification as indicator of cell death.

Cytokines and chemokines measurement

Chemokines and cytokines were measured by Luminex (Human XL cytokine Premixed Magnetic Luminex Performance Assay Kit (R&D Systems, bio-technique) according to the manufacturer's instructions. In brief, 50 µl of standard or supernatant inactivated with 1% NP40 for 10 minutes at 4°C were incubated with antibody-linked beads for 2 h. Then samples were washed three times with wash solution, and incubated for 1 h with biotinylated secondary antibodies. A final incubation of 30 min with streptavidin-PE preceded the acquisition on the Bioplex 200 (Biorad). At least 100 events were acquired for each analyte. Values below the standard curves were replaced by the lowest values of the concentrations measured.

Immunofluorescence and confocal analysis

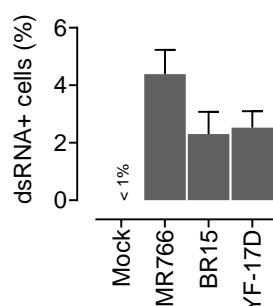
Freshly isolated pDCs were stained with the Cell Tracker Deep Red Dye (Termo Fisher Scientific) for 30 min at 37 °C. Labeled pDCs were co-cultured for 24 hours with previously seeded and infected Vero cells in glass coverslips. Cells were fixed with 37°C-prewarmed 4% PFA for 20 min at room temperature (RT) and permeabilized with 0.1% Triton X-100 in PBS for 4 min at RT. Fixed cells were stained overnight at 4°C using a polyclonal anti-ZIKV antibody provided by P.

Després (1:1000) in PBS-BSA. Then, cells were stained 20 min at RT with the secondary antibody donkey anti-mouse Alexa Fluor 488 IgG (1:1000) in PBS-BSA. Nuclei were stained with NucBlue (Thermo Fisher Scientific) for 20 min at RT. Lastly, coverslips were washed with BSA-free PBS and mounted with ProLong Glass antifade reagent (Fisher Scientific). Z-sections across cells at 0.5 μm increments were acquired with a Zeiss LSM 700 laser scanning confocal microscope equipped with a X63 objectives. Images were analyzed with the ICY software (icy.bioimageanalysis.org).

Statistical analysis

The data are presented as arithmetic mean \pm SD. Comparisons between different treatments have been analyzed by a one-way or two-way ANOVA tests as appropriate. Values of $p < 0.05$ were considered statistically significant for a post-hoc Tukey's test. Statistical analysis was performed using GraphPad Prism version 8 (GraphPad software, San Diego, CA).

SUPPLEMENTAL DATA



Supplemental figure.

Percentage of Vero cells hosting viral replication according to flow cytometry analysis using anti-dsRNA antibody (J2) at 12 hours post infection. Error bars represent the standard deviation of two experiments performed in triplicate.

REFERENCES

- Musso D, Gubler DJ. Zika Virus. *Clin Microbiol Rev*. 2016;29(3):487-524. doi: 10.1128/CMR.00072-15. PubMed PMID: 27029595; PubMed Central PMCID: PMC4861986.
- Dick GW, Kitchen SF, Haddow AJ. Zika virus. I. Isolations and serological specificity. *Trans R Soc Trop Med Hyg*. 1952;46(5):509-20. PubMed PMID: 12995440.
- Dick GW. Zika virus. II. Pathogenicity and physical properties. *Trans R Soc Trop Med Hyg*. 1952;46(5):521-34. PubMed PMID: 12995441.
- Bell TM, Field EJ, Narang HK. Zika virus infection of the central nervous system of mice. *Arch Gesamte Virusforsch*. 1971;35(2):183-93. PubMed PMID: 5002906.
- Duffy MR, Chen TH, Hancock WT, Powers AM, Kool JL, Lanciotti RS, et al. Zika virus outbreak on Yap Island, Federated States of Micronesia. *N Engl J Med*. 2009;360(24):2536-43. doi: 10.1056/NEJMoa0805715. PubMed PMID: 19516034.
- Zanluca C, Melo VC, Mosimann AL, Santos GI, Santos CN, Luz K. First report of autochthonous transmission of Zika virus in Brazil. *Mem Inst Oswaldo Cruz*. 2015;110(4):569-72. doi: 10.1590/0074-02760150192. PubMed PMID: 26061233; PubMed Central PMCID: PMC4501423.
- Ikejezie J, Shapiro CN, Kim J, Chiu M, Almiron M, Ugarte C, et al. Zika Virus Transmission-Region of the Americas, May 15, 2015-December 15, 2016. *Am J Transplant*. 2017;17(6):1681-6. doi: 10.1111/ajt.14333. PubMed PMID: 28544280.
- Cao-Lormeau VM, Blake A, Mons S, Lastere S, Roche C, Vanhomwegen J, et al. Guillain-Barre Syndrome outbreak associated with Zika virus infection in French Polynesia: a case-control study. *Lancet*. 2016;387(10027):1531-9. doi: 10.1016/S0140-6736(16)00562-6. PubMed PMID: 26948433; PubMed Central PMCID: PMC4544521.
- Victora CG, Schuler-Faccini L, Matijasevich A, Ribeiro E, Pessoa A, Barros FC. Microcephaly in Brazil: how to interpret reported numbers? *Lancet*. 2016;387(10019):621-4. doi: 10.1016/S0140-6736(16)00273-7. PubMed PMID: 26864961.
- Mlakar J, Korva M, Tul N, Popovic M, Poljsak-Prijatelj M, Mraz J, et al. Zika Virus Associated with Microcephaly. *N Engl J Med*. 2016;374(10):951-8. doi: 10.1056/NEJMoa1600651. PubMed PMID: 26862926.
- Driggers RW, Ho CY, Korhonen EM, Kuivaneen S, Jaaskelainen AJ, Smura T, et al. Zika Virus Infection with Prolonged Maternal Viremia and Fetal Brain Abnormalities. *N Engl J Med*. 2016;374(22):2142-51. doi: 10.1056/NEJMoa1601824. PubMed PMID: 27028667.
- Tappe D, Perez-Giron JV, Zammarchi L, Rissland J, Ferreira DF, Jaenisch T, et al. Cytokine kinetics of Zika virus-infected patients from acute to convalescent phase. *Med Microbiol Immunol*. 2016;205(3):269-73. doi: 10.1007/s00430-015-0445-7. PubMed PMID: 26702627; PubMed Central PMCID: PMC4867002.
- Zammarchi L, Stella G, Mantella A, Bartolozzi D, Tappe D, Gunther S, et al. Zika virus infections imported to Italy: clinical, immunological and virological findings, and public health implications. *J Clin Virol*. 2015;63:32-5. doi: 10.1016/j.jcv.2014.12.005. PubMed PMID: 25600600.
- Dowd KA, DeMaso CR, Pelc RS, Speer SD, Smith ARY, Goo L, et al. Broadly Neutralizing Activity of Zika Virus-Immune Sera Identifies a Single Viral Serotype. *Cell Rep*. 2016;16(6):1485-91. doi: 10.1016/j.celrep.2016.07.049. PubMed PMID: 27481466; PubMed Central PMCID: PMC45004740.
- Robbiani DF, Bozzacco L, Keeffe JR, Khouri R, Olsen PC, Gazumyan A, et al. Recurrent Potent Human Neutralizing Antibodies to Zika Virus in Brazil and Mexico. *Cell*. 2017;169(4):597-609 e11. doi: 10.1016/j.cell.2017.04.024. PubMed PMID: 28475892; PubMed Central PMCID: PMC5492969.
- Elong Ngono A, Vizcarra EA, Tang WW, Sheets N, Joo Y, Kim K, et al. Mapping and Role of the CD8(+) T Cell Response During Primary Zika Virus Infection in Mice. *Cell Host Microbe*. 2017;21(1):35-46. doi: 10.1016/j.chom.2016.12.010. PubMed PMID: 28081442; PubMed Central PMCID: PMC45234855.
- Grifoni A, Costa-Ramos P, Pham J, Tian Y, Rosales SL, Seumois G, et al. Cutting Edge: Transcriptional Profiling Reveals Multifunctional and Cytotoxic Antiviral Responses of Zika Virus-Specific CD8(+) T Cells. *J Immunol*. 2018;201(12):3487-91. doi: 10.4049/jimmunol.1801090. PubMed PMID: 30413672; PubMed Central PMCID: PMC6287102.
- Bowen JR, Quicke KM, Maddur MS, O'Neal JT, McDonald CE, Fedorova NB, et al. Zika Virus Antagonizes Type I Interferon Responses during Infection of Human Dendritic Cells. *PLoS Pathog*. 2017;13(2):e1006164. doi:

- 10.1371/journal.ppat.1006164. PubMed PMID: 28152048; PubMed Central PMCID: PMC5289613.
19. Wu Y, Liu Q, Zhou J, Xie W, Chen C, Wang Z, et al. Zika virus evades interferon-mediated antiviral response through the co-operation of multiple nonstructural proteins in vitro. *Cell Discov.* 2017;3:17006. doi: 10.1038/celldisc.2017.6. PubMed PMID: 28373913; PubMed Central PMCID: PMC5359216.
20. Luo H, Winkelmann ER, Fernandez-Salas I, Li L, Mayer SV, Danis-Lozano R, et al. Zika, dengue and yellow fever viruses induce differential anti-viral immune responses in human monocytic and first trimester trophoblast cells. *Antiviral Res.* 2018;151:55-62. doi: 10.1016/j.antiviral.2018.01.003. PubMed PMID: 29331320; PubMed Central PMCID: PMC5844857.
21. Gary-Gouy H, Lebon P, Dalloul AH. Type I interferon production by plasmacytoid dendritic cells and monocytes is triggered by viruses, but the level of production is controlled by distinct cytokines. *J Interferon Cytokine Res.* 2002;22(6):653-9. doi: 10.1089/10799900260100132. PubMed PMID: 12162875.
22. Blasius AL, Beutler B. Intracellular Toll-like Receptors. *Immunity.* 2010;32(3):305-15. doi: 10.1016/j.immuni.2010.03.012. PubMed PMID: WOS:000276125400005.
23. Kawai T, Akira S. Toll-like Receptors and Their Crosstalk with Other Innate Receptors in Infection and Immunity. *Immunity.* 2011;34(5):637-50. doi: 10.1016/j.immuni.2011.05.006. PubMed PMID: WOS:000291456500002.
24. Sun P, Fernandez S, Marovich MA, Palmer DR, Celluzzi CM, Boonnak K, et al. Functional characterization of ex vivo blood myeloid and plasmacytoid dendritic cells after infection with dengue virus. *Virology.* 2009;383(2):207-15. doi: 10.1016/j.virol.2008.10.022. PubMed PMID: 19013627.
25. Decembre E, Assil S, Hillaire ML, Dejnirattisai W, Mongkolsapaya J, Screaton GR, et al. Sensing of immature particles produced by dengue virus infected cells induces an antiviral response by plasmacytoid dendritic cells. *PLoS Pathog.* 2014;10(10):e1004434. doi: 10.1371/journal.ppat.1004434. PubMed PMID: 25340500; PubMed Central PMCID: PMC4207819.
26. Sinigaglia L, Gracias S, Decembre E, Fritz M, Bruni D, Smith N, et al. Immature particles and capsid-free viral RNA produced by Yellow fever virus-infected cells stimulate plasmacytoid dendritic cells to secrete interferons. *Sci Rep.* 2018;8(1):10889. doi: 10.1038/s41598-018-29235-7. PubMed PMID: 30022130; PubMed Central PMCID: PMC56052170.
27. Webster B, Werneke SW, Zafirova B, This S, Coleon S, Decembre E, et al. Plasmacytoid dendritic cells control dengue and Chikungunya virus infections via IRF7-regulated interferon responses. *Elife.* 2018;7. doi: 10.7554/eLife.34273. PubMed PMID: 29914621; PubMed Central PMCID: PMC6008049.
28. Bos S, Viranaicken W, Turpin J, El-Kalamouni C, Roche M, Krejbich-Trotot P, et al. The structural proteins of epidemic and historical strains of Zika virus differ in their ability to initiate viral infection in human host cells. *Virology.* 2018;516:265-73. doi: 10.1016/j.virol.2017.12.003. PubMed PMID: 29395111.
29. Li G, Bos S, Tsetsarkin KA, Pletnev AG, Despres P, Gadea G, et al. The Roles of prM-E Proteins in Historical and Epidemic Zika Virus-mediated Infection and Neurocytotoxicity. *Viruses.* 2019;11(2). doi: 10.3390/v11020157. PubMed PMID: 30769824.
30. Saidi H, Bras M, Formaglio P, Melki MT, Charbit B, Herbeuval JP, et al. HMGB1 Is Involved in IFN- α Production and TRAIL Expression by HIV-1-Exposed Plasmacytoid Dendritic Cells: Impact of the Crosstalk with NK Cells. *PLoS Pathog.* 2016;12(2):e1005407. doi: 10.1371/journal.ppat.1005407. PubMed PMID: 26871575; PubMed Central PMCID: PMC4752468.
31. Wu P, Wu J, Liu S, Han X, Lu J, Shi Y, et al. TLR9/TLR7-triggered downregulation of BDCA2 expression on human plasmacytoid dendritic cells from healthy individuals and lupus patients. *Clin Immunol.* 2008;129(1):40-8. doi: 10.1016/j.clim.2008.06.004. PubMed PMID: 18684674.
32. Mathan TS, Figdor CG, Buschow SI. Human plasmacytoid dendritic cells: from molecules to intercellular communication network. *Front Immunol.* 2013;4:372. doi: 10.3389/fimmu.2013.00372. PubMed PMID: 24282405; PubMed Central PMCID: PMC3825182.
33. Monel B, Compton AA, Bruel T, Amraoui S, Burlaud-Gaillard J, Roy N, et al. Zika virus induces massive cytoplasmic vacuolization and paraptosis-like death in infected cells. *EMBO J.* 2017;36(12):1653-68. doi: 10.15252/embj.201695597. PubMed PMID: 28473450; PubMed Central PMCID: PMC5470047.
34. Decalf J, Fernandes S, Longman R, Ahloulay M, Audat F, Lefrerre F, et al. Plasmacytoid dendritic cells initiate a complex chemokine and cytokine network and are a viable drug target in chronic HCV patients. *J Exp Med.* 2007;204(10):2423-37. Epub 2007/09/26. doi: 10.1084/jem.20070814. PubMed PMID: 17893202; PubMed Central PMCID: PMC2118448.

35. Brehin AC, Mouries J, Frenkiel MP, Dadaglio G, Despres P, Lafon M, et al. Dynamics of immune cell recruitment during West Nile encephalitis and identification of a new CD19+B220-BST-2+ leukocyte population. *J Immunol.* 2008;180(10):6760-7. PubMed PMID: 18453596.
36. Lazear HM, Govero J, Smith AM, Platt DJ, Fernandez E, Miner JJ, et al. A Mouse Model of Zika Virus Pathogenesis. *Cell Host Microbe.* 2016;19(5):720-30. doi: 10.1016/j.chom.2016.03.010. PubMed PMID: 27066744; PubMed Central PMCID: PMC4866885.
37. Shresta S, Kyle JL, Snider HM, Basavapatna M, Beatty PR, Harris E. Interferon-dependent immunity is essential for resistance to primary dengue virus infection in mice, whereas T- and B-cell-dependent immunity are less critical. *J Virol.* 2004;78(6):2701-10. PubMed PMID: 14990690; PubMed Central PMCID: PMC4353772.
38. Quicke KM, Suthar MS. The innate immune playbook for restricting West Nile virus infection. *Viruses.* 2013;5(11):2643-58. doi: 10.3390/v5112643. PubMed PMID: 24178712; PubMed Central PMCID: PMC4356407.
39. Morrison J, Laurent-Rolle M, Maestre AM, Rajsbaum R, Pisanelli G, Simon V, et al. Dengue virus co-opts UBR4 to degrade STAT2 and antagonize type I interferon signaling. *PLoS Pathog.* 2013;9(3):e1003265. doi: 10.1371/journal.ppat.1003265. PubMed PMID: 23555265; PubMed Central PMCID: PMC4361074.
40. Webster B, Assil S, Dreux M. Cell-Cell Sensing of Viral Infection by Plasmacytoid Dendritic Cells. *J Virol.* 2016;90(22):10050-3. doi: 10.1128/JVI.01692-16. PubMed PMID: 27605675; PubMed Central PMCID: PMC45105643.
41. Sun X, Hua S, Chen HR, Ouyang Z, Einkauf K, Tse S, et al. Transcriptional Changes during Naturally Acquired Zika Virus Infection Render Dendritic Cells Highly Conducive to Viral Replication. *Cell Rep.* 2017;21(12):3471-82. doi: 10.1016/j.celrep.2017.11.087. PubMed PMID: 29262327; PubMed Central PMCID: PMC5751936.
42. Silva MC, Guerrero-Plata A, Gilfoy FD, Garofalo RP, Mason PW. Differential activation of human monocyte-derived and plasmacytoid dendritic cells by West Nile virus generated in different host cells. *J Virol.* 2007;81(24):13640-8. doi: 10.1128/JVI.00857-07. PubMed PMID: 17913823; PubMed Central PMCID: PMC2168853.
43. Bruni D, Chazal M, Sinigaglia L, Chauveau L, Schwartz O, Despres P, et al. Viral entry route determines how human plasmacytoid dendritic cells produce type I interferons. *Sci Signal.* 2015;8(366):ra25. doi: 10.1126/scisignal.aaa1552. PubMed PMID: 25737587.
44. Colavita F, Bordoni V, Caglioti C, Biava M, Castilletti C, Bordin L, et al. ZIKV Infection Induces an Inflammatory Response but Fails to Activate Types I, II, and III IFN Response in Human PBMC. *Mediators Inflamm.* 2018;2018:2450540. doi: 10.1155/2018/2450540. PubMed PMID: 29967565; PubMed Central PMCID: PMC6008743.
45. Rossi SL, Tesh RB, Azar SR, Muruato AE, Hanley KA, Auguste AJ, et al. Characterization of a Novel Murine Model to Study Zika Virus. *Am J Trop Med Hyg.* 2016;94(6):1362-9. doi: 10.4269/ajtmh.16-0111. PubMed PMID: 27022155; PubMed Central PMCID: PMC4889758.
46. Kumar A, Hou S, Airo AM, Limonta D, Mancinelli V, Branton W, et al. Zika virus inhibits type-I interferon production and downstream signaling. *EMBO Rep.* 2016;17(12):1766-75. doi: 10.15252/embr.201642627. PubMed PMID: 27797853; PubMed Central PMCID: PMC45283583.
47. Bowen JR, Zimmerman MG, Suthar MS. Taking the defensive: Immune control of Zika virus infection. *Virus Res.* 2018;254:21-6. doi: 10.1016/j.virusres.2017.08.018. PubMed PMID: 28867493; PubMed Central PMCID: PMC5832569.
48. Rock J, Schneider E, Grun JR, Grutzkau A, Kuppers R, Schmitz J, et al. CD303 (BDCA-2) signals in plasmacytoid dendritic cells via a BCR-like signalosome involving Syk, Slp65 and PLCgamma2. *Eur J Immunol.* 2007;37(12):3564-75. doi: 10.1002/eji.200737711. PubMed PMID: 18022864.
49. Li L, Lok SM, Yu IM, Zhang Y, Kuhn RJ, Chen J, et al. The flavivirus precursor membrane-envelope protein complex: structure and maturation. *Science.* 2008;319(5871):1830-4. doi: 10.1126/science.1153263. PubMed PMID: 18369147.
50. Rey FA, Stiasny K, Heinz FX. Flavivirus structural heterogeneity: implications for cell entry. *Curr Opin Virol.* 2017;24:132-9. doi: 10.1016/j.coviro.2017.06.009. PubMed PMID: 28683393; PubMed Central PMCID: PMC6037290.
51. Sirohi D, Chen Z, Sun L, Klose T, Pierson TC, Rossmann MG, et al. The 3.8 Å resolution cryo-EM structure of Zika virus. *Science.* 2016;352(6284):467-70. doi: 10.1126/science.aaf5316. PubMed PMID: 27033547; PubMed Central PMCID: PMC4845755.
52. Davis CW, Mattei LM, Nguyen HY, Ansarah-Sobrinho C, Doms RW, Pierson TC. The location of asparagine-linked glycans on West Nile virions controls their interactions with CD209 (dendritic cell-specific ICAM-3 grabbing nonintegrin). *J Biol Chem.* 2006;281(48):37183-94. doi: 10.1074/jbc.M605429200. PubMed PMID: 17001080.

53. Davis CW, Nguyen HY, Hanna SL, Sanchez MD, Doms RW, Pierson TC. West Nile virus discriminates between DC-SIGN and DC-SIGNR for cellular attachment and infection. *J Virol.* 2006;80(3):1290-301. doi: 10.1128/JVI.80.3.1290-1301.2006. PubMed PMID: 16415006; PubMed Central PMCID: PMC1346927.
54. Navarro-Sanchez E, Altmeyer R, Amara A, Schwartz O, Fieschi F, Virelizier JL, et al. Dendritic-cell-specific ICAM3-grabbing non-integrin is essential for the productive infection of human dendritic cells by mosquito-cell-derived dengue viruses. *EMBO Rep.* 2003;4(7):723-8. doi: 10.1038/sj.embor.embor866. PubMed PMID: 12783086; PubMed Central PMCID: PMC1326316.
55. Tassaneetrithep B, Burgess TH, Granelli-Piperno A, Trumpfheller C, Finke J, Sun W, et al. DC-SIGN (CD209) mediates dengue virus infection of human dendritic cells. *J Exp Med.* 2003;197(7):823-9. doi: 10.1084/jem.20021840. PubMed PMID: 12682107; PubMed Central PMCID: PMC193896.
56. Miller JL, de Wet BJ, Martinez-Pomares L, Radcliffe CM, Dwek RA, Rudd PM, et al. The mannose receptor mediates dengue virus infection of macrophages. *PLoS Pathog.* 2008;4(2):e17. doi: 10.1371/journal.ppat.0040017. PubMed PMID: 18266465; PubMed Central PMCID: PMC193896.
57. Chen ST, Lin YL, Huang MT, Wu MF, Cheng SC, Lei HY, et al. CLEC5A is critical for dengue-virus-induced lethal disease. *Nature.* 2008;453(7195):672-6. doi: 10.1038/nature07013. PubMed PMID: 18496526.
58. Chen ST, Liu RS, Wu MF, Lin YL, Chen SY, Tan DT, et al. CLEC5A regulates Japanese encephalitis virus-induced neuroinflammation and lethality. *PLoS Pathog.* 2012;8(4):e1002655. doi: 10.1371/journal.ppat.1002655. PubMed PMID: 22536153; PubMed Central PMCID: PMC3334897.
59. Dzionek A, Sohma Y, Nagafune J, Cella M, Colonna M, Facchetti F, et al. BDCA-2, a novel plasmacytoid dendritic cell-specific type II C-type lectin, mediates antigen capture and is a potent inhibitor of interferon alpha/beta induction. *J Exp Med.* 2001;194(12):1823-34. PubMed PMID: 11748283; PubMed Central PMCID: PMC193584.
60. Bailey-Bucktrout SL, Caulkins SC, Goings G, Fischer JA, Dzionek A, Miller SD. Cutting edge: central nervous system plasmacytoid dendritic cells regulate the severity of relapsing experimental autoimmune encephalomyelitis. *J Immunol.* 2008;180(10):6457-61. PubMed PMID: 18453561; PubMed Central PMCID: PMC193584.
61. Lecoeur H, de Oliveira-Pinto LM, Gougeon ML. Multiparametric flow cytometric analysis of biochemical and functional events associated with apoptosis and oncosis using the 7-aminoactinomycin D assay. *J Immunol Methods.* 2002;265(1-2):81-96. Epub 2002/06/20. PubMed PMID: 12072180.

DISCUSSION

Zika is an unprecedented epidemiological phenomenon which surprised the world. For many years, it was considered a trivial virus responsible for only a handful of human infections, self-limited and benign, in Africa and Southeast Asia. Even its discovery was fortuitous, being the unexpected result of a YFV epidemiological campaign. But then, after decades of silent spread, a first epidemic broke out in Micronesia in 2007 – like a warning signal. A few years later, a sudden Zika outbreak of larger scale occurred in the Pacific islands before reaching Brazil in 2015. During this period, Zika was associated with severe neurological complications, highlighting its serious pathogenic potential for humans. Since its emergence, more than 80 countries and territories have been affected by the ZIKV pandemic, which is now recognized as a neurotropic and teratogenic virus. Joined in an unprecedented collective effort, scientific research teams from around the world studied the history and biology of ZIKV to understand how ZIKV emerged and turned into such an “epidemiological storm”.

One possibility was that ZIKV emergence and widespread dispersion throughout the tropics and subtropics were merely a consequence of the increasing population and distribution of competent mosquito vectors, increasing human population and urbanization, and growing global transport. The absence of anti-ZIKV immunity undoubtedly favored its emergence and was a key determinant for its maintenance and rapid spread among human. In addition, the immune background of ZIKV-affected populations likely influenced the infection success and/or outcome due to possible immune cross-reactions with related viruses. On the other hand, while ZIKV displays a similar structure to other flaviviruses, it also has specific attributes that may have improved its epidemiological success. For example, ZIKV is far more thermostable than DENV and hence keeps a substantial infectivity even when exposed to high temperatures¹. This high structural stability is in part due to the tighter arrangement of ZIKV surface proteins, and confers resistance to adverse physico-chemical conditions². This remarkable robustness allows the virus to survive in many body fluids including in the semen, which in turn increases its chance of sexual transmission³. However, since the environmental conditions were actually met, a question remains: why was Zika virus not recognized as pathogenic to humans before? Why did Zika emerge to cause severe outbreaks now?

While environmental factors undoubtedly support the process, the most likely explanation for ZIKV dramatic emergence and for the scope of resulting outbreaks is a modification of ZIKV intrinsic viral factors. The relevance of genetic changes as epidemic drivers has previously been demonstrated for other arboviruses such as WNV and CHIKV, for which mutations have been responsible for increased virogenesis and vector competence respectively^{4,5}. As an arbovirus, ZIKV evolution has been subject to unique selective pressures which may have favored the emergence of strains with increased epidemiological fitness. In this regard, it is likely that the scope of the current epidemic was partly facilitated by genetic determinants that improved ZIKV fitness and pathogenesis. In these last lines, I will explain how ZIKV findings, including ours, support this hypothesis.

Asian *versus* African ZIKV lineages: Can less be more?

Phylogenetic studies clearly show that ZIKV diverged into two lineages, African and Asian, with the latter including all epidemic strains. Whole genome comparative analysis performed between pre-epidemic and current ZIKV strains evidenced that genetic changes have occurred, several of which were conserved among the epidemic strains. Knowing this, our strategy has been to investigate the phenotype of two ZIKV strains temporally and geographically distant, in order to decipher whether Asian ZIKV strains are or not phenotypically different from the African ones. For that purpose, infectious molecular clones of MR766 and BeH819015 (BR15) strains were generated using the “infectious sub-genomic amplicons” method. Based on the same method, chimeric clones and mutants were also generated in order to study specific proteins or mutations. Owing that the ancestral prototype MR766 strain has never been associated with human infection cases, this strain was used as a reference in the experiments conducted to highlight epidemic strains features.

Phenotypic differences between ZIKV African and Asian lineage

In our studies, significant phenotypic differences were observed between African and Asian ZIKV strains. The molecular clone of MR766 replicated at higher titers and resulted in more apoptosis in epithelial and neuronal cell lines tested. These surprising differences were corroborated and repeatedly observed, in particular

in infected primary human cells relevant to ZIKV-related pathology, such as neural progenitor cells and placental trophoblasts^{6,7}. The African strains are also more pathogenic *in vivo*, in murine models^{8–10}. However, since immunocompetent mice are resistant to ZIKV infection (regardless of virus lineage), comparative trials were conducted in mouse models with innate immune deficiencies, particularly in type I interferon signaling pathways. In addition, the MR766 strain commonly used in these studies, was probably neuro- and mouse-adapted due to its 149 passages in suckling mice brains, which further emphasized the caution required for the extrapolation of results obtained in useful, but imperfect models. Nevertheless, these studies collectively highlighted intrinsic differences in the pathogenic properties of ZIKV strains of African and Asian lineages.

Accumulating evidence indicates that African strains are more cytopathic than Asian strains *in vitro* – a result which at first seems counter-intuitive but suggests a change in viral virulence factors. Actually, the "attenuated" phenotype of Asian strains (lower infection rates and virus production, and reduced induction of early cell death) is likely to contribute to a broader diffusion and to the establishment of a persistent infection, while African ZIKV strains may lead to a more acute or even restricted infection. This assumption is consistent with the results obtained from non-human primates (rhesus monkeys and cynomolgus), naïve to flavivirus exposure, which were subjected to African (Senegal and Nigeria) *versus* Asian (Puerto Rico, Thailand) lineage strains infection^{11,12}. Specifically, Rayner *et al.*¹¹ observed that, in contrast to the results obtained with the Asian strains infection^{13,14}, animals exposed to the African strain only presented low levels of viral RNA in serum samples with virtually no virus shedding in urine and saliva. In line with the low viremia detected, the immune response raised following African strain exposure was also low and insufficient to protect against a subsequent challenge with the Asian strain. Finally, apart from immunodeficient mice trials, both *in vitro* and *in vivo* studies support the hypothesis of viral genetic factors contributing to the differential infectivity of epidemic ZIKV strains.

The unforeseen effect of ZIKV structural proteins

The coding sequence of the structural proteins has accumulated a significant number of amino acid substitutions since the discovery of ZIKV in Uganda. In particular, prM and E proteins have undergone remarkable mutations, some of which *inter alia* led to a change in the structural conformation of both proteins. Given this, a part of my PhD research aimed to determine whether the structural proteins mutations could impact the ability of ZIKV epidemic strains to infect human cells. Through the development of a new set of chimeric molecular clones, we demonstrated that virions containing BR15 structural proteins were much less efficient in cell-attachment when compared to MR766. These unexpected results revealed a negative effect of the structural proteins on target cell susceptibility to the epidemic strains infection. The low binding rate of BR15 structural proteins has further been associated with a significant alteration in viral growth in epithelial and neuronal cells, pointing to a previously unrecognized role of structural proteins in cell permissiveness to Zika epidemic strains infection. Importantly, infection with virions containing BR15 structural proteins was not abortive in neuronal cells but rather resulted in the establishment of a basal infection with minimal loss of cell viability over at least seven days. Thus, the low binding rate of epidemic strains may represent a fitness advantage in increasing ZIKV capacity to initiate persistent infection in human target cells.

Molecular determinant of differential binding rate

As the capsid proteins are not part of the viral envelope, it is unlikely that changes in this protein were responsible for the reduced cell-attachment of epidemic ZIKV strains. Conversely, it was interesting to determine which amino-acid substitution(s) located in prM and E proteins support this phenomenon.

When virions undergo complete maturation, the peptide "pr", which concentrates the majority of ZIKV prM mutations, is detached from the virion surface which thus only contains the M protein embedded in the lipid membrane. However, if partial maturation occurs the latter remains and covers the fusion peptide. The first study characterizing the structure of ZIKV¹⁵ (French Polynesian strain 2013), revealed the presence of ZIKV particles with an irregular surface

indicating the production of a population of virions displaying a variable degree of maturation. This phenomenon is common in Flaviviruses and provides a greater fitness to DENV by facilitating infection through a cross-reaction involving antibodies directed against prM. In our study it seems unlikely that differences in binding correlate with a lower pr-M cleavage efficiency since the sequence of the furin cleavage site is strictly conserved between ZIKV strains. However, it is not excluded that prM act as a putative receptor-binding protein involved in ZIKV entry. Given that seven of the ten mutated residues mapped on the prM surface exposed in immature conformation, it is plausible that the prM of epidemic strains has evolved a unique interaction surface which influences the susceptibility of the cells. However, our results suggest that if these residues do affect the virus ability to enter the epithelial and neural cells tested, they are of minor importance when compared to the contribution of E protein.

In a comprehensive study targeting ZIKV prM, we demonstrated that binding rate was mainly determined by the envelope protein. Considering that the E protein is the main component of the viral envelope, it has always been recognized as the main mediator of flavivirus attachment. Specific structural elements of E have been implicated in the interaction with cellular attachment factors and receptors, including glycan(s) and domain III. During our studies we were unable to determine which residue(s) support the differential binding of epidemic strains precisely, but our results allowed the exclusion of seven out of sixteen mutations. In particular, we demonstrated that the "IVNDTGH" motif, which contains the unique E-glycosylation site of ZIKV, appears not to be involved in the decreased attachment capacity of epidemic strains to epithelial cells (See below). Therefore, it is likely that one or more of the following mutations identified in EDIII will support this phenotype: V317I, I341V, V343A, and D393E. The D393E mutation is particularly intriguing because it modifies the viral receptor sequence located in the fusion gene loop of EDIII which is known critical for the infection of mammalian and mosquito cells. However, if this mutation seems highly relevant, other changes should not be neglected, including those located on internal sites of E dimers. As a matter of fact, it is worth noting that seemingly cryptic sites can also be involved in cellular attachment due to their exposure during virus breathing or through allosteric changes triggered by a first ligand.

Table 9: Zika virus counteraction of antiviral response

VIRAL RESPONSE	VIRAL PROTEIN INVOLVED	MOLECULAR ACTION AND CONSEQUENCES	REFERENCE
Counteraction to activation of type 1 IFN	NS1, NS2A, NS2B, NS4A, NS4B, NS5	Targeting RIG-I pathway	10,16,17
Inhibition of IFN β production	NS1, NS4A, NS4B, NS5	NS4A and NS5 inhibit IRF3 and NF κ B; NS1 inhibits IRF3 IFN β production through binding to TBK1	18
Inhibition of JAK/STAT pathway	NS5, NS2B-NS3	NS5 binds to STAT2 for its proteasomal degradation; NS2B-NS3 impairs JAK-STAT signaling pathway by degrading Jak1	19–21
Inhibition of STING pathway	NS2B-NS3	Suppresses STING-dependent induction of innate immune responses by cleaving STING	22
Selective activation of type II IF signaling	NS5	NS5 promotes the formation of STAT1/STAT1 homodimers and activates type II IFN for viral replication	10
Induction of cellular autophagy	NS4A, NS4B	Inhibit Akt-mediated mTOR pathway through Tor1/TSC1 and Tip41	23,24
Subversion of HO-1 antiviral activity	Unspecified	ZIKV non-structural proteins modulates HO-1 expression to limit its antiviral effect	25

Determinants of ZIKV virulence

With the tremendous scientific effort done since 2016, many mechanisms and facets of Zika virus biology and pathogenesis have been uncovered. While the whole puzzle of ZIKV virulence is still not yet fully unraveled, we have learnt a great deal about the properties that allow the virus to alter cell function and overcome the many barriers and inhibitory effects it encounters. In addition, it is now possible to associate specific ZIKV proteins, or even mutations, with these specialized functions (Tables 9 and 10). Among these proteins, three are of particular interest to me and appear to be decisive viral factors involved in ZIKV pathogenicity and/or epidemiological fitness.

Table 10: Overview of Zika virus-induced cellular pathogenesis

CELLULAR PATHOGENESIS	VIRAL PROTEIN INVOLVED	MOLECULAR ACTION AND CONSEQUENCES	REFERENCE
Manipulation of cell cycle	E	E protein causes cell cycle arrest with accumulation of human fetal NCSs in G0 phase	26
Genotoxic effect	<i>undetermined</i>	ZIKV infection suppress pathways involved in chromosome replication and DNA damage and repair in neurospheres	27–29
Modulation of microRNA circuitry	E	E causes upregulation of mir-1273g-3p and mir-204-3p in human fetal NSCs which directly target important developmental genes. i.e. PAX3 (specification, migration, and differentiation of neural crest cells) and NOTCH2 (maintenance of proliferative state and inhibiting NSCs differentiation)	26
Suppression of host protein activity	NS2B-NS3	NS2B-NS3 cleaves key host proteins including, autophagy-related protein 16-1 (ATG16L1), eukaryotic translation initiation factor 4 gamma 1 (eIF4G1) and Septin-2. ATG16L1 and eIF4G1 mediate type-II interferon production and host-cell translation, respectively. ZIKV protease cleavage of Septin-2 led to cytokinesis defects and cell death in neural progenitor.	30,31

The E-glycosylation: a key factor for a broad diffusion

The E protein of all contemporary epidemic ZIKV strains contains a unique N-glycosylation site at position N154. While the origin of this modification is debated within the scientific community because of the putative 156T mutation, several studies, including ours, aimed to determine its biological relevance. *In vitro* studies showed that ZIKV E N-glycosylation has differential effects on the infection of mosquito *versus* human cells. Indeed, if the ablation of E-glycosylation had little impact on the permissiveness of human cells lines used as model of epithelial, neuronal or blood-brain barrier cells, it significantly increased infection of mosquito larvae cells (C6/36 and CCL-125)^{32–34}. Interestingly, Fontes-Garfias *et al.*³⁵, conducted the mirror study to ours using

mosquito cells and reported that the loss of the glycosylation site (mutation N154Q) led to increased binding rate and improved infectivity of ZIKV mutant progeny. These results, opposite to those observed in human cells, underline the strong host-specific effect of E-glycosylation.

In contrast, *in vivo* studies showed that ZIKV E-glycosylation was required for the infection of *Ae. aegypti* due to its critical contribution for antagonizing the immune system during mosquito midgut invasion, via the suppression of ROS production^{34,35}. Such *in vitro* and *in vivo* divergences have previously been encountered in the study of other flaviviruses. For example, the suppression of N153 E-glycosylation reduced DENV-2 replication in C6/36 cells^{36,37} but not in *Ae. aegypti* mosquitoes intra-thoracically inoculated³⁸. In the case of WNV, the elimination of glycosylation did not affect its replication in C6/36 cells, but significantly jeopardized its transmission to *Culex* mosquitoes^{39,40}. These differences point the limitations of *in vitro* systems out which, due to the lack of cellular factors and complex immune systems, do not allow accurate assessment of the biological impact of mutations.

Finally, ZIKV envelope N-glycosylation has been shown to be a key determinant of ZIKV virulence and neurotropism in infected mice. While the lack of glycosylation did not affect ZIKV capacity to replicate in brain tissue upon intracranial inoculation, its ability to gain access to the brain was impaired by subcutaneous injection⁴¹. These results are similar to those previously described for WNV and suggest that N154 is a critical determinant of neuroinvasiveness by ZIKV as well⁴⁰. The mechanism by which ZIKV enters the central nervous system through the peripheral entry route remains to be determined. However, it is likely that the virus gains access to target neural tissue either as cell-free virus, through disruption of the blood-brain barrier for example, or through infected immune cells able to circumvent this latter. This possibility is supported by the fact that ZIKV is a potent infectious agent of plasmacytoid dendritic cells. These sentinel immune cells are present in the skin, the main entry route of ZIKV infection, but are also the main CNS-infiltrating dendritic cell population⁴². Based on our results, pDCs are not selectively permissive to infection with epidemic ZIKV strain. Nevertheless, it is conceivable that the attenuated phenotype of epidemic strains could substantially increase the risk of pDC infection *in vivo* by

promoting implantation of the virus at the portal of entry. On the other hand, we showed that BR15 strain induces a higher expression of the CCR7 receptor on the surface of pDCs. CCR7 is a migration marker which promotes pDC trafficking through interaction with the ligands CCL19 and CCL21⁴³. This mechanism is particularly involved in the migration of pDCs from infected to secondary lymphoid tissues due to their high expression level of CCR7 ligands⁴³. An interesting point to note, is that CCL19 and CCL21 are also expressed in the blood vessels of the CNS, albeit in smaller amounts⁴⁴. Therefore, it is possible that infected pDCs serve as a Trojan horse for ZIKV entry into the CNS by taking advantage of the ability of specific blood-brain barrier components to attract CCR7-expressing cells.

Finally, current knowledge suggests that ZIKV unique N-glycosylation site at position N154 is a key viral factor facilitating ZIKV accessibility to target tissues. Considering that all epidemic ZIKV strains share this property, it could be involved both in the pathogenicity of the virus in humans and in its outstanding epidemiological fitness. As a matter of fact, this post-translational modification seems to be an essential step for viral transmission via *Ae. aegypti*, the main vector of epidemic ZIKV strains, as well as for the invasion of mammalian brain.

Is there only one mutation in prM involved in microcephaly?

As outbreaks spread, the spectrum of ZIKV pathogenicity was gradually uncovered, associating contemporary ZIKV strains with severe neurological defects in infants born to infected mothers. These strains belong to the Asian lineage and derive from a common ancestor which probably arrived in Southeast Asia in the 1960s. Yet, given that ZIKV had been circulating in Southeast Asia for many years, some researchers wondered why microcephaly was not detected earlier. The most probable explanation – besides a potential effect of herd immunity or protective cross-reactivity between heterologous flaviviruses – was that ZIKV acquired some adaptive mutations which resulted in pathologic manifestations in human fetal brain. From this hypothesis, Yuan *et al.*⁴⁵ investigated the impact of a mutation that presumably arose during the 2013 outbreak and which was conserved in strains associated with severe neurological complication in humans: the prM S17N (also referred to as S139N). On the basis

of their results, the authors published a report entitled "A single mutation in the prM protein of Zika virus contributes to fetal microcephaly". But is it really the fact of a single mutation? Despite their attractive title, it quickly appears that S17N is unlikely to be the only determinant of this severe outcome; if so, the title would instead be "A single mutation in the prM protein of Zika virus is responsible for fetal microcephaly". However, it is conceivable that this mutation exacerbates this phenomenon.

In our study focusing on ZIKV prM we showed that this viral protein is correlated with the viral permissiveness of human brain glial cell SNB-19 and with ZIKV-induced cytopathic effect. Surprisingly, we demonstrated that "pr", the cleaved peptide product of prM, was associated with ZIKV BR15-induced growth restriction and lower apoptotic cell death in human cell lines, including glial, neuronal and microvascular endothelial brain cells. These cytopathic effects were in line with the hypothesis that epidemic strains of ZIKV cause microcephaly by blocking the proliferation of embryonic neuronal cells²⁶. In our model, we identified a cluster of 4 mutated amino acids, including A26P but not S17N, to be involved in the previously described cytopathogenic effects, suggesting that the acquisition of these four mutations could contribute to the attenuated phenotype of epidemic ZIKV strains. Other experiments involving overexpression of BR15 prM displaying the reverse mutation at residue 17 (N17S) did not affect cytopathic effect in SNB-19. Overall, the combination of these findings suggests that mutations in the "pr" domain increase ZIKV ability to damage cells of the central nervous system.

On the other hand, the conclusions of Yuan *et al.* relied on results obtained upon ZIKV intra-cranial injection in neonatal mice. As a result, the virus was directly inoculated into target tissues and thus overcame the placental barrier through an artificial means. In this way it would be important to determine which viral factors support the crossing of this barrier, and hence allow the expression of the property associated with the prM 17N mutation. Ultimately it seems more plausible that each of these mutations, instead of function as a sole switch, endows ZIKV with enhanced virulence properties which, when expressed collectively, lead to severe microcephaly.

188V: ZIKV boarding pass by NS1

Another critical site involved in the pathogenesis of ZIKV is probably the residue 188 of the NS1 protein. Flavivirus NS1 is a viral glycoprotein expressed in multiple oligomeric forms that binds to intracellular membranes or cell surfaces. This protein is also secreted in the extracellular medium as a soluble lipoparticle and generally accumulates at high levels in human tissues and sera. The secretion of NS1 protein into the host circulatory system is also required for the effective infection of vector mosquitoes with DENV-2 and JEV during their blood meal⁴⁶. Indeed, NS1 is a potent inhibitor of ROS production and the JAK-STAT pathway which thus greatly helps mosquito-borne flaviviruses to overcome the gut immune barrier of their vector. Therefore, it is likely that the abundant secretion of NS1 is an evolutionary trait developed by flaviviruses to adapt to their multiple host environments.

In the case of ZIKV, a study conducted on AG6 mice, showed that the NS1 level in the serum of animals infected with ZIKV GZ01 - a strain isolated from a patient returned from Venezuela to China in 2016 - is higher than the NS1 level in mice infected by the strain isolated in Cambodia in 2010. As the NS1 of the most recent epidemic ZIKV strains differs from the one of anterior Asian strains by the only A188V mutation, the function of this residue was evaluated in mosquito transmission models. Using a mutant of the Cambodian ZIKV strain, Liu et al.⁴⁷ showed that the substitution of alanine with valine (A188V) resulted in higher NS1 antigenemia and enhanced virus transmission from mice to mosquitoes. Indeed, the authors showed that 188V leads to a higher prevalence of ZIKV-carrying mosquitoes in both mouse-mosquito and mosquito-mouse-mosquito transmission model. Taken together, these results suggest an important role for 188V in NS1 antigenemia in humans, and ZIKV transmission from humans to the vector.

Interestingly, multiple sequence alignment of ZIKV NS1 revealed that the strains from the African lineage have a valine in position 188. In contrast, ZIKV sequences belonging to the Asian lineage prior to 2012 displayed an alanine, which was then substituted by a valine in ZIKV strains associated to massive outbreaks. This suggests that ZIKV Asian lineage evolved during its spread from

Southeast Asia to the South Pacific islands to recover an ancestral residue. As a result, it is likely that 188V has enabled African strains to maintain by highly efficient enzootic or epizootic transmission cycles, but failed to be expressed in humans due to factors that prevent the establishment of human infection cycle. Conversely, the resurgence of 188V in a variant of ZIKV already capable of effective urban transmission cycle may have improved ZIKV transmission efficiency and, thereby, the prevalence of ZIKV-infected mosquitoes as well. Considering that ZIKV was previously responsible for a localized outbreak in Micronesia in 2007, one can speculate that the recovery of 188V is a potential explanation for the re-emergence of ZIKV.

In addition, flavivirus NS1 is a highly active viral protein known to interfere with the immune system by antagonizing antiviral activities such as the complement cascade in mammals, for example^{48,49}. In this regard it is of particular interest to highlight that 188V is also involved in the restriction of RLR-induced IFN- β production due to its inhibitory effect on the phosphorylation of TBK1¹⁸. Such antiviral signaling subversion can greatly facilitate viral replication and, if effective in humans, can promote successful ZIKV infection and viremia. Overall, 188V may have contributed by its synergistic effects to the re-emergence and spread of ZIKV by promoting its transmission from both human hosts and vector mosquitoes. Thus, A188V reversion appears to be an important factor in the recent and severe ZIKV outbreaks.

Concluding remarks: Did Zika mutate to cause severe diseases in humans and outbreaks?

As previously mentioned in the introduction of this manuscript, emerging events are the result of the convergence of several factors. Thus, as a multifactorial process, the sole ZIKV genetic changes are obviously not sufficient to explain the scope of recent severe outbreaks. However, these latter are definitely one of the main drivers for me. According to my doctoral research and the findings of other teams, ZIKV has actually accumulated mutations which certainly increased its pathogenic properties and transmissibility in both humans and mosquitoes. Among them, it is striking to note that E-glycosylation and NS1 118V might have already been expressed in ancestral strains of ZIKV; yet not associated with

epidemic likely because the genetic and/or environmental context at that time was not propitious. To my mind, ZIKV pathogenicity arose from subtle but important changes that, instead of endow ZIKV with a novel absolute capacity, allow the expression of “dormant” properties. Nevertheless, one should keep in mind that if epidemic ZIKV strains acquired the potential to be virulent, this precise feature is not only the fact of the virus but rather the host. Indeed, cases of dizygotic twins born to ZIKV-infected mothers have demonstrated that individual genetic background greatly influences the severity and outcome of ZIKV infection, even when infected with the same strain⁵⁰. This rare and unique cohort showed that CZS can affect one, but not the other twin, highlighting the existence of a genetic basis for CZS susceptibility.

Finally, if the precise reasons underlying the dramatic emergence and rapid ZIKV spread worldwide may never be known, this phenomenon undoubtedly result from the synchronicity of genetic changes with environmental and human factors. As discussed throughout this manuscript, mounting studies support the hypothesis that viral genetic changes contributed to ZIKV dramatic emergence. Moreover, it is likely that the combined effect of these mutations has triggered the expression of ZIKV neurotropism in humans, by facilitating a broader diffusion and the establishment of a persistent infection. But if we did learn a great deal about ZIKV after more than 2 years of intensive research, not all the mechanisms explaining its pathogenicity in humans have been deciphered. For instance, while the biological processes involved in the development of ZIKV-induced microcephaly are globally well characterized, our understanding of how ZIKV infection causes disorders of the peripheral nervous system is still limited. In the same way, although vertical transmission is considered as a hallmark of ZIKV, the identification of viral determinants supporting this unexpected route of transmission remains a great scientific challenge. On the other hand, if the effervescence associated with Zika has considerably faded, we would – in my opinion – be wrong to neglect it twice. As with WNV, for which the development of persistent neuropsychological impairment subsequent to infection was only detected *a posteriori*, it is probable that Zika virus still holds some surprises. If so, and if our knowledge on the spectrum of ZIKV pathogenicity is actually only the tip of the iceberg, what is underneath?

Personal remarks

To my mind, our current understanding of ZIKV evolution is hampered by the lack of strains and early research which aimed to characterize Zika virus. As a perfect example, ZIKV proved how a neglected virus could suddenly become a serious threat to human health. Unfortunately, Zika case is not unique and several other viruses, such as Ebola, have also caused highly threatening epidemics before attracting the attention of politicians and researchers. In a surge of idealism, I often wondered how many cases of emergence would it take for funders to learn the lesson? Because, as I wrote in this manuscript introduction, this tardive awareness clearly affects the responsiveness of the scientific community and could easily be minimized if more research programs focusing on "outsiders" pathogens were valued. Apart from this negative aspect, the urgency of Zika crisis was an enthralling scientific challenge to which I am proud to have modestly contributed. While Zika virus had devastating consequences, it also demonstrated the colossal investigative and response potential that the scientific community can provide when mobilized. Obviously not all things were perfect, but Zika was at the heart of a remarkable collaborative and multidisciplinary work.

On a personal level, my "crush" on Zika has been confirmed throughout my doctoral research and I am glad of all the things I learned. With this virus and the long discussions with Philippe and other passionate virologists, my interest in (flavi)viruses and virology has not stopped growing. My PhD was a wonderful adventure either from a scientific or from a human perspective. For this reason, I wanted to end this manuscript by expressing my deep gratitude to my supervisors ; thanks to them and all the opportunities they gave me, I feel I have found the profession I am made for.

REFERENCE

1. Xie, D.-Y. *et al.* A single residue in the α B helix of the E protein is critical for Zika virus thermostability. *Emerg. Microbes Infect.* **7**, 5 (2018).
2. Sirohi, D. & Kuhn, R. J. Zika Virus Structure, Maturation, and Receptors. *J. Infect. Dis.* **216**, S935–S944 (2017).
3. Kostyuchenko, V. A. *et al.* Structure of the thermally stable Zika virus. *Nature* **533**, 425–428 (2016).
4. Brault, A. C. *et al.* A single positively selected West Nile viral mutation confers increased virogenesis in American crows. *Nat. Genet.* **39**, 1162–1166 (2007).
5. Tsetsarkin, K. A., Vanlandingham, D. L., McGee, C. E. & Higgs, S. A single mutation in chikungunya virus affects vector specificity and epidemic potential. *PLoS Pathog.* **3**, e201 (2007).
6. Sheridan, M. A. *et al.* African and Asian strains of Zika virus differ in their ability to infect and lyse primitive human placental trophoblast. *PLOS ONE* **13**, e0200086 (2018).
7. Simonin, Y., van Riel, D., Van de Perre, P., Rockx, B. & Salinas, S. Differential virulence between Asian and African lineages of Zika virus. *PLoS Negl. Trop. Dis.* **11**, (2017).
8. Dowall, S. D. *et al.* A Susceptible Mouse Model for Zika Virus Infection. *PLoS Negl. Trop. Dis.* **10**, e0004658 (2016).
9. Tripathi, S. *et al.* A novel Zika virus mouse model reveals strain specific differences in virus pathogenesis and host inflammatory immune responses. *PLoS Pathog.* **13**, e1006258 (2017).
10. Lazear, H. M. *et al.* A Mouse Model of Zika Virus Pathogenesis. *Cell Host Microbe* **19**, 720–730 (2016).
11. Rayner, J. O. *et al.* Comparative Pathogenesis of Asian and African-Lineage Zika Virus in Indian Rhesus Macaque's and Development of a Non-Human Primate Model Suitable for the Evaluation of New Drugs and Vaccines. *Viruses* **10**, (2018).
12. Koide, F. *et al.* Development of a Zika Virus Infection Model in Cynomolgus Macaques. *Front. Microbiol.* **7**, 2028 (2016).
13. Aid, M. *et al.* Zika Virus Persistence in the Central Nervous System and Lymph Nodes of Rhesus Monkeys. *Cell* **169**, 610–620.e14 (2017).
14. Hirsch, A. J. *et al.* Zika Virus infection of rhesus macaques leads to viral persistence in multiple tissues. *PLOS Pathog.* **13**, e1006219 (2017).
15. Sirohi, D. *et al.* The 3.8 Å resolution cryo-EM structure of Zika virus. *Science* aaf5316 (2016). doi:10.1126/science.aaf5316
16. Kumar, A. *et al.* Human Sertoli cells support high levels of Zika virus replication and persistence. *Sci. Rep.* **8**, 5477 (2018).
17. Rossi, S. L. *et al.* Characterization of a Novel Murine Model to Study Zika Virus. *Am. J. Trop. Med. Hyg.* (2016). doi:10.4269/ajtmh.16-0111
18. Xia, H. *et al.* An evolutionary NS1 mutation enhances Zika virus evasion of host interferon induction. *Nat. Commun.* **9**, 414 (2018).
19. Wu, Y. *et al.* Zika virus evades interferon-mediated antiviral response through the co-operation of multiple nonstructural proteins in vitro. *Cell Discov.* **3**, 17006 (2017).
20. Grant, A. *et al.* Zika Virus Targets Human STAT2 to Inhibit Type I Interferon Signaling. *Cell Host Microbe* **0**, (2016).
21. Hertzog, J. *et al.* Infection with a Brazilian isolate of Zika virus generates RIG-I stimulatory RNA and the viral NS5 protein blocks type I IFN induction and signaling. *Eur. J. Immunol.* **48**, 1120–1136 (2018).
22. Ding, Q. *et al.* Species-specific disruption of STING-dependent antiviral cellular defenses by the Zika virus NS2B3 protease. *Proc. Natl. Acad. Sci.* **115**, E6310–E6318 (2018).
23. Li, G. *et al.* Characterization of cytopathic factors through genome-wide analysis of the Zika viral proteins in fission yeast. *Proc. Natl. Acad. Sci. U. S. A.* (2017). doi:10.1073/pnas.1619735114

24. Liang, Q. *et al.* Zika Virus NS4A and NS4B Proteins Deregate Akt-mTOR Signaling in Human Fetal Neural Stem Cells to Inhibit Neurogenesis and Induce Autophagy. *Cell Stem Cell* **19**, 663–671 (2016).
25. El Kalamouni, C. *et al.* Subversion of the Heme Oxygenase-1 Antiviral Activity by Zika Virus. *Viruses* **11**, (2018).
26. Bhagat, R. *et al.* Zika virus E protein alters the properties of human fetal neural stem cells by modulating microRNA circuitry. *Cell Death Differ.* **25**, 1837–1854 (2018).
27. Ghouzzi, V. E. *et al.* ZIKA virus elicits P53 activation and genotoxic stress in human neural progenitors similar to mutations involved in severe forms of genetic microcephaly and p53. *Cell Death Dis.* **8**, e2567 (2017).
28. Garcez, P. P. *et al.* Zika virus disrupts molecular fingerprinting of human neurospheres. *Sci. Rep.* **7**, 40780 (2017).
29. Devhare, P., Meyer, K., Steele, R., Ray, R. B. & Ray, R. Zika virus infection dysregulates human neural stem cell growth and inhibits differentiation into neuroprogenitor cells. *Cell Death Dis.* **8**, e3106 (2017).
30. Hill, M. E. *et al.* The Unique Cofactor Region of Zika Virus NS2B-NS3 Protease Facilitates Cleavage of Key Host Proteins. *ACS Chem. Biol.* **13**, 2398–2405 (2018).
31. Li, H. *et al.* Zika Virus Protease Cleavage of Host Protein Septin-2 Mediates Mitotic Defects in Neural Progenitors. *Neuron* (2019). doi:10.1016/j.neuron.2019.01.010
32. Gong, D. *et al.* High-Throughput Fitness Profiling of Zika Virus E Protein Reveals Different Roles for Glycosylation during Infection of Mammalian and Mosquito Cells. *iScience* **1**, 97–111 (2018).
33. Mossenta, M., Marchese, S., Poggianella, M., Slon Campos, J. L. & Burrone, O. R. Role of N-glycosylation on Zika virus E protein secretion, viral assembly and infectivity. *Biochem. Biophys. Res. Commun.* (2017). doi:10.1016/j.bbrc.2017.01.022
34. Wen, D. *et al.* N-glycosylation of Viral E Protein Is the Determinant for Vector Midgut Invasion by Flaviviruses. *mBio* **9**, e00046–18 (2018).
35. Fontes-Garfias, C. R. *et al.* Functional Analysis of Glycosylation of Zika Virus Envelope Protein. *Cell Rep.* **21**, 1180–1190 (2017).
36. Lee, E., Leang, S. K., Davidson, A. & Lobigs, M. Both E protein glycans adversely affect dengue virus infectivity but are beneficial for virion release. *J. Virol.* **84**, 5171–5180 (2010).
37. Mondotte, J. A., Lozach, P.-Y., Amara, A. & Gamarnik, A. V. Essential role of dengue virus envelope protein N glycosylation at asparagine-67 during viral propagation. *J. Virol.* **81**, 7136–7148 (2007).
38. Bryant, J. E. *et al.* Glycosylation of the dengue 2 virus E protein at N67 is critical for virus growth in vitro but not for growth in intrathoracically inoculated *Aedes aegypti* mosquitoes. *Virology* **366**, 415–423 (2007).
39. Moudy, R. M., Zhang, B., Shi, P.-Y. & Kramer, L. D. West Nile virus envelope protein glycosylation is required for efficient viral transmission by *Culex* vectors. *Virology* **387**, 222–228 (2009).
40. Beasley, D. W. C. *et al.* Envelope protein glycosylation status influences mouse neuroinvasion phenotype of genetic lineage 1 West Nile virus strains. *J. Virol.* **79**, 8339–8347 (2005).
41. Annamalai, A. S. *et al.* Zika Virus Encoding Nonglycosylated Envelope Protein Is Attenuated and Defective in Neuroinvasion. *J. Virol.* **91**, e01348–17 (2017).
42. Zozulya, A. L., Clarkson, B. D., Ortler, S., Fabry, Z. & Wiendl, H. The role of dendritic cells in CNS autoimmunity. *J. Mol. Med. Berl. Ger.* **88**, 535–544 (2010).
43. Seth, S. *et al.* CCR7 Essentially Contributes to the Homing of Plasmacytoid Dendritic Cells to Lymph Nodes under Steady-State As Well As Inflammatory Conditions. *J. Immunol.* **186**, 3364–3372 (2011).
44. Bielecki, B., Jatczak-Pawlik, I., Wolinski, P., Bednarek, A. & Glabinski, A. Central Nervous System and Peripheral Expression of CCL19, CCL21 and Their Receptor CCR7 in Experimental Model of Multiple Sclerosis. *Arch. Immunol. Ther. Exp. (Warsz.)* **63**, 367–376 (2015).

45. Yuan, L. *et al.* A single mutation in the prM protein of Zika virus contributes to fetal microcephaly. *Science* eaam7120 (2017). doi:10.1126/science.aam7120
46. Liu, J. *et al.* Flavivirus NS1 protein in infected host sera enhances viral acquisition by mosquitoes. *Nat. Microbiol.* **1**, 16087 (2016).
47. Liu, Y. *et al.* Evolutionary enhancement of Zika virus infectivity in *Aedes aegypti* mosquitoes. *Nature* **545**, 482–486 (2017).
48. Rastogi, M., Sharma, N. & Singh, S. K. Flavivirus NS1: a multifaceted enigmatic viral protein. *Virol. J.* **13**, (2016).
49. Chen, S., Wu, Z., Wang, M. & Cheng, A. Innate Immune Evasion Mediated by Flaviviridae Non-Structural Proteins. *Viruses* **9**, 291 (2017).
50. Caires-Júnior, L. C. *et al.* Discordant congenital Zika syndrome twins show differential in vitro viral susceptibility of neural progenitor cells. *Nat. Commun.* **9**, 475 (2018).

ANNEX

Viruses 2018, 10(5), 233; <https://doi.org/10.3390/v10050233>

PROBING MOLECULAR INSIGHTS INTO ZIKA VIRUS-HOST INTERACTIONS

Ina Lee¹, **Sandra Bos**², Ge Li ¹, Shusheng Wang¹, Gilles Gadea², Philippe Desprès²
and Richard Y. Zhao^{1,3,4,5,*}

1 Department of Pathology, University of Maryland School of Medicine, Baltimore, MD 21201, USA

2 Université de la Réunion, INSERM U1187, CNRS UMR 9192, IRD UMR 249, Unité Mixte Processus Infectieux en Milieu Insulaire Tropical, Plateforme Technologique CYROI, 94791 Sainte Clotilde, La Réunion, France

3 Department of Microbiology and Immunology, University of Maryland School of Medicine, Baltimore, MD 21201, USA

4 Institute of Global Health, University of Maryland School of Medicine, Baltimore, MD 21201, USA

5 Institute of Human Virology, University of Maryland School of Medicine, Baltimore, MD 21201, USA

**Author to whom correspondence should be addressed.*

Received: 5 April 2018 / Revised: 26 April 2018 / Accepted: 28 April 2018 / Published: 2 May 2018

Review

Probing Molecular Insights into Zika Virus–Host Interactions

Ina Lee ¹, Sandra Bos ² , Ge Li ¹, Shusheng Wang ¹, Gilles Gadea ² , Philippe Desprès ² and Richard Y. Zhao ^{1,3,4,5,*}

¹ Department of Pathology, University of Maryland School of Medicine, Baltimore, MD 21201, USA; ilee1@umm.edu (I.L.); GLi@som.umaryland.edu (G.L.); shushengwang018@gmail.com (S.W.)

² Université de la Réunion, INSERM U1187, CNRS UMR 9192, IRD UMR 249, Unité Mixte Processus Infectieux en Milieu Insulaire Tropical, Plateforme Technologique CYROI, 94791 Sainte Clotilde, La Réunion, France; sandrabos.lab@gmail.com (S.B.); gilles.gadea@inserm.fr (G.G.); philippe.despres@univ-reunion.fr (P.D.)

³ Department of Microbiology and Immunology, University of Maryland School of Medicine, Baltimore, MD 21201, USA

⁴ Institute of Global Health, University of Maryland School of Medicine, Baltimore, MD 21201, USA

⁵ Institute of Human Virology, University of Maryland School of Medicine, Baltimore, MD 21201, USA

* Correspondence: rzhao@som.umaryland.edu; Tel: +1-410-706-6301

Received: 5 April 2018; Accepted: 28 April 2018; Published: 2 May 2018



Abstract: The recent Zika virus (ZIKV) outbreak in the Americas surprised all of us because of its rapid spread and association with neurologic disorders including fetal microcephaly, brain and ocular anomalies, and Guillain–Barré syndrome. In response to this global health crisis, unprecedented and world-wide efforts are taking place to study the ZIKV-related human diseases. Much has been learned about this virus in the areas of epidemiology, genetic diversity, protein structures, and clinical manifestations, such as consequences of ZIKV infection on fetal brain development. However, progress on understanding the molecular mechanism underlying ZIKV-associated neurologic disorders remains elusive. To date, we still lack a good understanding of; (1) what virologic factors are involved in the ZIKV-associated human diseases; (2) which ZIKV protein(s) contributes to the enhanced viral pathogenicity; and (3) how do the newly adapted and pandemic ZIKV strains alter their interactions with the host cells leading to neurologic defects? The goal of this review is to explore the molecular insights into the ZIKV–host interactions with an emphasis on host cell receptor usage for viral entry, cell innate immunity to ZIKV, and the ability of ZIKV to subvert antiviral responses and to cause cytopathic effects. We hope this literature review will inspire additional molecular studies focusing on ZIKV–host Interactions.

Keywords: zika virus; ZIKV–host interactions; viral pathogenesis; cell surface receptors; antiviral responses; viral counteraction; cytopathic effects; microcephaly; ZIKV-associated neurologic disorders

1. Introduction

1.1. The Zika Virus (ZIKV): An Emerging Public Health Threat

The 2015 Zika virus (ZIKV) epidemic in the Americas surprised the world because of its rapid global spread and the findings that it associates with various neurologic disorders including microcephaly in newborns and Guillain–Barré syndrome (GBS) in adults. ZIKV was thought to be a mild virus that had little or no threat to humans. Through studies of this new ZIKV pandemic, we have now learned that ZIKV is a rather severe human pathogen that can cause significant neuropathology such as fetal microcephaly, GBS, and various other congenital neurologic and ocular disorders [1–5].

So, it begs the question of what has transformed a benign ZIKV over the past seventy years to generate the contemporary pathogenic ZIKV.

The goal of this article is to review the current literature on ZIKV–host interactions with a focus on molecular aspects. We herein summarize insights on host cell receptor usage for viral entry, cell innate immunity to ZIKV, and the ability of ZIKV to subvert antiviral responses and to cause cytopathic effects. The molecular mechanisms underlying these ZIKV–host interactions, and their potential impacts on ZIKV-induced fetal microcephaly or other neurologic disorders are discussed.

1.2. The Organization of Zika Virus

ZIKV belongs to the *flavivirus* genus of the *Flaviviridae* family which includes a number of medically important arboviruses such as Dengue Virus (DENV), Japanese Encephalitis Virus (JEV), and West Nile Virus (WNV). Structurally, ZIKV is similar to other flaviviruses. The nucleocapsid is approximately 25–30 nm in diameter, surrounded by a host membrane-derived lipid bilayer that contains envelope (E) and membrane (M) proteins. The virus particle is approximately 40–65 nm in diameter, with surface projections that measure roughly 5–10 nm [6], leading to an overall average size of 45–75 nm. The surface proteins are arranged in an icosahedral-like symmetry [7]. Like its flaviviral siblings, ZIKV contains a positive sense single-stranded RNA [ssRNA(+)] viral genome of approximately 10.7 kilobases (kb) (Figure 1). The genomic RNA is flanked by two terminal non-coding regions (NCR), i.e., the 5' NCR (107 nt) and the 3' NCR (428 nt) [8]. The ZIKV genome includes a single large open reading frame encoding a polyprotein of about 3300 amino acids, which is processed co- and post-translationally by viral and host proteases (PRs) to produce a total of fourteen immature proteins, mature proteins, and small peptides [9]. A total of ten mature viral proteins, i.e., three structural proteins (C, M, and E) and seven nonstructural (NS1, NS2A, NS2B, NS3, NS4A, NS4B, and NS5) proteins are produced after viral processing [6,9,10]. The 2K signal peptide, which is situated between NS4A and NS4B, plays a regulatory role in viral RNA synthesis and viral morphogenesis in other flaviviruses [11,12]. Among the structural proteins, the mature capsid (C) protein is produced by cleavage of the anchor-C (anaC) protein by a viral PR (anaC→C), which in turn triggers the cleavage of the precursor membrane (prM) protein by the host protease Furin. As a result, a mature membrane (M) protein and a Pr protein are produced (PrM→M + Pr) [11,13]. In the case of DENV, noninfectious and immature viral particles contain prM that forms a heterodimer with the E protein [14]. The transition of prM to M by Furin cleavage results in mature and infectious particles [15,16]. The E protein, composing the majority of the virion surface, is involved in binding to the host cell surface and triggering subsequent membrane fusion and endocytosis [8]. Post-translational processing of the non-structural protein region produces four viral enzymes, i.e., PR, helicase, methyl-transferase, and RNA-dependent RNA polymerase (RdRP). A fully active ZIKV PR consists of two protein components, namely the N-terminal domain of NS3 (NS3pro) and a membrane-associated NS2B cofactor [17,18]. The NS3pro is responsible for proteolytic processing of the viral polyprotein, whereas the NS2B cofactor is required for enhancing enzymatic activity and substrate specificity. The C-terminal domain of NS3 protein produces ZIKV helicase, which plays a critical role in NTP-dependent RNA unwinding and translocation during viral replication [19]. The methyl-transferase and RdRP are generated from the N-terminal and C-terminal of NS5, respectively. NS1, NS3, and NS5 are large proteins that are highly-conserved [6]. NS2A, NS2B, NS4A, and NS4B proteins are smaller, hydrophobic proteins [6]. The 3' NCR forms a loop structure that may play a role in translation, RNA packaging, cyclization, genome stabilization and recognition [8]. The 5' NCR allows translation via a methylated nucleotide cap or a genome-linked protein [7]. In addition, ZIKV produces abundant non-coding subgenomic flavivirus RNA (sfRNA) from the 3'UTR in infected cells, which may play a role in the viral life cycle and viral subversion of innate immunity [20].

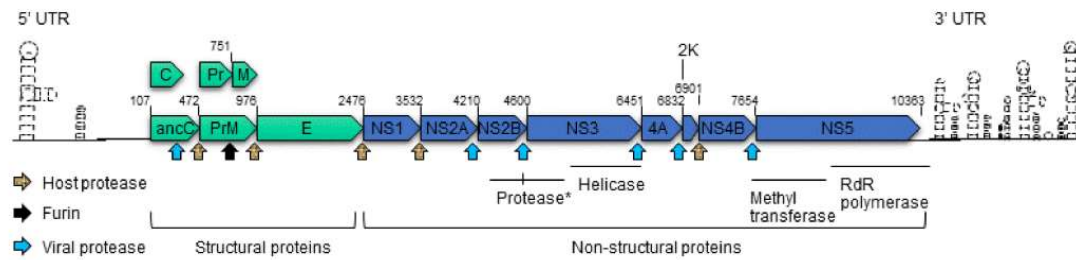


Figure 1. Schematic structure of the Zika virus genome. Each of the viral proteins is drawn based on the relative orientation in the RNA genome. The ZIKV viral protease, host protease and Furin protease are represented by different arrows, as shown. Each arrow points to the specific protease cleavage site. The numbers shown above each protein product indicate the start/end position. Abbreviations: ancC, anchored capsid protein C; C, capsid protein C; prM, precursor membrane protein; M, membrane protein; Pr, protein pr; E, envelope protein; NS, nonstructural protein; *, protease consists of N-terminal of NS3 and C-terminal NS2B as described in the text. C-terminal of NS3 encodes helicase; 2K, signal peptide 2K; NS5 encodes methyltransferase at its N-terminal end and RNA-dependent RNA (RdR) polymerase at its C-terminal end. UTR, untranslated region. The structures of 5' UTR and 3' UTR are based on [21]. The information of ZIKV protein products is based on [9].

1.3. The Infectious Cycle of ZIKV and Human Transmission

The ZIKV infectious cycle starts with the virus binding to host cell surface receptors and attachment factors via the E protein, leading to clathrin-dependent endocytosis. Internalized virus particles fuse with the endosomal membrane in a pH-dependent manner, releasing the genomic RNA into the cytoplasm of the host cell. The positive-sense viral genomic ssRNA is translated into a polyprotein that is subsequently cleaved to form structural and non-structural proteins. Viral replication takes place in intracellular membrane-associated compartments located on the surface of the endoplasmic reticulum (ER), resulting in a dsRNA genome synthesized from the genomic ssRNA(+) by viral RdRP. The dsRNA genome is subsequently transcribed and replicated, resulting in additional viral mRNAs/ssRNA(+) genomes. Immature virus particles are assembled within ER. They are then transported through the trans-Golgi network (TGN) where the fully mature infectious virus particles are formed as soon as prM is processed to M by a Furin-like protease. The new virus particles are released into the extracellular environment where they move on to a new infectious life cycle [7].

ZIKV is an arbovirus that is primarily transmitted to mammalian hosts by mosquito vectors from the *Aedes* (*Ae.*) genus including *Ae. africanus*, *Ae. aegypti*, *Ae. vitattus*, *Ae. furcifer*, *Ae. apicoargenteus*, and *Ae. luteocephalus* [22,23]. The incubation time for ZIKV in mosquito vectors is approximately 10 days [22]. Blood contact via blood transfusion or sexual contact is another route of ZIKV infection [24–26]. Consistent with this notion, human testis has been found to be a reservoir for ZIKV [22,27–29]. In addition, ZIKV can also be transmitted vertically from mother to child via placenta–fetal transmission [30,31]. This has become a main route for the development of fetal microcephaly [32,33].

1.4. A Brief History of ZIKV

The first ZIKV strain was isolated in 1947 from caged monkeys in the Zika forest of Uganda, Africa. A ZIKV strain MR766 (ZIKV_{MR766}) from that isolation was established and has been used since for research purpose [34]. Therefore, the ZIKV_{MR766} is often referred to as the historical or ancestral ZIKV strain. Initial characterization of ZIKV_{MR766} showed that it is highly neurotropic in mice, and no virus has been recovered from tissues other than the brains of infected mice [35]. That report further showed that mice at all ages were susceptible to ZIKV_{MR766} by intracerebral inoculations. In contrast, cotton-rats, Guinea pigs, and rabbits showed no sign of ZIKV_{MR766} infection by using the same intracerebral inoculations. Monkeys showed either mild fever (pyrexia) or no signs of infection.

Interestingly, mice younger than two weeks were highly susceptible to intraperitoneal inoculation, whereas mice older than two weeks can rarely be infected by the same route of intraperitoneal injection [35], suggesting established blood-brain barriers in the older mice may prevent ZIKV from accessing the brain.

In a different study, the effect of ZIKV infection on the central nervous system (CNS) of mice was examined by using intracerebral inoculation [36]. Histologic H & E staining showed that ZIKV infects the Ammon's horn (hippocampus proper) area of seven-day-old mouse brain. Detailed examination suggested that ZIKV infected pyriform cells of the Ammon's horn and induced hyperchromatic debris in those cells, suggesting possible DNA or chromosomal aberration. In addition, ZIKV induced gross enlargement (hypertrophy) of astroglial cells of the Ammon's horn, but had little effect on microglial cells of the same area [36]. Ultra-structural studies by electron microscopy (EM) further revealed that ZIKV replicates exclusively in the ER compartment of astroglial cells and neurons, an indication of membrane-associated viral replication [36].

Those early findings in the mouse model suggest that (1) ZIKV is a neurotropic virus with preference to embryonic brains [34,35], (2) ZIKV specifically infect astroglial cells and pyriform cells in the Ammon's horn, and (3) ZIKV primarily replicates in the ER network [36]. At the cellular level, ZIKV appeared to induce gross cell enlargement, chromosomal or DNA aberrations, and mitochondrial dysfunction [36]. Although early data showed that ZIKV was pathogenic to mice, there was no indication that ZIKV was pathogenic to humans [35]. Therefore, some types of virological change are likely to have taken place during the viral evolution in the past seventy years, leading to pathogenic ZIKV infection of humans.

The first ZIKV infection in human was documented in 1952 [34], and the virus was subsequently isolated from human hosts in Nigeria in 1968 [22]. Since then, multiple studies have confirmed the presence of ZIKV antibodies in human sera from a number of countries in Africa and Asia [22]. However, no severe diseases were clearly linked to those infections. In the recorded history, ZIKV infection appears to have migrated eastward from Africa. A number of outbreaks have taken place over the past seventy years including several minor outbreaks in 1977–1978 in Pakistan, Malaysia, and Indonesia. Two major outbreaks were documented in Yap Island of Micronesia in 2007, and in French Polynesia, New Caledonia, the Cook Islands, and Easter Island in 2013 and 2014 [26,37]. The affected individuals in those outbreaks were in the order of hundreds to thousands. However, in the most recent outbreak, ZIKV infection had been reported in eighty-five countries, territories, or subnational areas with an estimate of over 1.5 million affected individuals according to the World Health Organization (WHO). Brazil was the most affected country, with an estimated 440,000 to 1.3 million cases reported through December of 2015.

Although human ZIKV infection is mostly self-limiting, manifestations of neurological disorders such as GBS became increasingly apparent during the recent outbreaks in French Polynesia and Brazil [32,38]. The number of microcephaly in newborns also increased dramatically, which for the first time indicated a possible link between ZIKV infections and fetal malformations [32,39,40]. More than 4700 suspected cases of microcephaly were reported from mid-2015 through to January 2016 [41], spurring an unprecedented and world-wide effort to unravel this mystery. By March of 2016, the causal relationship between microcephaly in newborn and ZIKV infection was first established [32,39,40]. By April of 2016, a total of 3530 newborns with confirmed microcephaly were reported. In the same year, WHO declared an international public health emergency. In-depth research now shows that ZIKV infection is also associated with a number of other congenital and ocular diseases [1,2].

1.5. What Has Been Learned from the Recent ZIKV Break?

We have learned a great deal about the ZIKV and its etiology through the above described studies. The knowledge we have gained is that fetal microcephaly and other congenital malformations can indeed be caused by ZIKV infection [32,42,43]. Furthermore, those circulating and pathogenic ZIKV strains are most likely derived from the Asian lineage [44,45]. The Asian lineage is likely evolved

from the African lineage through viral gene mutations by adaptation of higher cytopathicity that led to enhanced viral pathogenicity. Particular efforts have been put to investigate whether the emergence of new ZIKV epidemic strains was associated with accumulation of specific mutations that would be the leading cause of increased pathogenic effects [44–46]. Also, investigations have been conducted to determine whether pathogenic strains of ZIKV could preferentially infect certain human tissues or cells, especially neural progenitor cells (NPCs) in the brain, or they have acquired greater virulence through accumulated effects of ZIKV gene mutations [47–49]. The antibody-dependent enhancement (ADE) may also contribute to the acquired virulence [50]. This scenario could occur if individuals have previously been exposed to other flaviviruses and have acquired antibodies that partially cross-react with ZIKV. Instead of neutralizing ZIKV, these antibodies could paradoxically augment ZIKV infectivity [50]. As a matter of fact, the opposite scenario has been observed in which pre-exposure of ZIKV was associated with enhanced DENV-2 infection *in vitro* [51] and in monkeys [52]. Therefore, enhanced ZIKV infection as the result of prior exposure of other flaviviral infection could certainly be feasible [53–56]. However, ADE is less likely to be the predominant mode of enhanced ZIKV pathogenicity in the recent break since ZIKV is known to cause fetal microcephaly in the absence of antibody response to other flaviviruses. We should also be mindful that despite these theories, we cannot exclude another possibility that ZIKV-induced microcephaly may not be the result of ZIKV evolution, but rather a reflection of the advanced technology in disease monitoring and diagnosis. In other words, microcephaly is intrinsic to all ZIKV strains but its evasion from public awareness could be due to the lack of sensitive detection methods in the past. This possibility may not totally be far-fetched, insofar that the very first ZIKV isolate, ZIKV_{MR766}, also induced microcephaly in animal and human brain-specific organoid models [40,43,57]. In fact, both African and Asian ZIKV strains (MR766, FSS13025, PF/2013/KD507, SZ01, and various epidemic Brazilian strains, e.g., ZIKV-BR/2015), have been shown to induce microcephaly-like phenotypes in animal and human brain-specific organoid models (Table 1) [40,43,57–59]. Nevertheless, virological activities of the ancestral ZIKV_{MR766} did appear to be different from Asian lineage in embryonic mouse brains [60]. Therefore, as it says that the devil is in the detail. It is very likely that the neurological defects caused by the epidemic Brazilian ZIKV in humans were attributed by subtle but important virological changes. Those newly adapted virological changes could include preferable infection to certain brain and neural cells such as hNPCs, persistent viral replication in host cells, and enduring neuropathic damages that lead to those observed ZIKV-associated neurological disorders. Further and detailed dissections of those virological traits certainly are warranted.

In short, even though we have learned a great deal about the ZIKV etiology, much still remains unknown. Some of the critical questions include; (1) what type of virological changes have taken place to result in increased viral pathogenicity, (2) which ZIKV protein(s) is responsible for the enhanced viral pathogenicity, and (3) how do the newly adapted ZIKV strains alter their interactions with host cells that lead to those neurologic defects? In particular, the specific mechanisms underlying the molecular actions of ZIKV-mediated neurologic disorders such as microcephaly and other neurologic disorders need to be thoroughly investigated.

Table 1. Zika viral strains that are known to cause microcephaly or microcephaly-like phenotypes.

ZIKV Strain	Model Used	Host/Location/Year	Microcephaly-Like Phenotypes	Reference
Human fetal tissue or organoid models				
MR766	Human brain-specific organoids	Rhesus monkey/Uganda/1947	Increased cell death and reduced proliferation, resulting in decreased neuronal cell-layer volume resembling microcephaly.	[40]
MR766	Human neurospheres and organoids	Rhesus monkey/Uganda/1947	Growth impairment of neurospheres and organoids	[43]
MR766	Human cerebral organoids	Rhesus monkey/Uganda/1947	Reduction of organoid growth and volume reminiscent of microcephaly via induction of TLR3	[57]
FSS 13025	Human brain-specific organoids	Human/Cambodia/2010	Increased cell death and reduced proliferation, resulting in decreased neuronal cell-layer volume resembling microcephaly.	[40]
ZIKV(BR)	Human organoids	Human/Brazil/2015	Reduction of proliferative zones and disrupted cortical layers; induction of apoptosis, autophagy and impaired neurodevelopment	[59]
KU527068	Aborted human fetal brain	Human/Brazil/2016	Microcephaly with calcification in the fetal brain and placenta	[32]
FB_GWUH	Aborted human fetal brain	Human/USA/2016	Fetal brain abnormalities with diffuse cerebral cortical thinning	[39]
Mouse models				
PF/2013/KD507	Mouse	Human/French Polynesia/2013	Fetal demise or intrauterine growth restriction	[33]
ZIKV(BR)	Mouse	Human/Brazil/2015	Intrauterine growth restriction, including signs of microcephaly and vertical transmission	[59]
SZ01	Mouse vertical transmission	Human/Samoa/2016	Infection of radial glia cells of dorsal ventricular zone of the fetuses resulting in reduced cavity of lateral ventricles and decreased cortical surface area	[40]
SZ01	Embryonic mouse brain	Human/Samoa/2016	Cell cycle arrest, apoptosis, and inhibition of NPC differentiation, resulting in cortical thinning and microcephaly	[61]
CAM/2010AndVEN/2016	Neonatal mouse brain	Human/Cambodia/2010 Human/Venezuela/2016	Neonatal ZIKV infection of VEN/2016 leads to more severe microcephaly than CAM/2010. VEN/2016 strain infection leads to stronger immune response, more severe calcification, more neuronal death and abolished oligodendrocyte development, but less activation of microglial cells.	[62]

Viral pathogenicity is normally referred to the state of a virus and its ability to cause disease. The attributes of viral pathogenicity are often constituted by the target of organ, tissue, and cells (cell tropism), the level and persistence of viral replication in host cells, and the ability of the virus to cause damage to host cells that is referred to as cytopathic effects (CPEs). Both historical and contemporary ZIKV strains have the capacity to replicate in brain-specific neuronal cells [34]. However, so far, only the epidemic strains were associated to congenital fetal microcephaly and other neurologic disorders, highlighting that viral factors other than the cell tropism are more likely contributing to the increased viral pathogenicity. Furthermore, multifactorial viral functions might have contributed to those ZIKV-associated diseases. Conceivably, it could be the changing balance in ZIKV–host interactions that leads to favorable and persistent ZIKV viral replication in host cells such as hNPCs, increased and lasting CPEs that ultimately contribute to those observed fetal development and neurologic disorders. In the following sections, we will discuss the molecular aspects of ZIKV–host interactions, which include (1) host target cells and cell surface receptors for viral entry, (2) host cellular and immune responses to ZIKV replications, (3) counteracting effects of ZIKV to host antiviral responses, and (4) ZIKV-induced cytopathic effects (restricted cell growth, cell cycle dysregulation, and cell death/apoptosis) that are all known contributing factors to fetal brain development and neurologic impairments [42,57,61].

2. Cellular Targets and Viral Entry

2.1. Cellular Targets

ZIKV primarily infects NPCs in embryonic brains [42,61,63]. In the adult brain, it also infects astroglial and microglial cells, and to lesser extent, neurons [36,42]. In addition, ZIKV infects other tissues such as skin (including dermal fibroblasts and epidermal keratinocytes), testis, and placenta (Table 2). As an arbovirus, ZIKV transmission is predominately through skin by mosquitoes such as *Ae. aegypti* and *Ae. africanus* [22,23]. Consistent with this route of transmission, immature and mature dendritic cells are susceptible to ZIKV infection [64–66]. ZIKV can also be transmitted through sexual contacts [24–26]. Infected Sertoli cells in human testis are known ZIKV reservoirs [27–29]. Several placenta-specific cells have been shown to be prone to ZIKV infection including Hofbauer cells, trophoblasts, and placental endothelial cells, supporting an important role of the placenta in transmitting ZIKV via blood to fetal brains [33,67,68]. In line with the idea that crossing the blood–brain barrier might be required to transmit the virus to the brain compartment [35], ZIKV persistently infects primary human brain microvascular endothelial cells (hBMECs) or established cell lines [69]. Interestingly, a hepatoma cell line Huh-7 appears to be highly permissive to ZIKV infection. However, liver has not yet been documented to be the target organ of ZIKV, even though DENV is well-known to infect liver [70,71].

2.2. The Cellular Receptors for ZIKV Entry

Flaviviruses enter host cells by clathrin-dependent endocytosis, which is initiated when viral particles interact with cell surface receptors. The cell surface receptors bind to the infectious viral particles and direct them to the endocytic pathway. Several cell surface receptors facilitate ZIKV viral entry (Table 2), which include the tyrosine-protein kinase receptor AXL, Tyro3, DC-SIGN, and TIM-1 [64,65]. AXL and Tyro3 are part of the TAM receptor tyrosine kinase family that normally binds to Gas6 and Pros1 ligands. These receptors are known to regulate an array of cellular activities including cell adhesion, migration, proliferation, and survival, as well as the release of inflammatory cytokines, which play pivotal roles in innate immunity [72]. DC-SIGN is an innate immune receptor present on the surface of both macrophages and dendritic cells (DCs). It recognizes a broad range of pathogen-derived ligands and mediates antigen uptake and signaling [73]. The TIM-1 receptor, also known as HAVcr-1 (Hepatitis A virus cellular receptor 1), plays an important role in host response to viral infection.

Even though all of the aforementioned cell surface receptors participate in ZIKV viral entry, they are not unique to ZIKV infection. For example, AXL, Tyro3, and DC-SIGN are used by Lassa virus [74]. The TIM-1 receptor mediates infections of the deadly Ebola virus [75]. In fact, both TAM and TIM families of phosphatidylserine receptors also mediate viral entry of other flaviviruses such as DENV [76] and WNV [77]. For instance, in the case of DENV, TIM receptors facilitate viral entry by directly interacting with virus-associated phosphatidylserine, whereas TAM-mediated infection relies on indirect viral recognition, in which the TAM ligand Gas6 acts as a bridging molecule by binding to phosphatidylserine within the viral particle [76]. Reviews of this topic can be found in [78,79].

Involvement of AXL, Tyro3, DC-SIGN, and, to a lesser extent, TIM-1 was initially described by Hamel et al. when they studied ZIKV entry in skin cells [64]. AXL was subsequently shown to be a prime target receptor for ZIKV viral entry in a variety of cell types including human endothelial cells (hECs) [61], neural stem cells [80], microglia and astrocytes [81], and oligodendrocyte precursor cells [82]. Examination of the AXL expression levels of diverse cell types suggests that AXL is highly expressed on the surface of human radial glial cells, astrocytes, hECs, oligodendrocyte precursor cells, and microglia in the developing human cortex as well as in progenitor cells of the developing retina [80,82]. Other ZIKV permissive and non-neuronal human cell types, which are known to express AXL, Tyro3, and/or TIM1 and likely to mediate viral entry, include placental cells, explants-cytotrophoblasts, endothelial cells, fibroblasts, and Hofbauer cells in chorionic villi as well as amniotic epithelial cells and trophoblast progenitors in amniochorionic membranes [83].

The susceptibility of human ECs to ZIKV positively correlates with the cell surface levels of AXL [61]. Gain- and loss-of-function tests revealed that AXL is required for ZIKV entry at a post-binding step, and small-molecule inhibitors of the AXL kinase significantly reduced ZIKV infection of hECs [61]. In human microglia and astrocytes of the developing brain, like DENV, AXL-mediated ZIKV entry requires the AXL ligand Gas6 to serve as a bridge linking ZIKV particles to glial cells [81]. Following binding, ZIKV is internalized through clathrin-mediated endocytosis and is transported to Rab5+ endosomes to establish productive infection. Downregulation of AXL by an AXL inhibitor R428 or an AXL decoy receptor MYD1 significantly reduced but did not abolish the ZIKV infection, suggesting the AXL receptor might be the primary but not the only receptor that is required for ZIKV infection [81]. Genetic knockdown of AXL in a glial cell line nearly abolished ZIKV infection [82]. It should be mentioned that elimination of any known entry receptor does not result in complete protection from viral infection, as flaviviruses use many different receptors, there is always redundancy and alternatives.

Interestingly, genetic ablation of the AXL receptor by CRISPR/CAS9 did not protect hNPCs and cerebral organoids from ZIKV Infection [84]. In particular, genetic ablation of AXL has no effect on ZIKV entry or ZIKV-mediated cell death in human induced pluripotent stem cell (iPSC)-derived NPCs or cerebral organoids. It is not yet clear what contributes to the observed discrepancy between this and other studies. One possibility is that ZIKV may use different cell surface receptors on iPSC-derived NPCs [84]. For example, TIM-1 plays a more prominent role than AXL in placental cells [83]. Duramycin, a peptide that binds phosphatidylethanolamine in enveloped viral particles and precludes TIM1 binding, reduced ZIKV infection in placental cells and explants. In a mouse study, comparison of homozygous or heterozygous AXL knock-out showed no significant differences in ZIKV viral replication and clinical manifestation, suggesting AXL is dispensable for ZIKV infection in those mice [85].

Table 2. Cellular targets and receptor usages.

Primary Cell	Receptor	References	
Brain			
Neural progenitor cells (NPCs)	AXL, TLR3	[80,84,85]	
Astroglial cells	AXL	[36,81,86–88]	
Microglial cells	AXL	[81]	
Placenta			
Hofbauer cells	AXL, Tyro3, TIM1	[67,68,83]	
Trophoblasts	AXL, Tyro3, TIM1, TLR3, TLR8	[67,68,83]	
Endothelial cells	AXL, Tyro3, TIM1	[33,83]	
Skin			
Dermal fibroblasts	AXL, TIM-1, TYRO3, TLR3, RIG-I, MDA5	[64,89]	
Epidermal keratinocytes	AXL, TIM-1, TYRO3, TLR3, RIG-I, MDA5	[64]	
Immune cells			
Immature dendritic cells	DC-SIGN	[64,65]	
Dendritic cells	DC-SIGN	[66]	
CD14 ⁺ monocytes	Unknown	[90–92]	
CD14 ⁺ CD16 ⁺ monocytes	Unknown	[91]	
Testis			
Sertoli cell	AXL	[28,93,94]	
Spermatozoa	Tyro3	[95,96]	
Kidney			
Renal mesangial cell	Unknown	[97]	
Glomerular podocytes	Unknown		
Renal Glomerular Endothelial Cell	Unknown		
Retina			
Retinal pericytes	Tyro3, AXL	[1,98]	
Retinal microvascular endothelial cells	Tyro3, AXL		
Permissive human cell lines			
Cell line	Origins	Permissiveness	References
SK-N-SH	Brain/Bone marrow	**	[99]
SH-SY5Y	Nerve	**	[100]
SF268	CNS in brain	***	[42,70]
HBMEC	Brain	***	[69,94]
SNB19	CNS in brain	***	[42]
Huh-7	Liver	***	[70]
HFF-1	Skin	***	[64]
A549	Lung	***	[100,101]
HOBIT	Osteoblast-like Cells	***	[102]

Note: **, moderate permissive; ***, highly permissive.

3. Cellular and Immune Responses to ZIKV Infection

Inflammation is one of the first line responses of the cellular immune system to viral infection, which is typically ignited by releasing cytokines including chemokines (Table 3). ZIKV triggers various host cell pro-inflammatory responses (Figure 2) [64,65,101,103]. For example, ZIKV stimulates CD8⁺ T cell-mediated polyfunctional immune responses to induce NF- κ B-mediated production of cytokines such as IL-1 β , IL-6, MIP1 α , as well as chemokines including IP10 and RANTES [87,103]

(Figure 2, left). These ZIKV-induced T cell immune responses are antiviral because when CD8+ isolates from previously ZIKV infected mice are introduced to naive mice prior to ZIKV infection, viral clearance is enhanced. Conversely, depletion of CD8+ T cells from infected animals compromises viral clearance [65]. ZIKV structural proteins (C, prM, and E) are the major targets of CD8+ T cell and CD4+ T cell responses [104].

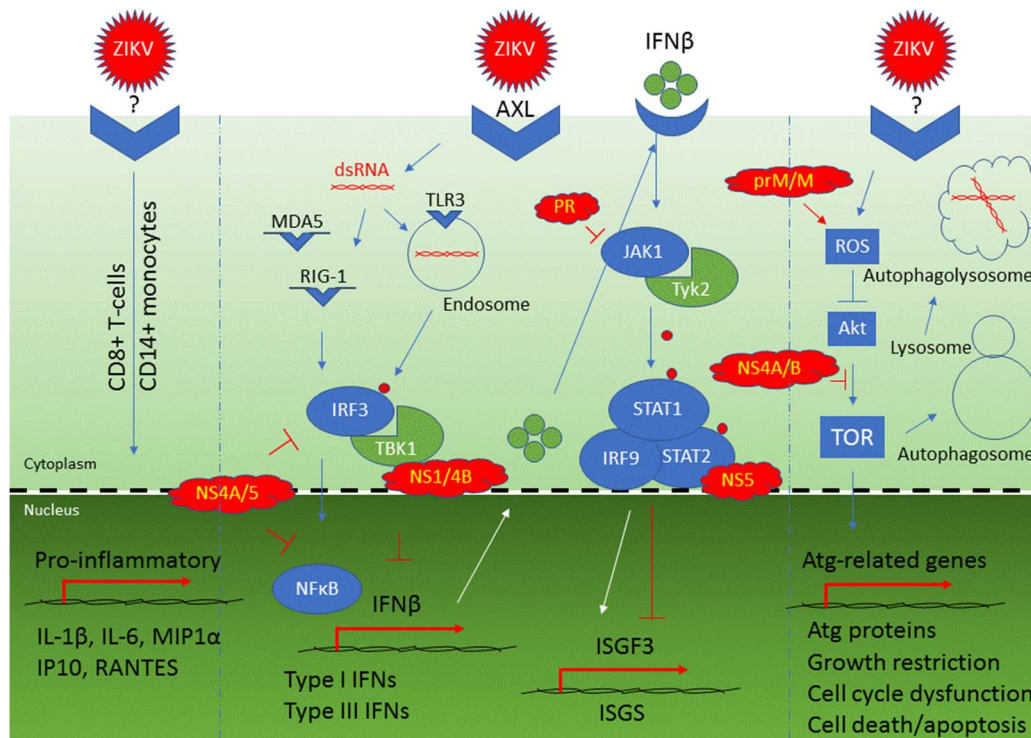


Figure 2. This figure illustrates Zika virus interactions with host cells. The Zika virus or proteins are colored in red. Cellular receptors or proteins that are affected by ZIKV are shown in blue. Cellular proteins shown in green are regulatory proteins such as kinases. Three Zika viruses are used here to show ZIKV-induced T-cell responses (left), ZIKV-mediated type I and type III IFNs productions (middle) and ZIKV-triggered autophagy (right). → indicates a positive interaction. denotes inhibitory action. Small red dots are used to indicate phosphorylation.

ZIKV also elicits humoral immune responses by producing protective and neutralizing antibodies in humans [34,45]. However, this antibody-mediated protection effect against ZIKV could be jeopardized in individuals who have previously been exposed to other flaviviruses such as DENV, which is the closest sibling of ZIKV. Pre-existing neutralizing antibodies against DENV presented in those individuals could, instead of neutralizing ZIKV, actually augment ZIKV infection and lead to more severe diseases [50]. This ADE effect of prior flaviviral infections on ZIKV pathogenicity has been thoroughly reviewed elsewhere [105,106].

Aside from ZIKV-mediated inflammatory and humoral responses, ZIKV also triggers a series of host cell innate immune responses, which are crucial for the recognition of viral invasion, activation of antiviral responses, and determination of the fate of viral infected cells (Figure 2, middle). Generally, primed by the pathogen-associated molecular pattern (PAMP) of different viruses, host cells recognize the invading virus by activating different types of pattern recognition receptors (PRRs), which could be cell surface receptors or endosomal receptors. For example, ZIKV is recognized by an endosomal toll-like receptor 3 (TLR3), which is a PRR that specifically recognizes dsRNA virus [57,64,65]. TLR3 belongs to a class of endosomal receptors that can be found in first line of defense cells such as macrophages or Langerhans cells. TLR3 activation plays a key role in host cell

innate immune responses to viral infection. Consistent with the innate immune responses to dsRNA virus, ZIKV-induced TLR3 activation promotes phosphorylation of interferon regulatory factor 3 (IRF3) by TBK1 kinase, leading to induction of type I interferon (IFN) signaling pathways [65,107]. This initiates a cascade that further activates cytoplasmic RIG-I-like receptors (RLRs) responses, subsequently inducing transcription of RIG-I, MDA5, and several type I and III IFN-stimulated genes including OAS2, ISG15, and MX1 [64]. Activation of the type I IFN signaling pathway results in production and secretion of IFN- β . Secreted IFN- β binding to IFN- β receptor activates JAK1 and Tyk2 kinases that in turn phosphorylate STAT1 and STAT2 (Figure 2, middle). Upon ZIKV infection, association of the phosphorylated STAT1/STAT2 heterodimer with IRF9 promotes ISRE3-mediated transcription of antiviral interferon stimulated genes (ISGS) [65]. One of the ISGS proteins, viperin (virus-inhibitory protein, endoplasmic reticulum-associated, IFN-inducible), shows strong antiviral activity against ZIKV. Specifically, it restricts ZIKV viral replication by targeting the NS3 protein for proteasomal degradation [108]. Therefore, the production of TLR3- and RIG-1/MDA5-mediated type I IFN production and subsequent activation of the JAK/STAT innate immune pathway confer increased resistance to ZIKV infection [109].

ZIKV is a membrane-associated virus that utilizes host ER for its replication and reproduction along the cellular secretory pathway. Through those cellular membrane interactions, ZIKV can trigger autophagy in a cell-dependent manner (Figure 2, right). This cellular process is normally involved in removal of aggregated or erroneously folded proteins through lysosomal degradation. Activation of cellular autophagy is a hallmark of flavivirus infection, which was thought to be part of the host innate immune response to eliminate invading intracellular pathogens [36,110–112]. Because autophagy activation could halt cellular growth and trigger apoptosis, ZIKV-induced autophagy was implicated in the ZIKV-mediated microcephaly [59,111,112]. Activation of autophagy elicits antiviral activities by removing viral proteins through reticulophagy, a selective form of autophagy that leads to ER degradation, or inclusion of viral proteins in autophagosomes destined for lysosomal degradation [113]. The ER-localized reticulophagy receptor FAM134B serves as a host cell restriction factor to ZIKV and other flaviviruses [114]. However, ZIKV-induced autophagy could be a double edged sword, which shows activities of both pro- and anti-ZIKV infection [113]. Activation of cellular autophagy counteracts ZIKV infection by actively removing viral proteins. As part of the host cell's antiviral responses, type I IFN signaling also limits ZIKV replication by promoting autophagic destruction of the viral NS2B/NS3pro protease in a STAT1-dependent manner [115]. Conversely, ZIKV takes advantage of autophagosome formation, whose presence was associated with enhanced viral replication [64]. ZIKV activates autophagy through the cellular mTOR stress pathway that connects oxidative stress and reactive oxygen species (ROS) production. This virus–host interaction appears to be highly conserved, as in human fetal neural stem cells, ZIKV triggers autophagy through inhibition of the mammalian mTOR pathway via AKT [111]. Similarly, in fission yeast cells, the ZIKV effect on TOR is mediated through a parallel pathway via Tor1 and Tip41, the human equivalents of TSC1 and TIP41 proteins [116,117]. Altogether, ZIKV infection elicits RIG-1/MDA5- and TLR3-mediated innate immune responses leading to releases of type I and type III IFNs to protect cells from viral invasion. ZIKV concurrently triggers cellular activation of the stress TOR signaling pathway that induces autophagy. The balance between pro- and anti-ZIKV activities of autophagy, at least in some cells, determines whether infected cells are protected through viral elimination, or destined to apoptosis as the result of viral propagation in host cells.

Table 3. Cellular antiviral responses and viral counteractions during Zika infection.

Cellular Antiviral Responses to Zika Infection			
Cellular Response	Cellular Protein Involved	Molecular Actions and Consequences	References
Pro-inflammatory CD8+ T-cell immune response	Cytokines: IL-1 β , IL-6, MIP1 α ; chemokines: IP-10, RANTES	T-cell mediated polyfunctional immune responses with releases of antiviral cytokines and chemokines	[65,103,118,119]
CD14+ monocytes and macrophages immune response	CXCL9, CXCL10, CXCL11, CCL5, IL-15	CD14+ monocytes prime NK cell activities during ZIKV infection	[92]
Humoral immune response	IgM, IgG	Production of neutralizing and protective antibodies to ZIKV	[120–122]
Cellular innate immune response: TLR3-mediated response	TLR3, IRF3, TBK1, type I IFNs, and IFN β	An early response that triggers IRF3 and recognizes ZIKV dsRNA in cytoplasm leading to activation of type I IFNs and IFN β production	[57,64,65]
Cellular innate immune response: RIG-1/MDA5-mediated response	RIG-1, MDA5, IRF-3, NF κ B, type I IFNs, and IFN β	Late responses that recognize ZIKV dsRNA and contribute to activation of type I IFNs and IFN β production	[64,65]
Type I and type III interferon activation	OAS2, ISG15, MX1	Production of IFN β as part of the cellular antiviral responses	[64]
Viral Counteraction			
Viral response	Viral protein involved	Molecular actions and consequences	References
Counteraction to activation of type I IFNs and IFN β production	NS1, NS2A, NS2B, NS4A, NS4B and NS5	Targeting RIG-1 pathway	[123–125]
Inhibition of IFN β production	NS1, NS4A, NS4B, NS5	NS4A and NS5 inhibit IRF3 and NF κ B; NS1 inhibits IRF3 IFN β production through binding to TBK1	[49]
Inhibition of the JAK/STAT pathway	NS5, PR	NS5 binds to STAT2 for its proteasomal degradation; PR inhibits JAK1 kinase	[115,126,127]
Selective activation of type II IFN signaling	NS5	NS5 promotes the formation of STAT1/STAT1 homodimers and activates type II IFN for viral replication	[123]
Induction of cellular autophagy	prM, M, NS1, NS2A, NS4A	In a yeast study, these ZIKV proteins induced cellular autophagy as indicated by formation of cytoplasmic puncta	[9]
Induction of cellular autophagy	NS4A, NS4B	Inhibit Akt-mediated mTOR pathway through Tor1/TSC1 and Tip41	[9,111]

4. Viral Counteraction to Host Antiviral Responses and ZIKV-Induced Cytopathic Effects

4.1. Viral Counteraction to Host Antiviral Responses

To establish successful viral infection, ZIKV has adopted various strategies to counteract host antiviral responses (Table 3). The final infection outcome depends on the balance between the host antiviral responses and the viral counteracting actions. A number of ZIKV-mediated counteracting actions are known. For example, once ZIKV infection is successfully established, it becomes resistant to IFN treatment, suggesting ZIKV might have deployed effective counteractive measures against host innate immune responses [101,125]. Resultant to this finding, no secreted type I and type III IFNs were detectable from ZIKV-infected cells [65]. Indeed, ZIKV impairs the induction of type I IFN by binding to IRF3, a member of the IRF family [49,125,128]. These ZIKV-mediated counteracting effects are achieved through multiple non-structural ZIKV proteins (NS1, NS2A, NS2B, NS4A, NS4B, and NS5). All of these ZIKV proteins suppress, to various degrees, IFN- β production by targeting distinct components of the RIG-I pathway [49]. For instance, the NS1, NS4A, and NS5 proteins specifically inhibit IRF3 and NF κ B [125], and the NS1 and NS4B proteins block IRF3 activation [49,115]. Interestingly, an A188V mutated NS1, which was found during the ZIKV epidemic starting in 2012, showed enhanced ability to block IFN- β induction, and facilitated mosquito-mediated virus transmission [49]. This acquired mutation enables NS1 binding to TBK1 and reduces TBK1 phosphorylation. Reversion of this mutation to the pre-epidemic genotype weakens the ability of ZIKV to counteract IFN- β production. Consistent with the idea that ZIKV blocks the IFN- β production through IRF3, IRF3 knockout cells lost this ZIKV effect [48,49].

ZIKV has also developed mechanisms to block the JAK/STAT pathway [65] (Figure 2, middle). For example, it blocks JAK1/Tyk2-mediated STAT1 and STAT2 phosphorylation resulting in ISGF3 transcription and ISGS translation shutdown [65]. On one hand, ZIKV utilizes its PR to inhibit JAK1 kinase [115]. On the other, ZIKV uses NS5 protein through direct binding to promote STAT2 proteasome-mediated degradation [125,126,128].

4.2. ZIKV-Induced Cytopathic Effects

Persistent viral replication and propagation inevitably confer adverse CPEs to host cells (Table 4). Like many other viruses, ZIKV encodes a limited number of proteins and, conceivably, has to rely on host cell resources to ensure its successful viral reproduction. Thus, a variety of devious approaches are utilized in order to commandeer host cell resources to create an environment for its own benefit. One common viral strategy is to deter host cell growth, or to subvert the host cell cycle into a specific phase whereby the virus gains optimal benefit by maximizing availability of cellular resources for its transcription, translation and assembly. This indeed is true for ZIKV in that ZIKV infection of hNPCs restricts cell growth and induces cell cycle dysfunction and apoptosis [42,61,63]. Further, these ZIKV-mediated CPEs appear to be associated with clinical neurological manifestations such as microcephaly [42,129]. For instance, ZIKV-induced CPEs correlate with the decrease of neuronal cell-layer volume of the brain organoids reminiscent of processes resulting in microcephaly, supporting that ZIKV-induced microcephaly is likely the result of ZIKV-mediated increase of CPEs [40,43,57,59].

Table 4. ZIKV proteins and associated cytopathic effects.

Protein	Primary Function	Main Phenotypes	References
Structural Proteins			
anaC	Anchored capsid protein	In the fission yeast cells, it restricts cellular growth and affects cell cycling. It also induces cellular oxidative stress leading to cell death.	[9]
C	Capsid protein	In the fission yeast cells, it restricts cellular growth. It also induces cellular oxidative stress leading to cell death; in hNPCs, it induces ribosomal stress and apoptosis.	[9,130]
prM	Precursor membrane protein	In the fission yeast cells, it restricts cellular growth and affects cell cycling. It also induces cellular oxidative stress and autophagy leading to cell death; a single prM mutation contributes to fetal microcephaly	[9,131]
M	Membrane protein	In the fission yeast cells, it restricts cellular growth and affects cell cycling. It also induces cellular oxidative stress and autophagy, leading to cell death.	[9]
Pr	Cleaved product from prM	Unknown	
E	Envelope protein	A putative cytopathic factor based on a yeast study. E protein facilitates viral entry. A single residue in the α B helix of the E protein is critical for Zika virus thermostability, and interaction with the host cell membrane.	[9,132]
Non-structural Proteins			
NS1	Viral replication, pathogenesis and immune evasion	In the fission yeast cells, it induces cellular oxidative stress and autophagy leading to cell death; An essential role in viral replication and immune evasion. It presents on the cell surface and presents as a dimer within cells, and as a hexamer once being secreted. NS1-mediated CPEs in mammalian cells have not yet been established.	[47–49,133]
NS2A	Unknown	In the fission yeast cells, it induces cellular oxidative stress and autophagy leading to cell death; ZIKV-encoded NS2A disrupts mammalian cortical neurogenesis by degrading adherens junction (AJ) proteins, leading to reduced proliferation and premature differentiation of radial glial cells and aberrant positioning of newborn neurons.	[131]
NS2B	Protease cofactor	In fission yeast cells, it restricts cellular growth. Forms a protease complex with NS3; a putative cytopathic factor based on a yeast study	[9,134]
NS3	Protease and helicase	NS3-mediated CPEs in mammalian cells have not yet been established.	[131]
NS4A	Viral RNA synthesis and viral morphogenesis	In the fission yeast cells, it restricts cellular growth and affects cell cycling. It also induces cellular oxidative stress and autophagy leading to cell death. It induces autophagy by inhibiting Atk-mediated TOR pathway through Tor1/TSC1 and Tip41 in both yeast and mammalian cells.	[9,111]
2K	A signal peptide	Viral RNA synthesis and viral morphogenesis. 2K-mediated CPEs have not yet been established.	[9,11,12]
NS4B	Viral RNA synthesis and viral morphogenesis	Synergistic to NS4A on inhibiting Akt-mediated TOR pathway	[111]
NS5	Methyltransferase; RNA-dependent polymerase	NS5-mediated CPEs in mammalian cells have not yet been established.	[128]

Although ZIKV confers various CPEs as described above, the identity of which ZIKV protein(s) is responsible, and the mechanism by which ZIKV mediates those effects, remains elusive. To assist in identifying which ZIKV viral protein(s) is responsible for those observed CPEs, we performed a genome-wide analysis of ZIKV proteins by using fission yeast (*Schizosaccharomyces pombe*) as a surrogate system [9,135]. Fission yeast is particularly useful here because the aforementioned ZIKV-mediated CPEs affect highly conserved cellular activities among all eukaryotes [136–139]. Each of the fourteen ZIKV viral cDNA encoding a specific protein or a small peptide was cloned into previously described fission yeast gene expression systems [140,141]. All of the ZIKV viral activities were measured simultaneously under the same inducible conditions, thus allowing concurrent functional characterization of each ZIKV protein. Consistent with the idea that ZIKV is a cell membrane-associated virus, and that the ER is the major “viral factory” [36,110,142], nine of the fourteen ZIKV proteins and peptides were found to associate with the ER network, including the nuclear membrane, ER, and Golgi [36,142,143]. Seven ZIKV proteins, including five mature and immature structural proteins (anaC/C, prM/M, and E), and two non-structural proteins (NS2B and NS4A), conferred a number of the same CPEs as reported in the ZIKV-infected mammalian cells infected by ZIKV [9,36,40,42,43]. Specifically, the ZIKV protein-producing yeast cells displayed restricted cellular growth, cellular autophagy, cell hypertrophy, cell cycle dysfunction, and cell death [9]. As described below, some of the same ZIKV protein-mediated CPEs have also been reported in mammalian cells.

4.3. The Structural Proteins

Cytopathic effects induced by ZIKV structural proteins are summarized in Table 4. Briefly, the yeast study showed that both the anaC and C proteins localize to the nuclei, triggering cellular oxidative stress leading to cell death [9]. Consistently, C protein is known to localize in the nucleus for other flaviviruses [144,145]. ZIKV C protein is present in human NPC nucleoli, sub-nuclear structures where ribosome biogenesis takes place, and also plays a role in cellular response to stress [130]. The presence of C protein in nucleoli was associated with activation of ribosomal stress and apoptosis [130]. Deleting part of the C protein prevented nucleolar localization, ribosomal stress, and apoptosis [130].

The E protein is a major viral surface protein that is responsible for the viral entry. Thus, it is a crucial viral determinant for initiating the ZIKV–host interaction. Comparison of E protein sequence and structure with that of other flaviviruses suggest ZIKV E protein is unique among flaviviruses, although some portions of it resemble its counterparts in WNV, JEV, and DENV [146,147]. During flaviviral assembly, E interacts with prM to form the prM-E heterodimers that protrude from the viral surface in the non-infectious and immature viral particles [14]. It is also involved in fusing the viral membrane with the host endosome membrane. As with other flaviviruses, the ZIKV E protein is glycosylated at amino acid N154. The E glycosylation appears to be critical for ZIKV infection of mammalian and mosquito cells, because a glycosylation mutant N154Q diminished oral infectivity by *Ae. aegypti* vector and showed reduced viremia and diminished mortality in mouse models [148]. Interestingly, knockout of E glycosylation does not significantly affect neurovirulence in mouse models [148]. While ZIKV encoding non-glycosylated E protein displayed attenuated and defective neuroinvasion when delivered subcutaneously, it replicated well following intracranial inoculation, suggesting possible involvement of E in passing through the blood-brain barrier [149]. Furthermore, ZIKV viral particles lacking the E protein glycan were still able to infect Raji cells expressing the lectin DC-SIGN receptor, indicating the prM glycan of partially mature particles can facilitate the viral entry [150]. The E protein, specifically its extended CD-loop, may confer viral stability, cell cycle-dependent viral replication, and in vivo pathogenesis, as shortening the CD-loop destabilizes the virus, and Δ 346 mutation in this loop disrupts thermal stability of the virus [151].

In DENV, the prM protein forms a heterodimer with the E protein and affects viral particle formation and secretion [14]. The resultant non-infectious and immature viral particles are transported through the TGN, where prM is cleaved by a host protease Furin, resulting in mature infectious

particles [15,16]. The transition from prM to M via the cleavage of host protease Furin is required for viral infectivity [11,13]. Therefore, both prM and M play important roles in viral pathogenesis. Consistent with the prM/M activities in host cells, in the yeast study, we showed that both prM and M proteins localize in ER [9]. Similarly, prM also localizes in ER in Vero cells [47]. In addition, the prM protein restricts cellular growth, and affects cell cycling leading to cell death in the yeast [9]. At the time of this writing, no description has yet been reported on the effect of individual prM or M protein on those basic cellular functions in mammalian cells. However, mutational analysis shows that the activity of prM protein contributes to fetal microcephaly [152]. Specifically, evolutionary analysis shows that a S139N substitution in the prM protein has persisted in the circulating ZIKV strains since the 2013 outbreak in French Polynesia to the subsequent spread to the Americas. A single serine(S)-to-asparagine(N) substitution (S139N) in the viral polyprotein of a presumably less neurovirulent Cambodian ZIKV_{FSS13025} strain [153], substantially increased ZIKV infectivity in both human and mouse NPCs, and led to more severe microcephaly in the mouse fetus, as well as higher mortality rates in neonatal mice [152]. Results of this study underscore the important contribution of prM to fetal microcephaly. However, the manner in which prM contributes to microcephaly, and the impact of S139N mutation on the prM function, are presently unknown. It is intriguing to note that residue 139 is actually located in the Pr region of the prM protein. Since neither prM nor Pr are present in the mature and infectious viral particles [15,16], it would be interesting to learn the molecular mechanism underlying the effect of the S139N mutation causing increased viral infectivity.

4.4. The Non-Structural Proteins

ZIKV PR, which consists of forty residues of the NS2B cofactor and the NS3pro domain of the NS3 [154], has been actively investigated for its PR activities (Table 4) [134,155,156]. In addition to ZIKV PR-mediated proteolysis for its own replication, ZIKV PR also cleaves the ER-localized reticulophagy receptor FAM134B to counteract host cell restriction through a selective form of autophagy known as reticulophagy [114]. Indeed, depletion of FAM134B by RNAi significantly enhanced ZIKV replication [114]. The production of the same PRs by other flaviviruses causes cell death by apoptosis [157,158]. However, whether ZIKV PR causes apoptosis is presently unknown. The yeast study showed that expression of the NS2B gene, which encodes the co-factor of the ZIKV PR, does induce cellular autophagy and cell death [9]. It would be of interest to test if fully active ZIKV PR can induce cell death in yeast and mammalian cells.

The NS4A protein, in conjunction with NS4B, activates cellular autophagy through inhibition of the mammalian TOR pathway via AKT [111]. Similarly, NS4A also inhibits the Tor1 pathway in the fission yeast. Furthermore, the yeast study showed that the inhibitory NS4A effect on TOR was mediated through Tor1 and Tip41, which are the human equivalents of TSC1 and TIP41 proteins [116,117].

Expression of NS2A reduces cell proliferation and causes premature differentiation of radial glial cells in the developing mouse brain [131]. In addition, NS2A interacts with adherens junction (AJ) proteins that are present at the epithelial–endothelial cell junctions, resulting in degradation and malformation of the AJ complex [131]. These NS2A-induced growth defect in the embryonic mouse cortex are unique to ZIKV, as the same effects were not seen in DENV. These NS2A effects could play a role in the pathogenic mechanism underlying ZIKV infection in the developing mammalian brain [131].

NS1 is a highly conserved protein among flaviviruses. It is an essential viral glycoprotein that plays a major role in virus–host interaction as it participates in viral replication, pathogenesis, and immune evasion [159]. As with other flaviviruses, NS1 is expressed at the cell surface and exists in diverse forms. Intracellular NS1 exists as a dimer that is required for viral replication, whereas the secreted NS1 hexamer interacts with host factors and plays a role in immune evasion [159,160]. Freire et al. [161] first revealed adaptation of the NS1 codon to human housekeeping genes in ZIKV Asian lineage, which could facilitate viral replication in humans. Indeed, an alanine(A)-to-valine(V)

amino acid substitution at residue 188 (A188V) of the NS1 protein was acquired by the ancient ZIKV strain since the turning of the century in Southeastern Asia. This A188V-carrying ZIKV strain circulated in that region before dissemination to Southern Pacific islands and the Americas [162]. Residue 188 is located within the interface of two NS1 monomers. However, this A188V substitution does not affect NS1 dimerization, instead increasing its secretability [48]. Strikingly, the A188V-carrying ZIKV epidemic strains were much more infectious in mosquitoes (*Ae. aegypti*) than the earlier Cambodia ZIKV_{FSS13025} strain, resulting in increased NS1 antigenemia. Enhancement of NS1 antigenemia in infected hosts promotes ZIKV infectivity and prevalence in mosquitoes, which could have facilitated transmission during the recent ZIKV epidemics [48]. Consistent with this idea, acquisition of the A188V substitution also correlates with enhanced ZIKV evasion of host interferon induction [49].

Interestingly, another pathogenic mutation T233A was isolated from the brain tissue of a ZIKV infected fetus with neonatal microcephaly [47]. The ZIKV NS1 T233A mutation, also located at the dimer interface, was not found in any other flaviviruses. This finding could potentially be significant because wildtype T233 organizes a central hydrogen bonding network at the NS1 dimer interface, while the T233A mutation disrupts this network and destabilizes the NS1 dimeric assembly in vitro [47]. However, the pathogenic potential of this mechanism has not yet been tested. Together, these studies on the NS1 protein suggest that ZIKV has acquired specific mutation(s) that increases its ability to evade host immune responses, and favors persistent viral replication, leading to enhanced viral pathogenicity.

5. Concluding Remarks

Since the global ZIKV pandemic in 2015, an unprecedented world-wide effort is being made to understand the ZIKV etiology and its associated human diseases. We have learned a great deal about its epidemiology, genetic diversity, viral pathogenicity, and clinical manifestations that are linked to ZIKV-associated human neurological diseases. In this article, we describe molecular interactions of ZIKV with its host cells. In particular, we briefly outline different cell types and receptors utilized by ZIKV for viral entry and infection. We then describe host cellular and immune responses to fight against ZIKV invasion. In response, ZIKV has adopted various counteracting strategies to defeat those host antiviral responses. The overall balance between host antiviral defenses and viral countermeasures determine the outcome of host cells, and the success of viral propagation and survival. Persistent viral replication and propagation inevitably damage human host cells, tissues, and organs, ultimately resulting in fetal microcephaly and a number of other neurologic disorders. Yet, we have only just begun to understand the molecular mechanisms underlying ZIKV interactions with host cells, and how those interactions relate to the observed neurological disorders caused by those newly adopted pathogenic ZIKVs. Much work is still needed to answer some of those same questions as we asked at the beginning, e.g., (1) what specific virological changes have taken place that transformed the ZIKV from a benign virus to a highly pathogenic virus, (2) how could viral mutations, such as those described in this review, alter the viral pathogenicity enabling recently observed neurological disorders, and (3) what specific changes in ZIKV–host interactions ultimately tilt the balance in favor of enhanced CPEs and viral pathogenicity? Ongoing and future research will no doubt continue to strive to provide answers to these questions. We hope this review will serve as a helpful reference to those who study ZIKV–host interactions, and that the information described herein will encourage additional studies focusing on the molecular mechanisms of this virus.

Acknowledgments: We want to thank all of those who have contributed our understanding of the emerging Zika virus especially those studies molecular mechanism underlying Zika virus–host interactions. We also want to apologize in advance if we have missed any important references that we should have included in this review. This work was supported in part by funding from the National Institute of Health (NIH R21 AI129369) and University of Maryland Medical Center (to R.Y.Z). This work was also supported by the ZIKAlert project (European Union–Région Réunion programme under grant agreement n° SYNERGY: RE0001902). S.B. has PhD degree scholarship from La Réunion Island University (Ecole Doctorale STS), funded by the French ministry MEESR.

Conflicts of Interest: The authors declare that there is no conflict of interest of any kind. The opinions expressed by the authors contributing to this journal do not necessarily reflect the opinions of the institutions with which the authors are affiliated.

Abbreviations

ADE	Antibody-dependent enhancement
CPE	Cytotoxic effect
CNS	Central nerve system
DC	Dendritic cell
DENV	Dengue virus
dsRNA	Double stranded RNA
ER	Endoplasmic reticulum
HAVcr-1	Hepatitis A virus cellular receptor 1
hEC	Human epithelial cell
hNPC	Human neural progenitor cell
hBMEC	Human brain microvascular endothelial cell
GBS	Guillain–Barré syndrome
IFN	Interferon
iPSC	Induced pluripotent stem cell
IRF3	Interferon regulatory factor 3
ISGS	Interferon stimulated genes
JEV	Japanese Encephalitis Virus
NPCs	Neural progenitor stem cells
PAMP	Pathogen-associated molecular pattern
PR	Protease
PRRs	Pattern recognition receptors
RdRP	RNA-dependent RNA polymerase
RLRs	RIG-I like receptors
sfRNA	Subgenomic flavivirus RNA
TGN	Trans-Golgi network
TLR3	Toll-like receptor 3
TOR	Target of rapamycin
WHO	World health organization
WNV	West Nile Virus
ZIKV	Zika virus

References

1. Zhao, Z.; Yang, M.; Azar, S.R.; Soong, L.; Weaver, S.C.; Sun, J.; Chen, Y.; Rossi, S.L.; Cai, J. Viral retinopathy in experimental models of zika infection. *Investig. Ophthalmol. Vis. Sci.* **2017**, *58*, 4355–4365. [[CrossRef](#)] [[PubMed](#)]
2. Sahiner, F.; Sig, A.K.; Savasci, U.; Tekin, K.; Akay, F. Zika virus-associated ocular and neurologic disorders: The emergence of new evidence. *Pediatr. Infect. Dis. J.* **2017**, *36*, e341–e346. [[CrossRef](#)] [[PubMed](#)]
3. Smith, D.W.; Mackenzie, J. Zika virus and Guillain-Barre syndrome: Another viral cause to add to the list. *Lancet* **2016**, *387*, 1486–1488. [[CrossRef](#)]
4. Wen, Z.; Song, H.; Ming, G.L. How does Zika virus cause microcephaly? *Genes Dev.* **2017**, *31*, 849–861. [[CrossRef](#)] [[PubMed](#)]
5. Carod-Artal, F.J. Neurological complications of Zika virus infection. *Expert Rev. Anti-Infect. Ther.* **2018**. [[CrossRef](#)] [[PubMed](#)]
6. Chambers, T.J.; Hahn, C.S.; Galler, R.; Rice, C.M. Flavivirus genome organization, expression, and replication. *Annu. Rev. Microbiol.* **1990**, *44*, 649–688. [[CrossRef](#)] [[PubMed](#)]
7. De Paula Freitas, B.; de Oliveira Dias, J.R.; Prazeres, J.; Sacramento, G.A.; Ko, A.I.; Maia, M.; Belfort, R., Jr. Ocular findings in infants with microcephaly associated with presumed Zika virus congenital infection in salvador, Brazil. *JAMA Ophthalmol.* **2016**, *134*, 529–535. [[CrossRef](#)] [[PubMed](#)]

8. Faye, O.; Freire, C.C.; Iamarino, A.; Faye, O.; de Oliveira, J.V.; Diallo, M.; Zanotto, P.M.; Sall, A.A. Molecular evolution of Zika virus during its emergence in the 20th century. *PLoS Negl. Trop. Dis.* **2014**, *8*, e2636. [[CrossRef](#)] [[PubMed](#)]
9. Li, G.; Poulsen, M.; Fenyvuesvolgyi, C.; Yashiroda, Y.; Yoshida, M.; Simard, J.M.; Gallo, R.C.; Zhao, R.Y. Characterization of cytopathic factors through genome-wide analysis of the zika viral proteins in fission yeast. *Proc. Natl. Acad. Sci. USA* **2017**, *114*, E376–E385. [[CrossRef](#)] [[PubMed](#)]
10. Harris, E.; Holden, K.L.; Edgil, D.; Polacek, C.; Clyde, K. Molecular biology of flaviviruses. *Novartis Found. Symp.* **2006**, *277*, 23–39, discussion 40, 71–23, 251–253. [[PubMed](#)]
11. Lobigs, M.; Lee, E.; Ng, M.L.; Pavy, M.; Lobigs, P. A flavivirus signal peptide balances the catalytic activity of two proteases and thereby facilitates virus morphogenesis. *Virology* **2010**, *401*, 80–89. [[CrossRef](#)] [[PubMed](#)]
12. Miller, S.; Kastner, S.; Krijnse-Locker, J.; Buhler, S.; Bartenschlager, R. The non-structural protein 4A of dengue virus is an integral membrane protein inducing membrane alterations in a 2K-regulated manner. *J. Biol. Chem.* **2007**, *282*, 8873–8882. [[CrossRef](#)] [[PubMed](#)]
13. Amberg, S.M.; Nestorowicz, A.; McCourt, D.W.; Rice, C.M. NS2B-3 proteinase-mediated processing in the yellow fever virus structural region: In vitro and in vivo studies. *J. Virol.* **1994**, *68*, 3794–3802. [[PubMed](#)]
14. Lin, J.C.; Lin, S.C.; Chen, W.Y.; Yen, Y.T.; Lai, C.W.; Tao, M.H.; Lin, Y.L.; Miaw, S.C.; Wu-Hsieh, B.A. Dengue viral protease interaction with NF- κ B inhibitor α/β results in endothelial cell apoptosis and hemorrhage development. *J. Immunol.* **2014**, *193*, 1258–1267. [[CrossRef](#)] [[PubMed](#)]
15. Stadler, K.; Allison, S.L.; Schalich, J.; Heinz, F.X. Proteolytic activation of tick-borne encephalitis virus by furin. *J. Virol.* **1997**, *71*, 8475–8481. [[PubMed](#)]
16. Elshuber, S.; Allison, S.L.; Heinz, F.X.; Mandl, C.W. Cleavage of protein prM is necessary for infection of BHK-21 cells by tick-borne encephalitis virus. *J. Gen. Virol.* **2003**, *84*, 183–191. [[CrossRef](#)] [[PubMed](#)]
17. Li, L.; Li, H.S.; Pauza, C.D.; Bukrinsky, M.; Zhao, R.Y. Roles of HIV-1 auxiliary proteins in viral pathogenesis and host-pathogen interactions. *Cell Res.* **2005**, *15*, 923–934. [[CrossRef](#)] [[PubMed](#)]
18. Melino, S.; Fucito, S.; Campagna, A.; Wrubl, F.; Gamarnik, A.; Cicero, D.O.; Paci, M. The active essential CFNS3d protein complex. *FEBS J.* **2006**, *273*, 3650–3662. [[CrossRef](#)] [[PubMed](#)]
19. Cao-Lormeau, V.M.; Blake, A.; Mons, S.; Lastere, S.; Roche, C.; Vanhomwegen, J.; Dub, T.; Baudouin, L.; Teissier, A.; Larre, P.; et al. Guillain-Barre syndrome outbreak associated with Zika virus infection in French polynesia: A case-control study. *Lancet* **2016**, *387*, 1531–1539. [[CrossRef](#)]
20. Goertz, G.P.; Abbo, S.R.; Fros, J.J.; Pijlman, G.P. Functional RNA during Zika virus infection. *Virus Res.* **2017**. [[CrossRef](#)] [[PubMed](#)]
21. Zhu, Z.; Chan, J.F.; Tee, K.M.; Choi, G.K.; Lau, S.K.; Woo, P.C.; Tse, H.; Yuen, K.Y. Comparative genomic analysis of pre-epidemic and epidemic zika virus strains for virological factors potentially associated with the rapidly expanding epidemic. *Emerg. Microbes Infect.* **2016**, *5*, e22. [[CrossRef](#)] [[PubMed](#)]
22. Hayes, E.B. Zika virus outside Africa. *Emerg. Infect. Dis.* **2009**, *15*, 1347–1350. [[CrossRef](#)] [[PubMed](#)]
23. Huang, Y.J.; Higgs, S.; Horne, K.M.; Vanlandingham, D.L. Flavivirus-mosquito interactions. *Viruses* **2014**, *6*, 4703–4730. [[CrossRef](#)] [[PubMed](#)]
24. Foy, B.D.; Kobylinski, K.C.; Chilson Foy, J.L.; Blitvich, B.J.; Travassos da Rosa, A.; Haddow, A.D.; Lanciotti, R.S.; Tesh, R.B. Probable non-vector-borne transmission of zika virus, Colorado, USA. *Emerg. Infect. Dis.* **2011**, *17*, 880–882. [[CrossRef](#)] [[PubMed](#)]
25. Mead, P.S.; Hills, S.L.; Brooks, J.T. Zika virus as a sexually transmitted pathogen. *Curr. Opin. Infect. Dis.* **2018**, *31*, 39–44. [[CrossRef](#)] [[PubMed](#)]
26. Musso, D.; Nhan, T.; Robin, E.; Roche, C.; Bierlaire, D.; Zisou, K.; Shan Yan, A.; Cao-Lormeau, V.M.; Broult, J. Potential for Zika virus transmission through blood transfusion demonstrated during an outbreak in French Polynesia, November 2013 to February 2014. *Eurosurveillance* **2014**, *19*. [[CrossRef](#)]
27. Govero, J.; Esakky, P.; Scheaffer, S.M.; Fernandez, E.; Drury, A.; Platt, D.J.; Gorman, M.J.; Richner, J.M.; Caine, E.A.; Salazar, V.; et al. Zika virus infection damages the testes in mice. *Nature* **2016**, *540*, 438–442. [[CrossRef](#)] [[PubMed](#)]
28. Ma, W.; Li, S.; Ma, S.; Jia, L.; Zhang, F.; Zhang, Y.; Zhang, J.; Wong, G.; Zhang, S.; Lu, X.; et al. Zika virus causes testis damage and leads to male infertility in mice. *Cell* **2017**, *168*, 542. [[CrossRef](#)] [[PubMed](#)]
29. Joguet, G.; Mansuy, J.M.; Matusali, G.; Hamdi, S.; Walschaerts, M.; Pavili, L.; Guyomard, S.; Prisant, N.; Lamarre, P.; Dejucq-Rainsford, N.; et al. Effect of acute Zika virus infection on sperm and virus clearance in body fluids: A prospective observational study. *Lancet Infect. Dis.* **2017**, *17*, 1200–1208. [[CrossRef](#)]

30. Cao, B.; Diamond, M.S.; Mysorekar, I.U. Maternal-fetal transmission of zika virus: Routes and signals for infection. *J. Interferon Cytokine Res.* **2017**, *37*, 287–294. [[CrossRef](#)] [[PubMed](#)]
31. Zanoluca, C.; de Noronha, L.; Duarte Dos Santos, C.N. Maternal-fetal transmission of the zika virus: An intriguing interplay. *Tissue Barriers* **2018**, *6*, e1402143. [[CrossRef](#)] [[PubMed](#)]
32. Mlakar, J.; Korva, M.; Tul, N.; Popovic, M.; Poljsak-Prijatelj, M.; Mraz, J.; Kolenc, M.; Resman Rus, K.; Vesnaver Vipotnik, T.; Fabjan Vodusek, V.; et al. Zika virus associated with microcephaly. *N. Engl. J. Med.* **2016**, *374*, 951–958. [[CrossRef](#)] [[PubMed](#)]
33. Miner, J.J.; Cao, B.; Govero, J.; Smith, A.M.; Fernandez, E.; Cabrera, O.H.; Garber, C.; Noll, M.; Klein, R.S.; Noguchi, K.K.; et al. Zika virus infection during pregnancy in mice causes placental damage and fetal demise. *Cell* **2016**, *165*, 1081–1091. [[CrossRef](#)] [[PubMed](#)]
34. Dick, G.W.; Kitchen, S.F.; Haddow, A.J. Zika virus. I. Isolations and serological specificity. *Trans. R. Soc. Trop. Med. Hyg.* **1952**, *46*, 509–520. [[CrossRef](#)]
35. Dick, G.W. Zika virus. II. Pathogenicity and physical properties. *Trans. R. Soc. Trop. Med. Hyg.* **1952**, *46*, 521–534. [[CrossRef](#)]
36. Bell, T.M.; Field, E.J.; Narang, H.K. Zika virus infection of the central nervous system of mice. *Arch. Gesamte Virusforsch.* **1971**, *35*, 183–193. [[CrossRef](#)] [[PubMed](#)]
37. Duffy, M.R.; Chen, T.H.; Hancock, W.T.; Powers, A.M.; Kool, J.L.; Lanciotti, R.S.; Pretrick, M.; Marfel, M.; Holzbauer, S.; Dubray, C.; et al. Zika virus outbreak on Yap Island, federated states of Micronesia. *N. Engl. J. Med.* **2009**, *360*, 2536–2543. [[CrossRef](#)] [[PubMed](#)]
38. Ios, S.; Mallet, H.P.; Leparc Goffart, I.; Gauthier, V.; Cardoso, T.; Herida, M. Current Zika virus epidemiology and recent epidemics. *Med. Mal. Infect.* **2014**, *44*, 302–307. [[CrossRef](#)] [[PubMed](#)]
39. Driggers, R.W.; Ho, C.Y.; Korhonen, E.M.; Kuivanen, S.; Jaaskelainen, A.J.; Smura, T.; Rosenberg, A.; Hill, D.A.; DeBiasi, R.L.; Vezina, G.; et al. Zika virus infection with prolonged maternal viremia and fetal brain abnormalities. *N. Engl. J. Med.* **2016**, *374*, 2142–2151. [[CrossRef](#)] [[PubMed](#)]
40. Qian, X.; Nguyen, H.N.; Song, M.M.; Hadiono, C.; Ogden, S.C.; Hammack, C.; Yao, B.; Hamersky, G.R.; Jacob, F.; Zhong, C.; et al. Brain-region-specific organoids using mini-bioreactors for modeling ZIKV exposure. *Cell* **2016**, *165*, 1238–1254. [[CrossRef](#)] [[PubMed](#)]
41. Victora, C.G.; Schuler-Faccini, L.; Matijasevich, A.; Ribeiro, E.; Pessoa, A.; Barros, F.C. Microcephaly in Brazil: How to interpret reported numbers? *Lancet* **2016**, *387*, 621–624. [[CrossRef](#)]
42. Tang, H.; Hammack, C.; Ogden, S.C.; Wen, Z.; Qian, X.; Li, Y.; Yao, B.; Shin, J.; Zhang, F.; Lee, E.M.; et al. Zika virus infects human cortical neural progenitors and attenuates their growth. *Cell Stem Cell* **2016**, *18*, 587–590. [[CrossRef](#)] [[PubMed](#)]
43. Garcez, P.P.; Loiola, E.C.; Madeiro da Costa, R.; Higa, L.M.; Trindade, P.; Delvecchio, R.; Nascimento, J.M.; Brindeiro, R.; Tanuri, A.; Rehen, S.K. Zika virus impairs growth in human neurospheres and brain organoids. *Science* **2016**, *352*, 816–818. [[CrossRef](#)] [[PubMed](#)]
44. Haddow, A.D.; Schuh, A.J.; Yasuda, C.Y.; Kasper, M.R.; Heang, V.; Huy, R.; Guzman, H.; Tesh, R.B.; Weaver, S.C. Genetic characterization of Zika virus strains: Geographic expansion of the Asian lineage. *PLoS Negl. Trop. Dis.* **2012**, *6*, e1477. [[CrossRef](#)] [[PubMed](#)]
45. Dowd, K.A.; DeMasos, C.R.; Pelc, R.S.; Speer, S.D.; Smith, A.R.Y.; Goo, L.; Platt, D.J.; Mascola, J.R.; Graham, B.S.; Mulligan, M.J.; et al. Broadly neutralizing activity of Zika virus-immune sera identifies a single viral serotype. *Cell Rep.* **2016**, *16*, 1485–1491. [[CrossRef](#)] [[PubMed](#)]
46. Anfasa, F.; Siegers, J.Y.; van der Kroeg, M.; Mumtaz, N.; Stalin Raj, V.; de Vrij, F.M.S.; Widagdo, W.; Gabriel, G.; Salinas, S.; Simonin, Y.; et al. Phenotypic differences between Asian and African lineage Zika viruses in human neural progenitor cells. *MSphere* **2017**, *2*. [[CrossRef](#)] [[PubMed](#)]
47. Wang, D.; Chen, C.; Liu, S.; Zhou, H.; Yang, K.; Zhao, Q.; Ji, X.; Chen, C.; Xie, W.; Wang, Z.; et al. A mutation identified in neonatal microcephaly destabilizes Zika virus NS1 assembly in vitro. *Sci Rep.* **2017**, *7*, 42580. [[CrossRef](#)] [[PubMed](#)]
48. Liu, Y.; Liu, J.; Du, S.; Shan, C.; Nie, K.; Zhang, R.; Li, X.F.; Zhang, R.; Wang, T.; Qin, C.F.; et al. Evolutionary enhancement of Zika virus infectivity in *Aedes aegypti* mosquitoes. *Nature* **2017**, *545*, 482–486. [[CrossRef](#)] [[PubMed](#)]
49. Xia, H.; Luo, H.; Shan, C.; Muruato, A.E.; Nunes, B.T.D.; Medeiros, D.B.A.; Zou, J.; Xie, X.; Giraldo, M.I.; Vasconcelos, P.F.C.; et al. An evolutionary NS1 mutation enhances Zika virus evasion of host interferon induction. *Nat. Commun.* **2018**, *9*, 414. [[CrossRef](#)] [[PubMed](#)]

50. Sariol, C.A.; Nogueira, M.L.; Vasilakis, N. A tale of two viruses: Does heterologous flavivirus immunity enhance Zika disease? *Trends Microbiol.* **2018**, *26*, 186–190. [[CrossRef](#)] [[PubMed](#)]
51. Kawiecki, A.B.; Christofferson, R.C. Zika virus-induced antibody response enhances dengue virus serotype 2 replication in vitro. *J. Infect. Dis.* **2016**, *214*, 1357–1360. [[CrossRef](#)] [[PubMed](#)]
52. George, J.; Valiant, W.G.; Mattapallil, M.J.; Walker, M.; Huang, Y.S.; Vanlandingham, D.L.; Misamore, J.; Greenhouse, J.; Weiss, D.E.; Verthelyi, D.; et al. Prior exposure to Zika virus significantly enhances peak Dengue-2 viremia in Rhesus macaques. *Sci. Rep.* **2017**, *7*, 10498. [[CrossRef](#)] [[PubMed](#)]
53. Dejnirattisai, W.; Supasa, P.; Wongwiwat, W.; Rouvinski, A.; Barba-Spaeth, G.; Duangchinda, T.; Sakuntabhai, A.; Cao-Lormeau, V.M.; Malasit, P.; Rey, F.A.; et al. Dengue virus sero-cross-reactivity drives antibody-dependent enhancement of infection with Zika virus. *Nat. Immunol.* **2016**, *17*, 1102–1108. [[CrossRef](#)] [[PubMed](#)]
54. Paul, L.M.; Carlin, E.R.; Jenkins, M.M.; Tan, A.L.; Barcello, C.M.; Nicholson, C.O.; Michael, S.F.; Isern, S. Dengue virus antibodies enhance Zika virus infection. *Clin. Transl. Immunol.* **2016**, *5*, e117. [[CrossRef](#)] [[PubMed](#)]
55. Londono-Renteria, B.; Troupin, A.; Cardenas, J.C.; Hall, A.; Perez, O.G.; Cardenas, L.; Hartstone-Rose, A.; Halstead, S.B.; Colpitts, T.M. A relevant in vitro human model for the study of Zika virus antibody-dependent enhancement. *J. Gen. Virol.* **2017**, *98*, 1702–1712. [[CrossRef](#)] [[PubMed](#)]
56. Cohen, J. Dengue may bring out the worst in Zika. *Science* **2017**, *355*, 1362. [[CrossRef](#)] [[PubMed](#)]
57. Dang, J.; Tiwari, S.K.; Lichinchi, G.; Qin, Y.; Patil, V.S.; Eroshkin, A.M.; Rana, T.M. Zika virus depletes neural progenitors in human cerebral organoids through activation of the innate immune receptor TLR3. *Cell Stem Cell* **2016**, *19*, 258–265. [[CrossRef](#)] [[PubMed](#)]
58. Hasan, S.S.; Miller, A.; Sapparapu, G.; Fernandez, E.; Klose, T.; Long, F.; Fokine, A.; Porta, J.C.; Jiang, W.; Diamond, M.S.; et al. A human antibody against Zika virus crosslinks the e protein to prevent infection. *Nat. Commun.* **2017**, *8*, 14722. [[CrossRef](#)] [[PubMed](#)]
59. Cugola, F.R.; Fernandes, I.R.; Russo, F.B.; Freitas, B.C.; Dias, J.L.; Guimaraes, K.P.; Benazzato, C.; Almeida, N.; Pignatari, G.C.; Romero, S.; et al. The Brazilian Zika virus strain causes birth defects in experimental models. *Nature* **2016**, *534*, 267–271. [[CrossRef](#)] [[PubMed](#)]
60. Shao, Q.; Herrlinger, S.; Zhu, Y.N.; Yang, M.; Goodfellow, F.; Stice, S.L.; Qi, X.P.; Brindley, M.A.; Chen, J.F. The African Zika virus MR-766 is more virulent and causes more severe brain damage than current Asian lineage and dengue virus. *Development* **2017**, *144*, 4114–4124. [[CrossRef](#)] [[PubMed](#)]
61. Li, C.; Xu, D.; Ye, Q.; Hong, S.; Jiang, Y.; Liu, X.; Zhang, N.; Shi, L.; Qin, C.F.; Xu, Z. Zika virus disrupts neural progenitor development and leads to microcephaly in mice. *Cell Stem Cell* **2016**, *19*, 120–126. [[CrossRef](#)] [[PubMed](#)]
62. Zhang, F.; Wang, H.J.; Wang, Q.; Liu, Z.Y.; Yuan, L.; Huang, X.Y.; Li, G.; Ye, Q.; Yang, H.; Shi, L.; et al. American strain of Zika virus causes more severe microcephaly than an old Asian strain in neonatal mice. *EBioMedicine* **2017**, *25*, 95–105. [[CrossRef](#)] [[PubMed](#)]
63. Shao, Q.; Herrlinger, S.; Yang, S.L.; Lai, F.; Moore, J.M.; Brindley, M.A.; Chen, J.F. Zika virus infection disrupts neurovascular development and results in postnatal microcephaly with brain damage. *Development* **2016**, *143*, 4127–4136. [[CrossRef](#)] [[PubMed](#)]
64. Hamel, R.; Dejarnac, O.; Wichit, S.; Ekcharyawat, P.; Neyret, A.; Luplertlop, N.; Perera-Lecoin, M.; Surasombatpattana, P.; Talignani, L.; Thomas, F.; et al. Biology of Zika virus infection in human skin cells. *J. Virol.* **2015**, *89*, 8880–8896. [[CrossRef](#)] [[PubMed](#)]
65. Bowen, J.R.; Zimmerman, M.G.; Suthar, M.S. Taking the defensive: Immune control of Zika virus infection. *Virus Res.* **2017**. [[CrossRef](#)] [[PubMed](#)]
66. Sun, X.; Hua, S.; Chen, H.R.; Ouyang, Z.; Einkauf, K.; Tse, S.; Ard, K.; Ciaranello, A.; Yawetz, S.; Sax, P.; et al. Transcriptional changes during naturally acquired Zika virus infection render dendritic cells highly conducive to viral replication. *Cell Rep.* **2017**, *21*, 3471–3482. [[CrossRef](#)] [[PubMed](#)]
67. Bayer, A.; Lennemann, N.J.; Ouyang, Y.; Bramley, J.C.; Morosky, S.; Marques, E.T., Jr.; Cherry, S.; Sadovsky, Y.; Coyne, C.B. Type III interferons produced by human placental trophoblasts confer protection against Zika virus infection. *Cell Host Microbe* **2016**, *19*, 705–712. [[CrossRef](#)] [[PubMed](#)]
68. Quicke, K.M.; Bowen, J.R.; Johnson, E.L.; McDonald, C.E.; Ma, H.; O’Neal, J.T.; Rajakumar, A.; Wrammert, J.; Rimawi, B.H.; Pulendran, B.; et al. Zika virus infects human placental macrophages. *Cell Host Microbe* **2016**, *20*, 83–90. [[CrossRef](#)] [[PubMed](#)]

69. Mladinich, M.C.; Schwedes, J.; Mackow, E.R. Zika virus persistently infects and is basolaterally released from primary human brain microvascular endothelial cells. *MBio* **2017**, *8*. [[CrossRef](#)] [[PubMed](#)]
70. Chan, J.F.; Yip, C.C.; Tsang, J.O.; Tee, K.M.; Cai, J.P.; Chik, K.K.; Zhu, Z.; Chan, C.C.; Choi, G.K.; Sridhar, S.; et al. Differential cell line susceptibility to the emerging Zika virus: Implications for disease pathogenesis, non-vector-borne human transmission and animal reservoirs. *Emerg. Microbes Infect.* **2016**, *5*, e93. [[CrossRef](#)] [[PubMed](#)]
71. Thepparit, C.; Smith, D.R. Serotype-specific entry of dengue virus into liver cells: Identification of the 37-kilodalton/67-kilodalton high-affinity laminin receptor as a dengue virus serotype 1 receptor. *J. Virol.* **2004**, *78*, 12647–12656. [[CrossRef](#)] [[PubMed](#)]
72. Lemke, G.; Burstyn-Cohen, T. Tam receptors and the clearance of apoptotic cells. *Ann. N. Y. Acad. Sci.* **2010**, *1209*, 23–29. [[CrossRef](#)] [[PubMed](#)]
73. Garcia-Vallejo, J.J.; Ambrosini, M.; Overbeek, A.; van Riel, W.E.; Bloem, K.; Unger, W.W.; Chiodo, F.; Bolscher, J.G.; Nazmi, K.; Kalay, H.; et al. Multivalent glycopeptide dendrimers for the targeted delivery of antigens to dendritic cells. *Mol. Immunol.* **2013**, *53*, 387–397. [[CrossRef](#)] [[PubMed](#)]
74. Shimojima, M.; Stroher, U.; Ebihara, H.; Feldmann, H.; Kawaoka, Y. Identification of cell surface molecules involved in dystroglycan-independent Lassa virus cell entry. *J. Virol.* **2012**, *86*, 2067–2078. [[CrossRef](#)] [[PubMed](#)]
75. Kondratowicz, A.S.; Lennemann, N.J.; Sinn, P.L.; Davey, R.A.; Hunt, C.L.; Moller-Tank, S.; Meyerholz, D.K.; Rennert, P.; Mullins, R.F.; Brindley, M.; et al. T-cell immunoglobulin and mucin domain 1 (TIM-1) is a receptor for zaire ebolavirus and lake victoria marburgvirus. *Proc. Natl. Acad. Sci. USA* **2011**, *108*, 8426–8431. [[CrossRef](#)] [[PubMed](#)]
76. Meertens, L.; Carnec, X.; Lecoin, M.P.; Ramdasi, R.; Guivel-Benhassine, F.; Lew, E.; Lemke, G.; Schwartz, O.; Amara, A. The TIM and TAM families of phosphatidylserine receptors mediate dengue virus entry. *Cell Host Microbe* **2012**, *12*, 544–557. [[CrossRef](#)] [[PubMed](#)]
77. Morizono, K.; Chen, I.S. Role of phosphatidylserine receptors in enveloped virus infection. *J. Virol.* **2014**, *88*, 4275–4290. [[CrossRef](#)] [[PubMed](#)]
78. Perera-Lecoin, M.; Meertens, L.; Carnec, X.; Amara, A. Flavivirus entry receptors: An update. *Viruses* **2013**, *6*, 69–88. [[CrossRef](#)] [[PubMed](#)]
79. Smit, J.M.; Moesker, B.; Rodenhuis-Zybert, I.; Wilschut, J. Flavivirus cell entry and membrane fusion. *Viruses* **2011**, *3*, 160–171. [[CrossRef](#)] [[PubMed](#)]
80. Nowakowski, T.J.; Pollen, A.A.; Di Lullo, E.; Sandoval-Espinosa, C.; Bershteyn, M.; Kriegstein, A.R. Expression analysis highlights AXL as a candidate Zika virus entry receptor in neural stem cells. *Cell Stem Cell* **2016**, *18*, 591–596. [[CrossRef](#)] [[PubMed](#)]
81. Meertens, L.; Labeau, A.; Dejarnac, O.; Cipriani, S.; Sinigaglia, L.; Bonnet-Madin, L.; Le Charpentier, T.; Hafirassou, M.L.; Zamborlini, A.; Cao-Lormeau, V.M.; et al. AXL mediates Zika virus entry in human glial cells and modulates innate immune responses. *Cell Rep.* **2017**, *18*, 324–333. [[CrossRef](#)] [[PubMed](#)]
82. Retallack, H.; Di Lullo, E.; Arias, C.; Knopp, K.A.; Laurie, M.T.; Sandoval-Espinosa, C.; Mancia Leon, W.R.; Krencik, R.; Ullian, E.M.; Spatazza, J.; et al. Zika virus cell tropism in the developing human brain and inhibition by azithromycin. *Proc. Natl. Acad. Sci. USA* **2016**, *113*, 14408–14413. [[CrossRef](#)] [[PubMed](#)]
83. Tabata, T.; Petitt, M.; Puerta-Guardo, H.; Michlmayr, D.; Wang, C.; Fang-Hoover, J.; Harris, E.; Pereira, L. Zika virus targets different primary human placental cells, suggesting two routes for vertical transmission. *Cell Host Microbe* **2016**, *20*, 155–166. [[CrossRef](#)] [[PubMed](#)]
84. Wells, M.F.; Salick, M.R.; Wiskow, O.; Ho, D.J.; Worringer, K.A.; Ihry, R.J.; Kommineni, S.; Bilican, B.; Klim, J.R.; Hill, E.J.; et al. Genetic ablation of AXL does not protect human neural progenitor cells and cerebral organoids from Zika virus infection. *Cell Stem Cell* **2016**, *19*, 703–708. [[CrossRef](#)] [[PubMed](#)]
85. Wang, Z.Y.; Wang, Z.; Zhen, Z.D.; Feng, K.H.; Guo, J.; Gao, N.; Fan, D.Y.; Han, D.S.; Wang, P.G.; An, J. AXL is not an indispensable factor for Zika virus infection in mice. *J. Gen. Virol.* **2017**, *98*, 2061–2068. [[CrossRef](#)] [[PubMed](#)]
86. Hamel, R.; Ferraris, P.; Wichit, S.; Diop, F.; Talignani, L.; Pompon, J.; Garcia, D.; Liegeois, F.; Sall, A.A.; Yssel, H.; et al. African and Asian Zika virus strains differentially induce early antiviral responses in primary human astrocytes. *Infect. Genet. Evol.* **2017**, *49*, 134–137. [[CrossRef](#)] [[PubMed](#)]

87. Stefanik, M.; Formanova, P.; Bily, T.; Vancova, M.; Eyer, L.; Palus, M.; Salat, J.; Braconi, C.T.; Zanotto, P.M.A.; Gould, E.A.; et al. Characterisation of Zika virus infection in primary human astrocytes. *BMC Neurosci* **2018**, *19*, 5. [[CrossRef](#)] [[PubMed](#)]
88. Chen, J.; Yang, Y.F.; Yang, Y.; Zou, P.; Chen, J.; He, Y.; Shui, S.L.; Cui, Y.R.; Bai, R.; Liang, Y.J.; et al. AXL promotes Zika virus infection in astrocytes by antagonizing type I interferon signalling. *Nat. Microbiol.* **2018**, *3*, 302–309. [[CrossRef](#)] [[PubMed](#)]
89. Persaud, M.; Martinez-Lopez, A.; Buffone, C.; Porcelli, S.A.; Diaz-Griffero, F. Infection by Zika viruses requires the transmembrane protein AXL, endocytosis and low pH. *Virology* **2018**, *518*, 301–312. [[CrossRef](#)] [[PubMed](#)]
90. Foo, S.S.; Chen, W.; Chan, Y.; Bowman, J.W.; Chang, L.C.; Choi, Y.; Yoo, J.S.; Ge, J.; Cheng, G.; Bonnin, A.; et al. Asian Zika virus strains target CD14⁺ blood monocytes and induce M2-skewed immunosuppression during pregnancy. *Nat. Microbiol.* **2017**, *2*, 1558–1570. [[CrossRef](#)] [[PubMed](#)]
91. Michlmayr, D.; Andrade, P.; Gonzalez, K.; Balmaseda, A.; Harris, E. CD14⁺ CD16⁺ monocytes are the main target of Zika virus infection in peripheral blood mononuclear cells in a paediatric study in Nicaragua. *Nat. Microbiol.* **2017**, *2*, 1462–1470. [[CrossRef](#)] [[PubMed](#)]
92. Lum, F.M.; Lee, D.; Chua, T.K.; Tan, J.J.L.; Lee, C.Y.P.; Liu, X.; Fang, Y.; Lee, B.; Yee, W.X.; Rickett, N.Y.; et al. Zika virus infection preferentially counterbalances human peripheral monocyte and/or NK cell activity. *MSphere* **2018**, *3*. [[CrossRef](#)] [[PubMed](#)]
93. Sheng, Z.Y.; Gao, N.; Wang, Z.Y.; Cui, X.Y.; Zhou, D.S.; Fan, D.Y.; Chen, H.; Wang, P.G.; An, J. Sertoli cells are susceptible to zikv infection in mouse testis. *Front. Cell. Infect. Microbiol.* **2017**, *7*, 272. [[CrossRef](#)] [[PubMed](#)]
94. Siemann, D.N.; Strange, D.P.; Maharaj, P.N.; Shi, P.Y.; Verma, S. Zika virus infects human sertoli cells and modulates the integrity of the in vitro blood-testis barrier model. *J. Virol.* **2017**, *91*. [[CrossRef](#)] [[PubMed](#)]
95. Salam, A.P.; Horby, P. Isolation of viable Zika virus from spermatozoa. *Lancet Infect. Dis.* **2018**, *18*, 144. [[CrossRef](#)]
96. Bagasra, O.; Addanki, K.C.; Goodwin, G.R.; Hughes, B.W.; Pandey, P.; McLean, E. Cellular targets and receptor of sexual transmission of Zika virus. *Appl. Immunohistochem. Mol. Morphol.* **2017**, *25*, 679–686. [[CrossRef](#)] [[PubMed](#)]
97. Alcendor, D.J. Zika virus infection of the human glomerular cells: Implications for viral reservoirs and renal pathogenesis. *J. Infect. Dis.* **2017**, *216*, 162–171. [[CrossRef](#)] [[PubMed](#)]
98. Roach, T.; Alcendor, D.J. Zika virus infection of cellular components of the blood-retinal barriers: Implications for viral associated congenital ocular disease. *J. Neuroinflamm.* **2017**, *14*, 43. [[CrossRef](#)] [[PubMed](#)]
99. Offerdahl, D.K.; Dorward, D.W.; Hansen, B.T.; Bloom, M.E. Cytoarchitecture of Zika virus infection in human neuroblastoma and aedes albopictus cell lines. *Virology* **2017**, *501*, 54–62. [[CrossRef](#)] [[PubMed](#)]
100. Bos, S.; Viranaicken, W.; Turpin, J.; El-Kalamouni, C.; Roche, M.; Krejbich-Trotot, P.; Despres, P.; Gadea, G. The structural proteins of epidemic and historical strains of Zika virus differ in their ability to initiate viral infection in human host cells. *Virology* **2018**, *516*, 265–273. [[CrossRef](#)] [[PubMed](#)]
101. Frumence, E.; Roche, M.; Krejbich-Trotot, P.; El-Kalamouni, C.; Nativel, B.; Rondeau, P.; Misse, D.; Gadea, G.; Viranaicken, W.; Despres, P. The south pacific epidemic strain of Zika virus replicates efficiently in human epithelial A549 cells leading to IFN- β production and apoptosis induction. *Virology* **2016**, *493*, 217–226. [[CrossRef](#)] [[PubMed](#)]
102. Colavita, F.; Musumeci, G.; Caglioti, C. Human osteoblast-like cells are permissive for Zika virus replication. *J. Rheumatol.* **2018**, *45*, 443. [[CrossRef](#)] [[PubMed](#)]
103. Tappe, D.; Perez-Giron, J.V.; Zammarchi, L.; Rissland, J.; Ferreira, D.F.; Jaenisch, T.; Gomez-Medina, S.; Gunther, S.; Bartoloni, A.; Munoz-Fontela, C.; et al. Cytokine kinetics of Zika virus-infected patients from acute to convalescent phase. *Med. Microbiol. Immunol.* **2016**, *205*, 269–273. [[CrossRef](#)] [[PubMed](#)]
104. Grifoni, A.; Pham, J.; Sidney, J.; O'Rourke, P.H.; Paul, S.; Peters, B.; Martini, S.R.; de Silva, A.D.; Ricciardi, M.J.; Magnani, D.M.; et al. Prior dengue virus exposure shapes T cell immunity to Zika virus in humans. *J. Virol.* **2017**, *91*. [[CrossRef](#)] [[PubMed](#)]
105. Elong Ngono, A.; Shresta, S. Immune response to dengue and Zika. *Annu. Rev. Immunol.* **2018**. [[CrossRef](#)] [[PubMed](#)]
106. Rey, F.A.; Stiasny, K.; Vaney, M.C.; Dellarole, M.; Heinz, F.X. The bright and the dark side of human antibody responses to flaviviruses: Lessons for vaccine design. *EMBO Rep.* **2018**, *19*, 206–224. [[CrossRef](#)] [[PubMed](#)]

107. Smith, J.L.; Jeng, S.; McWeeney, S.K.; Hirsch, A.J. A microRNA screen identifies the wnt signaling pathway as a regulator of the interferon response during flavivirus infection. *J. Virol.* **2017**, *91*. [[CrossRef](#)] [[PubMed](#)]
108. Panayiotou, C.; Lindqvist, R.; Kurhade, C.; Vonderstein, K.; Pasto, J.; Edlund, K.; Upadhyay, A.S.; Overby, A.K. Viperin restricts Zika virus and tick-borne encephalitis virus replication by targeting NS3 for proteasomal degradation. *J. Virol.* **2018**, *92*. [[CrossRef](#)] [[PubMed](#)]
109. Anglero-Rodriguez, Y.I.; MacLeod, H.J.; Kang, S.; Carlson, J.S.; Jupatanakul, N.; Dimopoulos, G. Aedes aegypti molecular responses to Zika virus: Modulation of infection by the toll and Jak/Stat immune pathways and virus host factors. *Front. Microbiol.* **2017**, *8*, 2050. [[CrossRef](#)] [[PubMed](#)]
110. Moran, M.; Delmiro, A.; Blazquez, A.; Ugalde, C.; Arenas, J.; Martin, M.A. Bulk autophagy, but not mitophagy, is increased in cellular model of mitochondrial disease. *Biochim. Biophys. Acta* **2014**, *1842*, 1059–1070. [[CrossRef](#)] [[PubMed](#)]
111. Liang, Q.; Luo, Z.; Zeng, J.; Chen, W.; Foo, S.S.; Lee, S.A.; Ge, J.; Wang, S.; Goldman, S.A.; Zlokovic, B.V.; et al. Zika virus NS4A and NS4B proteins deregulate Akt-mTOR signaling in human fetal neural stem cells to inhibit neurogenesis and induce autophagy. *Cell Stem Cell* **2016**, *19*, 663–671. [[CrossRef](#)] [[PubMed](#)]
112. Tetro, J.A. Zika and microcephaly: Causation, correlation, or coincidence? *Microbes Infect.* **2016**, *18*, 167–168. [[CrossRef](#)] [[PubMed](#)]
113. Chiramel, A.I.; Best, S.M. Role of autophagy in Zika virus infection and pathogenesis. *Virus Res.* **2017**. [[CrossRef](#)] [[PubMed](#)]
114. Lennemann, N.J.; Coyne, C.B. Dengue and Zika viruses subvert reticulophagy by NS2B3-mediated cleavage of FAM134B. *Autophagy* **2017**, *13*, 322–332. [[CrossRef](#)] [[PubMed](#)]
115. Wu, Y.; Liu, Q.; Zhou, J.; Xie, W.; Chen, C.; Wang, Z.; Yang, H.; Cui, J. Zika virus evades interferon-mediated antiviral response through the co-operation of multiple nonstructural proteins in vitro. *Cell Discov.* **2017**, *3*, 17006. [[CrossRef](#)] [[PubMed](#)]
116. Weisman, R.; Roitburg, I.; Schonbrun, M.; Harari, R.; Kupiec, M. Opposite effects of TOR1 and TOR2 on nitrogen starvation responses in fission yeast. *Genetics* **2007**, *175*, 1153–1162. [[CrossRef](#)] [[PubMed](#)]
117. Fenyvuesvolgyi, C.; Elder, R.T.; Benko, Z.; Liang, D.; Zhao, R.Y. Fission yeast homologue of Tip41-like proteins regulates type 2A phosphatases and responses to nitrogen sources. *Biochim. Biophys. Acta* **2005**, *1746*, 155–162. [[CrossRef](#)] [[PubMed](#)]
118. Elong Ngono, A.; Vizcarra, E.A.; Tang, W.W.; Sheets, N.; Joo, Y.; Kim, K.; Gorman, M.J.; Diamond, M.S.; Shresta, S. Mapping and role of the CD8⁺ T cell response during primary Zika virus infection in mice. *Cell Host Microbe* **2017**, *21*, 35–46. [[CrossRef](#)] [[PubMed](#)]
119. Zammarchi, L.; Tappe, D.; Fortuna, C.; Remoli, M.E.; Gunther, S.; Venturi, G.; Bartoloni, A.; Schmidt-Chanasit, J. Zika virus infection in a traveller returning to Europe from Brazil, March 2015. *Eurosurveillance* **2015**, *20*, 21153. [[CrossRef](#)] [[PubMed](#)]
120. Andrade, D.V.; Harris, E. Recent advances in understanding the adaptive immune response to Zika virus and the effect of previous flavivirus exposure. *Virus Res.* **2017**. [[CrossRef](#)] [[PubMed](#)]
121. Bardina, S.V.; Bunduc, P.; Tripathi, S.; Duehr, J.; Frere, J.J.; Brown, J.A.; Nachbagauer, R.; Foster, G.A.; Krysztof, D.; Tortorella, D.; et al. Enhancement of Zika virus pathogenesis by preexisting ant flavivirus immunity. *Science* **2017**, *356*, 175–180. [[CrossRef](#)] [[PubMed](#)]
122. Priyamvada, L.; Quicke, K.M.; Hudson, W.H.; Onlamoon, N.; Sewatanon, J.; Edupuganti, S.; Pattanapanyasat, K.; Chokephaibulkit, K.; Mulligan, M.J.; Wilson, P.C.; et al. Human antibody responses after dengue virus infection are highly cross-reactive to Zika virus. *Proc. Natl. Acad. Sci. USA* **2016**, *113*, 7852–7857. [[CrossRef](#)] [[PubMed](#)]
123. Lazear, H.M.; Govero, J.; Smith, A.M.; Platt, D.J.; Fernandez, E.; Miner, J.J.; Diamond, M.S. A mouse model of Zika virus pathogenesis. *Cell Host Microbe* **2016**, *19*, 720–730. [[CrossRef](#)] [[PubMed](#)]
124. Rossi, S.L.; Tesh, R.B.; Azar, S.R.; Muruato, A.E.; Hanley, K.A.; Auguste, A.J.; Langsjoen, R.M.; Paessler, S.; Vasilakis, N.; Weaver, S.C. Characterization of a novel murine model to study Zika virus. *Am. J. Trop. Med. Hyg.* **2016**, *94*, 1362–1369. [[CrossRef](#)] [[PubMed](#)]
125. Kumar, A.; Hou, S.; Airo, A.M.; Limonta, D.; Mancinelli, V.; Branton, W.; Power, C.; Hobman, T.C. Zika virus inhibits type-I interferon production and downstream signaling. *EMBO Rep.* **2016**, *17*, 1766–1775. [[CrossRef](#)] [[PubMed](#)]

126. Grant, A.; Ponia, S.S.; Tripathi, S.; Balasubramaniam, V.; Miorin, L.; Sourisseau, M.; Schwarz, M.C.; Sanchez-Seco, M.P.; Evans, M.J.; Best, S.M.; et al. Zika virus targets human Stat2 to inhibit type I interferon signaling. *Cell Host Microbe* **2016**, *19*, 882–890. [[CrossRef](#)] [[PubMed](#)]
127. Hertzog, J.; Dias Junior, A.G.; Rigby, R.E.; Donald, C.L.; Mayer, A.; Sezgin, E.; Song, C.; Jin, B.; Hublitz, P.; Eggeling, C.; et al. Infection with a Brazilian isolate of Zika virus generates RIG-I stimulatory RNA and the viral NS5 protein blocks type I IFN induction and signaling. *Eur. J. Immunol.* **2018**. [[CrossRef](#)] [[PubMed](#)]
128. Chaudhary, V.; Yuen, K.S.; Chan, J.F.; Chan, C.P.; Wang, P.H.; Cai, J.P.; Zhang, S.; Liang, M.; Kok, K.H.; Chan, C.P.; et al. Selective activation of type ii interferon signaling by Zika virus NS5 protein. *J. Virol.* **2017**, *91*. [[CrossRef](#)] [[PubMed](#)]
129. Nguyen, H.N.; Qian, X.; Song, H.; Ming, G.L. Neural stem cells attacked by zika virus. *Cell Res.* **2016**, *26*, 753–754. [[CrossRef](#)] [[PubMed](#)]
130. Slomnicki, L.P.; Chung, D.H.; Parker, A.; Hermann, T.; Boyd, N.L.; Hetman, M. Ribosomal stress and Tp53-mediated neuronal apoptosis in response to capsid protein of the Zika virus. *Sci. Rep.* **2017**, *7*, 16652. [[CrossRef](#)] [[PubMed](#)]
131. Yoon, K.J.; Song, G.; Qian, X.; Pan, J.; Xu, D.; Rho, H.S.; Kim, N.S.; Habela, C.; Zheng, L.; Jacob, F.; et al. Zika-virus-encoded NS2A disrupts mammalian cortical neurogenesis by degrading adherens junction proteins. *Cell Stem Cell* **2017**, *21*, 349–358 e346. [[CrossRef](#)] [[PubMed](#)]
132. Xie, D.Y.; Liu, Z.Y.; Nian, Q.G.; Zhu, L.; Wang, N.; Deng, Y.Q.; Zhao, H.; Ji, X.; Li, X.F.; Wang, X.; et al. A single residue in the alphab helix of the e protein is critical for Zika virus thermostability. *Emerg. Microbes Infect.* **2018**, *7*, 5. [[CrossRef](#)] [[PubMed](#)]
133. Brault, A.C.; Domi, A.; McDonald, E.M.; Talmi-Frank, D.; McCurley, N.; Basu, R.; Robinson, H.L.; Hellerstein, M.; Duggal, N.K.; Bowen, R.A.; et al. A zika vaccine targeting NS1 protein protects immunocompetent adult mice in a lethal challenge model. *Sci. Rep.* **2017**, *7*, 14769. [[CrossRef](#)] [[PubMed](#)]
134. Lei, J.; Hansen, G.; Nitsche, C.; Klein, C.D.; Zhang, L.; Hilgenfeld, R. Crystal structure of Zika virus NS2B-NS3 protease in complex with a boronate inhibitor. *Science* **2016**, *353*, 503–505. [[CrossRef](#)] [[PubMed](#)]
135. Bukrinsky, M. Yeast help identify cytopathic factors of zika virus. *Cell Biosci.* **2017**, *7*, 12. [[CrossRef](#)] [[PubMed](#)]
136. Nasmyth, K. A prize for proliferation. *Cell* **2001**, *107*, 689–701. [[CrossRef](#)]
137. Nurse, P. Cyclin dependent kinases and cell cycle control (nobel lecture). *ChemBiochem* **2002**, *3*, 596–603. [[CrossRef](#)]
138. Tooze, S.A.; Dikic, I. Autophagy captures the Nobel Prize. *Cell* **2016**, *167*, 1433–1435. [[CrossRef](#)] [[PubMed](#)]
139. Zhao, R.Y. Yeast for virus research. *Microb. Cell* **2017**, *4*, 311–330. [[CrossRef](#)] [[PubMed](#)]
140. Zhao, Y.; Elder, R.T.; Chen, M.; Cao, J. Fission yeast expression vectors adapted for positive identification of gene insertion and green fluorescent protein fusion. *Biotechniques* **1998**, *25*, 438–440, 442, 444. [[PubMed](#)]
141. Li, G.; Zhao, R.Y. Molecular cloning and characterization of small viral genome in fission yeast. *Methods Mol. Biol.* **2018**, *1721*, 47–61. [[PubMed](#)]
142. Romero-Brey, I.; Bartenschlager, R. Endoplasmic reticulum: The favorite intracellular niche for viral replication and assembly. *Viruses* **2016**, *8*, 160. [[CrossRef](#)] [[PubMed](#)]
143. Kaufusi, P.H.; Kelley, J.F.; Yanagihara, R.; Nerurkar, V.R. Induction of endoplasmic reticulum-derived replication-competent membrane structures by West Nile virus non-structural protein 4B. *PLoS ONE* **2014**, *9*, e84040. [[CrossRef](#)] [[PubMed](#)]
144. Sangiambut, S.; Keelapang, P.; Aaskov, J.; Puttikhunt, C.; Kasinrer, W.; Malasit, P.; Sittisombut, N. Multiple regions in dengue virus capsid protein contribute to nuclear localization during virus infection. *J. Gen. Virol.* **2008**, *89*, 1254–1264. [[CrossRef](#)] [[PubMed](#)]
145. Stock, N.K.; Escadafal, C.; Achazi, K.; Cisse, M.; Niedrig, M. Development and characterization of polyclonal peptide antibodies for the detection of yellow fever virus proteins. *J. Virol. Methods* **2015**, *222*, 110–116. [[CrossRef](#)] [[PubMed](#)]
146. Cox, B.D.; Stanton, R.A.; Schinazi, R.F. Predicting Zika virus structural biology: Challenges and opportunities for intervention. *Antivir. Chem. Chemother.* **2015**, *24*, 118–126. [[CrossRef](#)] [[PubMed](#)]
147. Kostyuchenko, V.A.; Lim, E.X.; Zhang, S.; Fibriansah, G.; Ng, T.S.; Ooi, J.S.; Shi, J.; Lok, S.M. Structure of the thermally stable zika virus. *Nature* **2016**, *533*, 425–428. [[CrossRef](#)] [[PubMed](#)]
148. Fontes-Garfias, C.R.; Shan, C.; Luo, H.; Muruato, A.E.; Medeiros, D.B.A.; Mays, E.; Xie, X.; Zou, J.; Roundy, C.M.; Wakamiya, M.; et al. Functional analysis of glycosylation of Zika virus envelope protein. *Cell Rep.* **2017**, *21*, 1180–1190. [[CrossRef](#)] [[PubMed](#)]

149. Annamalai, A.S.; Pattnaik, A.; Sahoo, B.R.; Muthukrishnan, E.; Natarajan, S.K.; Steffen, D.; Vu, H.L.X.; Delhon, G.; Osorio, F.A.; Petro, T.M.; et al. Zika virus encoding non-glycosylated envelope protein is attenuated and defective in neuroinvasion. *J. Virol.* **2017**, *91*. [[CrossRef](#)] [[PubMed](#)]
150. Goo, L.; DeMaso, C.R.; Pelc, R.S.; Ledgerwood, J.E.; Graham, B.S.; Kuhn, R.J.; Pierson, T.C. The Zika virus envelope protein glycan loop regulates virion antigenicity. *Virology* **2018**, *515*, 191–202. [[CrossRef](#)] [[PubMed](#)]
151. Gallichotte, E.N.; Dinno, K.H., 3rd; Lim, X.N.; Ng, T.S.; Lim, E.X.Y.; Menachery, V.D.; Lok, S.M.; Baric, R.S. CD-loop extension in Zika virus envelope protein key for stability and pathogenesis. *J. Infect. Dis.* **2017**, *216*, 1196–1204. [[CrossRef](#)] [[PubMed](#)]
152. Yuan, L.; Huang, X.Y.; Liu, Z.Y.; Zhang, F.; Zhu, X.L.; Yu, J.Y.; Ji, X.; Xu, Y.P.; Li, G.; Li, C.; et al. A single mutation in the prM protein of Zika virus contributes to fetal microcephaly. *Science* **2017**, *358*, 933–936. [[CrossRef](#)] [[PubMed](#)]
153. Shan, C.; Xie, X.; Muruato, A.E.; Rossi, S.L.; Roundy, C.M.; Azar, S.R.; Yang, Y.; Tesh, R.B.; Bourne, N.; Barrett, A.D.; et al. An infectious cDNA clone of Zika virus to study viral virulence, mosquito transmission, and antiviral inhibitors. *Cell Host Microbe* **2016**, *19*, 891–900. [[CrossRef](#)] [[PubMed](#)]
154. Mahawaththa, M.C.; Pearce, B.J.G.; Szabo, M.; Graham, B.; Klein, C.D.; Nitsche, C.; Otting, G. Solution conformations of a linked construct of the Zika virus NS2B-NS3 protease. *Antiviral Res.* **2017**, *142*, 141–147. [[CrossRef](#)] [[PubMed](#)]
155. Phoo, W.W.; Li, Y.; Zhang, Z.; Lee, M.Y.; Loh, Y.R.; Tan, Y.B.; Ng, E.Y.; Lescar, J.; Kang, C.; Luo, D. Structure of the NS2B-NS3 protease from Zika virus after self-cleavage. *Nat. Commun.* **2016**, *7*, 13410. [[CrossRef](#)] [[PubMed](#)]
156. Lee, H.; Ren, J.; Nocadello, S.; Rice, A.J.; Ojeda, I.; Light, S.; Minasov, G.; Vargas, J.; Nagarathnam, D.; Anderson, W.F.; et al. Identification of novel small molecule inhibitors against NS2B/NS3 serine protease from Zika virus. *Antiviral Res.* **2017**, *139*, 49–58. [[CrossRef](#)] [[PubMed](#)]
157. Shafee, N.; AbuBakar, S. Dengue virus type 2 NS3 protease and NS2B-NS3 protease precursor induce apoptosis. *J. Gen. Virol.* **2003**, *84*, 2191–2195. [[CrossRef](#)] [[PubMed](#)]
158. Yang, T.C.; Shiu, S.L.; Chuang, P.H.; Lin, Y.J.; Wan, L.; Lan, Y.C.; Lin, C.W. Japanese encephalitis virus NS2B-NS3 protease induces caspase 3 activation and mitochondria-mediated apoptosis in human medulloblastoma cells. *Virus Res.* **2009**, *143*, 77–85. [[CrossRef](#)] [[PubMed](#)]
159. Rastogi, M.; Sharma, N.; Singh, S.K. Flavivirus ns1: A multifaceted enigmatic viral protein. *Virol. J.* **2016**, *13*, 131. [[CrossRef](#)] [[PubMed](#)]
160. Viranaicken, W.; Ndebo, A.; Bos, S.; Souque, P.; Gadea, G.; El-Kalamouni, C.; Krejbich-Trotot, P.; Charneau, P.; Despres, P.; Roche, M. Recombinant Zika ns1 protein secreted from vero cells is efficient for inducing production of immune serum directed against NS1 dimer. *Int. J. Mol. Sci.* **2017**, *19*, 38. [[CrossRef](#)] [[PubMed](#)]
161. Freire, C.C.M.; Lamarino, A.; Neto, D.F.L.N.; Sall, A.A.; Zanutto, P.M.A. Spread of the pandemic Zika virus lineage is associated with NS1 codon usage adaptation in humans. *BioRxiv* **2015**. [[CrossRef](#)]
162. Delatorre, E.; Mir, D.; Bello, G. Tracing the origin of the NS1 A188V substitution responsible for recent enhancement of Zika virus Asian genotype infectivity. *Mem. Inst. Oswaldo Cruz* **2017**, *112*, 793–795. [[CrossRef](#)] [[PubMed](#)]



LIST OF PUBLICATIONS

— 2019 —

Li G[†] and **Bos S**[†], Tsetsarkin K A, Pletnev A G, Desprès P, Gadea G and Zhao R Y (2019) **The Roles of prM-E Proteins in Historical and Epidemic Zika Virus-mediated Infection and Neurocytotoxicity**. *Viruses* 11 157

— 2018 —

El Kalamouni C[†] and Frumence E[†], **Bos S**, Turpin J, Nativel B, Harrabi W, Wilkinson D A, Meilhac O, Gadea G, Desprès P, Krejbich-Trotot P and Viranaïcken W (2018) **Subversion of the Heme Oxygenase-1 Antiviral Activity by Zika Virus**. *Viruses* 11

Bos S, Gadea G and Despres P (2018a) **Dengue: a growing threat requiring vaccine development for disease prevention**. *Pathogens and Global Health* 0 1–12

Lee I, **Bos S**, Li G, Wang S, Gadea G, Desprès P and Zhao R Y (2018) **Probing Molecular Insights into Zika Virus–Host Interactions**. *Viruses* 10 233

Gaudry A, **Bos S**, Viranaïcken W, Roche M, Krejbich-Trotot P, Gadea G, Desprès P and El-Kalamouni C (2018) **The Flavonoid Isoquercitrin Precludes Initiation of Zika Virus Infection in Human Cells**. *International Journal of Molecular Sciences* 19 1093

Bos S, Viranaïcken W, Turpin J, El-Kalamouni C, Roche M, Krejbich-Trotot P, Desprès P and Gadea G (2018) **The structural proteins of epidemic and historical strains of Zika virus differ in their ability to initiate viral infection in human host cells**. *Virology* 516 265–73

— 2017 —

Viranaïcken W, Ndebo A, **Bos S**, Souque P, Gadea G, El-Kalamouni C, Krejbich-Trotot P, Charneau P, Desprès P and Roche M (2017b) **Recombinant Zika NS1 Protein Secreted from Vero Cells Is Efficient for Inducing Production of Immune Serum Directed against NS1 Dimer**. *International Journal of Molecular Sciences* 19

Viranaicken W, Nativel B, Krejbich-Trotot P, Harrabi W, **Bos S**, El Kalamouni C, Roche M, Gadea G and Desprès P (2017) **ClearColi BL21(DE3)-based expression of Zika virus antigens illustrates a rapid method of antibody production against emerging pathogens.** *Biochimie* 142 179–82

— 2016 —

Gadea G, **Bos S**, Krejbich-Trotot P, Clain E, Viranaicken W, El-Kalamouni C, Mavingui P and Desprès P (2016) **A robust method for the rapid generation of recombinant Zika virus expressing the GFP reporter gene.** *Virology* 497 157–62



American Society for Virology • University of Maryland

**WORKSHOP #22: FLAVIVIRUSES II—
MOLECULAR MECHANISMS OF INFECTION**

SUNDAY EVENING 7:00 PM

LOCATION: ST JOHN 1224

Convenor: Cara Pager

7:00–7:15 W22-1 **McDonald, E.M.**; Duggal, N.K.; Brault, A.C. (Centers for Disease Control and Prevention Division of Vector-Borne Infectious Diseases; Department of Biomedical Sciences and Pathobiology, Virginia Polytechnic Institute and State University)

Molecular Mechanisms of *In Utero* and Sexual Transmission of Zika Virus

7:15–7:30 W22-2 **Barnard, T.R.**; Rajah, M.M.; Sagan, S.M. (McGill University, Montreal, Canada)

Genetic Determinants of Zika Virus Fitness

7:30–7:45 W22-3 **Bos, S.**; Viranaicken, W.; Turpin, J.; El-Kalamouni, C.; Roche, M.; Krejbich-Trotot, P.; Despres, P.; Gadea, G. (Université de La Réunion, INSERM U1187, CNRS UMR 9192, IRD UMR 249, Unité Mixte Processus Infectieux en Milieu Insulaire Tropical, Plateforme Technologique CYROI, 97491, Sainte-Clotilde, La Reunion, France)

The Structural Proteins of Epidemic and Historical Strains of Zika Virus Differ in Their Ability to Initiate Viral Infection in Human Epithelial and Neuronal Cells

Abstract

Zika virus (ZIKV) is a mosquito-borne enveloped RNA virus belonging to flavivirus genus. In the past few years it has been associated with severe complications in humans, including neonatal birth defects and Guillain-Barré syndrome in adults, and became a major medical concern worldwide. ZIKV strains are divided into African and Asian genotypes, the latter being the leading cause of the major outbreaks. Faced with the increasing ZIKV threat, scientific efforts have been made to understand its pathogenicity. The characterization of epidemic ZIKV strains moved forward leading to the identification of molecular mechanisms involved in viral disease pathophysiology. In our study, efforts have been put to better understand the contribution of the structural proteins C, prM and E in the pathogenic properties of ZIKV epidemic strains. To this end, we generated the molecular clones BR15^{MC} derived from BeH819015 strain isolated in Brazil in 2015, and MR766^{MC} from African historical strain isolated in Uganda in 1947 using the ISA method-based inverse genetic strategy. A chimeric clone MR766/BR15^{CprME} containing the BeH819015 proteins C, prM, and E¹⁻⁴³⁷ was also constructed. The growths of the three viral clones were compared in human A549 and SH-SY5Y cells. Virus binding assay showed that ZIKV clones containing BeH819015 structural proteins were much less efficient in cell-attachment when compared to MR766^{MC}. The lower binding capacity of BeH819015 structural proteins was associated with a delay (A549 cells) or severe restriction (SH-SY5Y cells) in viral growth. ZIKV-mediated cell death and activation of innate immune responses were also delayed in A549 cells infected with BR15^{MC} or MR766/BR15^{CprME}. Among the diverging residues identified between MR766^{MC} and MR766/BR15^{CprME}, eleven amino acid substitutions could potentially be involved in the lower permissiveness of human host cells to BR15^{MC}. It is now crucial to determine which ones contribute to the permissiveness of human host-cells to ZIKV.

LETTRE D'ENGAGEMENT DE NON-PLAGIAT

Je, soussigné(e) Mme BOS Sandra en ma qualité de doctorant(e) de l'Université de La Réunion, déclare être conscient(e) que le plagiat est un acte délictueux passible de sanctions disciplinaires. Aussi, dans le respect de la propriété intellectuelle et du droit d'auteur, je m'engage à systématiquement citer mes sources, quelle qu'en soit la forme (textes, images, audiovisuel, internet), dans le cadre de la rédaction de ma thèse et de toute autre production scientifique, sachant que l'établissement est susceptible de soumettre le texte de ma thèse à un logiciel anti-plagiat.

Fait à Saint-Denis le : 30/04/2019

Signature :



Extrait du Règlement intérieur de l'Université de La Réunion
(validé par le Conseil d'Administration en date du 11 décembre 2014)

Article 9. Protection de la propriété intellectuelle – Faux et usage de faux, contrefaçon, plagiat

L'utilisation des ressources informatiques de l'Université implique le respect de ses droits de propriété intellectuelle ainsi que ceux de ses partenaires et plus généralement, de tous tiers titulaires de ces droits.

En conséquence, chaque utilisateur doit :

- utiliser les logiciels dans les conditions de licences souscrites ;
- ne pas reproduire, copier, diffuser, modifier ou utiliser des logiciels, bases de données, pages Web, textes, images, photographies ou autres créations protégées par le droit d'auteur ou un droit privatif, sans avoir obtenu préalablement l'autorisation des titulaires de ces droits.

La contrefaçon et le faux

Conformément aux dispositions du code de la propriété intellectuelle, toute représentation ou reproduction intégrale ou partielle d'une œuvre de l'esprit faite sans le consentement de son auteur est illicite et constitue un délit pénal.

L'article 444-1 du code pénal dispose : « Constitue un faux toute altération frauduleuse de la vérité, de nature à causer un préjudice et accomplie par quelque moyen que ce soit, dans un écrit ou tout autre support d'expression de la pensée qui a pour objet ou qui peut avoir pour effet d'établir la preuve d'un droit ou d'un fait ayant des conséquences juridiques ».

L'article L335_3 du code de la propriété intellectuelle précise que : « Est également un délit de contrefaçon toute reproduction, représentation ou diffusion, par quelque moyen que ce soit, d'une œuvre de l'esprit en violation des droits de l'auteur, tels qu'ils sont définis et réglementés par la loi. Est également un délit de contrefaçon la violation de l'un des droits de l'auteur d'un logiciel (...) ».

Le plagiat est constitué par la copie, totale ou partielle d'un travail réalisé par autrui, lorsque la source empruntée n'est pas citée, quel que soit le moyen utilisé. Le plagiat constitue une violation du droit d'auteur (au sens des articles L 335-2 et L 335-3 du code de la propriété intellectuelle). Il peut être assimilé à un délit de contrefaçon. C'est aussi une faute disciplinaire, susceptible d'entraîner une sanction.

Les sources et les références utilisées dans le cadre des travaux (préparations, devoirs, mémoires, thèses, rapports de stage...) doivent être clairement citées. Des citations intégrales peuvent figurer dans les documents rendus, si elles sont assorties de leur référence (nom d'auteur, publication, date, éditeur...) et identifiées comme telles par des guillemets ou des italiques.

Les délits de contrefaçon, de plagiat et d'usage de faux peuvent donner lieu à une sanction disciplinaire indépendante de la mise en œuvre de poursuites pénales.